

EXHIBIT 7



Brain wave synchronization and entrainment to periodic acoustic stimuli

Udo Will*, Eric Berg

School of Music, Cognitive Ethnomusicology, Ohio State University, 110 Weigel Hall, 1866 College Road, Columbus, OH 43210, USA

Received 4 January 2007; received in revised form 14 June 2007; accepted 12 July 2007

Abstract

As known, different brainwave frequencies show synchronies related to different perceptual, motor or cognitive states. Brainwaves have also been shown to synchronize with external stimuli with repetition rates of ca. 10–40 Hz. However, not much is known about responses to periodic auditory stimuli with periodicities found in human rhythmic behavior (i.e. 0.5–5 Hz). In an EEG study we compared responses to periodic stimulations (drum sounds and clicks with repetition rates of 1–8 Hz), silence, and random noise. Here we report inter-trial coherence measures taken at the Cz-electrode that show a significant increase in brainwave synchronization following periodic stimulation. Specifically, we found (1) a tonic synchronization response in the delta range with a maximum response at 2 Hz, (2) a phasic response covering the theta range, and (3) an augmented phase synchronization throughout the beta/gamma range (13–44 Hz) produced through increased activity in the lower gamma range and modulated by the stimulus periodicity. Periodic auditory stimulation produces a mixture of evoked and induced, rate-specific and rate-independent increases in stimulus related brainwave synchronization that are likely to affect various cognitive functions. The synchronization responses in the delta range may form part of the neurophysiological processes underlying time coupling between rhythmic sensory input and motor output; the tonic 2 Hz maximum corresponds to the optimal tempo identified in listening, tapping synchronization, and event-interval discrimination experiments. In addition, synchronization effects in the beta and gamma range may contribute to the reported influences of rhythmic entrainment on cognitive functions involved in learning and memory tasks.

© 2007 Elsevier Ireland Ltd. All rights reserved.

Keywords: Synchronization; Entrainment; Brainwaves; Auditory stimuli

Synchronization of oscillatory activities in distributed neural assemblies is a well-studied mechanism in the working of the brain. It can be understood as a reflection of the cooperative activity of neurons within distributed assemblies [10]. It entails the ideas that certain types of neural assemblies are characterized by synchronous activity of their constituent neurons, and that different EEG frequency components reveal synchronies related to different perceptual, motor or cognitive states [2,9,11,21]. Early in the history of human brain physiology it was demonstrated that brain activities could also synchronize to external stimuli [1,25]. Research using auditory stimuli has focused primarily on ‘steady-state auditory evoked potentials’ [8,9,16], working with stimulus repetition rates in the gamma range from 30 to 50 Hz. An area nearly absent from previous research is the synchronization of brainwaves to auditory stimuli with repetition rates below 10 Hz. This is somewhat surprising in view of a century of research on rhythmic sensorimotor synchronization [20,19],

and the overwhelming evidence for an optimal repetition rate in human repetitive perceptuo-motor behavior of 0.5 and 4 Hz (e.g. preferred tempo in listening to and in making of music, accuracy in detecting deviant event intervals, tapping synchronization, etc.) [6,24]. Recently, entrainment models of rhythmic motor behavior [12,13] have stimulated studies examining intrinsic rhythmicity and frequency coupling in neural systems as well as clinically applied synchronization research [23,22]. Despite the considerable number of studies, however, neurophysiological processes that underlie time coupling between rhythmic sensory input and motor output are still not well understood. The present study explores one aspect of this coupling by investigating whether brainwave oscillations synchronize to rhythmic auditory stimuli with stimulation rates of 1–8 Hz, a range most relevant to human repetitive sensorimotor behavior.

There has been only one previous study reporting a driving response of the EEG amplitude to acoustic stimuli with repetition rates from 3 to 8 Hz [15]. The study used direct, non-averaged EEG measurements, and it is unclear whether the identified responses were neurogenic in origin. Unfortunately, that study has never been replicated independently, probably

* Corresponding author. Tel.: +1 614 292 1585.

E-mail address: will.51@osu.edu (U. Will).

due to the fact that the experimental procedure applied does not easily lead to consistent analysis of the EEG amplitude periodicities: various studies have shown that auditory event related potentials attenuate with stimulus repetition and that degree of attenuation is affected by stimulation rate [14,17,7]. This reduced amplitude, together with the large variability of responses to repeated stimuli [3] causes considerable complications for standard ERP analysis in this experimental paradigm (continuous stimulation). We therefore decided to approach the question of EEG synchronization to periodic auditory stimulation by focusing on the analysis of stimulus related phase coherence.

In the present study we recorded EEGs from 10 subjects (5 females; mean age 26) who had been asked to listen to sound stimuli passively. Periodic acoustic stimuli consisted of clicks (0.005 s rectangular pulses) and drum sounds, each presented with repetition rates of 1–6, and 8 sounds/s (Hz); recordings with silence (no acoustic stimulation) and continuous pink noise (noise with an energy distribution matching human auditory frequency sensitivity) served as controls and reference measures. Subjects were seated in an upright chair, wearing an EEG cap and listening to the stimuli via headphones with eyes closed. The peak SPL for the click and drum sounds at headphones was adjusted to 79 dB. Continuous EEG recordings were made while subjects listened to 120-s periods of randomly selected periodic stimuli, silence, or pink noise. The presentation sequence of repetition rates and control trials was counterbalanced across subjects. EEGs were recorded from 19 non-polarizable Ag/AgCl electrodes (impedance < 5 k Ω) according to the international 10–20 system, referenced against common linked earlobes. Sampling rate was 256 Hz with a time constant of 0.3 s (upper frequency limit = 70 Hz). Data segments containing eye movements or voltage fluctuations > 250 μ V were excluded from further data processing. The analyses reported here were per-

formed on recordings from the vertex electrode (Cz) yielding largest responses.

Synchronization between periodic auditory stimuli and EEG responses was analyzed with the stimulus-locked inter-trial coherence (ITC) applied to 3-s epochs of the EEG recordings, with each epoch-start aligned with a stimulus onset. ITC, also referred to as “phase-locking factor” (Tallon-Baudry [21]), is a measure of consistency across epochs (or trials) of the EEG spectral phase at each frequency and latency window. Calculations for the spectral estimate of the normalized power spectrum were run on 3-s epochs using a three-cycle Hanning-windowed sinusoidal wavelet. ITC values were calculated for 21 EEG frequency bands (ten 1-Hz bands from 1 to 10 Hz, five 2-Hz bands from 12 to 20 Hz and six 4-Hz bands from 22 to 44 Hz). Because of the window effects only ITC values from the middle 1-s epoch were considered in the following. For each stimulus condition and frequency band we obtained epoch-length \times sample-rate = 256 ITC values. ITC calculations were done with our own MATLAB-script using the ‘phasecoher’ function from EEGLAB [5].

As the experimental paradigm does not allow for determination of a significance level for the ITC through comparison with a ‘pre-stimulus’ baseline we tested the significance in an analysis of variance of ITC values for the three experimental conditions (no stimulation, noise, and periodic stimulation). For this analysis ITC values were averaged over the 1-s epochs to obtain mean ITCs for each frequency band, stimulus condition, and subject.

Analysis of variance (ANOVA) of the mean ITC showed a significant effect for stimulus condition (periodic stimuli, noise, and silence), but not for EEG frequency bands (condition: $F(2, 9) = 79.06$, $p < 0.001$; frequency band: $F(20, 9) = 0.39$, $p = 0.9618$). The main effect for condition was due to increased phase coherence under periodic stimulation (Fig. 1a), whereas pink noise slightly reduced phase coherence in comparison

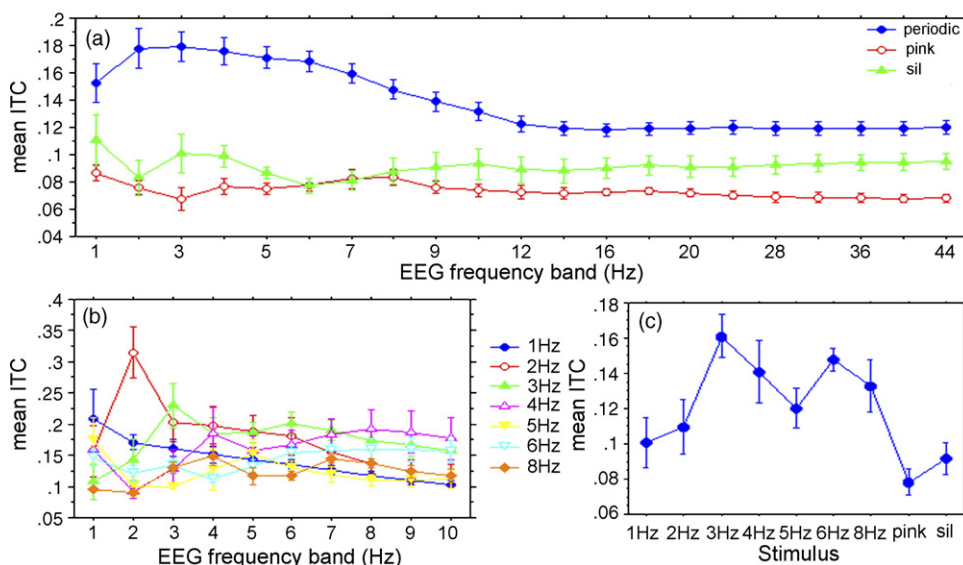


Fig. 1. Grand average ($n = 10$) of mean ITC. (a) Mean ITC for silent condition (sil), continuous pink noise stimulation (pink) and the mean for periodic stimulations (periodic) for all analyzed EEG frequency bands. (b) Mean ITC responses for 1–8 Hz repetition rates in the delta, theta, and alpha range. (c) Mean ITC in the lower gamma range (20 Hz). Error bars are ± 1 S.E.

with silence, the reduction being significant for the 14–44 Hz (beta and gamma) EEG bands (post-hoc Bonferroni–Dunn test: $p < 0.0001$). There was no significant interaction between factors condition and frequency band. Also, a post-hoc test did not show any significant differences between the effects of periodic drum and click stimuli ($F(1, 9) = 0.112$, $p > 0.7$).

Further analysis shows that the increase in inter-trial coherence is not just a consequence of the stimulus sequence but generated by specific brain responses to these stimuli:

- (1) If the mean ITC is analyzed with respect to stimulation rates (Fig. 1b and c) we find frequency specific maxima that cannot be explained in terms of stimulus characteristics (all periodic stimuli had constant duration and amplitude):
 - (a) Responses in the delta and theta range show a marked stimulus rate dependency, with rates from 1 to 5 Hz producing maxima in the respective EEG frequency bands and 2-Hz stimulations generating the largest responses (in the 2 Hz EEG band mean ITC for 2 Hz stimulation rates is about double than that for 1 or 3 Hz; Fig. 1b). This finding is incompatible with the idea that the increased ITC is a mere reflection of stimulus sequence.
 - (b) The increased coherence throughout the EEG frequency bands from 13 to 44 Hz also show stimulus rate dependency with an absolute maximum for 3 Hz and a second, smaller maximum for 6 Hz stimulus rates (Fig. 1c). A posthoc analysis for stimulus rate shows that mean ITC for 3 and 6 Hz in the 20 Hz EEG band are not only

significantly different from the silent and pink condition (Bonferroni–Dunn test $p < 0.0001$) but also from the 1 Hz stimulation (Bonferroni–Dunn test $p < 0.0001$), whereas mean ITCs for 1 and 2 Hz stimulation are not different from the control conditions (Bonferroni–Dunn test $p > 0.2$ for 1 Hz and $p > 0.06$ for 2 Hz).

- (2) Fig. 1b also suggests that the responses in the delta and theta range may be composite responses, consisting of frequency-band-specific components centered in the delta range and non-specific components with maxima in the theta band. Responses up to 5 Hz repetition rates each have a maximum in the corresponding frequency bands, with 2 Hz producing considerable larger values than the other rates (for 1–3 Hz the maxima are absolute, for 4 and 5 Hz relative). Stimulation rates of 6 and 8 Hz do not produce response peaks at the corresponding EEG frequency band but show relative maxima at the subharmonics of 3 and 4 Hz, respectively. All stimulation rates produce a second, broader response peak (only a raised level for 2 Hz stimuli) in the theta/alpha range.

Analysis of the actual time course of the ITC supports the idea of a composite response in the delta and theta range (Fig. 2): the frequency-specific peaks in the mean ITC responses are produced by a ‘tonic’ ITC component in the frequency band corresponding to the stimulation rate (marked by arrows in Fig. 2). This component has a pronounced maximum at around 2-Hz stimulation rate, falling off sharply at lower and higher rates. Such a response is obviously not a reflection of stimulus features: as a tonic

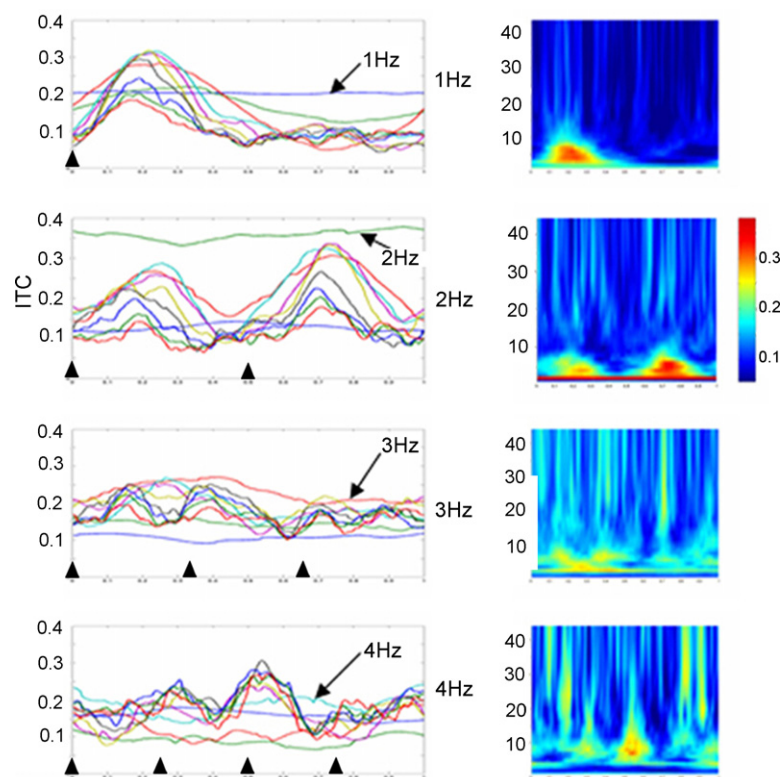


Fig. 2. Grand average ($n = 10$) of ITCs during 1 s EEG epochs for stimulus rates from 1 to 4 Hz. Left column: time/ITC plots for EEG frequency bands 1–10 Hz. Arrows point to the tonic component of the ITC response. Right column: time/EEG frequency bands (1–44 Hz) with ITC colour-coded. Triangles mark onsets of periodic stimuli.

response it shows no periodicities corresponding to the stimulus events and seems to be an induced response that, because of its frequency specificity, can be described as delta wave entrainment to the periodicity of the external acoustic stimuli. The second component is a phasic ITC response in all frequency bands above the band corresponding to the stimulation rate. The fact that its peak amplitude decreases with repetition rate might suggest that this component mainly reflects the coherence of stimulus-evoked activity as described in previous studies [14,17]. However, as it has been demonstrated that stimuli in a sequence – except for the first one – do not lead to stimulus related increase in spectral power [7], it is possible that the phasic response reflects a stimulus-induced activity. This stimulus-induced phase synchronization, however, instantly dissipates and does not lead to entrainment. The loss of stimulus evoked periodicity in the grand mean of this phasic response at rates higher than 2 Hz (see Fig. 2) seems to be due to several factors: higher stimulus rates reduce the amplitude of the evoked activity [14], and repeated stimulation leads to increased response variability [3]. As demonstrated in Fig. 3, this means that responses are not sharply time locked, and that there is subject specific variability in latency and amplitude of this response.

- (3) ITC time plots for the 14–44 Hz EEG bands (Fig. 4a) suggest that synchronization response in this range is different from those in the lower frequency ranges. Increased ITC in this range is marked by a strong 20–26 Hz modulation

(Fig. 4b), an activity that is also present in the absence of auditory stimulation (Fig. 4b). The modulation frequency appears to be independent of the stimulus repetition rate, but the degree of modulation is strongest for 3 Hz stimulation rates. The mean power spectral density of the 22–25 Hz modulation was found to be 12.5 dB higher (for the subject displayed in Fig. 4; mean = 7.2 dB for all 10 subjects) than in the silent condition. Additionally there is also a pronounced modulation by the periodic stimuli (Fig. 4a). For 3 Hz repetition rates the power spectral density of the 3 Hz modulation was found to be 19.3 dB higher (for the subject displayed in Fig. 4; mean = 12.7 dB for all 10 subjects) than in the silent condition. In contrast, non-periodic (noise) stimulation decreases the ongoing ‘background’ synchronization, as indicated by the above ANOVA (see Fig. 1a).

This study demonstrates some hitherto unknown synchronization responses of brainwaves to periodic auditory stimuli. Stimulation with repetition rates of 1–8 Hz leads to increased phase synchronization in all EEG frequency bands and three distinct components can be distinguished. The first is a tonic ITC response (i.e. not reflecting the periodicity of the stimulus sequence) in the delta range and appears to represent an ‘entrainment’ response: repetition rates between 1 and 5 Hz produce ITC response peaks in the corresponding EEG frequency bands and the response has an absolute maximum at around 2 Hz. This maximum corresponds well with the optimal rate (or tempo) identified in various studies on repetitive human

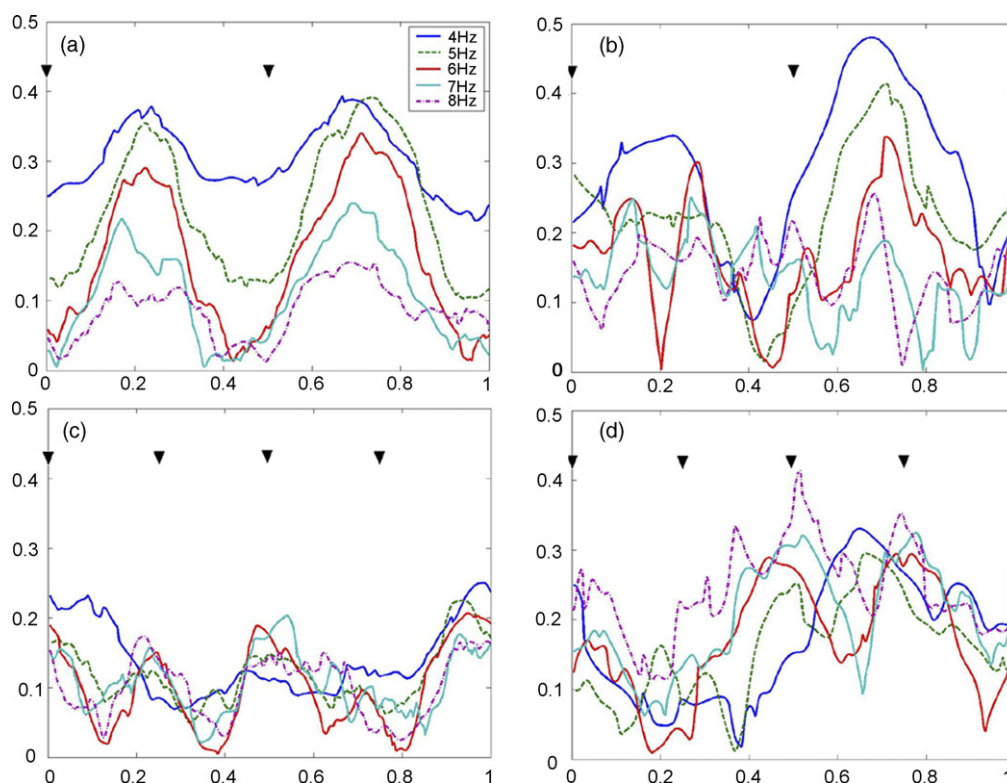


Fig. 3. Inter-subject variability of ITC responses in the theta band (4–8 Hz). Mean ITC responses for 120 1-s epochs from four subjects. (a, b) responses from two subjects for a stimulus rate of 2 Hz. Note the patterned response to the stimulus periods in subject b though all stimuli had constant amplitude. (c, d) responses from two different subjects for a stimulus rate of 4 Hz (the periodicity of the stimulus sequence is largely lost). Triangles mark onsets of periodic stimuli.

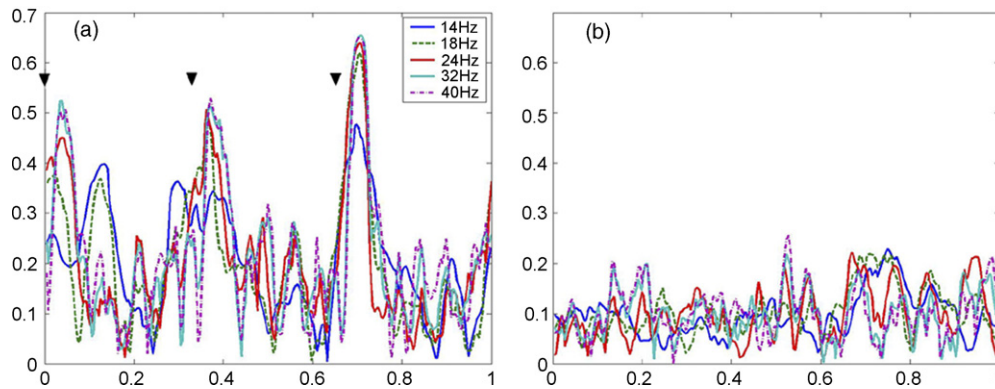


Fig. 4. Pattern of mean ITC responses in the beta and gamma bands for 120 1-s epochs from one subject (only five EEG bands are displayed: 14, 18, 24, 32, 40 Hz). (a) ITC responses for a stimulus rate of 3 Hz. Note increased modulation in low gamma range (ca. 20–26 Hz) that is also present in b, though with smaller amplitude. In addition there is a patterned modulation by the stimuli (3 Hz). (b) Background ITC for the silent condition is still modulated by ongoing activity in the low gamma range, though with considerably reduced amplitude. Triangles in (a) mark onsets of the periodic stimuli.

sensorimotor behavior (e.g. experiments on listening, tapping synchronization, and event-interval discrimination experiments) [24,6,12,13]. We suggest that this synchronization component forms an essential part of the neurophysiological processes underlying time coupling between rhythmic sensory input and motor output.

In contrast, the second component, a phasic response centered in the theta range, does not qualify as an entrainment response as all stimulus rates tested influence the ITC over a broad range of EEG frequencies. To a large part this component seems to reflect EEG activity induced by the sequence of stimuli. Loss of the stimulus periodicity in the grand average for stimulation rates larger than 2 Hz appears to be attributable to its reduced amplitude, considerable inter-subject variability, and the fact that it is not strictly time-locked. This variability in phase synchronicity is probably one of the chief reasons why previous analyses of auditory driving by 3–8 Hz stimuli, working with amplitude analysis of ERP, had not been very successful.

The third component, the synchronization responses in the 14–44 Hz EEG bands consist of an evoked (ITC modulation by the stimulus periodicity) and an induced (increased 20–26 Hz ITC modulation) subcomponent that have not been identified in studies using short stimulus sequences. Fuentemilla et al. [7], using three-stimuli trains with ISIs of 584-ms, did not find significant ERSP or ITC responses in the 20–49 Hz frequency range. These different results could be due to the slightly different analytical methods (ITC significance in Ref. [7] is calculated in reference to a 1000 ms pre-stimulus baseline) or, more likely, the different experimental design. As augmented synchronization in the 14–44 Hz EEG bands seems to be mediated by increased activity in the 20–26 Hz range, it seems possible that this is either not present in short stimulus sequences or rises to significance only under prolonged stimulation. This is supported by a recent study that reported gamma band responses to 60-tone acoustic stimulus trains with 390 ms ISIs [18]. The fact that these responses were also observed for omitted stimuli, together with the ‘mediated’ synchronization reported here, suggest that synchronization responses in the 14–44 Hz range may involve higher level of processing and hence may take part in

the reported influences of rhythmic ‘entrainment’ on cognitive functions involved in learning and memory tasks [22]. Başar-Eroglu and Başar [4] have shown that in cats visual and auditory stimuli evoke gamma responses in various brain regions. They demonstrated induced, evoked, and emitted gamma responses, the latter being bursts of gamma band oscillations time-locked to a stimulus (in a series of stimuli) that has not been presented. Their results suggest that these gamma activities may also be part of processes involved in anticipation, expectation and attention.

Acknowledgements

The research was supported by a grant from the Office of Research, Ohio State University, to U.W. Thanks to M. Jones, A. Neher, and S. Makeig for comments on various parts of this research.

References

- [1] E.D. Adrian, B.H.C. Matthews, The Berger rhythm: potential changes from the occipital lobes in man, *Brain* 57 (1934) 355–384.
- [2] A.P. Anokhin, W. Lutzenberger, N. Birbaumer, Spatiotemporal organization of brain dynamics and intelligence: an EEG study in adolescents, *Int. J. Psychophysiol.* 33 (1999) 259–273.
- [3] A. Arieli, A. Sterkin, A. Grinvald, A. Aertsen, Dynamics of ongoing activity: explanation of the large variability in evoked cortical activity, *Science* 273 (1996) 1868–1871.
- [4] C. Başar-Eroglu, E. Başar, A compound P300–40 Hz response of the cat hippocampus, *Int. J. Neurosci.* 60 (1991) 227–237.
- [5] A. Delorme, S. Makeig, EEGLAB: an open source toolbox for analysis of single trial EEG dynamics including independent component analysis, *J. Neurosci. Methods* 134 (2004) 9–21.
- [6] C. Drake, M.R. Jones, C. Baruch, The development of rhythmic attending in auditory sequences: attunement, referent period, focal attending, *Cognition* 77 (2000) 251–288.
- [7] L.I. Fuentemilla, J. Marco-Pallares, C. Grau, Modulation of spectral power and of phase resting of EEG contributes differentially to the generation of auditory event-related potentials, *Neuroimage* 30 (2006) 909–916.
- [8] R. Galambos, S. Makeig, P. Talmachoff, A 40 Hz auditory potential recorded from the human scalp, *Proc. Natl. Acad. Sci. U.S.A.* 78 (40) (1981) 2643–2647.

- [9] R. Galambos, S. Makeig, Dynamic changes in steady state potentials, in: E. Basar (Ed.), *Dynamics of Sensory and Cognitive Processing of the Brain*, Springer, Berlin, 1988, pp. 102–122.
- [10] J.H. Gruzeliier, New advances in EEG and cognition, *Int. J. Psychophysiol.* 24 (1996) 1–5.
- [11] W. Klimesch, EEG alpha and theta oscillations reflect cognitive and memory performance: a review and analysis, *Brain Res. Rev.* 29 (1999) 169–195.
- [12] E.W. Large, M.R. Jones, The dynamics of attending: How people track time-varying events, *Psychol. Rev.* 106 (1999) 119–159.
- [13] J.D. McAuley, M.R. Jones, Modeling effects of rhythmic context on perceived duration: a comparison of interval and entrainment approaches to short-interval timing, *J. Exp. Psychol. Hum. Percept. Perform.* 29 (2003) 1102–1125.
- [14] R. Näätänen, T. Picton, The N1 wave of the human electric and magnetic response to sound: a review and an analysis of the component structure, *Psychophysiology* 24 (4) (1987) 375–425.
- [15] A. Neher, Auditory driving observed with scalp electrodes in normal subjects, *Electroenceph. Clin. Neurophysiol.* 13 (1961) 449–451.
- [16] T.W. Picton, J. Vajsar, R. Rodriguez, K.B. Campbell, Reliability estimates for steady-state evoked potentials, *Electroencephalogr. Clin. Neurophysiol.* 68 (1987) 119–131.
- [17] J.J. Sable, K.A. Low, E.L. Maclin, M. Fabiani, G. Gratton, Latent inhibition mediates N1 attenuation to repeating sounds, *Psychophysiology* 41 (2004) 636–642.
- [18] J.S. Snyder, E.W. Large, Gamma-band activity reflects the metric structure of rhythmic tone sequences, *Cog. Brain Res.* 24 (2005) 117–126.
- [19] R.H. Stetson, A motor theory of rhythm and discrete succession, *Psychol. Rev.* 12 (250–270 (Part I); 293–350 (Part II)) (1905).
- [20] L.T. Stevens, On the time sense, *Mind* 11 (1886) 393–404.
- [21] C. Tallon-Baudry, O. Bertrand, C. Delpuech, J. Pernier, Stimulus specificity of phase-locked and non-phase-locked 40 Hz visual responses in human, *J. Neurosci.* 16 (13) (1996) 4240–4249.
- [22] M.H. Thaut, G.C. McIntosh, R.R. Rice, Rhythmic facilitation of gait training in hemiparetic stroke rehabilitation, *J. Neurol. Sci.* 151 (1997) 207–212.
- [23] M.T. Turvey, R.C. Schmidt, L.D. Rosenblum, Clock and motor components in absolute coordination of rhythmic movements, *Neuroscience* 33 (1989) 1–10.
- [24] L. Van Noorden, D. Moelants, Resonance in the perception of musical pulse, *J. New Music Res.* 28 (1) (1999) 43–66.
- [25] W.G. Walter, V.J. Dovey, H. Shipton, Analysis of electrical response of human cortex to photic stimulation, *Nature* 158 (1946) 340–341.

EXHIBIT 8

EFFECT OF LOW-LEVEL, LOW-FREQUENCY ELECTRIC FIELDS ON EEG
AND BEHAVIOR IN *MACACA NEMESTRINA*

R. J. GAVALAS, D. O. WALTER, J. HAMER AND W. ROSS ADEY

*Space Biology Laboratory, Brain Research Institute, University of California, Los Angeles, Calif.
90024 (U.S.A.)*

(Accepted September 12th, 1969)

INTRODUCTION

A series of preliminary experiments has been done in an attempt to determine whether or not low-level electric fields have an effect on behavior and/or patterns of electrical activity in the brain of monkeys.

Very few studies of this kind have been done on either animals or man. Experimentally produced changes in reaction time in humans exposed to low-level, low-frequency (less than 12 c/sec) fields have been reported^{7,9}. Changes in human reaction time have also been observed under low-frequency modulated magnetic fields⁶. Wever¹⁹ has described the modification of circadian periods of activity in man under weak 10 c/sec electric fields. It was not known what kind of primate behavior, if any, would be sensitive to field effects so that selection of a suitable behavioral task was a first consideration. Earlier pilot studies in this laboratory suggested that subjective time estimation in humans was influenced by the presence of fields. In the present study, we attempted to devise an analogous time estimation task suitable for use with monkeys, so that electrodes implanted deep in the brain could monitor brain electrical activity throughout the experiments. It is known that scheduling of reinforcements for a simple lever press can alter an animal's rate of response, or the timing of that response, or both. In the present study, monkeys were trained to press a lever under a variation of a fixed-interval (timing) schedule of reinforcement. Under this schedule there are no external cues or signals presented to the animal; he must 'time' his responses from the occurrence of his own last response. It is a schedule which has been widely employed in studies of animal behavior and has been especially useful in detecting effects of small dosages of drugs¹³. It was expected that if there were an effect of the fields it would be seen as a shift in the distribution of the monkey's interresponse times.

Other questions of research strategy arose; it was not obvious what brain structures, if any, would show an effect of the presence of the fields. Nor was it clear what kind of changes one might expect to see in the EEG — other than a possible direct driving by the applied field — or how to assess such changes. Consequently,

Brain Research, 18 (1970) 491–501

an array of 7 bipolar cortical and subcortical electrodes was implanted in the 1st monkey. A slightly different array was implanted in a 2nd monkey and electrode sites for the 3rd monkey were selected on the basis of results from the first 2. Computerized spectral analysis of the EEG was done and some special statistical tests were devised to compare fields-on vs. fields-off changes in EEG.

Low-level (2.8 V p-p) fields were used at 2 frequencies, both within the range of frequencies usually evaluated in EEG work (0–33 c/sec). In some of the experimental runs, 10 c/sec fields were used, to correspond to Hamer's earlier experiments⁸. In other runs, 7 c/sec fields were used because they were in the range of hippocampal theta (4–7 c/sec), a characteristic electrical activity of the brain that has been shown to be important in orienting and discriminating responses^{10,17}.

METHODS: EXPERIMENTAL DESIGN, BEHAVIORAL DATA ANALYSIS, AND EEG ANALYSIS

(1) *Experimental design*

Three pigtailed macaques were implanted with cortical and subcortical bipolar electrodes, and were adapted to Foringer monkey chairs. They were then trained to push a panel in front of them on a fixed interval-drl (differential reinforcement of low rates) limited hold schedule of reinforcement (drl-h schedule). The animal was gradually conditioned to wait 5 sec between pushes, and to push within a 2.5 sec reward-enable interval. If the animal pushed within the specified time interval, he was rewarded with a squirt of apple juice. If he pushed too early, or too late, he did not receive a reward, and the timer recycled to the beginning of another 5 sec interval. The behavioral task was completely automated with logic modules manufactured by B.R.S. Electronics. The monkeys were maintained throughout training and experiments on a standard controlled diet of monkey pellets, fruit, and restricted fluids. A liquid reinforcer was chosen in order to eliminate chewing artifacts in the EEG. The animal was trained until he was performing at a high rate of accuracy (70–80%) and his performance was relatively stable from one day to the next. All of the training was done in an isolated and sound-proofed booth. Task electronics and recording apparatus were in an outer room and the monkey's behavior was continuously monitored on closed-circuit TV.

After the animal was performing well, his behavioral records over a 24 h period were examined to determine periods of free responding during the day, and a 4 h segment of time was selected for scheduling daily experimental runs. The low-level (2.8 V p-p), low-frequency fields were administered by applying the voltage to 2 large metal plates, 40 cm apart, which were fastened to the monkey's chair so that the head of the animal was completely within the fields. Four hour daily tests with the fields on were randomly interspersed with 4 h daily control runs without the fields. A total of 20 such tests were done on the 3 well-trained monkeys. All monkeys were given 2 tests with 7 c/sec fields and 2 comparable control tests without fields. Two of the 3 monkeys were also given 2 tests with 10 c/sec fields and 2 control runs without the fields. EEG and behavioral data were continuously monitored throughout all runs.

In addition, EEG was monitored in 1 monkey during two 4 h non-performance runs (7 c/sec fields-on and fields-off) before he was trained to the drl-h task.

(2) *Data analysis of behavioral changes*

Interresponse time data (IRTs) were collected by the computer for each experimental run; each response of the animal was tallied as a function of time elapsed since the immediately preceding response. Two-tenths of a second bin widths were used; 144 bins were counted and interresponse times greater than that were tallied as 144 (28.8 sec). Mean and standard deviations were calculated for each 4 h run, and *t* tests were used to compare IRT distributions for experimental runs and the appropriate matched control runs.

(3) *Data analysis of EEG changes: spectral intensity, coherence, discriminant analysis*

EEG data were continuously recorded on a Grass polygraph and an Ampex analog tape recorder. In the 1st monkey (J) EEG was recorded from the left hippocampus, right hippocampus, right amygdala, midbrain reticular formation, right visual cortex, left visual cortex and motor cortex. In the 2nd monkey (Z) EEG was monitored from the right hippocampus, left hippocampus, left centre median, right visual cortex, and right amygdala. In the 3rd monkey (A) records were taken of the electrical activity of the right hippocampus, left hippocampus, right centre median, left centre median, right amygdala, and left amygdala.

Four sets of EEG data from comparable epochs from each day's run were selected for computer analysis. A set of correct (*i.e.*, properly timed) responses was selected from the beginning of the run and a 2nd set from the end of the run; similarly, a set of predominantly incorrect responses was sampled from the beginning of the run and a comparable set from the end of the run. Each epoch was approximately 80 sec in length. These epochs were spectrally analyzed in consecutive 10 sec samples and then averaged over the total 80 sec.

The selected data epochs were converted to digital form by the SDS 930 computer system of this laboratory and spectral analysis of this data was performed, using the BMDX92 program and the IBM 360/91 computer of the Health Sciences Computing Facility. Spectral resolution was set at 2 c/sec over the range 0–28 c/sec for survey purposes. Spectra and coherences¹⁸ were averaged for each structure, within condition, and plotted; spectra were converted before plotting to relative units (by dividing by the total intensity in that structure in that condition) in order to compensate for day-to-day variations in total intensity; the result is called 'percent power' at each frequency.

Spectral intensity. A specialized statistical test for the effect of the imposed field on recorded activity was devised as follows. In the frequencies from 4 to 20 c/sec, at least, the spectra were close to exponential in shape, in the absence of fields. If this were exactly true, the logarithm of the spectral curve would be a linear function of frequency, over this range. Then any activity contributed by the field would be

above the line containing those points not at the field frequency (or its harmonics). Accordingly, we tabulated the statistic ("peak quotient") for the 10 c/sec field.

$$\ln (S_{10}) = 1/2[\ln (S_{12}) + \ln (S_8)]$$

When the field was at 7 c/sec, more care was required. The 7 c/sec signal appeared both in the filter band centered at 6 c/sec and (to a lesser extent) in that centered at 8 c/sec. We chose to test only the value at 6 c/sec, and to compare it with the line based on 4 c/sec and 10 c/sec; thus, the peak quotient for the 7 c/sec field became

$$\ln (S_6) = [2/3 \ln (S_4) + 1/3 \ln (S_{10})]$$

The spectral estimates have a sampling distribution like $\chi^2/\text{d.f.}$, with d.f. calculated by the program (according to formulas adapted from Blackman and Tukey⁴) as approximately 200 in our case. Thus, the natural logarithm of a single spectral intensity has an approximately normal distribution, with variance 2/d.f., and a coefficient of skewness of -0.1 (ref. 1). Our peak quotient statistic, then, is close to normally distributed with variance 0.01. Its response to application of the field in the 2 experiments for each animal could be tested by the *t*-statistic, with the 2 fields-off values providing the mean corresponding to the null hypothesis of no effect of the field.

Coherence. An additional parameter calculated by the spectral analysis program is the coherence between the imposed field and the activity in each structure, as well as between the brain structures themselves. It is essentially analogous to the squared coefficient of correlation, and hence, a measure to the linear predictability between the 2 wave forms, taking into account spectral intensity, frequency and phase lag. Although the purity of the imposed sinusoidal field invalidates the usual distributional assumptions about the coherence statistic, we felt these results might be suggestive.

Discriminant analysis. In seeking for less obvious field effects, we applied stepwise discriminant analysis^{2,11} to spectral and cross-spectral parameters, with the exclusion of the frequency band containing the field frequency, or else of that band and all bands containing any harmonics of that frequency. Applications of this computer program, Discan (based on BMD 07M, Dixon⁵), to spectral analysis of EEGs have been described previously^{3,9,12,17}.

RESULTS

Behavioral data

Consistent differences in interresponse time distributions were observed in the 7 c/sec experiments. The 10 c/sec field condition failed to produce a reliable effect on the behavior. For one animal (Z) the mean interresponse time was unchanged by the 10 c/sec field; responses were slightly faster (but not significantly so) in the replication. In animal J, interresponse times were faster in the first 10 c/sec experiment and slower in the second.

Brain Research, 18 (1970) 491-501

EFFECT OF LOW-FREQUENCY FIELDS ON EEG AND BEHAVIOR

495

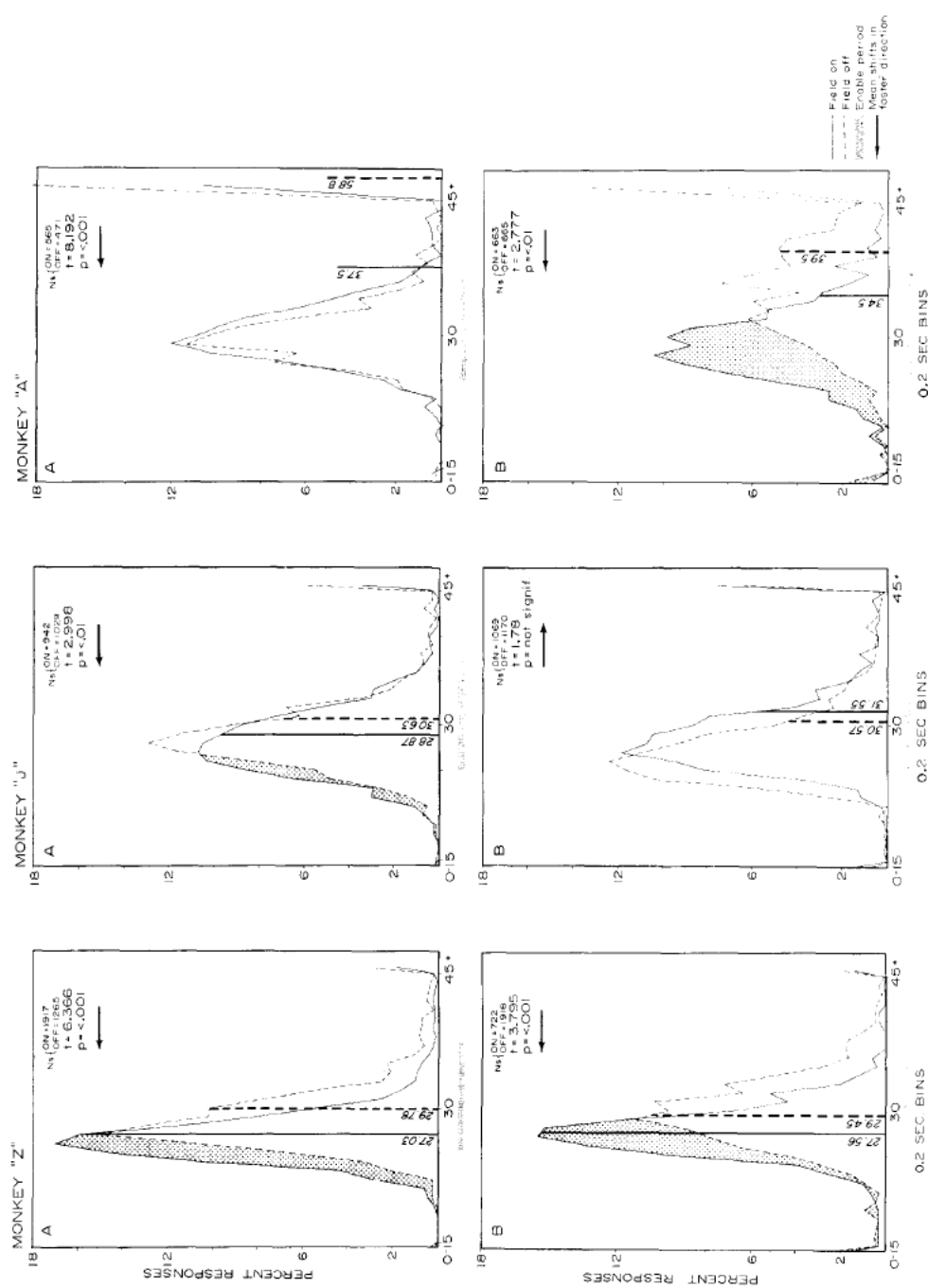


Fig. 1. Behavioral data showing shifts in interresponse time under 7 c/sec fields. The abscissa shows time between responses in 0.2 sec bins; the ordinate shows percent of total responses at each interval. (Note that only bins 15-45 are plotted; bins 0-14 were used in calculation of means and standard deviations.)

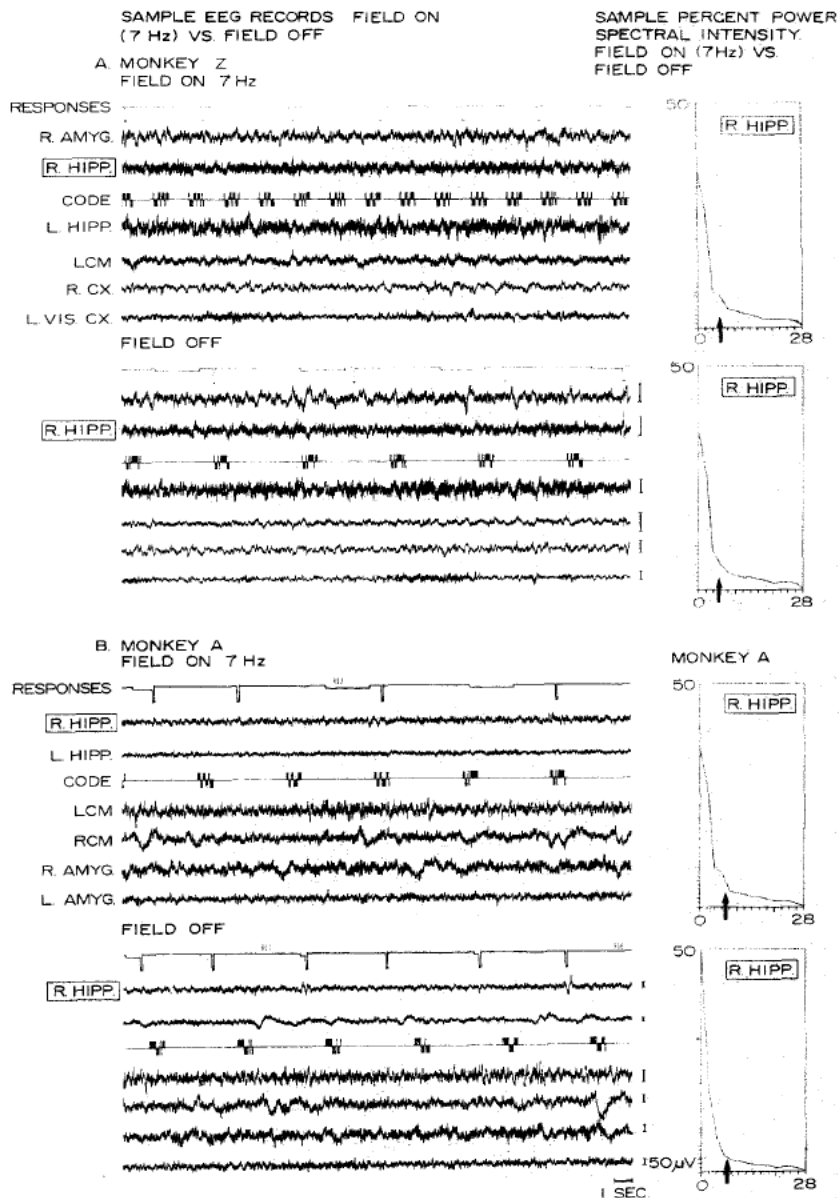


Fig. 2. Sample records of EEG and percent power graphs before conversion to peak quotients.

Under the 7 c/sec condition, however, rather large and consistent differences were observed in all animals. Animal Z showed a shift in mean interresponse time toward shorter IRTs; the difference was approximately 0.5 sec in the 1st experimental-control run. This finding was replicated in a 2nd experiment (see Fig. 1) and these dif-

Brain Research, 18 (1970) 491-501

EFFECT OF LOW-FREQUENCY FIELDS ON EEG AND BEHAVIOR

497

Performing DRL task. 80 sec. segments near end of the 4 hr. runs. Combined data from 2 experimental-control runs		7 CPS On vs. Off	10 CPS On vs. Off
<u>MONKEY J</u>	L. HIPPOCAMPUS	p = .048	p = .025
	R. HIPPOCAMPUS	p = .001	p = .011
	R. AMYGDALA	p = .003	p = .001
	(OTHER STRUCTURES OBSERVED: LMBRF, L.V. CX, R. M. CX, R.V. CX)		
<u>MONKEY Z</u>	R. HIPPOCAMPUS	p = .006	p = .020
	L. CENTRE MEDIAN	p = .001	p = .001
(OTHER STRUCTURES OBSERVED: AUD. CX, R.V. CX, R. AMYG, L. HIPP)			
<u>MONKEY A</u>	R. HIPPOCAMPUS	p = .001	No run
	L. HIPPOCAMPUS	p = .001	
	L. CENTRE MEDIAN	p = .059	
	(OTHER STRUCTURE OBSERVED: L. AMYG)		
Non-performing: Sitting quietly		7 CPS On vs. Off	
<u>MONKEY A</u>	R. HIPPOCAMPUS	p = .001	
	L. HIPPOCAMPUS	p = .036	
	R. CENTRE MEDIAN	p = .045	
	L. AMYGDALA	p = .003	
	(OTHER STRUCTURES OBSERVED: LCM, R. AMYG)		

Fig. 3. Significance levels for EEG peak quotients: fields-on vs. fields-off.

ferences were highly significant statistically ($P = 0.01$ or better). In general, the whole distribution was shifted towards faster responses, while overall number of responses did not increase or decrease consistently. For the 2nd animal (J), the IRT mean shifted significantly in the direction of faster responses in the 1st experiment; however, this difference was not replicated in the 2nd experiment. The 3rd animal (A), like the 1st, showed a shift in the direction of faster responses under the 7 c/sec field. This difference was statistically significant and was replicated in the 2nd experiment. Percent of correct responses (those falling between 5 and 7.5 sec) did not differ significantly under fields-on conditions for monkeys J and Z; monkey A, who had a large number of very long IRTs in the fields-off condition, showed gains of 16% correct and 21% correct when the fields were on. In summary, 5 of the 6 experiments showed a shift to significantly faster interresponse times under the 7 c/sec fields compared with fields-off performance. All of these mean differences were 0.4 sec or greater. Shifts in modal values also occurred in all 5 experiments and were all 0.2 sec or greater. The distributions and means for all monkeys are shown in Fig. 1. It may be observed that the overall output of responses and the variability of those responses differ considerably from monkey to monkey. Nevertheless, the direction of the mean shift under the fields is remarkably consistent and the size of the shift is relatively large.

EEG data

Visual inspection of the EEG data during the experiments did not reveal any marked effects due to the fields. An examination of the percent power graphs, however,

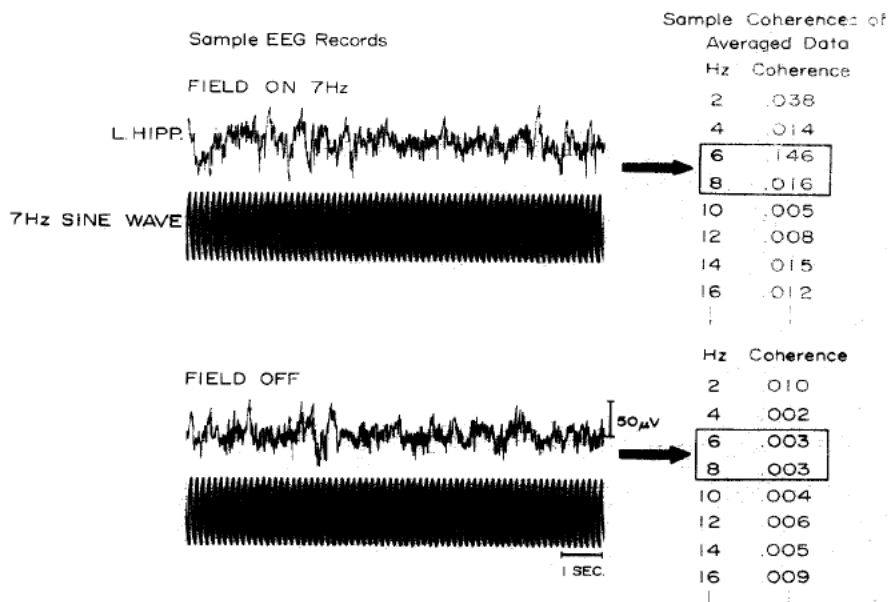


Fig. 4. Sample records of EEG and 7 c/sec sinusoidal wave form with corresponding coherence tables.

revealed small peaks in power from some brain structures at the fields frequency, for epochs of predominantly incorrect responses near the end of the run. A sample of EEG data and percent power graphs is shown in Fig. 2.

Peak quotients (as described in the Methods section) were compared via *t*-tests for these epochs in fields-on vs. fields-off conditions, for each animal and for each structure (see Fig. 3). In the 1st animal (J), significant differences were observed in the left hippocampus, the right hippocampus and the right amygdala for both the 7 c/sec and the 10 c/sec condition. In the 3rd animal (A), 7 c/sec fields only were tested. Differences at the 0.01 level or better were observed in right hippocampus, left hippocampus, and left centre median. EEG records were also evaluated for this animal while he was sitting quietly and before he had been trained to do the drl-h task. Differences in peak quotients for 7 c/sec fields-on vs. fields-off were observed in 4 of 6 structures tested: right hippocampus, right centre median, left hippocampus, and left amygdala.

Coherence measures between the 7 c/sec sinusoidal wave form and the responsive EEG structures were always higher for the fields-on condition than for the fields-off condition. Sample measures are shown in Fig. 4. Coherences between responsive brain structures did not reveal a consistent pattern of change.

No effects on EEG at non-field frequencies were visually noticeable, but the discriminant analysis program Discan (see Methods) was applied to the data of one animal (J), and identified strong driving (increased intensity and increased coherences) at harmonics of the field frequency. Although such harmonic response is perfectly

compatible with biological transduction^{15,16}, it does not exclude artifactual transduction. Further application of Discan, this time excluding all bands containing any harmonics of the field frequency, still showed a clear discriminability of fields-on from fields-off EEGs, principally in that intensity was raised in the fields-on condition, even in non-harmonic frequency bands.

DISCUSSION

The behavioral results suggest that imposing a 7 c/sec field on the performing animal resulted in shorter interresponse times. Results with 10 c/sec fields were not reliable. Experimental/control differences for the 7 c/sec runs were statistically significant for 5 of 6 experiments, and these differences could be observed in all 3 monkeys. In spite of large differences in total output of responses from monkey to monkey, the shift in interresponse times was very consistent (towards faster responses) and rather large (0.4 sec or greater).

Increases in EEG intensity (peak quotients) at the frequency of the fields were observed in all 3 animals in the hippocampus, and less consistently in the amygdala and centre median. These differences were observed both in the 7 c/sec and 10 c/sec conditions. Coherences between the sine wave and responsive brain structure at the fields frequency were always higher in the fields-on condition.

The analysis of the EEG data presents special problems. The difficulty of isolating effects of biological transduction from those of transduction at the electrode-tissue fluid interface is considerable, being almost parallel to the impossible question of 'what the tree looks like when no one is looking at it'. Nevertheless, the discriminant analysis program has provided preliminary evidence of subtle EEG changes at non-field frequencies that cannot be easily explained as electrode-tissue artifacts.

The concordance of evidence for a fields effect on behavior and on electrical activity of the brain is encouraging. We intend to pursue additional demonstrations of the same kind as well as others. One new technique to be applied is a frequency 'sweep' from 5 to 20 c/sec, with enough time spent at each frequency to allow coherence estimates to be reliably made there; our prediction is that, as occurred with whole-body vibration in the monkey¹⁶, and as seems to occur with sinusoidally modulated light stimulation in the human¹⁵ there will be a band of incoherent driving. It may even be possible to establish some specific non-linear model, along the lines successfully pursued by Spekreijse¹⁴ for the visual system.

SUMMARY

A series of experiments has been done to assess the effects of low-level, low-frequency electric fields on the behavior and EEG of monkeys. Three monkeys were implanted with subcortical and cortical EEG electrodes and trained to press a panel on a fixed interval-limited hold schedule. The monkeys were rewarded for pressing the panel once every 5 sec within a 2.5 sec enable period. After the animals were performing well, they were tested under low-level electric fields (2.8 V p-p);

the voltage was applied to 2 large metal plates 40 cm apart so that the monkey's head was completely within the field. Fields frequency was set at 7 or 10 c/sec within the range of typical EEG recording (0–33 c/sec). Four hour daily tests of fields-on were randomly interspersed with 4 h runs with fields-off. Under the 7 c/sec fields, the monkeys showed a significantly faster interresponse time in 5 of 6 experiments. Mean differences between fields-on and fields-off were 0.4 sec or greater. The 10 c/sec fields did not produce a reliable effect on behavior. Analysis of the EEG data showed a relative peak in power at the frequency of the fields (10 c/sec and 7 c/sec) for the hippocampus in all 3 monkeys. Similar peaks were seen less consistently in the amygdala and the centre median.

ACKNOWLEDGEMENTS

We gratefully acknowledge the support of ARPA Contract DADA 17-67-C-7124, NASA Grant NGR-05-007-195, and the assistance of the Health Sciences Computing Facility, supported by National Institutes of Health Grant FR-3.

Appreciation is expressed to Cavita Bloir for technical assistance in carrying out the experiments and to Joe Lucero for surgical implantation of the monkeys; Jacqueline Payne is credited with the illustrations. We are indebted to R. T. Kado for encouragement and assistance in the initial phases of the experiment.

REFERENCES

- 1 ABRAMOWITZ, M., AND STEGUN, I. A., *Mathematical Functions with Formulas, Graphs, and Math Tables*, U.S. Government Printing Office, 1964, p. 943.
 - 2 ANDERSON, T. W., *An Introduction to Multivariate Statistical Analysis*, Wiley, New York, 1958, Ch. 6, pp. 126–153.
 - 3 BERKHOUT, J., ADEY, W. R., AND CAMPEAU, E., Simian EEG activity related to problem solving during a simulated space flight, *Brain Research*, 13 (1969) 140–145.
 - 4 BLACKMAN, R. B., AND TUKEY, J. W., *The Measurement of Power Spectra*, Dover, New York, 1959, pp. 21–25.
 - 5 DIXON, W. J. (Ed.), *BMD Biomedical Computer Programs (2nd ed.)*, University of California Press, Los Angeles, Calif., 1967, pp. 214a–214t.
 - 6 FRIEDMAN, H., BECKER, R. O., AND BACHMAN, C. H., Effect of magnetic fields on reaction time performance, *Nature (Lond.)*, 213 (1967) 949–950.
 - 7 HAMER, J., Effects of low level, low frequency electric fields on human reaction time, *Commun. behav. Biol.*, 2 (1968) No. 2, Part A.
 - 8 HANLEY, J., WALTER, D. O., RHODES, J. R., AND ADEY, W. R., Chimpanzee performance data: computer analysis of electroencephalograms, *Nature (Lond.)*, 220 (1968) 879–881.
 - 9 KONIG, H., UND ANKERMULLER, F., Über den Einfluss besonders niederfrequenter elektrischer Vorgänge in der Atmosphäre auf den Menschen, *Naturwissenschaften*, 21 (1960) 486–490.
 - 10 RADULOVACKI, M., AND ADEY, W. R., The hippocampus and the orienting reflex, *Exp. Neurol.*, 12 (1965) 68–83.
 - 11 RAO, C. R., *Advanced Statistical Methods in Biometric Research*, Wiley, New York, 1952, Ch. 8, pp. 273–350.
 - 12 RHODES, J. M., WALTER, D. O., AND ADEY, W. R., Discriminant analysis of 'activated' EEG, *Psychon. Sci.*, 6 (1966) 439–440.
 - 13 SIDMAN, M., Techniques for assessing the effect of drugs on timing behavior, *Science*, 122 (1955) 925.
 - 14 SPEKREIJSE, H., *Analysis of EEG Responses in Man Evoked by Sine Wave Modulated Light*, Thesis, Junk, The Hague, 1966, 161 pp.
- Brain Research*, 18 (1970) 491–501

EFFECT OF LOW-FREQUENCY FIELDS ON EEG AND BEHAVIOR

501

- 15 VAN DER TWEEL, L. H., AND VERDUYN LUNEL, H. F. E., Human visual responses to sinusoidally modulated light, *Electroenceph. clin. Neurophysiol.*, 18 (1965) 587-598.
- 16 WALTER, D. O., AND ADEY, W. R., Linear and non-linear mechanisms of brain-wave generation, *Ann. N. Y. Acad. Sci.*, 128 (1966) 772-780.
- 17 WALTER, D. O., RHODES, J., AND ADEY, W. R., Discriminating among states of consciousness by EEG measurements, *Electroenceph. clin. Neurophysiol.*, 22 (1967) 22-29.
- 18 WALTER, D. O., RHODES, J. M., BROWN, D., AND ADEY, W. R., Comprehensive spectral analysis of human EEG generators in posterior cerebral regions, *Electroenceph. clin. Neurophysiol.*, 20 (1966) 224-237.
- 19 WEVER, R., Einfluss schwacher elektro-magnetischer Felder auf die circadiane Periodik des Menschen, *Naturwissenschaften*, 1 (1968) 29-33.

Brain Research, 18 (1970) 491-501

EXHIBIT 9

EFFECTS OF MODULATED VERY HIGH FREQUENCY FIELDS ON
SPECIFIC BRAIN RHYTHMS IN CATS

S. M. BAWIN, R. J. GAVALAS-MEDICI AND W. R. ADEY

*Department of Anatomy and Brain Research Institute, University of California, Los Angeles, Calif.
90024 (U.S.A.)*

(Accepted January 25th, 1973)

SUMMARY

The effects of exposures to low intensity (1 mW/sq.cm or less), very high frequency (VHF) (147 MHz) electrical fields, amplitude-modulated at biological frequencies (1-25 Hz), were studied on untrained and conditioned chronically implanted cats. The fields were applied between two aluminum plates (identical voltages, 180° phase shift) firmly anchored to the floor of an isolation booth, especially designed for use of VHF fields. The animals were restrained in a hammock, the longitudinal axis of the body kept parallel to the field plates. EEG and EOG were recorded through a system of low pass filters on a Model 6 Grass electroencephalograph and an Ampex FR 1100 tape recorder; behavior was continuously observed through a closed circuit TV.

A series of animals was operantly trained to produce specific transient brain rhythms following periodic (every 30 sec) presentations of a light flash stimulus. The levels of performance were established (visual and spectral analysis) during conditioning and extinction schedules for a series of cats submitted to VHF fields amplitude-modulated at the dominant frequencies of the selected transient patterns and for a control group, in the absence of fields. The irradiated animals differed markedly from the control group in the rate of performance, accuracy (in terms of frequency bandwidth) of the reinforced patterns and resistance to extinction (minimum of 50 days *versus* 10 days).

The specificity of the frequency of the modulation was tested on another group of untrained animals where spontaneous transient patterns were used to trigger for short epochs (20 sec following every burst) the VHF fields amplitude-modulated at various frequencies. The experimental results indicated clearly that the fields were acting as reinforcers (increasing the rate of occurrence of the spontaneous rhythms) only when modulated at frequencies close to the biologically dominant frequency of the selected intrinsic EEG rhythmic episodes.

Various possible routes of interaction between the external fields and the CNS are discussed, and the hypothesis is offered that the amplitude-modulated VHF fields could influence the excitability of neuronal membranes.

INTRODUCTION

The damaging effects of ionizing electromagnetic radiations on biological systems have been intensively studied since the turn of the century. Little attention has been paid to the other end of the spectrum where radiations have millimetric to kilometric wavelengths. A new interest in possible implications of prolonged exposure to radio-frequency radiations arose from the rapid development of high powered equipment that followed World War II and the consequent widening of its domain of application (military, medical, industrial and scientific). During the past 25 years, numerous investigations have been made with fields mainly in the micro-wave range at intensities from 1 to 100 mW/sq. cm on humans, animals and protein suspensions *in vitro*.

A wide range of effects have been reported, including severe damage to the lens of the eye and to the testes, decreased amino acid incorporation in testes and liver, alterations in electrophoretic, immunologic and enzymatic activities of proteins, disintegration of myelin and denaturation of the collagen in the peripheral nervous system, disturbance in the vegetative nervous system, various cardiovascular changes and behavioral reactions such as avoidance, struggling or hypoactivity. These have been attributed mainly to thermal effects. Even the phenomena of pearl-chain formation in protein cultures and orientation of micro-organism in the presense of electromagnetic fields^{21,51} have been subjected to criticism and re-evaluation on grounds that they may be attributable to heating.

There is persistent controversy over thermal *versus* non-thermal effects, even though there is no clear evidence of biologically significant temperature changes in tissues exposed to low level irradiations in the radio-frequency range. Effects have been reported in low to moderately high levels of irradiations, where the fields did not obviously interact with the biological material via the thermal route for auditory responses^{15,40,41,52}, brain stem and cortical evoked responses^{16,54}, changes in reaction time in humans and animals^{18,20,27,34,59}, escape reactions in birds⁶¹⁻⁶³, dogs and cats^{35,36}, hypoactivity in rats^{12,28,29,33}, and alterations of conditioned responses^{24,59,60}.

Very few studies have dealt with the effects of electromagnetic fields on brain wave patterns. Much of the pertinent work has been done by Soviet and East European investigators. Their results as presented in translation are often obscure and generally refer to short latency synchronization of the cortical EEG^{3,4,8,19,25,26,53}. To the best of our knowledge, Gavalas *et al.*¹⁸ were the first to report specific changes in brain electrical activity of monkeys subjected to low level, low frequency electrical fields (7 Hz sine waves, 2.8 V p-p applied between large metal plates placed parallel and 40 cm apart). In addition to behavioral changes (shifts toward shorter inter-response times), spectral analysis of EEG samples taken after 3 or 4 h of exposure

revealed power peaks at 6–8 Hz in some specific brain locations (hippocampus, amygdala and centrum medianum). These pioneer studies strongly suggest that very low power electric fields are able to enhance or drive specific brain rhythms.

From the survey of the available literature it appears that the pulse repetition rate (or the frequency of carrier wave modulation) of high frequency radiation is a very important parameter among the field conditions eliciting behavioral and CNS effects. The results described in Gavalas' experiment were best developed after several hours of exposure. As a means of possibly reducing the time of exposure for a reliable, detectable change to occur, we decided to use weak VHF fields (147 MHz, intensity less than 1 mW/sq. cm) amplitude-modulated over a wide, low frequency range (0–30 Hz).

The possible impact of these electric fields amplitude-modulated at various biological frequencies was tested on conditioned (experiment I) and spontaneous (experiment II) transient EEG patterns.

MATERIAL AND METHODS

(A) Implantation of recording electrodes

Twelve adult female cats were chronically implanted with bipolar electrodes. The electrodes consisted of two parallel wires (enamelled stainless steel, 33-gauge, Driver Harris Co.) glued on a nichrome strut (20-gauge) and insulated with Epoxylite (The Epoxylite Corporation, South El Monte, Calif.) through 10 baking periods of 20 min (170 °C). The wires were cut 3–4 mm from the end of the strut and insulation stripped from the tip to provide a recording surface.

The implantation of electrodes was carried out stereotactically under pentobarbital anesthesia (30 mg/kg body weight, i.p.). The electrode coordinates were chosen from Snider and Niemer's⁵⁶ stereotaxic atlas of the cat brain. Bipolar electrodes were implanted in the caudate nucleus (CdN), amygdala (Amyg), nucleus ventralis anterior of the thalamus (VA), centrum medianum (CM), hippocampus (Hipp), midbrain reticular formation (MBRF) and presylvian gyrus (PSG). Stainless steel screws were inserted through the cranium to make light contact with the dura mater. Two enamelled wires for monitoring eye movements were tied to the orbicularis oculi muscle on each side and led subcutaneously to the connecting plug on the skull. The animals were sacrificed at the end of the experiment, the brains fixed in formalin and cut in sections 80 μ m thick for identification of the electrode positions.

(B) VHF fields exposure techniques

An isolation booth (2.4 m \times 2.4 m \times 2.0 m) has been designed especially for use with VHF test fields. It was built with a frame of wood and covered inside and outside by No. 10 mesh copper screening. Lighting was provided by three 12 V, 25 W lamps, supplied by a 12 V battery (situated outside the room); light intensity was adjustable from the outside. Adequate ventilation was provided by a 2400 liter/

min blower forcing air into the booth and by a 1500 liter/min blower serving as a suction fan. A closed circuit TV camera was mounted on the wall of the room to allow behavioral observation of the animals. Power supply, transmitter and modulation function generator were located outside the shielded room. The power supply was designed to provide modulated high voltage to the transmitter (Viking 6 N 2, E. F. Johnson Company, Waseca, Minn.). The function generator (Model 202A, Hewlett Packard, Palo Alto, Calif.) provided sine waves for amplitude-modulation of the VHF carrier wave.

The fields were applied between two aluminum plates (area 4100 sq. cm) firmly anchored to a wooden board attached to the floor in the center of the screened room. The flared configuration of the plates aimed at a uniform distribution of the applied voltages. The unbalanced coaxial transmission line from the transmitter was coupled to the plates by means of a 'balun' (coaxial cable, half a wavelength long) connecting the feeding point of one plate to the other, so that identical voltages were applied to the two plates with a 180° phase shift. A delta system of impedance matching minimized the standing-wave ratio on the transmission line and associated reflection of energy toward the transmitter. The transmitter output, at 147 MHz, was monitored by an inline wattmeter (Bird Electronic Corporation, Cleveland, Ohio, Model 43 Thruline). The output of the unmodulated VHF carrier was adjusted to provide adequate power on the field plates (maximum 1 mW/sq. cm) after deduction of the estimated losses in the room (40% of the total power output). Modulation percentage (up to 90%) of the VHF field was measured with a Tektronix type 360 indicator, connected through a diode detector to a wire loop (2 mm diameter) mounted on the wall inside the screened room. All lines were brought in and out of the booth through low pass filters of the 'feed through' type (approximately 120 dB attenuation at 147 MHz).

A wooden frame (a replica of a Horsley-Clarke stereotaxic apparatus) was mounted on a table between the field plates. The ear bars were used to restrain the animals. They were fitted in a cylinder cemented at the front of the implant, thus avoiding any painful pressure in the ear canals. The animals were free to sit or lie but no lateral movement of the head was possible. Microdot cables (Microdot Corporation, Pasadena, Calif.) connected the plugs attached to the skull to a board fixed in the ceiling of the booth. The lines were filtered as they exited from the roof and were then fed through another set of low pass filters, first into a Model 6 Grass electroencephalograph, then through R6 reverbers into an Ampex FR 1100 tape-recorder.

(C) Testing protocols

Experiment I: effects of electric fields on conditioned brain patterns

To minimize interferences with the VHF fields, due to behavioral responses and/or gross body movements, we decided to directly condition specific patterns in specific brain locations, and to consider the overt behavior as a correlate of the conditioned responses^{7,13,14,57,58}. The animals were trained in an operant conditioning procedure with a negative reinforcement (electrical stimulation) applied directly

in the brain (frontal eye field of the PSG) as the unconditional stimulus (US). This US appeared unpleasant, although behaviorally, it produced only ocular movements^{43,46,50,67}. The patterns to be manipulated by means of operant reinforcement were selected during movement free periods, in order to place some limitation on behavior³⁹.

The operant schedule was first tested on two animals to maximize the efficiency of the procedure which was subsequently applied to 5 other cats.

The training paradigm consisted of a series of 100 flashes presented at fixed intervals (30 sec), followed (2.5 sec later) by electrical stimulation of the frontal eye field. The flashes (1 μ m sec, $18 \cdot 10^6$ beam candle) were delivered by a Strobotac type 1531-A (General Radio Co., Concord, Mass.) located in front and on the left (45° angle) of the fixed animal's head. A Grass stimulator (Model S4, Grass Instrument Co., Quincy, Mass.) coupled to the brain tissue through an isolation transformer (General Radio GR 587A), was used for stimulation of the frontal eye fields. The stimulator output was manually controlled by a switch. The stimulus was applied for 400 msec at a frequency of 400 pulses/sec. The duration of the pulses was 0.5 msec and the intensity of the current, measured with a 10 Ω series resistance was in the range of 300–500 μ A⁴⁶.

The patterns to be reinforced were selected from any one of the brain locations surveyed, during two control sessions of 50 min each (days 1 and 2). This selection was somewhat arbitrary. However, the same general principles were applied in each case: (a) the rhythms were always visually detectable from the background electroencephalographic activity; (b) the frequency bandwidth of the signals was narrow (desirably less than ± 2 Hz from the dominant frequency); (c) assuming a mean duration of 0.5 sec, the probability that at least one burst would be present in any 2.5 sec interval was never less than one-quarter. During two other sessions (days 3 and 4), two series of 100 flashes were presented to the animals. The operant response was defined as the occurrence of the selected patterns during the 2.5 sec epochs following the presentation of the flash (CS). The operant level was determined by averaging the number of operant responses from day 4 and day 2 (with a pulse as a flash stimulus marked on the recording). The criterion for conditioning, arbitrarily chosen in advance, required that the conditioned levels of performance at least doubled the pre-conditioning levels of occurrence of the patterns following the flash presentations.

In the first part of this experiment (part A) the animals were trained in the absence of fields during 10 daily sessions of 50 min each. They were then submitted to an extinction schedule (where the flashes alone were presented) during which they were tested every other day. The operant responses were considered extinguished when the performances were stabilized for 3 consecutive sessions at baseline levels.

During the second phase (part B) the animals were first reconditioned, using the same avoidance technique, during 4 sessions. They were then divided into two groups. The first series (2 cats) was overtrained for 6 days in the absence of fields before being resubmitted to extinction. The other series (3 cats) was irradiated continuously within session, with VHF fields amplitude-modulated at the dominant frequency of the par-

ticular EEG response under training, during overtraining and extinction. These animals were tested every 2 days during the first 20 days of extinction and every 3 days thereafter until return to operant levels. Daily performance was assessed by visual analysis of the EEG records. EEG epochs of 2.5 sec were selected for spectral analysis. These records covered 3 phases of training: at initial operant levels (specific rhythm pattern in epochs following the presentation of the flash); during the conditioning sessions (epochs following the US, responses and errors); and during extinction⁶⁹.

The data were processed at the Computing Facility of the U.C.L.A. Center for the Health Sciences (BMDX program IBM 360/91). The spectral resolution was set at 1.0 Hz over the range 0–32 Hz. The autospectra of the various structures surveyed were averaged in groups of 20, for each condition studied, within a particular session. The grouping of these separate epochs thus produced a sufficiently long data train to statistically validate 1.0 Hz spectral resolution for the bandwidth 0–32 Hz. The absolute power densities of each frequency band were normalized to the total power in each structure, and then displayed as 'per cent power' graphs.

Experiment II: effects of electrical fields on spontaneous transient EEG rhythms

Two animals were used in this complementary study. Two different patterns occurring in two different brain locations were selected for each animal in preliminary testing sessions. The selected EEG channels were filtered through two analog frequency-selectors (Universal active filters, Model FS61, Kinetic Technology Inc., Santa Clara, Calif.) externally tuned by coupled RC elements. The attenuation curves, regulated by external resistors, were set at the highest possible resolution (attenuation of 12 dB for frequencies 1.7 Hz away from the dominant rhythm). Triggering levels were experimentally adjusted, so that only clearly visible patterns were detected by the filter (peak of the attenuation curve). Both animals were then subjected to two baseline sessions of 50 min each, in the absence of fields. During the following days, the imposition of the VHF fields, amplitude-modulated at various frequencies, was sequentially triggered by the rectified output of each filter via an intermediate operational amplifier. The fields were applied during the whole length of each burst (minus the inherent filter delay) and during the first 20 sec following it. The occurrence of a second or third burst during the fields-on epochs recycled the chain of events, so that every occurrence was similarly reinforced. A final control was then made, during which neither filter triggered the VHF fields. The integrated filter outputs (negative pulse), recorded together with the ongoing EEG, were measured (in sec) and summed for each session.

RESULTS

Experiment I

(A) Operant conditioning of specific transient brain rhythms

(1) *Behavior.* All animals followed very similar behavioral patterns during

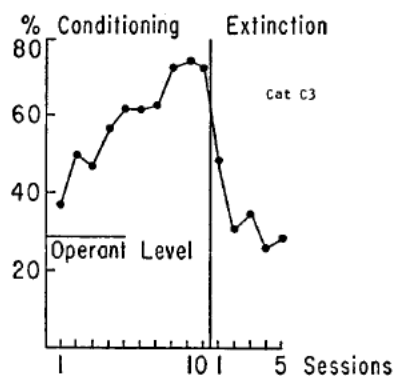


Fig. 1. Performances of cat C3 (centrum medianum—14 Hz) during conditioning and extinction. Data normalized over the total number of CS presentations within session.

their first conditioning and extinction. They rapidly learned to use the intertrial intervals to shift position and relax, while the onset of the flash would immediately stop any behavioral activity for a few seconds. The level of motor activity increased during the first days of extinction. Following that rebound in free behavior the animals started to ignore the CS and progressively shifted from their fixed 'performing' attitude towards complete relaxation, spindle and slow wave sleep.

Learning and extinction curves were practically identical for all animals. Fig. 1 illustrates the level of performance in the case of animal C3 (centrum medianum rhythm) during training and extinction; the data were normalized over the total number of CS presentations within a session. Less than 7 sessions were required for the animals to double their operant levels (criterion of conditioning). They were then overtrained 3 or 4 days, during which the performances stabilized and remained at 70–80% until day 10. The extinction profiles were very sharp in each case. The performances dropped rapidly to baseline levels in less than 6 days (third extinction session).

(2) *Transient rhythms analysis.* The most clearly visible rhythms were found in the visual cortex (cats C1, C2 and C5), the hippocampus (cats C4, C5, and C7) and the centrum medianum (cats C3 and C6).

The fully developed responses exhibited increased amplitude and sharply defined peak frequencies, i.e., 16, 6 and 3 Hz in the visual cortex, 4.5–3 Hz in the hippocampus and 13–16 Hz in the centrum medianum.

Fig. 2 illustrates a conditioned response in the centrum medianum (cat C6) together with its autospectral profile (average of 20 epochs of 2.5 sec each). At the end of extinction, amplitudes were again similar to those during pre-conditioning sessions and the spectral profiles shifted from sharply defined peaks to more or less extended plateaux or to different frequencies.

(B) *Effects of amplitude-modulated VHF fields on conditioned brain rhythms*

(1) *Behavior.* All 5 animals (as previously mentioned, C1 and C2 were excluded

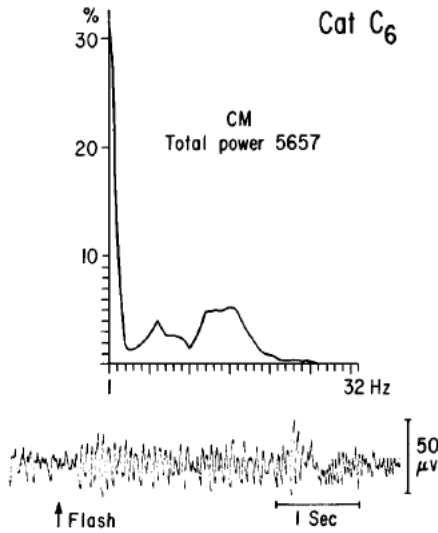


Fig. 2. Centrum medianum patterns and their spectral profile (average of 20 epochs of 2.5 sec each) Cat C6. Conditioning day 10.

from this phase of the experiment) doubled their extinction (and operant) levels in 4 days, at a much faster rate than during the first conditioning.

Two cats (C3 and C7) served as controls and were overtrained (sessions 5–10) then extinguished in the absence of fields. The 3 other animals (C4, C5 and C6) were irradiated with the 147 MHz fields, (amplitude-modulated at 4.5 Hz, 3 Hz and 14 Hz, respectively) during overtraining and extinction.

The two control cats maintained regular levels of performance during the training sessions, but never exceeded their previous achievement. There were long periods of time where the animals would not perform at all due to sleep or inattention. The extinction conducted in the absence of fields was again very rapid. The performances dropped to 40% during the first session. Thereafter, both animals alternated epochs of spindle, slow wave and paradoxical sleep until the end of the experiment (5 sessions, 10 days).

By contrast, the irradiated cats remained quiet but fully awake during the 6 overtraining sessions. The performances presented irregular peaks and eventually all levels were equal if not superior to the highest scores obtained during the first conditioning. These conditions remained unchanged during the first part of the extinction schedule (25 days for cat C4, 40 days for C5 and C6). Drowsiness, slow wave sleep and REM epochs then started to occur at the end of the testing periods until approximately day 55 when this behavior was suddenly replaced again by alertness and restlessness. The animals ceased performing and returned to their behavior at operant levels, characterized by periods of high activity, alternating with epochs of drowsiness. They completely ignored the flash in the last 3 sessions. Fig. 3 compares the recon-

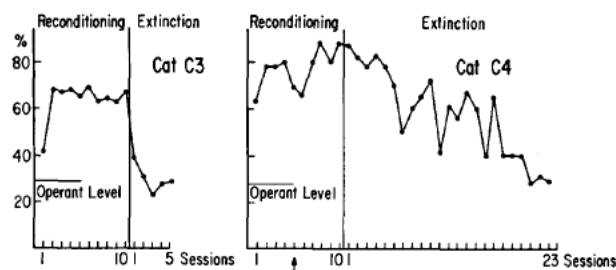


Fig. 3. Comparison of performance of cats C3 (centrum medianum 14 Hz—no field) and C4 (hippocampus 4.5 Hz—VHF field amplitude-modulated at 4.5 Hz) during reconditioning and extinction. Data normalized over the total number of CS presentations within session. The arrow indicates the first day of exposure to the fields.

ditioning and extinction curves of cats C4 (VHF field amplitude-modulated at 4.5 Hz) and C3 (control).

(2) *Transient rhythms analysis.* All patterns were well developed and very similar to the previous fully conditioned response on day 4 of the retraining schedule.

The profile of the response in the two control cats remained stable during over-training (day 5–10) in the absence of fields. Spectral analysis merely confirmed the visual observations, that is, the peaks of the responses (13–14 Hz in CM, cat C3; 4 Hz in Hipp, cat C7) were still clearly defined but the background EEG activity was slower and of higher amplitude than in the first training schedule. Without reinforcement, these responses extinguished readily, as in the first extinction.

The patterns of the responses of the irradiated animals (C4, C5 and C6) contrasted sharply with the low EEG background activity and the generalized high amplitude seen in the two control animals.

Spectral analysis revealed subtle but very interesting changes in the reinforced patterns of the cats exposed to the fields in the finding of a concentration of power densities around the imposed frequency of the modulation.

Daily controls with the fields amplitude-modulated at different frequencies for short epochs of time and with brief field-off conditions failed to produce any changes or any artifactual patterns in those highly stable responses. No change was ever elicited in the recorded brain activities by application of fields in the absence of conditioning procedure.

Fig. 4 is a comparison of the autospectra of the hippocampal activities of animal C4 in the cases of correct and incorrect responses during irradiation with the fields modulated at 4.5 Hz (peak frequency of the response). It can be seen that the peak shifted away from the imposed frequency when the animal was not performing. The hippocampal responses shifted to 2–3 Hz as the performances returned to operant levels.

The first exposure to the VHF fields, modulated at 3 Hz, produced sharp responses with peaks at 2 Hz in the hippocampus and visual cortex of cat C5. During the following sessions, the hippocampal rhythms shifted towards 3 Hz but the cortical

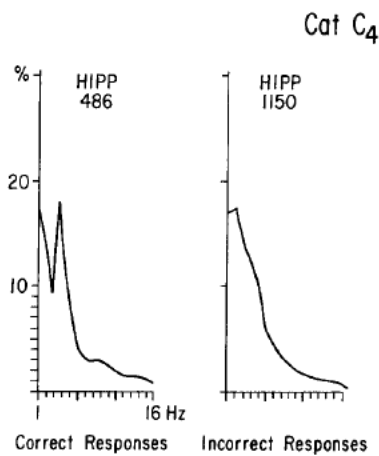


Fig. 4. Comparison of the autospectra (average of 20 epochs of 2.5 sec each) of the hippocampal patterns (cat C₄) in cases of correct and incorrect responses during exposures to VHF fields amplitude-modulated at 4.5 Hz. Reconditioning day 5.

activity remained centered at 2 Hz. Fig. 5 compares the autospectra of the visual cortex and hippocampus in cases of correct and incorrect responses during the fourth day of irradiation.

The reconditioned centrum medianum pattern of cat C₆ was centered around 12 Hz. During the first exposure to the fields modulated at 14 Hz, the response appeared as a plateau between 13 and 15 Hz, and in subsequent sessions, this plateau narrowed to a sharp peak at 14 Hz. Fig. 6 compares the autospectra of the centrum

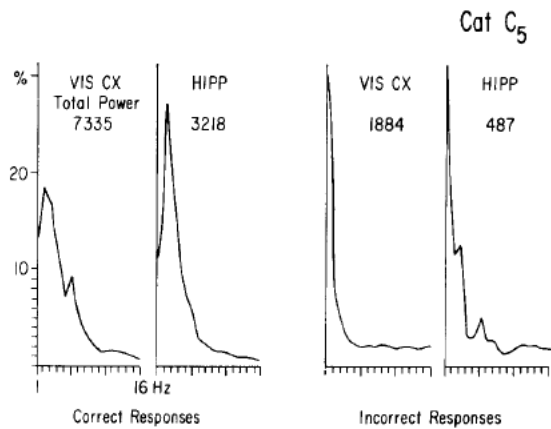


Fig. 5. Comparison of the autospectra (average of 20 epochs of 2.5 sec each) of cortical and hippocampal patterns of cat C₅ in cases of correct and incorrect responses during exposure to VHF fields amplitude-modulated at 3 Hz. Reconditioning day 8.

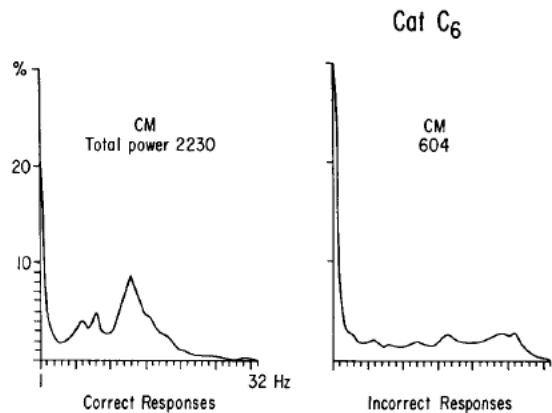


Fig. 6. Comparison of the autospectra (average of 20 epochs of 2.5 sec each) of the centrum medianum patterns of cat C6 in cases of correct and incorrect reponses during exposures to VHF fields amplitude-modulated at 14 Hz.

medianum activities in cases of responses and errors, during the tenth day of the extinction schedule.

Experiment II

Two mutually exclusive rhythms (14 Hz in centrum medianum and 10 Hz in presylvian gyrus, cat R1) and two concurrent patterns (13 Hz in caudate nucleus and 4 Hz in centrum medianum, cat R2) were selected for manipulation in the VHF fields.

Experimental schedules were drawn up for each animal and are presented below.

Cat R1	
Session	Experimental condition
1 and 2	Control — no field.
3 and 4	14 Hz filter triggering VHF fields amplitude-modulated at 14 Hz.
5 and 6	10 Hz filter triggering VHF fields amplitude-modulated at 10 Hz.
7 and 8	10 Hz filter triggering VHF fields amplitude-modulated at 3 Hz.
9	Control — no field.
Cat R2	
Session	Experimental condition
1 and 2	Control — no field.
3 and 4	4 Hz filter triggering VHF fields amplitude-modulated at 4 Hz.
5 and 6	13 Hz filter triggering VHF fields amplitude-modulated at 13 Hz.
7	Control — no field.

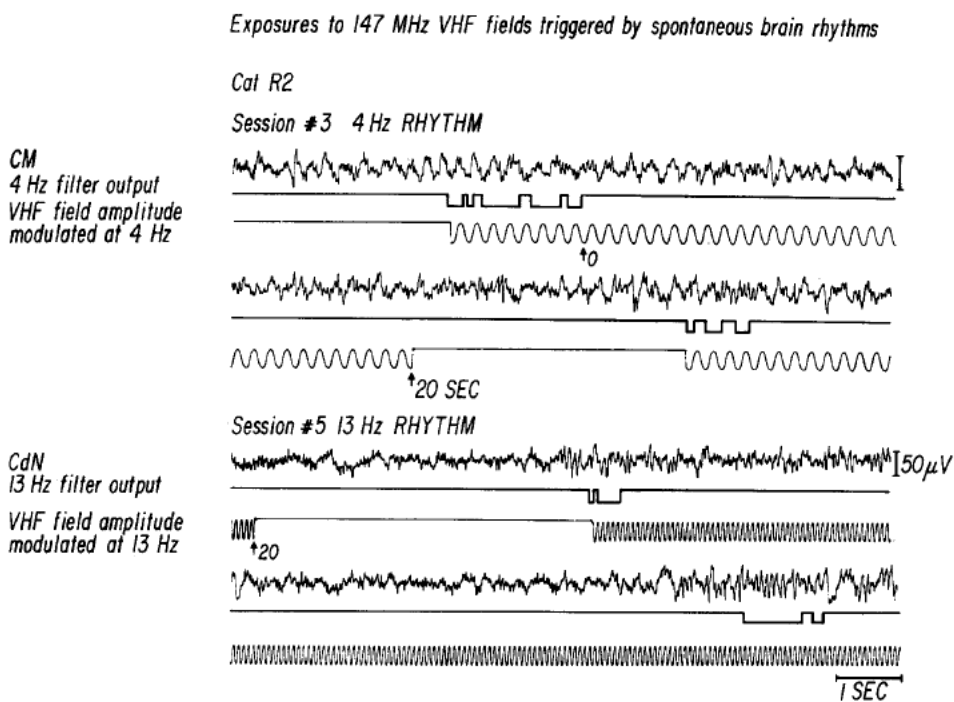


Fig. 7. Selected patterns and mechanisms of reinforcement. Cat R2. Sessions III and V.

Fig. 7 illustrates the two patterns selected in animal R2, together with the integrated filter outputs and the triggered fields.

There were no significant changes in the total filter outputs and in the rates of occurrence of the transient bursts in either cat during the first two control sessions. These values were thus grouped and averaged over the two days for each animal.

Both animals reacted similarly to the imposition of the fields, even though the experimental conditions were purposely made different:

- (1) Two fields-on sessions were required before substantial, reliable changes from the baselines occurred.
- (2) The shifts from one modulation frequency to another (session 5) induced temporary increases in the previously enhanced rhythms (14 Hz in cat R1, 4 Hz in cat R2) which disappeared during the second exposure to the new modulations.
- (3) The following increases of the total filter outputs (in sec) of the reinforced patterns were due to increases of the rates of occurrence of these rhythms; the mean durations of the bursts remained unchanged.
- (4) The mean lengths of the fields-on epochs increased steadily with the performances (in terms of the number of spontaneous bursts) of the animals.
- (5) During the last session, in the absence of fields, all outputs returned to the previous control values.

ELECTRIC FIELDS AND BRAIN RHYTHMS

377

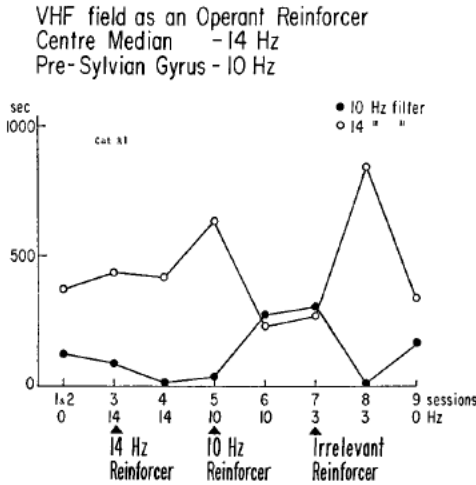


Fig. 8. Selective reinforcement of intrinsic EEG rhythmic episodes by VHF fields. Cat R1. Experimental conditions: no field (0), VHF fields amplitude-modulated at 14 Hz, 10 Hz and 3 Hz (see text).

The imposition of the fields modulated at a frequency (3 Hz) different from the triggering one (10 Hz, cat R1, sessions 7 and 8) lead to dramatic decrease of the 10 Hz rhythm (presylvian gyrus) and increase of the non-reinforced patterns (14 Hz, centrum medianum). These results provided strong evidence that the modulation was indeed responsible for enhanced and decreased occurrence of rhythm seen in previous sessions. This experiment was not repeated with the second animal since, in this case, both rhythms were present at the same time in the EEG and still selectively reinforced by the two different modulations with performances identical to those seen in cat R1.

Fig. 8 illustrates the experiment for cat R1. The total time recorded for each filter during each session is shown on the ordinate. The experimental conditions for each day are symbolized on the abscissa by the symbols: 0 (no fields), 10 Hz, 14 Hz and 3 Hz (frequency of the amplitude-modulation).

DISCUSSION

The experimental data indicate that low level VHF fields, amplitude-modulated at specific frequencies, produce marked effects on conditioned specific brain rhythms (enhanced regularity of the patterns, sharpening of the spectral peaks around the central frequency of the response, extremely prolonged resistance to extinction). These effects cannot be attributed to the conditioning procedure, since the results started to diverge from the two controls only after imposition of the fields. Nor can they be attributed to the choice of brain location (and/or task) since the two control cats were conditioned to produce responses similar to those of the irradiated animals. The innumerable tests conducted within every session (variation of the frequencies of modula-

tion and field-off conditions imposed for short epochs), the sharp contrasts in the EEG between correct *versus* incorrect responses, the finding that the specific activities were localized in the structures subjected to reinforcement together with the eventual return to baselines, strongly suggest a genuine biological transduction in the CNS, which could be described as an enhancement of frequency-related biological rhythms.

The results obtained in the second experiment indicate that it is indeed possible to selectively enhance various brain rhythms by reinforcing their spontaneous occurrence with short irradiations by the fields, amplitude-modulated at appropriate frequencies. Therefore, the hypothesis is offered that the fields were acting as effective contingent reinforcers in both experiments.

The shielding wires were continued up to the animal's head, leaving only very short lengths of unshielded conductor between the leads and the brain. Therefore, they provided adequate attenuation for the fields picked up by the inner conductor. Also, taking into account the considerable mismatch of impedance between recording cables, electrodes and brain tissue, we concluded that the antenna effects on the leads could induce only very small potentials at the tip of the electrodes.

Nevertheless, spectral analysis might be expected to reveal residual voltages so induced and rectified at the electrode-tissue contact. Such effects would be expected to appear uniformly at all electrodes and to be present, unchanged, during the fields exposure.

In fact, no evidence of generalized or sustained artifact was seen in any animals. The EEG changes reported here were anatomically localized, highly specific in terms of frequency and associated with transient patterns. Therefore, we feel confident that the tissue effects are not attributable to direct injection of field voltages via electrodes.

The possibility of thermal effects due to overall or local heating seems equally remote. First, the fields intensities used in all experiments were of the order of 1 mW/sq. cm of field plate area, or less. The heat production resulting from exposures to incident power density of this order has been estimated to be less than 10% of the average basal metabolic rate and therefore almost insignificant³⁷. Secondly, theoretical calculation of the distribution of heating potentials induced by electromagnetic energies have shown that 'hot spots' were generated inside conducting spheres (5 cm radius, electrical characteristics similar to those of biological tissues) only for frequencies well above 250 MHz, the maximum effects being seen around 900 MHz³⁰. Third, diffuse heating could hardly explain the prolonged resistance to extinction followed by return to baseline in the conditioned animals and the selective increase of the rate of occurrence of spontaneous transient EEG rhythms.

On the other hand, it is clear that these effects may have been mediated via peripheral receptors. The current controversy regarding peripheral *versus* central receptors cannot yet be resolved. It can only be stated that we do not yet know of transducers that could relay specific information about the frequency of the modulation of the VHF fields, only to localized brain structures involved in frequency related activity. Destruction of visual, olfactory, vestibular and auditory inputs, or hypothalamic and thalamic (posterolateral ventral nucleus) lesions and sections of the spinal cord at the level of C1 have been reported to be without significant influence

on the observed fields effects^{5,16,26}. Evoked responses in the cortex of the dog⁵⁴ and in the cat's brain stem¹⁶ were elicited by pulsed electromagnetic exposure. In the latter case, the response was abolished by careful shielding of the head alone. These experimental findings seem to be in favor of a more direct action of the fields upon the CNS.

Nevertheless, Schwan⁴⁹ calculated (by direct application of Laplace's equation) the potential evoked across a biological membrane by microwave fields perpendicular to the nerve axis. He found values 10^5 – 10^6 times smaller than the resting potential and therefore concluded that 'according to all modern concepts of neurophysiology about excitation, this just cannot stimulate nerves'. It is not clear, however, what was meant exactly by stimulation or excitation of a biological membrane. The fact that extracellular electrical fields influence the activity of adjacent neurons has been repeatedly evidenced during the past 15 years. For example, Terzuolo and Bullock⁶⁴ showed that extracellular voltage gradients as low as 1 mV/mm alter firing rate in the stretch receptor neurons of the crayfish and Nelson³⁸ reported comparable findings in the spinal motoneurons of the cat. In Nelson's study, the estimated external field strength was of the order of 5–10 mV/mm and short latency facilitation was observed in the single motoneurons tested during synchronous antidromic stimulation of many adjacent neurons. The author suggested that neuronal geometrical organization, as seen in the cerebrum and the hippocampus, could be much more favorable for electrical interaction between cells or groups of cells than the amorphous arrangement of spinal cord neurons. For the whole organism, Rommel and McCleave⁴⁴ have reported that a DC gradient as small as $6 \mu\text{V}/\text{cm}$ is an effective conditional stimulus in the eel, again raising the question of central *versus* peripheral receptors.

There is evidence in the literature that slow potentials, originating in neurons, may combine extracellularly to form electroencephalographic signals. Prominent extracellular positive potentials were recorded synchronously with long latency, long duration, postsynaptic potentials evoked in thalamic neurons during recruiting responses⁴². These positive waves were attributed to the summation of postsynaptic potentials of the involved neurons. Slow membrane fluctuations (3–5 Hz; 5–36 mV) synchronous with the electroencephalographic theta rhythms were observed in pyramidal hippocampal neurons¹⁷. Similar fluctuations were observed in cortical neurons of the cat by Elul^{9,11}. The spontaneous variations of the resting potential were found to resemble and parallel the EEG recorded in the same area (sensorimotor cortex). The amplitude distribution of the EEG was found to follow a normal curve while the neuronal distribution was definitively non-Gaussian. This seems to indicate that the neuronal generators involved in the formation of the local EEG are independent or at least non-linearly related. On the other hand, brief periods of EEG synchronization during spindle sleep and mental task performances^{2,10} were characterized by skewed amplitude distributions and similar statistical analyses have been conducted on the human alpha rhythm by Saunders⁴⁵ to lead to comparable results. In addition to the work of Fujita and Sato¹⁷ on the hippocampal electroencephalographic and intracellular activities, oscillatory neuronal rhythms have been recorded and compared with the electroencephalographic patterns in cortical and pyramidal tract neurons^{6,23}, and it seems reasonable to acknowledge the existence of brief transient epochs

where the EEG and neuronal activity could be strongly correlated. If the EEG signals picked up by a macroelectrode reflect the slow undulations of the membrane potential of a surrounding population of neurons, rhythmic electroencephalographic patterns could result, for example, from transient increase (in a limited frequency bandwidth) of one activity shared by this population or from an increase in the number of neuronal generators involved in frequency-related activities.

Our data do not provide any specific information about the mechanism underlying the formation of the EEG, nor do they indicate ways in which neuronal susceptibility to surrounding electric fields may occur. The following short discussion is thus necessarily based on previous hypotheses and assumptions.

Schwan⁴⁹ has shown that electromagnetic radiations below 300 MHz readily penetrate biological material, while most energy of higher frequency signals is absorbed in skin. VHF fields would thus infiltrate the tissues with the depth of penetration proportional to the inverse square root of the frequency, assuming a fairly constant tissue resistivity in that frequency range. So, an amplitude-modulated 147 MHz field could by its mere presence in the extracellular space, play the role of one or many wave generators and contribute to the total electrical activity seen by the tip of the electrode. New induced activity was never seen in any brain structure under study, while pre-existing rhythms were repeatedly and exclusively enhanced by exposure to fields modulated at the dominant frequency of the transient bursts. This does not preclude a non-biological interference. It is possible that the field's strength is insufficient to become the dominant component in the medium, but might be large enough to contribute to an existing energy band (creating an artificial cooperativeness among frequency-related energies). This possibility cannot be excluded but it does not explain the increase in the spontaneous occurrence of short patterns, as seen when the fields were tentatively used as reinforcers, nor the differences seen in the performances and behavior of the two groups of conditioned animals.

The power absorbed as a function of the depth has been calculated for typical living material by Vogelmann⁶⁶. It was shown that for a 10 mW/sq. cm field intensity in air, the power even in the first 0.1 cu. cm of tissue would never exceed 1 mW for a cross section of 1 sq. cm at all frequencies below 3 GHz. The maximum field strength induced in the tissues by VHF fields of 1 mW/sq. cm intensity would be of the order of 10–20 mV/mm, thus in the same range as the extracellular electrical fields recorded around the spinal neurons.

The mechanisms of interaction between intercellular low electrical fields and neuronal membranes remain to be elucidated. However, some hypotheses can be made in the light of the relatively new concepts of a 'greater membrane of brain cells' as described by Lehninger³¹ and Schmitt⁴⁷. This greater membrane is composed of a lipid-protein inner layer (inner zone) and a diffuse external coat of polysaccharides, glycoproteins and lipoproteins. It is suggested that conformational changes (resulting, for example, from interference with external cations and water) taking place in the outer layer could induce conformational changes in the inner zone proteins.

The existence of an 'electrogenic protein' undergoing conformational changes in the presence of electrical forces had been postulated by Schmitt and Davison⁴⁸ in

1965; the underlying assumption was that those changes would affect the triggering of membranous pores, therefore modulating the excitability of the cell. Extensive studies of these membranous proteins (for example: Wallach and Zahler⁶⁸; Lenard and Singer³²; Singer and Nicholson⁵⁵) led to a new model of the inner zone of the greater membrane. In this model phospholipid bilayers alternate with globular protein sections, the polar end of the proteins being in contact with the aqueous phase, the hydrophobic end being hidden inside the membrane. Protein-protein interaction as well as oligosaccharide-protein interaction could thus occur in the outer layer to form glycoproteins and lipoproteins, as suggested by Schmitt⁴⁷ in 1969. A model proposed by Adey¹, and based on the greater membrane concept, envisages a modification of calcium binding to polyanionic macromolecules on dendritic structures in the genesis of slow waves in dendrites of cerebral neurons. It also envisages a role for calcium in 'membrane amplification' by cooperative processes as a possible basis for susceptibility of central neurons to weak environmental electric fields.

Possible mechanisms of interaction of electromagnetic fields with molecular systems have been proposed, notably by Vogelhut⁶⁵ and Illinger²². Illinger's studies, based on quantum-mechanical models, suggested that biological interactions between RF radiations and biopolymers could occur through segmental rotation of the random coils of the molecules (resulting in fluctuations from the equilibrium distribution of tertiary structures) and/or through quasi-rotational motion of the water molecules forming a sheath about the helical structure (primary and secondary structures) of the biopolymers. The importance of the water-bound molecules was similarly stressed by Vogelhut⁶⁵ who suggested that the variations in the transport properties of the membranes under RF radiations were due to transformation of the hydrated water phase of the globular proteins. Here, hydration states are sharply dependent on divalent cation binding, particularly of calcium.

There exists, therefore, a possibility that an externally applied electrical field could influence the activity or excitability of a population of cells, and that the changes seen in the gross recordings would reflect true neuronal phenomena.

ACKNOWLEDGEMENTS

This investigation was supported in part by the Air Force Office of Scientific Research of the Office of Aerospace Research under Contract 44620-70-C-0017; by the National Aeronautics and Space Administration under Grant NGR 05-007-195; by the Office of Naval Research under Contract N00014-69-A-0200-4037; and by the Marie Curie Fellowship of the AAUW, 1971-1972.

Grateful thanks is given to Mr. R. Stahl and Mr. P. Kaminsky for the design of the VHF equipment, Mrs. M. Peppel for the editing of the manuscript, Mrs. J. Sells for the preparation of illustrations; and to Mrs. M. Lee for the histological preparations.

REFERENCES

- 1 ADEY, W. R., Organization of brain tissue: is the brain a noisy processor? *Int. J. Neurosci.*, 3 (1972) 271-284.
- 2 ADEY, W. R., ELUL, R., WALTER, R. D., AND CRANDALL, P. H., The cooperative behavior of neuronal populations during sleep and mental tasks, *Proc. Amer. Electroenceph. Soc.*, (1966) 86.
- 3 BARANSKI, S., AND EDELWEIN, Z., Electroencephalographical and morphological investigation upon the influence of microwaves on the central nervous system, *Acta physiol. pol.*, 18 (1967) 517-532.
- 4 CHIZHENKOVA, R. A., The role of different brain formations in EEG reactions of rabbits to a constant magnetic field and electromagnetic fields of ultra high and supra high frequencies, *Zh. vyssh. nerv. Deyat. Pavlova*, 17 (1967) 313-321.
- 5 CHIZHENKOVA, R. A., Electrical reaction of the rabbit cerebral cortex to various electromagnetic fields, *Zh. vyssh. nerv. Deyat. Pavlova*, 17 (1967) 1083-1090.
- 6 CREUTZFELDT, O. D., WATANABE, S., AND LUX, H. D., Relations between EEG phenomena and potentials of single cortical cells. II. Spontaneous and convulsoid activity, *Electroenceph. clin. Neurophysiol.*, 20 (1966) 19-37.
- 7 DELGADO, J. M. R., JOHNSON, V. S., WALLACE, J. D., AND BRADLEY, R. J., Operant conditioning of amygdala spindling in the free chimpanzee, *Brain Research*, 22 (1970) 347-362.
- 8 EDELWEIN, Z., An attempt to assess the functional state of the cerebral synapses in rabbits exposed to chronic irradiation with microwaves, *Acta physiol. pol.*, 19 (1968) 897-906.
- 9 ELUL, R., Dipoles of spontaneous activity in the cerebral cortex, *Exp. Neurol.*, 6 (1962) 285-299.
- 10 ELUL, R., Specific site of generation of brain waves, *Physiologist*, 7 (1964) 125.
- 11 ELUL, R., Brain waves: intracellular recording and statistical analysis help clarify their physiological significance. In *Proceedings of the 1966 Rochester Conference on Data Acquisition and Processing in Biology and Medicine*, Vol. 5, Pergamon Press, Oxford, 1968, pp. 93-115.
- 12 ERSHOVA, L. K., AND DUMANSKII, YU. D., Cortical biopotentials in rabbits under the effect of low intensity electromagnetic fields with radio frequency waves, *Fiziol. Zh. (Kiev)*, 15 (1969) 777-780.
- 13 FOX, S. S., AND AHN, H., Identification of functional bioelectric configurations in spontaneous activity of the brain. In *First Annual Meeting of the Society for Neurosciences*, Washington, D.C., 1971, p. 81.
- 14 FOX, S. S., AND RUDELL, A. P., Operant controlled neural event: formal and systematic approach to electrical coding of behavior in brain, *Science*, 162 (1968) 1299-1302.
- 15 FREY, A. H., Human auditory system response to modulated electromagnetic energy, *J. appl. Physiol.*, 17 (1962) 689-692.
- 16 FREY, A. H., Brain stem evoked responses associated with low-intensity pulsed UHF energy, *J. appl. Physiol.*, 23 (1967) 984-988.
- 17 FUJITA, Y., AND SATO, T., Intracellular records from hippocampal pyramidal cells in rabbit during theta rhythm activity, *J. Neurophysiol.*, 27 (1964) 1011-1025.
- 18 GAVALAS, R. J., WALTER, D. O., HAMER, J., AND ADEY, W. R., Effect of low-level, low-frequency electric fields on EEG and behavior in *Macaca nemestrina*, *Brain Research*, 18 (1970) 491-501.
- 19 GVOZDIKOVA, A. M., ANAN'EV, V. M., ZENINA, I. N., AND ZAK, V. I., Sensitivity of the rabbit's central nervous system to a continuous super-high frequency electromagnetic field, *Biul. eksp. Biol. Med.*, 58 (1964) 63-68.
- 20 HAMER, J., Effects of low level, low frequency electric fields on human reaction time, *Commun. behav. Biol.*, 2 (1968) No. 2A.
- 21 HELLER, S. H., Cellular effects of microwave radiation. In S. F. CLEARY (Ed.), *Symposium Proceedings. Biological Effects and Health Implications of Microwave Radiations*, BRH/DBE 70-2, PB 193898, Rockville, Md., 1970, pp. 116-121.
- 22 ILLINGER, K. H., Molecular mechanisms for microwave absorption in biological systems. In S. F. CLEARY (Ed.), *Symposium Proceedings. Biological Effects and Health Implications of Microwave Radiation*, BRH/DBE 70-2, PB 193898, Rockville, Md., 1970, pp. 112-115.
- 23 JASPER, H., AND STEFANIS, C., Intracellular and oscillatory rhythms in pyramidal tract neurons in the cat, *Electroenceph. clin. Neurophysiol.*, 18 (1965) 541-553.
- 24 JUSTESEN, D. R., AND KING, N. W., Behavioral effects of low level microwave irradiation in the closed-space situation. In S. F. CLEARY (Ed.), *Symposium Proceedings. Biological Effects and Health Implications of Microwave Radiation*, BRH/DBE 70-2, PB 193898, Rockville, Md., 1970, pp. 154-179.

- 25 KHOLODOV, YU. A., Changes of electrical activity of rabbit cerebral cortex in the action of UHF electromagnetic fields, *Biul. eksp. Biol. Med.*, 56 (1963) 42-46.
- 26 KHOLODOV, YU. A., Influence of a UHF EM field on the electrical activity of a neurally isolated strip of the cortex of the brain, *Biul. eksp. Biol. Med.*, 57 (1964) 98-101.
- 27 KONIG, H., AND ANKERMULLER, F., Über den Einfluss besonders niederfrequenter elektrischer Vorgänge in der Atmosphäre auf den Menschen, *Naturwissenschaften*, 21 (1960) 486-490.
- 28 KORBEL, S. F., Behavioral effects of low intensity UHF radiation. In S. F. CLEARY (Ed.), *Symposium Proceedings. Biological Effects and Health Implications of Microwave Radiation*, BRH/DBE 70-2, PB 193898, Rockville, Md., 1970, pp. 180-184.
- 29 KORBEL, S. F., AND FINE, H. L., Effects of low intensity UHF radio fields as a function of frequency, *Psychonom. Sci.*, 9 (1967) 527-528.
- 30 KRITIKOS, H. N., AND SCHWAN, H. P., Hot spots generated in conducting spheres by electromagnetic waves and biological implications, *IEEE Trans. Biomed. Engng.*, BME-19 (1972) 53-58.
- 31 LEHNINGER, A. L., The neuronal membrane, *Proc. nat. Acad. Sci. (Wash.)*, 60 (1968) 1055-1101.
- 32 LENARD, J., AND SINGER, S. J., Protein conformation in cell membrane preparations as studied by optical rotatory dispersion and circular dichroism, *Proc. nat. Acad. Sci. (Wash.)*, 56 (1966) 1828-1835.
- 33 LOVANOVA, YE. A., Survival and development of animals with various intensities and durations of the influence of UHF. In A. A. LETAVET AND Z. V. GORDON (Eds.), *Biological Action of Ultrahigh Frequencies*, Academy of Medical Sciences, Moscow, 1960, pp. 52-56.
- 34 LOVANOVA, YE. A., AND TOLGSKAYA, M. S., Change in the higher nervous activity and interneuron connections in the cerebral cortex of animals under the influence of UHF. In A. A. LETAVET AND Z. V. GORDON (Eds.), *Biological Action of Ultrahigh Frequencies*, Academy of Medical Sciences, Moscow, 1960, pp. 69-74.
- 35 MCAFFEE, R. D., Physiological effects of thermode and microwave stimulation of peripheral nerves, *Amer. J. Physiol.*, 203 (1962) 374-378.
- 36 MICHAELSON, S., DUNDERO, R., AND HOWLAND, J. W., The biological effects of microwave irradiation in the dog. In *Proceedings of the Second Annual Tri-Service Conference on Biological Effects of Microwave Energy*, Defense Documentation Center, Alexandria, Va., 1958, pp. 175-188.
- 37 MUMFORD, W. W., Heat stress due to RF radiation. In S. F. CLEARY (Ed.), *Symposium Proceedings. Biological Effects and Health Implications of Microwave Radiation*, BRH/DBE 70-2, PB 193898, Rockville, Md., 1970, pp. 21-34.
- 38 NELSON, P. G., Interaction between spinal motoneurons of the cat, *J. Neurophysiol.*, 29 (1966) 275-287.
- 39 OLDS, J., AND HIRANO, T., Conditioned responses of hippocampal and other neurons, *Electroenceph. clin. Neurophysiol.*, 26 (1969) 159-166.
- 40 PRESMAN, A. S., The role of electromagnetic fields in physiological processes, *Biofizika*, 1 (1964) 131-134.
- 41 PURAHICK, H. K., AND LAWRENCE, J. L., Modulated alternating current energy to stimulate audition in totally deaf humans, *25th Annual Meeting of the Aerospace Medical Association*, Miami, Fla., (1964).
- 42 PURPURA, D. P., AND COHEN, B., Intracellular recording from thalamic neurons during recruiting responses, *J. Neurophysiol.*, 25 (1962) 621.
- 43 ROBINSON, D. A., AND FUCHS, A. F., Eye movement evoked by stimulation of frontal eye fields, *J. Neurophysiol.*, 32 (1969) 637-648.
- 44 ROMMEL, S. A., JR., AND MCCLEAVE, J. D., Oceanic electric fields: perception by American eels?, *Science*, 176 (1972) 1233-1235.
- 45 SAUNDERS, M. G., Amplitude probability density studies on alpha and alpha-like patterns, *Electroenceph. clin. Neurophysiol.*, 15 (1963) 761-767.
- 46 SCHLAG, J., AND SCHLAG-REY, M., Induction of oculomotor responses by electrical stimulation of the prefrontal cortex in the cat, *Brain Research*, 22 (1970) 1-13.
- 47 SCHMITT, F. O., Brain cell membranes and their microscopic environment, *Neurosci. Res. Progr. Bull.*, 7 (1969) 281-300.
- 48 SCHMITT, F. O., AND DAVISON, P. F., Brain and nerve proteins: functional correlates. Role of protein in neural function, *Neurosci. Res. Progr. Bull.*, 3 (1965) 1-87.
- 49 SCHWAN, H. P., Interaction of microwave and radio frequency radiations with biological systems. In S. F. CLEARY (Ed.), *Symposium Proceedings. Biological Effects and Health Implications of Microwave Radiation*, BRH/DBE 70-2, PB 193898, Rockville, Md., 1970, pp. 13-20.

- 50 SCOLLO-LAVIZZARI, G., Anatomische und physiologische Beobachtungen über das frontale Augenfeld der Katze, *Helv. physiol. pharmacol. Acta*, 22 (1964) C42-C43.
- 51 SHER, L. D., AND SCHWAN, H. P., *Mechanical Effects of AC Fields on Particles Diffused in a Liquid: Biological Implications*, Ph. D. dissertation, Univ. Penn., Philadelphia, Contract AF 30 (602), ONR Techn. Rep. 37, 1963.
- 52 SHEYVENKHMEN, B. YU., Effects of the action of an ultra-high frequency field on the audio sensitivity during application of electrodes in the zone of projection of the aural zone of the cortex, *Probl. Fiziol. Akustiki*, 1 (1949) 122-127.
- 53 SHLIAFER, T. P., AND IAKOVLEA, M. I., Influence of electromagnetic fields of ultra-high frequencies on impulse activity of the cerebral cortex neurons, *Fiziol. Zh. (Leningr.)*, 55 (1969) 16-21.
- 54 SIMON, R. C., AND HOSHIKO, M., Evaluation of electrostimulation of hearing by evoked potential. In N. L. WULFSOHN AND A. SANCES, JR. (Eds.), *The Nervous System and Electric Currents, Vol. 12*, Plenum Press, New York, 1971, pp. 15-18.
- 55 SINGER, S. J., AND NICOLSON, G. L., The fluid mosaic model of the structure of cell membranes, *Science*, 175 (1972) 720-730.
- 56 SNIDER, R. S., AND NIEMER, W. T., *A Stereotaxic Atlas of the Cat Brain*, Univ. Chicago Press, Chicago, 1961.
- 57 STERMAN, M. B., HOWE, R. C., AND MACDONALD, L. R., Facilitation of spindle-bursts sleep by conditioning of electroencephalographic activity while awake, *Science*, 167 (1970) 1146-1148.
- 58 STERMAN, M. B., WYRICKA, W., AND CLEMENTE, C. D., EEG correlates of behavioral inhibition, *Condit. Reflex*, 4 (1969) 124-125.
- 59 SUBBOTA, A. G., The effect of a pulsed super-high frequency SHF electromagnetic field on the higher nervous activity of dogs, *Biul. eksp. Med.*, 46 (1958) 1206-1211.
- 60 TALLARICO, R., AND KETCHUM, J., Effect of microwaves on certain behavior patterns of the rat. In C. SUSSKIND (Ed.), *Proceedings of the Third Annual Tri-Service Conference on Biological Effects of Microwave Radiating Equipments*, Defense Documentation Center, Alexandria, Va., 1959, pp. 75-76.
- 61 TANNER, J. A., Effect of microwave radiation on birds, *Nature (Lond.)*, 210 (1966) 636.
- 62 TANNER, J. A., AND ROMERO-SIERRA, C., Bird feathers as sensory detectors of microwave fields. In S. F. CLEARY (Ed.), *Symposium Proceedings. Biological Effects and Health Implications of Microwave Radiation*, BRH/DBE 70-2, PB 193898, Rockville, Md., 1970, pp. 185-187.
- 63 TANNER, J. A., ROMERO-SIERRA, C., AND DAVIE, S. J., Non-thermal effects of microwave radiation on birds, *Nature (Lond.)*, 216 (1967) 1139.
- 64 TERZUOLO, C. A., AND BULLOCK, T. H., Measurement of imposed voltage gradient adequate to modulate neuronal firing, *Proc. nat. Acad. Sci. (Wash.)*, 42 (1956) 687-694.
- 65 VOGELHUT, P. O., Interaction of microwave and radio frequency radiation with molecular systems. In S. F. CLEARY (Ed.), *Symposium Proceedings. Biological Effects and Health Implications of Microwave Radiation*, BRH/DBE 70-2, PB 193898, Rockville, Md., 1970, pp. 98-100.
- 66 VOGELMAN, J. H., Physical characteristics of microwave and other radio-frequency radiation. In S. F. CLEARY (Ed.), *Symposium Proceedings. Biological Effects and Health Implications of Microwave Radiation*, BRH/DBE 70-2, PB 193898, Rockville, Md., 1970, pp. 7-12.
- 67 WAGMAN, I. H., Eye movements induced by electrical stimulation of cerebrum in monkeys and their relationship to bodily movements. In M. B. BENDER (Ed.), *The Oculomotor System*, Hoeber, New York, 1964, pp. 18-39.
- 68 WALLACH, D. F. H., AND ZAHLER, P. H., Protein conformation in cellular membranes, *Proc. nat. Acad. Sci. (Wash.)*, 56 (1966) 1552-1559.
- 69 WALTER, D. O., Spectral analysis for electroencephalograms: mathematical determination of neurophysiological relationships from records of limited duration, *Exp. Neurol.*, 8 (1963) 155-181.

EXHIBIT 10



Frequency-specific responses in the human brain caused by electromagnetic fields

Glenn B. Bell ^a, Andrew A. Marino ^{a,*}, Andrew L. Chesson ^b

^a Department of Orthopaedic Surgery, ^b Neurology Section, Department of Medicine, Louisiana State University Medical Center, P.O. Box 33932, Shreveport, LA 71130-3932, USA

(Received 4 August 1993; revised 25 October 1993; accepted 12 November 1993)

Abstract

The effects of 1.5- and 10-Hz electromagnetic fields (EMFs), 0.2–0.4 gauss, on the intrinsic electrical activity of the human brain at these frequencies was studied. Each of 19 subjects exposed for 2-sec epochs exhibited altered brain electrical activity at the frequency of the EMF during the time of stimulation, as determined by spectral analysis of the electroencephalogram. Since brain activity at specific frequencies could be altered by applied EMFs, the results suggest that it may be possible to use EMFs to determine whether particular intrinsic frequencies subserve specific physiological or behavioral responses.

Key words: EEG; Electromagnetic field; EMF; Magnetic field; Brain; Power spectra; Fourier transformation

1. Introduction

Human brain electrical activity manifested in the electroencephalogram (EEG) consists primarily of frequencies below 20 Hz (Niedermeyer 1987). The question whether these frequencies directly mediate behavioral and physiological effects, or are epiphenomena, has not been resolved (Adey 1970). Externally applied electromagnetic fields (EMFs) may provide a means to alter specific intrinsic frequencies by driving or otherwise interacting with physiological oscillations within the brain, thereby permitting direct assessment of their biological significance in both normal and pathological processes.

EMFs at 2–12 Hz have been reported to affect behavior in man and animals (Hamer 1968; Gavalas et al. 1970; Gavalas-Medici and Day-Magdaleno 1976; Wever 1987), and several animal studies suggest that EMFs can specifically alter brain electrical activity. A relative peak in spectral power was seen in monkeys at the frequency of the EMF (Gavalas et al. 1970), and EMFs amplitude-modulated at 3–14 Hz were reported to reinforce the occurrence of spontaneous rhythms in

cats when the EMF frequency was tuned to the frequency of the intrinsic rhythm (Bawin et al. 1973). EMFs at 5–10 Hz altered intrinsic EEG power in rabbits at the frequency of stimulation (Bell et al. 1992a).

EMFs at 35–40 Hz (Bell et al. 1991) and 60 Hz (Bell et al. 1992b) can non-specifically alter human brain activity, but the effects of EMFs on EEG power at the frequency of stimulation have not previously been described. We report here that human subjects exposed to EMFs exhibited changes in the EEG at the frequency of stimulation.

2. Methods

EMF exposure

Magnetic fields were produced using a pair of coils, each 130 cm in diameter and consisting of 250 turns of copper wire; the coils were maintained parallel and separated by 65 cm (the Helmholtz condition) using a wooden frame. The coil current was obtained from a signal generator (Model 182A, Wavetek, San Diego, CA), and amplifier (Model 7500, Krohn-Hite, Avon, MA), and controlled by a computer-based timing circuit. The subjects sat between the coils (sagittal plane

* Corresponding author. Tel.: (318) 674-6180. Fax: (318) 674-6186.

Table 1

Subject Characteristics and Exposure Conditions

The subjects were clinically normal at the time they entered the study except for those with the listed complaints

Subject (age, sex)	Magnetic field (Gauss)	Frequency (Hz)	Complaint
1 22 F	0.2–0.8	10	None
2 30 M	0.2–0.8	10	None
3 31 F	0.2–0.8	10	None
4 30 M	0.2–0.8	10	None
5 25 F	0.2–0.8	10	None
6 62 M	0.2–0.8	10	None
7 27 M	0.2–0.8	10	None
8 26 F	0.2–0.8	10	Seizures
9 28 F	0.2–0.8	10	Seizures
10 21 M	0.2–0.8	10	Numbness
11 31 F	0.2–0.8	1.5	None
12 30 M	0.2–0.8	1.5	None
13 22 F	0.2–0.8	1.5	None
14 31 F	0.2–0.8	1.5	None
15 35 M	0.2–0.8	1.5	None
16 30 M	0.2–0.8	1.5	None
17 34 M	0.2–0.8	1.5	Seizures
18 51 M	0.2–0.8	1.5	Dizziness
19 42 M	0.2–0.8	1.5	Seizures

perpendicular to the coil axis) on a wooden chair in a dark room with their eyes closed. The head and upper chest were within a magnetic-field region that was uniform to within 5% of its predetermined value (within 20% when the thorax and pelvis are included); the field at the feet was about half of that at the head. The average background 60-Hz magnetic field was about 0.1 mG.

The equipment that powered the coils and recorded the EEG was located 15 m from the room occupied by the subjects. The room was partially soundproofed, but occasional sounds that occurred irregularly in an adjacent corridor could be heard in the room. There were no visual, auditory, or tactile cues to the subjects that indicated the presence of the magnetic field.

Subjects

Thirteen normal (non-symptomatic) subjects were chosen from the general population, and 6 symptomatic subjects were selected from among those with neurological complaints who underwent a clinical EEG as a diagnostic procedure (Table 1). The symptomatic subjects were identified for possible inclusion by an EEG technician, who noted the presence of a well-developed occipital alpha rhythm during the clinical EEG. Subjects having this finding were asked to participate in the study, and those consenting and willing to remain in the laboratory area after completion of their clinical EEG, were utilized. No subject who had a seizure during the clinical EEG, or who had persistent focal or generalized slowing was used. All clinical EEGs were normal except for that from one subject (No. 17,

Table 1), which exhibited intermittent, dysrhythmic activity, as later interpreted by the neurologist reading the clinical tracings and blinded to whether the subject was a study participant. The results were analyzed without respect to age, sex, or the presence of symptoms.

The study was approved by the Institutional Review Board for Human Research of the Louisiana State University Medical Center.

EEG measurement

Gold-plated surface electrodes 1 cm in diameter (Grass Instrument Co., Quincy, MA) were placed at C₃, C₄, P₃, P₄, O₁, and O₂ (10–20 system); to facilitate quantitative comparisons, the electrodes were referred to a common point (linked ears were chosen for convenience), and the ground was placed on the forehead. Electrode impedances were measured before and after each recording, using an electrode impedance meter (Grass Model EZM 5A, Grass Instrument Co., Quincy, MA); typically, the impedances were 2–3 k Ω .

The EEG was filtered to pass 0.3–35 Hz, and then the signal was split and simultaneously recorded on an electroencephalograph (Model 6, Grass Instrument Co., Quincy, MA) and stored on a 40-Mbyte hard drive after sampling at 200 Hz; the stored data was analyzed on a mainframe computer using commercial software (SAS Institute, Inc., Austin, TX). Trials containing obvious movement artifacts were identified on the written record, and the corresponding digitized data was deleted.

The aim was to determine whether brief exposure to an EMF having a frequency of an intrinsic brain rhythm produced an alteration in the EEG at the frequency of stimulation during the application of the field. Characteristic frequencies within the Δ (1.5 Hz) and α (10 Hz) bands were therefore chosen for study, and fields ≤ 0.8 gauss were used to avoid the production of magnetophosphenes, which can occur at stronger fields.

A method of analysis was developed to control for Faraday-type induction which occurs in the human head in the presence of a magnetic field. Since the inductive signal is proportional to the rate of change of magnetic flux (Serway, 1990), by applying a relatively strong magnetic field (0.8 gauss rms) and measuring the induced signal under the assumption that the contribution of the EEG was negligible, the strength of the induced signal at lower fields could be determined on the basis of proportionality.

Consider a pair of surface electrodes attached to a volume electrical conductor (Fig. 1A). Application of $B_0(f_0)$, a uniform magnetic field at frequency f_0 , results in an inductive signal superimposed on the noise ($B = 0$) signal. The electrode voltage is amplified and Fourier-transformed to produce the power spectrum. Let $P(B_0, f_0)$ be the coefficient of the power spectrum

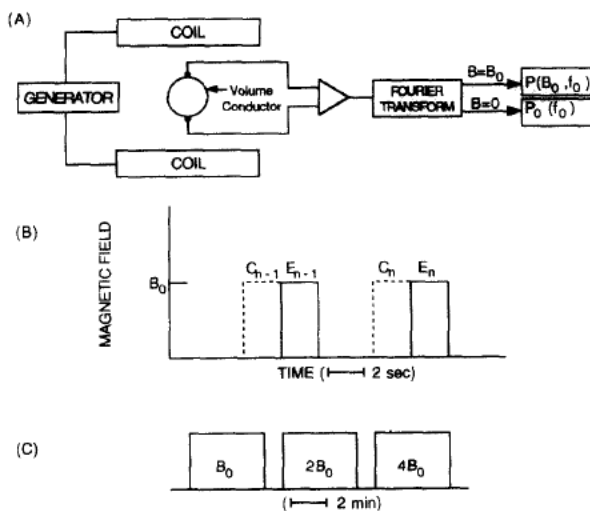


Fig. 1. Characterization of the signal induced in a volume conductor by a magnetic field. B_0 induces a voltage that is amplified and Fourier-transformed. $P(B_0, f_0)$ is the power at f_0 measured during application of B_0 ; $P_0(f_0)$ is measured in the absence of the field. Measurements were made during application of B_0 , $2B_0$, and $4B_0$ in consecutive time intervals (blocks). For human subjects, the order of field presentation was varied randomly from subject to subject. Within each block the field was on for 2 sec and off for 5 sec (the B_0 block is illustrated). C_n and E_n are the control and exposed epochs in the n th trial ($n = 50$). For human subjects, the EEG at f_0 during the exposed epochs at B_0 and $2B_0$ was compared with the power in the corresponding control epochs, after the former were corrected for the inductive signal (determined using $4B_0$).

at f_0 ; it can be expressed as the sum of $P_{B_0}(f_0)$ and $P_0(f_0)$, the contributions due to the field and the noise, respectively (Oppenheim and Schaffer 1975). $P_{B_0}(f_0)$ can therefore be determined from the difference in Fourier coefficients between field and no-field epochs.

$$P_{B_0}(f_0) = P(B_0, f_0) - P_0(f_0) \quad (1)$$

For a sinusoidal magnetic field, the inductive signal is directly proportional to the product of frequency and field strength; the Fourier coefficient of the induced signal is therefore proportional to the product of the squares of frequency and field strength (Serway 1990). Differences defined as in Eq. 1 but formed at $2B_0$ and $4B_0$ therefore correspond to 4 times and 16 times the difference observed at B_0 , respectively;

$$4P_{B_0}(f_0) = P(2B_0, f_0) - P_0(f_0) \quad (2)$$

$$16P_{B_0}(f_0) = P(4B_0, f_0) - P_0(f_0) \quad (3)$$

If the volume conductor is the head of a human subject, and the voltage is the EEG measured from any pair of electrodes during application of the field, the Fourier coefficient corresponding to an exposed epoch can formally be considered to be the sum of three contributions: the inductive signal, the EEG that would be present if no magnetic field were applied, and a

putative effect of the field on the EEG. When modified to allow for an effect of the field (μ_1 and μ_2 at B_0 and $2B_0$, respectively), Eqs. 1 and 2 can be rewritten

$$[P(B_0, f_0) - P_{B_0}(f_0)] - P_0(f_0) + \mu_1 = 0 \quad (4)$$

$$[P(2B_0, f_0) - 4P_{B_0}(f_0)] - P_0(f_0) + \mu_2 = 0 \quad (5)$$

where $P_0(f_0)$ now represents the sum of the signals due to the control EEG and noise.

If

$$[P(B_0, f_0) - P_{B_0}(f_0)] - P_0(f_0) \neq 0 \quad (6)$$

it follows that $\mu_1 \neq 0$. Similarly, if

$$[P(2B_0, f_0) - 4P_{B_0}(f_0)] - P_0(f_0) \neq 0 \quad (7)$$

then $\mu_2 \neq 0$. Thus, an effect of the magnetic field (B_0 , $2B_0$) on EEG activity (μ_1 , $\mu_2 \neq 0$) can be inferred from a comparison between $P_0(f_0)$ and the EEG power measured during application of the field but corrected for the inductive signal ($[P(B_0, f_0) - P_{B_0}(f_0)]$, $[P(2B_0, f_0) - 4P_{B_0}(f_0)]$). If, after subtracting the inductive signal, the EEG power were the same as that in the absence of the field, it would follow that the field had no effect on the EEG; otherwise, the null hypothesis must be rejected.

A trial consisted of the presentation of the magnetic field for 2 sec, followed by an interstimulus period of 5 sec (Fig. 1B). $P(B_0, f_0)$ and $P(2B_0, f_0)$ were computed for each exposure epoch in a series of 50 trials; $P(f_0)$ was determined from the 2-sec intervals immediately preceding each of the exposure epochs. Since EEG power was generally negligible in comparison with the inductive signal caused by $4B_0$, $P_{B_0}(f_0)$ could best be estimated from Eq. 3 (highest signal-to-noise ratio). $[P(B_0, f_0) - P_{B_0}(f_0)]$ and $[P(2B_0, f_0) - 4P_{B_0}(f_0)]$ were each compared with $P_0(f_0)$ using the Wilcoxon signed rank test (Pfurtscheller and Aranibar 1977) at a significance level of $P < 0.05$. If statistically significant differences were found in the EEG from a particular electrode, it was inferred that the subject responded to the presence of the field by exhibiting altered brain electrical activity at f_0 . The analysis was performed for each of the 6 electrodes (referred to linked ears) for each subject, using 50 trials with $B_0 = 0.2$ gauss and 50 additional trials with $2B_0 = 0.4$ gauss. The overall procedure is depicted in Fig. 1.

Saline, tap water and a melon were used to evaluate the accuracy of the measuring system and the validity of the procedure for determining the effect of field strength on the magnitude of the inductive signal. For measurements in saline and tap water, 6 measuring electrodes were attached to the curved surface of a plastic cylinder (20 cm in diameter), which was immersed in either normal saline or tap water. The electrodes were placed in one plane, with spatial separations and locations that approximately corresponded

Table 2

Evaluation of the method of measuring spectral power during application of a magnetic field

Fields of 0.2, 0.4 and 0.8 gauss at either 1.5 or 10 Hz were applied to normal saline, tap water, and a melon, as depicted in Fig. 1. The power at the frequency of the applied field (averaged over 50 2-sec epochs) was computed for electrodes located to correspond to the indicated standard (10–20 system) EEG electrodes. The measurements obtained at 0.2 and 0.4 gauss are expressed as a percent difference relative to that obtained at 0.8 gauss, taking into account the expected proportional differences between different field strengths. The results are expressed in terms of the percent difference (PD) between the observed (O) and expected (E) values: $PD = 100 \times |(O - E)/E|$. Individual measurements were reproducible to within 5%. Electrode resistances 0.1–0.2 k Ω , 1–2 k Ω , 2–3 k Ω for saline, tap water, and melon, respectively

Electrode	Percent difference in spectral power (%)									
	1.5 Hz				10 Hz					
	Saline		Tap		Saline		Tap		Melon	
	0.2 G	0.4 G	0.2 G	0.4 G	0.2 G	0.4 G	0.2 G	0.4 G	0.2 G	0.4 G
C ₃	5.1	6.6	10.9	3.0	6.1	2.3	7.6	4.0	15.0	4.2
C ₄	2.3	0.0	16.1	7.8	9.7	3.7	7.8	7.4	5.6	5.6
P ₃	7.1	14.3	7.0	0.0	10.8	8.7	6.6	3.8	11.2	21.5
P ₄	8.7	6.5	3.3	0.8	6.1	2.3	5.3	2.9	18.5	1.6
O ₁	18.8	2.2	4.8	7.4	16.9	7.7	2.2	9.1	13.7	7.7
O ₂	1.1	2.5	3.1	7.4	8.3	3.1	8.0	4.0	3.8	4.0
Mean \pm SE	6.7 \pm 1.1%				7.4 \pm 1.0%					

to the central, parietal, and occipital electrodes on the human subjects. All measurements were referred to a single reference electrode, located anteriorly, and in the same plane as the measuring electrodes. The locations of the electrodes on the melon were also similar to the electrode locations on the human subjects.

3. Results

The contribution of the inductive signal in each of the passive conductors was found by applying 0.8 gauss and using Eq. 3, and the value thus determined (the expected value) was compared with those found during application of 0.2 and 0.4 gauss, respectively, using Eqs. 1 and 2 (the observed values). The inductive signal at 0.2 and 0.4 gauss was essentially as expected on the basis of the assumption of a proportional response (Table 2); the mean percent differences for the 3 conductors were 7.4 and 6.7% at 10 Hz and 1.5 Hz, respectively. Thus, the response of the measuring system to induced signals in passive conductors was pro-

portional to the square of the field strength and frequency, as expected.

Typical results obtained from a human subject using 10 Hz are shown in Table 3, which lists the mean 10-Hz power from the control and exposed epochs from subject No. 1, after correction for the inductive signal. The 10-Hz power during the control epochs measured from C₃ and C₄ was 454 and 768 μV^2 , respectively; during application of the field the corresponding values were 1514 and 3756 μV^2 , and each of the distributions differed significantly from their corresponding controls as determined by the Wilcoxon test. Significant differences were also found at the other electrodes during application of 0.2 gauss, and at the C and P electrodes during application of 0.4 gauss. The results for all 10 subjects exposed to the 10-Hz field are summarized in Fig. 2, which gives the observed significant changes in spectral power caused by the magnetic field, expressed in terms of the magnitude of the percent difference between the observed and expected values. The 10-Hz field produced significant effects in the 10-Hz EEG power from 1 or more electrodes in 8

Table 3

EEG spectral power at 10 Hz in subject no. 1 exposed to 10-Hz magnetic fields

The absolute value of the mean \pm SE are listed for the Control epochs [$P_0(10)$] and for the exposed epochs after correction for the inductive signal [$P(0.2,10) - P_{0,2}(10)$], and [$P(0.4,10) - 4P_{0,2}(10)$]. The distributions were compared using the Wilcoxon test

Electrode	Spectral power at 10 Hz (μV^2)					
	0.2 gauss			0.4 gauss		
	Control	Exposed	P	Control	Exposed	P
C ₃	454 \pm 82	1514 \pm 350	(0.002)	407 \pm 55	15321 \pm 1004	(0.0001)
C ₄	768 \pm 162	3756 \pm 418	(0.0001)	443 \pm 68	14820 \pm 1119	(0.0001)
P ₃	704 \pm 164	307 \pm 139	(0.0001)	453 \pm 68	522 \pm 529	(0.04)
P ₄	1282 \pm 327	603 \pm 130	(0.0001)	822 \pm 174	2004 \pm 376	(0.0001)
O ₁	793 \pm 101	2326 \pm 485	(0.0001)	1100 \pm 222	604 \pm 1592	(0.47)
O ₂	797 \pm 127	6907 \pm 648	(0.0001)	2038 \pm 643	2287 \pm 2368	(0.99)

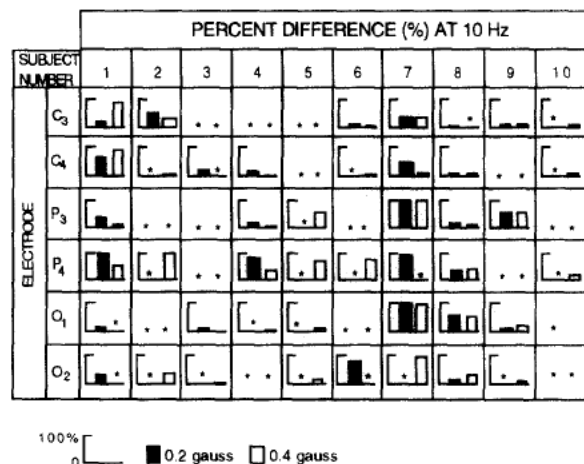


Fig. 2. Change in spectral power of human subjects at 10 Hz during application of a 10-Hz magnetic field. The results are expressed in terms of the percent difference between the observed and expected power. The solid and open bars correspond to 0.2 and 0.4 gauss, respectively. Data from nonsignificant comparisons are omitted (indicated by asterisks). Percent differences greater than 100% are shown as 100%.

of 10 subjects exposed to 0.2 gauss, and in all 10 subjects when exposed to 0.4 gauss.

Table 4 shows typical results obtained during application of 1.5 Hz, and the results for all 1.5-Hz subjects are summarized in Fig. 3. Significant effects on EEG power from 1 or more electrodes was found in 6 of 9 subjects exposed at 0.2 gauss, and in all 9 subjects at 0.4 gauss (Fig. 3).

In all 4 of the field conditions studied, statistically significant responses were usually observed at 2 or more electrodes (Fig. 4).

4. Discussion

In each subject, the magnetic field altered ongoing brain activity at the frequency of stimulation from one or more electrodes (Figs. 2 and 3). The effect was more

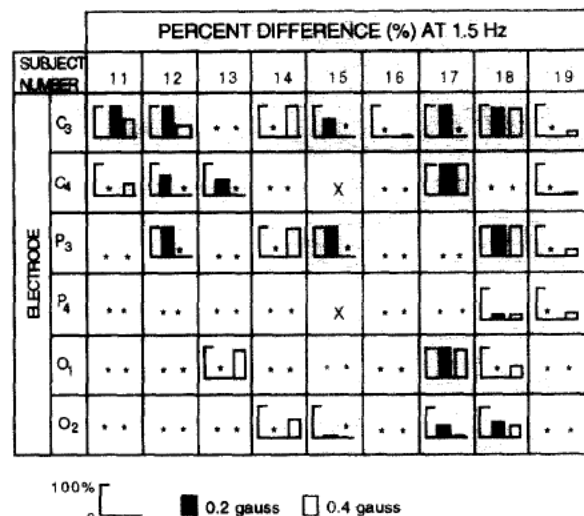


Fig. 3. Change in spectral power of human subjects at 1.5 Hz during application of a 1.5-Hz magnetic field. The results are expressed in terms of the percent difference between the observed and expected power. The solid and open bars correspond to 0.2 and 0.4 gauss, respectively. Data from nonsignificant comparisons are omitted (indicated by asterisks). Percent differences greater than 100% are shown as 100%. X, data not recorded.

likely at 10 Hz compared with 1.5 Hz, and more likely at 0.4 gauss compared with 0.2 gauss (Fig. 4), but the strength of the effect was not proportional to either frequency or field strength (Figs. 2 and 3). A possible source of error that could vitiate these inferences would be the existence of passive contributions to the signal during presentation of the magnetic field other than Faraday induction. If so, every comparison between field-on and field-off groups of data would be biased because no corrections were applied for non-inductive signals. But non-inductive contributions were not seen during measurements of the passive volume conductors, where the observed signal was as expected on the basis of induction alone to within an average of about 7%. Consequently, any putative non-inductive contribution must be such that it exists only for some volume

Table 4
EEG spectral power at 1.5 Hz in subject no. 11 exposed to 1.5-Hz magnetic fields
The absolute value of the mean \pm SE are listed for the control epochs [$P_0(1.5)$] and for the exposed epochs after correction for the inductive signal [$P(0.2,1.5) - P_{0.2}(1.5)$], and [$P(0.4,1.5) - 4P_{0.2}(1.5)$]. The distributions were compared using the Wilcoxon test

Electrode	Spectral power at 1.5 Hz (μV^2)					
	0.2 gauss			0.4 gauss		
	Control	Exposed	P	Control	Exposed	P
C ₃	3836 \pm 551	2013 \pm 618	(0.003)	3656 \pm 893	674 \pm 756	(0.007)
C ₄	2111 \pm 318	1898 \pm 369	(0.50)	2391 \pm 272	1548 \pm 503	(0.05)
P ₃	2895 \pm 419	3223 \pm 634	(0.91)	3662 \pm 679	2942 \pm 611	(0.15)
P ₄	2133 \pm 352	2664 \pm 601	(0.94)	3002 \pm 464	1775 \pm 458	(0.13)
O ₁	2845 \pm 448	4343 \pm 798	(0.23)	4251 \pm 655	4500 \pm 876	(0.70)
O ₂	3304 \pm 702	3483 \pm 634	(0.92)	4412 \pm 705	4857 \pm 932	(0.55)

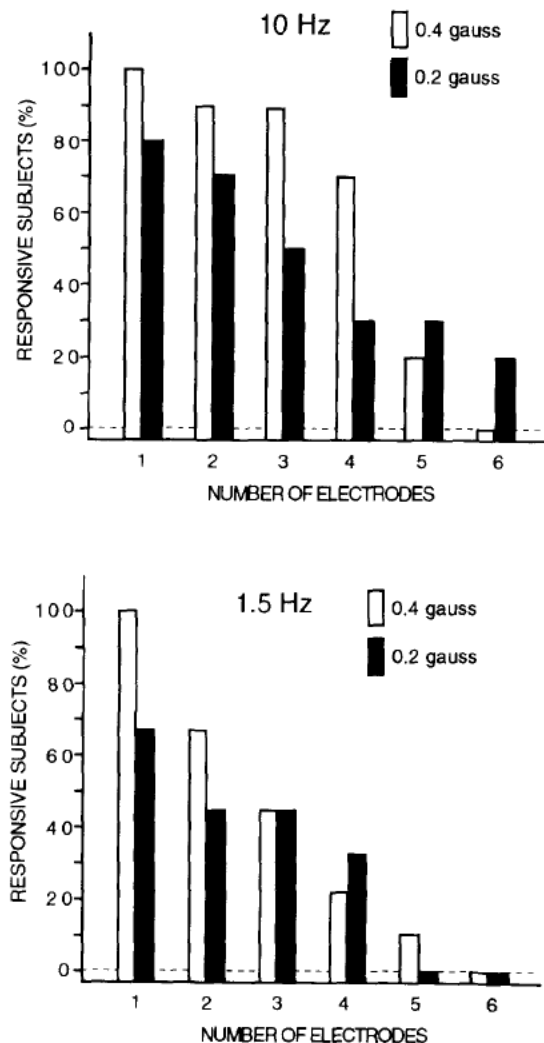


Fig. 4. Percent of subjects that manifested a significant response to a field at 1 or more electrodes, as a function of the number of electrodes.

conductors (the human head) and not others (saline, tap water, and a melon). Further, if non-inductive signals were present during measurement of the EEG, they must have (1) occurred in some subjects and not others, (2) occurred at some electrodes and not others, and (3) been independent of field strength; these characteristics seem incompatible with passive physical systems. Other potential sources of error include artifacts due to movement of the head or electrode wires, and interference due to respiration. There is, however, no reason to expect that such events occurred differently or more often in exposed than control epochs; uncontrolled motion would therefore have biased the results toward acceptance of the null hypothesis.

Neither age, sex nor the presence of symptoms had any apparent differential role in the elaboration of the

observed effects, but the number of subjects within each such class was too small to permit reliable evaluation of class-specific effects. The question whether the effects were due to a direct interaction or were a consequence of an alerting response were not addressed in this study.

Examples of specific frequencies within the central nervous system in relation to particular biological endpoints include 8–9 Hz in the relaxed state and 1–2 Hz in deep sleep. In general, however, it is not clear how most of the various frequencies that can be extracted from the EEG using techniques such as the fast Fourier transform should be regarded. They may originate from relatively monochromatic physiological oscillators, or perhaps they are merely mathematical constructs useful for representing the sum of myriad post-synaptic potentials and action potentials that propagate to the scalp by volume conduction. The results reported here indicate that the external EMF was transduced, resulting in an alteration in the EEG at the frequency of stimulation. Thus, if electrophysiological activity at a particular frequency were a part of the mechanistic chain leading to a particular response, then observations of the response could be used to assess CNS function. Time-estimation tasks, for example, appear to be particularly sensitive to specific EMF frequencies (Medici 1988).

The locus of EMF transduction is still undetermined, but it occurred during a 2-sec exposure epoch, thereby suggesting that it is in a neural or perineural cell. The transduction mechanism may involve sub-threshold changes in cell membrane potential (unpublished data).

In summary, the EMF affected the EEG at the frequency of stimulation in all subjects tested; the spectral power depended on both the subject and the conditions of measurement, and there was a nonlinear relationship between field strength and the magnitude of the response. Similar results were found previously in rabbits exposed to 1–1.5 gauss, 5–10 Hz (Bell et al., 1992a). The similarity in the responses observed in the animal and human studies may indicate that the mechanism of interaction of the EMF with neural tissue is similar in the two species. Thus, the rabbit may be an appropriate species for studying mechanistic and dosimetric aspects of tissue-EMF interactions.

References

- Adey, W.R. (1970) Cerebral structure and information storage. *Prog. Physiol. Psychol.*, 3: 181–200.
- Bawin, S.M., R.J. Gavalas-Medici and W.R. Adey (1973) Effects of modulated very high frequency fields on specific brain rhythms in cats. *Brain Res.*, 58: 365–384.
- Bell, G., A. Marino, A. Chesson and F. Struve (1991) Human sensitivity to weak magnetic fields. *Lancet*, 338: 1521–1522.

- Bell, G., A. Marino, A. Chesson and F. Struve (1992a) Electrical states in the rabbit brain can be altered by light and electromagnetic fields. *Brain Res.*, 570: 307–315.
- Bell, G., A. Marino and A. Chesson (1992b) Alterations in brain electrical activity caused by magnetic fields: detecting the detection process. *Electroenceph. Clin. Neurophysiol.*, 83: 389–397.
- Gavalas, R.J., D.O. Walter, J. Hamer and W.R. Adey (1970) Effect of low-level, low-frequency electric fields on EEG and behavior in *Macaca nemestrina*. *Brain Res.*, 18: 491–501.
- Gavalas-Medici, R. and S.R. Day-Magdaleno (1976) Extremely low frequency, weak electric fields affect schedule-controlled behavior of monkeys. *Nature*, 261: 256–259.
- Hamer, J. (1968) Effects of low-level, low-frequency electric fields on human reaction time. *Commun. Behav. Biol.*, 2: 217–222.
- Medici, R. (1988) Behavioral measures of electromagnetic field effects. In: A. Marino (Ed.), *Modern Bioelectricity*, Marcel Dekker, New York, NY, pp. 557–585.
- Niedermeyer, E. (1987) The normal EEG of the waking adult. In: E. Niedermeyer and F.H. Lopes da Silva (Eds.), *Electroencephalography*, 2nd edn., Urban and Schwarzenberg, Baltimore, MD.
- Oppenheim, A.V. and R.W. Schaffer (1975) *Digital Signal Processing*. Prentice-Hall, Englewood Cliffs, NJ.
- Pfurtscheller, G. and A. Aranibar (1977) Event-related cortical desynchronization detected by power measurements of scalp EEG. *Electroenceph. Clin. Neurophysiol.*, 42: 817–826.
- Serway, R.A. (1990) *Physics for Scientists and Engineers*. Saunders, Philadelphia, PA.
- Wever, R.A. (1987) The electromagnetic environment and the circadian rhythms of human subjects. In: M. Grandolfo, S.M. Michaelson and A. Rindi (Eds.), *Biological Effects and Dosimetry of Static and ELF Electromagnetic Fields*, Plenum Press, New York, NY.

EXHIBIT 11

Resting EEG Effects During Exposure to a Pulsed ELF Magnetic Field

Charles M. Cook,^{1,2} Alex W. Thomas,^{1,2} Lynn Keenlside,¹ and Frank S. Prato^{1,2}

¹Department of Nuclear Medicine, Lawson Health Research Institute,
St. Joseph's Health Care (London), London, Ontario, Canada

²The Department of Medical Biophysics, University of Western Ontario, London,
Ontario, Canada

Continuing evidence suggests that extremely low frequency magnetic fields (ELF MFs) can affect animal and human behavior. We have previously demonstrated that after a 15 min exposure to a pulsed ELF MF, with most power at frequencies between 0 and 500 Hz, human brain electrical activity is affected as measured by electroencephalography (EEG), specifically within the alpha frequency (8–13 Hz). Here, we report that a pulsed ELF MF affects the human EEG during the exposure period. Twenty subjects (10 males; 10 females) received both a magnetic field and a sham session of 15 min in a counterbalanced design. Analysis of variance (ANOVA) revealed that alpha activity was significantly lower over the occipital electrodes (O1, Oz, O2) [$F_{1,16} = 5.376$, $P < .01$, $\eta^2 = 0.418$] after the first 5 min of magnetic field exposure and was found to be related to the order of exposure (MF-sham vs. sham-MF). This decrease in alpha activity was no longer significant in the 1st min post-exposure, compared to sham ($P > .05$). This study is among the first to assess EEG frequency changes during a weak ($\pm 200 \mu T_{pk}$), pulsed ELF MF exposure. *Bioelectromagnetics* 26:367–376, 2005.

© 2005 Wiley-Liss, Inc.

Key words: alpha activity; electromagnetic field; occipital; EEG; ELF

INTRODUCTION

Research examining the electrical activity on the human brain, as measured by electroencephalography (EEG), has found a number of effects within specific frequency bands after brief extremely low frequency magnetic field (ELF MF) exposures [Cook et al., 2002; Hamblin and Wood, 2002; Mann and Roschke, 2004], however, there are still inconsistencies found during replication attempts [Krause et al., 2004]. We have recently found that after exposure to a pulsed MF, the EEG was affected [Cook et al., 2004] in a manner consistent with a number of other publications [Bell et al., 1991, 1994; Lyskov et al., 1993a,b; Huber et al., 2000, 2002; Krause et al., 2000a,b; Lebedeva et al., 2001; Croft et al., 2002; D'Costa et al., 2003]. Specifically, it has been found that alpha activity (8–13 Hz) over occipital-parietal regions tends to be significantly higher after MF exposure compared to sham exposure.

One drawback to the cited studies, including our own, is that the results tend to be post hoc, where an effect is found after a brief MF exposure. One question that remains to be explored is exactly “when” this effect may be occurring. With respect to our most recent study, we found an increase in occipital alpha activity (8–13 Hz) after 15 min of pulsed MF exposure. Unfortunately, due to the extreme interference of the

pulsed MF with the recording of the EEG in that experimental design, we were unable to examine exactly when, or if, this effect occurred during the exposure. The question remains, do weak ($\pm 200 \mu T_{pk}$) pulsed ELF MFs affect the EEG during the exposure? Is it consistent with the response in the post-exposure

The Supplementary Material referred to in this article can be accessed at www.interscience.wiley.com/jpages/0197-8462/suppmat.

Grant sponsor: Canadian Foundation for Innovation (CFI); Grant sponsor: Ontario Research and Development Challenge Fund (ORDCF); Grant sponsor: Plunkett Foundation; Grant sponsor: Ontario Innovation Trust (OIT); Grant sponsor: Lawson Health Research Institute; Grant sponsor: Canadian Institutes of Health Research (CIHR) (to F.S.P.); Grant sponsor: CIHR doctoral research award (C.M.C.).

*Correspondence to: Charles M. Cook, Room H-512, Department of Nuclear Medicine and MR, Lawson Health Research Institute, St. Joseph's Health Care (London), 268 Grosvenor Street, London, Ontario, Canada N6A 4V2. E-mail: ccook@lri.sjhc.london.on.ca

Received for review 17 June 2004; Final revision received 14 January 2005

DOI 10.1002/bem.20113

Published online 10 May 2005 in Wiley InterScience (www.interscience.wiley.com).

period (higher 8–13 Hz activity) or is there a different response during the exposure period? Our current study was designed to answer this question.

METHODS

Subjects

Subjects (ages 20–38; 10 males/10 females) were recruited from staff and students at Lawson Health Research Institute. The research protocol was approved by the University of Western Ontario Review Board for health sciences research involving human subjects.

Procedure

The methodology used in the present study has been extensively described in Cook et al. [2004]. Briefly, subjects were informed that participation in the experiment involved two sessions, one consisting of a 15 min exposure to a pulsed ± 200 μ T MF and the other session consisting of 15 min sham exposure. This was counterbalanced across subjects for order and randomly presented (sham-MF $n = 10$; MF-sham $n = 10$). Using a standard crossover design, experiments were run approximately 1 week apart (7 ± 2 days). Subjects were fitted with the EEG recording apparatus and seated within the exposure device [Thomas et al., 2001a]. Subjects were told that the session would begin recordings with eyes open, followed by eyes closed for the duration of the experiment until instructed to open their eyes (see Table 1). They were instructed to relax, but to not fall asleep. Any subject who did fall asleep was to be excluded from the study. The experiment consisted of 5 min of pre-exposure baseline EEG (2.5 min eyes open and then 2.5 min eyes closed) followed by either 15 min of MF or sham exposure.

Exposure Apparatus

Subjects were seated in the magnetic field exposure system that consists of three orthogonal square Helmholtz-like coils with 2, 1.75, and 1.5 m sides (10 turns of 8 G stranded conductor per coil with an incorporated high temperature, non-conductive cooling/heating tube wound on Lexan[®] frames). Each of the three coil pairs was driven by a constant current amplifier via a digital-to-analog converter [Thomas et al., 2001a]. Only the vertical coil pair was powered

during exposure for this experiment; all other coils were unpowered. With respect to the production of any auditory artifacts, the apparatus showed no acoustic noise production above ambient (< 64 db ambient, 20 Hz–18 kHz) during pulsed magnetic field exposure (± 200 μ T_{pk}). There was minimal possibility of olfactory artifacts due to amplifier heating, as neither the coils or the constant current amplifiers (Model 7780E6; Techtron Div., Crown International, Elkhart) used for the production of the magnetic fields are being driven near to capacity [Thomas et al., 2001a].

Pulsed Magnetic Field Design

The pulsed magnetic field used in the current study (Thomas et al., 1999; US Patent no. 6,234,953) has been utilized in a number of previous studies [Thomas et al., 1997a,b, 1998, 2001b] (Fig. 1). The rationale for the design and utilization of the pulsed magnetic field was extensively discussed in Cook et al. [2004].

Electrophysiological Measures

EEG was recorded from 14 Ag/AgCl electrodes from the occipital (O1, Oz, O2), parietal (P3, Pz, P4), central (CPz, C3, Cz, C4), and frontal regions (FCz, F3, Fz, F4) with a Quik-cap (Neuroscan Labs, Sterling, VA). Reference was to linked ears and also included a forehead ground (AFz). Vertical electrooculogram (EOG) was recorded to control for eye movement artifacts. Data acquisition was provided by a Scan 4.3 Workstation through Grass Model 12 Neurodata Acquisition System (Astro-Med, West Warwick, RI), continuously sampled at 1024 Hz (i.e., 1024 samples per s) and band-pass filtered from 0.1–300 Hz with a 60 Hz notch filter. Data was stored and analyzed offline. Data was further band-pass filtered at 1.5–80 Hz to further remove low and high frequency noise.

In order to facilitate the acquisition of EEG data during the MF exposure, a “gate” or “restore” device was designed to turn off or disconnect the input signal to the EEG amplifier and restore the signal to a zero baseline in response to interference. This device utilized the trace restorer function within the Grass Model 12 amplifiers. Normally, when large transient voltages or signals cause the amplifiers to block, the trace restore button can be depressed which will return the amplifiers to the normal zero volts. When the button is released, the amplifiers continued normal recording.

TABLE 1. Overview of the Procedure

Pre-exposure eyes open baseline	Pre-exposure eyes closed baseline	Magnetic field/sham	EEG sampling period	Post-exposure eyes closed baseline	Post-exposure eyes open baseline
2.5 min	2.5 min	15 min	5 min	2.5 min	2.5 min

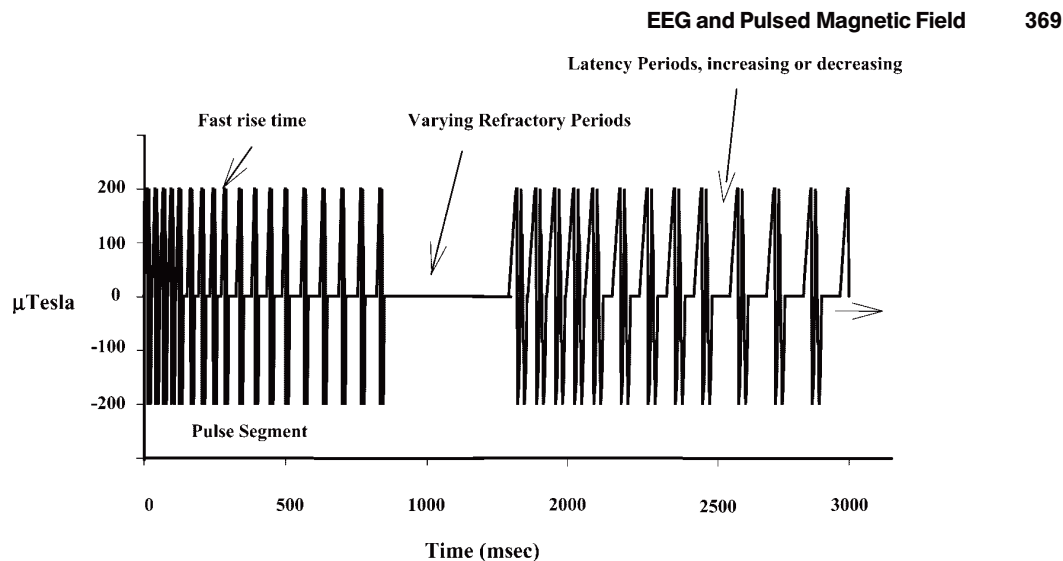


Fig. 1. The pulsed magnetic field design. The design is made of individual pulses, each of which are doublet, combined in an 853 ms segment, which includes 18 pulses. Each pulse has a maximum rise time of 1 ms resulting in a maximum time-changing magnetic field rate of 0.4 T/sec. In between segments are varying refractory periods of 110, 220, 330 ms followed by a longer fourth refractory period of 5000 ms after which (853 ms) begins another pulse segment. During this 5000 ms refractory period, 4.095 s epochs of EEG data were collected. This pattern was repeated for 15 min.

Our “restore” device utilized the external connection for this amplifier function. The Techtron amplifier input pulsed magnetic field waveform was rectified (full wave) and integrated (10–20 ms) to produce a “blanking signal.” This blanking signal (transistor-transistor logic, TTL) was connected to the trace restore input of the EEG amplifier (Grass Model 12), which disconnected the EEG input and zeroed the output. Sensitivity was set for ~25% of the peak input signal, that is, it protected the EEG at anything over 25% of the peak pulsed magnetic field exposure and released it if less (see Supplementary Fig. 1 for a block diagram, which is available at www.interscience.wiley.com/jpages/0197-8462/suppmat). At the end of the pulsed magnetic field waveform, the blanking signal was released and the EEG resumed normal recording. The deadtime has been measured to be less than 50 ms. The selection of the EEG epoch occurred 50 ms after the end of the pulse sequence to ensure no interference in the data (Fig. 2).

The blanking circuit’s primary purpose was to allow the acquisition of EEG data during the entire refractory period between magnetic field pulses. However, it also significantly limited injected current in the electrode cap. The measured voltage from the pulse on the EEG record was roughly 150 μ V with most peaking below 100 μ V. In comparison to Cook et al. [2004], where no blanking circuit was utilized, the Grass amplifier saturated at 250 μ V. If we consider

worst case 1000 μ V induced voltage in Cook et al. [2004], and we assume that the resistance at the scalp is zero and the Grass input impedance is 1 M Ω , then from Ohm’s law we get 1×10^{-9} A (1000 pA) induced current flowing through the subject. With the blanking circuit, this value is reduced by at least a factor of 10 (<100 pA) due to the open input circuit of the Grass amplifier.

Resting EEG Analysis

Pre- and post-exposure. For the periods outside of the MF/sham exposure, 1 min of artifact-free EEG data (lacking obvious muscle/movement artifacts) was sampled from each of the four baseline periods (eyes open/closed, pre-/postexposure), with 1 min sampled from the beginning of the data period immediately post-MF/sham exposure and a 2nd min taken from the end of the 5 min sampling period (see Table 1). The 1 min periods were subjected to ocular artifact rejection (vertical eye movements) and then epoched into 2047 ms periods. After baseline and artifact correction (rejection criteria, ± 100 μ V), the 2047 ms sweeps (consisting of 2048 data points) were averaged in the frequency domain (Fast Fourier Transform; Hanning window; 10%). The EEG was evaluated over the spectrum 4–35 Hz for changes within three EEG frequency bands: θ (4–7 Hz), α (8–13 Hz), and β (14–35 Hz).

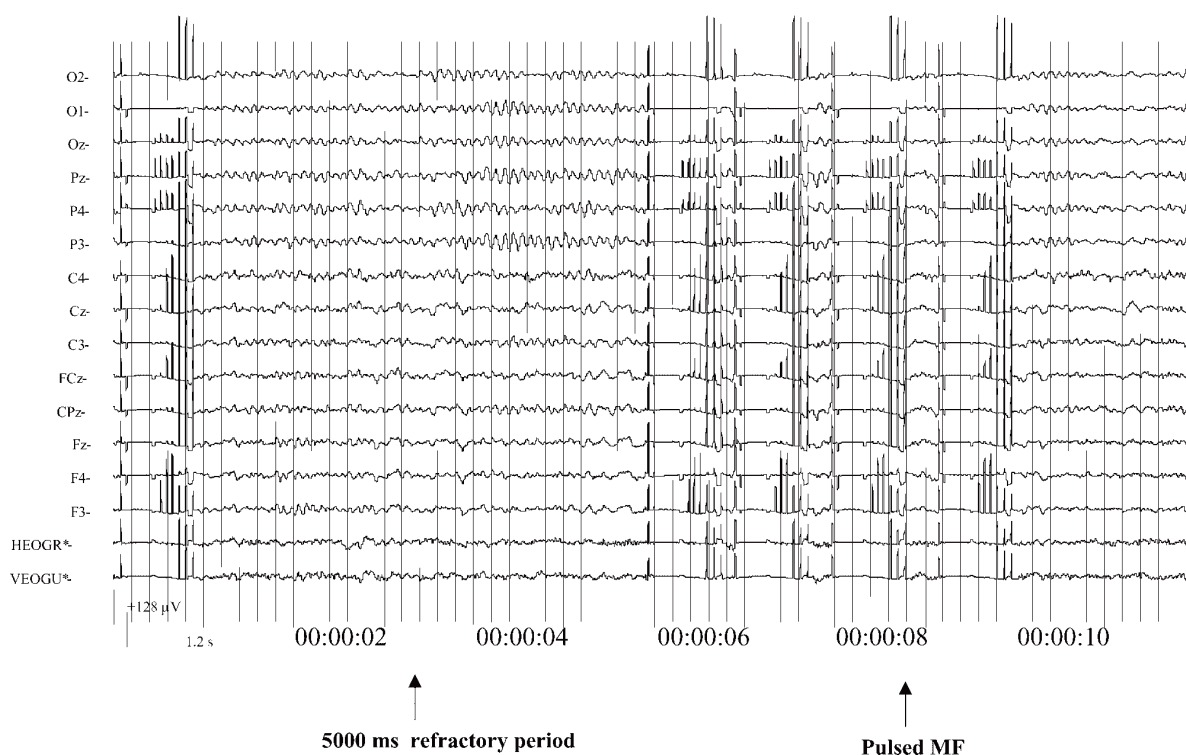


Fig. 2. Example of EEG trace. Input signal is reconnected allowing a restoration of the EEG signal after the zeroed baseline and allowing us to collect a large sweep of EEG data (the 5000 ms refractory period) not contaminated by the pulsed MF.

During MF and sham exposure. For the 15 min MF exposure period, 98 5000 ms blocks of data were sampled. The precise time period associated with each of the 98 MF blocks was time-matched to the corresponding sham session for selection of 98 sham blocks. Therefore, each subject had a grand total of 196 EEG blocks (98 MF; 98 sham). After selection, the 5000 ms blocks were epoched into 4095 ms periods. Those contaminated by obvious signs of muscle/motor artifacts were rejected from the analysis (rejection criteria, $\pm 100 \mu\text{V}$). After baseline correction, the 4095 ms sweeps (consisting of 4096 data points) were subject to Fast Fourier Transform (Hanning window; 10%). The EEG was evaluated over the spectrum 4–35 Hz for changes within three EEG frequency bands: θ (4–7 Hz), α (8–13 Hz), and β (14–35 Hz).

Statistical Analyses

Pre- and post-exposure. Amplitude-frequency values were subjected to statistical analyses using analysis of variance (ANOVA) with a significance level set at 0.05 (SPSS, Statistical Packages for Social Sciences, SPSS version 10, SPSS, Inc., Chicago, IL, USA). Decided a priori, separate ANOVAs (Bonferroni corrected, mixed

design with one level repeated), examining the individual frequency (θ , α , β) at each set of electrodes (O1, Oz, O2; P3, Pz, P4; CPz, C3, Cz, C4; FCz, F3, Fz, F4) from each epoch (eyes closed preexposure; 1 min post-MF and sham exposure; eyes closed post-exposure) by sex (male and female), and by order of presentation (sham-MF or MF-sham). The rationale for statistical analyses has been described previously in Cook et al. [2004]. All figures display means with error bars representing 1 SE of the mean.

During MF and sham exposure. The 15 min exposure period for MF and sham was blocked into approximately 5 min increments, creating a 1st, 2nd, and 3rd exposure period. As with the pre- and post-exposure data, amplitude-frequency values were then subjected to ANOVA (Bonferroni corrected, mixed design with one level repeated) examining the individual frequency (θ , α , β) at each set of electrodes (O1, Oz, O2; P3, Pz, P4; CPz, C3, Cz, C4; FCz, F3, Fz, F4).

Comparisons between pre- and post-exposure and during. Note that there are differences in the number of data points used between in the pre- and post-exposure sweeps (2048 points), and sweeps acquired during the

MF and sham (4096 points). This results in different scaling of the sums within the three EEG frequency bands. If a simple discrete Fourier Transform had been applied, the sweeps acquired “during” the MF and sham would, theoretically, have an amplitude $\sqrt{2}$ greater than the sweeps acquired in the pre- and post-exposure period [Hoch and Stern, 1996]. However, given the additional filtering needed to avoid artifacts in the computed frequency distributions (Hanning window, digital filtering), this scaling factor across all EEG frequency bands is no longer correct. Hence no “post scaling” of the summed frequency bands was performed, and the absolute amplitudes between “pre and postexposure” sweeps and those sweeps acquired “during” the exposure should not be compared.

RESULTS

Pre-exposure

(a) Baseline eyes open period: a significant sex difference was found in the amount of frontal (F3, Fz, F4) beta activity (14–35 Hz) ($F_{1,16} = 7.715$, $P < .05$, partial $\eta^2 = 0.325$) with female subjects displaying higher frontal β during the eyes open period in both sham ($F_{1,19} = 7.823$, $P < .05$) and MF sessions ($F_{1,19} = 4.675$, $P < .05$). (b) Baseline eyes closed period: no significant differences existed in the eyes closed period between MF and sham exposure for any condition, frequency or regions ($P > .05$).

During MF/Sham Exposure

After blocking the 15 min exposure into 1st, 2nd, and 3rd periods (each period equivalent to 5 min), a significant three-way interaction was found between condition (MF/sham) and exposure order, and time period (0–5, 5–10, 10–15 min) for occipital (O1, Oz, O2) theta activity (4–7 Hz) ($F_{2,15} = 4.469$, $P < .05$, partial $\eta^2 = 0.373$). Post hoc t -test indicated that the source of the interaction was in the “sham-MF” exposure order, with the 2nd period (5–10 min) ($t_{19} = 2.915$, $P < .05$), and 3rd period (10–15 min) ($t_{19} = 3.290$, $P < .01$) of the MF condition having significantly higher theta activity than the 1st period of the sham condition (Fig. 3). There were also differences between exposure order for the two 3rd period shams. Subjects exposed to “MF-sham” exposure order displayed higher theta activity during the 3rd period (10–15 min) than subjects in the “sham-MF” order, although, this was marginally significant ($t_{19} = 2.089$, $P = .051$). There was a marginal overall difference between sham exposures (MF-sham and sham-MF) with a tendency for higher overall theta activity in those exposed to MF-sham compared to sham-MF

EEG and Pulsed Magnetic Field 371

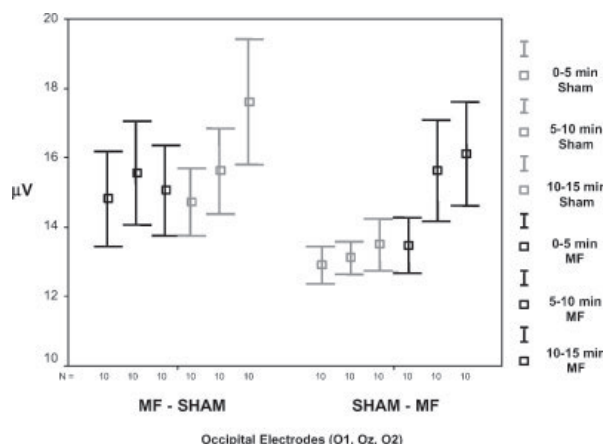


Fig. 3. Theta activity (4–7 Hz) over the occipital electrodes (O1, Oz, O2). Fifteen minute exposure is decomposed into 1st, 2nd, and 3rd periods (each period equivalent to 5 min). A significant three-way interaction was found between condition (MF/sham) and exposure order, and time period (0–5, 5–10, 10–15 min) for occipital (O1, Oz, O2) theta activity (4–7 Hz) ($F_{2,15} = 4.469$, $P < .05$, partial $\eta^2 = 0.373$). Post hoc t -test indicated that the source of the interaction was in the “sham-MF” exposure order with the 2nd period (5–10 min) ($t_{19} = 2.915$, $P < .05$), and 3rd period (10–15 min) ($t_{19} = 3.290$, $P < .01$) of the MF condition having significantly higher theta activity than the 1st period (0–5 min) of the sham condition.

($t_{19} = 1.992$, $P = .06$). Over the frontal electrodes (F3, Fz, F4), there was significantly higher theta activity over the entire 15 min MF exposure compared to sham ($F_{1,16} = 4.813$, $P < .05$, partial $\eta^2 = 0.231$).

A significant three-way interaction between condition (MF/sham), exposure period (0–5, 5–10, 10–15 min), and exposure order (MF-sham/sham-MF) was found for occipital (O1, Oz, O2) alpha activity (8–13 Hz) ($F_{1,16} = 5.376$, $P < .05$, partial $\eta^2 = 0.418$). Post hoc t -test indicated that the subjects in the MF-sham exposure order displayed significantly lower occipital alpha activity during 2nd period (5–10 min) of MF exposure compared to the 1st period (0–5 min) ($t_{19} = 3.813$, $P < .01$) and 3rd period (10–15 min) ($t_{19} = 3.462$, $P < .01$) (Fig. 4). Another significant three-way interaction between condition (MF/sham), exposure period (1st, 2nd, 3rd), and exposure order (MF-sham/sham-MF) was found for alpha activity (8–13 Hz) over the parietal electrodes (P3, Pz, P4) ($F_{1,16} = 4.384$, $P < .05$, partial $\eta^2 = 0.369$). Post hoc t -test again indicated that the subjects in the “MF-sham” exposure order displayed significantly lower occipital alpha activity during 2nd period (5–10 min) of MF exposure compared to the 1st period (0–5 min) ($t_{19} = 3.449$, $P < .01$), and 3rd period (10–15 min) ($t_{19} = 2.989$, $P < .05$) (see Supplementary Fig. 2).

An interaction was also found between sex (male/female) and exposure period (MF-sham/sham-MF) for

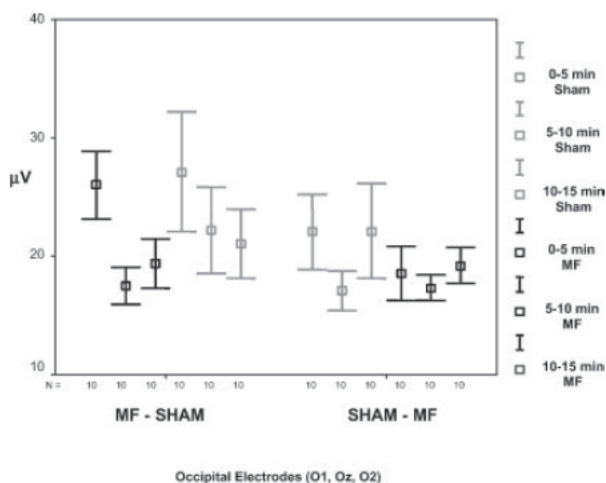


Fig. 4. Alpha activity (8–13 Hz) over the occipital electrodes (O1, Oz, O2). Fifteen minute exposure is decomposed into 1st, 2nd, and 3rd periods (each period equivalent to 5 min). A significant three-way interaction was found between condition (MF/sham), exposure period (0–5, 5–10, 10–15 min), and exposure order (MF-sham/sham-MF) ($F_{1,16} = 5.376$, $P < .05$, partial $\eta^2 = .418$). Post hoc t -test indicated that the subjects in the MF-sham exposure order displayed significantly lower occipital alpha activity during 2nd period (5–10 min) of MF exposure compared to the 1st period (0–5 min) ($t_{19} = 3.813$, $P < .01$), and 3rd period ($t_{19} = 3.462$, $P < .01$).

occipital (O1, Oz, O2) beta activity (14–35 Hz) ($F_{1,16} = 4.925$, $P < .05$, partial $\eta^2 = 0.396$). Post hoc t -test indicated that female subjects displayed significantly lower beta activity during the 2nd exposure period (5–10 min) compared to the 1st period (0–5 min) for both MF ($t_{19} = 3.696$, $P < .01$) and sham exposure ($t_{19} = 3.073$, $P < .05$) (Supplementary Fig. 3). When directly comparing the 2nd period exposure periods, it was found that female subject's beta activity was lower during the 2nd period of MF exposure compared to sham ($t_{19} = 2.622$, $P < .05$).

Post-exposure

“5 min Sampling Period” (1st and 5th min of this period were sampled, see Table 1).

- (a) In the 1st min post-exposure there was a significant main effect of exposure condition for beta activity (14–35 Hz) over the frontal electrodes (F3, Fz, F4) with higher beta activity after the MF compared to sham exposure ($F_{1,16} = 4.633$, $P < .05$, partial $\eta^2 = 0.226$). An interaction was also noted between condition (MF/sham) and exposure order (MF-sham/sham-MF) for beta activity over the frontal region ($F_{1,16} = 5.478$, $P < .05$, partial $\eta^2 = 0.255$). Post hoc t -test indicated that during the “sham-MF” exposure, there was significantly

higher beta activity during the MF exposure compared to sham ($t_{19} = 3.039$, $P < .05$) (Supplementary Fig. 4). A marginally significant main effect of exposure condition was found for theta activity (4–7 Hz) over the frontal region (F3, Fz, F4) ($F_{1,16} = 4.353$, $P = .053$, partial $\eta^2 = 0.214$) with higher theta activity after the MF compared to the sham exposure.

- (b) For the 5th min of the sampling period, there were no significant effects found for any condition, frequency or region.
- (c) In the 2.5 min postexposure baseline period (approximately 7 min post-exposure), there was a significant main effect of exposure condition for theta activity over the frontal electrodes (F3, Fz, F4) with higher theta activity after the MF compared to sham exposure ($F_{1,16} = 4.904$, $P < .05$, partial $\eta^2 = 0.235$).
- (d) When subjects were asked to open their eyes, there were no significant differences between MF and sham sessions for any condition, frequency or region ($P > .05$). (For a summary of results, see Table 2.)

DISCUSSION

We have determined there are a number of significant changes in the frequency content of the EEG that occur during a 15 min pulsed MF exposure. Most significantly, we found that alpha activity (8–13 Hz) over the occipital and parietal region significantly decreases after 5 min of pulsed MF exposure and is dependent on the order of exposure (MF followed by sham exposure) (Fig. 3). This was also noted over the parietal electrodes (P3, Pz, P4) (Supplementary Fig. 2). Further frequency changes were noted within the occipital region, with significantly higher theta activity (4–7 Hz) after 5 min of pulsed MF exposure, which was also dependent on exposure order (sham followed by MF exposure). A significant sex difference was also found for occipital beta activity (14–35 Hz) with female subjects displaying significantly lower beta after 5 min of MF exposure compared to sham (Supplementary Fig. 3). We also found significant overall increase in θ (4–7 Hz) activity over the frontal electrodes (F3, Fz, F4) for the entire 15 min MF period compared to sham exposure.

Current Results in Comparison With Cook et al. [2004]

Although, there were differences in the exposure characteristics between this experiment and our previous study (the longer refractory period), it is of

TABLE 2. Summary of Pulsed MF Results Upon Electroencephalogram

Pre exposure eyes open baseline	Pre exposure eyes closed baseline	Magnetic field/sham	EEG sampling period	Postexposure eyes closed baseline	Postexposure eyes open baseline
2.5 min ↓ in occipital beta activity during both sham/MF in males	2.5 min No significant differences	15 min overall ↑ frontal theta activity during 15 min MF	5 min ↑ in frontal θ 1st min post-MF exposure	2.5 min ↑ in frontal θ ~7 min post-MF exposure	2.5 min No significant differences
		↑ occipital θ during MF (sham-MF exp order) (Fig. 3) ↓ in occipital (Fig. 4) and parietal α (Suppl Fig. 2) after 5 min of MF exposure (MF-sham exp order) ↓ in occipital β after 5 min of MF in female subjects (Suppl Fig. 3)	↓ beta activity 1st min post-MF exposure (Suppl Fig. 4)		

interest to compare the results. We were previously limited to examining the post-exposure period (Table 1) to assess the effects of the pulsed MF, while in the current experiment we were able to track changes in the EEG during the entire exposure period. However, most of the significant changes observed during the pulsed MF exposure were transient. The decrease in occipital alpha activity did not persist during the post-exposure period, when it was no longer significantly different from sham levels. This is somewhat puzzling as the post-exposure period is where the changes in alpha activity were noted in our other experiment, as well as in a large number of previous publications [Bell et al., 1991, 1994; Lyskov et al., 1993a,b; Huber et al., 2000, 2002; Krause et al., 2000a,b; Lebedeva et al., 2001; Croft et al., 2002; D’Costa et al., 2003]. The interaction between exposure order and occipital theta activity was also no longer significant in the 1st min post-exposure. Only the higher amount of frontal theta activity found during the entire 15 min MF exposure persisted into the 1st min of the post-exposure period, but only as a marginally significant result ($P = .053$). Coinciding with the higher frontal theta activity in the 1st min post-MF exposure was a significant increase in frontal beta activity (14–30 Hz) that was also related to exposure order (sham-MF) (Supplementary Fig. 4). There was no evidence of changes in frontal theta and beta activity in Cook et al. [2004].

As we continued to track any changes in EEG frequency over the post-exposure period, all significant differences between MF and sham were no longer evident approximately 4 min after the end of the exposure period. By the post-exposure baseline period, approximately 7 min post-MF, there again was significantly higher frontal theta activity compared to sham. Increasing theta activity over anterior brain regions has been interpreted as a correlate of decreasing arousal, that is, subjective sleepiness [Strijkstra et al., 2003]. Coupled with the high degree of frontal beta activity, this could be interpreted as an effort to maintain wakefulness [Strijkstra et al., 2003]. However, no subjects were excluded for falling asleep in the current study, as there was no behavioral evidence of sleep (video monitors indicated all subjects remained seated in an upright position) and all were immediately responsive to verbal requests made by the experimenter. Subjects were also queried at the cessation of the experiment, whether they had fallen asleep at any time. All subjects reported feeling drowsy but indicated they had not fallen asleep, a similar observation from our previous experiment.

We also observed a pre-exposure difference during the “eyes open” baseline recording period (Table 2) with

female subjects displaying significantly greater frontal beta activity (14–35 Hz). It would appear that this difference was maintained during the exposure period, as only female subjects displayed a significant decrease in beta activity during the first 5 min of MF exposure with no changes noted in male subjects. No significant differences during the “eyes open” baseline period at the end of the experiment were evident, nor were any differences found in our previous study. Overall, it would appear that our present results examining the effects of pulsed MFs upon the EEG do not coincide with any of our previous findings [Cook et al., 2004].

Significant Changes During Pulsed Magnetic Field Exposure

The most significant observation in the current experiment was the effect on the occipital alpha activity, occurring after the first 5 min of pulsed MF exposure. This again highlights the significance of this frequency band in studies of MF exposure [Bell et al., 1991, 1994; Lyskov et al., 1993a,b; Huber et al., 2000, 2002; Lebedeva et al., 2001; Croft et al., 2002; D’Costa et al., 2003; Cook et al., 2004]. What separates this observation from previous studies is that we observed the change during the presentation of the pulsed MF. This also corresponds to the behavioral results of Thomas et al. [2001b], where an effect was noted upon human standing balance (with eyes closed) within 5 min of pulsed MF exposure.

To further examine this result, the three 5-min periods were then roughly decomposed into individual 1 min increments to track any changes within the three periods. It is quite evident that the changes occur within the first 5 min of MF exposure period and significantly decreases over the next several minutes compared to a sham exposure (Supplementary Fig. 5).

In Cook et al. [2004], we noted that occipital alpha activity tended to decrease from the pre-exposure eyes closed baseline to 1st min post-exposure (Table 1). When similar time points were compared, 1 min after both sham and MF, we found that the alpha activity was higher post-MF compared to sham, differing in the “magnitude” of the decrease. Our current results also indicated that occipital and parietal alpha activity decreases from the pre-exposure eyes closed baseline to 1st min post-exposure. Most importantly, we have found that it decreases significantly based upon MF exposure and the order of presentation (Fig. 4). When occipital alpha is assessed in the 1st min post-exposure, no differences are seen between MF and sham, in contrast to our previous results [Cook et al., 2004].

An interesting aspect of the current results was the number of effects associated with the order of exposure. Both occipital theta and alpha activity were found to be

dependent upon the order of exposure to the pulsed MF or the sham. For occipital theta activity, subjects assigned to receive a sham exposure in their first session, followed by pulsed MF in their second session, displayed significantly lower variability than subjects who received the MF during their first session, followed by sham (Fig. 3). Frontal beta activity in the 1st min post-exposure was also found to be higher post-MF, but only if the subjects were first assigned to receive sham and received the MF during their second session (Supplementary Fig. 4). As noted earlier, subjects displayed decreases in occipital alpha activity, but only when assigned to receive the pulsed MF exposure in their first session (Fig. 4).

These observations would suggest an effect upon the brain’s network for “novelty” or “familiarity” assessment. The brain’s response to a novel situation is relatively specific, with reductions in regional cerebral blood flow occurring in response to repeat situations [Habib, 2002]. It has been known for a long time that organisms react differently to new and unexpected stimuli than to otherwise identical but old and expected ones. Research examining these responses has been classified under “orienting response,” habituation, and novelty detection. Generally, most research on novelty is based upon recognition memory, whereby sets of stimuli, for example, visual stimuli, pictures, are presented to a subject over repeat sessions. The response observed in our study is somewhat more complex. We are studying the dynamics of the brain in response to a pulsed MF, one that is not “consciously” perceived on the part of the subject. The brain’s assessment of “novelty” in our experiment is the procedure itself. The appearance of any overt or defined experimental condition is absent from this study, with both sessions appearing to be identical to the subject. If repeated exposure to a consciously perceived stimuli is associated with decreases in blood flow within specific regions [Habib, 2002], one conclusion that could be drawn is that we are demonstrating a significant “priming” effect in the resting EEG that is dependent on the order of exposure to the MF.

The relationship between novelty, orienting responses, and priming is subtle, but is probably best conceived as the response of an organism to old versus new stimuli and is thought to be part of the implicit memory system [Thayer and Friedman, 2002; Henson, 2003]. Habituation is the result of repeated exposure to a stimulus without meaningful consequences. It has been proposed that this results in a decreased neural response due to a reallocation of attentional resources; as the novelty decreases, the attention processing will also decrease [Simpson et al., 2001a,b; Feinstein et al., 2002]. It would appear that the effect of the MF on

occipital alpha activity is also conditionally related to the state of the individual at a specific point in time. This “rest state” of the brain (resting awake with eyes closed) has been extensively studied using fMRI and PET [Raichle et al., 2001]. One current idea regarding the functional significance of this brain network is that it relates to memory processing and orientation to the external environment [Gusnard and Raichle, 2001]. Subsequent exposures to a specific contextual event, that is, the experimental situation, may ultimately lead to blood flow reductions within these brain regions and hence, interact with our MF effects upon the EEG.

If this is the case, it would appear that the exposure order is a significant variable to consider in future studies as the “initial conditions” would appear to be very sensitive to the subsequent measurements. This observation has been taken for granted in a number of studies examining psychological variables, such as episodic memory, pain perception etc., but has not been, prior to our study, noted in experiments examining magnetic field effects on human cognition/perception or electrophysiology. This may be an important factor leading to discrepant results between human experiments in bioelectromagnetics.

One question the current experiment raises is why the modification of the pulsed magnetic field design garnered significantly different results from Cook et al. [2004]? As noted earlier, we modified the original design by extending the refractory period from 1200 to 5000 ms to allow the collection of larger EEG sweeps. We hypothesized that this extension would be marginal in terms of effect. This hypothesis now appears incorrect, as the effect upon occipital alpha activity noted in Cook et al. [2004] did not replicate despite the nearly identical experimental design. By increasing the refractory period to 5000 ms, we decreased the true exposure period. In Cook et al. [2004], the pulse sequence contained 170 periods of 1200 ms each, while the current experimental sequence contained 98 periods of 5000 ms each.

If we consider the evoked potential literature, changing the refractory period of the stimulus can markedly change the amplitudes of the evoked potentials [Raij et al., 2003]. The refractory period concept from evoked potential research derives from studies of single nerve cells where there is a recovery cycle or refractory period following an action potential, during which time, further stimulation will not result in an action potential [Budd et al., 1998]. How exactly this observation may relate to the current results is a matter of speculation, as we were not able to measure the EEG during the pulsed MF in our previous study [Cook et al., 2004]. Experiments are now needed to assess whether the effects upon the EEG, noted here after 5 min of pulsed MF exposure

(5000 ms refractory), are evident for the original pulsed MF sequence (1200 ms refractory) where we have noted our previous behavioural and EEG results.

CONCLUSION

Occipital alpha activity (8–13 Hz) was found to decrease during exposure to a pulsed ELF MF compared to a sham exposure. This effect was found after the first 5 min of a 15 min pulsed ELF MF exposure and was dependent on the MF/sham order of exposure. To our knowledge this study is among the first to track human EEG frequency changes during exposure to a pulsed magnetic field. Discrepancies between our current findings and the results of our previous experiment [Cook et al., 2004] suggest the EEG changes may be sensitive to the characteristics of the magnetic field pulse train.

ACKNOWLEDGMENTS

Special thanks to J. Davis for technical and computer assistance.

REFERENCES

- Bell GB, Marino AA, Chesson AL. 1991. Alterations in brain electrical activity caused by magnetic fields: Detecting the detection process. *Electroencephalogr Clin Neurophysiol* 83: 389–397.
- Bell GB, Marino AA, Chesson AL. 1994. Frequency-specific responses in the human brain caused by electromagnetic fields. *J Neurol Sci* 123:26–32.
- Budd TW, Barry RJ, Gordon E, Rennie C, Michie PT. 1998. Decrement of the N1 auditory event-related potential with stimulus repetition: Habituation vs. refractoriness. *Int J Psychophysiol* 31:51–68.
- Cook CM, Thomas AW, Prato FS. 2002. Human electrophysiological and cognitive effects of exposure to ELF magnetic and ELF modulated RF and microwave fields: A review of recent studies. *Bioelectromagnetics* 23:144–157.
- Cook CM, Thomas AW, Prato FS. 2004. Resting EEG is affected by exposure to a pulsed ELF magnetic field. *Bioelectromagnetics* 25:196–203.
- Croft RJ, Chandler JS, Burgess AP, Barry RJ, Williams JD, Clarke AR. 2002. Acute mobile phone operation affects neural function in humans. *Clin Neurophysiol* 113:1623–1632.
- D’Costa H, Trueman G, Tang L, Abdel-rahman U, Abdel-rahman W, Ong K, Cosic I. 2003. Human brain wave activity during exposure to radiofrequency field emissions from mobile phones. *Australas Phys Eng Sci Med* 26:162–167.
- Feinstein JS, Goldin PR, Stein MB, Brown GG, Paulus MP. 2002. Habituation of attentional networks during emotion processing. *Neuroreport* 13:1255–1258.
- Gusnard DA, Raichle ME. 2001. Searching for a baseline: Functional imaging and the resting human brain. *Nat Rev Neurosci* 2:2685–2694.
- Habib R. 2002. On the relation between conceptual priming, neural priming, and novelty assessment. *Scand J Psychol* 242:187–195.

- Hamblin DL, Wood AW. 2002. Effects of mobile phone emissions on human brain activity and sleep variables. *Int J Radiat Biol* 78:659–669.
- Henson RN. 2003. Neuroimaging studies of priming. *Prog Neurobiol* 70:53–81.
- Hoch JC, Stern A. 1996. NMR data processing. Cambridge, Massachusetts: Wiley-Liss.
- Huber R, Graf T, Cote KA, Wittmann L, Gallmann E, Matter D, Schuderer J, Kuster N, Borbely AA, Achermann P. 2000. Exposure to pulsed high-frequency electromagnetic field during waking affects human sleep EEG. *Neuroreport* 11: 3321–3325.
- Huber R, Treyer V, Borbely AA, Schuderer J, Gottselig JM, Landolt HP, Werth E, Berthold T, Kuster N, Buck A, Achermann P. 2002. Electromagnetic fields, such as those from mobile phones, alter regional cerebral blood flow and sleep and waking EEG. *J Sleep Res* 11:289–295.
- Krause CM, Sillanmaki L, Koivisto M, Haggqvist A, Saarela C, Revonsuo A, Laine M, Hamalainen H. 2000a. Effects of electromagnetic fields emitted by cellular phones on the electroencephalogram during a visual working memory task. *Int J Radiat Biol* 76:1659–1667.
- Krause CM, Sillanmaki L, Koivisto M, Haggqvist A, Saarela C, Revonsuo A, Laine M, Hamalainen H. 2000b. Effects of electromagnetic field emitted by cellular phones on the EEG during an auditory memory task. *Neuroreport* 11:761–764.
- Krause CM, Haarala C, Sillanmaki L, Koivisto M, Alanko K, Revonsuo A, Laine M, Hamalainen H. 2004. Effects of electromagnetic field emitted by cellular phones on the EEG during an auditory memory task: A double blind replication study. *Bioelectromagnetics* 25:33–40.
- Lebedeva NN, Sulimov AV, Sulimova OP, Kotrovskaya TI, Gailus T. 2001. Cellular phone electromagnetic field effects on bioelectric activity of human brain. *Crit Rev Biomed Eng* 29: 125–133.
- Lyskov E, Juutilainen J, Jousmaki V, Hanninen O, Medvedev S, Partanen J. 1993a. Influence of short-term exposure of magnetic field on the bioelectrical processes of the brain and performance. *Int J Psychophysiol* 14:227–231.
- Lyskov EB, Juutilainen J, Jousmaki V, Partanen J, Medvedev S, Hanninen O. 1993b. Effects of 45-Hz magnetic fields on the functional state of the human brain. *Bioelectromagnetics* 14: 87–95.
- Mann K, Roschke J. 2004. Sleep under exposure to high-frequency electromagnetic fields. *Sleep Med Rev* 8:95–107.
- Raichle ME, MacLeod AM, Snyder AZ, Powers WJ, Gusnard DA, Shulman GL. 2001. A default mode of brain function. *Proc Natl Acad Sci USA* 98:676–682.
- Raij TT, Vartiainen NV, Jousmaki V, Hari R. 2003. Effects of interstimulus interval on cortical responses to painful laser stimulation. *J Clin Neurophysiol* 20:73–79.
- Simpson JR, Snyder AZ, Gusnard DA, Raichle ME. 2001a. Emotion-induced changes in human medial prefrontal cortex: I. During cognitive task performance. *Proc Natl Acad Sci USA* 98:683–687.
- Simpson JR, Drevets WC, Snyder AZ, Gusnard DA, Raichle ME. 2001b. Emotion-induced changes in human medial prefrontal cortex: II. During anticipatory anxiety. *Proc Natl Acad Sci USA* 98:688–693.
- Strijkstra AM, Beersma DG, Drayer B, Halbesma N, Daan S. 2003. Subjective sleepiness correlates negatively with global alpha (8–12 Hz) and positively with central frontal theta (4–8 Hz) frequencies in the human resting awake electroencephalogram. *Neurosci Lett* 340:17–20.
- Thayer JF, Friedman BH. 2002. Stop that! Inhibition, sensitization, and their neurovisceral concomitants. *Scand J Psychol* 43: 123–130.
- Thomas AW, Kavaliers M, Prato FS, Ossenkopp KP. 1997a. Antinociceptive effects of a pulsed magnetic field in the land snail, *Cepaea nemoralis*. *Neurosci Lett* 222:107–110.
- Thomas AW, Kavaliers M, Prato FS, Ossenkopp KP. 1997b. Pulsed magnetic field induced “analgesia” in the land snail, *Cepaea nemoralis*, and the effects of mu, delta, and kappa opioid receptor agonists/antagonists. *Peptides* 18:703–709.
- Thomas AW, Kavaliers M, Prato FS, Ossenkopp KP. 1998. Analgesic effects of a specific pulsed magnetic field in the land snail, *Cepaea nemoralis*: Consequences of repeated exposures, relations to tolerance and cross-tolerance with DPDPE. *Peptides* 19:333–342.
- Thomas AW, Prato FS, Kavaliers M, Persinger MA. 1999. Low Frequency magnetic field designed pulses for therapeutic use. U.S. Patent #6,234,953 and International PCT/CA97/00388 1996,1997,1998,1999.
- Thomas AW, Drost DJ, Prato FS. 2001a. Magnetic field exposure and behavioral monitoring system. *Bioelectromagnetics* 22: 401–407.
- Thomas AW, Drost DJ, Prato FS. 2001b. Human subjects exposed to a specific pulsed (200 microT) magnetic field: Effects on normal standing balance. *Neurosci Lett* 297:121–124.

EXHIBIT 12

Intern. J. Neuroscience, 117:1341–1360, 2007
Copyright © 2007 Informa Healthcare
ISSN: 0020-7454 / 1543-5245 online
DOI: 10.1080/00207450600936882

informa
healthcare

ELECTROENCEPHALOGRAPHIC, PERSONALITY, AND EXECUTIVE FUNCTION MEASURES ASSOCIATED WITH FREQUENT MOBILE PHONE USE

MARTIJN ARNS

Brain Resource International Database
Brain Resource Company B.V.
Nijmegen, The Netherlands

GILLES VAN LUIJTELAAR

NICI, Radboud University Nijmegen
Department of Biological Psychology
Nijmegen, The Netherlands

ALEX SUMICH

REBECCA HAMILTON

EVIAN GORDON

Brain Resource International Database
Brain Resource Company
Sydney, Australia

Received 1 June 2006.

This study was kindly funded by the BIAL foundation (grant # 81/02). Data from The Brain Resource International Database was generously provided by the Brain Resource Company Pty Ltd. The authors also thank local BRC clinics for data collection, Tim Leslie at BRC Sydney for developing a robust method for scoring all Alpha Peak Frequency data and Nick Cooper for the second peak alpha analysis of the data.

All scientific decisions are made independent of Brain Resource Companies's commercial decisions via the independently operated scientific division, BRAINnet (www.brainnet.org.au), which is overseen by the independently funded Brain Dynamics Centre and scientist members.

Address correspondence to Drs. M.W. Arns, Brain Resource Company B.V./Brainquiry B.V., Toernooiveld 100, 6525 EC Nijmegen, The Netherlands. E-mail: marns@qeeq.nl

The present study employs standardized data acquired from the Brain Resource International Database to study the relationship between mobile phone usage, personality, and brain function ($n = 300$). Based on the frequency and duration of mobile phone usage, three groups were formed. The findings suggest a subtle slowing of brain activity related to mobile phone use that is not explained by differences in personality. These changes are still within normal physiological ranges. Better executive function in mobile phone users may reflect more focused attention, possibly associated with a *cognitive training* effect (i.e., frequently making phone calls in distracting places), rather than a direct effect of mobile phone use on cognition.

Keywords cognition, EEG slowing, GSM, mobile phone, neuropsychology, personality

INTRODUCTION

Industry sources suggested that there will be over one billion mobile phone (MP) users worldwide by 2005 (Repacholi, 2001). Reviews of the effects on general health, including carcinogenic potency, of the 900–1800 MHz electromagnetic fields (EMF) emitted by MPs find no significant adverse affects (the Dutch Health Council, 2002; Independent Expert Group on Mobile Phones [IEGMP], 2000). Three primary theories of the potential effects of EMF on biological tissue are (1) the activation of endogenous opioids; (2) the induction of electrical fields in the brain; and (3) thermal radiation (Banik et al., 2003). To date little experimental evidence is available to support the former two theories (Repacholi, 2001). However, studies suggest EMF produced by MP may cause a change in temperature of biological tissue (van Leeuwen et al., 1999). The radiation produced by MP changes the skin's temperature by .25 degrees and the brain's temperature by .12 degrees Celsius. However, this is suggested to have no real effects on health (van Leeuwen et al., 1999; Bernardi et al., 2000; Wainwright, 2000; Wang & Fujiwara, 1999). Nevertheless, given that phones are often used in close proximity to the head, it is important to investigate whether long-term and/or frequent MP use have any specific effects on brain function through heat radiation or otherwise.

The direct effects of MP-use *during* use (i.e., acute effects) on brain function have been investigated using neuropsychological and neurophysiological techniques. Evidence suggests an association between acute MP use and enhanced scores on cognitive tests. For example, exposure to a field that simulates MP use decreases reaction times (Preece et al., 1999; Koivisto et al., 2000) and enhances performance in attention tasks without an increase in the

number of errors made (Lee et al., 2001; 2003; Koivisto et al., 2000). These results have been mostly interpreted as being due to small increases in brain temperature that lead to increased metabolic activity and thus faster reaction times. Thus, EMF may also have potentially beneficial effects on brain function that could be developed as treatment for functional brain disorders.

Electroencephalographic (EEG) studies show an increase in alpha EEG power, mainly in the parietal and occipital areas during exposure to a MP-“like” field; during wakefulness (Croft et al., 2002; Schulze et al. 1996; Mann & Röschke, 1996; Krause et al., 2000) and sleep (Lebedeva et al., 2001; Borbély et al., 1999; Huber et al., 2000; 2002a; 2002b). Furthermore, increases in theta power (Lebedeva et al., 2001) and modulation of high frequency induced brain activity (Eulitz et al., 1998) have been reported during MP exposure. In contrast, other studies find no significant effects of MP exposure on spectral measures of the wake and sleep EEG (Röschke & Mann, 1997; Wagner et al., 2000; Eulitz et al., 1998). In more controlled studies, Krause et al. (2004) and Haarala et al. (2003) failed to replicate previous findings. Thus, if present, the acute effects of MP-use on EEG, memory or reaction time may be small, variable and not easily replicable. Thus, results of the acute effects of an MP-“like” field on brain function are inconclusive and reasons for the aforementioned inconsistencies are unclear.

The relationship between the cumulative long-term and/or frequent use of MP use on brain function and information processing has not been reported. Such a study would require an expensive, complex longitudinal study. Given current inconsistencies in the aforementioned studies of acute effects, it is unclear whether such expense would be warranted. Therefore, the current epidemiological study was designed to gather pilot data and explore the association between long-term and/or frequent MP-use, brain function, and personality. Thus, the Brain Resource International Database (also see www.brainnet.org.au) was used to investigate personality, neuropsychological performance, and brain function as a function of self-reported mobile phone use in a large group of healthy subjects. In addition, the current study aimed to identify appropriate measures of brain function and/or possible confounding variables associated with long-term regular MP use that could be incorporated into a future study.

MATERIALS AND METHODS

Subjects

Three hundred right-handed healthy individuals were used in this study (see Table 1 for subject characteristics). Database exclusion criteria included

Table 1. Group characteristics

	“Naïve MP user group”	“Intermediate MP user group”	“Heavy MP user group”	<i>p</i> -value
Gender				0.756
F	51	52	47	
M	49	48	53	
Age (years)				0.170
Mean	31.67	29.70	28.47	
SD	11.79	13.00	11.45	
Education (years)				0.269
Mean	13.66	13.02	12.78	
SD	3.64	3.93	4.29	
RUI***				0.000
Mean	—	2.08	13.74	
SD	—	1.002	13.107	

a personal or family history of mental illness, brain injury, neurological disorder, serious medical condition, drug/alcohol addiction; and a family history of genetic disorder. Six laboratories (New York, Rhode Island, Nijmegen, London, Adelaide, and Sydney) participated using standardized data acquisition techniques (identical amplifiers, standardization of other hardware, paradigm details, software acquisition, and task instructions). Interlab reliability measures were high and are reported elsewhere. All subjects voluntarily gave written informed consent, and local medical ethical approval was obtained for all clinics. Subjects were required to refrain from caffeine, alcohol, and smoking for at least 2 h prior to testing.

Grouping of Participants According to Mobile Phone Use

Table 2 shows the self-report questionnaire used to quantify the extent of mobile phone use by participants. This questionnaire was developed as part of the Brain Resource International Database. Currently reliability and validity data for this questionnaire are not available. A measure of Recent Usage Intensity (RUI) was computed based on number of phone calls per day (question 1) × duration of phone calls (question 2) × total time of mobile phone use (question 3). Three MP user groups of equal size (*n* = 100) were formed based on the RUI. The top-100 users were identified *Heavy-users*. A *Naïve user* group consisted of 100 subjects who answered Q0 with “no” (did not use mobile phone). An *Intermediate-user* group consisted of 100 subjects randomly

Table 2. Self-report questionnaire used to quantify the extent of mobile phone use by subjects

Question	Answer
Q0: Do you use a mobile phone?	Yes/no
Q1. How often do you use a mobile phone (to make or receive a call)?	(5) Many times a day (4) A few times a day (3) Once a day (2) Once every few days (1) Once a week or less
Q2. What would be the duration, on average, of each call?	(1) Less than 5 minutes (2) 5–10 minutes (3) 10–15 minutes (4) 15–20 minutes (5) greater than 20 minutes
Q3. How much time, on average, would you spend on the mobile phone each day?	(1) Less than 10 minutes (2) 10–30 minutes (3) 30–60 minutes (4) 60–90 minutes (5) greater than 90 minutes
Q4. How many years have you been using a mobile phone?	(5) Less than 1 year (4) 1–2 years (3) 2–3 years (2) 3–5 years (1) Greater than 5 years

Scores for the individual answers are between brackets.

selected from the remaining subjects who answered Q0 with “yes.” Table 1 shows the demographic characteristics of the subjects included in the study.

Subjects were seated in a sound and light attenuated room, controlled at an ambient temperature of 22°C. Personality, electroencephalographic, and neuropsychology assessments were completed in order.

Personality

NEO–FFI (Five Factor Inventory) (Costa & McCrae, 1992) was used to measure five personality traits including conscientiousness, agreeableness, neuroticism, extraversion, and openness.

Electroencephalographic Data Acquisition

Participants were seated in a sound and light attenuated room, controlled at an ambient temperature of 22°C. EEG data were acquired from 28 channels: Fp1, Fp2, F7, F3, Fz, F4, F8, FC3, FCz, FC4, T3, C3, Cz, C4, T4, CP3, CPz,

CP4, T5, P3, Pz, P4, T6, O1, Oz, and O2 (Quikcap; NuAmps; 10–20 electrode international system). Data were referenced to linked mastoids with a ground at AFz. Horizontal eye-movements were recorded with electrodes placed 1.5 cm lateral to the outer canthus of each eye. Vertical eye movements were recorded with electrodes placed 3 mm above the middle of the left eyebrow and 1.5 cm below the middle of the left bottom eye-lid. Skin resistance was $< 5 \text{ K Ohms}$ and above 1 K Ohm for all electrodes. A continuous acquisition system was employed and EEG data were EOG corrected offline (Gratton et al., 1983). The sampling rate of all channels was 500 Hz. A low pass filter with attenuation of 40 dB per decade above 100 Hz was employed prior to digitization.

The EEG data were recorded for 2 min during each of two conditions: eyes open (EO) and eyes closed (EC). Subjects were asked to sit quietly. During EO subject were asked to fix their eyes on a red dot presented on a computer screen.

Electroencephalographic Variables

Average power spectra were computed for each condition (EO, EC). Each two minute epoch was divided into adjacent intervals of four seconds. Power spectral analysis was performed on each four- second interval by first applying a Welch window to the data, and then performing a Fast Fourier Transform (FFT).

The power was calculated in the four frequency bands for both conditions, delta (1.5–3.5 Hz), theta (4–7.5 Hz), alpha (8–13 Hz), and beta (14.5–30 Hz). These power data were then square-root transformed in order to fulfill the normal distributional assumptions required for parametric statistical analysis.

Electrode Sites

Given that right (T4, T6) and left temporal (T3, T5) areas are in close proximity to the ears and therefore more susceptible to the effects of MP use, EEG measures were taken from these areas. However, midline areas (FCz, Cz, CPz, Pz) were also examined as a measure of overall brain function. Data from other sites were not examined in the current study.

Alpha peak frequency data were scored using a robust algorithm and manually checked by an independent scorer.

Neuropsychology

Neuropsychological assessment was completed using a touch screen monitor. Measures included: Visual working memory, Digit Span (forward and reverse),

Table 3. Neuropsychological tests assessed and the according variables

Task	Measure
Visual span of attention	Number correct
Digit span	Number correct
Reverse digit span	Number correct
Word interference	Number correct for word condition; number correct for color condition, <i>word interference score</i> (number correct for word condition—number correct for color condition)
Switching of attention test (A and B)	Number completed, number of errors

Word Interference test (equivalent to the Stroop test), and Switching of Attention test part A and B (equivalent to the WAIS Trails A and B) (see Gordon, 2003 and Gordon et al., 2005 for details of these tests). All tests were fully computerized and subjects’ responses were recorded via touch-screen presses. Reliability and validity data on these tasks are reported elsewhere (Gordon et al., 2005; Clark et al., 2006; Williams et al., 2005; Paul et al., 2005). Variables measured by each test are displayed in Table 3.

STATISTICAL ANALYSIS

Missing Values

If missing values were present for a given statistical test, those cases were excluded for that analysis. The number of missing values per group are included in the Results sections.

Analysis

All statistics were performed using SPSS 11.5.1 for Windows. Differences between RUI groups in age, education, and personality scores were tested using one-way Analyses of Variance (ANOVA). Bonferroni tests were used for post-hoc analysis. Differences between groups in categorical variables (Sex and RUI) were tested using Kruskal-Wallis nonparametric test.

Multivariate Analysis of Variance (MANOVA, Pillai’s Trace) were used to test for group differences in scores on neuropsychology tests with RUI as a between groups variable and neuropsychology tests as a within subjects variable. Bonferroni tests were used in post-hoc analysis. Univariate ANOVAs were then used to test for differences between RUI groups on individual tests.

Any significant differences in personality profile were taken into account by including these measures as covariates in these MANOVAs and ANOVAs

EEG Data

MANOVA (using Pillai’s Trace) was used to test group differences in power with the within groups variables *Task* (EO/ EC), *Electrode Location* (Left Temporal, Central, and Right Temporal) and *Frequency Band* (delta, theta, alpha, and beta) and between groups variable *RUI Group* (Naïve, Intermediate, and Heavy user group). Significant interactions were further explored using within-group MANOVAs, and via simple contrasts for the between subject factor. Alpha peak frequency was analyzed in the same way, replacing EEG frequency with alpha peak frequency. As with neuropsychology analyses, any significant differences in personality profile were taken into account by including these measures as covariates.

RESULTS

Table 1 shows means, *SDs*, and *p* values of sex, age, education, and RUI naïve, intermediate, and heavy users. There were no differences between the three groups with respect to age, sex, and education. However, there were differences between the groups for mobile phone use (RUI), indicating that the groups differed only in mobile phone use and not on other variables such as age, sex, and years of education.

Personality

Table 4 displays the personality characteristics of the three groups. There was one missing value (.33%) due to incomplete data acquisition of the NEO FFI. There was a significant main effect of *MP group* for Extraversion ($F = 4.407$; $df = 2, 296$ $p = .013$) and Openness ($F = 3.520$; $df = 2, 296$; $p = .031$). Pair wise contrasts revealed that the Heavy User Group scored higher on Extraversion as compared to the Naïve User Group ($p = .010$). No significant differences were seen in contrasts for openness. Therefore, Extraversion and Openness where used as covariates in further analyses as described in the following sections.

Neuropsychology

Significant findings for neuropsychology variables are presented in Figure 1. A significant difference was seen for *RUI group* in overall neuropsychological

Table 4. NEO FFI results for the three groups (Costa & McCrae, 1992)

	“Naïve user group”	“Intermediate user group”	“Heavy user group”	<i>p</i> -value
<i>n</i> =	100	99	100	
Neuroticism				0.906
Mean	18.90	18.54	18.89	
SD	6.30	6.70	6.79	
Extraversion*				0.013
Mean	29.04	30.44	31.35	
SD	4.90	5.77	5.91	
Openness*				0.031
Mean	31.60	31.44	29.56	
SD	6.56	6.15	5.38	
Agreeableness				0.650
Mean	31.69	31.83	30.69	
SD	6.22	5.83	5.66	
Conscientiousness				0.552
Mean	30.59	31.70	31.14	
SD	7.28	7.44	6.26	

performance ($F = 1.763$; $df = 18, 574$; $p = .026$). Univariate ANOVA’s revealed that there was a significant effect on the Word Interference Score ($F = 3.654$, $df = 2, 294$, $p = .027$) with the heavy user group showing the highest interference score, (i.e., least interference). However, post-hoc tests

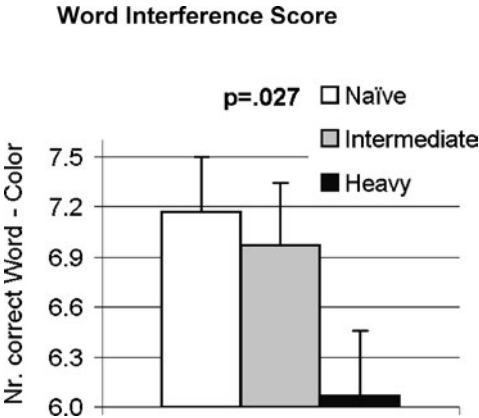


Figure 1. Difference on the Word Interference Score between the three MP user groups. Heavy mobile phone users show less interference than the other two groups (error bars are S.E.M.).

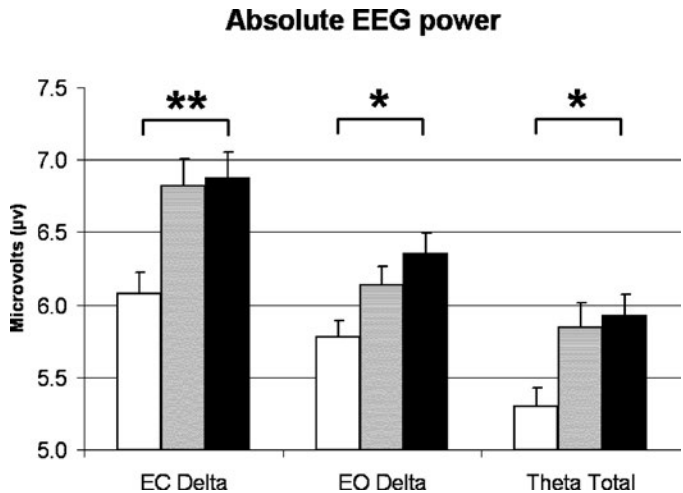


Figure 2. Findings for the EEG data across the groups. Note that all observed differences show dose-response like profiles (* $p < .05$; ** $p < .010$; *** $p = .001$). EC and EO stand for eyes-closed and eyes-open condition).

failed to reach significance. No significant differences were found between the user groups on any other neuropsychology measures.

EEG

Figure 2 shows the significant findings for Delta power (during Eyes Closed and Eyes Open) and Theta Power (average for Eyes open and Eyes Closed). Figure 3 shows mean alpha peak frequency for EO and EC at left temporal, central, and right temporal sites. Figure 4 shows the significant findings for mean alpha peak frequency for EO (average of combined sites).

Multivariate analysis revealed a significant effect of condition (EO/EC) ($F = 3.877$; $df = 1, 293$; $p = .050$), electrode location ($F = 9.798$; $df = 2, 292$; $p < .000$), and EEG frequency ($F = 3.571$; $df = 3, 291$; $p = .014$). There was no significant main effect for RUI. The Location X Extraversion interaction was significant ($F = 3.521$; $df = 2, 292$; $p = .031$). Significant first-order interactions were found between Condition and EEG frequency band ($F = 2.843$; $df = 3, 291$; $p = .038$) and between EEG frequency and RUI group ($F = 2.252$; $df = 6, 584$; $p = .037$). RUI group effects for the separate frequency bands are reported in what follows.

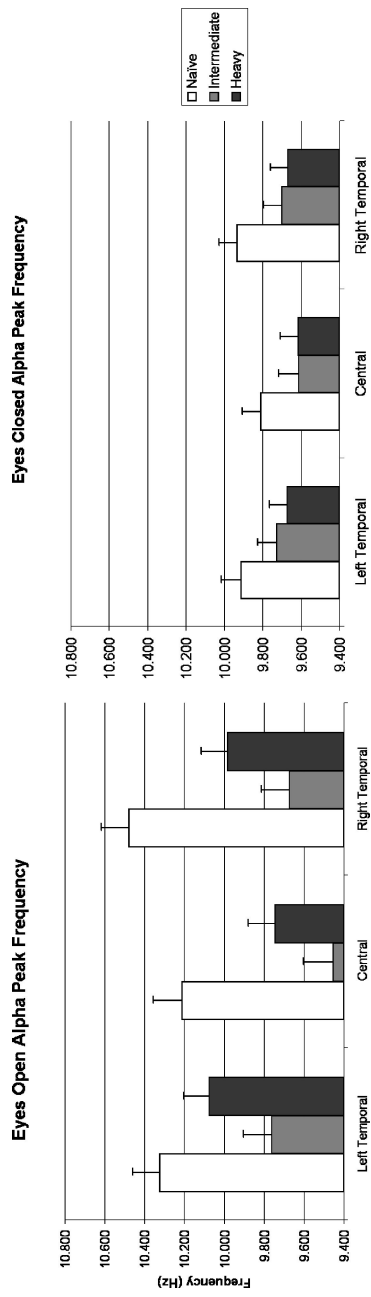


Figure 3. The consistent decreased peak alpha frequency for the mobile phone user groups compared to naive users for the three locations. Note the fact that during eyes open EEG the alpha peak frequency for both mobile phone user groups is decreased, but only for the intermediate group significantly so. Correlational analysis revealed that the alpha peak frequency correlated significantly to RUI, thereby supporting the fact that this effect is related to mobile phone use.

1351

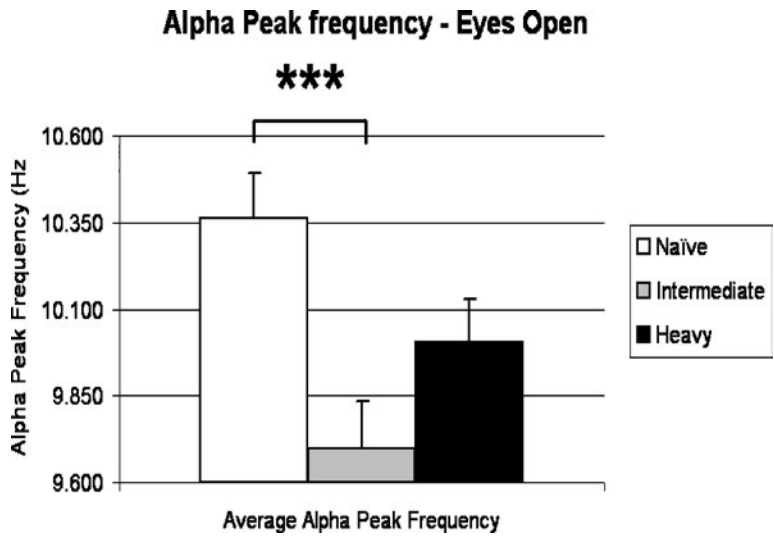


Figure 4. Significant effect for alpha peak frequency during eyes open EEG.

Delta

Significant differences in delta power were found for electrode location ($F = 12.078$; $df = 2, 293$; $p < .000$) and RUI ($F = 4.570$; $df = 2, 294$; $p = .011$). A significant interaction was seen for Condition X RUI group ($F = 4.467$; $df = 2, 294$; $p = .012$). Thus, separate analyses were performed for EO and EC.

Eyes Closed—Delta. For the eyes-closed condition MANOVA revealed an effect of electrode location ($F = 7.163$; $df = 2, 293$; $p = .001$) and Group ($F = 5.223$; $df = 2, 294$; $p = .006$). Delta was higher at the Central sites as compared to the temporal sites. Contrasts revealed that the heavy user group had more delta than the naïve user group ($p = .007$).

Eyes Open—Delta. For the eyes-open condition MANOVA revealed an effect of electrode location ($F = 14.712$; $df = 2, 293$; $p < .000$) and Group ($F = 3.421$; $df = 2, 294$; $p = .034$). Delta was higher at the central sites as compared to the temporal sites. Contrasts revealed that the heavy user group had more delta than the naïve user group ($p = .011$).

Theta

Multivariate analysis revealed an effect of Condition ($F = 4.910$; $df = 1, 294$; $p = .027$), electrode position ($F = 12.102$; $df = 2, 293$; $p < .000$) and Group

($F = 3.552$; $df = 2$; 294 ; $p = .030$). Theta was higher at the central sites as compared to the temporal sites and theta was also higher during eyes closed condition. Contrasts revealed that the heavy user group differed from the naïve user group ($p = .023$), with the heavy user group showing increased theta power.

Alpha and Beta

Multivariate analysis revealed a significant effect of Location ($F = 4.163$; $df = 2$, 293 ; $p = .016$) for alpha power. Alpha power was increased at central compared to temporal sites. No significant effects were seen for beta.

Alpha Peak Frequency

Figure 3 shows the results for alpha peak frequency for all three locations during both eyes-open and eyes-closed condition. Figure 4 shows the significant findings for alpha peak frequency during eyes-open.

The following percentages of missing values were reported for this analysis naïve 14%; intermediate 18% and heavy 19%. The main effect for RUI was close to significance ($F = 2.957$; $df = 2$; $p = .054$). Multivariate analysis revealed a significant interaction between Condition and RUI ($F = 3.452$; $df = 2$; 244 ; $p = .033$). EO and EC conditions were therefore analyzed separately.

Eyes Closed

The following percentages of missing values were reported for this analysis: naïve 5%; intermediate 7%; and heavy 6%. Multivariate analysis showed no significant effect for RUI group ($F = 1.491$; $df = 1$; $p = .227$).

Eyes Open

The following percentages of missing values were reported for this analysis: naïve 12%; intermediate 15%; and heavy 16%. MANOVA revealed a significant effect for RUI group ($F = 5.986$; $df = 2$; $p = .003$). Post hoc analysis demonstrated that the naïve group had significantly higher alpha peak frequency compared to the intermediate group ($p = .001$), but did not significantly differ from the heavy user group ($p = .106$).

Bivariate non-parametric correlations (Kendall's tau_b) revealed a significant correlation between RUI score and eyes-open alpha peak frequency at

central ($r = -.093$, $p = .028$) and right ($r = -.114$, $p = .009$) areas and between right-temporal eyes-open alpha peak frequency and Openness ($r = .084$; $p = .044$). The correlation was not significant between eyes-open alpha peak frequency and NEO FFI scores, education, age, sex, or neuropsychological indices of executive function.

DISCUSSION

This pilot study sought to investigate the relationship between long-term MP use and brain function employing an epidemiological approach. MP-use was associated with EEG slowing as demonstrated by increased delta and theta power and decreased alpha peak frequency in MP users. Furthermore, heavy MP use was associated with less interference on the word interference test, as well as increased extraversion and decreased openness.

Increased delta and theta EEG activity were observed during both eyes open and eyes closed conditions over all three regions in participants who reported heavy usage of mobile phones. The data used in this study were all EOG corrected, therefore these increases in Theta and Delta cannot be explained by differences in eye movements or EOG artefacts. Both mobile phone user groups, compared to naïve users, showed decreased alpha peak frequency—only significantly so for the intermediate user group—particularly during eyes-closed condition. This suggests a general slowing of the EEG, related to mobile phone use (increase in slow EEG activity, decreased EEG peak frequency). Figure 3 shows that the decrease in alpha peak frequency during eyes-open is more pronounced for the intermediate group than the heavy group. Therefore, it could be questioned whether this effect is really related to mobile phone use. However, a highly significant negative correlation was seen between RUI and eyes-open alpha peak frequency for the central and right temporal regions. Indeed, the study also found a correlation between Openness and eyes-open alpha peak frequency; however, this correlation was less significant, smaller and only present for the right temporal region. The fact that eyes-open alpha peak frequency did not significantly correlate with other NEO FFI scores or the interference score further adds to this. Therefore, these effects cannot easily be explained by differences between groups in personality or neuropsychological results. Nor are they likely to be due to education or age, as groups did not significantly differ on these variables. Thus, an association between MP-use and alpha peak frequency is supported. However, it is difficult to draw firm conclusions about causality in the current

study, which was epidemiological and used self-reported questionnaires of MP-use rather than directly measuring EMF exposure levels.

Heavy mobile phone users performed better on the Word Interference test, a measure of executive function. Results suggest heavy mobile phone users experience less interference on the color condition, reflecting better executive function. This supports previous studies that report an increase in performance on attention tests with acute exposure to MPs (Lee et al., 2001; 2003; Koivisto et al., 2000; Krause et al., 2000b). These studies suggest increased performance on attention may be due to an acute local increase in temperature by EMFs emitted by the MP. However, in the current epidemiological study subjects were not acutely exposed to a MP. Therefore, results cannot be attributed to an acute increase in temperature. Current results suggest that, as well as the acute effects seen in previous experimental studies, chronic changes in neuropsychological performance are associated with increased MP use. Future studies should explore whether these are due to EMF exposure or some other as yet unknown variable. For example, heavy mobile phone users may more often make phone calls in busy environments (e.g., in a train, shop, street), which would require focused attention on the conversation while filtering out irrelevant environmental information. This may act as a kind of cognitive training that could have the effect of enhancing focused attention. Alternatively, people who are able to focus on using the phone in busy environments may be more likely to use phones frequently. Longitudinal studies are required to confirm the causal direction of the relationship between control of attention and frequent MP use. Other tasks and modalities used to measure controlled attention (e.g., P300 event-related potential) could also be used to understand the current results better.

Finally, heavy mobile phone users were found to be more extraverted and less open compared to naïve mobile phone users. This finding probably reflects a preexisting trait difference between heavy and naïve MP users, and could reflect the fact that some jobs (e.g., executives, salesmen) use mobile phones more frequently. It can also be expected that extraverts tend to communicate more often with other people compared to introverts, which could involve frequent mobile phones use.

Some studies have sought to establish a relationship between personality and EEG measures. For example Stough et al. (2001) found a positive correlation between theta EEG power and Openness for all cortical regions. In contrast, a negative correlation was found between theta power and Openness in the current study. The results also show heavy mobile phones users scored lower on Openness but had greater overall theta EEG. Tran et al. (2001) found that extraverts showed increased alpha power in frontal but not posterior regions.

Schmidtke and Heller (2004) found a negative correlation between alpha power at T5 and T6 and neuroticism, but no correlations for Extraversion. The present authors have covaried for the preexisting differences in Extraversion and Openness. This, together with the earlier summarized findings makes it implausible that personality alone could have accounted for the relationship between mobile use and EEG in the current study.

Previous studies investigating acute EMF effects on EEG have most consistently found an increase in alpha EEG activity (Waking EEG: Croft et al., 2002; Schulze et al., 1996; Mann & Röschke, 1996; Krause et al., 2000; Lebedeva et al., 2001; Borbély et al., 1999; Huber et al., 2000, 2002a, 2002b). Results from lower frequencies are less consistent. Croft et al. (2002) found a decrease in delta power during EMF exposure. However, Kramarenko and Tan (2003) found small bursts of slow waves in the delta–theta range after 15–20 s of mobile phone use that is consistent with the increase in delta and theta seen in the current study. Huber et al. (2000) and Borbély et al. (1999) found no effect in alpha peak frequency in response to acute EMF exposure. However, Kramarenko and Tan (2003) found an increase in the median EEG frequency. It could be speculated that although increases in EEG frequency are seen in acute MP use, or in response to EMF exposure, decreases in resting EEG frequency may follow frequent use. Clearly, further studies investigating both acute and long-term frequent use should be conducted.

EEG slowing is seen in a number of pathological conditions including Alzheimer's (Rodriguez et al., 1999). However, the change in EEG power in the current study was small. The increase in delta power in MP users for eyes-closed and eyes-open was 13.1% and 9.8%, respectively; theta power was increased with 11.8%; and alpha peak frequency was decreased with 6.4% (intermediate user group) and 3.4% (heavy user group). Thus values reported in the current study are within normal variation and are not considered pathological.

Previous studies suggested that the main effect of EMF on biological tissue is due to heat exchange (IEGMP, 2000; Health Council, 2002; van Leeuwen et al., 1999; Bernardi, et al., 2000; Wainwright, 2000; Wang & Fujiwara, 1999). However, whether changes in brain temperature of this small magnitude have the kinds of long-term and widespread effects seen in the current study is yet to be confirmed. If the current findings are due to thermal effects, local effects would be expected, given that the effect of heat exchange diminishes exponentially over distance. However, the observed effects in this study were consistent over all areas (bilateral temporal and central areas).

Recent studies suggest alternative explanations of altered brain activity in response to MP use. Using PET scans, Huber et al. (2002) found that MP

use alters regional cerebral blood flow in the dorsolateral prefrontal cortex of the exposed hemisphere (and not in the temporal regions). Furthermore, they compared the effects of a pulse modulated signal (MP signal) to a continuous signal with the same characteristics, and found that pulse modulation was critical for reported EMF changes in brain function. Furthermore, their results suggest that changes were not due to a thermal effect, which was equal for both signals. Concordantly, although Kramarenko and Tan (2003) found a main effect over the exposed temporal regions, significant EEG slowing was also seen at F7 and F8, which may reflect dorsolateral prefrontal cortex function. This suggests that EMF has a direct effect on brain function, but cannot be explained by a thermoregulatory effect (Kramarenko & Tan, 2003). These studies only came to the authors' knowledge after the data analysis was finished, hence this article has not included frontal sites in the data analysis, because—at that time—there was no evidence for mechanisms other than thermal effects.

MPs are relatively new to the market. It is not surprising then that in the current study the average duration of having used a mobile phone was relatively brief in all groups (heavy users = 2.4 years; intermediate-users = 1.8 years). Although a causal relationship needs to be confirmed by future research, if the relationship between MP-use and brain function found in the current study is in fact due to EMF or some other aspect of MP-use, the question must be asked as to how these effects would change over a period of 5 or even 10 years of use. A follow-up study investigating brain function in this group at later time points would be useful in this respect.

The current epidemiological study should be considered as a pilot to further longitudinal research and requires replication using larger numbers and independent samples. Nevertheless, it suggests a relationship between MP-use and subtle EEG slowing, and between MP-use and enhanced executive function. The nature of the effect is still unclear and no conclusions can be drawn with respect to adverse health effects or whether this effect reflects an adaptive brain response. It should also be noted that the questionnaire used in the current study has not been fully validated and only gives a crude indication of MP use. Future studies should therefore incorporate more accurate and validated measures of the extent of MP use and extend the number of recording sites to include frontal areas.

REFERENCES

- Banik, S., Bandyopadhyay, S., & Ganguly, S. (2003). Bioeffects of microwave—a brief review. *Bioresource Technologies*, 87, 155–159.

- Bernardi, P., Cavagnaro, M., Pisa, S., & Piuze, E. (2000). Specific absorption rate and temperature increases in the head of a cellular-phone user. *IEEE Transactions on Microwave Theory and Techniques*, 48, 1118–1126.
- Borbély, A. A., Huber, R. H., Graf, T., Fuchs, B., Gallmann, E., & Achermann, P. (1999). Pulsed high-frequency electromagnetic field affects human sleep and sleep electroencephalogram. *Neuroscience Letters*, 275, 207–210.
- Clark, C. R., Paul, R. H., Williams, L. M., Arns, M., Fallahpour, K., Handmer, C., & Gordon, E. (2006). Development of ageing across the lifespan using common neuropsychological indices on an automated test battery. *Archives of Clinical Neuropsychology*,
- Costa, Jr., P. T., & McCrae, R. R. (1992). *NEO PI-R: Professional manual (Revised NEO Personality Inventory (NEO PI-R) and NEO Five-Factor Inventory (NEO-FFI))*. Odessa, FL: Psychological Assessment Resources, Inc.
- Croft, R. J., Chandler, J. S., Burgess, A. P., Barry, R. J., Williams, J. D., & Clarke, A. R. (2002). Acute mobile phone operation affects neural function in humans. *Clinical Neurophysiology*, 113, 1623–1632.
- Dutch Health Council. (2002). *Mobiele telefoons; een gezondheidskundige analyse*. Den Haag: Dutch Health Council publicatie nr. 2002/01
- Eulitz, C., Ullsperger, P., Freude, G., & Elbert, T. (1998). Mobile phones modulate response patterns of human brain activity. *Neuroreport*, 9, 3229–3232.
- Gordon, E. (2003). Integrative neuroscience in psychiatry: The role of a standardized database. *Australasian Psychiatry*, 11(2), 156–163.
- Gordon, E., Cooper, N., Rennie, C., Hermens, D., & Williams, L. (2005). Integrative neuroscience: The role of a standardized database. *Clinical EEG and Neuroscience*, 36, 64–75.
- Gratton, G., Coles, M. G., & Donchin, E. (1983). A new method for off-line removal of ocular artifact. *Electroencephalography and Clinical Neurophysiology*, 55, 468–484.
- Haarala, C., Bjornberg, L., Ek, M., Laine, M., Revonsuo, A., Koivisto, M., & Hamalainen, H. (2003). Effect of a 902 MHz electromagnetic field emitted by mobile phones on human cognitive function: A replication study. *Bioelectromagnetics*, 24(4), 283–288.
- Huber, R., Graf, T., Cote, K. A., Wittmann, L., Gallmann, E., Matter, D., Schuderer, J., Kuster, N., Borbely, A. A., & Achermann, P. (2000). Exposure to pulsed high-frequency electromagnetic field during waking affects human sleep EEG. *Neuroreport*, 11, 3321–3325.
- Huber, R., Borbély, A. A., Gottselig, J. M., Kuster, N., Landolt, H. P., Schuderer, J., Werth, E., & Achermann, P. (2002a). Electromagnetic fields and the sleep EEG: Effect of signal modulation. *European Sleep Research Society, JSR*, 11, 106: 213.
- Huber, R., Treyer, V., Borbély, A. A., Schruderer, J., Gottselig, J. M., Landolt, H. P., Werth, E., Berthold, T., Kuster, N., Buck, A., & Achermann, P. (2002b).

- Electromagnetic fields, such as those from mobile phones, alter regional cerebral blood flow and sleep and waking EEG. *Journal of Sleep Research*, 11, 289–295.
- IEGMP. (2000). Mobile phones and health. Report of an independent expert group on mobile phones. UK Minister of Public Health. National Radiological Protection Board, Chilton, Oxon. Available at www.iegmp.org.uk
- Koivisto, M., Revonsuo, A., Krause, C. M., Haarala, C., Sillanmäki, L., Laine, M., & Hämäläinen, H. (2000). Effects of 902 MHz electromagnetic field emitted by cellular phones on response times in humans. *Neuroreport*, 11, 413–415.
- Koivisto, M., Krause, C. M., Revonsuo, A., Laine, M., & Hämäläinen, H. (2000). The effects of electromagnetic field emitted by GSM phones on working memory. *Neuroreport*, 11(8), 1641–1643.
- Kramarenko, A. V., & Tan, U. (2003). Effects of high-frequency electromagnetic fields on human EEG: A brain mapping study. *International Journal of Neuroscience*, 113, 1007–1019.
- Krause, C. M., Sillanmäki, L., Koivisto, M., Häggqvist, A., Saarela, C., Revonsuo, A., Laine, M., & Hämäläinen, H. (2000). Effects of electromagnetic fields emitted by cellular phones on the electroencephalogram during a visual working memory task. *International Journal Radiation Biology*, 76(12), 1659–1667.
- Krause, C. M., Haarala, C., Sillanmäki, L., Koivisto, M., Alanko, K., Revonsuo, A., Laine, M., & Hämäläinen, H. (2004). Effects of electromagnetic field emitted by cellular phones on the EEG during an auditory memory task: A double blind replication study. *Bioelectromagnetics*, 25(1), 33–40.
- Lebedeva, N. N., Sulimov, A. V., Sulimova, O. P., Korotkovskaya, T. I., & Gailus, T. (2001). Investigation of brain potentials in sleeping humans exposed to the electromagnetic field of mobile phones. *Critical Reviews in Biomedical Engineering*, 29, 125–133.
- Lee, T. M. C., Ho, S. M. Y., Tsang, L. Y. H., Yang, S. H., Li, L. S., Chan, C. C., & Yang, S. Y. (2001). Effect on human attention of exposure to the electromagnetic field emitted by mobile phones. *Neuroreport*, 12, 729–731.
- Lee, T. M. C., Lam, P. K., Yee, L. T. S., & Chan, C. C. H. (2003). The effect of the duration of exposure to the electromagnetic field emitted by mobile phones on human attention. *Neuroreport*, 14, 1361–1364.
- Mann, K., & Röschke, J. (1996). Effects of high-frequency electromagnetic fields on human sleep. *Neuropsychobiology*, 33, 41–47.
- Repacholi, M. H. (2001). Health risks from the use of mobile phones. *Toxicology Letters*, 13, 323–331.
- Rodriguez, G., Copello, F., Vitali, P., Perego, G., & Nobili, F. (1999). EEG spectral profile to stage Alzheimer's disease. *Clinical Neurophysiology*, 110, 1831–1837.
- Röschke, J., & Mann, M. (1997). No short-term effects of digital mobile radio telephone on the awake human electroencephalogram. *Bioelectromagnetics*, 18, 172–176.

- Schmidtke, J. I., & Heller, W. (2004). Personality, affect and EEG: Predicting patterns of regional brain activity related to extraversion and neuroticism. *Personality and Individual Differences*, in press.
- Schulze, S., Krafczyk, S., Botzel, K., Brix, J., & Matthes, R. (1996). *Pulsed microwaves modulate EEG-activity in the alpha Band*. *Epilepsy by: Electroencephalography and Clinical Neurophysiology*, 99(4), 318–319.
- Stough, C., Donaldson, C., Scarlata, B., & Ciorciari, J. (2001). Psychophysiological correlates of the NEO PI-R Openness, Agreeableness and Conscientiousness: Preliminary results. *International Journal of Psychophysiology*, 41, 87–91.
- Tran, Y., Craig, A., & McIsaac, P. (2001). Extraversion-introversion and 8–13 Hz waves in frontal cortical regions. *Personality and Individual Differences*, 30, 205–215.
- Van Leeuwen, G. M. J., Lagendijk, J. J. W., van Leersum, B. J. A. M., Zwamborn, A. P. M., Hornsleth, S. N., & Kotte, A. N. T. J. (1999). Calculation of change in brain temperature due to exposure to a mobile phone. *Physical and Medical Biology*, 44, 2367–2379.
- Wagner, P., Röschke, J., Mann, K., Fell, J., Hiller, W., Frank, C., & Grözing, M. (2000). Human sleep EEG under the influence of pulsed radio frequency electromagnetic field: Results from polysomnographies using submaximal high power flux densities. *Neuropsychobiology*, 42, 207–212.
- Wainwright, P. (2000). Thermal effects of radiation from cellular telephones. *Physical Medicine Biology*, 45, 2363–2372.
- Wang, J., & Fujiwara, O. (1999). FDTD computation of temperature rise in the human head for portable telephones. *IEEE Trans Microwave Theory Tech*, 47, 1528–1534.
- Williams, L. M., Simms, E., Clark, C. R., Paul, R. H., Rowe, D. L., & Gordon, E. (2005). The test-retest reliability of a standardized neurocognitive and neurophysiological test battery. *International Journal of Neuroscience*, 115, 1605–1630.

EXHIBIT 13

SHORT COMMUNICATION

Enhancing cognitive performance with repetitive transcranial magnetic stimulation at human individual alpha frequency

Wolfgang Klimesch,¹ Paul Sauseng¹ and Christian Gerloff²¹Department of Physiological Psychology, Institute of Psychology, University of Salzburg, Hellbrunnerstr. 34, A-5020 Salzburg, Austria²Department of Neurology, Cortical Physiology Research Group, University of Tuebingen Medical School, Hoppe-Seyler-Str. 3, 72076 Tuebingen, Germany

Keywords: alpha, EEG, mental rotation, oscillations, rTMS

Abstract

We applied rapid-rate repetitive transcranial magnetic stimulation (rTMS) at individual alpha frequency (IAF) to improve cognitive performance by influencing the dynamics of alpha desynchronization. Previous research indicates that a large upper alpha power in a reference interval preceding a task is related to both large suppression of upper alpha power during the task and good performance. Here, we tested the hypothesis that rTMS at individual upper alpha frequency (IAF + 1 Hz) can enhance alpha power in the reference interval, and can thus improve task performance. Repetitive TMS was delivered to the mesial frontal (Fz) and right parietal (P6) cortex, and as sham condition with 90°-tilted coil (P6 position). The behavioural effect was assessed in a mental rotation task. Further control conditions were rTMS at a lower IAF (IAF – 3 Hz) and at 20 Hz. The results indicate that rTMS at IAF + 1 Hz can enhance task performance and, concomitantly, the extent of task-related alpha desynchronization. This provides further evidence for the functional relevance of oscillatory neuronal activity in the alpha band for the implementation of cognitive performance.

Introduction

Associations between cognitive performance and endogenous modulations of oscillatory neuronal activity in the individual alpha frequency (IAF) range have been established in a number of studies (see Klimesch, 1999). If these associations are functionally relevant (rather than mere epiphenomena), then it should be possible to influence cortical oscillations and thereby modulate behavioural performance. Here we tested the hypothesis that repetitive transcranial magnetic stimulation (rTMS) can induce predictable changes in oscillatory cortical activity and improve performance in a mental rotation task.

Transcranial magnetic stimulation (TMS) has been used in various ways to interfere with cortical function. It has the potential to disrupt cortical functions in a target region of interest (for a recent review see Hallet, 2000). This ability to create a temporary ‘virtual brain lesion’ allows to study the causal role of the affected region for complex motor (Gerloff *et al.*, 1997) and cognitive processes (for a review see Jahanshahi & Rothwell, 2000). As an example, TMS applied over V5 can interfere selectively with the perception of motion of a stimulus without impairing its recognition (for a review see, e.g. Walsh & Cowey, 1998).

Transcranial magnetic stimulation has also been used to improve brain function (for a recent review see Triggs & Kirshner, 2001). Thereby, one important parameter is the frequency of repeatedly delivered single TMS pulses (rTMS). At frequencies of 5 Hz and higher, rTMS transiently enhances cortical excitability (Pascual-Leone *et al.*, 1994),

whereas slow rTMS at a frequency of about 1 Hz induces a transient suppression of excitability (Chen *et al.*, 1997a). Another important factor is the temporal relationship between task performance and magnetic stimulation. Application of fast rTMS (at a frequency of 5 Hz or higher) during task performance (or the presentation of the task relevant stimulus) usually has detrimental effects on cognitive processes (Grafman *et al.*, 1994; Wassermann *et al.*, 1999). If, however, fast rTMS is delivered in a period preceding a task (Hamilton & Pascual-Leone, 1998; Mottaghy *et al.*, 1999; Triggs *et al.*, 1999; Evers *et al.*, 2001; Sparing *et al.*, 2001) or in short periods during processing of a task (Boroojerdi *et al.*, 2001), enhanced performance can be observed. Facilitating effects have also been reported when single pulse TMS is used with a long interstimulus interval (500 ms or more) before task onset (Töpper *et al.*, 1998).

In the present study, we applied rTMS at IAF to enhance cognitive performance. The rationale of the experimental procedure is derived from three basic findings about the human electroencephalogram (EEG) alpha rhythm (for an extensive review of the following findings cf. Klimesch, 1999). First, interindividual differences in mean or peak alpha frequency are large (7–13 Hz; mean for young adults is about 10 Hz) and are related to memory performance and the speed of information processes. Second, the extent of alpha reactivity [as measured, e.g. by event-related desynchronization (ERD); cf. ref. Pfurtscheller & Aranibar, 1977] depends on the amplitude of alpha oscillations during a resting or reference period that precedes task performance. In a series of studies, we have shown that cognitive performance is related to the extent of ERD, which in turn depends on the extent of power in a resting or test interval. Subjects with large alpha power tend to exhibit a pronounced ERD and both measures are associated with good

Correspondence: Dr Wolfgang Klimesch, as above.
E-mail: wolfgang.klimesch@sbg.ac.at

Received 16 September 2002, revised 17 December 2002, accepted 20 December 2002

cognitive performance in a variety of different tasks (Neubauer *et al.*, 1995). Thus, large resting (or reference) alpha power and a large ERD are associated with good cognitive performance. Third, these findings are frequency sensitive. They can be observed in a narrow upper alpha band (width of 2 Hz) but only if frequency boundaries are adjusted to IAF (e.g. for a subject with fast IAF of 12 Hz, the upper alpha band is 12–14 Hz).

On the basis of these findings, our conclusion was that a period of pronounced (upper) alpha activity – preceding task performance – is associated both with a large ERD (alpha suppression or reactivity) and good performance. Thus, the logic underlying the present experiment was to apply rTMS at individual upper alpha frequency (IAF + 1 Hz) in a period preceding task performance. Because the human alpha rhythm (as measured by scalp EEG) shows a clear association with visual information processing demands, we used a mental rotation task and applied rTMS at IAF + 1 Hz over a right parietal (P6) and a frontal site (Fz). These sites were selected because functional magnetic resonance imaging studies have shown repeatedly that the superior-parietal lobule (BA 7) – particularly in the right hemisphere – plays a significant role in mental rotation (e.g. Richter *et al.*, 2000; Thomsen *et al.*, 2000). There is also evidence that the lateral premotor and supplementary motor area (lateral and medial BA 6) is involved (Richter *et al.*, 2000). Control conditions were rTMS at IAF – 3 Hz (lower alpha, individually adjusted) and at 20 Hz (beta frequency, not adjusted individually). We expected that compared with the control conditions, subjects would show improved mental rotation performance, increased upper alpha power during a reference period (preceding the task) and increased ERD (larger suppression) during task performance in the experimental condition (rTMS at IAF + 1 over the right parietal cortex).

It is interesting to note that almost all studies reporting facilitating effects (ignoring those exploiting the potential of disinhibition) applied rTMS at a frequency that either equals mean alpha frequency (which is about 10 Hz) (Hamilton & Pascual-Leone, 1998; Wassermann *et al.*, 1999), harmonics of alpha at 20 Hz (Mottaghy *et al.*, 1999; Triggs *et al.*, 1999; Sparing *et al.*, 2001) or subharmonics like 5 Hz (Boroojerdi *et al.*, 2001). Thus, the facilitating effects of these studies may have been already been, at least in part, because of the influence of IAF.

Materials and methods

Subjects

Experiments were carried out at the Department of Neurology, University of Tübingen Medical School. They were performed in accordance to standard safety guidelines (Chen *et al.*, 1997b) and the Code of Ethics of the World Medical Association and were approved by the Institutional Review Board of the University of Tuebingen. In Experiment 1, a sample of 16 subjects (six healthy males with a mean age of 26.7 years, range 22–29 years and ten females with a mean age of 23.1 years, range 18–30 years) was used. Because one female subject did not tolerate rTMS, 15 subjects remained for data analysis. In Experiment 2, a different sample of six subjects (three healthy males with a mean age of 27.3 years, range 24–29 years and three females with a mean age of 24.7 years, range 20–30 years) was used. All subjects were right handed, had normal or corrected to normal vision and were paid for participation. They participated after giving written informed consent.

Stimulus presentation and cognitive tasks

Stimuli were line drawings of cubes that were modified versions of the subtest mental rotation of the IST-70 (a standard German intelligence test). The cubes had different symbols on each side. On each trial a set of six cubes (three in an upper and three in a lower row) were presented on a computer monitor. The target cube always appeared in the middle position of the first row and was marked by a surrounding square. Subjects had to decide which of the other five cubes matched the mentally rotated target. They were instructed to perform the task as fast and accurately as possible. The six cubes remained on the screen until the subject responded by pressing one of five buttons. A single trial started with a warning signal (i.e. the visual presentation of the letters ‘TMS’) for 1000 ms. Then, the train of 24 TMS pulses was delivered starting at the offset of the warning signal. Immediately after the last TMS pulse, the cubes were presented. The next trial started 11 600 ms after the subject responded.

The set of six cubes were presented in nine blocks, each consisting of eight trials. Analogous to the IST-70, the target cube differed for a series of sets (trials) whereas the five test cubes remained the same. For construction of the trials, we used a sample of nine series with eight sets. In each of the eight sets the target cube was different, but the other five cubes remained the same. The sequence of blocks was randomized between subjects. Dependent variables were reaction time and percentage correct answers calculated separately for each block of trials.

rTMS protocol

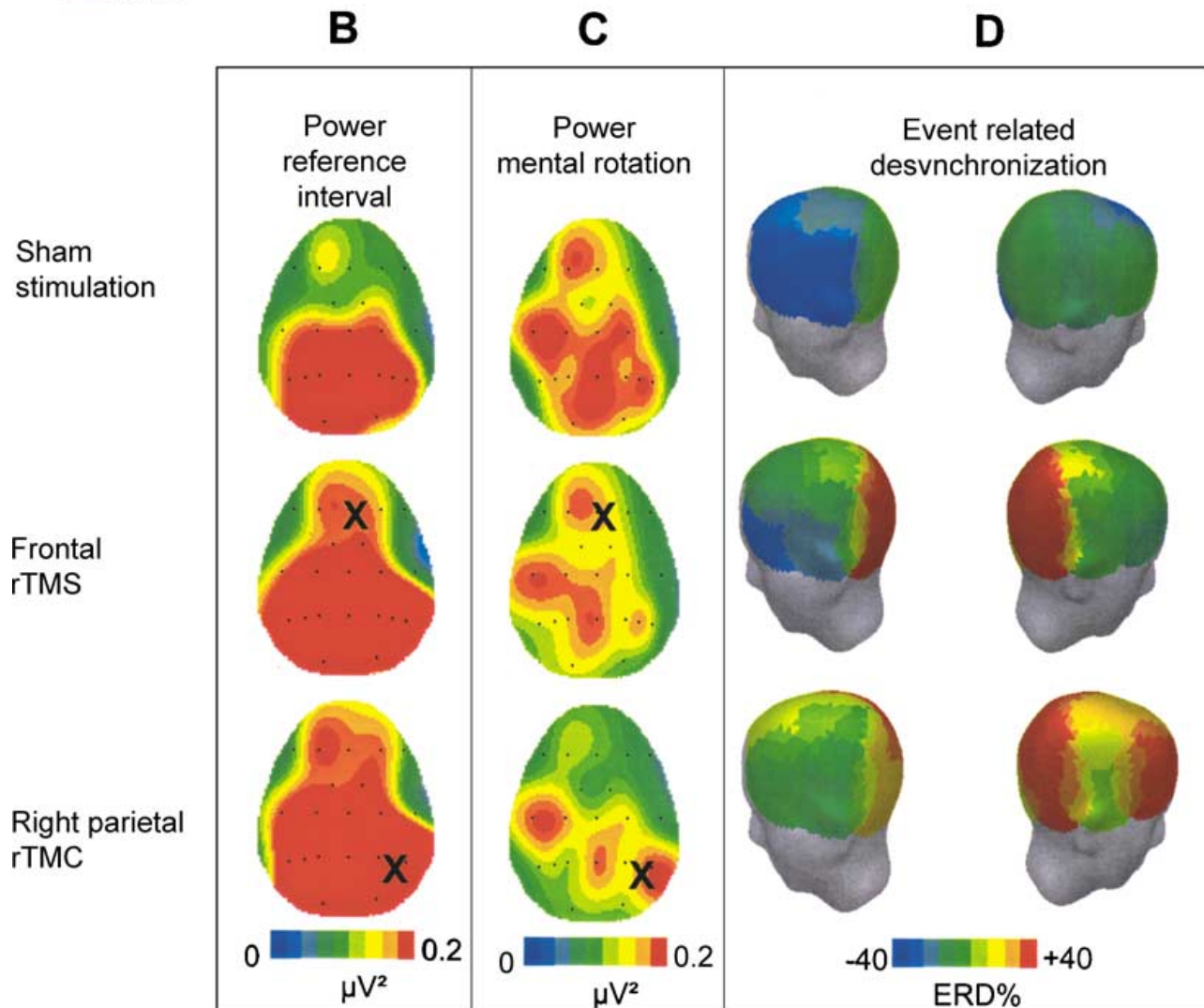
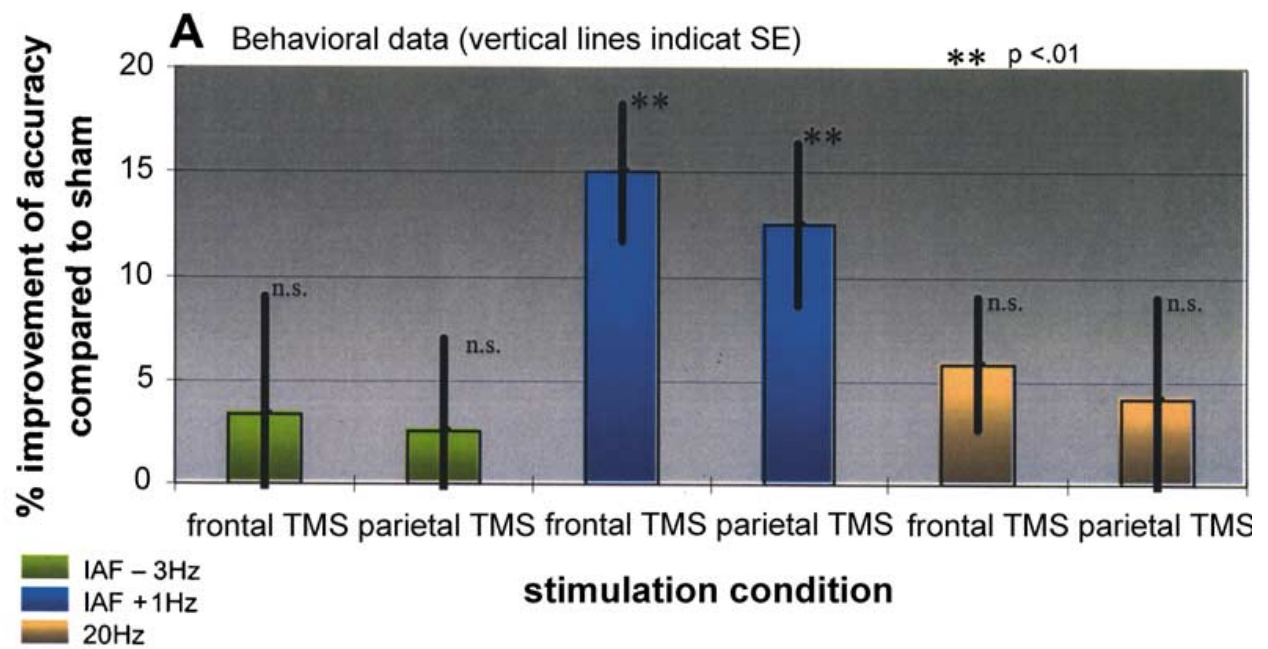
A MagStim Rapid stimulator (MagStim, Whitland, UK) with a 70-mm figure-8 coil was used. Locations for rTMS stimulation were determined according to the international 10–20 system. In the experimental condition, rTMS was applied at P6 (above the intraparietal sulcus), at Fz and rotated by 90° over P6 for sham. This experimental manipulation is termed the stimulation condition. The output strength of the rTMS was set to 110% of the subjects’ motor threshold, defined as the intensity needed for eliciting motor evoked potentials of at least 50 μ V recorded at the thumb of the left hand in 50% (5/10) of single pulses delivered to the contralateral motor cortex. The electromyogram was recorded from two bipolar Ag–AgCl electrodes over the left abductor pollicis brevis muscle (band pass, 5–200 Hz; sample rate, 1000 Hz). Mean intensity for rTMS was 57.3% of maximal stimulator output. Sham served as the control condition in which the sensory effects of rTMS were simulated to some extent without interfering with cortical processes. Subjects could not be aware of whether a stimulation condition was real or not because conditions were applied in a randomized way, subjects could not see the coil and were not informed about the existence of placebo stimulation.

In order to keep the total ‘energy’ applied to the cortex by rTMS constant for the different frequencies (see below), a fixed number of 24 pulses was delivered in each condition. Thus, the duration of pulse trains varied between 1.2 to ~4.8 s (depending on IAF and condition). No rTMS was given during execution of the task.

Experiments 1 and 2

Both experiments started with the recording of the EEG to determine IAF. Experiment 1 served to assess cognitive performance and Experiment 2 to monitor changes in ERD and absolute band power (for the reference and test interval). In Experiment 1 the three stimulation

FIG. 1. (A) Task performance increases after repetitive transcranial magnetic stimulation (rTMS) (A). The rTMS induced improvement of accuracy of mental rotation is significant for individual alpha frequency (IAF) + 1 Hz only. The influence of rTMS at individual upper alpha frequency (IAF + 1 Hz) on the EEG is depicted in the lower panel. The results for the reference interval (a time period preceding rTMS), the test interval (time period during task performance) and event-related desynchronization (ERD) are shown in B, C and D, respectively. Note the rTMS-induced increase in power during reference and decrease during test.



conditions (Fz, P6, sham) were combined with three stimulation frequencies resulting in nine blocks of experimental conditions. Stimulation frequencies were IAF + 1 Hz, IAF – 3 Hz, and 20 Hz. The nine blocks of trials were assigned randomly to each of the nine experimental conditions. In order to increase the number of trials for the analysis of the EEG, only stimulation frequency at IAF + 1 Hz was used, but three blocks of trials were presented under each of the three stimulation conditions in Experiment 2. In Experiment 1, the electrodes were removed before delivering rTMS. In Experiment 2, the electrodes remained on the subject's scalp throughout the entire session. The IAF was determined for right parietal sites on the basis of power spectra (obtained from a 3-min resting period with eyes closed, preceding the performance of the experiment) as the peak frequency within 7 and 14 Hz (IAF \pm SD, measured at rest was 9.7 ± 1.57 Hz).

EEG recording

EEG signals were amplified by a Neuroscan 32 channel amplifier system (Neuroscan, El Paso, TX, USA). They were recorded referentially against a common linked earlobe reference (impedance <3 k Ω) from 21 Ag AgCl electrodes according to the international 10/20 system. Sampling rate was 250 Hz, upper frequency limit was 40 Hz. The electro-oculogram (EOG) was recorded from two additional electrodes. Data were converted to a digital format via a 32-channel A/D converter. Sampling rate was 250 Hz.

EEG data analysis for Experiment 2

Absolute band power (for the reference and test interval) and ERD were calculated in individually determined frequency bands. The reference interval consisted of a period of 3 s starting 5 s before the onset of the warning signal, and the test interval consisted of the first 3 s following presentation onset of the cubes. In these time windows epochs of 1024 ms were used for averaging. Thus for each stimulation condition and subject 72 (3×24) epochs remained for analysis. All of the epochs in each condition were carefully checked individually for artifacts (eye blinks, horizontal and vertical eye movements, muscle artifacts, etc.) by visual inspection. Epochs that were associated even with small changes in the horizontal or vertical EOG-channel within the reference and test interval (see below) were rejected. The average number of artifact-free trials for the three stimulation conditions (Fz, Pz and sham) were 30.8, 30.4, and 35.1, respectively. During the rTMS train the EEG amplifier was blocked.

The ERD is the percentage change in test power with respect to a reference interval (Pfurtscheller & Aranibar, 1977):

$$\text{ERD} = 100 \times [(\text{reference} - \text{test power})/\text{reference power}]$$

Frequency bands were determined individually for each subject *i*, by using individual alpha frequency IAF(*i*) as a cut-off point between the lower and upper alpha band. Four EEG frequency bands were analysed: Theta, IAF(*i*) – 6 Hz to IAF(*i*) – 4 Hz; lower-1 alpha, IAF(*i*) – 4 Hz to IAF(*i*) – 2 Hz; lower-2 alpha, IAF(*i*) – 2 Hz to IAF(*i*); and upper alpha, IAF(*i*) to IAF(*i*) + 2 Hz. Mean alpha frequency at rest was 10.25 ± 1.05 Hz.

Statistical analysis

We have focused on the comparison between stimulation at Fz, P6 and sham. One-way ANOVAs with the factor stimulation condition (Fz, Pz, sham) were used to analyse the behavioural data (percentage of correct responses and reaction time) of Experiment 1. Separate ANOVAs were carried out for each dependent variable and stimulation frequency. For Experiment 2, we performed two-way ANOVAs with the factors

stimulation condition (Fz, Pz, sham) and recording site (the entire set of 21 electrode sites) to analyse ERD in the four EEG bands. The Greenhouse Geisser correction was applied. Significance level was set at 5%. For Experiment 2, again separate ANOVAs were carried out for each dependent variable (ERD, reference and test power).

Results

Behavioural data

Performance (percentage correct responses) increased significantly only after rTMS at IAF + 1 Hz as indicated by the significant factor stimulation condition ($F_{2,28} = 8.86$, $P < 0.01$; cf. Fig. 1). *Post hoc* Scheffé tests indicate significant differences between stimulation at Fz and sham ($P < 0.01$) as well as P6 and sham ($P < 0.01$) but not between P6 and Fz. No significant changes in performance were induced with stimulation frequencies at IAF – 3 Hz, or 20 Hz. No significant effects were found for reaction time in any condition.

EEG data: ERD

From the four EEG bands analysed, only the upper alpha and lower-2 alpha band showed significant results. Compared with sham, rTMS at IAF + 1 Hz, induced a significant increase in lower-2 and upper alpha desynchronization (ERD) during mental rotation. For the ERD in the lower-2 alpha band, the only significant effect was found for factor stimulation condition ($F_{2,10} = 5.68$, $P < 0.05$). Scheffé tests revealed a significantly larger ERD only at P6 ($P < 0.05$) compared to sham. For the upper alpha band factor stimulation condition ($F_{2,10} = 8.82$, $P < 0.05$) reached significance. Again, no other variance sources were significant. Scheffé tests show a significant increase between rTMS at Fz and sham ($P < 0.05$) as well as P6 and sham ($P < 0.01$). No significant difference was found between P6 and Fz. Figure 1D indicates that the increase in upper alpha ERD during rTMS stimulation is a result of both decreased poststimulus power (Fig. 1C) and increased reference power (Fig. 1B). For ERD/ERS in the remaining two EEG bands (lower-1 alpha and theta) none of the variance sources reached significance.

EEG data: band power in reference and test interval

For band power values in the reference and test interval, only one significant effect of factor stimulation condition was found ($F_{2,10} = 5.44$, $P < 0.05$). This was obtained for the lower-2 alpha band during the test interval. Scheffé tests revealed a significantly lower band power after stimulation at P6 as compared with Fz ($P < 0.05$). Factor recording site reached significance in all but two cases (lower-2 alpha, reference and upper alpha, test interval). In none of the cases did the interaction between the two factors reach significance. Because factor 'recording site' reflects the usual pattern of topographical differences, these findings will not be considered in the following.

Discussion and conclusions

As predicted, rTMS delivered at the subjects' IAF at Fz and P6 lead to a significant improvement in mental rotation performance when compared with sham. This most likely because of the fact that both frontal and parietal sites play an important role in mental rotation (Richter *et al.*, 2000; Thomsen *et al.*, 2000).

The influence of rTMS at IAF on EEG parameters mimicked exactly that situation which we know is typical for good performance: increased reference power, decreased test power and, consequently, a large ERD. It is important to note that the influence of rTMS was not restricted to the time period immediately following the delivery of pulses (i.e. to the test interval) but could be observed also in the

reference interval that followed the last rTMS stimulation after an inter-trial interval of about 30 s (depending on the reaction time). Most interestingly, the direction of change in power is different in the reference and test interval. In the same way as we know from EEG studies, good performance was related to increased alpha band power in a reference, but decreased band power during a test period (for an extensive review see Klimesch, 1999). Thus, we conclude that rTMS at IAF improves performance by way of those factors that are known to be of importance under normal conditions.

The physiological nature of those mechanisms underlying the rTMS-related improvements are not known. It could be assumed that during rTMS cortical networks are put in a state of 'resonance', in a similar way as was observed for photic driving (Silberstein, 1995; Hermann, 2001). However, little is known about the dynamic changes in spontaneous electrocortical activity during and immediately after rTMS.

The present findings suggest that the relationship between the dynamics of alpha desynchronization and cognitive performance is not correlative but causal in nature. Consequently, rTMS at IAF might even be useful as a therapeutic tool for patients with cortical dysfunctions. The timing of the rTMS application relative to the task will be critical and future research is necessary to clarify this aspect.

Acknowledgements

This research was supported by the Austrian 'Fonds zur Förderung der wissenschaftlichen Forschung', Project P-13047 to W.K. C.G. was supported by the Deutsche Forschungsgemeinschaft (grant SFB 550/C5).

Abbreviations

ANOVA, analysis of variance; EEG, electroencephalogram; EOG, electro-oculogram; ERD, event-related desynchronization; IAF, individual alpha frequency; rTMS, repetitive transcranial magnetic stimulation; TMS, transcranial magnetic stimulation.

References

- Boroojerdi, B., Phipps, M., Kopylev, L., Wharton, C.M., Cohen, L.G. & Grafman, J. (2001) Enhancing analogic reasoning with rTMS over the left prefrontal cortex. *Neurology*, **56**, 526–528.
- Chen, R., Classen, J., Gerloff, C., Celnik, P., Wassermann, E.M., Hallett, M. & Cohen, L.G. (1997a) Depression of motor cortex excitability by low frequency transcranial magnetic stimulation. *Neurology*, **48**, 1398–1403.
- Chen, R., Gerloff, C., Classen, J., Wassermann, E.M., Hallett, M. & Cohen, L.G. (1997b) Safety of different inter-train intervals for repetitive transcranial magnetic stimulation and recommendations for safe ranges of stimulation parameters. *Electroencephalogr. Clin. Neurophysiol.*, **105**, 415–421.
- Evers, S., Böckermann, I. & Nyhuis, W. (2001) The impact of transcranial magnetic stimulation on cognitive processing: an event-related potential study. *Neuroreport*, **12**, 2915–2918.
- Gerloff, C., Corwell, B., Chen, R., Hallett, M. & Cohen, L.G. (1997) Stimulation over the human supplementary motor area interferes with the organization of future elements in complex motor sequences. *Brain*, **120**, 1587–1602.
- Grafman, J., Pascual-Leone, A., Alway, D., Nichelli, P., Gomez-Tortosa, E. & Hallett, M. (1994) Induction of a recall deficit by rapid-rate transcranial magnetic stimulation. *Neuroreport*, **5**, 1157–1160.
- Hallett, M. (2000) Transcranial magnetic stimulation and the human brain. *Nature*, **406**, 147–150.
- Hamilton, R.H. & Pascual-Leone, A. (1998) Cortical Plasticity associated with Braille reading. *Trends Cogn. Sci.*, **2**, 168–174.
- Hermann, C.S. (2001) Human EEG responses to 1–100 HZ. Flicker: resonance phenomena in visual cortex and their potential correlation to cognitive phenomena. *Exp. Brain Res.*, **137**, 346–353.
- Jahanshahi, M. & Rothwell, J. (2000) Transcranial magnetic stimulation studies of cognition: an emerging field. *Exp. Brain Res.*, **131**, 1–9.
- Klimesch, W. (1999) EEG alpha and theta oscillations reflect cognitive and memory performance: a review and analysis. *Brain Res. Brain Res. Rev.*, **29**, 169–195.
- Mottaghy, F.M., Hungs, M., Brüggmann, M., Sparing, R., Boroojerdi, B., Foltys, H., Huber, W. & Töpper, R. (1999) Facilitation of picture naming after repetitive transcranial magnetic stimulation. *Neurology*, **53**, 1806–1812.
- Neubauer, A., Freudenthaler, H.H. & Pfurtscheller, G. (1995) Intelligence and spatiotemporal patterns of event-related desynchronization (ERD). *Intelligence*, **20**, 249–266.
- Pascual-Leone, A., Valls-Sole, J. & Wassermann, E.M. (1994) Responses to rapid-rate transcranial magnetic stimulation of the human motor cortex. *Brain*, **117**, 847–858.
- Pfurtscheller, G. & Aranibar, A. (1977) Event-related cortical desynchronization detected by power measurements of the scalp EEG. *Electroencephalogr. Clin. Neurophysiol.*, **42**, 817–826.
- Richter, W., Somorjai, R., Summers, R., Jarmasz, M., Menon, R.S., Gati, J.S., Georgopoulos, A.P., Tegeler, C., Urgubil, K. & Kim, S.G. (2000) Motor area activity during mental rotation studied by time-resolved single-trial fMRI. *J. Cogn. Neurosci.*, **12**, 310–320.
- Silberstein, R.B. (1995) Steady state visually evoked potentials, brain resonances and cognitive processes. In Nunez, P.L. (ed.), *Neocortical Dynamics and Human EEG Rhythms*. Oxford University Press, New York, pp. 272–303.
- Sparing, R., Mottaghy, F.M., Hungs, M., Brüggmann, M., Foltys, H., Huber, W. & Töpper, R. (2001) Repetitive transcranial magnetic stimulation effects on language function depend on the stimulation parameters. *J. Clin. Neurophysiol.*, **18**, 326–330.
- Thomsen, T., Hugdahl, K., Ersland, L., Barndton, R., Lundervold, A., Smievoll, A.I., Roscher, B.E. & Sundberg, H. (2000) Functional magnetic resonance imaging (fMRI) study of sex differences in a mental rotation task. *Med. Sci. Monit.*, **6**, 1186–1196.
- Töpper, R., Mottaghy, F.M., Brüggmann, M., Noth, J. & Huber, W. (1998) Facilitation of picture naming by focal transcranial magnetic stimulation of Wernicke's area. *Exp. Brain Res.*, **121**, 371–378.
- Triggs, W.J. & Kirshner, H.S. (2001) Improving brain function with transcranial magnetic stimulation? *Neurology*, **56**, 429–430.
- Triggs, W.J., McCoy, K.J.M., Greer, R., Rossi, F., Bowers, D., Kortenkamp, S., Nadeau, S., Heilman, K. & Goodman, W.K. (1999) Effects of left frontal transcranial magnetic stimulation on depressed mood, cognition and corticomotor threshold. *Biol. Psychiatry*, **45**, 1440–1446.
- Walsh, V. & Cowey, A. (1998) Magnetic stimulation studies of visual cognition. *Trends Cogn. Sci.*, **2**, 103–110.
- Wassermann, E.M., Blaxton, T.A., Hoffman, E.A., Berry, C.D., Oletsky, H., Pascual-Leone, A. & Theodore, W.H. (1999) Repetitive transcranial magnetic stimulation of the dominant hemisphere can disrupt visual naming in temporal lobe epilepsy patients. *Neuropsychologia*, **37**, 537–544.

EXHIBIT 14



US 20050256539A1

(19) **United States**(12) **Patent Application Publication**(10) **Pub. No.: US 2005/0256539 A1****George et al.**(43) **Pub. Date:****Nov. 17, 2005**

(54) **METHODS AND SYSTEMS FOR USING
TRANSCRANIAL MAGNETIC
STIMULATION TO ENHANCE COGNITIVE
PERFORMANCE**

Publication Classification(51) **Int. Cl.⁷** **A61N 1/00**(52) **U.S. Cl.** **607/2; 600/13**

(76) **Inventors:** **Mark S. George**, Sullivan's Island, SC
(US); **Daryl E. Bohning**, Warren, CT
(US)

(57) **ABSTRACT**

Correspondence Address:
NEEDLE & ROSENBERG, P.C.
SUITE 1000
999 PEACHTREE STREET
ATLANTA, GA 30309-3915 (US)

Methods and systems are provided for using transcranial magnetic stimulation (TMS) to enhance cognitive performance of at least one subject. At least one neural circuit is located in the brain of the subject, which is activated when the subject performs a predetermined task. Functional magnetic resonance imaging maps may be used to scan and generate maps of the interested neural circuits so as to locate proper neural circuits responsible for a predetermined task. An electromagnetic coil is positioned over a region on the scalp of the subject corresponding to the at least one neural circuit in the brain of the subject. A transcranial magnetic stimulation is delivered from the coil to the region on the scalp of the subject to induce current to flow in the brain that causes neuronal depolarization in the brain and effectuates a change in the performance of the predetermined task by the subject.

(21) **Appl. No.:** **10/509,262**(22) **PCT Filed:** **Mar. 25, 2003**(86) **PCT No.:** **PCT/US03/09463****Related U.S. Application Data**

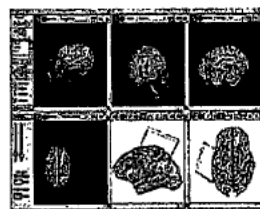
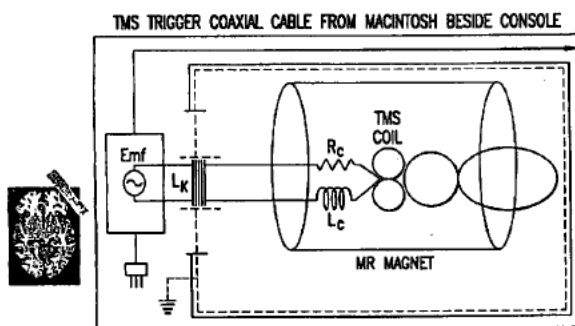
(60) Provisional application No. 60/367,520, filed on Mar. 25, 2002.

**Individualized Imaging of
Cognitive Circuit During a Behavior**

(fMRI)



**Individual Placement
Of TMS Coil over region
(Frameless Stereotaxy in Lab)**

**Improved Performance?**

**Put it all together in the scanner
Use Interleaved TMS/fMRI to
Test circuitry theories,
And effect on performance, and
Rationally design man-portable TMS**

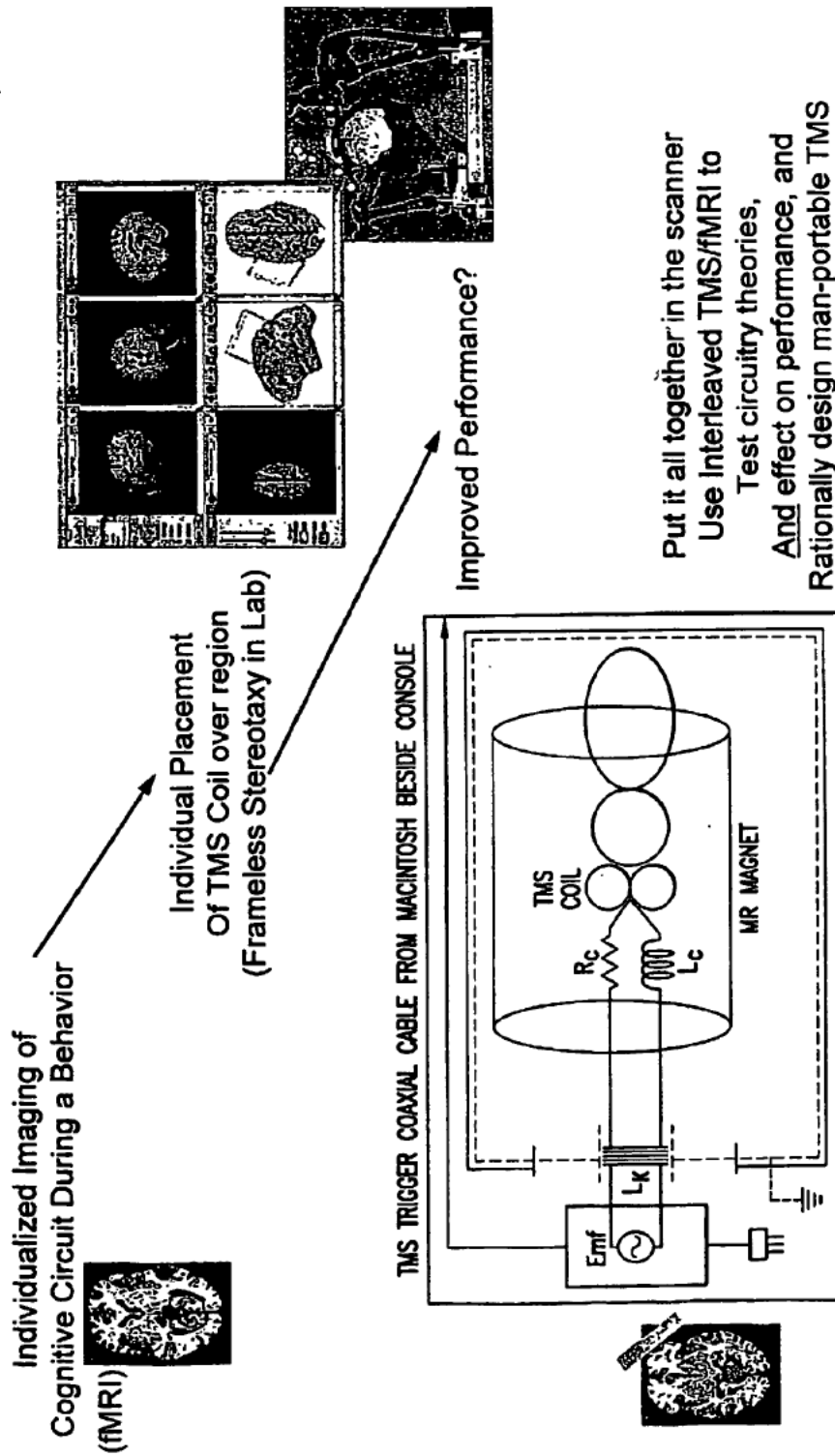


FIG. 1

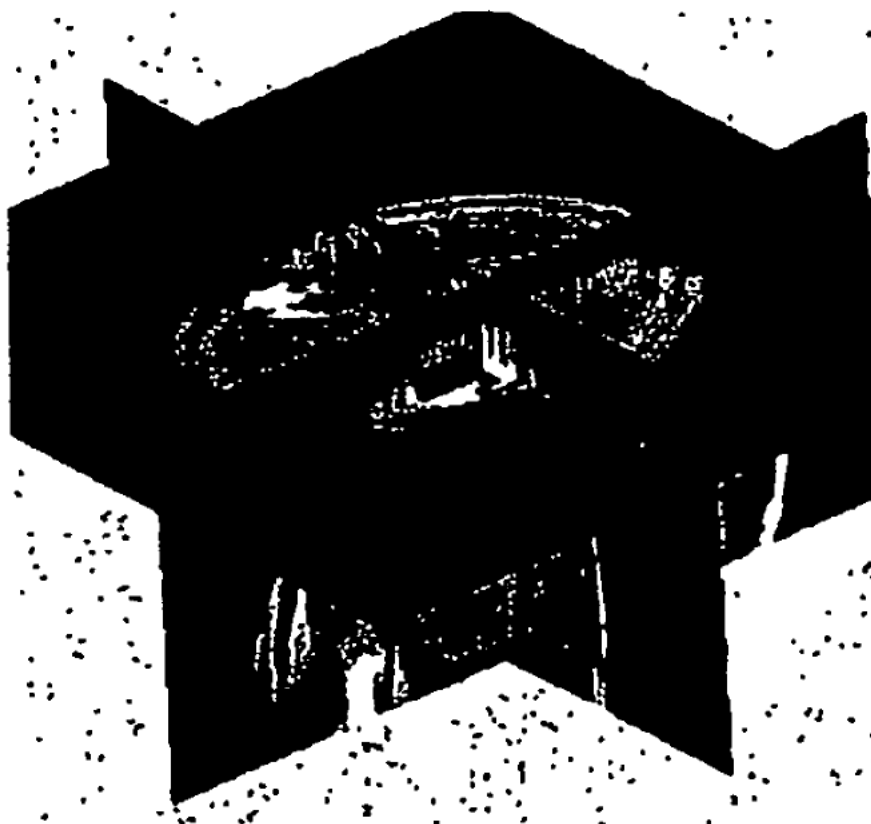


FIG. 2

Patent Application Publication Nov. 17, 2005 Sheet 3 of 11 US 2005/0256539 A1

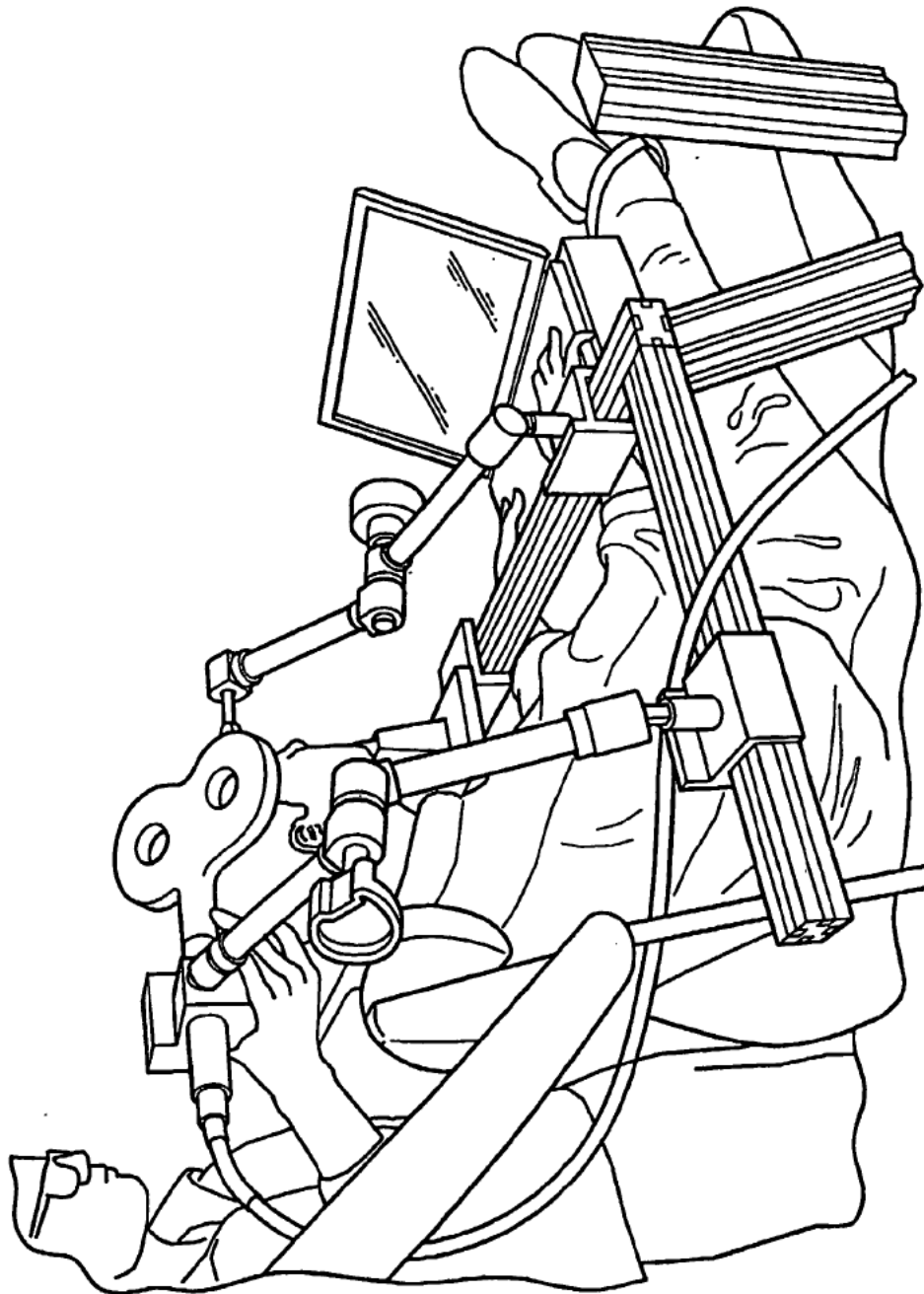


FIG. 3

fMRI GUIDED TMS DURING THE STERNBERG IN ONE SUBJECT

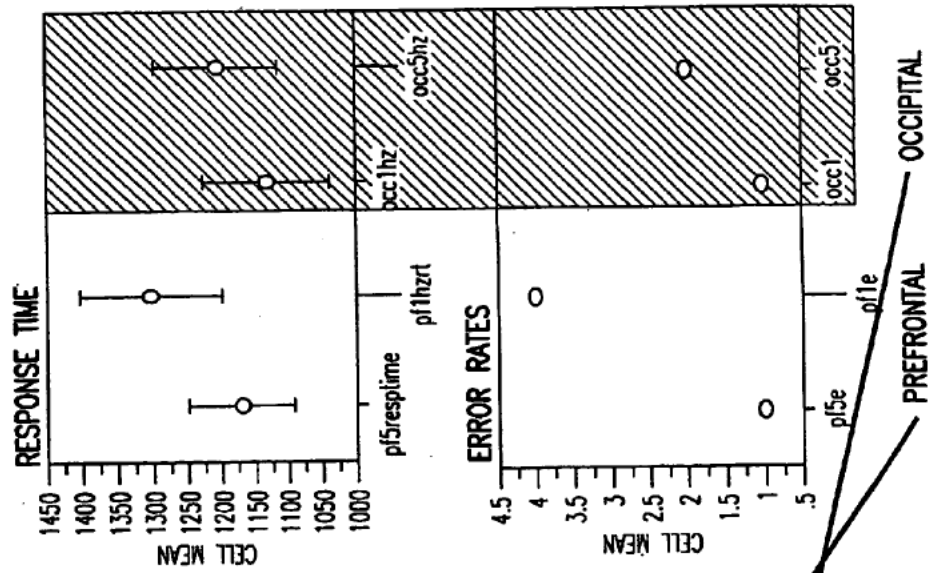


FIG.4

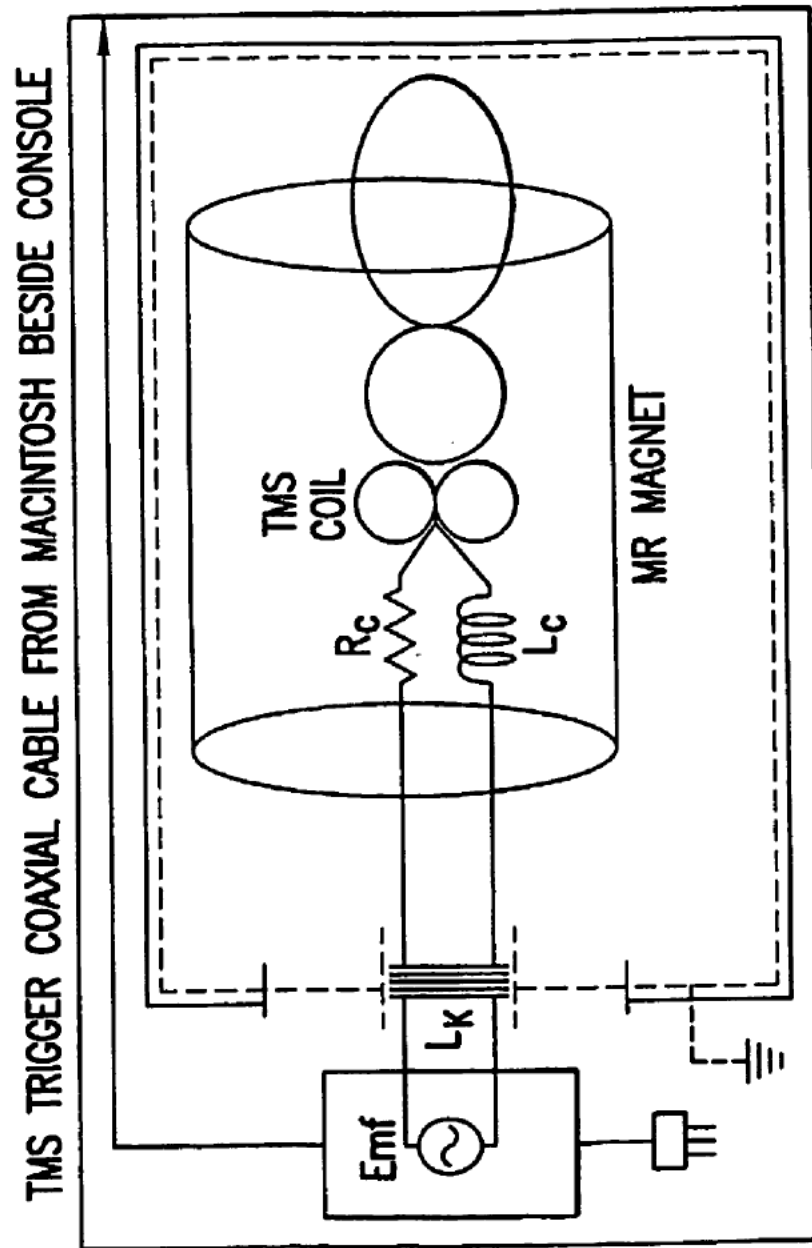


FIG.5

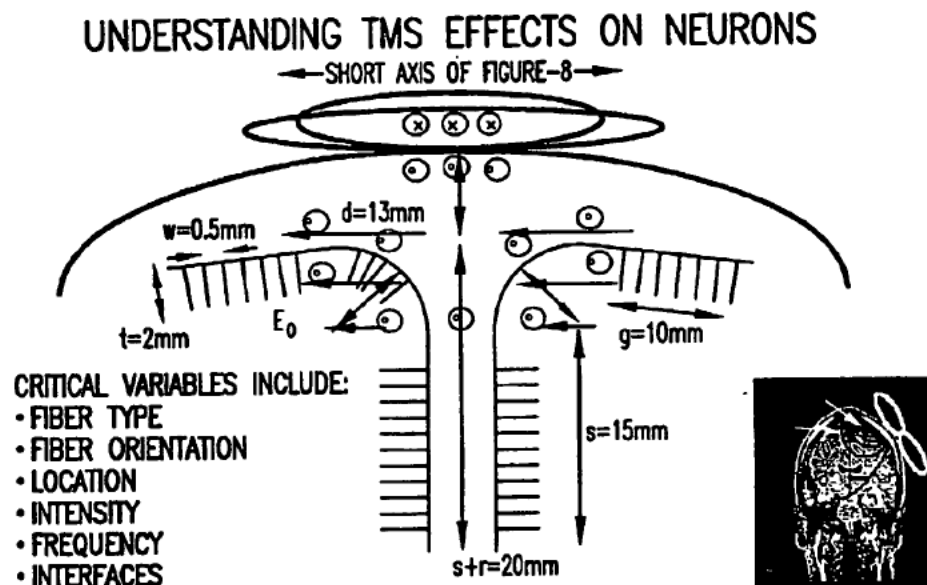


FIG.6

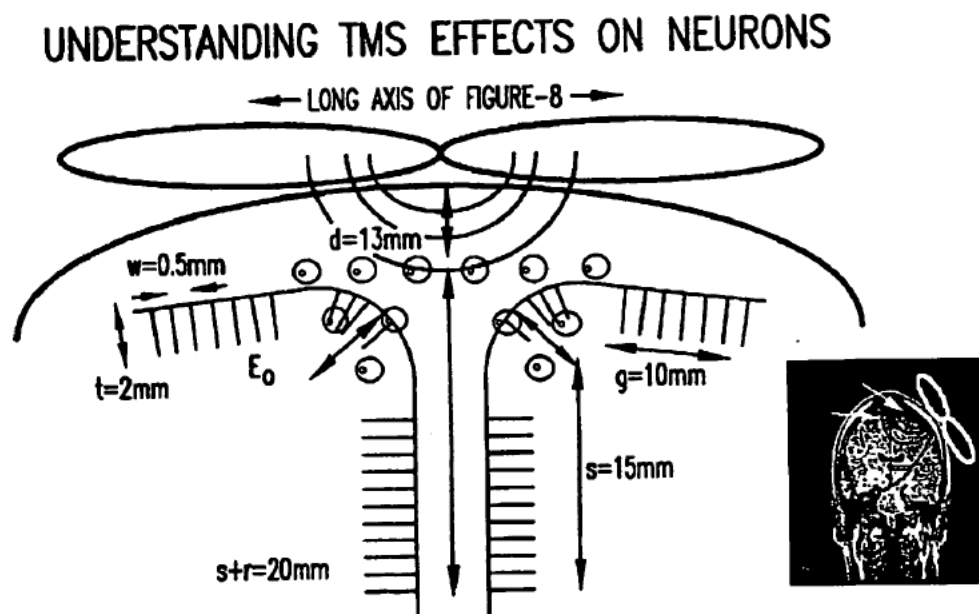
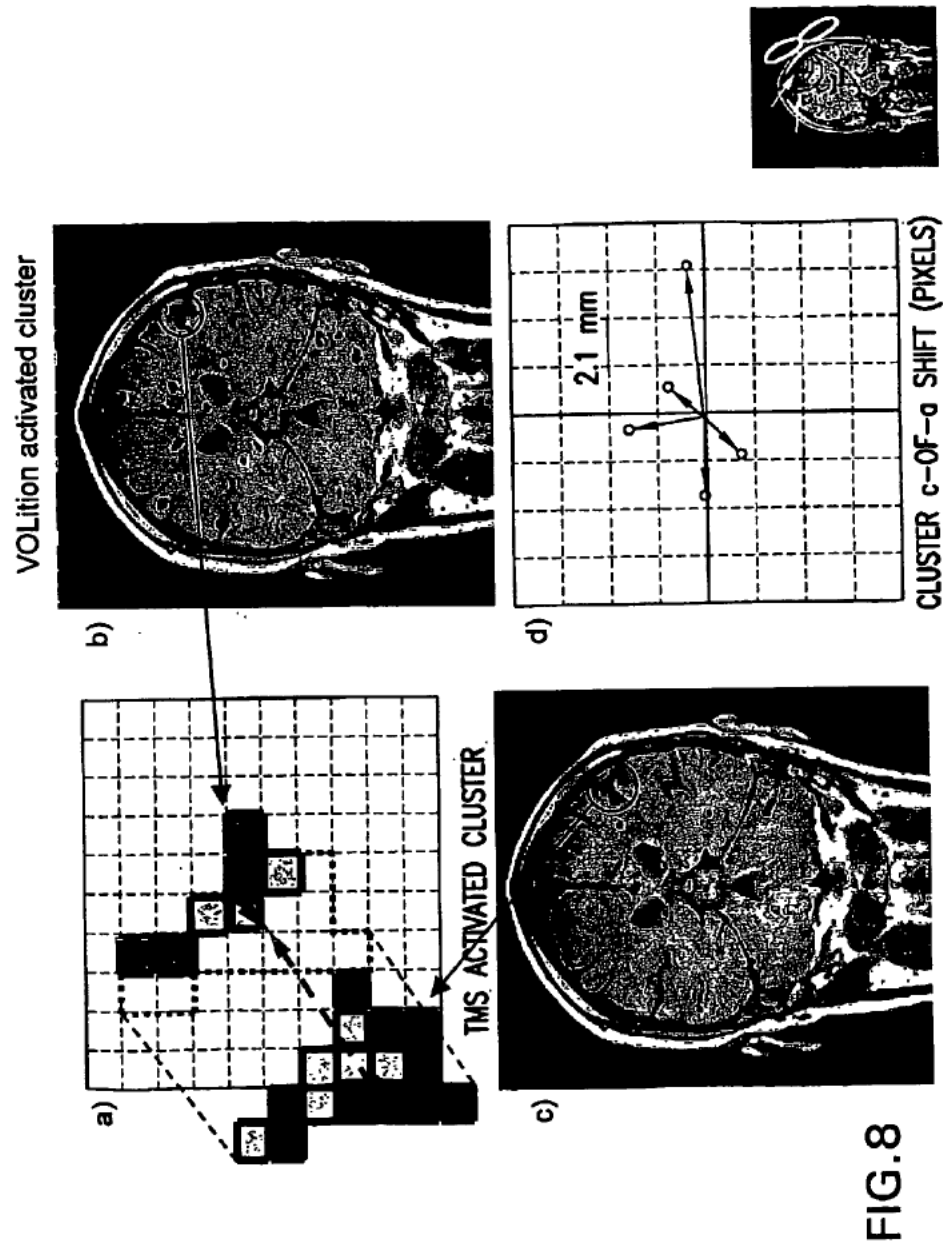


FIG.7



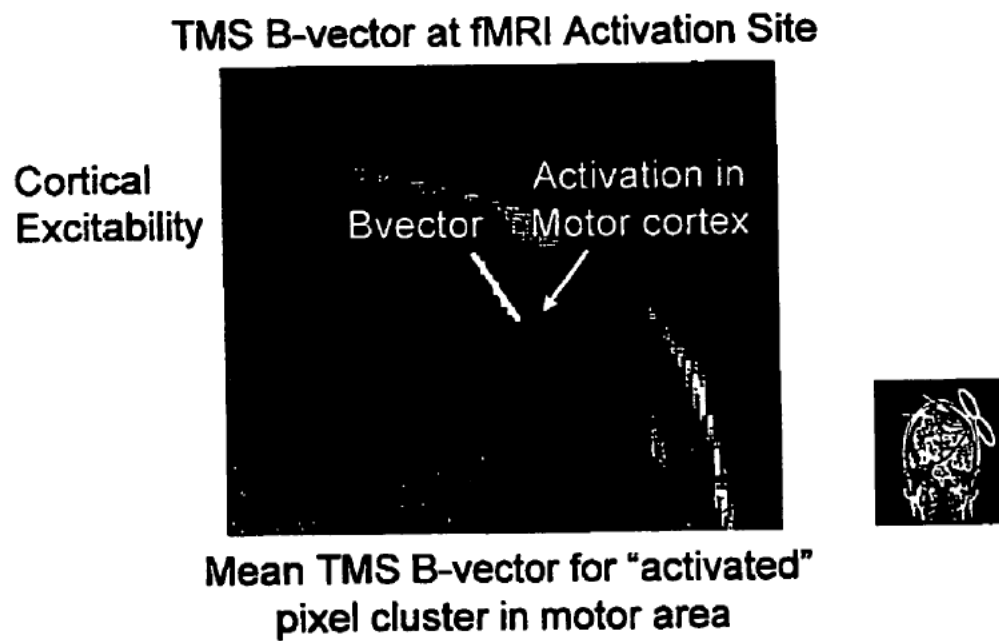
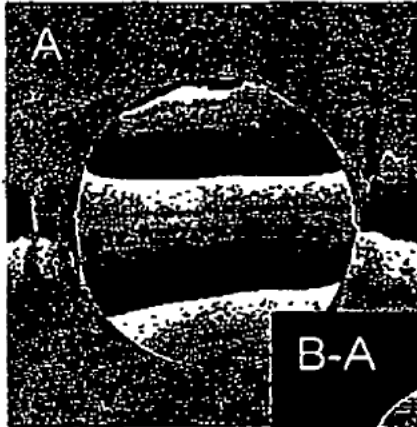


FIG.9

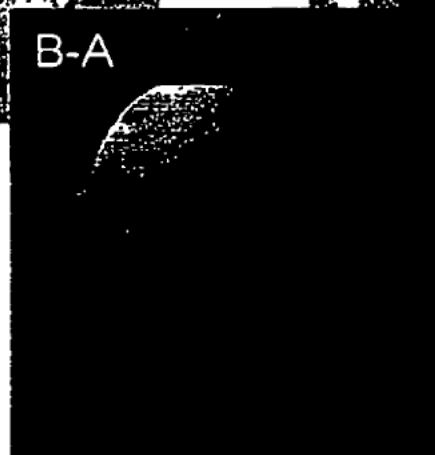
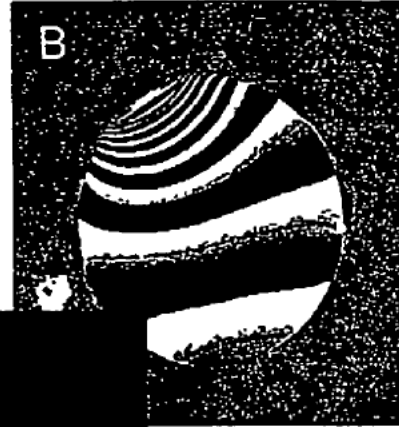
Patent Application Publication Nov. 17, 2005 Sheet 10 of 11 US 2005/0256539 A1

Using Conventional MRI To Image the Magnetic Field of TMS

TMS coil current OFF!



TMS coil current ON!



B-A= Phase Map of
Magnetic Field

FIG. 10

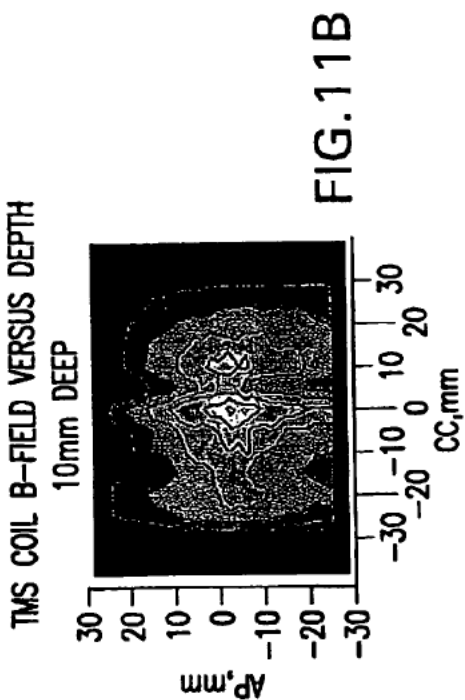


FIG.11B

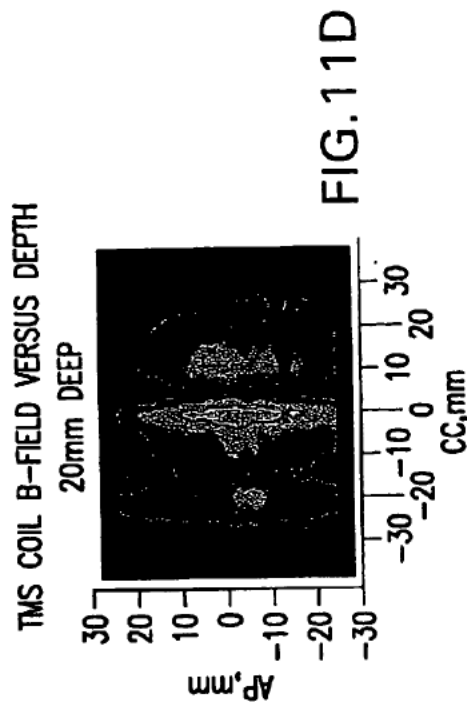


FIG.11D

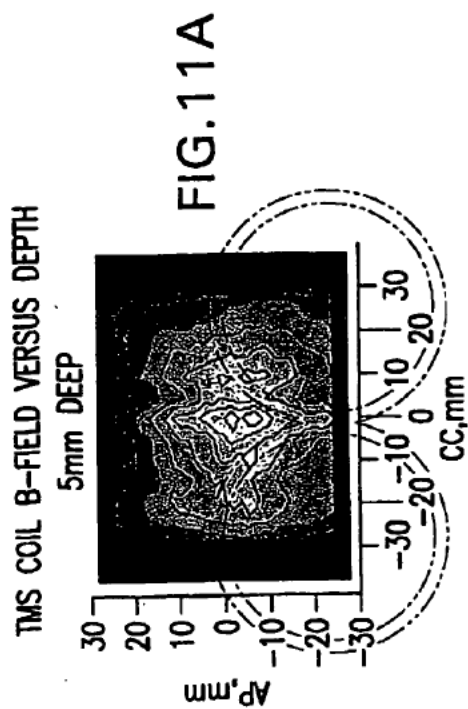


FIG.11A

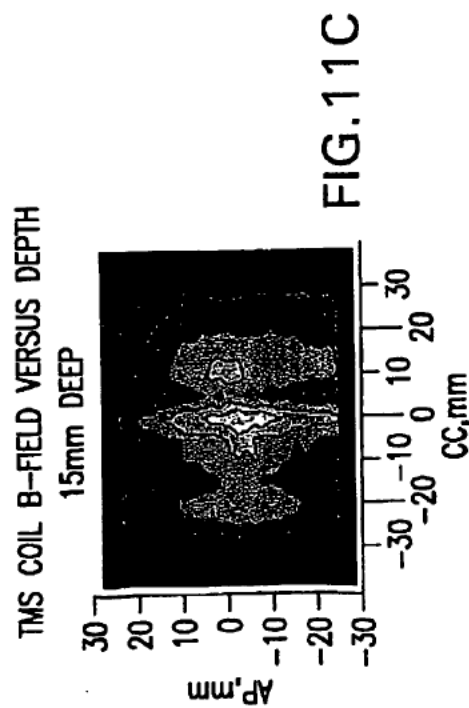


FIG.11C

US 2005/0256539 A1

Nov. 17, 2005

1

METHODS AND SYSTEMS FOR USING TRANSCRANIAL MAGNETIC STIMULATION TO ENHANCE COGNITIVE PERFORMANCE

BACKGROUND

[0001] The present invention generally relates to the use of transcranial magnetic stimulation to enhance performance. More particularly, the present invention relates to methods and systems for using transcranial magnetic stimulation to enhance cognitive performance of one or more subjects.

[0002] For over a century, it has been recognized that electricity and magnetism are interdependent (Maxwell's equations) (Bohning, 2000). Passing current through a coil of wire generates a magnetic field perpendicular to the current flow in the coil. If a conducting medium, such as the brain, is adjacent to the magnetic field, current will be induced in the conducting medium. The flow of the induced current will be parallel, but opposite in direction, to the current in the coil (Cohen et al., 1990; Brasil-Neto et al., 1992; Saypol et al., 1991; Roth et al., 1991). Thus, transcranial magnetic stimulation (hereinafter "TMS") has been referred to as "electrode-less" electrical stimulation to emphasize that the magnetic field acts as the medium between electricity in the coil and induced electrical currents in the brain.

[0003] TMS involves placing an electromagnetic coil on the scalp. Subjects are awake and alert. There is some discomfort, in proportion to the muscles that are under the coil and to the intensity and frequency of stimulation. Subjects usually notice no adverse effects except for occasional mild headache and discomfort at the site of the stimulation.

[0004] High intensity current is rapidly turned on and off in the coil through the discharge of capacitors. This produces a time-varying magnetic field that lasts for about 100-200 microseconds. The magnetic field typically has a strength of about 2 Tesla (or 40,000 times the earth's magnetic field, or about the same intensity as the static magnetic field used in clinical MRI). The proximity of the brain to the time-varying magnetic field results in current flow in neural tissue.

[0005] The technological advances made in the last 15 years have led to the development of magnetic stimulators that produce sufficient current in brain to result in neuronal depolarization. Neuronal depolarization can also be produced by electrical stimulation, with electrodes placed on the scalp (referred to as transcranial electric stimulation ("TES")). Importantly, unlike electrical stimulation, where the skull acts as a massive resistor, magnetic fields are not deflected or attenuated by intervening tissue. This means that TMS can be more focal than TES. Furthermore, for electrical stimulation to achieve sufficient current density in brain to result in neuronal depolarization, pain receptors in the scalp must be stimulated (Saypol et al., 1991).

[0006] A striking effect of TMS occurs when one places the coil on the scalp over the primary motor cortex. A single TMS pulse of sufficient intensity causes involuntary movement. The magnetic field intensity needed to produce motor movement varies considerably across individuals and is known as the motor threshold (Kozel et al., 2000; Pridmore et al., 1998). Placing the coil over different areas of the motor cortex causes contralateral movement in different

distal muscles, corresponding to the well-known homunculus. TMS can be used to map the representation of body parts in the motor cortex on an individual basis. Subjectively, this stimulation feels much like a tendon reflex movement. Thus, a TMS pulse produces a powerful but brief magnetic field which passes through the skin, soft tissue and skull and induces electrical current in neurons, causing depolarization which then has behavioral effects (body movement).

[0007] Single TMS over the motor cortex can produce simple movements. Over the primary visual cortex, TMS can produce the perception of flashes of light or phosphenes (Amassian et al., 1995). To date, these are the 'positive' behavioral effects of single pulse TMS. Other immediate behavioral effects are generally disruptive. Interference with, and perhaps augmentation of, information processing and behavior is especially likely when TMS pulses are delivered rapidly and repetitively. Repeated rhythmic TMS is called repetitive TMS (rTMS). If the stimulation occurs faster than once per second (1 Hz) it is modified as fast rTMS.

[0008] rTMS at frequencies of around 1 Hz has been shown to produce inhibition of the motor cortex. rTMS at higher frequencies of several minutes has been shown to excite the underlying cortex for several minutes. Manipulations of frequency and intensity may produce distinct patterns of facilitation (fast rTMS) and inhibition (slow rTMS) of motor responses with distinct time courses. These effects may last beyond the duration of the rTMS trains with enduring effects on spontaneous neuronal firing rates. Determining whether, in fact, lasting increases and decreases in cortical excitability can be produced as a function of rTMS parameters, and whether such effects can be obtained in areas outside of the motor cortex, are of key importance.

[0009] As indicated above, TMS is generally safe with no side effects except mild headache in about 5% of subjects. However, higher frequency TMS can produce seizures. With the publication of safety tables in 1998, there have been no unintended seizures produced in the world (Wassermann et al., 1996b; Wassermann, 1997; Wassermann et al., 1996a). Animal studies, along with human post-mortem and brain imaging studies (Nahas et al., 2000a), have all failed to find any pathological effects of TMS (Lorberbaum & Wassermann, 2000).

[0010] TMS evoked motor responses result from direct excitation of corticospinal neurons at or close to the axon hillock. It is thought that the TMS magnetic field induces an electrical current in superficial cortex. The TMS magnetic field declines exponentially with distance from the coil. This limits the area of depolarization with current technology to a depth of about 2-cm below the brain's surface. Nerve fibers that are parallel to the TMS coil (perpendicular to the magnetic field) are more likely to depolarize than those perpendicular to the coil. It is thought as well that bending nerve fibers are more susceptible to TMS effects than straight fibers (Amassian et al., 1995).

[0011] Conventional TMS coils are either round, or in the shape of a figure eight (Cohen et al., 1990). The figure eight designs are more focal than the round coils. Most coils are mere copper wire either alone or wrapped around a solid metal core. Because most coils are inefficient, they produce heat as a byproduct. The solid coils are more efficient, without a heating problem. Other manufacturers have used

US 2005/0256539 A1

2

Nov. 17, 2005

water cooling (Cadwell) or air cooling (Magstim) to deal with this issue. DARPA materials science research might drastically improve the current technology.

[0012] The peak effect of TMS can be localized to within less than a millimeter in terms of functional location. More work is needed in terms of actually understanding the exact location of TMS effects (Bohning et al., 2001; Bohning et al., 1997). There is much debate about whether one could devise an array of coils in such a way as to stimulate deep in the brain without overwhelming superficial cortex.

[0013] Although current TMS technology has shown that it can interrupt and facilitate many behaviors, several technical issues limit the field. Current coils are bulky and hard to focus. Because of the materials used, they overheat and require large capacitors. It is not clear whether one could stimulate deeper in the brain with current designs. Finally, TMS at present is limited to single TMS applications. There has been virtually no work done on producing arrays of TMS coils that are discharged in a coordinated fashion. Such an array would likely vastly open up new TMS vistas (including defense applications).

[0014] Most studies with TMS have shown that high frequency TMS can interrupt a higher cognitive function. It is relatively easy to produce speech arrest by stimulating over the motor speech area (Broca's). Speech arrest occurs only for the moment of stimulation. With the MUSC team as consultants, Drs. Stern and Lisanby at Columbia are using this 'knockout lesion' ability of TMS to understand the neural circuits used in response to sleep deprivation. There are also some studies using precisely timed single pulse TMS for augmentation of function. But as with the other potential applications, this requires precise timing (Grafinan, 2000). Precisely timing TMS bursts with stimulus presentation would thus be more difficult to adapt to warfare conditions.

[0015] At the recent CAPS teaming workshop, two different Armed Forces Representatives highlighted the need for 'non-pharmacological' approaches to boosting cognitive performance. There is thus likely only a small psychological hurdle for general warfighter acceptance of these techniques, should we succeed in finding ways of using TMS to enhance performance at baseline or following sleep deprivation. This general warfighter acceptance is remarkable given how revolutionary these concepts are, compared with the status quo. These representatives, when asked why there might be such easy acceptance of TMS in the battlefield, responded that TMS made sense in terms of focal delivery of the needed changes, without distribution throughout the whole body (e.g. lack of side effects), and the ability to turn the device on and off without worry about lingering half-lives.

[0016] Thus, there is a huge need for radical new approaches (as highlighted in the CAPS announcement). Human limitations on performance are now the rate limiting aspects of most weapons systems and warfare capability. There is thus also likely easy acceptance of TMS, if the necessary background work shows that it can improve performance. The potential impact on DOD could thus be huge. If TMS is found to boost normal performance, or even slightly restore performance in the face of sleep deprivation, there will undoubtedly be many other potential military and non-military applications. The design of man-portable TMS

systems would provide the foundation for a revolution in the field of TMS, with profound impact on therapeutic applications as well.

[0017] Therefore, there is a need to develop new methods and systems that can utilize TMS to deliver stimulation to proper neural circuits of a living being to enhance cognitive performance of the living being.

SUMMARY

[0018] According to a first aspect of the invention, methods for using TMS to enhance cognitive performance are provided. According to a first embodiment, a method for enhancing cognitive performance includes the steps of locating at least one neural circuit in the brain of a subject, which is activated when the subject performs a predetermined task, positioning an electromagnetic coil over a region on the scalp of the subject corresponding to the at least one neural circuit in the brain of the subject, delivering a transcranial magnetic stimulation from the coil to the region on the scalp of the subject, inducing a current to flow in the brain, causing neuronal depolarization in the brain, and effectuating a change in the performance of the predetermined task by the subject.

[0019] According to another embodiment, a method of using TMS to enhance cognitive performance in a plurality of subjects, such as human beings, includes the steps of dividing the plurality of subjects into groups, subjecting each of the groups into a first state and a second state, locating at least one neural circuit in the brain of a subject in the group corresponding to one of the first state and the second state, which is activated when the subject performs a predetermined task under one of the first state and the second state, positioning an electromagnetic coil over a region on the scalp of the subject corresponding to the at least one neural circuit in the brain of the subject, delivering a transcranial magnetic stimulation from the coil to the region on the scalp of the subject, inducing a current to flow in the brain, causing neuronal depolarization in the brain, and effectuating a change in the performance of the predetermined task by the subject under one of the first state and the second state. In one embodiment, the first state is a state at which a subject is at rest, and the second state is a state at which a subject is sleep-deprived. fMRI can be utilized to identify different neural circuits associated with different subject at a state, wherein the neural circuits are activated while a predetermined task is performed. TMS can then be delivered to proper neural circuits to restore and/or retrain the circuits to enhance the performance.

[0020] According to yet another embodiment, a method of using TMS to enhance cognitive performance in at least one subject includes the steps of during a behavior individualized imaging of at least one cognitive neural circuit, locating the at least one cognitive neural circuit, individually positioning an electromagnetic coil over a region on the scalp of the subject corresponding to the at least one cognitive neural circuit, and delivering a stimulation through the electromagnetic coil to the at least one cognitive neural circuit to affect the behavior related to the at least one cognitive neural circuit. Individualized imaging can be performed by an fMRI scanner, and the electromagnetic coil is associated with a TMS system, which are interleaved to provide synergistic stimulation(s).

US 2005/0256539 A1

Nov. 17, 2005

3

[0021] In another aspect, a system of using TMS to enhance cognitive performance is provided. In one embodiment, the system includes means for locating at least one neural circuit in the brain of a subject, which is activated when the subject performs a predetermined task, an electromagnetic coil that can be positioned over a spot on the scalp of the subject corresponding to the at least one neural circuit in the brain of the subject, means for delivering a transcranial magnetic stimulation from the coil to the spot on the scalp of the subject so as to induce a current to flow in the brain, cause neuronal depolarization in the brain, and effectuate a change in the performance of the predetermined task by the subject. The locating means includes an fMRI system that can be utilized to scan and generate maps of the interested neural circuits so as to locate proper neural circuits responsible for a predetermined task. Additionally, the system includes a computer having a CPU and one or more memory devices to, among other things, coordinate the operation among the different parts of the system, optimize the operation parameters such as TMS use parameters, and facilitate the TMS delivering.

[0022] In another embodiment, a portable system of using TMS to enhance cognitive performance in at least one subject includes an energy source, such as a battery, a CPU, a database having fMRI maps of neural circuits corresponding to a plurality of tasks stored therein, and a movable electromagnetic coil. The CPU is electrically coupled to the energy source and communicates with the database, which is associated with a memory device of the CPU, or alternatively with a separate memory device, or both. The movable electromagnetic coil is electrically coupled to the energy source and communicates with the CPU. In operation, when a subject is to perform a predetermined task, the CPU communicates with the database and selects one or more fMRI maps of one or more neural circuits corresponding to the predetermined task. The CPU then communicates with the movable electromagnetic coil so that the electromagnetic coil to be positioned over a region on the scalp of the subject according to the selected one or more fMRI maps. Proper transcranial magnetic stimulation from the coil is then delivered to the region on the scalp of the subject so as to induce a current to flow in the brain, cause neuronal depolarization in the brain, and effectuate a change in the performance of the predetermined task by the subject. The subject can be a person or an animal. The system can be constructed within a frame that is portable. Alternatively, the system can have an array of TMS coils, each being able to deliver TMS individually or in coordination.

[0023] These and other aspects will become apparent from the following description of the preferred embodiment taken in conjunction with the following drawings, although variations and modifications may be effected without departing from the spirit and scope of the novel concepts of the disclosure.

BRIEF DESCRIPTION OF THE DRAWINGS

[0024] FIG. 1 is a flow chart schematically showing one method of using TMS to improve cognitive performance according to an exemplary embodiment.

[0025] FIG. 2 shows an exemplary transverse structural scan of a subject.

[0026] FIG. 3 illustrates how a TMS is placed over a subject according to an exemplary embodiment.

[0027] FIG. 4 shows exemplary reaction times and error rates for one subject.

[0028] FIG. 5 illustrates a TMS in cooperation with a fMRI scan according to an exemplary embodiment.

[0029] FIGS. 6 and 7 schematize and scale exemplary relationships between the magnetic field of a TMS coil and induced currents v. brain activation, respectively.

[0030] FIG. 8 illustrates shows exemplary results relating to the relative positions of TMS-induced thumb movement and a similar movement executed volitionally.

[0031] FIG. 9 illustrates an exemplary image of the brain with the fMRI activation in the motor cortex superimposed.

[0032] FIG. 10 illustrates how to use MRI to image the magnetic field of TMS according to an exemplary embodiment.

[0033] FIG. 11 shows the magnetic field of a TMS coil on surfaces at different depths according to exemplary embodiments.

DETAILED DESCRIPTION

[0034] Several exemplary embodiments of the invention are now described in detail. Referring to the drawings, like numbers indicate like parts throughout the views. As used in the description herein and throughout the claims that follow, the meaning of "a," "an," and "the" includes plural reference unless the context clearly dictates otherwise. Also, as used in the description herein and throughout the claims that follow, the meaning of "in" includes "in" and "on" unless the context clearly dictates otherwise.

[0035] Overview

[0036] Recent researches suggest the potential of TMS technologies. Topper et al. have shown that stimulation over temporal lobe facilitates or improves picture naming (Topper et al., 1998). Grafman et al. have recently shown that stimulation over the prefrontal cortex, and not sham stimulation, improves analogous reasoning (Boroojerdi et al., 2001). The same NIH group has shown that 1 Hz TMS for 10 minutes can transiently suppress motor cortex or visual cortex activity, for up to 20 minutes following stimulation.

[0037] However, there has never been a systematic, large-scale attempt to understand these phenomena and hence to use the TMS technologies in real world applications. This invention represents exciting improvements in the field and provides methods and system for ways of delivering TMS to improve performance. Several aspects, applications, and embodiments of the present invention are reviewed as follows.

[0038] In one application, prior to engaging in a task, a subject such as a soldier has TMS applied to the appropriate region, with improved cognition for a short amount of time so as to improve the subject's performance in the task. A slight modification would be to have intermittent stimulation while performing the task at low intensities that does not interfere with cognition, which in fact improves reasoning.

[0039] According to exemplary embodiments, this and other applications can be realized through:

[0040] 1. Improvements in TMS technology as discussed below; and

US 2005/0256539 A1

Nov. 17, 2005

4

- [0041] 2. A series of TMS studies and/or experiments performed according to exemplary embodiments in healthy adults providing novel methods, procedure(s) and discoveries:
- [0042] a. A series of excitatory TMS over prefrontal or other regions of the brain to improve cognitive reasoning for a period of time at a first state of mind such as being awake;
 - [0043] b. Whether this improvement is measurable on tests resembling real word conditions such as combat conditions and whether it degrades accuracy;
 - [0044] c. Finding and optimizing use parameters for achieving this and other effects;
 - [0045] d. Locating other regions where intermittent stimulation might improve cognitive reasoning; and
 - [0046] e. Repeat all of the above in subjects who are in the second state of mind such as sleep deprived.
- [0047] In other words, according to exemplary embodiments, TMS and fMRI may be used to understand the neural circuits involved and to apply TMS at proper regions in order to produce these effects (Nahas et al, 2000b; George & Bohning, 2000; Bohning et al, 2000a; Bohning et al, 2000b; and Bohning et al, 1998).
- [0048] Thus, the present invention greatly advances the TMS field, with spin-offs in the use of TMS as a neuroscience tool, in the ability to use TMS in other cognitive applications, and in advancing TMS as a potential therapy for neuropsychiatric disorders. Some of these spin-offs include:
- [0049] Materials science—New types of TMS coils are made from new materials that have different electrical conductivity and may be made to stimulate deeper into brain than presently possible;
 - [0050] Size of TMS devices—New types of TMS coils are made in ways that are smaller, without the inefficiencies that generate heat;
 - [0051] Arrays—A plurality of TMS coils are coordinated in an array to stimulate multiple regions in precisely timed ways. Arrays may be received in a helmet for portability. Such a helmet may have many overlapping figure eight regions that are controlled from an external device such as a central control center; and
 - [0052] Portability—In one embodiment of the present invention, the stimulators; capacitors and energy source are able to be placed in combat areas in a portable device without sacrificing other functions.
- [0053] Furthermore, among other things, the present invention demonstrates, using one representative task (such as the Sternberg), whether and how TMS at different use parameters can be used to improve performance. Interestingly, even in studies over the motor cortex, there has not been a synthetic systematic examination of TMS use parameters on a behavior.
- [0054] In sum, the present invention has the potential to revolutionize this very promising young field of TMS applications.
- [0055] In one aspect, the invention relates to a method of determining TMS Use Parameters. The measures here are performance data while healthy subjects are performing the Sternberg (Study 1A1) and having TMS delivered over candidate or control regions, at different TMS use parameters. Specifically, response time (milliseconds) and error rates are measured. This will be done both at rest and with partial sleep deprivation (4 hours of sleep) (Study 1A4).
- [0056] A separate set of data contains the fMRI brain maps of regions activated during the Sternberg at baseline. These fMRI brain maps can be used to guide the TMS placement, as well as to determine the physical dimensions of a man-portable TMS system that, for example, do not need to have each soldier perform an fMRI activation map at the field.
- [0057] Another set of data contains the fMRI brain maps of regions activated during the Sternberg while TMS is being applied within the scanner (1A5). These maps may help in understanding how TMS is modifying the brain during task performance, and to generate hypotheses about secondary sites where TMS might be applied in order to even further boost performance.
- [0058] Generation alone of these three data sets (behavioral dose response with focused, image guided application; data on the variation across subjects in the physical location of this function; data on how TMS applied at a key site modifies brain activity) represents a remarkable and never before completed advancement for science.
- [0059] In another aspect, the invention relates to provide several man-portable TMS coil systems. In one embodiment of the present invention, this section of work provides three models of potential TMS systems. Using high power computers, each design is tested using computer modeling for basic design issues such as (weight, heat generation, internal stresses, the amount of induced electrical current it could deliver within the brain), and the power needed to run such a system. This results in a series of design drawings of several TMS options, and formal white paper discussions of each area under testing (coil, power systems, etc). The designs can be optimized by optimizing the use parameters needed to improve cognition—(e.g. frequency, intensity, total dose, temporal relationship of TMS to task performance), as well as information derived from the model testing.
- [0060] Among other things, the present invention has several advantages over the prior art as discussed below. Many of the prior art studies focused on pharmacological agents to improve performance, with little focus on where in the brain the compound is acting to improve performance. (It was interesting to note the general level of acceptance from military spokesman about the preference for non-pharmacological (i.e. TMS) CAP boosts over pharmacological approaches). On the other hand, many groups proposed using functional brain imaging (PET or fMRI) to understand CAP variables, but without discrete methods of acting on this circuit or systems level knowledge. This invention is unique in that it directly translates systems level circuit findings from functional brain imaging, and then uses this knowledge to apply TMS to improve performance.

US 2005/0256539 A1

5

Nov. 17, 2005

[0061] There are others who are proposing to use TMS in other applications. Importantly, the other proposals lack the design and testing elements of how to translate TMS into real world such as war fighter applications. Their approaches also focus on understanding sleep deprivation effects, while this invention has improved baseline or near baseline functioning.

[0062] Thus, the present invention is unique and highly relevant to the CAPS mission. One aspect of the present invention is to determine if TMS can boost performance on a sleep-deprivation sensitive task at baseline (or under minimal degradation of performance), and then build a system that may allow this to be translated to the field.

[0063] In one embodiment of the present invention, fMRI image is used to guide placement of the TMS coil so that the TMS coil is located at an important region for the behavior. This maximizes the efficiency of finding performance enhancing TMS use parameters. Another aspect of the present invention involves examining the fMRI activation maps and determining probabilistic rules for TMS application, which may solve how one can translate these initial image guided effects with a simpler to use formula for large-scale production.

[0064] In sum, the present invention provides a revolutionary new approach to boosting cognitive performance, TMS, both at baseline and then potentially during periods of sleep deprivation. It uses high-tech functional brain imaging and frameless stereotaxy to explore TMS use parameters over fMRI identified critical regions, and then uses a very unique technology, interleaved TMS within an fMRI scanner, to fully explore potential ways of using TMS to boost performance.

[0065] Methods and System for Determining TMS Use Parameters

[0066] According to an exemplary embodiment, a series of TMS studies or experiments may be conducted with the goal of determining whether TMS can enhance cognitive performance. The task that is used for these studies is the Sternberg task. This is chosen because it is easily performed, with a large body of literature, is stable over time and largely immune from learning and order effects, and is sensitive to changes in sleep, with measurable decreases in task performance following sleep deprivation. Alternatively, other tasks can be chosen and/or used.

[0067] Determining TMS use parameters involves a series of TMS studies in the BSL and the CAIR 3T fMRI scanner, specially built for interleaved TMS/fMRI studies. The studies flow logically from one to the next, and are linked one on the next, although only 1A3 is truly conditional on prior results. They involve a common task, and a common method of delivering TMS to a particular region. The different studies are labeled as follows:

- [0068] 1A1—TMS during Sternberg; 30 subjects
- [0069] 1A2—TMS preceding Sternberg; 30 subjects
- [0070] 1A3—Replication and refinement of TMS effects; 60 subjects (conditional)
- [0071] 1A4—Testing TMS effects with minor sleep deprivation; 60 subjects

[0072] 1A5—Using interleaved TMS/fMRI to understand TMS effects and find synergistic stimulation (20 subjects)

[0073] 2A6—Using previously acquired fMRI scans to determine the probabilistic method of applying TMS in a man-portable system

[0074] 2A7—Testing whether probabilistic TMS placement is as effective as fMRI guided

[0075] 2A8—Testing whether similar effects are found in women.

[0076] Note that the number of subjects for each study can be modified to include less or more subjects.

[0077] These studies are performed according to the embodiments of the present invention. Most of these studies involve methods recently worked out according to the present invention as illustrated in FIG. 1, which is discussed in detail below.

[0078] fMRI Scan. Within a 1.5 Tesla Philips MRI scanner, subjects were given a high-resolution structural MRI scan, followed by an echoplanar BOLD fMRI scan. During the fMRI scan, subjects had their heads constrained and were able to view stimuli through MRI compatible 3-D goggles. They were also able to respond to stimuli using a two-button response pad. Subjects were then shown the Sternberg task, or a control task including seeing objects and responding to their physical location. The task and control stimuli were presented in block designs of 26 seconds each, alternating over 10 minutes. Subjects were trained on the Sternberg task prior to MRI scanning.

[0079] Image Data Analysis. Images were then transferred from the Philips to a computer system such as the MUSC MAIAL Sun systems. There they were inspected for artifacts, and corrected for motion across the 10 minutes. They were spatially and temporally smoothed using SPM within the software MEDx. Staying within the person's own brain space (that is, not transforming the data to a common brain space), t-tests were performed on the data to discern brain regions that were significantly more active during the Sternberg task than during the control condition. Regions that were significant at the $p < 0.001$ level were then subjected to a cluster analysis of $p < 0.05$. These functional difference maps were then overlaid on the same person's structural MRI scan. The MUSC MAIAL has the ability to perform this series of steps in less than 24 hours. FIG. 2 shows a transverse structural scan of a subject. Also shown are the brain regions that are significantly more active while performing the Sternberg compared to the control task ($p < 0.001$ for display).

[0080] Frameless Stereotaxy. Within the BSL—The MUSC BSL is a beta test site for a frameless stereotaxy system such as one developed at McGill University (Brainsight). These merged structure/function Sternberg images are then transferred to the BSL Brainsight system. The subject is then placed in a modified dental chair with passive head immobilization system. The subject's brain is then stereotactically linked to the fMRI image. The TMS coil is then placed over the subject's brain region, overlying the prefrontal area of maximal activation during the Sternberg minus control conditions as shown in FIG. 3. The TMS coil

US 2005/0256539 A1

Nov. 17, 2005

6

is also positioned over a region in the secondary occipital cortex not activated in the fMRI images.

[0081] Sternberg Testing with TMS using different use parameters. Then, with the TMS coil positioned over the candidate region or control region, in a randomized, counterbalanced manner, the subject performs the Sternberg with TMS applied at different use parameters. FIG. 4 shows the reaction times and error rates for one subject who was stimulated over the prefrontal or occipital regions, each at high frequency (5 Hz) or low frequency (1 Hz), all at 110% of MT.

[0082] Follow-up Testing using the Interleaved TMS/fMRI technique. Once a TMS use parameter is found that has a significant positive effect, then subjects can be placed within the fMRI scanner as shown in FIG. 5, and will perform the Sternberg task, with and without TMS applied to the region. This allows an understanding of how TMS is acting to improve behavior, and it may also identify secondary sites where TMS might be applied with synergistic effects.

[0083] Applicants have spent several years reasoning through the most efficient methods for rationally determining how to apply TMS in cognitive paradigms. The method described herein shows the approach that the applicants determined as the most logical, and the most efficient, at determining how to use TMS to modify cognition and improve performance. This individual fMRI based method of TMS placement, although technically complex, completely solves the issue of where to apply the TMS. With this method, there is no question that the TMS is being delivered at the appropriate location. One can then begin a rational dose finding exploration. When specific dose or use parameter effects are found, the same images that were used to guide the TMS placement in individuals can be examined for probabilistic rules about where to apply TMS short of within individual fMRI guidance.

[0084] Several studies or experiments performed according to exemplary embodiments involving TMS delivered over fMRI identified regions to test if there are frequencies that enhance performance are now described in more detail.

[0085] Subjects: For all experiments in this aspect of the present invention, the applicants recruit healthy young men (age 18-35), with the following inclusion and exclusion criteria: No history of major head trauma or seizures; Medically healthy; No brain diseases; No metal objects in their bodies prohibiting an MRI scan; No history of Substance Abuse; Urine drug screen negative.

[0086] Subjects are studied while free of alcohol or coffee for the day, in a non-sleep deprived state.

[0087] Also, several studies presented here are not involving female subjects. This has several advantages. First, there may be gender differences in regional brain activity and response to TMS. We would have to immediately double our sample sizes and all dosing work. Further, brain excitability and response to TMS changes slightly over the menstrual cycle, and we would need to perform studies in women timed in conjunction with the menstrual cycle. However, the methods and systems described herein can be applied to female subjects.

[0088] Subjects are invited to come to the BSL for initial screening. There they may give written informed consent,

undergo a history and physical examination, undergo minor initial cognitive testing, be trained on the Sternberg, and may provide a urine sample for drug screen.

[0089] On the second visit they may then have an fMRI brain scan (3.0 Tesla, Philips MRI scanner). This gives a high quality structural scan for Brainsight registration, and gives circuit information about Sternberg task performance. This information can be processed in near real-time (24 hours) in the MAIAL, using MEDx and SPM. This generates an activation map within each individual, merged onto that person's brain.

[0090] Two days later they return to the BSL where they will then participate in the following TMS techniques. Motor threshold is determined using standard techniques. In the following, several experiments are described:

[0091] Study 1A1. 30 subjects, each studied twice TMS During the Sternberg. In a complex, 6-hour study, subjects have the Magstim figure eight coil placed over the prefrontal regions identified on MRI scanning. TMS is delivered in the following matrix, with the following 3 variables tested (intensity, frequency, and region): The intensities tested will be—90, 110, 120% of MT. The frequencies tested are 1, 5, 10 Hz. Other frequency values can also be chosen. All epochs last about 10 minutes, with a 10-minute rest. This gives $3 \times 3 \times 2 = 18$ combinations of these variables. 18×20 minutes = 360 minutes (or 6 hours). Studies normally start at 8 am and proceed for 2, 3-hour blocks, with a 30-minute lunch break in between. A standard lunch is provided. Each subject then returns for another similar day, separated by at least one-day rest. The order of variables are randomized and counterbalanced. Performing the same studies twice on each individual can help reduce noise and standard deviation and greatly enhance the ability to find TMS induced cognitive improvement, if it exists.

[0092] TMS is delivered regardless of whether the Sternberg stimulus is being displayed, the interstimulus interval is on, or a response is needed. The reasoning for this is that if TMS needs to be that precisely coupled to stimulus processing, it is unlikely to have field applications.

[0093] Reaction Time and Error Rates: Data obtained for each subject averaged across the two days by condition (e.g. prefrontal 110% MT 5 Hz results from each day will be summed and averaged within each subject). These mean RT and error rates are analyzed using a 3 factor ANOVA testing for location (prefrontal or occipital control), frequency (1, 5, 10), or intensity (90%, 110%, 120% MT). Post-hoc tests are utilized to explore behavioral trends within each factor.

[0094] Sample Sizes and Power: 30 subjects, each with two TMS day-long sessions, provide ample power to detect improvement in Sternberg performance. Note that if positive effects are found, these are subject to later replication, so this sample size is designed to be able to identify an effect, if it exists. This can be tested later for replication. Sample sizes of 20-30 have been used in the literature to show TMS effects on cognition of 10% or more. A formal power analysis reveals that if there is a 5% variation of Sternberg performance across the variables, a sample of 30 subjects will have an Alpha of 0.05 and a 95% power to detect a 5% improvement as a function of one of the 3 factors (intensity, site, frequency). Further, for all effects found, these are tested for replication in a separate cohort (See Study1A3 below).

US 2005/0256539 A1

Nov. 17, 2005

7

[0095] Study 1A2: 30 subjects are split in 2 groups. TMS before Sternberg is being performed. Data from the Queen Square group over motor cortex and from Cohen and colleagues over both motor and occipital cortex have shown that TMS can be delivered before a cognitive task, with resulting lasting effects for up to an hour. In many ways, delivering TMS before a behavior in a real world setting such as a combat setting is advantageous to performing it during the behavior.

[0096] In a similar, 6 hour study, 15 initial subjects have the Magstim figure eight coil placed over the prefrontal site or the occipital cortex. TMS are delivered in the following matrix, with the following 3 variables tested (intensity, frequency, region): In this study, TMS is delivered during the 10 minutes immediately preceding the Sternberg task. There will be no TMS during the actual task. Rather, subjects are examined for lasting effects of TMS delivered before the task. The intensities tested are—90, 110, 120% of MT. The frequencies tested are 1, 5, 10 Hz. All epochs will last 10 minutes, with a 10 minute rest. This gives $3 \times 3 \times 2 = 18$ combinations of these variables. $18 \times 20 \text{ minutes} = 360 \text{ minutes}$ (or 6 hours). Studies normally start at 8 am and proceed for 2, 3-hour blocks, with a 30-minute lunch break in between. Each subject then returns for another similar day, separated by at least one day off. The order of variables are randomized and counterbalanced. Performing the same studies twice on each individual helps reduce noise and standard deviation and greatly enhances the ability to find TMS induced cognitive improvement. Again, other sets of testing parameters can be utilized to provide new set of data.

[0097] Results are analyzed in the first 15 subjects using the 3 factor ANOVA described above. These variables can be examined and predict the use parameters in the next 15 subjects. In this study, the same methods as above are used, except the frequency and intensity with the best effect are utilized, and a new variable of time preceding task is introduced. Thus there is one frequency and one intensity. TMS will be delivered for variable amounts of time (10 min, 20 min, 30 min) and variable times before the Sternberg (10 min, 20 min, 30 min).

[0098] Again, these response data (reaction time, error rate) are analyzed using repeated measures ANOVA examining for dose and time from TMS.

[0099] Study 1A3: Study 1A3 is designed to, among other things, examine replication and refinement of TMS effects. If significant effects are found with either Study 1A1 (During) or 1A2 (Preceding) or both, an attempt is made to replicate these in an independent cohort and examine TMS effects with parameters in the same neighborhood. Thus, these conditional studies in 30 subjects are designed to replicate and extend any findings that might be observed in the initial studies. To do so, an additional 30 subjects are recruited and TMS are performed either during or before the Sternberg so as to explore the neighboring use parameters. For example, if prefrontal TMS 1 Hz, MT were found to enhance the Sternberg during performance, one would retest this, and add the conditions of 1.5 Hz, 0.5 Hz, 90% MT and 110% MT.

[0100] These studies (1A1, 1A2, 1A3) are designed to be performed in subjects who are not sleep deprived. One can question, however, whether effects found in these subjects are able to be applied to the CAP mission of improving

performance during sleep deprivation, which is for each subject a different state from the state where a subject is not sleep deprived. It is possible, although unlikely, that a TMS effect seen in non-sleep deprived conditions might have a paradoxical effect in sleep deprived conditions. More likely is another scenario where TMS is able to have little or a marginal effect under optimum conditions, but a greater effect in slightly degraded conditions. The following two studies are similar to the above studies, but differ in that subjects are admitted overnight to a test facility such as the GCRC and then awakened at 3 am, thus ensuring that they are partially sleep deprived during the TMS session the following day.

[0101] Study 1A4 (during and before Sternberg, with partial sleep deprivation): 60 subjects. The same studies as described above are done with subjects who are partially sleep-deprived. That is, subjects are admitted to the GCRC and awakened at 3 am, and then have testing done on the day following sleep deprivation. They will be sent home for a normal night's sleep, then readmitted the following night and retested, thus having a second day of repeated mild partial sleep deprivation. These studies are needed even if large performance enhancing TMS effects are seen in the earlier, non-sleep deprived studies. These subjects would be run in this study for safety and to make sure that TMS stimulation parameters that are helpful in non sleep-deprivation are not problematic or worsening in sleep deprived individuals.

[0102] Study 1A5: 20 subjects. Study 1A5 utilizes TMS within the fMRI scanner to examine effects found. When significant effects are found in any of the Studies 1A1, 1A2 and 1A3, as they do, TMS is then performed within the fMRI scanner at the location with use parameters found to have a behavioral effect. This study provides valuable information about how TMS is producing its effects, and might indicate other regions where TMS could be applied in a synergistic fashion in addition to prefrontal stimulation. This study may also aid greatly in understanding how focal or diffuse the TMS application might be in order to achieve behavioral effects.

[0103] In doing so, TMS is administered within the fMRI scanner at the use parameters found in the earlier studies, while subjects are performing the Sternberg task. Data analysis is performed similar to that used to determine the optimum spot for TMS placement.

[0104] Study 2A6: To answer how precise must the placement be to achieve enhancement in performance, Study 2A6 is designed to perform image data analysis. Thus, in this study, no new subjects, but examination of imaging data previously acquired. If performance effects are found using the very precise anatomical precision method, there is a need to see if TMS can be done in a less precise anatomic location method. The functional imaging scans obtained in the earlier parts of the Studies 1A1-1A5 will be analyzed in MedX to generate a probabilistic rule for how imprecise to place the TMS coil and still improve performance. This may involve examining the range of regions identified as critical in Sternberg performance across subjects and then morphing individual brain scans into a common brain space.

[0105] Study 2A7: Among other things, study 2A7 is designed to test whether probabilistic TMS placement is as effective as fMRI guided. In this study, the rule generated in

US 2005/0256539 A1

8

Nov. 17, 2005

Study 1A6 is directly tested in a new cohort of 30 subjects. The use parameters are those previously identified as optimum for maximizing effects. The variable to be explored here is location of the TMS coil—fMRI guidance, versus the rule-based algorithm identified above. In addition to a direct test of the proposed algorithm, TMS is systematically delivered in 1-mm increments away from the MRI identified region, to assess how imprecise the TMS application might be.

[0106] Study 2A8: Among other things, Study 2A8 is designed to test whether similar effects are found in women. In one embodiment, the test group includes 30 women. In particular, before a TMS system could be used in the military, it would be important to determine if similar effects are seen in women. Thus, in 30 women screened as above, they would have TMS applied in the manner determine in Study 1A1-1A5 testing to have optimum effects.

[0107] An Experiment:

[0108] In yet another experiment/study, a plurality of subjects was divided into two groups. The first group contained 6 subjects with clear improvements in the Sternberg (RT) with the prefrontal TMS. The second group contained 6 subjects with clear worsening. Each group then was monitored for each subject's activity during the Sternberg within the fMRI, wherein no TMS was applied. Data was obtained and then analyzed to show that the TMS prefrontal improves (the first group) used prefrontal cortex and cingulated during the Sternberg; in contrast, those in the second group whom TMS did not improve RT, or even worsened it, did not use prefrontal and cingulated but instead used parietal and visual cortex (and/or maybe basal ganglia). Thus, different people use different neural circuits, both at rest and when sleep deprived, and these circuits can be identified and selected by fMRI, which in turn allows TMS to be used to either restore function or train or refrain circuits according to the present invention.

[0109] B. Designing A Portable TMS System

[0110] Another aspect of the present invention relates to a portable TMS system that can be used in real world situations to enhance cognitive performance. To achieve effective TMS with a man-portable system, there are 3 major considerations: 1) physical size of the TMS "coil", 2) device positioning, and 3) power requirements. With all three, there are conflicting demands on the system. A small sized "coil" would be more portable, but, if too small, might not be effective at stimulating the brain. A system that would allow the coil's position to range over an area would make it possible to accommodate the varied brain anatomy of different people, but would likely be more bulky and complex. Increased power demands almost always introduce complexity and weight, but decreasing the power of the system would also likely mean that greater accuracy would be required in coil positioning.

[0111] Improved understanding of the absolute requirements for effective TMS gained in practicing the present invention provides clearly defined constraints for the design, and innovations in materials and/or design, though not eliminating these conflicts, may reduce them so that a practical man-portable TMS system is achievable according to the present invention.

[0112] A portable TMS system according to an exemplary embodiment, takes into consideration at least some of the following:

[0113] 1) TMS anatomical characterization, i.e., where in the cerebral cortex does neuronal discharge occur: a) sulcus, b) crown of gyrus, c) transition zone, or d) a combination of them;

[0114] 2) TMS physical characterization, i.e. functional relation between TMS "coil" field and degree of neuronal activation;

[0115] 3) TMS "coil" coverage requirements, i.e. a) localized or nonlocalized stimulations, b) single or multiple stimulation sites, c) field profile requirements, full widths at half maximum (FWHM): W_x, W_y, W_z ;

[0116] 4) TMS "coil" positioning requirements, i.e. must the coil position be adjustable to accommodate different brain anatomy, range of movement: $R\phi, R\theta, Rr$;

[0117] 5) Magnetic field characteristics of concept coils: standard figure-8, modified figure-8, programmable lattice, spinning magnet, moving magnet, and phased-array;

[0118] 6) Conductivity model of human brain;

[0119] 7) Electric field characteristics of concept coils: standard figure-8, modified figure-8, programmable lattice, spinning magnet, moving magnet, and phased-array;

[0120] 8) Induced current characteristics of concept coils: standard figure-8, modified figure-8, programmable lattice, vibrating permanent magnet, and phased-array;

[0121] 9) TMS induced current measurement project: To determine if TMS induced currents might be mapped in-vivo;

[0122] 10) Power requirements for TMS stimulator;

[0123] 11) Preliminary design for reduced power TMS stimulator; and

[0124] 12) Concepts for man-portable power supply.

[0125] Some aspects of design characteristics of a portable TMS system according to an exemplary embodiment are discussed in more detail below.

[0126] Magnetic Field and Induced Currents Versus Brain Activation

[0127] Better data is needed on the relationship between the magnetic field of the TMS coil and the induced currents, and, in turn, the anatomy of cerebral cortex and the actual depolarization of neurons in cerebral cortex. FIGS. 6 and 7 schematize and scale these relationships for orthogonal orientations of a standard figure-8 TMS coil to help more quantitatively define some of the factors involved in TMS, factors which will likely constrain the design of a man-portable TMS system. This provides information about where one needs to stimulate, how focal the stimulations needs to be, and the preferred direction of the induced electric fields. It gives information on the variation in brain anatomy between individuals. Combining this information,

US 2005/0256539 A1

9

Nov. 17, 2005

one can get an idea of the required size of the “coil” and if it will be necessary to position it differently for different brain anatomies, i.e., if one size fits all, or if one needs to custom fit the “coil” to each person. It also provides information about the field intensities that must be produced, and how they must be directed relative to the relevant structures in the brain. This is important for deciding on a configuration for the coil as well as the power requirements.

[0128] Data about size and location of TMS Performance related activations and coil position relative to activation are also needed. Data may come from BrainSight data from Studies 1A1-1A5. This information tells one about the importance of position, i.e., is the effect sensitive to position, or can a generalized stimulation be used.

[0129] Data about spatial variation of relevant brain structures are obtained to tell one whether a single configuration is sufficient, or, at the other extreme, if the coil must be customized for or adaptable to each individual. This largely involves a comprehensive literature review of published data (human and animal) and then examination of the BrainSight data being collected in Study 1A2-1A5 subjects.

[0130] Data about magnetic field vector at activation site can be obtained from two ways. First, phase maps and TMS/fMRI data from past studies are utilized: Using data from previous TMS/fMRI studies over motor cortex, the relative displacements of TMS coil, motor cortex, and fMRI activation will be obtained. These will then be combined with simulations of the TMS coils magnetic field and knowledge of the anatomy of motor cortex to gain a better understanding of the relationship between magnetic field and cerebral cortex for optimum stimulations. FIG. 8 shows exemplary results according to the present invention. The relative positions of TMS-induced thumb movement and a similar movement executed volitionally are determined (Bohning et al., 2000). Coil and magnetic field distributions may be added to complete the picture relating activation and magnetic field. FIG. 9 shows more of this preliminary work on this problem, an image of the brain with the fMRI activation in motor cortex superimposed and an arrow indicating the directions and magnitude of the magnetic field at the center of the fMRI activation.

[0131] Additionally, the computed B-field of the coil combined with BrainSight Data from Studies 1A1-1A5 can be utilized. As in the above case, this can provide data about the relative displacements of the TMS coil stimulation and the area of activation in motor cortex. Though it may not show the area of activation as does fMRI activation, it can show the position of the TMS coil position at which the maximum motor evoked potentials (MEPs) were induced relative to brain anatomy. This facilitates one to tie magnetic field to area of cerebral cortex in which neuronal discharge occurs as well as the anatomical structure.

[0132] Magnetic Field, Electric Field and Induced Current Simulations for Different Coil Designs

[0133] The field patterns of the different coil configurations are a major factor in either eliminating a particular coil design or selecting it for further development. In one embodiment, the coil is capable of stimulating the desired area(s) effectively, and if focal rather than diffuse stimulation is desired, it must not stimulate other areas.

[0134] Field Simulations are performed for standard figure-8, modified figure-8, programmable lattice, vibrating

“crescent” permanent magnet, and phased-array. The simulations will be similar, except that the electric field induction is caused by the movement by the vibrating permanent magnets, rather than by current pulses as in the figure-8 and lattice coil. Alternatively, field simulations can be conducted on computer models.

[0135] B-field phase maps are utilized as well. The coils magnetic field pattern can be measured using MRI phase maps to check the computed magnetic fields (Bohning et al., 1997). FIG. 10 illustrates the principle, and FIG. 11 shows brain images on which a surface approximately 2 cm below the scalp, about the depth of most TMS and at different depths.

[0136] MRI segmentation into gray and white matter and CSF for conductivity volume map are used in the present invention. Moreover, phase map fMRI technique is used to advance understanding in this area.

[0137] Induced E-Field Simulations:

[0138] The induced E-field may be computed in a plane parallel to a simple figure-8 coil and homogeneous medium. It would be necessary to do this for a volume encompassing the areas of the brain to be stimulated and extend the calculations to, at least, a three component model of brain tissue, i.e., gray and white matter and CSF.

[0139] Induced J-Currents Simulations:

[0140] Induced currents actually cause the neuronal discharge associated with the activation.

[0141] Induced E-Field and Induced J-Currents Versus Brain Anatomy Mapping:

[0142] It has been estimated that the transmembrane current flow needed to depolarize the membrane is caused by the spatial derivative of the electric field along the axon, dE/dx , (Reilly 1992; Abdeen and Stuchly 1994; Garnham et al. 1995) and that the peak spatial derivative needed to achieve stimulation is approximately 5 kV/m^2 (Rudiak and Marg 1994). Our simulations along with previously acquired data and data from the above studies should make it possible for us to check and extend these observations.

[0143] Power Requirements:

[0144] Based on the strength-duration relation for neuronal depolarization,

$$\begin{aligned} Q(t) &= Q_0 \left[1 + \frac{\Delta t}{\Delta t_0} \right] \\ J(t) &= J_0 \left[1 + \frac{\Delta t}{\Delta t_0} \right] \end{aligned}$$

[0145] where Q_0 =minimum threshold depolarization charge density for nonleaky membranes

[0146] J_0 =rheobase, the minimum stimulus current density that can attain threshold at infinite duration

[0147] Δt_0 =the strength-duration time constant (chronaxie) ($\approx 150 \mu\text{s}$, Barker et al., 1991) and our estimates of induced currents, we will attempt to adjust the TMS pulse waveform to increase depolarization efficiency and reduce power consumption.

US 2005/0256539 A1

Nov. 17, 2005

10

[0148] Moving Magnet Induction

[0149] Though there are no resistive losses due to large currents, the “moving” magnets have to be moved in approximately a quarter of a millisecond. This will require some sort of electromechanical device, which itself will consume power, to overcome the coil’s inertia, move it a short distance and then return, which could be cumbersome and fragile. A magnet spinning at high speed, would require neither a large current, nor the generation of the forward and backward impulses of a pulsed system, but would require power to bring the spinning magnet up to speed and keep it there and would generate current continuously not pulses. There would also be a problem with the gyroscopic effect of any magnet, large enough to stimulate the brain, spinning at high speed. In addition, there is no data on the stimulation pattern of such a TMS “coil”, so extensive simulations would be necessary. However, these concepts should not be rejected out of hand, and the information gained through the associated simulations would increase our understanding of the magnetic fields and induced currents of any design.

[0150] Electronic Induction

[0151] Though the absolute power requirements will only be known once the TMS performance studies have been completed, to tell us the frequency and duration of stimulation, it is certain that we will be aiming at the absolute minimum power per pulse required for effective stimulation. This can be explored by 1) reducing resistive and inductive power loss in the “coil” and 2) altering pulse waveform for more efficient excitations, and resonant stimulator power. Resistive and inductive loss reduction will be sought through the uses of new “coil” materials, e.g., silver and/or room temperature superconductors, and “coil” conformation changes to confine losses to those associated with currents induced in the brain. We also explore the use of an impedance matching gel filled liner to take shape of head to see if this may improve current distribution or reduce power consumption. The shorter the stimulating waveform, the less power that is required to induce neuronal discharge, hence we design a stimulator power supply that puts out shorter waveforms, and, operates in a “resonant” mode to recapture the returning pulse.

[0152] Stimulation Control

[0153] According to exemplary embodiments, for stimulation control, the following are provided and modeled: a means for controlling the TMS stimulation, stimulation pattern control, and programmable lattice coil position control, which can be merely a means of activating the lattice elements to create a coil of a particular size at a particular position, or, it can include a test sequence for customizing the coil to accommodate individual anatomy.

[0154] Coil Designs, i.e., Possible Solution Devices

[0155] The following designs are modeled according to exemplary embodiments:

- [0156]** Standard figure-8;
- [0157]** Modified figure-8;
- [0158]** Programmable Lattice;
- [0159]** Vibrating magnets; and

[0160] MEMs—Micro-electromechanical Devices—
Assess possible application in cortical stimulation phased array.

[0161] According to exemplary embodiments, several (at least 3) prototypes of the portable TMS system are produced and tested in conditions gradually approaching actual combat. The initial testing would be done in the BSL using military simulator computer programs. If these were successful, then testing would be performed in the actual field.

[0162] For each prototype delivered, the device is tested for performance capabilities (e.g., Tesla generated, heating, weight, etc.). Then, the prototype is used in the BSL on subjects and record performance behavior and other side effects.

[0163] Prototype 1 will be performance tested in the BSL, likely using flight simulators or submarine simulators, as well as the Sternberg task, by using likely simulators would be those involving long range flight simulators, or Advanced SEAL Delivery Systems.

[0164] Prototype 2 would be field tested in an armed services testing lab, and Prototype 3 would be tested in actual field conditions. Testing would be done under optimum and mildly sleep deprived conditions. Initial testing (prototype 1) would be done on healthy young men or women. Later testing would involve trained warfighters. Prototypes would be evaluated as well for safety (neuro-psychological and behavioral as well as for the device itself).

[0165] In summary, the present invention provides, among other things, the following:

- [0166]** 1) fMRI images: In one example, a series of fMRI activation maps in 120 healthy young men while performing the Sternberg task. These maps would show how much the functional localization of the Sternberg task varies across individuals.
- [0167]** 2) TMS use parameter dose response performance data, both at baseline and after partial sleep deprivation; a detailed dose finding study of whether and how TMS might modify Sternberg performance if delivered during the task or before it. These TMS effects would be understood both at baseline and under conditions of partial sleep deprivation.
- [0168]** 3) Interleaved TMS/fMRI maps showing how TMS applied at key regions modifies circuit behavior and changes performance.
- [0169]** 4) Design maps and models of Man-portable TMS Systems: These would be detailed and able to be presented to industry for prototype construction.
- [0170]** 5) 3 working prototypes of a man-portable TMS system.
- [0171]** 6) Detailed data on whether and how these systems perform in simulator and field testing.
- [0172]** 7) Improved understanding of how to create TMS systems for mass use without the need for individual fMRI guidance of TMS placement.
- [0173]** 8) Understanding of whether TMS works at these parameters in women as well as men.

US 2005/0256539 A1

Nov. 17, 2005

11

[0174] This body of work has the potential for revolutionizing the approach to enhancing cognitive performance by focusing on brain circuits and minimally invasive brain stimulation.

[0175] While there have been shown preferred and alternate embodiments of the present invention, it is to be understood that certain changes can be made in the form and arrangement of the elements of the system and steps of the method as would be known to one skilled in the art without departing from the underlying scope of the invention as described herein. Furthermore, the embodiments described above are only intended to illustrate the principles of the present invention and are not intended to limit the scope of the invention.

[0176] Moreover, the texts and drawings of the Appendix are incorporated into the application by reference as an integral part of the application. Additionally, the documents listed in the Appendix are incorporated into the application by reference.

What is claimed is:

1. A method for using transcranial magnetic stimulation to enhance cognitive performance, comprising the steps of:

locating at least one neural circuit in the brain of a subject, which is activated when the person performs a predetermined task;

positioning an electromagnetic coil over a region on the scalp of the subject corresponding to the at least one neural circuit in the brain of the subject; and

delivering a transcranial magnetic stimulation from the coil to the region on the scalp of the person to induce current to flow in the brain that causes neuronal depolarization in the brain and effectuates a change in the performance of the predetermined task by the subject.

2. The method of claim 1, wherein the subject is a human being.

3. A method for using transcranial magnetic stimulation to enhance cognitive performance in a plurality of subjects, comprising the steps of:

dividing the plurality of subjects into groups,

subjecting each of the groups into a first state and a second state,

locating at least one neural circuit in the brain of a subject in the group corresponding to one of the first state and the second state, which is activated when the subject performs a predetermined task under one of the first state and the second state,

positioning an electromagnetic coil over a region on the scalp of the subject corresponding to the at least one neural circuit in the brain of the subject, and

delivering a transcranial magnetic stimulation from the coil to the region on the scalp of the subject to induce a current to flow in the brain that causes neuronal depolarization in the brain and effectuates a change in the performance of the predetermined task by the subject under one of the first state and the second state.

4. The method of claim 3, wherein the subjects are human beings.

5. The method of claim 3, wherein the first state is a state in which a subject is at rest, and the second state is a state in which a subject is sleep-deprived.

6. The method of claim 3, wherein functional magnetic resonance imaging maps are used to identify different neural circuits associated with different subject on a state, wherein the neural circuits are activated while a predetermined task is performed.

7. The method of claim 6, wherein transcranial magnetic stimulation is delivered to proper neural circuits to restore and/or retrain the circuits to enhance the performance.

8. A method of using transcranial magnetic stimulation to enhance cognitive performance in at least one subject, comprising:

during a behavior individualized imaging of at least one cognitive neural circuit, locating the at least one cognitive neural circuit, individually positioning an electromagnetic coil over a region on the scalp of the subject corresponding to the at least one cognitive neural circuit, and delivering a stimulation through the electromagnetic coil to the at least one cognitive neural circuit to affect the behavior related to the at least one cognitive neural circuit.

9. The method of claim 8, wherein individualized imaging can be performed by a functional magnetic resonance imaging scanner.

10. The method of claim 8, wherein the electromagnetic coil is interleaved with a transcranial magnetic stimulation system to provide synergistic stimulation(s).

11. A system for using transcranial magnetic stimulation to enhance cognitive performance in at least one subject, comprising:

means for locating at least one neural circuit in the brain of a subject, which is activated when the subject performs a predetermined task,

an electromagnetic coil that can be positioned over a spot on the scalp of the subject corresponding to the at least one neural circuit in the brain of the subject, and

means for delivering a transcranial magnetic stimulation from the coil to the spot on the scalp of the subject so as to induce a current to flow in the brain, cause neuronal depolarization in the brain, and effectuate a change in the performance of the predetermined task by the subject.

12. The system of claim 11, wherein the locating means includes a functional magnetic resonance imaging system that can be utilized to scan and generate maps of the interested neural circuits so as to locate proper neural circuits responsible for a predetermined task.

13. The system of claim 11, further comprising a computer having a CPU and one or more memory devices to coordinate the operation among the different parts of the system, optimize the operation parameters, and facilitate the transcranial magnetic stimulation delivering.

14. The system of claim 13, wherein the operation parameters are transcranial magnetic stimulation parameters.

15. A portable system for using transcranial magnetic stimulation to enhance cognitive performance in at least one subject, the system comprising:

a CPU;

an energy source electrically coupled to the CPU;

US 2005/0256539 A1

Nov. 17, 2005

12

a database in communication with the CPU and having functional magnetic resonance imaging (fMRI) maps of neural circuits corresponding to a plurality of tasks stored therein; and

a movable electromagnetic coil electrically coupled to the energy source and in communication with the CPU, wherein when a subject is to perform a predetermined task, the CPU selects one or more fMRI maps of one or more neural circuits from the corresponding to the predetermined task from the database and causes the movable electromagnetic coil to be positioned over a region on the scalp of the subject according to the selected one or more fMRI maps, and the movable electromagnetic coil delivers transcranial magnetic stimulation to the region on the scalp of the subject so as to induce a current to flow in the brain, cause neuronal depolarization in the brain, and effectuate a change in the performance of the predetermined task by the subject.

16. The system of claim 15, wherein the energy source is a battery.

17. The system of claim 15, wherein the database is associated with a memory device of the CPU and/or a separate memory device.

18. The system of claim 15, wherein the subject is a person.

19. The system of claim 15, wherein the subject is an animal.

20. The system of claim 15, wherein the system is constructed within a frame that is portable.

21. The system of claim 15, wherein the system comprises an array of transcranial magnetic stimulation coils, each being able to deliver transcranial magnetic stimulation individually or in coordination.

* * * * *

EXHIBIT 15

Therapeutic Effects of Individualized Alpha Frequency Transcranial Magnetic Stimulation (α TMS) on the Negative Symptoms of Schizophrenia

Yi Jin^{1,2}, Steven G. Potkin², Aaron S. Kemp²,
Steven T. Huerta², Gustavo Alva², Trung Minh Thai²,
Danilo Carreon², and William E. Bunney, Jr.²

²Department of Psychiatry and Human Behavior,
University of California, Irvine, School of Medicine

Previous research in clinical electroencephalography (EEG) has demonstrated that reduction of alpha frequency (8–13 Hz) EEG activity may have particular relevance to the negative symptoms of schizophrenia. Repetitive Transcranial Magnetic Stimulation (rTMS) was utilized to investigate this relationship by assessing the therapeutic effects of stimulation set individually at each subject's peak alpha frequency (α TMS). Twenty-seven subjects, with predominantly negative symptom schizophrenia, received 2 weeks of daily treatment with either α TMS, 3 Hz, 20 Hz, or sham stimulation bilaterally over the dorsolateral prefrontal cortex. Individualized α TMS demonstrated a significantly larger ($F_{3,33} = 4.7$, $p = .007$) therapeutic effect (29.6% reduction in negative symptoms) than the other 3 conditions ($< 9\%$). Furthermore, these clinical improvements were found to be highly correlated ($r = 0.86$, $p = .001$) with increases (34%) in frontal alpha amplitude following α TMS. These results affirm that the resonant features of alpha frequency EEG play an important role in the pathophysiology of schizophrenia and merit further investigation as a particularly efficacious frequency for rTMS treatments.

Key words: alpha rhythm/ α TMS/schizophrenia/EEG/transcranial magnetic stimulation

Introduction

As introduced by Anthony Barker in 1985, transcranial magnetic stimulation (TMS) offers a noninvasive method of inducing electrical activation of the brain. In accordance with the principles of electromagnetic induction,

a high voltage pulse of electricity passed through a coil placed adjacent to the scalp can generate a brief magnetic field perpendicular to the electric current flow. The magnetic field, in turn, will pass through the skull unimpeded and induce a secondary electric current in the brain.¹ The secondary current has exactly the same alternating rate with opposite direction as the original pulses in the coil. These features of electromagnetic stimulation have provided us with a unique tool to perturb or tune electric oscillatory activities in the brain.

Primarily utilized as a probe for cortical mapping of distributed neural circuits and associated cognitive, motor, or behavioral functions, TMS has proven to be an invaluable addition to the tools of functional brain research.² Of particular relevance to the current investigation, however, are the recent attempts to explore the therapeutic potential of the method as a unique treatment modality for a variety of neuropsychiatric disorders.³ Repetitive TMS (rTMS), which refers to the use of grouped pulses of stimulation employed at precise frequencies to achieve a constant train of activation over brief periods of a treatment session, has become the most widely explored method of administration.

Within established rTMS treatment parameters, however, there still remains considerable uncertainty as to how best to optimize therapeutic efficacy for the various illnesses under investigation. Among such stimulation parameters that require optimization are

1. Frequency—Higher frequencies (> 10 Hz) have been commonly believed to increase cortical excitability, while lower frequencies are thought to act as inhibitory;
2. Intensity—Generally quantified for each individual as a percentage of the threshold at which motor activity can be elicited (~ 1 –2 Tesla);
3. Duration—To reduce risk of seizure or muscle tension pain, pulse trains are normally brief (1–2 seconds), and intertrain intervals are generally 30–60 seconds; and
4. Site of Stimulation—Varies depending on patient population or specific brain functions under investigation. Central to the current study was the question of what would be the optimal stimulation frequency to use in the treatment of the negative symptoms of schizophrenia.

¹To whom correspondence should be addressed; e-mail: yjin@uci.edu.

While rTMS has been extensively studied in the treatment of depression and other disorders, there has been only a limited number of reports on its clinical effects in the treatment of schizophrenia.⁴ Using low frequency (1 Hz) stimulation over left temporoparietal cortex, Hoffman et al.⁵ reported statistically significant decreases in auditory hallucinations in schizophrenia as compared with sham stimulation. These results have also been replicated by d'Alfonso et al.⁶ using similar treatment parameters. Geller et al.⁷ found beneficial effects of slow (1 Hz) rTMS at suprathreshold intensity through a nonfocal stimulation over vertex, which affected both hemispheres in 10 subjects with schizophrenia. In contrast to the low frequency approach, Rolnik et al.⁸ used a fast rate rTMS of 20 Hz at 80% motor threshold (MT) in a small group of patients with schizophrenia and found that 2 weeks of daily treatment over left dorsolateral prefrontal cortex (DLPFC) significantly reduced the psychotic symptoms, as indicated by the reduction of Brief Psychiatric Rating Scale (BPRS) scores, whereas depressive and anxiety symptoms did not change significantly. With similar stimulation frequency and intensity (20 Hz and 80% MT), Cohen et al.⁹ reported their findings in schizophrenia with predominant deficit syndromes, demonstrating that bilateral fast rTMS of prefrontal area might be beneficial to patients by reducing their negative symptoms.

While various parameters and their combination need to be more fully investigated, the present study was designed to compare the efficacy of different frequencies of rTMS in treating schizophrenic subjects with predominant negative symptoms, a complex syndrome that includes social withdrawal, affective flattening, poor motivation, and apathy. Compared with low (3 Hz) and high (20 Hz) frequencies, we hypothesized that frontal lobe rTMS with individualized stimulus rate at subjects' peak alpha EEG frequency (8–13 Hz) would be most effective as a treatment. This hypothesis is based on a well-documented EEG finding that patients with schizophrenia have reduced alpha activity (power and coherence) at rest¹⁰ or during sensory and cognitive stimulations.^{11,12} Studies have also shown that the decrease in alpha power was associated with patients' psychotic symptoms^{13,14} and that the clinical improvement in negative symptoms following clozapine treatment was correlated with the degree of photically driven alpha EEG normalization in the frontal cortex.^{15,16} Considering the resonant features of alpha EEG oscillation,^{17,18} the reported intra-individual stability of alpha peak frequencies,^{19,20} and the purported association of reduced alpha activity to schizophrenia symptomatology, we predicted that the stimulus rate of rTMS set individually at each subject's intrinsic peak alpha frequency would increase frontal alpha activity and, consequently, reduce the clinical symptoms.

Methods

Subjects

Twenty-seven patients diagnosed with schizophrenia (age: 37.7 ± 9.0 years old; sex: 18 males, 9 females) presenting predominantly negative symptoms and stabilized on current antipsychotic medications for at least 30 days were enrolled in the study at the outpatient clinic of the University of California, Irvine, Neuropsychiatric Center. Each patient received a structured interview with 2 research psychiatrists and met the DSM-IV diagnostic criteria for schizophrenia or schizoaffective disorder. Severity of symptoms was evaluated by the Positive and Negative Syndrome Scale (PANSS). During the subject recruitment, a minimum score of 20 on the PANSS negative symptom subscale and a maximum score of 19 on the positive symptoms subscale were required at baseline. Patients who met any of the following criteria were excluded: significant physical illness in the 4-week period preceding the start of the study, current diagnosis or past history of epilepsy or indication of seizure proneness on EEG screening, major head trauma, progressive neurological diseases, high dose (> 400 mg) clozapine in the past 3 months, electric convulsion treatment in history, present history of any other psychiatric diagnosis, drug dependence, or toxic psychosis in the preceding 8 weeks. Each patient provided fully informed, institutional review board–approved, written consent before participation in any study procedures.

Procedure

Four rTMS treatments with 3 different frequencies and a sham stimulus were included in a double-blind crossover design. Each patient had an equal chance to be assigned into 2 study groups, each of which included 2 treatments (ie, alpha/sham or 3 Hz/20 Hz). Patients were kept blind to the treatment condition for the duration of the study. Treatment order of the combinations was random. Each treatment consisted of 10 daily sessions during a 2-week period, with 2 weeks of no treatment between conditions. Patients' current antipsychotic treatments were kept unchanged during the rTMS study. In each daily treatment session, a CADWELL 9-cm circular coil was placed on the middle of the forehead with the side edges reaching the areas of F₃ and F₄ EEG electrode locations. Stimulation was given 2 seconds per minute for 20 consecutive minutes per session at an intensity of 80% motor threshold, a minimal magnetic pulse that reliably induced visible contra lateral thumb movement (average intensity: 149.5 joules per pulse). The frequencies for the active stimuli were 3 Hz, individualized alpha (8–13 Hz) and 20 Hz. Rate for the alpha frequency stimulation was determined at the nearest integer of each patient's average alpha peak frequency, obtained from 5 frontal EEG leads (F₇, F₃, F_z, F₄, F₈). Sham stimulation was given by applying an unplugged coil to the forehead and an activated coil left 2 feet away behind the patient.

During the EEG recording, patients were in a supine position and asked to relax with their eyes closed throughout the testing period. Nineteen EEG electrodes (Ag–Ag Cl) were used according to the International 10–20 system and referenced to linked mastoids. Electro-oculograms (EOGs) from the outer canthus of both eyes were recorded simultaneously to monitor eye movements. The impedance of each electrode was lower than 5 K Ω . Two minutes of EEG epochs were collected and digitized by a 16-bit A/D (analog/digital) converter at the rate of 256 Hz and further processed digitally by Neurodata Inc (QND 10.2) data acquisition system. Sixty seconds of artifact free epochs were utilized for fast Fourier transformations (FFT). FFT window was set at 512 data points with 80% overlap.

Severity of psychosis, depression, and movement disorders were assessed with PANSS, Montgomery-Asberg Depression Rating Scale (MADRS), Barnes Akathisia Rating Scale (BARS), and Simpson-Angus Scale (SAS), respectively. All rating scales and EEGs were administered at screening, baseline (immediately prior to first treatment), immediately following the fifth and tenth treatments, and after 2 weeks of washout for each condition. While the technician administering the rTMS procedures (SH) could not be blinded, the evaluating physicians (AG, TT, and DC), EEG technicians (YJ and AK), and patients remained unaware of the type of treatment throughout the duration of the study. A priori categorical definition for clinical response was $> 30\%$ baseline-to-posttreatment reduction, or < 16 at the end of second phase treatment when baseline score was lower than 20 on PANSS negative symptom subscale.

Statistical Analyses

Clinical data were analyzed on an intent-to-treat basis with the last observation carried forward. Patients with a baseline and at least 1 additional set of completed assessments (at least 5 treatment sessions) were included in the analysis of mean treatment effect. Efficacy in clinical ratings was evaluated by using analyses of variance (ANOVA). The models included 1 between-subjects factor of treatment, and 2 within-subjects factors of time and treatment order. Covariance for the baseline was used when significant group difference was found at the baseline. The Kruskal-Wallis test was used for post hoc comparisons of clinical responsive among treatment groups.

Raw EEG data were edited offline by an experienced technician who was blind to the treatment conditions to eliminate any significant ($> 3^\circ$ arc) eye movements or any other type of apparent artifact. Twenty-four to thirty artifact-free epochs (512 data points per epoch) in each recording channel were calculated by a fast Fourier transform (FFT) routine to produce a power spectrum with $\frac{1}{2}$ Hz frequency resolution, through which 5 consecutive EEG bands (δ : 0.5–4.0 Hz, θ : 4.5–7.5 Hz,

α : 8.0–13.0 Hz, and β : 13.5–30.0 Hz) were yielded. Peak frequency and power density of each band were automatically calculated. In this study only the alpha band was reported. Variable for each channel was normalized by dividing power in every frequency band by the total energy across the entire spectrum and presented as relative power density. To further reduce the data, FFT coefficients from 19 EEG channels were clustered into 3 regional measures on both hemispheres, namely, the frontal, temporal, and parieto-occipital areas. Multivariate analysis of variance (MANOVA) with repeated measures was used to determine the main effect interactions. This model included 1 grouping factor (treatment) and 3 within-factors (time, brain region, and hemisphere). Huyhn-Feldt adjustments for degree of freedom were applied when the assumption of variance-covariance matrix to be circular in form was violated. Pearson correlation coefficients were used to test the association between changes in EEG and negative symptoms.

Results

Twenty patients finished at least 1 phase of treatment, resulting in 11 cases in the α TMS group, 8 in the sham group, 9 in the 3 Hz group, and 9 in the 20 Hz group. Before the completion of phase 1, 3 patients dropped out from the high-frequency group, 2 from the low-frequency group, 1 from the alpha frequency group, and 1 from the sham group because of the discomfort of the stimulation or the exacerbation of psychotic symptoms during the treatment. No adverse effects were found to be directly related to the rTMS in any treatment group. Two major positive results are summarized as follows:

1. Patients' negative symptoms were greatly reduced with α TMS (Figure 1). Compared with sham ($8\% \pm 0.2$) and both low- ($9\% \pm 0.12$) and high-frequency ($-4\% \pm 0.18$) rTMS groups, individualized α TMS (mean stimulus rate: 8.6 Hz ± 0.8) produced significantly greater reduction ($29.6\% \pm 0.27$) of PANSS negative symptom scores ($F_{3,33} = 4.7$, $p = .007$). There was no significant main effect interaction among factors of treatment order, evaluation time, and group. Using $> 30\%$ improvement or < 16 endpoint rating on PANSS negative symptoms criteria, we further observed that 6 of 11 patients responded to the alpha treatment, while only 1 responded to the low-frequency, 1 to sham, and none to the high-frequency stimulation. A Kruskal-Wallis test showed the group asymmetry among the 4 treatments to be highly significant ($\chi^2 = 9.33$, $p = .009$). There was no statistical significance among the groups in positive symptom changes. Treatment effects on depressive symptoms (MADRS) and movement scales (BARS, SAS) were also not statistically significant.

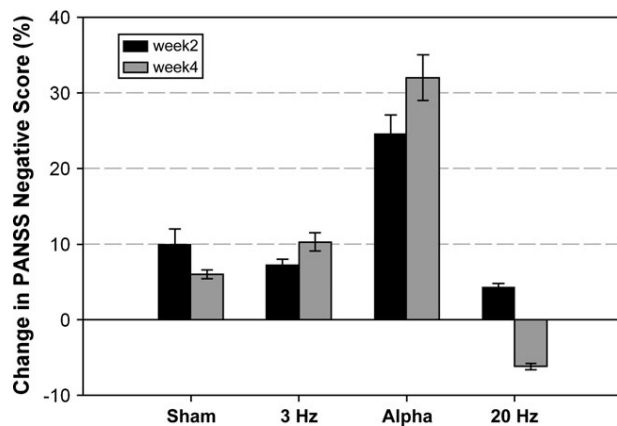


Fig. 1. Clinical response to rTMS at 3 Hz ($n = 9$), 20 Hz ($n = 9$), alpha frequency ($n = 11$), and sham ($n = 8$) immediately following 2 weeks of treatment (Week 2) and after an additional 2 weeks following end of treatment (Week 4). The level of response is shown as percent decrease (improvement) from baseline Positive and Negative Syndrome Scale (PANSS) negative symptom subscale scores.

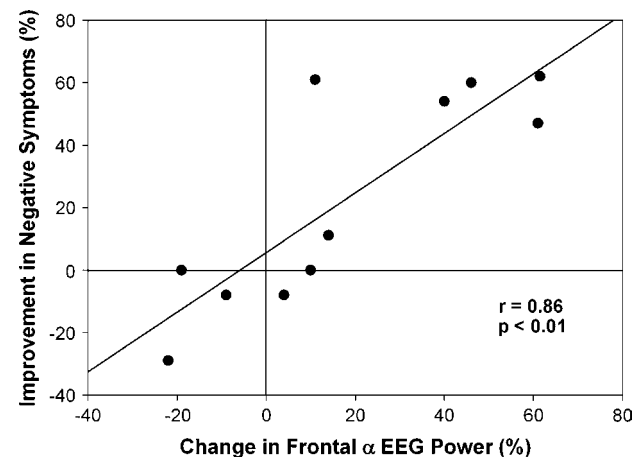


Fig. 2. Percent improvements in the Positive and Negative Syndrome Scale (PANSS) negative symptom subscale were significantly correlated with changes in the alpha band (α : 8–13 Hz) EEG in the frontal cortex of those patients receiving the individualized α TMS. Such correlations were not found for any of the other treatment groups or cortical regions examined.

2. EEG change following α TMS predicted clinical improvement (Figure 2). The individualized α TMS produced a marked increase ($34\% \pm 0.3$) in power of the alpha EEG activity, primarily in the frontal area, while there were no significant EEG changes in sham (0 ± 0.19), low-frequency ($14\% \pm 0.31$), or high-frequency treatment groups ($6\% \pm 0.32$). Analysis of variance with repeated measure (MANOVA) revealed a significant difference among the treatment groups ($F_{2,126} = 3.27$, $p = .03$). Correlational analyses demonstrated that improvements in negative symptoms following α TMS treatment were highly associated with the degree of alpha EEG power increment in the frontal lobe ($r = 0.86$, $p = .001$) but not in the central, temporal, or parieto-occipital areas. These data suggest that the more alpha power increased in the frontal lobe following α TMS, the greater the improvement in negative symptoms.

Discussion

While the parameter choice of rTMS treatment for psychosis remains controversial, our study using individualized alpha frequency and motor threshold-based intensity demonstrated a significant therapeutic effect on the negative symptoms of schizophrenia. These improvements were highly correlated with the degree of patients' alpha EEG enhancement in the frontal areas. These findings are consistent with our previous studies showing that the effects of antipsychotic treatment with clozapine on negative symptoms were predicted by the degree of alpha EEG normalization.^{15,16}

Findings of the present study also support an important notion that EEG of alpha band has strong resonant

features that can be tuned or perturbed with proper stimulation.^{17,18,21} In addition to sensory stimulations,^{21,22} direct electromagnetic manipulations of brain activity also appear to be an effective method of evoking resonant responses, as long as the stimulation rates are close enough to the intrinsic frequency of the alpha rhythm. We find these results to be particularly interesting given that an increasing number of studies have shown that high-order cognitive functions may be carried out by coherent neural processing across multiple regions in the brain,^{23,24} where alpha EEG may provide a gating mechanism for the synchrony among different areas.²⁵ It has been demonstrated, for example, that when a cat has been stimulated with a sensory stimulation, an increased coherence in the alpha range between all structures in the visual pathway, hippocampus, and reticular formation could be observed.²⁶ Furthermore, Klimesch, Schimke, and Pfurtscheller²⁷ and others²⁸ have provided clear evidence of a positive, consistent relationship between working memory performance and mean alpha activity.

On the other hand, patients with schizophrenia often have some degree of power or coherence reduction in alpha-band EEG activity,¹⁰ particularly during perceptual or cognitive activation.^{11,12} Using a visual stimulation paradigm with repetitive light flashing, we have demonstrated that alpha EEG photic driving is a reliable and specific index in studies of mental disorders.²⁰ Compared to normal subjects, drug-free schizophrenic individuals have significantly reduced power density in the alpha EEG photic responses.^{19,20} Furthermore, we have found that the reduced EEG photic driving in schizophrenics could be normalized by effective treatment with clozapine. The increment of the EEG photic driving produced by clozapine was positively correlated with

patients' clinical improvement in negative symptoms, assessed by BPRS. Patients who clinically responded to the treatment had significantly greater increase in photic driving than those who did not respond.^{15,16} Consistent with these discoveries, the present study demonstrated for the first time that direct manipulation with α TMS could alter the alpha EEG based on the physics of resonance and improve negative symptoms in schizophrenia. It suggests strongly that alpha EEG and negative symptoms may have a causal relationship and, therefore, further investigations are needed.

Some limitations of the current study should also be discussed before any conclusions can be drawn. Cross-over design has its economic benefit when the sample size is small. The drawback, however, is the potential confound of carryover effects, which may significantly alter the results. In the present study a 2-week break between different stimulations might not have been enough to completely wash out the carryover effects. Also, to solve the common problem of residual magnetic field in sham stimulus when a tilted coil is applied, we used an unplugged coil. Although the acoustic effect was presented by another active coil in close proximity, the somatic sensation of scalp muscle contractions was missing. A third limitation was the uncontrolled ongoing medication. Although patients in this study all met the predefined clinical criteria of stability on their current dose, the possibility of an rTMS-drug interaction could not be entirely excluded. Furthermore, a more rigorous assessment of the merits of utilizing individualized α TMS must also include a condition with the stimulus rate fixed at a frequency within the alpha band (8–13 Hz) to determine whether the selection of individualized alpha would have a superior effect to fixed frequencies in this range, as hypothesized.

Conclusion

Drawing on previous findings linking a reduction in the power density and coherence of alpha frequency EEG with the negative symptoms of schizophrenia, this study hypothesized that the use of individualized alpha frequency rTMS would provide a superior treatment effect than other stimulation frequencies. It was proposed that the resonant “tuning” of the peak alpha oscillations would serve to increase the power density in this frequency range and thereby improve the negative symptoms. The results have provided support for these hypotheses and are interpreted as further evidence to the critical relationship of alpha-rhythm oscillations to the pathophysiology of schizophrenia. Furthermore, these findings suggest that the use of alpha frequency as a stimulation parameter for rTMS merits further controlled trials to more thoroughly investigate its potential efficacy as a treatment for the negative symptoms of schizophrenia.

Acknowledgments

Support for this project was provided by a competitive research grant from the Stanley Medical Research Institute, 5430 Grosvenor Lane, Suite 200, Bethesda, MD 20814–2142.

References

1. Roth BJ, Saypol JM, Hallett M, Cohen LG. A theoretical calculation of the electric field induced in the cortex during magnetic stimulation. *Electroencephalogr Clin Neurophysiol*. 1991;81(1):47–56.
2. Walsh V, Pascual-Leone A. *Neurochronometrics of Mind: TMS in Cognitive Science*. Cambridge, Mass: MIT Press; 2003.
3. George MS, Belmaker RH. *Transcranial Magnetic Stimulation in Neuropsychiatry*. Washington, DC: American Psychiatric Press; 2000.
4. George MS, Lisanby SH, Sackeim HA. Transcranial magnetic stimulation: applications in neuropsychiatry [comment]. *Arch Gen Psychiatry*. 1999;56:300–311.
5. Hoffman RE, Hawkins KA, Gueorguieva R, et al. Transcranial magnetic stimulation of left temporoparietal cortex and medication-resistant auditory hallucinations. *Arch Gen Psychiatry*. 2003;60:49–56.
6. d'Alfonso AAL, Aleman A, Kessels RPC, et al. Transcranial magnetic stimulation of left auditory cortex in patients with schizophrenia: effects on hallucinations and neurocognition. *J Neuropsychiatry Clin Neurosci*. 2002;14(1):77–79.
7. Geller V, Grisaru N, Abarbanel JM, Lemberg T, Belmaker RH. Slow magnetic stimulation of prefrontal cortex in depression and schizophrenia. *Prog Neuropsychopharmacol Biol Psychiatry*. 1997;21:105–110.
8. Rollnik JD, Huber TJ, Mogk H, et al. High frequency repetitive transcranial magnetic stimulation of the dorsolateral prefrontal cortex in schizophrenic patients. *Neuroreport*. 2000;11(18):4013–4015.
9. Cohen E, Bernardo M, Masana J, et al. Repetitive transcranial magnetic stimulation in the treatment of chronic negative schizophrenia: a pilot study. *J Neurol Neurosurg Psychiatry*. 1999;67:129–130.
10. Stevens JR, Livermore A. Telemetered EEG in schizophrenia: spectral analysis during abnormal behaviour episodes. *J Neurol Neurosurg Psychiatry*. 1982;45:385–395.
11. Colombo C, Gambini O, Macciardi F, et al. Alpha reactivity in schizophrenia and in schizophrenic spectrum disorders: demographic clinical and hemispheric assessment. *Int J Psychophysiol*. 1989;7:47–54.
12. Hoffman R, Buchsbaum M, Escobar M, Makuch R, Neuchterlein K, Guich S. EEG coherence of prefrontal areas in normal and schizophrenia males during perceptual activation. *J Neuropsychiatry Clin Neurosci*. 1991;3:169–175.
13. Omori M, Koshino Y, Murata T, et al. Quantitative EEG in never-treated schizophrenic patients. *Biol Psychiatry*. 1995;38:305–309.
14. Merrin EL, Floyd TC. Negative symptoms and EEG alpha in schizophrenia: a replication. *Schizophr Res*. 1996;19:151–161.
15. Jin Y, Potkin SG, Sandman C. Clozapine increases EEG photic driving in clinical responders. *Schizophr Bull*. 1995;21:263–268.
16. Jin Y, Potkin SG, Sandman CA, Bunney WE Jr. Topographic analysis of EEG photic driving in patients with

- schizophrenia following clozapine treatment. *Clin Electroencephal.* 1998;29:73 78.
17. Jin Y, Potkin SG, Rice D, et al. Abnormal EEG responses to photic stimulation in schizophrenic patients. *Schizophr Bull.* 1990;16:627 634.
 18. Jin Y, Sandman CA, Wu JC, Bernat J, Potkin SG. Topographic analysis of EEG photic driving in normal and schizophrenic subjects. *Clin Electroencephal.* 1995;26:102 107.
 19. Kondacs A, Szabo M. Long-term intra-individual variability in the background EEG in normals. *Clin Neurophysiol.* 1999; 110:1708 1716.
 20. Salinsky MC, Oken BS, Morehead L. Test-retest reliability in EEG frequency analysis. *Electroencephalogr Clin Neurophysiol.* 1991;79(5):382 392.
 21. Jin Y, Castellanos A, Solis ER, Potkin SG. EEG resonant responses in schizophrenia: a photic driving study with improved harmonic resolution. *Schizophr Res.* 2000;44:213 220.
 22. Jin Y, Potkin SG, Sandman CA, Bunney WE Jr. Electroencephalographic photic driving in patients with schizophrenia and depression. *Biol Psychiatry.* 1997;41:496 499.
 23. Llinás RR. The intrinsic electrophysiological properties of mammalian neurons: insights into central nervous system function. *Science.* 1988;242:1654 1664.
 24. Basar E. *Brain Function and Oscillations.* Berlin: Springer-Verlag; 1998.
 25. Wiener N. Rhythms in physiology with particular reference to electroencephalography. *Proc Rudolf Virchow Med Soc City N Y.* 1957;16:109 124.
 26. Basar E, Demir N, Gönder A, Ungan P. Combined dynamics of EEG and evoked potentials: I. studies of simultaneously recorded EEG-EPograms in the auditory pathway, reticular formation, and hippocampus of the cat brain during the waking stage. *Biol Cybernetics.* 1979;34:1 19.
 27. Klimesch W, Schimke H, Pfurtscheller G. Alpha frequency cognitive load and memory performance. *Brain Topogr.* 1993; 5(3):241 251.
 28. Clark R, Veltmeyer M, Hamilton R, et al. Spontaneous alpha peak frequency predicts working memory performance across the age span. *Int J Psychophysiol.* 2004;53:1 9.

EXHIBIT 16

Transcranial magnetic stimulation: a historical evaluation and future prognosis of therapeutically relevant ethical concerns

Jared C Horvath,¹ Jennifer M Perez,¹ Lachlan Forrow,² Felipe Fregni,³
Alvaro Pascual-Leone¹

¹Berenson-Allen Center for Noninvasive Brain Stimulation, Beth Israel Deaconess Medical Center and Harvard Medical School, Boston, USA

²Beth Israel Deaconess Medical Center and Harvard Medical School, Boston, USA

³Laboratory of Neuromodulation, Spaulding Rehabilitation Hospital, Boston, USA

Correspondence to

Mr J C Horvath, Berenson-Allen Center for Noninvasive Brain Stimulation, Beth Israel Deaconess Medical Center and Harvard Medical School, 330 Brookline Ave KS-158, Boston, MA 02215, USA; jhorvat2@bidmc.harvard.edu

Received 1 September 2010

Revised 14 October 2010

Accepted 31 October 2010

Published Online First

24 November 2010

ABSTRACT

Transcranial Magnetic Stimulation (TMS) is a non-invasive neurostimulatory and neuromodulatory technique increasingly used in clinical and research practices around the world. Historically, the ethical considerations guiding the therapeutic practice of TMS were largely concerned with aspects of subject safety in clinical trials. While safety remains of paramount importance, the recent US Food and Drug Administration approval of the Neuronetics NeuroStar TMS device for the treatment of specific medication-resistant depression has raised a number of additional ethical concerns, including marketing, off-label use and technician certification. This article provides an overview of the history of TMS and highlights the ethical questions that are likely arise as the therapeutic use of TMS continues to expand.

INTRODUCTION

Transcranial Magnetic Stimulation (TMS) is a non-invasive neurostimulatory and neuromodulatory technique increasingly used in clinical and research practices around the world. Although originally developed as a diagnostic tool, TMS can transiently or lastingly modulate cortical excitability (either increasing or decreasing it) via the application of localised magnetic field pulses. This and other neurobiological effects can be leveraged for therapeutic applications in neurology, psychiatry and rehabilitation. Historically, the ethical considerations guiding the therapeutic practice of TMS were largely concerned with aspects of subject safety in clinical trials. While safety remains of paramount importance, the recent US Food and Drug Administration (FDA) approval of the Neuronetics Inc. (Malvern, PA, USA) NeuroStar TMS device for the treatment of specific medication resistant depression has raised a number of additional ethical concerns. Some of these are derivatives of previously identified issues, but others, such as marketing, off label use and technician certification, have not been well explored. As the therapeutic potential for TMS expands to include a wide range of neuropsychiatric conditions, including those where patients have few alternative treatment options, ethical issues are likely to continue to grow rapidly. This article provides an overview of the historical, present and future ethical issues associated with the therapeutic use of TMS and discusses ways in which these issues might be addressed.

A TMS PRIMER

TMS is a neurophysiologic technique that allows for non-invasive stimulation of the human brain.^{1,2} Introduced approximately 25 years ago, TMS can be combined with various brain mapping methodologies (eg, electroencephalography, positron emission tomography or functional MRI), to study intra-cortical excitation and inhibition balance, cortico-cortical and cortico-subcortical connectivity and interactions, and brain plasticity. Repetitive transcranial magnetic stimulation (rTMS) has been shown to transiently disrupt neuronal activity for periods exceeding stimulation duration. This modulated brain activity may prove useful in both the determination of causal relationships between focal brain activity and emergent behaviour as well as in the treatment of numerous neurological and psychiatric illnesses.

The physical principles of TMS were discovered in 1881 by English physicist Michael Faraday, who observed that a pulse of electric current passing through a wire coil generates a magnetic field. The rate of change of this magnetic field determines the induction of a secondary current in a nearby conductor. During TMS, the stimulating coil is held over a subject's head and produces an electric current in the subject's brain via electro-magnetic induction. This current in turn depolarises neurons and can generate various physiological and behavioural effects depending on the targeted brain area. Because magnetic fields can pass the skull with almost no resistance, TMS can induce relatively large currents in targeted cortical areas.

The design of magnetic stimulators is relatively straightforward, consisting of a main unit and a stimulating coil. The main unit is composed of a charging system, one or more energy storage capacitors, a discharge switch and circuitry used to control pulse shape, energy recovery and other variable functions. The factors essential to the effectiveness of a magnetic stimulator are the speed of magnetic field rise time and the maximisation of the peak coil energy. Therefore, large energy storage capacitors and efficient energy transfer from the capacitor to the coil are important (typically energy storage capacity is around 2000J with a 500J transfer from the capacitor to the stimulating coil in less than 100 microseconds via a *thyristor*, an electrical device capable of switching large currents in a short time). The peak discharge current needs to be several thousand amperes in order to induce currents in the brain of sufficient magnitude to depolarise neural elements (about 10 mA/cm²).

Clinical ethics

The precise mechanisms underlying the neural effects of TMS are largely unknown.¹ Currents induced by TMS typically flow parallel to the plane of the stimulation coil. Therefore, in contrast with electrical cortical stimulation, TMS preferentially activates neural elements oriented horizontally to the brain surface. However, exactly which neural elements are activated remains unclear and, in fact, might vary across different brain regions and different subjects. Recent animal studies have begun probing these important mechanistic questions.^{3–5}

PRE-HISTORY OF TMS: AN ETHICAL PERSPECTIVE

The field of electrophysiology was born in 1771 with the discovery of bioelectricity by the Italian physician Luigi Galvani. Soon thereafter, Galvani's nephew, Giovanni Aldini, began touring the European countryside promoting his belief that bioelectricity could unlock the secrets to dead tissue reanimation. To prove his theory, Aldini staged macabre public demonstrations during which, via the application of direct electric current, he induced muscular contractions in dead animals, and, in 1803, the lifeless body of executed convict George Forster.⁶ Through this incident, several important ethical considerations began to emerge. Scientific advancements may harness great potential, but this does not exempt scientists from asking whether such potentialities *should* be explored. How might a system of ethics be maintained that serves to protect research subjects and to protect the integrity of and respect for both science and mankind?

In 1874, scientific exploration of bioelectricity within muscles and nerve fibres reached an apex when American physician Robert Bartholow applied electrical current to the exposed dura of Cincinnati housewife Mary Rafferty. After successful induction of slight muscular twitches, Bartholow increased the applied current until distress, convulsion and eventually, coma were reported.^{7–8} Rafferty died 72 h later. This incident highlights a dilemma pervasive throughout medical science: in the quest for knowledge, too often experimenters can become blind to the potentially deleterious effects of their actions. Over zealousness often clouds typically sound judgement, illustrating the importance of and need for outside, independent risk to benefit assessment. Today such assessment is provided by the Institutional Review Boards. However, the responsibility for the proper conduct and sound ethical grounding of a given experiment ultimately remains in the hands of the investigators.

The development of electroconvulsive therapy (ECT) in 1937 ushered the field of brain stimulation into the modern 'medical device' age. Developed by Italian physicians Cerletti and Bini, ECT was intended to treat the manic symptoms of schizophrenic inpatients. However, as the popularity of the device grew, practitioners quickly elevated ECT to the status of psychiatric panacea. This gross overuse led to a plethora of serious adverse psychological and physical side effects, thereby creating a strong negative public attitude towards the therapy. In 1976, in reaction to public backlash against ECT and similar treatments, the FDA assumed regulatory control over all emerging medical devices. Interestingly, ECT (along with several other brain stimulation devices on the market prior to government intercession) today remains out of the purview of FDA regulation. Although ECT is considered by many to be a highly effective treatment for depression,⁹ its use remains impacted by unfavourable public opinion. An important charge for the FDA is to oversee the cautious development and implementation of novel therapies so as to assure efficacy and preclude preventable complications due to practitioner misuse that may substantiate a stigmatisation that can limit their acceptance by patients who

could potentially benefit from their use (as exemplified by ECT misuse in the 40s and 50s).

In 1972, another incident in the annals of brain stimulation raised relevant therapeutic ethical concerns. Building upon Jose Delgado's work with behaviour modification in animals via deep brain electrical stimulation, two doctors from Tulane University attempted to 'cure' a patient of his homosexuality. Combining electrical stimulation of *patient B 19's* septum with forced heterosexual interactions (provided by a female prostitute), Drs Moan and Heath reported a 10 month eradication of homosexual behaviour.¹⁰ Here we see what many modern practitioners consider the darkest hour for brain stimulation. When contemplating this event, it is important to remember that our ethical perception is inextricably linked to the often shifting social definitions of the core concepts of health and disease. It is important, therefore, to remain cognisant of the sociological factors that may colour our opinion and, whenever possible, attempt to remain pluralistic when constructing any ethical framework (See Figure 1).

THE EVOLUTION OF TMS

The first reliable transcranial magnetic brain stimulator was developed by Anthony Barker and colleagues and was introduced to the world in 1984–1985. Since that time, TMS has gone through several major stages of development, each defined by unique achievements and concomitant considerations.

Establishing diagnostic utility

In the late 1970s, a handful of clinicians began using transcranial electric stimulation to diagnostically measure motor conduction time in patients suffering from multiple sclerosis. This technique, although efficacious, was limited by the extreme discomfort it elicited in patients and subjects. TMS provided a propitious solution to this problem: via single pulse stimulation, practitioners could perform similar motor conduction time tests in a much safer, far less painful manner.¹¹ Over the ensuing years, physician interest in TMS remained largely within the realm of diagnostics.

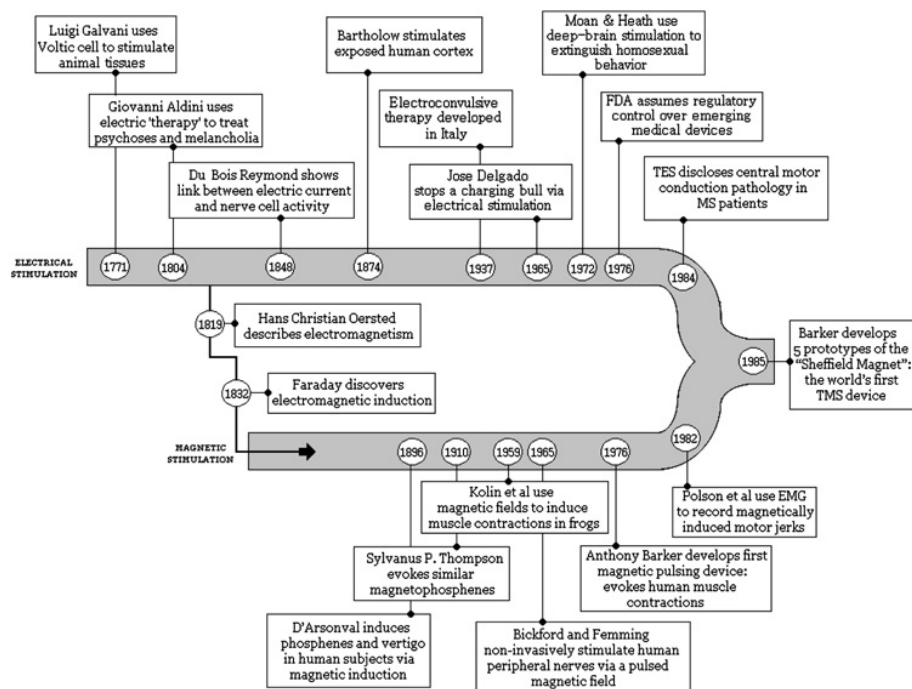
The major ethical considerations during this first stage of TMS concerned overall device safety. Because TMS originated as a diagnostic and investigational device, not many animal models were developed to study short or long term effects. As such, TMS practitioners promoted the field rather cautiously (as compared with ECT). A keen focus was maintained on patient reported side effects, especially those related to or resembling seizure activity.

Exploring therapeutic possibilities

In 1991 the journal *Neurology* published an article by Dr Alvaro Pascual Leone *et al*, entitled *Induction of speech arrest and counting errors with rapid rate transcranial magnetic stimulation*.¹² This paper was one of the first to use an rTMS paradigm. Qualitatively different from previous single pulse methodologies, rTMS allowed for a more sustained neurological intervention. This new paradigm opened the door for researchers to conduct more nuanced studies of cognitive function and neural interaction. In 1994, Pascual Leone *et al* reported that rTMS could generate lasting cortical effects that remained after the cessation of stimulation (lasting between 3 and 4 min).¹³ This ability to induce sustained physiological and cognitive effects made rTMS a tool conducive to the field of therapeutic medicine.

The expansion of TMS from single pulse indication to repetitive pulse intervention greatly increased the number of TMS ethical concerns. In addition to lasting matters of safety,

Figure 1 A timeline of notable uses and discoveries in electrical and magnetic stimulation leading up to the development of the first reliable magnetic brain stimulator in 1984–1985.



practitioners and clinicians were suddenly confronted with innumerable clinical considerations, including which disorders might be responsive to stimulatory treatment, issues of patient response patterns, and potential interactions between rTMS and medication. Even as labs elsewhere continued to generate ever increasing numbers of active rTMS studies, practitioners undertook the daunting but necessary task of conducting Phase I research.^{14–16}

The clinical push

One of the first proof of principle TMS studies specifically focused on a therapeutic application of repetitive TMS in a neuropsychiatric disease was published by Kolbinger *et al*, who examined the effects of rTMS on 15 patients suffering from drug resistant depression.¹⁷ Of the 10 patients receiving non sham stimulation, all showed significant improvement.

This transition to proof of principle studies did not eradicate previous ethical concerns; rather, it added new considerations to the ever relevant previous concerns. The inclusion of lengthy and repetitive patient treatment protocols (as opposed to transitory research protocols) raised questions about the long term cortical effects of TMS. The apprehension felt by many clinicians and scientists was reflected in a letter entitled *Shocking Safety Concerns*,¹⁸ published several months after a successful proof of principle trial conducted by Pascual Leone *et al*.¹⁹ In this missive, Browne gave voice to the fear that history might repeat itself in the later phase realisation of a treatment's detrimental effects (eg, prolonged use of Vioxx, a drug prescribed for the acute treatment of pain, was found to increase the risk of heart disease only after the drug had been widely used).²⁰ Due in large part to the concerns voiced by Brown and others, TMS practitioners largely agreed that, in order to maintain a circum spect developmental trajectory, it was imperative to outline universal safety and procedural standards.

To this end, a group of leading TMS authorities convened in 1996 and published the first detailed safety and ethical guidelines for TMS in both the clinical and the laboratory setting.²¹

Perhaps borrowing a lesson from the unchecked stimulation methodologies of the past (eg, ECT), this assemblage set out written standards which would serve to maintain prudence and discretion in a field that could easily be derailed by one or two rogue practitioners. Despite the relative nascence of the TMS device, the International Federation of Clinical neurophysiology demonstrated foresight by adopting and implementing these standards worldwide (although, to be fair, these guidelines did not cover all the aspects of TMS safety, such as long term effects).

Clinical expansion

With safety guidelines in place and numerous successful proof of principle trials affirming potential benefits, TMS became more established. Clinics offering off label therapies for myriad neurological and psychological pathologies began appearing worldwide.^{22–23}

As is common with novel treatments, initial rTMS patient populations consisted primarily of patients who had exhausted other, more established forms of treatment. As such, for many patients, rTMS became a 'last hope' intervention, which raises an ethical issue relevant to many young technologies: when a treatment population consists of desperate individuals willing to endure potentially unsafe procedures to obtain relief, an objective focus on potential signs of diminished autonomy as a result of neuropsychiatric illness, desperation or both, becomes doubly important. This is especially true when obtaining informed consent.^{24–25} This problem may be further aggravated by patients seeking and receiving misleading information via secondary sources such as the internet. Therefore, additional safeguards may need to be instituted to avoid potential problems or mistakes when exploring novel treatment methods within vulnerable populations.

As rTMS became more widespread, on label treatment for depression was approved by the regulatory agencies of numerous countries, including Brazil, Israel, Australia and Canada. This swift expansion created an explosion of ethical concerns in the

Clinical ethics

world of brain stimulation. How are practical guidelines to be enforced with the migration of patients over borders to obtain treatment unavailable in their home countries? How is honesty to remain in side effect reporting when said reports directly affect business? These questions remain important today and the need to revisit and continually update TMS safety guidelines and recommendations for global clinical implementation is imperative.

In addition to clinical expansion, practitioners developed various new stimulation paradigms impacting the risk to benefit profile of TMS. For example, theta burst stimulation, a high frequency stimulatory pattern, can induce rapid long term potentiation and long term depression effects via the mimicry of powerful brain oscillations. Theta burst stimulation allows for longer lasting and more profound modulation of cortical excitability with shorter stimulation duration. Consider also varied coil shapes, varied stimulation pulse characteristics, varied stimulation sites and varied power levels, and a picture of TMS as a broad, permutated methodology begins to emerge. With this breadth, issues of proper technician and practitioner procedural training and certification became important. With increasing numbers of individuals seeking TMS therapy, ensuring patients received the best possible treatment by a doctor well versed in both the appropriate methodology and all relevant device considerations became of paramount concern (and remains so today).

2008 Consensus conference

The guidelines established in 1998 for the application of TMS in research and clinical settings were reviewed in a consensus conference which took place in 2008. The resulting publication updated limits for the combination of rTMS frequencies, intensities and train durations to reduce risk of seizure induction.²⁶ The article provided the scientific community with an up to date evaluation of the safety record of research and clinical applications of TMS. In addition, the article introduced several important questions, such as the use of novel parameters, while underscoring several long standing questions that remained unanswered, such as the risk of TMS in patients with neuro psychiatric disorders.

In the decade spanning the conferences, the uses of TMS expanded exponentially, growing to include new research applications, clinical applications and cross modality integration (including combining TMS with electroencephalography, positron emission tomography, and functional MRI). Despite these advancements, the initial safety guidelines developed at the 1998 conference were found to have stood the test of a decade's worth of work. While standards must continue to be regularly reviewed and updated, the safety record of TMS to date confirms that potential future ethical problems can often be largely avoided with proper 'preventive ethics' foresight and restraint in the present.²⁷

FDA APPROVAL

In 2007, O'Reardon *et al* published the results of an industry sponsored, multisite, randomised clinical trial in which 301 patients with major depression, who had previously failed to respond to *at least one* adequate antidepressant treatment trial, underwent either active or sham TMS over the left dorsolateral prefrontal cortex.²⁸ The patients, who were medication free at the time of the study, received TMS five times per week over 4–6 weeks. The data demonstrated that a sub population of patients, those who were relatively less resistant to medication (having failed not more than two good pharmacological trials),

showed a statistically significant improvement on several secondary outcome measures. Supported by these results, Neuronetics Inc, the study sponsoring company, obtained approval from the FDA for the clinical treatment of specific forms of medication refractory depression (FDA approval K061053).

FDA approval (granted in October 2008) was limited to the NeuroStar TMS device (manufactured by Neuronetics Inc) for the protocol of stimulation employed in the study (high frequency, 10 Hz—rTMS applied daily for 4–6 weeks at supra threshold intensity) within a highly specific subpopulation of patients (adults who have failed to achieve satisfactory improvement from one, but no more than one, adequate antidepressant medication trial).

When research studies are sponsored by industries, one must consider scientific rigour and issues of conflicting interest. Ensuring research remains free of undue influence is critical, but there are certain circumstances in which industry sponsorship may not be a detrimental occurrence. For example, with FDA approval granted to Neuronetics, the door has opened for additional companies, devices and treatments to receive serious FDA consideration. More importantly, patients who once lacked an efficacious, safe treatment option now have an alternative with proper risk to benefit balance assurances.

Recently, a National Institutes of Health sponsored, multi site TMS depression trial was undertaken.²⁹ The researchers were able to successfully reproduce the results from the earlier Neuronetics study. In addition to strengthening the therapeutic profile of TMS, this outcome proved important for three additional reasons: first, with a National Institutes of Health sponsored trial, much of the potential for researcher and patient bias was eliminated. Second, with successful replication, many questions and/or concerns engendered from the earlier industry sponsored trial were assuaged. Finally, the risk of false positive findings from the initial trial was greatly decreased.

The narrow FDA approved on label indication poses ethical questions. The patient criteria leave many potential patients to consider off label options. Also, studies have revealed that the benefits of rTMS treatment may lapse after 4–6 months.³⁰ Unfortunately, the FDA has not approved long term TMS maintenance and care. This leaves the issues of prolonged symptom alleviation and continued treatment up for ethical debate. As TMS continues to advance as a therapeutic option, such questions will undoubtedly become increasingly common. As such, we must ensure that naturalistic studies are officially reported so as to increase the pool of analysable safety data.³¹

The existing safety guidelines for TMS differentiate between relative and absolute contraindications, thus providing important guidance in selection of suitable TMS candidates. Patients exhibiting relative contraindications may have, for example, a history of epilepsy or lesions of the brain; they may also be taking medication that lowers the seizure threshold. Patients with an absolute contraindication to TMS are those patients who have implanted metallic hardware in close contact to the discharging coil (eg, cochlear implants). Performing TMS on patients demonstrating an absolute contraindication carries the risk of inducing malfunctioning of such implanted devices.²⁶ Therefore, when it comes to deciding whether a patient is eligible for TMS, the risk to benefit ratio is crucial, and the clinician or investigator should carefully weigh the presence of both types of contraindications while assessing whether TMS is appropriate. However, because TMS data is still limited, more concrete recommendations are not possible at this time.

In the USA, FDA approval does not ensure coverage by health insurance companies. Thus, not all patients who meet the FDA guidelines and may benefit from TMS can afford to be treated. Likewise, many patients seeking off label therapy cannot afford treatment, as neither on or off label TMS is covered by health insurance in the USA. This leaves payment options to the individual clinics. Is there a way for clinics to set pricing so all patients in need, regardless of socioeconomic status, can access treatment? Although this concern may only be pertinent under the present US healthcare system, as TMS continues to advance as a treatment option, economic questions unique to each country's individual medical structure will undoubtedly become increasingly common and must be addressed.

Another subject worth exploring pertains to TMS advertisements. FDA approval comes with the privilege of therapeutic advertising for on label application of rTMS for depression. However, advertisement can also attract patients who may want off label rTMS use. Who should the advertisements target? How should the disclosure of side effects be dealt with? Surely TMS treatment for depression can be made appealing based on what it *does not* do (eg, it does not cause some of the side effects associated with other common antidepressant medications), but perhaps it would be more prudent to market TMS for what the literature indicates it *can* do. Even though they would almost certainly be non binding, consensus standards regarding the content of promotional advertising for TMS would be beneficial before practitioners or companies move forward (See Figure 2).

Present and future ethical considerations for the scientific use of TMS

As the clinical and research utility of TMS grows, questions concerning treatment guidelines must be considered. What criteria should we adopt before recommending TMS as a possible treatment for depression or other neuropsychological diseases? Of course, all pertinent information—small effect sizes

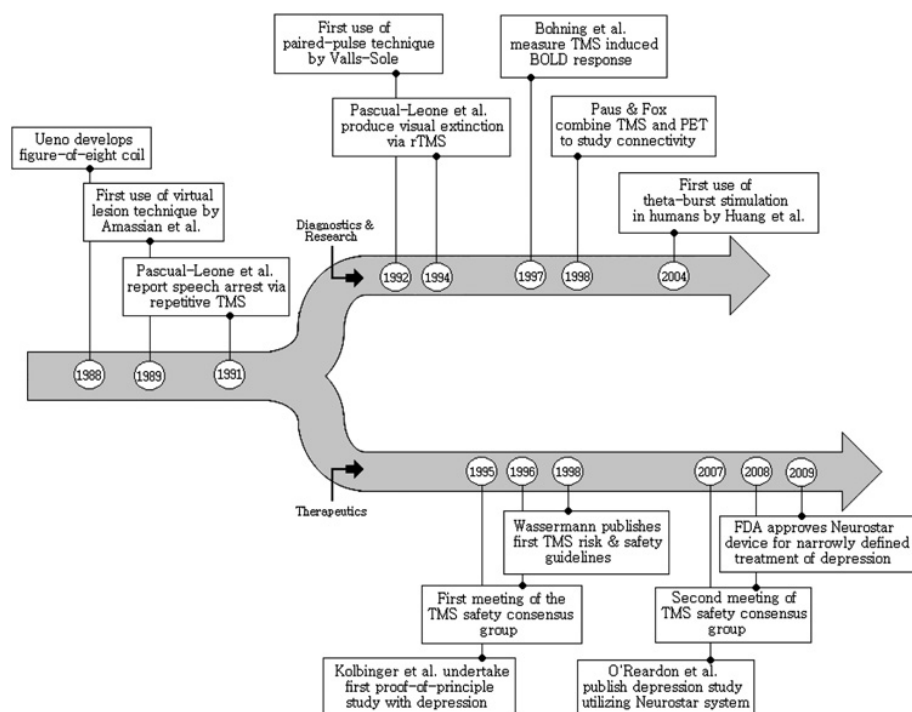
in TMS trials, safety data, alternative treatments, even potential future effects—must be fully disclosed to the patient. The truth about what TMS can and cannot offer must be explicitly stated, and every effort to balance a patient's hopes and expectations with the unpredictable reality of science must be made. Perhaps it would be useful to create an easily accessible website providing the public with up to date TMS information from objective and authoritative sources.

Similarly, as the risk to benefit ratio depends on inter individual differences, practitioners are needed with experience with TMS and with the relevant patient population. Ultimately this requires the development of universal training guidelines and accreditation requirements for TMS clinicians. Who should deliver TMS? How should we ensure practitioners are using TMS correctly and safely? Currently, there are no TMS training requirements, although it is advised that practitioners be well versed in the basics of brain physiology and TMS mechanisms, protocols and safety issues.²⁶ It is apparent, though, that stronger regulations, or at least guidelines, are needed.

In neuroscientific research settings, TMS can occasionally produce seemingly detrimental effects, most typically mild and transient memory deficits. In studies designed to explore these effects on performance tasks, the effects are brief and do not raise particular safety issues.²⁶ Still, these studies challenge the risk to benefit ratio. To what extent is it ethical to induce changes in a subjects' brain if the benefit is strictly increased scientific knowledge? Taken one step further, if a therapeutic paradigm is developed that largely mimics one of these research protocols, there is a possibility transient deficits may be produced in the clinic. Although it is not always possible to translate effects generated in healthy populations to clinical patients, the inclusion of cognitive interference on the list of possible treatment side effects is worthy of consideration and discussion.

Finally, recent research combining TMS with genetic testing has revealed that the therapeutic utility of rTMS, particularly in the treatment of drug resistant patients, might be increased by

Figure 2 A timeline of the ethical progression of TMS, highlighting some of the important diagnostic, research, and therapeutic developments in the field.



Clinical ethics



Figure 3 The compiling nature of ethical considerations.

identifying genetic predictors of certain rTMS effects. Combining TMS with genetic testing, though, presents compound ethical challenges: one must keep in mind the ethical considerations applicable to TMS research while evaluating the complex host of issues pertaining to genetic testing. Current research suggests that genetic factors may influence the response to TMS, but is the current evidence strong enough to merit genetic testing on all TMS subjects? The broad range of genetic factors, epigenetic effects and TMS parameters leaves scientists with an intricate array of testing possibilities. Given the postulated role of synaptic plasticity in brain injury and disease, and the epidemiologic evidence concerning the role of BDNF in the synaptic plasticity of the adult brain,³² there does seem to be a potential therapeutic potential for future interventions. However, that potential comes at a cost. Genetic material must first be obtained (and drawing blood certainly poses a discomfort for research participants) and then stored. To address some of these issues, Knoppers and Chadwick highlight the notion of honest and reciprocal exchange between researcher and participant.³³ The autonomy and the contribution of the research participant must be recognised and respected to the fullest in protocols calling for genetic testing. Informed consent and communication with potential participants must be clear, and the objectives transparent. Moreover, participants should fully understand that they have the option to take part in a protocol, and that they can decide whether to have their DNA banked, coded, analysed, even replicated and potentially commercialised.

CONCLUSION

As TMS continues to gain momentum in the field of therapeutic medicine, it is likely to pave the way to additional future non invasive brain stimulation and neuromodulation techniques. For example, transcranial direct current stimulation is a rapidly expanding non invasive brain stimulation method that is even easier to apply than TMS and a lot more accessible given much lower device costs. Therefore, we must remain vigilant and use lessons of the past to continually reflect upon current issues of safety and ethics of non invasive brain stimulation. Our ethical perspective will inevitably evolve with changes in cultural and societal values, but hopefully the issues we have outlined here will provide a strong foundation for approaching the future. As in any discussion, the most essential questions are not those we have the answers to, but rather those which remain uncertain. Should we fail to ask and carefully consider these questions proactively, we risk effecting serious adverse consequences within one or more patients due to future TMS mal use. If this happens, the entire field may be frozen by outcries of public criticism reminiscent of the overwhelmingly negative perceptions that continue to plague ECT even today. Given the potential of TMS and non invasive brain stimulation in general, this would be a tragic occurrence—possibly depriving a large

patient population of significant therapeutic benefit. Fortunately, because such a situation is so clearly foreseeable, it is also largely preventable if we act without delay²⁷ (See Figure 3).

Competing interests None.

Provenance and peer review Not commissioned; externally peer reviewed.

REFERENCES

1. Pascual-Leone A, Davey M, Wassermann EM, et al. *Handbook of Transcranial Magnetic Stimulation*. London: Edward Arnold, 2002.
2. Walsh V, Pascual-Leone A. *Neurochronometrics of Mind: Transcranial Magnetic stimulation in Cognitive Science*. Cambridge, MA: MIT Press, 2003.
3. Allen EA, Pasley BN, Duong T, et al. Transcranial magnetic stimulation elicits coupled neural and hemodynamic consequences. *Science* 2000;**317**: 1918–21.
4. Wagner T, Valero-Cabre A, Pascual-Leone A. Noninvasive human brain stimulation. *Ann Rev Biomed Eng* 2007;**9**:527–65.
5. Valero-Cabre A, Pascual-Leone A, Rushmore RJ. Cumulative sessions of repetitive transcranial magnetic stimulation (rTMS) build up facilitation to subsequent TMS-mediated behavioral disruptions. *Eur J Neurosci* 2008;**27**:765–74.
6. Parent A. Giovanni Aldini: from animal electricity to human brain stimulation. *Can J Neurol Sci* 2004;**31**:576–84.
7. Zago S, Ferrucci R, Fregni F, et al. Bartholow, Sciamanna, Alberti: pioneers in the electrical stimulation of the exposed human cerebral cortex. *Neuroscientist* 2008;**14**:521–8.
8. Harris LJ, Almerigi JB. Probing the human brain with stimulating electrodes: the story of Robert Bartholow's experiment on Mary Rafferty. *Brain and Cogn* 2009;**70**:92–115.
9. Surgeon General. *Mental Health: A Report of the Surgeon General. Chapter 4: adults and mental health*: <http://surgeongeneral.gov>, 1999 (accessed 14 Feb 2010).
10. Moan CE, Heath RG. Septal stimulation for the initiation of heterosexual activity in a homosexual male. *J Behav Ther Exp Psychiatry* 1972;**3**:23–30.
11. Green RM, Pascual-Leone A, Wassermann EM. Ethical guidelines for rTMS research. *IRB: A Review of Human Subjects Research* 1997;**19**(2):1–7.
12. Pascual-Leone A, Gates JR, Dhuna A. Induction of speech arrest and counting errors with rapid-rate transcranial magnetic stimulation. *Neurology* 1991;**41**:697–702.
13. Pascual-Leone A, Valls-Sole J, Wassermann EM, et al. Responses to rapid-rate transcranial magnetic stimulation of the human motor cortex. *Brain* 1994;**117**:847–58.
14. Counter SA, Borg E, Lofquist L, et al. Hearing loss from the acoustic artifact of the coil used in extracranial magnetic stimulation. *Neurology* 1990;**40**:1159–62.
15. Dhuna AK, Gates JR, Pascual-Leone A. Transcranial magnetic stimulation in patients with epilepsy. *Neurology* 1991;**41**:1067–72.
16. Pascual-Leone A, Houser CM, Reese K, et al. Safety of rapid-rate transcranial magnetic stimulation in normal volunteers. *Electroencephalogr Clin Neurophysiol* 1993;**89**:120–30.
17. Kolbinger HM, Hoflich G, Hufnagel A, et al. Transcranial magnetic stimulation (TMS) in the treatment of major depression: a pilot study. *Hum Psychopharmacol—Clin Exp* 1995;**10**:305–10.
18. Brown P. Shocking safety concerns. *Lancet* 1996;**348**:959.
19. Pascual-Leone A, Rubio B, Pallardo F, et al. Rapid-rate transcranial magnetic stimulation of left dorsolateral prefrontal cortex in drug-resistant depression. *Lancet* 1996;**348**:233–7.
20. Mukherjee D, Nissen S, Topol EJ. Risk of Cardiovascular Events Associated with Selective COX-2 Inhibitors. *JAMA* 2001;**286**:954–9.
21. Wassermann EM. Risk and safety of repetitive transcranial magnetic stimulation: report and suggested guidelines from the International Workshop on the Safety of Repetitive Transcranial Magnetic Stimulation, June 5–7, 1996. *Electroencephalogr Clin Neurophysiol* 1998;**108**:1–16.
22. Wassermann EM, Lisanby SH. Therapeutic application of repetitive transcranial magnetic stimulation: a review. *Clin Neurophysiol* 2001;**112**:1367–77.
23. Kobayashi M, Pascual-Leone A. Transcranial magnetic stimulation in neurology. *Lancet Neurol* 2003;**2**:145–56.
24. Minogue BP, Palmer-Fernandez G, Udell L, et al. Individual autonomy and the double blind controlled experiment: the case of desperate volunteers. *J Med Philos* 1995;**20**:43–55.
25. Miller FG, Brody H. A critique of clinical equipoise: Therapeutic misconception in the ethics of clinical trials. *Hastings Cent Rep* 2003;**33**:19–28.
26. Rossi S, Hallett M, Rossini PM, et al. Safety, ethical considerations, and application guidelines for the use of transcranial magnetic stimulation in clinical practice and research. *Clin Neurophysiol* 2009;**120**:2008–39.
27. Forrow L, Arnold RM, Parker LS. Preventive ethics; expanding the horizons of clinical ethics. *J Clin Ethics* 1993;**4**:287–94.
28. O'Reardon JP, Solvason HB, Janicak PG, et al. Efficacy and safety of transcranial magnetic stimulation in the acute treatment of major depression: a multisite randomized control trial. *Biol Psychiatry* 2007;**62**:1208–16.
29. George MS, Lisanby SH, Avery D, et al. Daily left prefrontal transcranial magnetic stimulation therapy for major depressive disorder: a sham controlled randomized trial. *Arch Gen Psychiatry* 2010;**67**:507–16.
30. Demirtas-Tatlidede A, Mechanic-Hamilton D, Press DZ, et al. An open-label, prospective study of repetitive transcranial magnetic stimulation (rTMS) in the

- long-term treatment of refractory depression: reproducibility and duration of the antidepressant effect in medication-free patients. *J Clin Psychiatry* 2008;**69**:930–4.
31. **Cohen RB**, Boggio PS, Fregni F. Risk factors for relapse after remission with repetitive transcranial magnetic stimulation for the treatment of depression. *Depress Anxiety* 2009;**26**:682–8.
 32. **Klein JA**, Chan S, Pringle E, *et al.* BDNF Val66Met polymorphism is associated with modified experience-dependent plasticity in human motor cortex. *Nat Neurosci* 2006;**9**:735–7.
 33. **Knoppers BM**, Chadwick R. Human genetic research: emerging trends in ethics. *Genetics* 2005;**6**:75–9.

EXHIBIT 17

Transcranial Magnetic Stimulation in Psychiatry: Historical Reflections and Future Directions

Sarah H. Lisanby

The history of transcranial magnetic stimulation (TMS) in psychiatry spans disciplines, continents, and decades, and it upended prevailing dogma. Initially developed as a tool to probe the motor system in neurology, TMS induces electricity in the brain without inducing a seizure (when given within safety limits). TMS made its debut in 1985 in the United Kingdom when the prevailing dogma in psychiatry was that a seizure is necessary for the therapeutic effects of electroconvulsive therapy (ECT). The idea of treating depression with electricity alone without inducing a seizure was viewed with skepticism. Fortunately, a group of pioneering researchers across several countries in the early 1990s saw TMS as a promising means of treating severe depression without the cognitive side effects of ECT. Borrowing methods used to study the motor system (a large round coil positioned on the vertex) and the fastest repetition rate available to them in 1993 (0.25–0.5 Hz), a team in Germany treated 2 patients with treatment-resistant depression, one of whom showed benefit (1). In 1994, a group in Israel took a similar approach in 10 patients with depression and 10 patients with schizophrenia (2). In 1995, a team from Germany and Austria reported significant antidepressant effects of this approach in a randomized controlled trial (3). That same year, researchers in the United States took a different approach—informed by neuroimaging findings in depression, they used the more focal figure-8 coil to target the left dorsolateral prefrontal cortex using the higher repetition rate that was available then (20 Hz repetitive TMS) and reported significant antidepressant effects in an open-label trial (4). In 1996, a team in Spain reported the first randomized controlled trial of repetitive TMS targeting the dorsolateral prefrontal cortex for depression (5). Numerous randomized controlled trials, meta-analyses, and an industry-sponsored pivotal trial later, the U.S. Food and Drug Administration cleared TMS for the treatment of depression in adults in 2008. Subsequent clearances followed, for presurgical mapping in 2009, migraine with aura in 2013, obsessive-compulsive disorder in 2019, smoking cessation in 2020, and comorbid anxiety in major depressive disorder in 2021. How did we get here, and what have we learned along the way? This commentary touches on a few lessons from the past that may be useful to reflect on as TMS reaches its fifteenth year after U.S. Food and Drug Administration clearance.

Design, and Redesign, With the Brain in Mind. The first TMS device was designed nearly 4 decades ago by Barker, Jalinous, and Freeston, a team of engineers working at the University of Sheffield. The ability of TMS to noninvasively

map the homunculus, induce phosphenes, arrest speech, and other early marvels transformed our ability to map brain-behavior relationships in humans. However, when we open the box of TMS, literally, and examine its circuit topology, we see that it was not entirely designed with the brain in mind. The dampened cosine waveform, which is the shape of the electric field induced when the capacitor is discharged through the stimulating coil, is not efficient in inducing neuronal depolarization. Electrical stimulation devices use square waves because they are efficient at inducing action potentials. It turns out that it is possible to redesign TMS circuit topology to induce near rectangular waveforms and have user control of pulse width and shape. Controllable pulse parameter TMS (cTMS) devices offering this ability are now available for research applications, and new devices with even more flexibility are in development (6).

Another aspect of TMS device design that has been taken as a given is the clicking noise generated by the vibration of the coil when it is discharged. This clicking causes artifacts in TMS–functional magnetic resonance imaging and TMS-evoked potential recording, and it impacts attention and other factors that can confound TMS experiments. It turns out that through pulse shape control, careful selection of materials, and other engineering decisions made with the human auditory system in mind, quieter devices and coils can be developed (7).

Given the scalp sensation and clicking artifacts, sham approaches are needed to mimic the ancillary effects of TMS. Earlier approaches to sham (tilting the coil off the head) failed to blind the operator, but even worse, some induced significant currents in the brain and hence were not biologically inert (8). Contemporary approaches to sham (e.g., electrical stimulation of the scalp coupled with metal shields that block the magnetic field from the coil) are advances in many respects; however, we should remember to evaluate whether the scalp electrical stimulation may introduce new confounds that may have some degree of biological activity. Redesigned TMS systems are needed to enable active TMS that lacks scalp sensation and clicking artifacts (or at least minimizes them) so that the need to reproduce these sensory effects in the sham condition is alleviated. This could greatly simplify the interpretation of TMS–functional magnetic resonance imaging and TMS-evoked potential recording paradigms.

Dose Matters, and It Is Complicated. Early studies used a low number of pulses and a limited number of treatment days, while later studies found better responses by increasing the number of pulses per day and number of days per course. There was also an early appreciation that frequency mattered.

Commentary

High frequencies were excitatory and low frequencies were inhibitory, so the dogma went. Now we know that the temporal aspects of dose are more complex, and that nested temporal patterns, such as theta burst stimulation, can enhance the potency of TMS. What was less appreciated in the early days were the other 2 key elements of dosing: spatial and contextual (9). With the advent of electric field (e-field) modeling, the impact of coil placement and orientation on the spatial distribution of the electric field induced in the brain became apparent and enabled greater precision in targeting paradigms. E-field modeling, coupled with new developments in modeling the neuronal response to stimulation, may enable more accurate approaches to individualize TMS dosing for brain regions outside of the motor cortex than the motor threshold.

As for the contextual aspects of dosing, we knew early on that TMS effects depend on what the brain is doing at the time of stimulation. The simplest example of this is the impact of muscle tone on motor threshold. Demonstrating that this facilitation of effects can extend beyond the motor system, we reported that working memory task performance during precisely timed and targeted TMS enhanced working memory function (10). We extended this work by individually targeted TMS coupled with concurrent cognitive therapy as a novel approach to treating depression (11).

Optimizing dose to improve efficacy may be key to maximizing the clinical impact of TMS. The initial industry-sponsored pivotal trial of TMS for depression failed to meet its primary endpoint but achieved U.S. Food and Drug Administration clearance based on a subset analysis showing that active and sham separated in patients who had failed a single antidepressant medication (12). Label expansion to patients who had not responded to more than one trial was later achieved through a pooled analysis of the industry trial combined with the National Institute of Mental Health (NIMH)-supported Optimization of TMS for the Treatment of Depression (OPT-TMS) study. Rather than using ever-larger sample sizes to detect small effect sizes, developing approaches to increase effect sizes through dose optimization may have more clinical impact, as we have seen with the Stanford Neuromodulation Therapy trial (13). Not only are more potent dosing strategies good for signal enhancement in clinical trials, but they also increase the likelihood and speed of response for patients who have serious and disabling conditions. We also learned the hard way that adult dosing does not always work in adolescents, a trial that also highlighted the need to address sham response (14).

Targeting Is a Moving Target. In the early days, targeting was simple: find the motor cortex by triggering a thumb twitch and measure 5 cm anteriorly to target the dorsolateral prefrontal cortex. While easy to implement and replicate, this method yielded tremendous variation across individuals. Now we know that identifying the target, and reaching it reliably and selectively, is challenging. Targets may be individual brain areas, distributed networks, or neural oscillations. Targets may be reached directly or trans-synaptically. Structural and functional image guidance is increasingly being used to individualize targeting. While these developments have improved the spatial precision and rigor of TMS studies, we should

remember that they also have limitations and costs. The test-retest reliability of the imaging paradigm and analytic pipeline used to identify the individualized network to target should be evaluated, documented, and reported (15). As we gain precision in targeting networks, we may need to rethink how to match our clinical outcome assessments to capture what the targeted network actually does rather than focusing exclusively on DSM diagnoses that may not map well onto the targeted circuit. The Research Domain Criteria platform may be helpful in this regard, both for conceptualizing targets linked to specific domains of function and for selecting readouts to demonstrate target engagement.

Future Directions and Funding Opportunities. There remains much work to be done for TMS to fully realize its potential in psychiatry. Important research gaps include TMS paradigms that are safe and effective for treating children and adolescents; practical, plausible, and biologically inactive sham conditions; unpacking studies to determine the individual contributions of image guidance and accelerated dosing paradigms; optimizing multimodal paradigms that combine TMS with concurrent cognitive interventions; and understanding how TMS works at a cellular and biophysical level. The NIMH created new programs to support neuromodulation research, including the [Neuromodulation and Neurostimulation Program](#), the [Multimodal Neurotherapeutics Program](#), and the [Novel Pharmacologic and Device-based Intervention Program for Pediatrics](#). The National Institute of Mental Health [Clinical Trials Pipeline](#) has funding opportunities that support device-based interventions across the phases of intervention development. The National Institutes of Health (NIH) BRAIN Initiative has a funding opportunity to examine the mechanisms of action of neuromodulation at a biophysical level ([RFA-NS-20-006](#)). While more research is needed, history shows us that TMS has been a success story in psychiatry, which bodes well for its future.

Acknowledgments and Disclosures

This work was supported by NIMH Intramural Research Program Grant No. ZIAMH002955.

SHL is inventor on patents and patent applications on electrical and magnetic brain stimulation therapy systems held by the NIH and Columbia University (no royalties). The opinions expressed in this article are the author's own and do not reflect the views of the NIH, the Department of Health and Human Services, or the United States government.

Article Information

From the Noninvasive Neuromodulation Unit, Experimental Therapeutics and Pathophysiology Branch, National Institute of Mental Health, Bethesda, Maryland.

Address correspondence to Sarah H. Lisanby, M.D., at Sarah.Lisanby@NIH.gov.

Received Apr 11, 2023; revised and accepted May 3, 2023.

References

1. Höflich G, Kasper S, Hufnagel A, Ruhmann S, Möller H-J (1993): Application of transcranial magnetic stimulation in treatment of drug-resistant major depression—A report of 2 cases. *Hum Psychopharmacol* 8:361–365.

2. Grisaru N, Yaroslavsky U, Abarbanel J, Lamberg T, Belmaker RH (1994): Transcranial magnetic stimulation in depression and schizophrenia. *Eur Neuropsychopharmacol* 4:287–288.
3. Kolbinger HM, Höflich G, Hufnagel A, Müller H-J, Kasper S (1995): Transcranial magnetic stimulation (TMS) in the treatment of major depression—A pilot study. *Hum Psychopharmacol* 10:305–310.
4. George MS, Wassermann EM, Williams WA, Callahan A, Ketter TA, Basser P, *et al.* (1995): Daily repetitive transcranial magnetic stimulation (rTMS) improves mood in depression. *Neuroreport* 6:1853–1856.
5. Pascual-Leone A, Rubio B, Pallardo F, Catala MD (1996): Rapid-rate transcranial magnetic stimulation of left dorsolateral prefrontal cortex in drug-resistant depression. *Lancet* 348:233–237.
6. Peterchev AV, Goetz SM, Westin GG, Luber B, Lisanby SH (2013): Pulse width dependence of motor threshold and input-output curve characterized with controllable pulse parameter transcranial magnetic stimulation. *Clin Neurophysiol* 124:1364–1372.
7. Zeng Z, Koponen LM, Hamdan R, Li Z, Goetz SM, Peterchev AV (2022): Modular multilevel TMS device with wide output range and ultrabrief pulse capability for sound reduction. *J Neural Eng* 19:(2):10.1088/1741-2552/ac572c.
8. Lisanby SH, Gutman D, Luber B, Schroeder C, Sackeim HA (2001): Sham TMS: Intracerebral measurement of the induced electrical field and the induction of motor-evoked potentials. *Biol Psychiatry* 49:460–463.
9. Deng Z-D, Luber B, Balderston NL, Velez Afanador M, Noh MM, Thomas J, *et al.* (2020): Device-based modulation of neurocircuits as a therapeutic for psychiatric disorders. *Annu Rev Pharmacol Toxicol* 60:591–614.
10. Luber B, Stanford AD, Bulow P, Nguyen T, Rakitin BC, Habeck C, *et al.* (2008): Remediation of sleep-deprivation-induced working memory impairment with fMRI-guided transcranial magnetic stimulation. *Cereb Cortex* 18:2077–2085.
11. Luber BM, Davis S, Bernhardt E, Neacsu A, Kwapil L, Lisanby SH, Strauman TJ (2017): Using neuroimaging to individualize TMS treatment for depression: Toward a new paradigm for imaging-guided intervention. *Neuroimage* 148:1–7.
12. Lisanby SH, Husain MM, Rosenquist PB, Maixner D, Gutierrez R, Krystal A, *et al.* (2009): Daily left prefrontal repetitive transcranial magnetic stimulation in the acute treatment of major depression: Clinical predictors of outcome in a multisite, randomized controlled clinical trial. *Neuropsychopharmacology* 34:522–534.
13. Cole EJ, Phillips AL, Bentzley BS, Stimpson KH, Nejad R, Barmak F, *et al.* (2022): Stanford Neuromodulation Therapy (SNT): A double-blind randomized controlled trial. *Am J Psychiatry* 179:132–141.
14. Croarkin PE, Elmaadawi AZ, Aaronson ST, Schrodt GR Jr, Holbert RC, Verdoliva S, *et al.* (2021): Left prefrontal transcranial magnetic stimulation for treatment-resistant depression in adolescents: A double-blind, randomized, sham-controlled trial. *Neuropsychopharmacology* 46:462–469.
15. Cash RFH, Cocchi L, Lv J, Wu Y, Fitzgerald PB, Zalesky A (2021): Personalized connectivity-guided DLPFC-TMS for depression: Advancing computational feasibility, precision and reproducibility. *Hum Brain Mapp* 42:4155–4172.

EXHIBIT 18



Prog. Neuro-Psychopharmacol. & Biol. Psychiat. 1997, Vol. 21, pp. 105-110
Copyright © 1997 Elsevier Science Inc.
Printed in the USA. All rights reserved
0278-5846/97 \$32.00 + .00

PII S0278-5846(96)00161-3

SLOW MAGNETIC STIMULATION OF PREFRONTAL CORTEX IN DEPRESSION AND SCHIZOPHRENIA

¹VADIM GELLER, ¹NIMROD GRISARU, ²JACOB M ABARBANEL,
¹TAMARA LEMBERG and ¹ROBERT H BELMAKER

¹Ministry of Health Mental Health Center, Faculty of Health Sciences
Ben Gurion University of the Negev, Beersheva Israel

²Department of Neurology, Kaplan Hospital, Rehovot, Israel

(Final form - October 1996)

Abstract

Vadim Geller, Nimrod Grisaru, Jacob M Abarbanel, Tamara Lemberg and Robert H Belmaker: Slow Magnetic Stimulation of Prefrontal Cortex in Depression And Schizophrenia. *Prog Neuro-Psychopharmacol. & Biol. Psychiatry* 1997, **21**, pp. 105-110. Copyright © 1997 Elsevier Science Inc.

- 1 The authors used transcranial magnetic stimulation (TMS) of pre-frontal cortex to study mood changes in 10 depressed patients and 10 schizophrenic patients.
- 2 A slow rate of stimuli was used, one per 30 seconds; maximal intensity of about 2 Tesla was given for 30 stimuli, 15 on each side of the brain.
- 3 No side effects were seen and at least three depressed patients and two schizophrenic patients appeared to improve, at least transiently.
- 4 These results suggest that rapid rate TMS may not be necessary to elicit mood effects.

Keywords: depression, frontal lobe, schizophrenia, transcranial magnetic stimulation,

Abbreviations: Brief psychiatric rating scale (BPRS), diagnostic statistical manual (DSMIII-R), electroconvulsive stimulation (ECS), electro convulsive therapy (ECT), electroencephalograph (EEG), Hamilton Depression scale (HDS), Hertz (Hz), institutional review board (IRB), transcranial magnetic stimulation (TMS)

Introduction

Transcranial magnetic stimulation (TMS) of the brain is a new but widespread neurological diagnostic procedure (Hallet and Cohen, 1989). Stimulation by rapid millisecond length magnetic pulses over the motor cortex can cause muscle contraction in the contralateral arm or leg, depending on the area of motor cortex stimulated. Parkinsonian patients have been reported to show less

akinesia (enhanced reaction time) after TMS (Pascual-Leone *et al.*, 1994a; Pascual-Leone *et al.*, 1994b). Slow TMS was effective in a single pulse, as was rapidly repeated TMS. A preliminary trial with a single session of 30-50 single TMS stimuli of 100% intensity (≈ 2 Tesla) of 10 schizophrenic patients and 10 depressed patients over the motor cortex revealed some antidepressant effect in 3 patients and improvement in 1 chronic schizophrenic patient (Grisaru *et al.*, 1994). Repeated daily slow TMS stimulation of motor cortex to 2 depressed patients helped one patient (Hoflich *et al.*, 1993), and a controlled trial of low intensity vs high intensity slow TMS in 10 depressed patients treated daily for five days over the motor cortex with 250 pulses at 0.5 Hz near motor threshold revealed some clinical benefit (Kolbinger *et al.*, 1995). More recently, George *et al.* (1995) and Pascual-Leone *et al.*, (1996) have reported that rapid TMS unilaterally over left prefrontal cortex to depressed patients caused improvement in a controlled design. High frequency (10-20 Hz) and long stimulation time (20 trains of 2-10 sec each) were used but with low power (80-90% of motor threshold).

Daily TMS to rats enhances apomorphine-induced stereotypy, reverses immobility in the Porsolt swim test, and increases seizure threshold, all effects similar to ECS in rats (Fleischmann *et al.*, 1995). Rapid TMS (25 Hz for 2 sec) has more marked effects in animal models than slow TMS (Fleischmann *et al.*, 1994; Fleischmann *et al.*, 1995, Fleischmann *et al.*, 1996) but slow TMS in humans can be given at full 2-2.5 Tesla intensity, unlike rapid TMS (George *et al.*, 1995) which cause seizures if given at full intensity and above threshold of rapidity (Pascual-Leone *et al.*, 1993). Thus slow TMS may have therapeutic potential and should not be ignored in favor of rapid TMS.

Since TMS over the motor cortex causes some discomforting motor movement, and since pre-frontal cortex is more often implicated in psychopathology of both depression and schizophrenia (Buchsbaum *et al.*, 1984), the authors decided to study TMS of pre-frontal cortex in these illnesses. Some of this data has been recently reviewed (Grisaru *et al.*, 1995).

Methods

Subjects. Ten consenting depressed patients (DSM-III-R - Diagnostic Statistical Manual) and 10 consenting chronic schizophrenic patients (DSM-III-R) participated after approval of the protocol by the IRB and the Ministry of Health. MAGSTIM 200 was used by an expert neurologist. Patients were evaluated with the Hamilton Depression Scale (HDS) (Hamilton, 1967) for the 10 depressed patients or Brief Psychiatric Rating Scale (BPRS) (Overall and Gorham 1962) for the 10 schizophrenic patients before and then after 24 hr, 6 days and 28 days after a single TMS session. Ongoing antidepressant or antipsychotic treatment was not altered before TMS treatment. None of the patients had previously received TMS (Grisaru *et al.*, 1994).

Study Procedure. Patients were given 15 stimuli over the frontal area on each side for a total of 30 stimuli in a single session. A 14 cm diameter coil was located above the orbital area on the C₃ or C₄ EEG point. Patients were given a 100% stimulus intensity, 2.5 tesla for 1 millisecond each stimulus. Stimuli were given every 30 seconds for 15 minutes. Total stimuli were 30.

Results

Tables 1 and 2 summarize the results. Among both depressed and schizophrenic patients several patients showed some improvement after the single session of TMS. Depressed patient SB reported an immediate lifting of mood within hours after TMS. His continued improvement, however, cannot be separated from concurrent antidepressant treatment. Depressed patient JR also showed an immediate lifting of mood but his continued improvement cannot be separated from concurrent antidepressant treatment. Patient DH showed increased tension and depression after the TMS session, but then improved on the standard treatment in a manner parallel to her past responses. Depressed patient MS also had an immediate lifting of mood and then continued to improve on conventional antidepressants. Depressed patient AT had three previous psychotic depressions that responded slowly to imipramine plus haloperidol. After TMS he appeared to improve more rapidly than in the past and was transferred the next day to an open ward. Patient JW had not responded to two weeks of standard antidepressants in a closed ward but seemed to respond rapidly after TMS. Patient PB showed increased tension and crying after TMS, and CB, ZK and RG had no response whatsoever.

Table 1
HDS after TMS in Depression

Name	Age	Sex	DX	Before	2 hrs after	7 days after	28 days after
SB	33	M	BP, dep	32	18	24	7
JR	27	M	UP	18	4	9	1
DH	36	F	SA, dep	30	35	28	12
MS	40	F	UP	18	2	8	20
AT	37	M	PD	31	22	20	17
CB	49	M	BP, dep	22	18	28	26
JW	42	M	PD	35	21	33	15
ZK	53	F	PD	44	43	41	40
RG	40	F	BP, dep	35	31	32	27
PB	37	F	UP	12	11	12	---

BP = bipolar; PD = psychotic depression; SA = schizoaffective, UP = unipolar

Schizophrenic patient AS had mood lifting after TMS but no lasting effect. Schizophrenic patient MJ had no immediate effect and some later improvement appeared consistent with his usual course of

illness. IZ had a marked temporary improvement the day after TMS and then rapid relapse; OZ reacted similarly. Patient LD after TMS improved rapidly concurrently with clozapine treatment despite a previous slow response to clozapine. Other schizophrenic patients showed no response to TMS.

Table 2
BPRS after TMS in Schizophrenia

Name	Age	Sex	DX	Before	24 hrs after	7 days after	28 days after
SJ	38	M	schiz	38	35	37	37
MJ	28	M	schiz	62	62	55	46
AS	39	M	schiz	52	34	46	36
IZ	31	M	schiz	49	35	42	39
SH	30	M	schiz	57	51	50	55
OZ	34	M	schiz	49	33	43	39
OB	43	F	schiz	71	71	70	---
SJ	35	M	schiz	57	53	54	40
LD	33	M	schiz	57	45	34	39
EB	41	F	schiz	43	40	41	---

Discussion

This uncontrolled study cannot prove antidepressant or antischizophrenic efficacy of frontal lobe magnetic stimulation. A striking immediate lifting of mood for several hours was noted in many patients. No serious negative side effects were observed, and results appear comparable to that of motor cortex TMS (Grisaru *et al.*, 1994; Hoflich *et al.*, 1993; Koblinger *et al.*, 1995) with the advantage that there is no motor discomfort. It is often emphasized that ECT requires convulsion for clinical efficacy (Potter and Rudofsky, 1993). However, magnetic stimulation is more penetrating than electrical stimulation and may cause neuronal depolarization in critical brain structures without causing convulsion (Hallett and Cohen, 1989). The early history of ECT required numerous trials before the present variants of electrode placement became accepted, and TMS research is at a very early stage. Recent controlled studies in depression suggests that rapid TMS over left cortex induces a mood elevation but rapid TMS over right cortex does not (George *et al.*, 1995; Pascual-Leone *et al.*, 1996); this laterality will have to be studied in future clinical research. Studies of rapid TMS are usually limited to 80% of motor threshold or roughly 50% of machine intensity. The present study of slow TMS provides preliminary data on high intensity (100% machine power) TMS to frontal cortex.

Conclusion

Comparison of effects of slow TMS, as in the present study where a 100% intensity stimulus was given every 30 seconds, with rapid TMS, as in the study of George et al. (1995) where a 80% of motor threshold stimulus was given 20 times per second, will require empirical studies in the future.

Acknowledgments

Supported by a NARSAD Senior Investigator Award to RH Belmaker.

References

- BUCHSBAUM MD, DELISI LE, HOLCOMB HH, CAPPELLETTI J, KING AC, JOHNSON J, HAZLETT E, DOWLING-ZIMMERMAN S, POST RM, MORIHISA J, CARPENTER W, COHEN R, PICKAR D, WEINBERGER DR, MARGOLIN R, KESSLER RM (1984). Anteroposterior gradients in cerebral glucose use in schizophrenia and affective disorders. *Arch Gen Psychiatry* **4**: 1159-1166.
- FLEISCHMANN A, PROLOV K, ABARBANEL J and BELMAKER RH (1995). The effect of transcranial magnetic stimulation of rat brain on behavioral models of depression. *Brain Research* **699**: 130-132.
- FLEISCHMANN A, STEPPEL J, LEON A and BELMAKER RH (1994). The effect of transcranial magnetic stimulation compared with electroconvulsive shock on rat apomorphine-induced stereotypy. *Euro Neuropsychopharmacol* **4**: 449-450.
- FLEISCHMANN A, TALPALAR AE, GROSSMAN Y, SILVERBERG D and BELMAKER RH (1996). Antidepressant potential of transcranial magnetic stimulation in rat models: comparison of slow versus rapid magnetic stimulation. In: Montgomery S and Halbreich U (eds) *Pharmacotherapy of Mood and Cognition*. American Psychiatric Press. (In press).
- GEORGE MS, WASSERMAN EM, WILLIAMS WA, CALLAHAN A, KETTER TA, BASSER P, HALLET M and POST RM (1995). Daily repetitive transcranial magnetic stimulation (rTMS) improves mood in depression. *NeuroReport* **6**: 14.
- GRISARU N, ABARBANEL JM and BELMAKER RH (1995). Slow magnetic stimulation of motor cortex and frontal lobe in depression and schizophrenia. *Acta Neuropsychiatrica* (special issue). **7**: S21-S23.
- GRISARU N, YAROSLAVSKY U, ABARBANEL J, LAMBERG T and BELMAKER RH (1994). Transcranial magnetic stimulation in depression and schizophrenia. *European Neuropsychopharmacology* **4**: 287-288.
- HALLET M and COHEN LG (1989). Magnetism: A new method for stimulation of nerve and brain. *JAMA* **262**: 538-54.
- HAMILTON M (1967). Development of a rating scale for primary depressive illness. *Br J Soc Clin Psychol* **6**: 278-296.

- HOFLICH G, KASPER S, HUFNAGEL A, RUHRMANN S and MOLLER HJ (1993). Application of transcranial magnetic stimulation in treatment of drug-resistant major depression - a report of two cases. *Human Psychopharmacol* **8**: 361-365.
- KOLBINGER HM, HOFLICH G, HUFNAGEL A, MOLLER HJ and KASPER S (1995). Transcranial magnetic stimulation (TMS) in the treatment of major depression - a pilot study. *Human Psychopharmacology* **10**: 305-310.
- OVERALL JE and GORHAM DR (1962). The brief psychiatric rating scale. *Psychol Rep* **10**: 799-812.
- PASCUAL-LEONE A, HOUSER CM, REESE K, SHOTLAND LI, GRAFMAN J, SATO S, VALLS-SOLE J, BRASIL-NETO JP, WASSERMANN EM, COHEN LG and HALLETT M (1993). *Electroencephalo Clin Neurophysiol* **89**: 120-130.
- PASCUAL-LEONE A, RUBIO B, PALLARDO F and CATALA MD (1996). Beneficial effect of rapid-rate transcranial magnetic stimulation of the left dorsolateral prefrontal cortex in drug-resistant depression. *Lancet* **348**: 223-237.
- PASCUAL-LEONE A, VALLS SOLE J, BRASIL NETO JP, CAMMAROTA A, GRAFMAN J and HALLET M (1994b). Akinesia in Parkinson's disease, part 2: Effects of subthreshold repetitive transcranial motor cortex stimulation. *Neurology* **44**: 892-898.
- PASCUAL-LEONE A, VALLS SOLE J, BRASIL NETO JP, COHEN LG and HALLET M (1994a). Akinesia in Parkinson's disease, part 1: Shortening of simple reaction time with focal, single-pulse TMS. *Neurology* **44**: 884-891.
- POTTER WZ, AND RUDORFER MV (1993). Electroconvulsive therapy-A modern medical procedure. *N Eng J Med* **328**: 882-883.

Inquiries and reprint requests should be addressed to:

Professor RH Belmaker
Beersheva Mental Health Center
PO Box 4600
BEERSHEVA
Israel

EXHIBIT 19



Contents lists available at ScienceDirect

Journal of Neuroscience Methods

journal homepage: www.elsevier.com/locate/jneumeth

Analytic consistency and neural correlates of peak alpha frequency in the study of pain

Natalie J. McLain, Moheb S. Yani, Jason J. Kutch^{*}

Division of Biokinesiology and Physical Therapy, University of Southern California, Los Angeles, CA, USA

ARTICLE INFO

Keywords:

EEG
fMRI
Peak alpha frequency
Biomarker
Processing
Pain

ABSTRACT

Background: Several studies have found evidence of reduced resting-state peak alpha frequency (PAF) in populations with pain. However, the stability of PAF from different analytic pipelines used to study pain has not been determined and underlying neural correlates of PAF have not been validated in humans.

New method: For the first time we compare analytic pipelines and the relationship of PAF to activity in the whole brain and thalamus, a hypothesized generator of PAF. We collected resting-state functional magnetic resonance imaging (rs-fMRI) data and subsequently 64 channel resting-state electroencephalographic (EEG) from 47 healthy men, controls from an ongoing study of chronic prostatitis (a pain condition affecting men). We identified important variations in EEG processing for PAF from a review of 17 papers investigating the relationship between pain and PAF. We tested three progressively complex pre-processing pipelines and varied four post-processing variables (epoch length, alpha band, calculation method, and region-of-interest [ROI]) that were inconsistent across the literature.

Results: We found a single principal component, well-represented by the average PAF across all electrodes (grand-average PAF), explained > 95% of the variance across participants. We also found the grand-average PAF was highly correlated among the pre-processing pipelines and primarily impacted by calculation method and ROI. Across methods, interindividual differences in PAF were correlated with rs-fMRI-estimated activity in the thalamus, insula, cingulate, and sensory cortices.

Conclusions: These results suggest PAF is a relatively stable marker with respect to common pre and post-processing methods used in pain research and reflects interindividual differences in thalamic and salience network function.

1. Introduction

Chronic pain is very impactful. A challenge of studying chronic pain is that it is an inherently subjective experience. Therefore, identifying objective markers is a pressing need. Markers of particular interest would be those that could measure the predisposition to developing chronic pain. Resting-state peak alpha frequency (PAF) measured from electroencephalography (EEG) has been proposed as such a marker (Furman et al., 2019). Previous work has also shown that resting-state PAF is reduced in populations with neuropathic pain in persistent abdominal pain as a result of chronic pancreatitis (Vries et al., 2013), neuropathic pain as a result of spinal cord injury (Boord et al., 2007; Sato et al., 2017), and increased subjective perception of tonic heat pain (Nir et al., 2010; Raghuraman et al., 2019). Interindividual differences in PAF may relate to awareness and the sampling of sensory inputs

(Angelakis et al., 2004; Mierau et al., 2017), and thus may reflect an individual's response to acute pain in a way that may influence the transition to chronic pain.

However, the existing literature is not conclusive in establishing a relationship between PAF and pain: studies on chronic back pain (Schmidt et al., 2012), central neuropathic pain in multiple sclerosis patients (Krupina et al., 2019), and persistent pain after breast cancer treatment (van den Broeke et al., 2013) did not find a relationship between slowed PAF and pain. Together the positive and negative findings of the existing literature are often interpreted as suggesting either a differential relationship between PAF and pain of different origins, or as lack of a strong relationship between PAF and pain altogether. Within the pain field there is also substantial variation in how PAF is computed and interpreted, which complicates the comparison of results across studies.

^{*} Correspondence to: University of Southern California, 1540 E. Alcazar Street, CHP 155, Los Angeles, CA 90033, USA.

E-mail address: kutch@usc.edu (J.J. Kutch).

<https://doi.org/10.1016/j.jneumeth.2021.109460>

Received 24 May 2021; Received in revised form 10 December 2021; Accepted 21 December 2021

Available online 24 December 2021

0165-0270/© 2021 Published by Elsevier B.V.

In order to interpret and compare results across the field in a meaningful way, we must first be certain that differences in findings are not simply a byproduct of differences in processing pipelines. While previously published papers have focused on developing a method that best estimates the “true” PAF value (Corcoran et al., 2018), the goal of this paper is instead to analyze previously employed methods and determine whether differences in processing decisions may impact the final PAF calculation. We reviewed 17 papers with complete available methods investigating the relationship between PAF and pain and found that there were major differences in data filtering, whether data were re-referenced, what kind of artifact removal was performed, epoching, alpha band bounds, and formula for calculating PAF. Furthermore, comparisons between PAF and other measures of neural activity are infrequent, limiting the interpretation of PAF in terms of underlying cortical and subcortical activity patterns. The thalamus is a hypothesized generator of the alpha rhythm and has been implicated in alpha rhythm alterations, but the association between thalamic activity and PAF in humans has not been thoroughly explored.

Given these uncertainties, in this study we aimed to assess the robustness of PAF to three different pre-processing pipelines as well as four processing variables (seven epoch lengths, two formulas for calculating PAF, three different alpha bands, and five regions-of-interest [ROIs]: grand-average, frontal, parietal, occipital, sensorimotor) representative of what is currently being used in the pain literature. Additionally, we aimed to associate PAF with fractional amplitude of low-frequency fluctuations (fALFF), a resting-state functional magnetic resonance imaging (rs-fMRI)-derived measure of local activity. To accomplish these aims, we analyzed data from 47 healthy men, a subset of an ongoing study of urologic chronic pelvic pain. The dataset included 64-channel resting-state electroencephalographic (EEG) and resting-state functional magnetic resonance imaging (rs-fMRI) from all participants. We first ran three of the most representative EEG pre-processing pipelines and then varied post-processing parameters (epoch length, PAF formula, alpha band bounds, and ROI) as determined by our review of the PAF and pain literature. We then determined whether there was a relationship between the ROI averages and whole brain as well as thalamic activity in healthy men.

2. Methods

2.1. Participants

Forty-seven healthy men who were the control group with complete EEG and rs-fMRI data for an ongoing study of chronic prostatitis were entered into this study. Participants were included if they were older than 18 years of age, able to participate in the informed consent process, safe to be scanned by magnetic resonance imaging, had no diagnosis of chronic prostatitis, had no active urinary, anal, or genital infection, and no severe, urgent, or debilitating medical condition. All aspects of the study conformed to the principles described in the Declaration of Helsinki and were approved by our Institutional Review Board. All participants provided informed consent. The final group of participants was 35.10 ± 13.30 years old (mean \pm SD, range, 22.89–63.56 years).

2.1.1. EEG collection and analysis

Continuous EEG data was collected using a 64-channel, ANT Neuro gel-based electrode cap with sintered Ag/AgCl electrodes. The online reference was placed at the right mastoid. Signal was acquired with eego sports acquisition software (v1.2.1) from an Ant Neuro eego Sports amplifier (product number ee-202) at a sampling rate of 2048 Hz. Impedances for all electrodes were kept below 15 k Ω .

Participants were lying supine and told to keep their head as still as possible, relax, and not go to sleep. Participants were then told to follow automated, alternating voice commands to open or close their eyes. The continuous recording was annotated at the beginning of each eyes-open/eyes-closed epoch: in total, there were ten minutes of continuous EEG

data with non-overlapping, one-minute epochs marked for five eyes-open and five eyes-closed periods.

All offline data processing was performed with EEGLAB v13.6.5.b and MATLAB (R2018b) scripts.

Parameters for the EEG analysis were based on a review of 17 papers investigating the relationship between chronic pain and PAF (Björk et al., 2009; Boord et al., 2007; Corlier et al., 2021; Furman et al., 2020, 2019, 2018; Krupina et al., 2019; Ngernyam et al., 2015; Nir et al., 2010; Raghuraman et al., 2019; Sato et al., 2017; Schmidt et al., 2012; Simis et al., 2021; van den Broeke et al., 2013; Vries et al., 2013; Vuckovic et al., 2018, 2014). Papers were selected from an initial search in Pubmed with the following search terms: EEG AND (alpha frequency OR peak frequency) AND pain AND (human OR patient) NOT review. In addition, a filter for only papers available in English was applied. This produced 214 titles and abstracts that were screened. Animal research and research from non-applicable fields such as sleep and anesthesiology were excluded at this step, as were protocol-only publications. We also excluded magnetoencephalography (MEG) papers at this step. While the collection setup and final data set in EEG and MEG are highly similar, the underlying physiological process recorded is quite different. The two modalities are subject to slightly different sets of noise/processing issues and we elected to focus exclusively on EEG to ensure results were not confounded by including processing parameters for two different modalities (Cohen and Cuffin, 1983; Cuffin and Cohen, 1979; Molins et al., 2008; Muthuraman et al., 2015). 134 articles remained after this step. Full-text articles were then assessed for eligibility and further exclusions were made for no PAF calculation ($n = 87$), no pain score and/or pain population ($n = 10$), no resting-state PAF ($n = 12$), never relating pain to resting-state PAF ($n = 7$), and no full version available ($n = 2$). At this step, a total of 118 articles were excluded, and one additional article was identified and added through review of literature references in the screened papers. The remaining 17 articles are the ones discussed in this paper and summarized in Table 1 and Supplementary Table 1. A flow diagram with the complete information on the conducted search and selection process can be found in Supplementary Fig. 1. As indicated in Supplementary Table 1, this analysis includes papers of varying clinical and healthy populations, as well as papers that did and did not find a relationship between PAF and pain.

Analysis of EEG data processing parameters was conducted in two steps: pre-processing (time-series de-noising) and post-processing (data reduction to summary measures). First, three representative pipelines of pre-processing steps/variables were compared to determine the initial impact on PAF calculation. Second, post-processing variables (epoch length, PAF formula, alpha band bounds, and ROI) were varied for the cleaned data and compared in a sensitivity analysis to determine their impact on PAF calculation. If the pre-processing pipelines from the first step were found to have a significant effect on PAF, the second step would be performed individually for each of the three pre-processing pipelines.

2.1.2. Pre-processing comparison

For all three pipelines, signal for all eyes open/closed epochs was bandpass filtered from 1 to 100 Hz. These low and high pass cutoffs were determined by taking the mode of the low and high pass cutoffs in the 17 articles reviewed. During collection, each non-overlapping, one-minute epoch was marked as eyes-open or eyes-closed by the experimenter. During processing, recorded data was inspected to verify eyes-open/eyes-closed epochs were in the correct order/marked correctly. Incorrectly marked epochs were removed from the data set before further analysis. The first and last 10% of each 60-second epoch was removed, leaving five 48-second, eyes-closed epochs for further analysis. Each epoch was then processed through three different, progressively complex pre-processing pipelines:

Table 1

Processing data from the 17 articles reviewed. General abbreviations: NS not stated, NA not applicable; preprocessing abbreviations: CA common average, GC Gratton & Coles, VI visual inspection; post processing abbreviations: COG center of gravity, GA grand-average, ROI region of interest.

Paper	Not varied in our analysis			Varied in Preprocessing		Varied in post-processing				
	Eye State	Bandpass	Notch	Re-Reference	Noise removal	Epoch length	Epoch overlap	Alpha band	Peak or COG	GA, ROI, channel
Boord et al. (2007)	Both	0–500 Hz	no	no	ICA	2 s	No	8–13 Hz	peak	GA, channel
Björk et al. (2009)	Closed	0.5–70 Hz	50 Hz	CA	VI	4 s	no	8–13 Hz	peak	channel
Nir et al. (2010)	Closed	0.15–100 Hz	50 Hz	no	"artifact rejection program" (max voltage step 50uV)	1 s	No	7.5–12 Hz	peak	channel
Schmidt et al. (2012)	Closed	1–30 Hz	no	CA	GC, VI	4 s	2 s	4–12 Hz* *	both	ROI, GA
van den Broeke et al. (2013)	Closed	0.1–30 Hz	no	no	GC, VI	4 s	No	7–13 Hz	COG	ROI
deVries et al. (2013)	Closed	1–120 Hz	no	Mean of mastoids	GC, VI, rejected if > 200 uV amp or voltage steps > 50 uV	10 s	No	7.5–13 Hz	COG	ROI, GA
Vuckovic et al. (2014)	Both	1 Hz	48–52 Hz	CA	VI, amplitude ≥ 100 μV or present across all electrodes removed; ICA	2 s	1 s	8–12 Hz	peak	GA, channel
Ngernyam et al., 2015	Closed	0.1–70 Hz	no	no	VI, ICA	2 s	No	4–13 Hz* *	peak	ROI
Sato et al. (2017)	Closed	.5–70 Hz	no	no	Amplitudes > 80 μV rejected	2 s	1 s	7–14 Hz	both	ROI
Furman et al. (2018)	Closed	5–16 Hz	no	no	gamma band-based ICA	5 s	No	9–11 Hz	COG	ROI
Vuckovic et al. (2018)	Both	0.5–60 Hz	50 Hz	CA	VI, amplitude ≥ 100 μV or present across all electrodes removed; ICA	NS	NS	8–13 Hz	peak	channel
Furman et al. (2019)	Closed	2–100 Hz	50 Hz	CA	PCA, VI	5 s	No	8–12 Hz	COG	ROI
Raghuraman et al. (2019)	Closed	0.5–100 Hz	no	NA; surface Laplacian	ICA	5 s	No	7.4–12 Hz	COG	channel
Furman et al. (2020)	Closed	0.2–100 Hz	no	no	VI, PCA	5 s	No	9–11 AND 8–12 Hz	COG	ROI
Krupina et al., 2020	Closed	0.5–30 Hz	50 Hz	no	VI, BRAINSYS algorithm (4–5 SD=artifact)	4 s	No	8–13 Hz	peak	ROI
Corlier et al. (2021)	Closed	NS	no	CA	semi-automated FASTER toolbox, VI	4 s	NS	7–13 Hz	COG	ROI
Simis et al. (2021)	Closed	1–40 Hz	no	no	VI	5 s	2.5 s	8–12.9 Hz	peak	ROI
Current paper	Closed	1–100 Hz	60 Hz	CA	MARA, Amplitudes > 80 μV rejected	2,4,5, 10, 30, 45,48 s	No	7.5–13 Hz 8–12 Hz 9–11 Hz	Both	ROI, GA

- Notch:** A notch filter was applied from 58 to 62 Hz to attenuate electrical noise in the bandpassed EEG signal. A version of the data preprocessed up to this step was stored for later analysis.
- ReRef+Notch:** The notch pre-processed data was further pre-processed by re-referencing the EEG data to the common average of each participant's electrodes. A version of the data preprocessed up to this step was stored for later analysis. Of the 17 papers reviewed, only seven re-referenced their EEG data (Björk et al., 2009; Corlier et al., 2019; Furman et al., 2019; Schmidt et al., 2012; Vries et al., 2013; Vuckovic et al., 2018, 2014).
- MARA+ReRef+Notch:** Notch/bandpass filtered data was further pre-processed by ICA analysis to prepare data for automated artifact removal via the Multiple Artifact Rejection Algorithm (MARA): Artifact rejection was performed in an automated manner using MARA within EEGLAB (Winkler et al., 2014, 2011). As in the original applications of MARA, we used the default MARA setting and rejected any components with artifact probabilities greater than 0.5 (i.e., more than 50% likely to be an artifact component) (Gabard-Durnam et al., 2018; Winkler et al., 2014, 2011). After artifact removal, each channel's signal was re-referenced to the common average of all channels for each participant.

Data from all three pipelines was then processed in the same way to calculate PAF, detailed below.

Bounds for the alpha band vary across sources: initially an alpha band of 7.5–13 Hz was determined to best cover the distribution represented in Table 1. Papers examining the theta-alpha range were not included in the initial alpha band determination (Ngernyam et al., 2015;

Schmidt et al., 2012). Follow-up sensitivity analyses were performed on an additional two alpha bands (further discussed in the post-processing section below). Only eyes-closed data was used for the calculation of PAF, in keeping with the majority of the 17 papers reviewed and previous work investigating the predictive value of individual alpha frequency (Corlier et al., 2019): only three papers reported results for resting-state PAF from eyes-open data (Boord et al., 2007; Vuckovic et al., 2018, 2014). The power spectral density (PSD) with normalized units of the EEG frequencies for each eyes-closed epoch were computed in MATLAB. Epochs with peak-to-peak amplitude exceeding 80 mV were completely excluded from further analysis, in line with the more conservative (Sato et al., 2017) of the two articles that reported using amplitude cutoffs as part of EEG pre-processing (Sato et al., 2017; Vries et al., 2013). Initially, center of gravity (COG), as reported in Furman et al. (2019), was used to determine the peak alpha frequency (7.5–13 Hz) for each epoch at each electrode. In brief, COG takes the weighted sum of the alpha spectrum divided by the total power, resulting in the "center" of the spectral power between 7.5 and 13 Hz. The following equation was used:

$$\text{COG} = \frac{\sum_{i=1}^n f_i \times a_i}{\sum_{i=1}^n a_i}$$

f_i is the i th frequency bin including and above 7.5 Hz, n is the number of frequency bins between 7.5 and 13 Hz, and a_i is the spectral amplitude for f_i .

Six of the 17 papers reviewed used COG to determine PAF (Furman

et al., 2020, 2019, 2018; Raghuraman et al., 2019; van den Broeke et al., 2013; Vries et al., 2013) and three included measurements for both the dominant peak of spectral density and COG method (Corlier et al., 2021; Sato et al., 2017; Schmidt et al., 2012). Eight of the 17 papers reviewed determined PAF by selecting the frequency of the highest power in the alpha band (also known as “peak picking”) (Björk et al., 2009; Boord et al., 2007; Krupina et al., 2019; Ngernyam et al., 2015; Nir et al., 2010; Simis et al., 2021; Vuckovic et al., 2018, 2014). See comparisons in Table 1. COG is thought to be a more stable measure, particularly in cases where there are multiple peaks within the band of interest (Brötzner et al., 2014; Klimesch, 1999, 1997; Klimesch et al., 1993). Analysis of how peak picking and COG measures of PAF differ within individuals, especially in combination with other varied post-processing parameters, however, has not yet been conducted. Therefore, we will revisit and vary the calculation method (peak picking versus COG) in the post-processing section.

PAF was then averaged across all remaining epochs at each electrode for spatial distribution of PAF values (*topographic PAF*) and further averaged across all electrodes to compute the *grand-average PAF* for each participant. Headmaps for topographic PAF were visualized using the EEGLAB function *topoplot*.

2.1.3. Post-processing comparison

Because the three pre-processing pipelines showed very little variation in grand-average and topographic PAF, we selected the most comprehensive pipeline (Notch+ReRef+MARA) to serve as the “synthesized literature pipeline” (SLP), a baseline analysis process we used to compare four post-processing parameters that varied the most across the reviewed papers: epoch length, alpha band range, COG versus peak picking methods for determining PAF, and ROI. SLP parameters are preprocessing with Notch+ReRef+MARA pipeline, epoch length=48 s, alpha band= 7.5–13 Hz, and ROI=grand-average. Epoch lengths in the reviewed papers ranged from 2 s to 30 s (Table 1), making the 48 s in our synthesized literature pipeline epochs much longer than what is commonly used in the field. Epoch overlap also varied across papers but compared to epoch length, was far less variable: only four papers used epochs that overlapped, and all four used epochs that overlapped by 50% (Sato et al., 2017; Schmidt et al., 2012; Simis et al., 2021; Vuckovic et al., 2014). Two papers did not report if their epochs were overlapping (Corlier et al., 2021; Vuckovic et al., 2018). All remaining papers used non-overlapping epochs, as reported in Table 1.

We performed a sensitivity analysis representative of the epoch lengths used in the reviewed papers (Table 1), ranging up to the length used in our own calculation. The final set of values used was 2 s, 4 s, 5 s, 10 s, 30 s, 45 s, and 48 s (SLP). We varied these epoch lengths individually for both the COG and peak picking methods of PAF calculation, keeping the alpha band at the synthesized literature pipeline range (7.5–13 Hz). Epochs with peak-to-peak amplitude exceeding 80 mV were excluded from further analysis. Therefore, varying the epoch length also affected the amount of data removed by the 80 mV cutoff. Grand-average PAF was then calculated using both peak picking and COG for each epoch at each electrode before being averaged at each electrode and then across all electrodes. The range of PAF values across the epoch lengths was calculated for each participant (separately for peak picking and COG) as well as the range for each participant when comparing peak picking and COG for the synthesized literature pipeline values (epoch length=48 s). If either variable at this step (COG versus peak picking or epoch length) was found to significantly impact the final, grand-average PAF value, it would be carried forward to the next step: varying alpha band bounds.

Because there was little effect of epoch length, but an apparent effect of COG versus peak picking for PAF calculation, we used the synthesized literature pipeline with the original 48-second epochs to vary alpha band range and COG versus peak picking for PAF calculation. Sensitivity analysis for the alpha range was performed on 7.5–13 Hz (SLP), and 8–12 Hz and 9–11 Hz to reflect a comparison performed in Furman et al.

(2019). Epochs with peak-to-peak amplitude exceeding 80 mV were excluded from further analysis. Grand-average PAF was then calculated using both peak picking and COG for each of the three alpha bands for each epoch at each electrode before being averaged at each electrode and then across all electrodes. The range of PAF values within each subject was calculated for each of the three alpha bands. Alpha band was also found to impact grand-average PAF calculation. The grand-average PAF values from COG versus peak picking for all three alpha bands were carried forward to be analyzed with the fMRI data (described in Section 2.3).

Because there is variation across publications in the final PAF measure used (grand-average versus ROI and channel level, see Table 1) we selected four representative electrode ROIs from the papers reviewed. Of the 17 papers reviewed, 11 used ROI analysis. The four most common and consistent ROIs can be summarized with four electrode combinations: frontal (F3, Fz, F4, Fp1, Fp2), parietal (CP3, CPz, CP4, P3, Pz, P4), occipital (O1, Oz, O2), and sensorimotor (C3, Cz, and C4). We calculated the average across each of these ROIs using the SLP with both COG and peak picking calculation methods to compare against the grand-average measure. These four average PAF values were carried forward to be analyzed in a separate fMRI analysis alongside the grand-average.

2.2. MRI collection and analysis

2.2.1. MRI acquisition and pre-processing

On the same day but before EEG collection, we collected resting-state functional magnetic resonance imaging (rs-fMRI) data using a 3 Tesla MRI scanner (Siemens Magnetom Prisma). To spatially align the rs-fMRI data, we also acquired a structural image with a T1-weighted magnetization prepared rapid gradient-echo sequence (MP-RAGE): repetition time 2300 ms, echo time 2.98 ms, slice thickness 1 mm, 240 slices, 256×256 mm voxel matrices, and $1 \times 1 \times 1$ mm voxel size. The resting scans were acquired with the participant resting in a supine position, eyes closed, for 10 min in 36-slice whole-brain volumes with repetition time 2000 ms, echo time 28 ms, slice thickness 4 mm, 220×220 mm voxel matrices, $3.4 \times 3.4 \times 4.0$ mm voxel size, and flip angle 77 degrees. All neuroimaging pre-processing was performed using fMRIprep 1.5.8 as we have described previously (Mawla et al., 2020).

2.2.2. Assessment of local activity

We assessed local activity in discrete brain regions using the Amplitude of Low Frequency Fluctuations (ALFF). ALFF is a local measure of spontaneous brain activity, which is computed from the power spectrum of the BOLD signal. Fractional ALFF (fALFF) accounts for physiological confounds and individual differences by examining power in the frequency range of interest compared to power in the total frequency range. Here we focused on slow-5 oscillations (0.01–0.027 Hz) (Mawla et al., 2020) - decreased relative power in this frequency band has been associated with increases in neural activity (Kilpatrick et al., 2014; Mawla et al., 2020; Yani et al., 2019). In order to generate slow-5 fALFF images, the 3dRSFC function in the Analysis of Functional NeuroImages (AFNI) software package was used to compute the fractional power in the slow-5 band while spatially smoothing to 6 mm FWHM and removing the effect of 12 parameters with linear regression (six head motion time series and six aCompCor time series) (Mawla et al., 2020).

2.2.3. fMRI motion assessment

We assessed head motion using Framewise Displacement (FD), and planned to exclude any participants with gross head motion defined as average FD exceeding 0.55 mm based on recent recommendation (Parkes et al., 2018; Van Dijk et al., 2012). Of the 47 participants, none had gross head motion exceeding this limit. As an additional precaution, average FD from each participant was included as a confounding variable in the statistical analysis below.

2.3. Statistics

We ran a principal components analysis (PCA) on the topographic PAF at each electrode for every participant using the *pca* function in MATLAB to determine whether or not PAF is low dimensional and, if so, if grand-average is a good, low dimensional representation of the data. We examined the percentage of the total variance explained by each principal component to assess the independence of topographic PAF across all electrodes. We then examined the principal components scores, to determine if the component explaining the most variance aligned with grand-average PAF. We then tested the hypothesis that grand-average PAF would be consistent across the above-described three pre-processing pipelines by calculating the Spearman's ranked correlation coefficient between each of the three possible pairs of pipelines.

fMRI statistics were carried out using FEAT (FMRI Expert Analysis Tool) Version 6.00, part of FSL (FMRIB's Software Library, www.fmrib.ox.ac.uk/fsl). We tested the hypothesis that PAF is associated with thalamic activity by masking slow-5 fALFF data to the entire thalamus as defined by the Harvard Oxford Atlas in FSL (HarvardOxford-sub-prob2mm_thalamus) and performed linear regression analyses to assess the association between the masked slow-5 fALFF images and grand-average PAF values. We additionally performed this analysis on the unmasked/whole-brain slow-5 fALFF images. If grand-average PAFs from the three pre-processing pipelines tested were significantly different, we planned to run this analysis for each of the three pipelines. If they were found to be similar, we planned to only use grand-average PAF from the most comprehensive pipeline (MARA+ReRef+Notch). Likewise, we planned to run the analysis for only the post-processing variables (epoch length, alpha bounds, COG versus peak picking, ROI) that proved to have a significant impact on the final grand-average PAF calculation. Therefore, the final analysis included grand-average PAF values from the MARA+ReRef+Notch pipeline for all three alpha bands examined, using both peak picking and COG to calculate the PAF. ROI for both peak picking and COG were examined in a second fMRI analysis. Using OLS (ordinary least squares) simple mixed effects, grand-average PAF was included as a regressor with average FD from each participant included in the model as a regressor of no interest. Z-statistic images were thresholded using cluster correction determined by $Z > 2.3$ and a corrected cluster significance threshold of $P = 0.05$ (Worsley, 2001). If the fMRI analysis with the grand-average PAF values showed a significant impact of any of the post-processing variables on identified neural correlates, those post-processing variables would also be carried forward to the EEG ROI fMRI analysis.

The EEG ROI fMRI analysis was an OLS fMRI analysis similar to the grand-average analysis described above. Each EEG ROI average PAF was entered as the covariate of the slow-5 fALFF data to further determine if the EEG ROIs had separate neural correlates. Because the alpha bands in the first fMRI analysis had increasingly fewer correlates as they became narrower but otherwise overlapped, while the two calculation methods potentially highlighted different neural structures, we carried forward only the alpha band from the SLP (7.5–13 Hz, epoch length=48 s, COG used to calculate PAF) was 1.5%, and no more than half the data was removed for any one subject. Specifically for the purpose of

visualizing the distribution of grand-average and topographic PAF values, we split the MARA+ReRef+Notch data into the highest 16, lowest 16, and remaining middle 15 grand-average PAF value individuals. We color-coded the distribution of the grand-average PAF for all participants (Fig. 1a.), and plotted the averaged scalp maps (topographic PAF values, Fig. 1b) and power spectra averaged across all electrodes (Fig. 1c) for the highest and lowest 16 individuals. The grand-average PAF value was 10.50 ± 0.14 (mean \pm SD) for the highest 16 participants and 9.67 ± 0.30 (mean \pm SD) for the lowest 16 participants. These distinct peaks are also visible in the averaged power spectrum data (across all epochs and electrodes) for the highest and lowest 16 participants (Fig. 1c). The remaining middle participants had a mean grand-average PAF value of 10.17 ± 0.07 (mean \pm SD). Note that these high, low, and middle groupings were used only for visualization, and no further statistics were run/no group differences were calculated.

We then split and plotted the grand-average and topographic PAF data in the same way for each of the three pipelines (Fig. 2a and b.). Note that the top half of the third column of Fig. 2 is the same data from Fig. 1a and b. Results for each measure (grand-average and topographic PAF) appear to be highly similar across all three pre-processing pipelines. Using the data from all 47 participants, the MARA+ReRef+Notch pipeline produced a mean grand-average PAF value of 10.11 ± 0.40 Hz (mean \pm SD) and had a range of 9.24–10.79 Hz. The ReRef+Notch pipeline produced a mean grand-average PAF value for all participants of 10.10 ± 0.38 Hz (mean \pm SD) and had a range of 9.23–10.70 Hz. The Notch pipeline produced a mean grand-average PAF value for all participants of 10.07 ± 0.33 Hz (mean \pm SD) and had a range of 9.31–10.61 Hz.

The principal components analysis revealed that > 95% of the

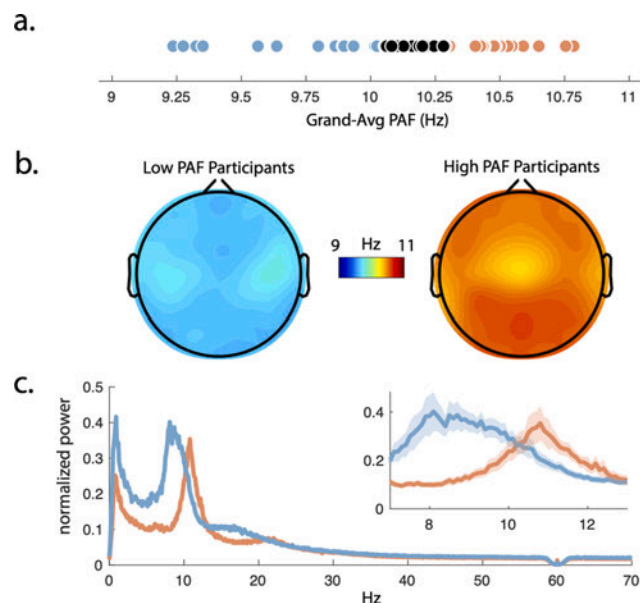


Fig. 1. 64 channel EEG data run through the most comprehensive pre-processing pipeline, MARA+ReRef+Notch, was used to examine differences in individuals with high and low grand-average PAF values. Participants were split into three groups based on their grand-average PAF, with distribution shown for the lowest 16 PAF individuals in blue, the highest 16 in orange, and the remaining, middle 15 in black (a). The PAF averaged across all epochs at each electrode was then further averaged across the lowest and highest 16 participants and plotted topographically on headmaps (b). Averaged power spectra across all epochs and electrodes for the lowest and highest 16 participants were then plotted to illustrate the differing peaks (c), which match up with PAF distributions in (a). An inset shows the data zoomed into just the alpha band, 7.5–13 Hz, with standard error shaded (c). (For interpretation of the references to color in this figure, the reader is referred to the web version of this article.)

3. Results

All processing variables of interest are reported in Table 1, and information about subject populations (sample size, clinical versus healthy, pathology if applicable) as well as the relationship between PAF and pain are reported in Supplementary Table 1. Detailed criteria and steps for the literature review process are reported in Supplementary Fig. 1.

The mean number of ICs removed using MARA for all participants was 27.85 ± 9.54 (mean \pm STD). The total amount of data removed due to the 80 mV cutoff for the SLP (alpha 7.5–13 Hz, epoch length=48 s, COG used to calculate PAF) was 1.5%, and no more than half the data was removed for any one subject. Specifically for the purpose of

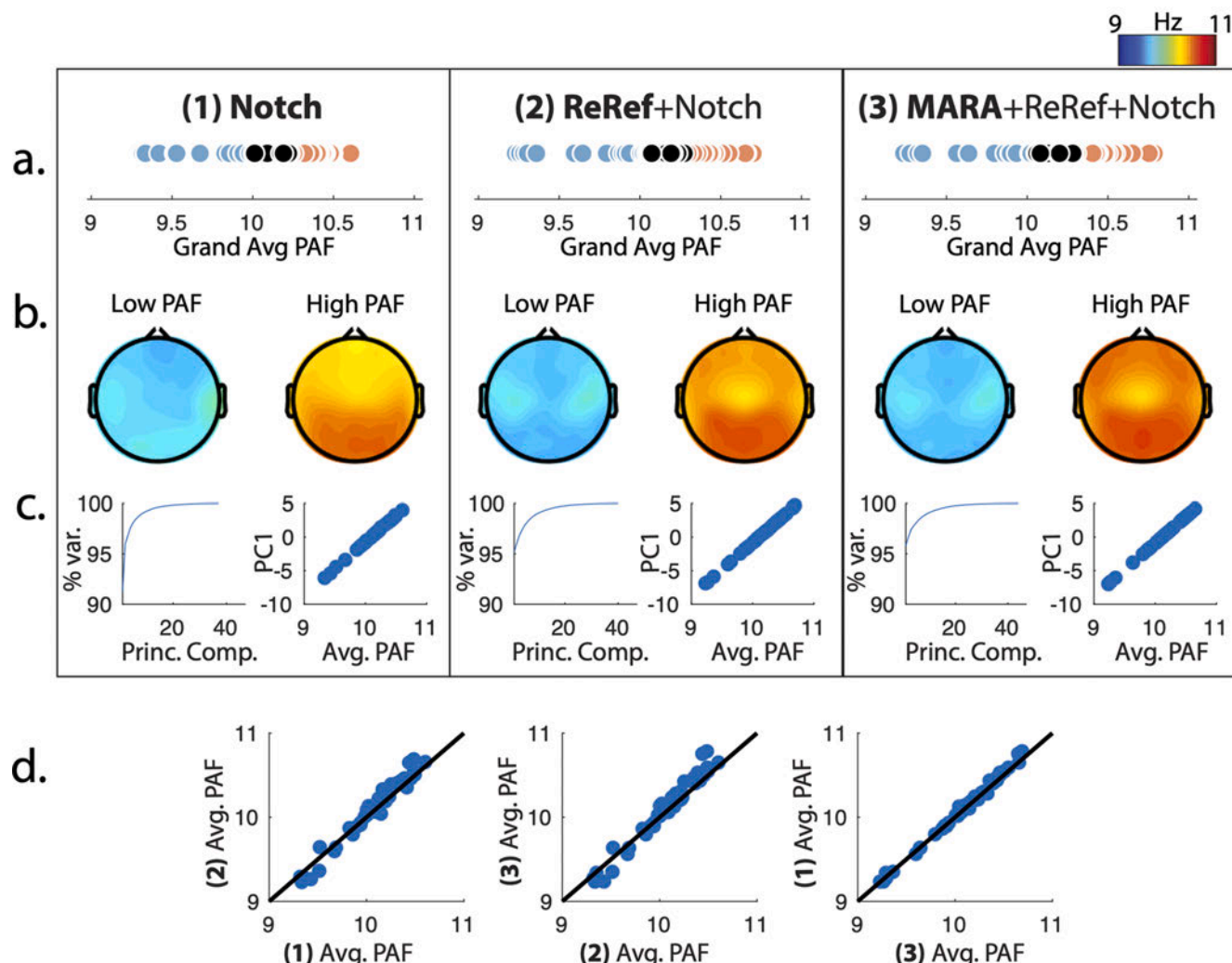


Fig. 2. EEG data run through each of the three pre-processing pipelines was compared. Participants were divided based on their grand-average PAF values calculated with the MARA+ReRef+Notch pipeline into the lowest 16, highest 16, and remaining middle 15. The distributions of PAF values are shown for each group, with the lowest 16 in blue, the highest 16 in orange, and the middle 15 in black (a). PAF data for the lowest and highest 16 participants was then averaged at each electrode and plotted topographically on headmaps (b). Principal components analysis was run on all participants (c). It was discovered that over 95% of the variance for the topographic PAF data from all three pre-processing pipelines was explained by a single principal component, PC1. The weights for PC1 align well with the grand-average PAF for each individual (c). The three possible combinations of pre-processing pipelines were then compared and found to be highly correlated, with a Spearman's ranked correlation coefficient of > 0.95 for all three comparisons (d). a-d all indicate a high degree of similarity between the data from each pre-processing pipeline in terms of grand-average PAF, topography, and variance. (For interpretation of the references to colour in this figure, the reader is referred to the web version of this article.)

variance for the topographic PAF values for all three pre-processing pipelines was explained by a single component (Fig. 2c). This component aligned well with the grand-average of PAF, as confirmed by plotting the first principal component score (PC1) against the grand-average PAF for each participant (Fig. 2c). Additionally, each participant's grand-average PAFs for each of the three pipelines were plotted against one another to ensure that the distribution of individual scores lined up (Fig. 2d). All three methods showed strong agreement between participant scores ($\rho > 0.97$ for all three pre-processing pipeline comparisons: Notch and ReRef+Notch $\rho = 0.980$, Notch and MARA+ReRef+Notch $\rho = 0.982$, ReRef+Notch and MARA $\rho = 0.995$).

Because of the high degree of similarity between all three pre-processing pipelines, the sensitivity analysis for epoch length, alpha band bounds, COG versus peak picking, and ROI for PAF calculation was only performed on preprocessed EEG spectra from the MARA+ReRef+Notch pipeline.

The total amount of data removed due to the 80 mV cutoff was 1.4%

for 45 s epochs, 1.3% for 30 s epochs, 0.58% for 10 s epochs, 0.4% for 5 s epochs, 0.3% for 4 s epochs, and 0.2% for 2 s epochs. No more than half the data was removed in any one subject, with the max percentage of data removed for any one subject decreasing with shorter epoch lengths. We plotted the values of grand-average PAF for all seven epoch lengths (2 s, 4 s, 5 s, 10 s, 30 s, 45 s, and 48 s/synthesized literature pipeline) for both peak picking (Fig. 3a) and COG PAF values (Fig. 3b). Additionally, the grand-average PAF for peak picking versus COG when keeping the epoch length constant (SLP, epoch length=48 s) were plotted (Fig. 3c). The mean range of PAF values in a specific subject across epoch lengths was 0.28 ± 0.16 Hz when peak picking was used and 0.08 ± 0.05 when COG was used. The mean range of values within a subject for peak picking versus COG was 0.51 ± 0.40 Hz. There was little effect of epoch length, but an apparent effect of COG versus peak picking for grand-average PAF calculation, being particularly pronounced for participants at either extreme of the group PAF range (Fig. 3b). Only peak picking versus COG was carried forward to the

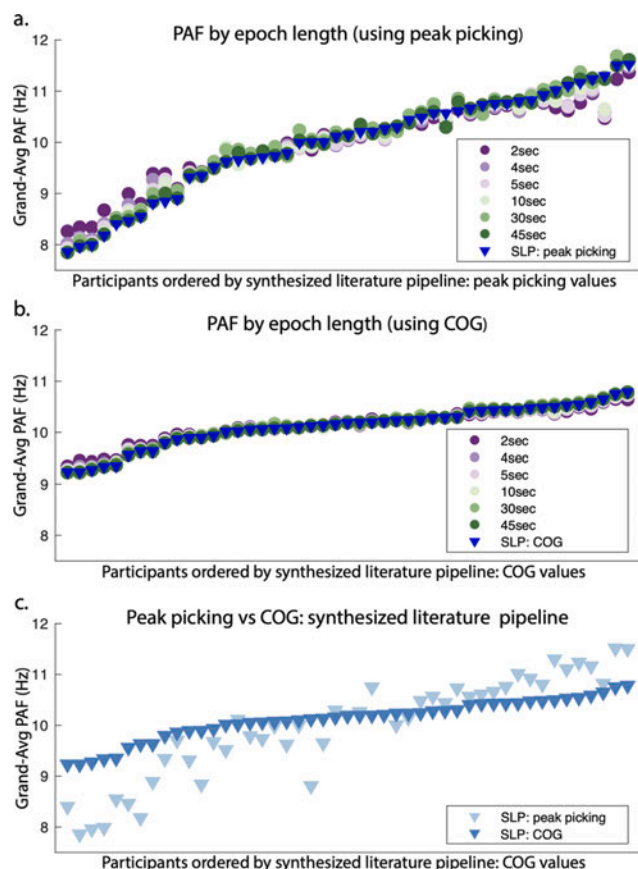


Fig. 3. Cleaned EEG data from the MARA+ReRef+Notch pipeline was used to calculate grand-average PAF using seven epoch lengths representative of what was used in the 17 articles reviewed. The synthesized literature pipeline (SLP) is the grand-average PAF from 48 s epoching and alpha 7.5–13 Hz as done in Figs. 1 and 2. Peak picking (a) and COG (b) were used separately across the varied epoch lengths and SLP to calculate grand-average PAF. Each point along the x-axis is an individual subject, and they are ascendingly ordered by SLP grand-average PAF value with peak picking in (a) and SLP with COG in (b) and (c). When epoch length was held constant at 48 s (SLP) and calculation method was varied, a substantial difference was observed in many participants (c). Across the five tested epoch lengths, the mean range of grand-average PAF values for each participant was 0.28 ± 0.16 Hz when calculated with peak picking (a) and 0.08 ± 0.05 when calculated with COG (b). When epoch length was held constant at 48 s (SLP), the mean difference of grand-average PAF values was 0.51 ± 0.40 Hz when calculated using peak picking and COG for each participant (c).

alpha band bound sensitivity analysis.

The comparison of grand-average PAF for the three alpha bands (8–12 Hz, 9–11 Hz, and 7.5–13 Hz/synthesized literature pipeline) was plotted for both peak picking (Fig. 4a) and COG (Fig. 4b) grand-average PAF. The mean range of grand-average PAF values in a specific subject across the three alpha bands was 0.38 ± 0.42 Hz when peak picking was used and 0.27 ± 0.17 when COG was used (mean \pm SD). There was a moderate effect of alpha band bounds on the final grand-average PAF calculation (Fig. 4). Peak picking versus COG and the three alpha bands were carried forward to the fMRI analysis.

The ROI averages and grand-average PAF (referred to collectively as the five ROIs) were highly correlated within calculation method (Table 3): all combinations of averages had correlation coefficients over 0.89 when calculated with peak picking and over 0.91 when calculated with COG. As with the other comparisons of peak picking and COG, peak picking values were far more variable across ROIs within participants. When plotting all five ROI averages across all participants, there was an

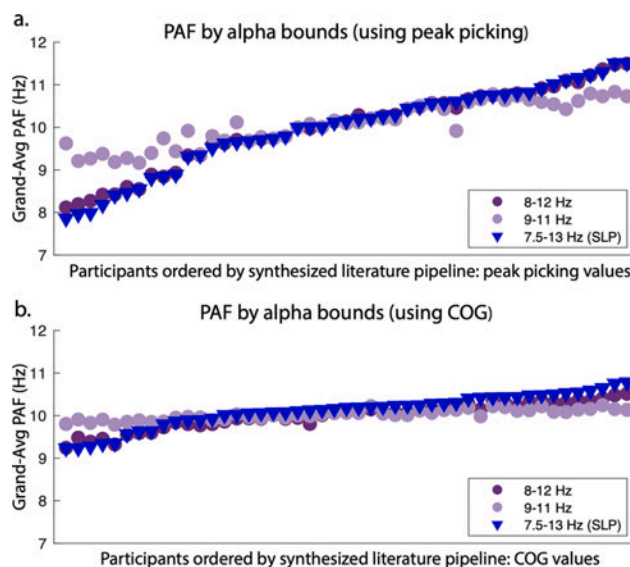


Fig. 4. Cleaned EEG data from the MARA+ReRef+Notch pipeline was used to calculate grand-average PAF using three alpha bands: 7.5–13 Hz (synthesized literature pipeline), and 8–12 Hz and 9–11 Hz. The synthesized literature pipeline (SLP) is the grand-average PAF from 48 s epoching and alpha 7.5–13 Hz as done in Figs. 1 and 2. Peak picking (a) and COG (b) were used separately across the varied alpha bands to calculate grand-average PAF. Each point along the x-axis is an individual subject, and they are ascendingly ordered by SLP grand-average PAF value with peak picking in (a) and SLP with COG in (b). There is a moderate difference within participants. Across the three alpha bands tested, the mean range of the grand-average PAF values for each participant was 0.38 ± 0.42 Hz when calculated with peak picking (a) and 0.27 ± 0.17 when calculated with COG (b).

apparent difference between sensorimotor and the other four ROIs for both calculation methods (Fig. 6). The average range of PAF values in an individual across the five ROIs was 0.72 ± 0.43 for peak picking and 0.51 ± 0.46 for COG. However, when the sensorimotor ROI was removed from the analysis, the range dropped to 0.28 ± 0.23 for peak picking and 0.11 ± 0.06 for COG. To obtain a comparison point for the parameters varied above, we reviewed the difference between healthy populations and pain populations as well as more pain-sensitive versus less pain-sensitive groups in healthy populations in the 17 papers reviewed. We found that, when reported, the average difference between slow and fast PAF groups is nearly 1 Hz (Supplementary Table 1).

The first slow-5-PAF analysis was run only on the data from the MARA+ReRef+Notch pipeline, varying the bounds of the alpha band and COG versus peak picking for PAF calculation. Cluster maxima are reported in Table 2. From the masked data, a slow-5 cluster in the left thalamus was negatively associated with grand-average PAF values from the MARA+ReRef+Notch pipeline for alpha band = 7.5–13 Hz, COG and peak picking, and alpha band = 8–12 Hz, peak picking only ($Z > 2.3$; cluster significance: $p < 0.05$, corrected) (Fig. 5). Cluster maxima are reported in Table 2. From the whole brain data, slow-5 clusters in the insula, cingulate, and sensory cortices were also negatively associated with grand-average PAF values for nearly all of the alpha band-PAF calculation combinations. In particular, the insula (COG) and cingulate (peak picking) for alpha bands 7.5–13 Hz and 8–12 Hz, as well as sensory cortices for all three bands. Alpha band 9–11 Hz paired with the COG calculation was the only set of grand-average PAF values that produced no neural correlates (Table 2, Fig. 5).

The neural correlates of the five ROIs from the second fMRI analysis heavily overlapped with one another (Fig. 7, Table 4), with no clear spatial distinction. There was a fairly consistent negative association between PAF in the five ROIs and slow-5 fALFF in the thalamus and sensory cortices. There was also a negative association between PAF and

Table 2

Cluster maxima coordinates for significant clusters from the fMRI-PAF analysis. Includes association with grand-average PAF values calculated from all three tested alpha bands (7.5–13 Hz, 8–12 Hz, and 9–11 Hz), with both peak picking and COG. Locations reported as Montreal Neurological Institute (MNI) co-ordinates, with regions identified using the Harvard-Oxford Cortical Structural and Juelich Histological Atlases.

	x (mm)	y (mm)	z (mm)	size (voxels)	z-score
7.5–13 Hz, peak picking					
Thalamus	-6	-16	4	135	4.06
Sensory cortex	44	-8	24	460	3.97
	-64	-22	12	274	4.32
Cingulate	-6	22	28	255	5.14
7.5–13 Hz, COG					
Thalamus	-6	-18	4	104	3.86
Insula	-40	-12	-12	398	4.26
Sensory cortex	-68	-20	16	312	4.3
	44	-8	24	302	3.95
Insula	34	0	-10	262	4.26
8–12 Hz, peak picking					
Thalamus	-6	-16	4	121	3.99
Sensory cortex	44	-8	24	404	3.85
	-64	-20	12	271	4.25
Cingulate	-6	22	28	251	5.05
8–12 Hz, COG					
Sensory cortex	-64	-20	12	293	3.99
Insula	-40	-12	-12	282	3.94
9–11 Hz, peak picking					
Sensory cortex	-64	-22	12	207	4.12

slow-5 fALFF in other regions that varied across ROIs. The cingulate stayed specific to the peak picking method (associated only with the parietal and grand-average ROIs). The insular cluster, however, now shows up for both COG and peak picking: there is a negative association between PAF and insula in almost all COG ROIs (besides sensorimotor), but PAF is also negatively associated with insula in the sensorimotor and occipital peak picking ROIs. Additionally, the peak picking sensorimotor ROI produced new clusters in the brainstem not found with any of the other ROIs. Overall, however, the neural correlates for the five averages were highly similar to one another for both the peak picking and COG calculation methods. The sensorimotor ROI had the least overlap with the other four ROIs, corresponding to the patterns seen in the average ROI PAF data (Table 3).

4. Discussion

Despite the novelty and promise of PAF, a few key issues complicate the interpretation of past data and comparison across publications in the pain field. The first issue is a lack of consistency in the pre-processing pipelines and post-processing variables for EEG data. We reviewed 17 papers investigating the relationship between PAF and pain and found that there were major differences in how labs were pre-processing their data, (re-referencing, artifact removal, etc), epoch length, bounds of the alpha band, COG versus peak picking for PAF calculation, and ROI versus grand-average summary measures (Table 1). Heterogeneity in the pre-processing pipelines makes it difficult to tease apart whether differences in past findings are truly attributable to applications in different types of pain populations, or simply an artifact of differences in data processing. As such, it is necessary to determine how robust PAF is against different types of processing.

Additionally, there is little accompanying neuroimaging data to support the theoretical mechanisms behind PAF. While several papers in humans and animals have investigated the relationship between the alpha rhythm more broadly speaking and potential generators in the brain through neuroimaging and single-cell recording (Hughes and Crunelli, 2005), there has been little validation of similar ideas for PAF specifically. One paper identified an association between cerebral blood flow and PAF in the thalamus, insula, and other cortical and subcortical structures, but it has yet to be replicated (Jann et al., 2010). As such, it is

uncertain what physiological changes underlie altered PAF: proponents of thalamocortical dysrhythmia suggest decreased PAF is a result of the interaction between the thalamus and cortex, with high threshold bursting in a subset of thalamocortical neurons slowing as a result of reduced modulatory corticothalamic feedback (Hughes et al., 2004; Silva et al., 1980). This, however, has yet to be substantiated in human models (Hughes and Crunelli, 2005) and recent work in human intracranial recordings (Halgren et al., 2019) and EEG power analysis in source space (Ta Dinh et al., 2019) casts doubt on the thalamus as the primary alpha rhythm pacemaker.

The findings of this study address both primary concerns. Our results indicate that PAF is indeed robust against the tested EEG data pre-processing pipelines but may be sensitive to certain post-processing variables (specifically calculation method and ROI). However, across methods, interindividual differences in PAF were correlated with rs-fMRI-estimated activity in the thalamus, insula, cingulate, and sensory cortices. The mean grand-average PAF values from the most comprehensive pipeline in this study (MARA+ReRef+Notch), 10.11 ± 0.34 Hz, as well as the range, 9.24–10.79 Hz, line up well with previous investigations of the stability and standard values for resting-state PAF in healthy individuals (Furman et al., 2019; Haegens et al., 2014).

In summary of our analysis, varying pre-processing pipeline had little to no effect on grand-average PAF values, epoch length had an effect of 0.28–0.08 Hz (peak picking and COG), alpha band had an effect of 0.38–0.27 Hz (peak picking and COG), ROIs had an effect of 0.72–0.51 Hz (peak picking and COG) with sensorimotor included and 0.28–0.11 Hz (peak picking and COG) without sensorimotor, and peak picking versus COG had an effect of 0.51 Hz. Reviewing the difference between healthy populations and pain populations as well as more pain-sensitive versus less pain-sensitive groups in healthy populations, we found that, when reported, the average difference between slow and fast PAF groups is nearly 1 Hz (Supplementary Table 1). This is substantially larger than the difference between PAF calculations for the factors varied in this paper, apart from peak picking versus COG, the difference between ROIs when sensorimotor is included, and, to a lesser extent, alpha band bounds. Together, these findings provide evidence that grand-average PAF is generally a suitable summary measure for capturing interindividual differences in PAF, but care should be taken when comparing across papers that differ on multiple high impact variables (particularly peak picking versus COG and sensorimotor ROI versus grand average of other examined ROIs).

Given that resting-state PAF is often thought to capture trait rather than state information, and that our analysis found very little effect of epoch length, longer epochs may be more appropriate to capture a reliable, individual marker. Previous findings indicate test-retest reliability for PAF generally increases with increased epoch length up to 40–60 s (Gudmundsson et al., 2007; Salinsky et al., 1991). However, groups working with limited data should consider that with increasing epoch length, more data may be lost depending on the method of data cleaning. Additionally, it is worth noting that stationarity in our EEG signal is likely less of a concern than it would be in task-based or otherwise non-resting-state data. Epoch overlap also varied across papers but compared to epoch length in the 17 papers reviewed, was far less variable and is likely a smaller concern (Table 1). The bounds of the alpha band used (a concern echoed in (Corcoran et al., 2018)), the use of peak picking or COG to calculate the PAF value at each epoch, and some ROIs had a more apparent effect on the calculation of the grand-average PAF.

In the pain literature, the summary values reported for PAF are not consistent: grand-average was used in four papers, ROI was used in 11 papers, and channel analysis was used in six papers (with two using a combination of grand-average and ROI and two using a combination of grand-average and channel) (Table 1). However, the ROIs also used an average across all the electrodes of interest, papers often only include one or two ROIs, and two of the ROI papers noted that the PAF group differences were seen across all electrodes. Our analysis found that over

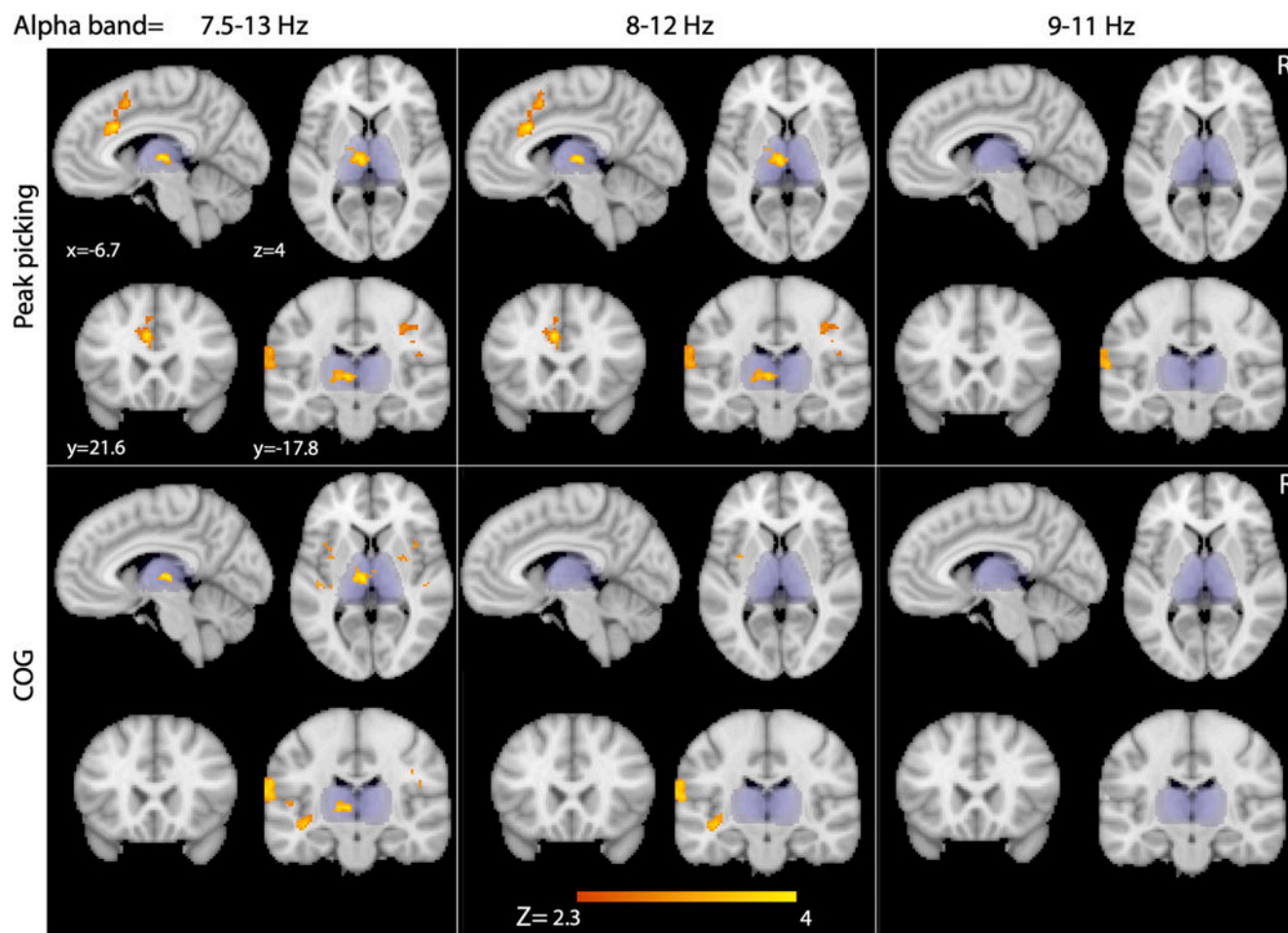


Fig. 5. Grand-average PAF values for each participant from the MARA+ReRef+Notch pipeline varied across three alpha bands (7.5–13 Hz, and 8–12 Hz and 9–11 Hz.) and two calculation methods (peak picking versus COG) were associated with slow-5 fALFF data using ordinary least squares regression on both whole brain and masked thalamic data. The area covered by the thalamic mask is indicated in blue. Slow-5 clusters in nodes of the salience network (insula, cingulate, and sensory cortex) and the left thalamus were negatively associated with grand-average PAF values ($Z > 2.3$; cluster significance: $p < 0.05$, corrected), but shows some variation across the different alpha bands and calculation methods. Alpha 9–11 Hz paired with COG was the only analysis that produced no neural correlates with slow-5 fALFF data. (For interpretation of the references to colour in this figure, the reader is referred to the web version of this article.)

95% of the variance in the EEG data from all three pre-processing pipelines was explained by the grand-average PAF of each individual. This lines up well with previously published data that peak frequency in the alpha and beta band have high inter-individual variation compared to intraindividual variation, giving them strong discriminating ability when classifying individuals based on EEG data (Grosfeld et al., 1976). In order to address any variation between topographic PAF values, in addition to our PCA analysis, we analyzed average PAF values from four representative electrode ROIs: frontal, parietal, occipital, and sensorimotor. This analysis showed that mean PAF in each of these regions was highly correlated for both PAF calculation methods (peaking picking and COG). When plotting the averages for the four ROIs and grand-average across participants, however, there did appear to be a difference between the sensorimotor ROI and other ROIs examined. This is reflected in the calculation of PAF range across ROIs within each participant: excluding sensorimotor from this calculation produces a large reduction in range of PAF values.

Our results also indicate a significant relationship ($p < 0.001$) between grand-average PAF from multiple post-processing variable combinations and interindividual differences in activity in a cluster in the left thalamus as well as left insula, right cingulate, and bilateral sensory cortex (coordinates reported in Table 2). The findings in Fig. 5 illustrate that even with variation in high impact post-processing variables, many

of the same neural correlates are still found, the clusters in the thalamus and sensory cortices being particularly robust against post-processing variations. The insula, cingulate, and thalamus are also nodes in the salience network (Hegarty et al., 2020), indicating a positive relationship between salience network activity and PAF. Our results do, however, indicate that different calculation methods for PAF (peak picking versus COG) may tap into different structures within the salience network: the grand-average COG analysis produced clusters in the insula that were not found in the peak picking analysis, and the grand-average peak picking analysis produced clusters in the cingulate that were not found in the COG analysis. Previous work using mean regional cerebral blood flow in healthy adults also found an association between COG PAF and the thalamus and insula, but not the cingulate (Jann et al., 2010), which aligns well with our findings. The specificity of these clusters to a particular calculation method, however, is less distinct in the ROI analysis (discussed below). Further investigation is warranted.

When conducting the fMRI analysis on the PAF averages from the five ROIs (the grand-average plus four representative ROIs), the results are fairly consistent. There is no apparent spatial distinction between the neural correlates of the five ROIs. While there are some differences, the correlates from the ROIs largely overlap, with the clusters in the thalamus and sensory cortices being the most consistent. The sensorimotor ROI, particularly for the peak picking calculation method, had the most

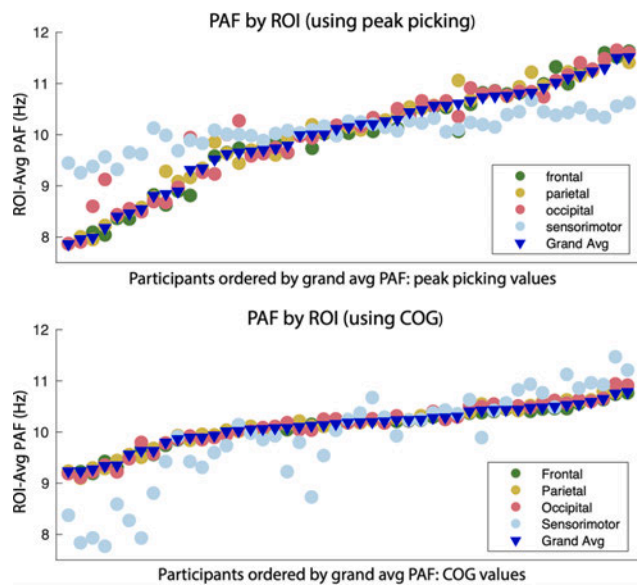


Fig. 6. Cleaned EEG data from the MARA+ReRef+Notch pipeline was used to calculate the average PAF across four representative electrode ROIs. These values were plotted along with the grand-average PAF values. Processing variables were held at the SLP (epoch length 48 s, alpha band 7.5–13 Hz), but with separate calculations for both peak picking (a) and COG (b) across the five measures (four ROIs, one grand-average). Each point along the x-axis is an individual subject, and they are ascendingly ordered by grand-average PAF value (SLP) with peak picking (a) and COG (b). Summary statistics and correlation coefficients are reported in Table 3.

divergent neural correlates. This lines up with the sensitivity analysis that suggests the mean from the sensorimotor ROI greatly increases the range of PAF values across all ROIs within participants and is the least correlated with the other four (Table 3, Fig. 6).

In the COG analysis, all ROIs besides the sensorimotor were associated with clusters in the sensory cortex, insula, and the thalamus. The peak picking results, while still overlapping, were slightly less consistent: the cingulate cluster shows up only for the grand-average and parietal ROIs, while the occipital and sensorimotor ROIs are associated with insular clusters that do not appear in the grand-average analysis. The sensorimotor ROI from the peak picking analysis additionally has some clusters that are not associated with any of the other four ROIs (most noticeably, one cluster in the brainstem). Despite these differences, there is no clear-cut indication of divergent neural correlates from ROI analysis alone. Rather, the associated clusters are highly overlapping across ROIs.

Calculation method in particular seems to have a large impact on the final PAF calculation that is consistent for all post-processing parameters varied in this paper: COG measures produce less variability across participants' grand-average PAF, but also compresses the range of grand-average PAF values. Given the fMRI findings that additionally suggest a potential difference in the neural correlates for grand-average COG versus peak picking (insula versus cingulate), care should be taken in future studies to select the most appropriate calculation method. While COG may be more stable, it is possible that it may also make inter-individual differences harder to detect.

PAF has great potential as a biomarker for pain sensitivity and/or chronic pain states. Therefore, it is important to establish whether PAF can be reliably compared across publications and better understand the neural mechanisms underlying interindividual differences. A decreased PAF has been associated with neuropathic pain in persistent abdominal pain as a result of chronic pancreatitis (Vries et al., 2013), neuropathic pain as a result of spinal cord injury (Boord et al., 2007; Sato et al., 2017), decreases in pain following an anodal tDCS intervention in spinal

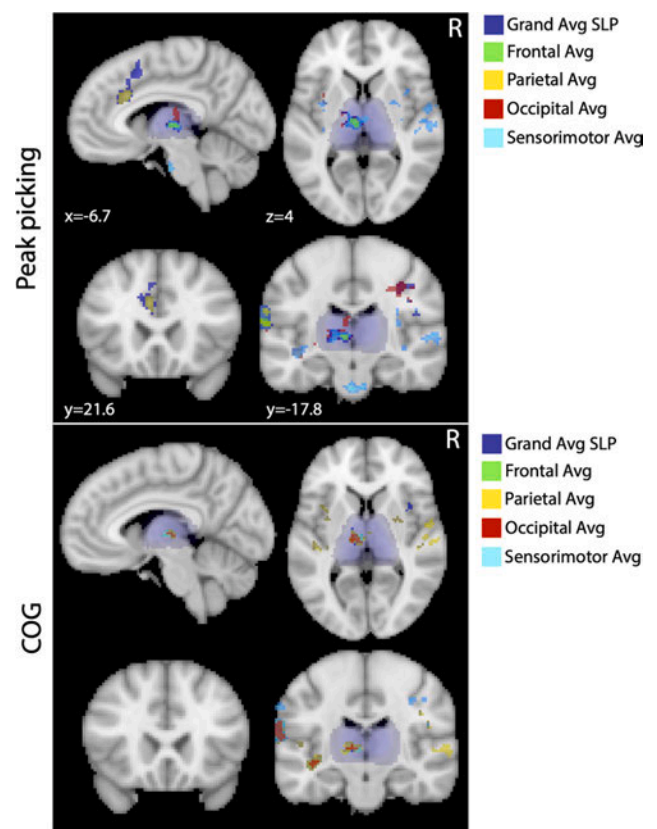


Fig. 7. Average PAF values for each participant from the MARA+ReRef+Notch pipeline were calculated for four representative ROIs (frontal, parietal, occipital, sensorimotor) and the grand-average using two calculation methods (peak picking versus COG). These values were associated with slow-5 data using ordinary least squares regression on both whole brain and masked thalamic data. The area covered by the thalamic mask is indicated in blue. Slow-5 clusters in nodes of the salience network (insula, cingulate, and sensory cortex) and the left thalamus were negatively associated with grand-average PAF values ($Z > 2.3$; cluster significance: $p < 0.05$, corrected) from most of the ROIs. There is some variation across ROIs, but largely overlapping neural correlates are highlighted. (For interpretation of the references to colour in this figure, the reader is referred to the web version of this article.)

cord injury/bilateral neuropathic pain (Ngernyam et al., 2015), and subjective perception of tonic heat pain (Nir et al., 2010; Raghuraman et al., 2019). Recent literature has also suggested that individual peak alpha frequency may be a stable biomarker that indicates who is susceptible to developing chronic pain conditions, with lower pain-free, PAF predicting increased average pain experienced in an induced, progressive muscle pain model (Furman et al., 2019). This study in particular makes PAF an attractive marker, as it suggests PAF may be able to identify those at risk of developing chronic pain conditions before the onset of pathology. This attribute could be extremely useful in identifying individuals who need increased attention following events such as surgery and directing brain-based interventions such as neuromodulation (Corlier et al., 2019).

PAF is additionally attractive as a marker because it has been shown to be highly heritable through the use of twin studies (Posthuma et al., 2001; van Beijsterveldt and van Baal, 2002) and generally stable over time in healthy adults, displaying high test-retest reliability over a span of six months and remaining consistent before and after 100 h of cognitive intervention/training across those six months (Grandy et al., 2013). Experiments looking at changes in PAF over the course of several days or weeks show that it is largely stable within individuals.

However, there is still debate about whether PAF is a marker for pain

Table 3

Summary statistics and matrix of Pearson's correlation coefficient for electrode ROIs (four most common ROIs in the PAF-pain literature reviewed). All correlations were significant at the $p < 0.001$ level.

Peak picking							
ROI	Mean	SD	1.	2.	3.	4.	5.
1. Grand avg	9.969	1.002	–	–	–	–	–
2. Frontal	9.939	1.045	0.9898	–	–	–	–
3. Parietal	10.030	1.021	0.9913	0.9752	–	–	–
4. Occipital	10.047	0.987	0.9722	0.9644	0.9507	–	–
5. Sensorimotor	10.082	0.337	0.9226	0.9112	0.9215	0.8867	–
COG							
ROI	Mean	SD	1.	2.	3.	4.	5.
1. Grand avg	10.114	0.399	–	–	–	–	–
2. Frontal	10.100	0.401	0.9964	–	–	–	–
3. Parietal	10.141	0.430	0.9931	0.9843	–	–	–
4. Occipital	10.135	0.447	0.9906	0.9902	0.9792	–	–
5. Sensorimotor	9.881	0.961	0.9320	0.9240	0.9318	0.9128	–

Table 4

Cluster maxima coordinates for significant clusters from the slow-5 fALFF with EEG ROI analysis. Includes clusters associated with ROI average PAF values calculated from all four tested regions (frontal, parietal, occipital, sensorimotor), for both peak picking and COG. Locations reported as Montreal Neurological Institute (MNI) coordinates, with regions identified using the Harvard-Oxford Cortical Structural and Juelich Histological Atlases.

	x (mm)	y (mm)	z (mm)	size (voxels)	z- score
COG					
Frontal					
Thalamus	-6	-18	4	20	3.84
Sensory Cortex	-68	-20	16	113	4.24
Insula	-40	-12	-12	68	4.23
Parietal					
Thalamus	-6	-18	4	105	3.8
Insula	-40	-12	-12	417	4.31
	34	0	-10	214	4.23
Primary auditory cortex	42	-26	8	236	3.79
Sensory Cortex	44	-8	24	205	3.99
	-64	-16	22	277	4.3
Occipital					
Thalamus	-10	-16	4	21	3.88
Sensory Cortex	-68	-20	16	120	4.32
Insula	-40	-12	-10	84	4.22
Sensorimotor					
Thalamus	-6	-16	4	31	4.17
Sensory cortex	44	-8	24	336	3.95
	-64	-22	12	310	4.4
Peak picking					
Frontal					
Thalamus	-6	-16	4	20	3.78
Sensory Cortex	-64	-22	12	70	4.24
Parietal					
Sensory Cortex	-64	-22	12	87	4.15
Cingulate	-6	22	28	63	5.28
Occipital					
Thalamus	-10	-16	4	21	3.88
Sensory Cortex	-68	-20	16	120	4.32
Insula	-40	-12	-10	84	4.22
Sensorimotor					
Thalamus	-6	-18	4	125	3.67
Insula	-40	-12	-12	303	4.45
	34	-12	10	292	3.88
	34	0	-10	265	3.89
Superior parietal lobule	22	-54	64	219	3.41
Brainstem	-2	-16	-34	207	4.44
Inferior parietal lobule	62	-32	14	201	3.4
Sensory cortex	44	-8	24	197	4.38
	-66	-22	12	282	4.27

sensitivity/chronic pain at all and if it is, whether it might be specific to certain types of pain. Studies on chronic back pain (Schmidt et al., 2012), central neuropathic pain in multiple sclerosis patients (Krupina

et al., 2020), and persistent pain after breast cancer treatment (van den Broeke et al., 2013) did not find a relationship between slowed PAF and pain. While it was excluded from the analysis in this paper because it did not contain detailed methods for calculation of PAF but instead used peak frequency (defined as being in the 6–14 Hz range), Ta Dinh et al. (2019) has the largest sample size of any peak frequency-pain study discussed in this paper (101 pain patients, 84 healthy controls). This study found no difference in peak frequency between healthy controls and chronic pain groups. However, it also included a variety of pain conditions with widely ranging scores for painDETECT, a questionnaire used to assess the likelihood of a neuropathic pain component (Freynhagen et al., 2006). Much of the discussion around discrepancies in findings for the PAF-pain relationship relates to the type of pain condition being studied, particularly neuropathic versus non-neuropathic. The multiple interpretations of Ta Dinh et al. (2019)'s outcomes further support the need to understand whether differences in findings for PAF-pain relationships stem from true population differences, a lack of a relationship altogether, or from the processing decisions discussed in this paper.

Our study indicates a negative association between slow-5 band activity in the thalamus and grand-average PAF. Previous studies have indicated that increases in fALFF across the low frequency spectrum (0.01–0.1 Hz) have a positive correlation with brain activity measured through other markers such as glucose metabolism and cerebral blood flow (Aiello et al., 2015; Wang et al., 2021). However, studies looking at fALFF in the slow-5 band (0.01–0.027 Hz) specifically indicate that decreased relative power in this frequency band is associated with increases in neural activity (Kilpatrick et al., 2014; Mawla et al., 2020; Yani et al., 2019). Interpreting our results based on previous slow-5 data, it potentially indicates a positive association between grand-average PAF and salience and thalamic activity. This would align with previous studies that have found a positive relationship between alpha band activity and thalamic activity (Goldman et al., 2002; Schwab et al., 2015; Jann et al., 2010). Additionally, one paper reported an inverse relationship between alpha power and thalamic glucose metabolism (Lindgren et al., 1999). The relationship between neural activity and PAF is likely complex and will need further validation.

While the thalamic mask used in our analysis encompassed both sides of the thalamus (left and right), our thalamic results were largely lateralized to the left thalamus in both the grand-average and ROI analysis. While this finding is somewhat unusual, the lateralization is not entirely novel. A previous MEG paper found that, in contrast to our findings, when comparing neuropathic and non-neuropathic ankylosing spondylitis patients, a significant increase in normalized alpha power for the NP participants was found only in right thalamus and right insula after correcting for multiple frequencies (Kisler et al., 2020). There are no obvious explanations for this lateralization in the literature, therefore more neuroimaging work will be required to understand these differences.

Though our findings support the relationship between grand-average PAF and thalamic and salience network activity, there is still uncertainty about the interpretation of PAF and its neural underpinnings. While PAF is understood to reflect attention and alertness, this interpretation is largely based on task-based EEG measures and understanding of the alpha band more generally (Mierau et al., 2017; Saalman et al., 2012; Stein et al., 2000). It is not yet clear what resting-state PAF value reflects. In a review of the literature surrounding shifts in PAF under a host of different testing and intervention conditions, Mierau et al., 2017 suggested that interindividual differences in PAF may serve as a stable neurophysiological marker, or a brain “trait” reflecting differences in individual biology, while intraindividual differences in PAF, especially over shorter timescales, reflect brain “state,” or adaptations in response to different tasks and conditions (Mierau et al., 2017).

PAF will generally increase as task demands increase, with differing PAF modulation across electrodes reflecting the cortical networks that are engaged or disengaged with specific tasks. It follows that PAF may be responsible for or involved in the sampling or processing frequency of cortical neurons (Mierau et al., 2017). Nir et al. (2010), who collected continuous EEG during application of a tonic, painful temperature stimulus, found that participants who experienced more pain had greater increases in PAF in temporal ROIs contralateral to stimulus. By contrast, those with certain chronic pain conditions or who are more susceptible to experiencing high levels of pain have lower resting-state PAF than controls. Shifts to lower PAF are also associated with schizophrenia spectrum disorder, obsessive compulsive disorder, and depressive disorder patient populations (Schulman et al., 2011). Of particular importance, there is significant evidence to suggest that PAF decreases with increased age (Chiang et al., 2011; Osaka et al., 1999; Clark et al., 2004). In this paper’s fMRI analysis, we are not associating PAF with a clinical feature, but instead directly relating two different brain measures. Therefore, while our age range was large (22.89–63.56 years), we did not include a correction for age. Thus, while our study supports the theory that PAF is related to thalamic and salience network activity, further research is needed to understand what differences in PAF indicate about interindividual differences in brain function.

One potential limitation of our fMRI findings is the z-threshold used. We have used the $z > 2.3$ threshold in previous work using fALFF to map activity changes related to natural bladder filling, and derived expected regions based on animal models (Mawla et al., 2020). Threshold is important to consider and may lead to false-positive results (Eklund et al., 2016), but no z-threshold has been established for fALFF data. Our current findings appear to be plausible given the association between PAF and pain as well as the association between pain and the salience network [see next paragraph and Kutch et al. (2017)], but the effect of z-threshold should be carefully considered in future studies.

Review of the literature surrounding the salience network suggests it as a potential mediator between bottom-up and top-down signals (Menon and Uddin, 2010). The anterior insula in particular has been shown to be involved in mediating attention, detecting salient stimuli, initiating control signals, and focusing attention on external stimuli. The thalamus is also part of the salience network (Hegarty et al., 2020), and is known to be involved in bottom-up pain processing for both nociceptive and neuropathic pain (Ab Aziz and Ahmad, 2006).

In summary, we provide evidence that PAF is robust against many common differences in EEG data processing with the second-largest healthy sample of the 17 papers included in the development of our pipelines and sensitivity analysis. This supports comparing across past studies investigating the relationship between PAF and pain, although special attention should be given to papers that differ on multiple high impact variables (alpha bounds, ROI, and COG versus peak picking). Additionally, we provide further evidence in support of the relationship between PAF and thalamic activity, as well as a relationship between PAF and the salience network, that is generally robust across ROIs. We provide support for PAF as a robust neural activity marker and grand-average PAF as a suitable summary measure for capturing variation in

individuals’ PAF data across the scalp. More information is needed about the nature of the relationship between PAF and thalamic and salience network activity, as well as the neural mechanisms reflected in interindividual differences in PAF.

CRedit authorship contribution statement

Natalie McLain: Conceptualization, Methodology, Formal analysis, Visualization, Writing – original draft. **Moheb Yani:** Software, Formal analysis, Investigation, Writing – Review & Editing. **Jason Kutch:** Conceptualization, Methodology, Software, Writing – original draft, Funding acquisition.

Declaration of Competing Interest

The authors declare that they have no known competing financial interests or personal relationships that could have appeared to influence the work reported in this paper.

Acknowledgements

We would like to thank Arike Coker for manuscript support and helpful discussions. This work was supported, in part, by grants DK110669 and DK121724 from the National Institute of Diabetes and Digestive and Kidney Diseases (NIH/NIDDK).

Appendix A. Supporting information

Supplementary data associated with this article can be found in the online version at doi:10.1016/j.jneumeth.2021.109460.

References

- Ab Aziz, C.B., Ahmad, A.H., 2006. The role of the thalamus in modulating pain. *Malays. J. Med. Sci.* 13, 11–18.
- Aiello, M., Salvatore, E., Cachia, A., Pappata, S., Cavaliere, C., Prinster, A., Nicolai, E., Salvatore, M., Baron, J.-C., Quarantelli, M., 2015. Relationship between simultaneously acquired resting-state regional cerebral glucose metabolism and functional MRI: a PET/MR hybrid scanner study. *Neuroimage* 113, 111–121.
- Angelakis, E., Lubar, J.F., Stathopoulou, S., Kounios, J., 2004. Peak alpha frequency: an electroencephalographic measure of cognitive preparedness. *Clin. Neurophysiol.* 115, 887–897.
- Björk, M.H., Stovner, L.J., Nilsen, B.M., Stjern, M., Hagen, K., Sand, T., 2009. The occipital alpha rhythm related to the “migraine cycle” and headache burden: a blinded, controlled longitudinal study. *Clin. Neurophysiol.* 120, 464–471.
- Boord, P., Siddall, P.J., Tran, Y., Herbert, D., Middleton, J., Craig, A., 2007. Electroencephalographic slowing and reduced reactivity in neuropathic pain following spinal cord injury. *Spinal Cord* 46, 118–123.
- Brötner, C.P., Klimesch, W., Doppelmayr, M., Zauner, A., Kerschbaum, H.H., 2014. Resting state alpha frequency is associated with menstrual cycle phase, estradiol and use of oral contraceptives. *Brain Res* 1577, 36–44.
- Cohen, D., Cuffin, B.N., 1983. Demonstration of useful differences between magnetoencephalogram and electroencephalogram. *Electroencephalogr. Clin. Neurophysiol.* 56, 38–51.
- Corcoran, A.W., Alday, P.M., Schlesewsky, M., Bornkessel-Schlesewsky, I., 2018. Toward a reliable, automated method of individual alpha frequency (IAF) quantification. *Psychophysiology* 55, e13064.
- Corlier, J., Carpenter, L.L., Wilson, A.C., Tirrell, E., Gobin, A.P., Kavanaugh, B., Leuchter, A.F., 2019. The relationship between individual alpha peak frequency and clinical outcome with repetitive Transcranial Magnetic Stimulation (rTMS) treatment of Major Depressive Disorder (MDD). *Brain Stimul.* 12, 1572–1578.
- Corlier, J., Tadayonnejad, R., Wilson, A.C., Lee, J.C., Marder, K.G., Ginder, N.D., Wilke, S.A., Levitt, J., Krantz, D., Leuchter, A.F., 2021. Repetitive transcranial magnetic stimulation treatment of major depressive disorder and comorbid chronic pain: response rates and neurophysiologic biomarkers. *Psychol. Med.* 1–10.
- Cuffin, B.N., Cohen, D., 1979. Comparison of the magnetoencephalogram and electroencephalogram. *Electroencephalogr. Clin. Neurophysiol.* 47, 132–146.
- Eklund, A., Nichols, T.E., Knutsson, H., 2016. Cluster failure: Why fMRI inferences for spatial extent have inflated false-positive rates. *Proc. Natl. Acad. Sci. US A* 113, 7900–7905.
- Freyhagen, R., Baron, R., Gockel, U., Tölle, T.R., 2006. painDETECT: a new screening questionnaire to identify neuropathic components in patients with back pain. *Curr. Med. Res. Opin.* 22, 1911–1920.
- Furman, A.J., Meeker, T.J., Rietschel, J.C., Yoo, S., Muthulingam, J., Prokhorenko, M., Keaser, M.L., Goodman, R.N., Mazaheri, A., Seminowicz, D.A., 2018. Cerebral peak

- alpha frequency predicts individual differences in pain sensitivity. *Neuroimage* 167, 203–210.
- Furman, A.J., Prokhorenko, M., Keaser, M.L., Zhang, J., Chen, S., Mazaheri, A., Seminowicz, D.A., 2020. Sensorimotor peak alpha frequency is a reliable biomarker of prolonged pain sensitivity. *Cereb. Cortex*. <https://doi.org/10.1093/cercor/bhaa124>.
- Furman, A.J., Thapa, T., Summers, S.J., Cavaleri, R., Fogarty, J.S., Steiner, G.Z., Schabrun, S.M., Seminowicz, D.A., 2019. Cerebral peak alpha frequency reflects average pain severity in a human model of sustained, musculoskeletal pain. *J. Neurophysiol.* <https://doi.org/10.1152/jn.00279.2019>.
- Gabard-Durnam, L.J., Mendez Leal, A.S., Wilkinson, C.L., Levin, A.R., 2018. The harvard automated processing pipeline for electroencephalography (HAPPE): Standardized processing software for developmental and high-artifact data. *Front. Neurosci.* 12, 97.
- Goldman, R.I., Stern, J.M., Engel Jr, J., Cohen, M.S., 2002. Simultaneous EEG and fMRI of the alpha rhythm. *NeuroReport*. <https://doi.org/10.1097/01.wnr.0000047685.08940.d0>.
- Grandy, T.H., Werkle-Bergner, M., Chicherio, C., Schmiedek, F., Lövdén, M., Lindenberger, U., 2013. Peak individual alpha frequency qualifies as a stable neurophysiological trait marker in healthy younger and older adults. *Psychophysiology* 50, 570–582.
- Grosfeld, F.M., Jansen, B.H., Hasman, A., Visser, S.L., 1976. La reconnaissance des individus à l'intérieur d'un groupe de 16 sujets normaux. *Rev. Electroencephalogr. Neurophysiol. Clin.* 6, 295–297.
- Gudmundsson, S., Runarsson, T.P., Sigurdsson, S., Eiriksdottir, G., Johnsen, K., 2007. Reliability of quantitative EEG features. *Clin. Neurophysiol.* 118, 2162–2171.
- Haegens, S., Cousijn, H., Wallis, G., Harrison, P.J., Nobre, A.C., 2014. Inter- and intra-individual variability in alpha peak frequency. *Neuroimage* 92, 46–55.
- Halgren, M., Ulbert, I., Bastuji, H., Fabó, D., Eröss, L., Rey, M., Devinsky, O., Doyle, W.K., Mak-MacCully, R., Halgren, E., Wittner, L., Chauvel, P., Heit, G., Eskandar, E., Mandell, A., Cash, S.S., 2019. The generation and propagation of the human alpha rhythm. *Proc. Natl. Acad. Sci. USA* 116, 23772–23782.
- Hegarty, A.K., Yani, M.S., Albishi, A., Michener, L.A., Kutch, J.J., 2020. Saliency network functional connectivity is spatially heterogeneous across sensorimotor cortex in healthy humans. *Neuroimage* 221, 117177.
- Hughes, S.W., Crunelli, V., 2005. Thalamic mechanisms of EEG alpha rhythms and their pathological implications. *Neuroscientist* 11, 357–372.
- Hughes, S.W., Lörincz, M., Cope, D.W., Blethyn, K.L., Kékesi, K.A., Rheinallt Parri, H., Juhász, G., Crunelli, V., 2004. Synchronized oscillations at α and θ frequencies in the Lateral Geniculate Nucleus. *Neuron*. [https://doi.org/10.1016/s0896-6273\(04\)00191-6](https://doi.org/10.1016/s0896-6273(04)00191-6).
- Jann, K., Koenig, T., Dierks, T., Boesch, C., Federspiel, A., 2010. Association of individual resting state EEG alpha frequency and cerebral blood flow. *Neuroimage* 51, 365–372.
- Kilpatrick, L.A., Kutch, J.J., Tillisch, K., Naliboff, B.D., Labus, J.S., Jiang, Z., Farmer, M.A., Apkarian, A.V., Mackey, S., Martucci, K.T., Clauw, D.J., Harris, R.E., Deusch, G., Ness, T.J., Yang, C.C., Maravilla, K., Mullins, C., Mayer, E.A., 2014. Alterations in resting state oscillations and connectivity in sensory and motor networks in women with interstitial cystitis/painful bladder syndrome. *J. Urol.* 192, 947–955.
- Kisler, L.B., Kim, J.A., Hemington, K.S., Rogachov, A., Cheng, J.C., Bosma, R.L., Osborne, N.R., Dunkley, B.T., Inman, R.D., Davis, K.D., 2020. Abnormal alpha band power in the dynamic pain connectome is a marker of chronic pain with a neuropathic component. *Neuroimage Clin.* 26, 102241.
- Klimesch, W., 1999. EEG alpha and theta oscillations reflect cognitive and memory performance: a review and analysis. *Brain Res. Brain Res. Rev.* 29, 169–195.
- Klimesch, W., 1997. EEG-alpha rhythms and memory processes. *Int. J. Psychophysiol.* [https://doi.org/10.1016/s0167-8760\(97\)00773-3](https://doi.org/10.1016/s0167-8760(97)00773-3).
- Klimesch, W., Schimke, H., Pfurtscheller, G., 1993. Alpha frequency, cognitive load and memory performance. *Brain Topogr.* 5, 241–251.
- Krupina, N.A., Churyukanov, M.V., Kukushkin, M.L., Yakhno, N.N., 2019. Central neuropathic pain and profiles of quantitative electroencephalography in multiple sclerosis patients. *Front. Neurol.* 10, 1380.
- Kutch, J.J., Ichesco, E., Hampson, J.P., Labus, J.S., Farmer, M.A., Martucci, K.T., Ness, T.J., Deusch, G., Apkarian, A.V., Mackey, S.C., Klumpp, D.J., Schaeffer, A.J., Rodriguez, L.V., Kreder, K.J., Buchwald, D., Andriole, G.L., Lai, H.H., Mullins, C., Kusek, J.W., Landis, J.R., Mayer, E.A., Clemens, J.Q., Clauw, D.J., Harris, R.E., MAPP Research Network, 2017. Brain signature and functional impact of centralized pain: a multidisciplinary approach to the study of chronic pelvic pain (MAPP) network study. *Pain* 158, 1979–1991.
- Lindgren, K.A., Larson, C.L., Schaefer, S.M., Abercrombie, H.C., Ward, R.T., Oakes, T.R., Holden, J.E., Perlman, S.B., Benca, R.M., Davidson, R.J., 1999. Thalamic metabolic rate predicts EEG alpha power in healthy control subjects but not in depressed patients. *Biol. Psychiatry*. [https://doi.org/10.1016/s0006-3223\(98\)00350-3](https://doi.org/10.1016/s0006-3223(98)00350-3).
- Mawla, I., Schrepf, A., Ichesco, E., Harte, S.E., Klumpp, D.J., Griffith, J.W., Strachan, E., Yang, C.C., Lai, H., Andriole, G., Magnotta, V.A., Kreder, K., Clauw, D.J., Harris, R.E., Quentin Clemens, J., Richard Landis, J., Mullins, C., Rodriguez, L.V., Mayer, E.A., Kutch, J.J., 2020. Natural bladder filling alters resting brain function at multiple spatial scales: a proof-of-concept MAPP Network Neuroimaging Study. *Sci. Rep.* <https://doi.org/10.1038/s41598-020-76857-x>.
- Menon, V., Uddin, L.Q., 2010. Saliency, switching, attention and control: a network model of insula function. *Brain Struct. Funct.* 214, 655–667.
- Mierau, A., Klimesch, W., Lefevre, J., 2017. State-dependent alpha peak frequency shifts: experimental evidence, potential mechanisms and functional implications. *Neuroscience* 360, 146–154.
- Molins, A., Stufflebeam, S.M., Brown, E.N., Hämäläinen, M.S., 2008. Quantification of the benefit from integrating MEG and EEG data in minimum l2-norm estimation. *Neuroimage* 42, 1069–1077.
- Muthuraman, M., Moliadze, V., Mideksa, K.G., Anwar, A.R., Stephani, U., Deuschl, G., Freitag, C.M., Siniatchkin, M., 2015. EEG-MEG integration enhances the characterization of functional and effective connectivity in the resting state network. *PLoS One* 10, e0140832.
- Ngernyam, N., Jensen, M.P., Arayawichanon, P., Auvichayapat, N., Tiamkao, S., Janjarasjitt, S., Punjaruk, W., Amatachaya, A., Aree-uea, B., Auvichayapat, P., 2015. The effects of transcranial direct current stimulation in patients with neuropathic pain from spinal cord injury. *Clin. Neurophysiol.* 126, 382–390.
- Nir, R.-R., Sinai, A., Raz, E., Sprecher, E., Yarnitsky, D., 2010. Pain assessment by continuous EEG: association between subjective perception of tonic pain and peak frequency of alpha oscillations during stimulation and at rest. *Brain Res.* 1344, 77–86.
- Parkes, L., Fulcher, B., Yücel, M., Fornito, A., 2018. An evaluation of the efficacy, reliability, and sensitivity of motion correction strategies for resting-state functional MRI. *Neuroimage* 171, 415–436.
- Posthuma, D., Neale, M.C., Boomsma, D.I., de Geus, E.J., 2001. Are smarter brains running faster? Heritability of alpha peak frequency, IQ, and their interrelation. *Behav. Genet.* 31, 567–579.
- Raghuraman, N., Wang, Y., Schenk, L.A., Furman, A.J., Tricou, C., Seminowicz, D.A., Colloca, L., 2019. Neural and behavioral changes driven by observationally-induced hypoalgesia. *Sci. Rep.* 9, 19760.
- Saalmann, Y.B., Pinsk, M.A., Wang, L., Li, X., Kastner, S., 2012. The pulvinar regulates information transmission between cortical areas based on attention demands. *Science* 337, 753–756.
- Salinsky, M.C., Oken, B.S., Morehead, L., 1991. Test-retest reliability in EEG frequency analysis. *Electroencephalogr. Clin. Neurophysiol.* 79, 382–392.
- Sato, G., Osumi, M., Morioka, S., 2017. Effects of wheelchair propulsion on neuropathic pain and resting electroencephalography after spinal cord injury. *J. Rehabil. Med.* 49, 136–143.
- Schmidt, S., Naranjo, J.R., Brenneisen, C., Gundlach, J., Schultz, C., Kaube, H., Hinterberger, T., Jeanmonod, D., 2012. Pain ratings, psychological functioning and quantitative EEG in a controlled study of chronic back pain patients. *PLoS ONE*. <https://doi.org/10.1371/journal.pone.0031138>.
- Schulman, J.J., Cancro, R., Lowe, S., Lu, F., Walton, K.D., Llinás, R.R., 2011. Imaging of thalamocortical dysrhythmia in neuropsychiatry. *Front. Hum. Neurosci.* 5, 69.
- Schwab, S., Koenig, T., Morishima, Y., Dierks, T., Federspiel, A., Jann, K., 2015. Discovering frequency sensitive thalamic nuclei from EEG microstate informed resting state fMRI. *Neuroimage* 118, 368–375.
- Silva, F.H.L. da, da Silva, F.H.L., Vos, J.E., Mooibroek, J., van Rotterdam, A., 1980. Relative contributions of intracortical and thalamo-cortical processes in the generation of alpha rhythms, revealed by partial coherence analysis. *Electroencephalogr. Clin. Neurophysiol.* [https://doi.org/10.1016/0013-4694\(80\)90011-5](https://doi.org/10.1016/0013-4694(80)90011-5).
- Simis, M., Pacheco-Barrios, K., Uygur-Kucukseymen, E., Castelo-Branco, L., Battistella, L.R., Fregni, F., 2021. Specific electroencephalographic signatures for pain and descending pain inhibitory system in spinal cord injury. *Pain. Med.* <https://doi.org/10.1093/pm/pnab124>.
- Stein, A., von, von Stein, A., Sarnthein, J., 2000. Different frequencies for different scales of cortical integration: from local gamma to long range alpha/theta synchronization. *Int. J. Psychophysiol.* [https://doi.org/10.1016/s0167-8760\(00\)00172-0](https://doi.org/10.1016/s0167-8760(00)00172-0).
- Ta Dinh, S., Nickel, M.M., Tiemann, L., May, E.S., Heitmann, H., Hohn, V.D., Edenharter, G., Utpadel-Fischler, D., Tölle, T.R., Sauseng, P., Gross, J., Ploner, M., 2019. Brain dysfunction in chronic pain patients assessed by resting-state electroencephalography. *Pain* 160, 2751–2765.
- van Beijsterveldt, C.E.M., van Baal, G.C.M., 2002. Twin and family studies of the human electroencephalogram: a review and a meta-analysis. *Biol. Psychol.* [https://doi.org/10.1016/s0301-0511\(02\)00055-8](https://doi.org/10.1016/s0301-0511(02)00055-8).
- van den Broeke, E.N., Wilder-Smith, O.H.G., van Goor, H., Vissers, K.C.P., van Rijn, C.M., 2013. Patients with persistent pain after breast cancer treatment show enhanced alpha activity in spontaneous EEG. *Pain. Med.* 14, 1893–1899.
- Van Dijk, K.R.A., Sabuncu, M.R., Buckner, R.L., 2012. The influence of head motion on intrinsic functional connectivity MRI. *Neuroimage* 59, 431–438.
- Vries, M.D., De Vries, M., Wilder-Smith, O., Jongsma, M., Van den Broeke, E., Arns, M., Van Goor, H., Van Rijn, C., 2013. Altered resting state EEG in chronic pancreatitis patients: toward a marker for chronic pain. *J. Pain. Res.* <https://doi.org/10.2147/jpr.s50919>.
- Vuckovic, A., Hasan, M.A., Fraser, M., Conway, B.A., Nasserolleslami, B., Allan, D.B., 2014. Dynamic oscillatory signatures of central neuropathic pain in spinal cord injury. *J. Pain.* 15, 645–655.
- Vuckovic, A., Jairees, M., Purcell, M., Berry, H., Fraser, M., 2018. Electroencephalographic predictors of neuropathic pain in subacute spinal cord injury. *J. Pain.* 19, 1256.e1–1256.e17.
- Wang, J., Sun, H., Cui, B., Yang, H., Shan, Y., Dong, C., Zang, Y., Lu, J., 2021. The relationship among glucose metabolism, cerebral blood flow, and functional activity: a Hybrid PET/fMRI Study. *Mol. Neurobiol.* <https://doi.org/10.1007/s12035-021-02305-0>.
- Winkler, I., Brandl, S., Horn, F., Waldburger, E., Allefeld, C., Tangermann, M., 2014. Robust artifactual independent component classification for BCI practitioners. *J. Neural Eng.* 11, 035013.

N.J. McLain et al.

Journal of Neuroscience Methods 368 (2022) 109460

Winkler, I., Haufe, S., Tangermann, M., 2011. Automatic classification of artifactual ICA-components for artifact removal in EEG signals. *Behav. Brain Funct.* 7, 30.

Worsley, K.J., 2001. Statistical analysis of activation images. In: Jezzard, P., Matthews, P. M., Smith, S.M. (Eds.), *Functional MRI: An Introduction to Methods*. Oxford Scholarship Online.

Yani, M.S., Fenske, S.J., Rodriguez, L.V., Kutch, J.J., 2019. Motor cortical neuromodulation of pelvic floor muscle tone: potential implications for the treatment of urologic conditions. *Neurourol. Urodyn.* 38, 1517–1523.

EXHIBIT 20



Full-length review

EEG alpha and theta oscillations reflect cognitive and memory performance: a review and analysis

Wolfgang Klimesch *

Department of Physiological Psychology, Institute of Psychology, University of Salzburg, Hellbrunnerstr. 34, A-5020 Salzburg, Austria

Accepted 24 November 1998

Abstract

Evidence is presented that EEG oscillations in the alpha and theta band reflect cognitive and memory performance in particular. Good performance is related to two types of EEG phenomena (i) a tonic increase in alpha but a decrease in theta power, and (ii) a large phasic (event-related) decrease in alpha but increase in theta, depending on the type of memory demands. Because alpha frequency shows large interindividual differences which are related to age and memory performance, this double dissociation between alpha vs. theta and tonic vs. phasic changes can be observed only if fixed frequency bands are abandoned. It is suggested to adjust the frequency windows of alpha and theta for each subject by using individual alpha frequency as an anchor point. Based on this procedure, a consistent interpretation of a variety of findings is made possible. As an example, in a similar way as brain volume does, upper alpha power increases (but theta power decreases) from early childhood to adulthood, whereas the opposite holds true for the late part of the lifespan. Alpha power is lowered and theta power enhanced in subjects with a variety of different neurological disorders. Furthermore, after sustained wakefulness and during the transition from waking to sleeping when the ability to respond to external stimuli ceases, upper alpha power decreases, whereas theta increases. Event-related changes indicate that the extent of upper alpha desynchronization is positively correlated with (semantic) long-term memory performance, whereas theta synchronization is positively correlated with the ability to encode new information. The reviewed findings are interpreted on the basis of brain oscillations. It is suggested that the encoding of new information is reflected by theta oscillations in hippocampo-cortical feedback loops, whereas search and retrieval processes in (semantic) long-term memory are reflected by upper alpha oscillations in thalamo-cortical feedback loops. © 1999 Elsevier Science B.V. All rights reserved.

Keywords: EEG; ERD; Alpha; Theta; Oscillation; Memory; Hippocampus; Thalamus

Contents

1. Introduction	170
1.1. Cognitive and memory performance: introductory remarks	170
1.2. Alpha and theta: some basic aspects	171
1.3. Definition of frequency bands	172
1.4. Oscillatory components in the EEG	174
2. Tonic changes and differences in the alpha and theta frequency range	174
2.1. Age related changes and performance related differences in alpha frequency	175
2.2. Age related changes in alpha and theta power	176
2.3. Age related changes in alpha and theta reactivity	178
2.4. Changes in alpha and theta power during the wake–sleep cycle	178
2.5. Alpha power in congenital blindness	181
3. Interim discussion	181
4. Event-related (phasic) changes in the alpha and theta band	182
4.1. Desynchronization in the lower alpha band reflects attention	183
4.2. Desynchronization in the upper alpha band reflects semantic memory performance	185
4.3. Synchronization in the theta band reflects episodic memory and the encoding of new information	187
4.4. The relationship between desynchronization, synchronization and absolute power	189

* Fax: +43-662-8044-5126; e-mail: wolfgang.klimesch@sbg.ac.at

5. General conclusions and physiological considerations	189
Acknowledgements	191
References	191

1. Introduction

In a physiological sense, EEG power reflects the number of neurons that discharge synchronously. Because brain volume and the thickness of the cortical layer is positively correlated with intelligence (e.g., Refs. [12,165]) it is tempting to assume that EEG power too, is a measure that reflects the capacity or performance of cortical information processing. Although it will be argued that this is in principle the case, it must be emphasized that power measurements are strongly affected by a variety of unspecific factors such as the thickness of the skull or the volume of cerebrospinal fluid, by methodological and technical factors (such as interelectrode distance or type of montage) but also by more specific factors such as age, arousal and the type of cognitive demands during actual task performance.

It is the purpose of the present article to show that EEG power is indeed related to cognitive and memory performance, but in a complex and partly non-linear way. Within the alpha frequency range EEG power is positively related to cognitive performance and brain maturity, whereas the opposite holds true for the theta frequency range. Alpha and theta reactivity as well as event-related changes in alpha and theta band power show yet another pattern of results. During actual task demands the extent of alpha power suppression is positively correlated with cognitive performance (and memory performance in particular) whereas again the opposite holds true for the theta band. Here, the extent of theta synchronization is related to good performance. The review which focuses on the theta and alpha frequency range considers first tonic changes in power (such as age related differences in the EEG) and then phasic or event-related changes.

1.1. Cognitive and memory performance: introductory remarks

Two basic aspects of memory processes will be distinguished [66]. The first refers to processes of the working memory system (WMS), the second to that of the long-term memory system (LTMS). Probably any cognitive process depends on the resources of both systems. As an example, let us consider an every day cognitive process such as recognizing a familiar object. The basic idea here is that after a sensory code is established, semantic information in long-term memory (LTM) is accessed which is used to identify the perceived object. If the matching process

yields a positive result, the object is recognized which in turn leads to the creation of a short-term memory (STM) code. In this case, bottom up pathways are activated which are similar or identical to those which would serve to retrieve information from LTM. This classical explanation of encoding still reflects the current view, which was originally stated by Shiffrin and Geisler [137]: “The process of encoding is essentially one of recognition: the appropriate image or feature is contacted in LTM and then placed (i.e., copied) in STM” (p. 55). Complex cognitive processes such as speaking and thinking may also be described in terms of a close interaction between the WMS and LTMS. The basic difference to the foregoing example is that a sensory code is lacking and that a code is generated in STM which in the case of speaking represents a ‘plan’ of what to say. The codes generated in STM trigger search processes in LTM to retrieve the relevant knowledge about the appropriate semantic, syntactic and articulatory information. This latter idea is similar to Baddeley’s concept of working memory, which comprises an attentional controller, the central executive and subsidiary slave systems [3,4].

In the WMS, encoding has two different meanings, one refers to episodic, the other to sensory-semantic information. The encoding of sensory information (as a process of recognition) always aims at the semantic understanding of perceived information which is first processed in the LTMS. Because of this close relation between sensory and semantic encoding we will use the term sensory-semantic code. The creation of a new code comprises episodic information, which according to Tulving (e.g., [158]), is that type of contextual information which keeps an individual autobiographically oriented within space and time. Because time changes the autobiographical context permanently, there is a permanent and vital need to update and store episodic information. Thus, the formation of episodic memory traces is one of the most important tasks of the WMS.

Cognitive performance is closely related and linked to the performance of the WMS and LTMS. As an example, most intelligence tests comprise subtests measuring memory span (an important function of the WMS) and tests such as judging analogies (which reflect an important aspect of semantic LTMS). The increase in cognitive performance from childhood to puberty as well as the decrease in performance during the late lifespan is, most likely, due or at least closely linked to performance changes in the WMS and LTMS.

With respect to the functional anatomy of memory, there is good evidence that brain structures that lie in the medial temporal lobe (comprising the hippocampal formation) and prefrontal cortex support various functions of the WMS (cf. the reviews in Refs. [102,140,141] and findings about the contribution of the hippocampal region for the generation of event-related potentials in the human scalp EEG during novelty detection [85,86]). Studies focusing on the ontogeny of human memory indicate that the hippocampus matures relatively early in postnatal life, whereas the prefrontal cortex which is important for the development of an increased memory span matures much later (cf. Refs. [109,57] for reviews). Although many aspects of memory develop early in childhood (up to an age of about 2 or 3 years) it is not yet known when memory is fully matured. As will be discussed in Section 5, there is good evidence that a complex structure of feedback loops (or 'reentrant loops'; [37]) connecting the hippocampus with different cortical regions and the prefrontal cortex in particular may provide the anatomical basis for the WMS. It appears likely that these feedback loops develop and become increasingly differentiated with increasing age over the entire time span of childhood and possibly early adulthood. The increase in EEG frequency during that life period may (besides other factors) reflect this process of brain maturation. The basic assumption is that the better these feedback loops become integrated and interconnected with other brain areas, the faster the frequency of EEG oscillations will be.

1.2. Alpha and theta: some basic aspects

Alpha is (with the exception of irregular activity in the delta range and below) the dominant frequency in the human scalp EEG of adults. It is manifested by a 'peak' in spectral analysis (cf. Fig. 1) and reflects rhythmic 'alpha waves' which are known since Berger (e.g., Ref. [10]). The fact that alpha clearly is an oscillatory component of the human EEG has led to a recent 'renaissance' in the interest of EEG alpha activity [5,8,7,9].

Frequency and power are closely interrelated measures. Usually, alpha frequency is defined in terms of peak or gravity frequency within the traditional alpha frequency range (f_1 to f_2) of about 7.5–12.5 Hz. Peak frequency is that spectral component within f_1 to f_2 which shows the largest power estimate (cf. Fig. 1A). Alpha frequency can also be calculated in terms of gravity (or 'mean') frequency which is the weighted sum of spectral estimates, divided by alpha power: $(\sum(a(f) \times f)) / (\sum a(f))$. Power spectral estimates at frequency f are denoted $a(f)$. The index of summation is in the range of f_1 to f_2 . Particularly if there are multiple peaks in the alpha range (for a classification see e.g., Ref. [39]), gravity frequency appears the more adequate estimate of alpha frequency.

As is well known from animal research, unlike alpha in the human scalp EEG, theta is the dominant rhythm in the

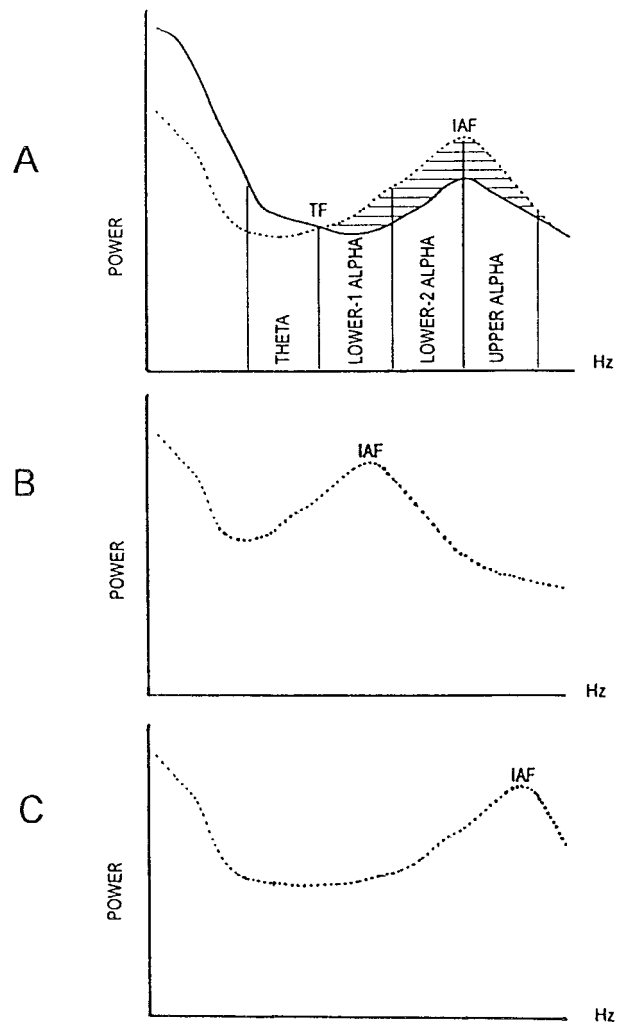


Fig. 1. Individual alpha frequency (IAF) varies to a large extent even in a sample of age matched subjects as the three power spectra indicate. Depending on their memory performance and other factors, IAF lies in the range of about 9.5–11.5 Hz for young healthy adults. (A) If power spectra are calculated separately for a resting period in which subjects are in a state of alert wakefulness (dotted line) and during actual task performance (e.g., memorizing visually presented words), alpha power becomes suppressed, but theta power increases (bold line). That frequency where the two spectra intersect marks the transition frequency (TF) between the theta and alpha band. Experiments from our laboratory have shown that TF lies almost 4 Hz below IAF and that the lower alpha band (which can be further divided in two subbands) is somewhat wider than the upper alpha band. (B) Alpha power of a subject with a very slow alpha rhythm will fall outside the fixed frequency window of the traditional alpha band of about 7.5–12.5 Hz. As an example, if IAF in (A) is 10 Hz and in (B) only 8 Hz, the lower alpha band in (B) will already comprise that frequency range which is the theta band in (A), whereas the upper alpha band in (B) will fall in the frequency range of the lower alpha band in (A). Similar problems arise, if IAF lies already at the upper frequency limit of the alpha band. (C) For a subject with a very fast IAF of about 11.5 Hz or more, almost the entire frequency range of the traditional alpha band (7.5–12.5 Hz) would actually fall in the range of the lower alpha band of that subject. It is therefore of crucial importance to adjust frequency bands individually for each subject, by using IAF as the cut off point between the lower and upper alpha band (see text).

hippocampus of lower mammals. Its frequency ranges from about 3 to 12 Hz (e.g., Ref. [95]) and, thus, shows a much wider frequency range than in humans where theta lies between about 4 to 7.5 Hz. Its wide frequency range and large power make it easy to observe frequency and power changes in animals. This is in sharp contrast to the human scalp EEG, where—without the help of sophisticated methods—changes in theta frequency are very difficult or almost impossible to detect. The question, thus, is whether there is a physiological criterion that allows us to decide which frequency marks the transition between alpha and theta oscillations.

Alpha and theta respond in different and opposite ways. The crucial finding is that with increasing task demands theta synchronizes, whereas alpha desynchronizes (cf. the bold in relation to dotted line in Fig. 1A). This fact is documented in reviews on event-related desynchronization (ERD) [122,67,68], as well as by a variety of studies using other experimental approaches (e.g., Ref. [45,46,95,99, 131,133,129]). If EEG power in a resting condition is compared with a test condition, alpha power decreases (desynchronizes) and theta power increases (synchronizes). Classical findings demonstrate that the decrease in alpha power (suppression of the alpha rhythm) can be observed primarily when subjects close their eyes. More recent evidence, however, suggests that attentional and semantic memory demands are powerful factors which lead to a selective suppression of alpha in different ‘subbands’ and that the well described effects of visual stimulation (e.g., eyes open vs. closed) represent just a special class of sensory-semantic task demands (see Section 4 and Refs. [72,75,78–81]). As already emphasized, encoding of sensory information always aims to extract the meaning of the perceived information which is stored in semantic LTM. Thus, there is a close relation between sensory and semantic encoding.

As Fig. 1 illustrates, that frequency in the power spectra which marks the transition from theta synchronization to alpha desynchronization may be considered the individual transition frequency (TF) between the alpha and theta band for each subject. When using this method to estimate TF, we have found that TF shows a large interindividual variability (ranging from about 4 to 7 Hz) which is significantly correlated with alpha peak frequency [76]. Preliminary evidence for a covariation between theta and alpha frequency was already found by Klimesch et al. [75] and is further documented by Doppelmayr et al. [34]. These findings indicate that theta frequency (as measured by TF) varies as a function of alpha frequency and suggest to use alpha frequency as a common reference point for adjusting different frequency bands not only for the alpha, but theta range as well. For estimating theta power, the individual determination of frequency bands may even be more important because otherwise the effects of theta synchronization are masked by alpha desynchronization particularly in the range of TF (cf. Fig. 1B,C).

1.3. Definition of frequency bands

Because alpha frequency varies to a large extent as a function of age, neurological diseases, memory performance (see Section 2.1 below), brain volume [115,114] and task demands [73], the use of fixed frequency bands does not seem justified. As an example, an elderly subject with bad memory performance may show a peak frequency of 7 Hz or lower [16]. When strictly applying the rule that alpha peak frequency is that spectral component within $f1 = 7.5$ and $f2 = 12.5$ Hz which shows maximal power, we would arrive at the conclusion that the obtained frequency indicates theta instead of alpha frequency. Fortunately, as discussed in the previous section, there is a physiological criterion which allows us to answer this question. If EEG power around 7 Hz would desynchronize during a test—as compared to a resting condition (cf. Fig. 1A)—we still would accept that a peak frequency of 7 Hz indicates alpha but not theta frequency.

This example documents the necessity to define the alpha band individually for each subject as that range ($f1$ to $f2$) ‘around’ the individual dominant EEG frequency (above the lower delta range) that desynchronizes during task demands. In order to avoid confusions with traditional measures, we use the term individual alpha frequency (IAF) to denote the individual dominant (peak or gravity) EEG frequency (in the range of $f1$ to $f2$) of a single subject. The crucial point, of course, is the exact location and individual definition of the frequency limits $f1$ and $f2$. For $f1$, TF is a good estimate, but for $f2$ an obvious physiological criterion is lacking. An indirect way to solve this problem is to define the frequency limits of the lower alpha band by $f1$ and IAF and to assign the ‘remaining’ part of the alpha frequency range (which equals [alpha frequency window] – [IAF – $f1$]) to the upper band. Results from our laboratory indicate that the lower alpha band has a width of about 3.5–4 Hz. Accordingly, the upper alpha band (the frequency range above IAF) is a rather narrow band of 1 or 1.5 Hz, if it is assumed that the alpha frequency window has a width of about 5 Hz. Experimental findings (discussed in detail in Section 4 below) indicate that the upper alpha band—defined as a band of 2 Hz above IAF—responds selectively to semantic LTM demands and behaves in a completely different and sometimes opposite way as the lower alpha band (see also the review in Ref. [121]). Furthermore and most importantly, it was found that the lower alpha band (a band of 4 Hz below IAF) reflects different types of attentional demands. Thus, it was broken down into two subbands of 2 Hz each which are termed lower-1 and lower-2 alpha (see Fig. 1 and Section 4).

In summarizing, when using IAF as an anchor point, it proved useful to distinguish three alpha bands (with a width of 2 Hz each), two lower alpha bands (below IAF) and one upper alpha band (above IAF). The theta band is defined as the frequency band of 2 Hz which falls below

TF. As for the upper frequency limit of the upper alpha band, there are no clear criteria for the lower frequency limit of the theta band. In any case, however, it is important to emphasize that the use of narrow frequency bands reduces the danger that frequency specific effects go undetected or cancel each other. Thus, broad band analyses must be interpreted with great caution. The implication is that an unbiased estimate of alpha and theta power can be obtained only, if the traditional fixed band analyses are abandoned and if narrow frequency bands are adjusted to the individual alpha frequency of each subject. However, the vast majority of studies use broad, instead of narrow alpha bands (cf. Table 1) which in addition are not adjusted individually.

The suggested definition of frequency bands is based on physiological criteria (such as TF and IAF) and on the functional significance of narrow frequency bands (see Section 4). An alternative way to define EEG frequency bands is to analyze the covariance of spectral estimates by multivariate statistical methods such as factor analysis. The crucial question here is whether the activities in different frequency bands vary independently. With respect to the traditional theta and alpha frequency range, results from

factor analyses show at least three independent factors, one for theta, one for the lower alpha band and another for the upper alpha band (see e.g., Ref. [106] and the summary in Ref. [96]). However, the frequency limits vary considerably between studies. As an example, Wieneke (reported in Ref. [96]) found a factor covering the frequency range of 6–9 Hz, which was termed ‘theta’ whereas within that same frequency range, Mecklinger et al. [106] extracted one component which they classified as ‘lower alpha’. Divergent results from factor analyses are due to the type of power measurements (spectral estimates may be expressed in terms of relative or absolute power), type of derivation (e.g., monopolar [referential], bipolar, Laplacian), electrode location, task type (resting condition with eyes open or closed or performance of some task), the selected sample of subjects, and finally the method used to extract and rotate factors. It also should be emphasized that factor analyses are usually performed on the basis of a correlation matrix which was obtained by correlating spectral estimates over a sample of n subjects. Done in this way, the extracted factors represent average frequency ranges of that particular sample. However, factor analysis could also be used for an individual definition of fre-

Table 1
EEG alpha activity: frequency limits and peak (#) or gravity (*) frequency

Ref. no./author	Broad band	Subbands	Der.	N	Age	α -frequency
[1] Alloway et al.	8–12	–	M	10	29–62	–
[2] Anokhin and Vogel	8–13	–	M	101	20–45	–
[11] Besthorn et al.	–	7.5–9.5; 9.5–12.5	M	92	59–78	–
[14] Boiten et al.	8–13	–	M	8	22–29	–
[16] Brenner et al.	–	8.0–9.9; 10–12.9		119	51–89	6–14,r
[17] Breslau et al.	8.2–12.9	–	M	33	18–78	–
[24] Chiamonti et al.	8–11.5	–	M	55	51–81	–
[27] Coben et al.	8–13	–	B	127	64–83	6.9–9.3*
[36] Duffy et al.	8–11.75	–	M	63	30–80	7.5–13#,r
[44] Gevins et al.	8–13	–	M	55	–	–
[55] Hartikainen et al.	7.6–13.9	–	B	52	33–78	9.6–10.1#
[61] Jausovec	7.5–13	–	M	60	18–19	–
[62] John et al.	7.5–12.5	–	B	648	1–21	–
[65] Kaufman et al.	8–12	–	MEG	3	–	–
[87] Könönen and Partanen	7.6–13.9	–	B	54	23–80	–
[89] Krause et al.	–	8–10; 10–12	M	10	23–41	–
[99] Marciani et al.	8–12.5	–	C	60	19–89	–
[117] Obrist et al.	–	–		57	65–84	7.5–9.2#
[124] Pfurtscheller	–	1 or 2 Hz bands	M, B	§	§	–
[132] Salenius et al.	7–14 Hz	–	MEG	13	20–49	9.3–11#,r
[134] Schmid et al.	7.4–12.5	–	B	536	5–11	–
[139] Somsen et al.	7.5–12.5	–	M	142	5–12	4.5–10#
[146] Sterman et al.	–	2 Hz bands 5–15	M	26	25–39	–
[153] Széles et al.	8–13	–	M	58	53–78	–
[156] Torres et al.	–	–	M	182	48–88	9.4\$,S.D. = 1
[157] Torsvall and Akerstedt	8–11.9	–	B	11	27–58	–
[162] Wada et al.	7.5–12.5	–	M	264	3–26	–
[164] Wieneke et al.	–	3 db below peak	M	110	18–50	9.9#,S.D. = 1
[166] Williamson et al.	8–13	–	MEG	§	§	–

Der. = Derivation; M = monopolar; B = bipolar; C = Common average reference; N = sample size; §, Reviewed data; r, range for lowest and highest frequency; \$, Dominant frequency, defined by period of alpha wave.

quency bands, if the EEG of a single subjects is used and if spectral estimates are correlated over a series of n trials (epochs).

Even if frequency bands are defined individually for each subject, it must be emphasized that EEG frequencies vary between recording sites. As an example, it is well known that alpha waves occur primarily during wakefulness over the posterior regions of the head and can be best seen with eyes closed and under conditions of physical relaxation and mental inactivity [110]. The frequency of alpha waves is faster at posterior and slower at anterior recording sites. It would, thus, be desirable to adjust frequency bands not only individually for each subject but also for each recording site. For practical reasons, this has not yet been done.

1.4. Oscillatory components in the EEG

In an empirical sense, an oscillatory component is defined by the presence of a rhythmic activity in the EEG which is manifested by a 'peak' in spectral analysis. In contrast to theta, alpha as the dominant rhythmic activity, characterized by sinusoidal wave forms, clearly meets this definition. In the human EEG of young healthy adults, there are at least two other oscillatory components, the mu rhythm and the third rhythm. The mu rhythm (mu stands for motor) has an arch-shaped wave morphology, appears over the motor area and becomes suppressed (desynchronized) during motor related task demands (see the extensive work of Pfurtscheller et al., e.g., Ref. [125]). Other terms are 'arcade', 'comb' or 'wicket' rhythm, 'central', 'rolandic' and 'somatosensory' alpha (cf. the review in Ref. [110] p. 137f). The third rhythm which is not detectable in the scalp EEG (but e.g., by the use of epidural electrodes or magnetoencephalography [MEG]) is independent from the (posterior) alpha and mu rhythm and appears over the midtemporal region [110]. In emphasizing the fact that (in the MEG) this rhythm is best seen over the auditory cortex in the temporal lobe, Hari [51] uses the term 'tau' rhythm (tau stands for temporal). There is some evidence that the tau rhythm becomes suppressed during acoustic but not visual stimulation (cf. the review in Hari et al. [52]). Because the focus of this review is on theta and alpha activity with respect to cognitive performance and memory, the mu and third rhythm will not be considered.

Despite the fact that theta does not meet the criteria for an oscillatory component in the EEG, it may still be argued that activity within the individually defined theta band reflects oscillatory processes. In a theoretical sense, the EEG can be conceived of a linear superposition of a set of different sine waves (oscillatory components). In addition, there are more specific arguments which are based on empirical evidence:

1. With the help of sophisticated methods, theta peaks can be found in the human scalp EEG of young healthy adults [45].

Table 2

Double dissociation between tonic and phasic (event-related) changes in alpha and theta power with respect to cognitive performance

	Increasing performance		Decreasing performance	
	Theta power	Alpha power	Theta power	Alpha power
Tonic change	Decreases	Increases	Increases	Decreases
Phasic change	Increases	Decreases	Decreases	Increases

Tonic changes are discussed in Section 2, phasic changes in Section 4 below.

A phasic change is measured as an increase or decrease in band power during task performance as compared to a reference or resting period (cf. Fig. 7).

2. Theta frequency (as measured by TF) covaries with alpha frequency (as measured by IAF [34,76]).
3. Theta and alpha band power are related to each other, although in a reciprocal or 'opposite' way (see Sections 2–4 below and Table 2),
4. Animal research has shown that theta clearly is an oscillatory component of the hippocampal EEG which is related to memory processes (see e.g., the review by Miller [107] and Section 5 below),
5. Research from our laboratory indicates that theta band power increases in response to memory demands just as hippocampal theta in animals does (see Sections 4.3 and 5 below).

Thus, the concepts of desynchronization and synchronization will also be used for the (individually defined) theta band. In a similar way, these concepts will be applied to the different subbands of alpha. Visual inspection of 'alpha waves' in the EEG may invite the misleading interpretation that there is only a single rhythm which may just vary in frequency. As the results from factor analyses have shown, there are at least two independent components of alpha activity which must be distinguished. Based on physiological and experimental evidence, many authors meanwhile assume that there is an entire population of different alpha rhythms (e.g., Refs. [6,166,167]). Thus, it seems quite obvious to assume that during desynchronization different alpha rhythms in different subbands start to oscillate with different frequencies (for more details see Section 5).

2. Tonic changes and differences in the alpha and theta frequency range

The type of EEG changes or differences which are discussed in the following sections may be termed 'tonic' in order to contrast them from 'phasic' changes. Phasic (or event-related) changes in the EEG are more or less under volitional control and occur at a rapid rate, whereas tonic changes are not (or less) under volitional control and occur at a much slower rate. Phasic changes in the EEG are task and/or stimulus related. Tonic changes, on the other hand,

occur over the life cycle and in response to circadian rhythms, fatigue, distress, neurological disorders, etc.

2.1. Age related changes and performance related differences in alpha frequency

It is a well documented fact that alpha frequency changes with age. From early childhood up to puberty alpha frequency increases, but then starts to decline with age. For children, Hughes [60] reports that alpha frequency for 1, 3, 9 and 15-year olds increases from about 5.5 to 8, 9 and 10 Hz, respectively. Similar estimates were reported by Somsen et al. [139] and Niedermeyer [112]. It should be noted, however, that the increase in alpha frequency and changes in alpha power are not linear, but occur in several growth spurts [38,59,155]. Within the age range of adult subjects Köpruner et al. [88] have found a linear relationship (alpha peak frequency = $11.95 - 0.053 \times \text{age}$) between age and alpha frequency. According to this relationship a young adult of, e.g., 20 years has an expected peak frequency of 10.89 Hz, whereas a 70 year old subject shows a drop of 2.65 Hz down to a frequency of 8.24 Hz. It is important to note that even in a sample of age-matched subjects, interindividual differences are about as large as age-related differences. When interindividual variability is described

in terms of a normal distribution [67], about a third of young adults are expected to show a difference in alpha frequency of more than 2 Hz.

With respect to an age related decrease in alpha frequency there is some discussion about its general validity. As an example, Duffy et al. [36] report only a slight and non-significant drop in alpha peak frequency. Closer inspection of their results, however, reveal that their finding is due to a lack of decrease in alpha frequency during the early and middle adult age range (from about 30 to 50 years). For older subjects, a drop of about 1 Hz was found between 60 and 80 year olds. Other studies have found evidence that an age related decrease in alpha frequency may not be due to age per se but instead to age related neurological diseases [58,156] or to a lack of school education (cf. Ref. [53]). Nonetheless, changes in alpha frequency as schematically depicted in Fig. 2 give a good overall picture of the respective results reported in the literature.

The findings of several experiments suggest that alpha frequency is an indicator for the speed of cognitive and memory performance in particular. Early findings reported by Surwillo [147–152] indicate that alpha frequency is significantly correlated with the speed of information processing as measured by reaction times (RT). Subjects with

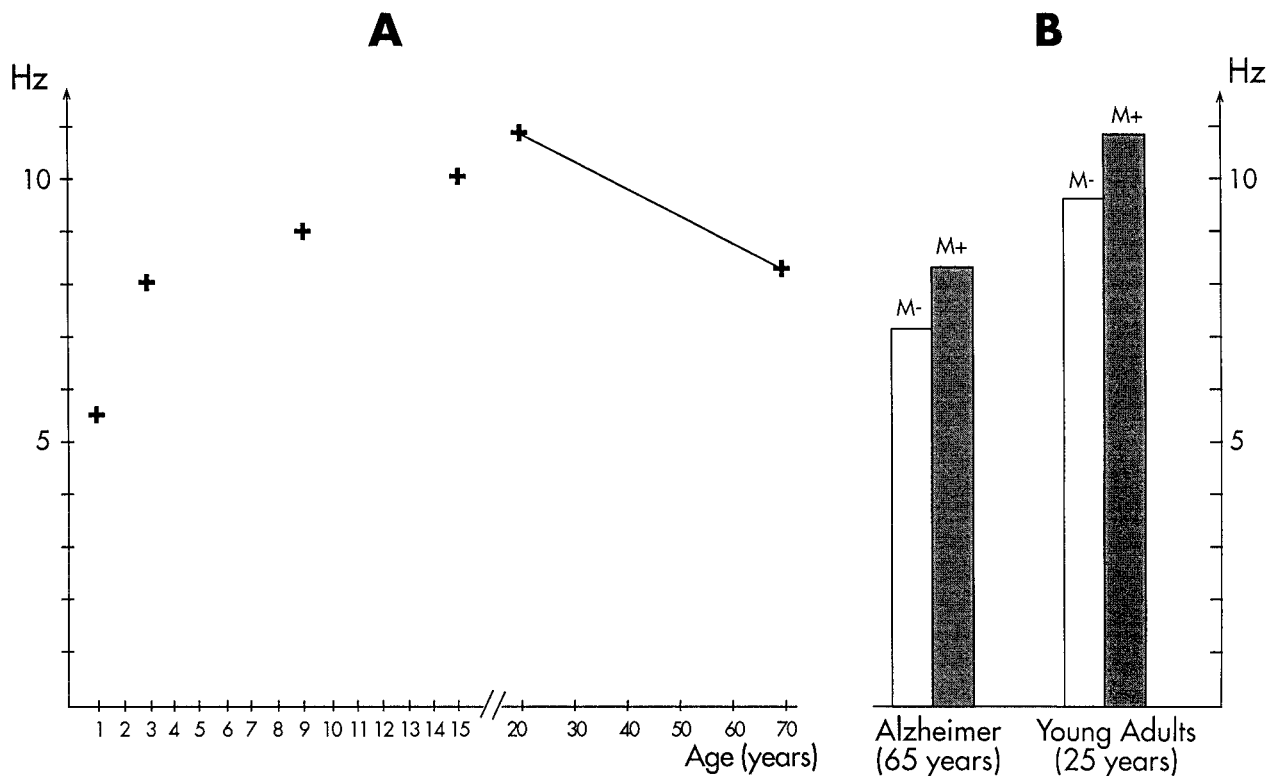


Fig. 2. Interindividual differences in alpha frequency are large and vary with age and memory performance. (A) From early childhood to puberty, alpha frequency increases from about 5.5 to more than 10 Hz but then starts to decrease with age. This decrease in alpha frequency may be due to age related neurological diseases or even to the lack of 'mental training' in the later lifespan but not to age per se. (B) As compared to bad memory performers, good performers have a significantly higher alpha frequency. This holds true not only for young and healthy subjects (e.g. Refs. [69,71,73] but even for Alzheimer demented subjects [71].

high alpha frequency show fast RTs, whereas slow subjects have low alpha frequency (for similar results see also Ref. [77]). These findings are in good agreement with the results from a variety of experiments from our laboratory which revealed that alpha frequency of good memory performers is about 1 Hz higher than that of age-matched samples of bad performers [67,68,70,71,73,74]. Because good performers are faster in retrieving information from memory [66] than bad performers, these data too indicate that alpha frequency is related to the speed of information processing or reaction time. These results also suggest that alpha frequency should be related to intelligence which indeed seems to be the case ([2]). All of these findings are based on interindividual differences in alpha frequency. In contrast, intraindividual or task related shifts in alpha frequency appear not to be related to the speed of information processing [76] because an asymmetric desynchronization in the broad alpha band (favoring the lower or upper band) will lead to a shift in power and, thus, to a distorted estimate of alpha frequency.

In summarizing, the reported findings suggest that alpha frequency is an indicator of cognitive and memory performance. This conclusion is also supported by the fact that alpha frequency increases from early childhood to adulthood and then decreases with age over the remaining life span in a similar way as brain volume and general cognitive performance does (e.g., Refs. [12,165]).

2.2. Age related changes in alpha and theta power

The extent of age related frequency and power changes in children are depicted in Fig. 3A (data are from Somsen et al. [139]). At an age of 12 years (dashed line) children show already a well developed alpha peak at about 10 Hz. In contrast, for 7-year old children, two different peaks, a theta peak (centered at 4.5 Hz) and an alpha peak (located at about 9 Hz) can be observed. As compared to younger children, 12-year olds exhibit a strong decrease in theta power and a pronounced increase in upper alpha power.

When broad band differences within the traditional frequency ranges (cf. the vertical lines in Fig. 1) are calculated, the age related increase in absolute alpha power is blurred. The reason for this is that due to an increase in alpha frequency, peak alpha power shifts towards higher frequencies. As a consequence, the upper alpha band shows an increase in power whereas the opposite holds true for the lower alpha band (cf. Fig. 3A). Thus, for the broad alpha frequency range, little or no age related differences are obtained. Misleading interpretations that arise from this fact can easily be demonstrated by considering the results of a broad band analysis as depicted in Fig. 4 (data are again from Somsen et al. [139]). Age related changes in broad band absolute power (delta: 1.5–3.5 Hz, theta: 3.5–7.5 Hz, alpha: 7.5–12.5 Hz, beta: 12.5–22.5 Hz) indicate large differences in the delta and theta but no changes (or

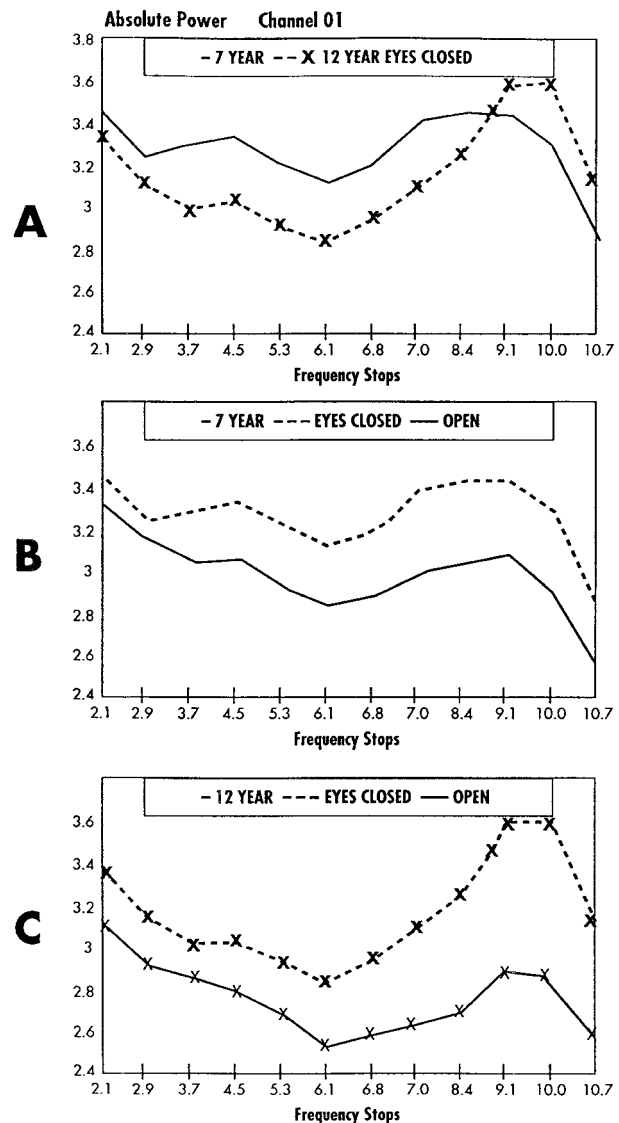
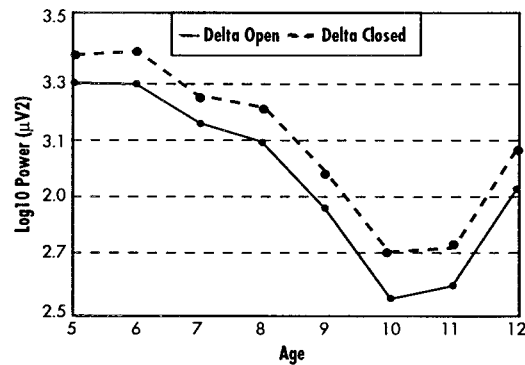


Fig. 3. Power spectra for 7 and 12 year old children (data replotted from Ref. [139], p. 201; reprinted with permission). (A) As compared to young children, older children show a pronounced increase in upper alpha power and a strong decrease in theta and delta power. Power suppression during eyes opening is smaller for young (B) as compared to older children (C).

even a slight decrease) in the alpha band (cf. the left part of Fig. 4). If relative, instead of absolute power is calculated, a different pattern of results emerges as the diagrams in the right part of Fig. 4 indicate. Here, in agreement with the data of Fig. 3, delta and theta power decreases, whereas alpha power increases. The reason for this difference between absolute and relative power can easily be explained when considering the fact that relative power measurements tend to give larger estimates for the dominant frequency range (where absolute power is largest) and lower estimates for frequencies which fall outside this range. As a consequence, when alpha becomes the dominant frequency with increasing age, relative power measurements will show a pronounced age related increase in

Absolute Power



Relative Power

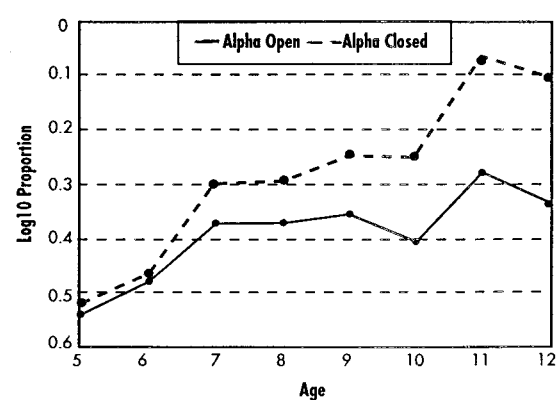
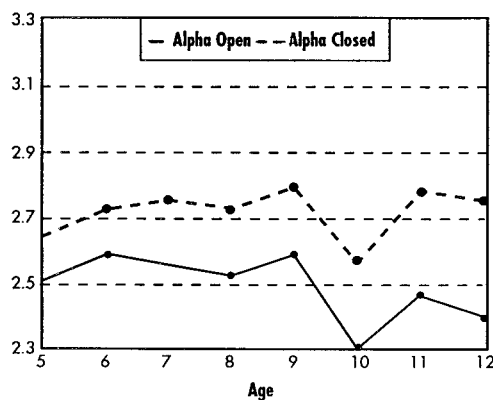
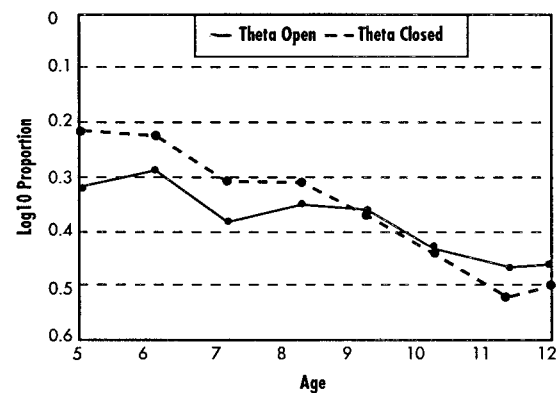
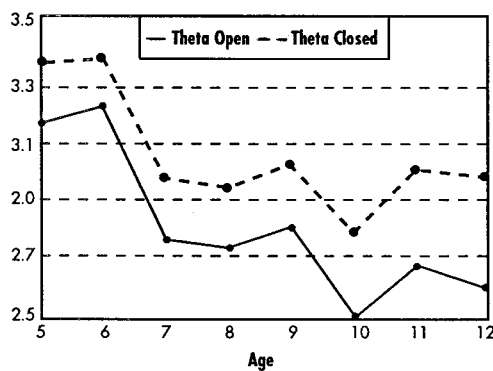
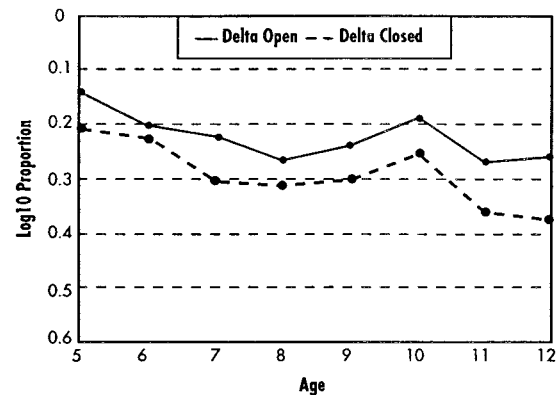


Fig. 4. Differences between age related changes in absolute and relative power (broad band analysis; data replotted from Ref. [139], pp 194–195; reprinted with permission). Because individual alpha frequency changes with age (cf. Fig. 2) and because broad band analyses use fixed frequency windows, the strong age related increase in upper alpha power is blurred (cf. Fig. 1). Relative power measures give better estimates for the alpha band because (i) they yield larger measures for the dominant frequency range and because (ii) with increasing age, alpha power becomes the dominant frequency in the EEG.

alpha power. This divergence in age related changes in absolute broad band and relative alpha power were obtained by many other studies (e.g., Ref. [54]).

The findings reported by Somsen et al. [139] are in good agreement with earlier studies. It has been shown repeatedly that absolute power in the delta and theta band

decrease with age while relative alpha power (or absolute upper alpha power) increases [42,53,54,62,63,105]. Studies investigating developmental changes in topography have found that the increase in alpha power starts at posterior derivations and ends at more anterior recording sites ([43], for similar results see also Ref. [162]). The increase in

alpha power is even more remarkable, if one considers findings reported by Yordanova and Kolev [169] which indicate that phase locking in the alpha frequency range also increases with age.

The conclusion from the studies reviewed so far is that the mature brain at or beyond an age of about 16 is characterized by an increase in absolute power in the upper alpha band but by a decrease in theta and delta power as compared to a less developed brain in younger children. A series of other studies support this view and show further that children with poor education [53], with reading writing/disabilities [54], with spelling disabilities [21] or with other types of neurological disorders [134] show significantly more delta and theta but less alpha power (for a review see also Ref. [134]).

For older subjects (about 50 years and older) a variety of studies have found age related changes in EEG power (e.g., Refs. [26,103,116,164] and the reviews in Refs. [110–112,160]). Most of these studies show a general slowing of the EEG with a pronounced power increase in the slow frequency ranges of about 7 Hz and below and a decrease in higher frequencies of about 7 Hz and higher (e.g., Refs. [26,101,116,117]).

A very similar pattern of results is obtained for cognitively impaired or demented subjects. As compared to age matched controls, the EEG of demented subjects is characterized by an increase in theta, a decrease in alpha power and alpha blocking and a forward shift in alpha activity from posterior to more anterior recording sites (e.g., Refs. [11,24,27,64] p. 995, [138,153]). It should be noted, however, that a few studies report that demented [16] or old subjects [87] show even an increase in alpha power. In the study of Brenner et al. [16] this effect was restricted to the lower alpha band. Könönen and Partanen [87] used a bipolar montage and, thus, their findings reflect effects that are topographically restricted and may, thus, not be related to changes in absolute or relative power as reported in other studies (cf. the overview in Table 1).

Reports on age related changes in alpha and theta power must be interpreted with caution because most of the studies used broad band analyses within fixed frequency windows. In older subjects at an age of about 60–70 years alpha frequency lies between 8.5 to 9 Hz. As a consequence, the traditional alpha range of 7.5–12.5 Hz will miss most of the ‘real alpha range’ (cf. Fig. 1B,C) and will instead reflect only a small part of the ‘real’ upper alpha band. On the other hand, the traditional theta band of 4–7.5 Hz will reflect most of the slowed alpha activity. Thus, an age related decrease in alpha may be masked by an age related increase in theta. Depending on the age of the subjects and their averaged alpha frequency, some studies report either a lack of an age related change in the alpha band (e.g., Ref. [99]) or even an increase (e.g., Ref. [16]) which might actually be due to an increase in theta.

In summarizing, the reported findings suggest that alpha (particularly in the range of the upper alpha band) and

theta change with age in a nonlinear and opposite way. There is a strong increase in alpha but decrease in theta and delta from early childhood to adulthood. During adulthood alpha and theta power may remain comparatively stable but at least beyond the age of 50 or 60 years [17] a period of a pronounced decrease in alpha and increase in theta power can be observed which may well be due to age related neurological disorders and not to age per se [58,55]. It is interesting to note that sedative drugs (benzodiazepines or barbiturates) which are known to cause different degrees of amnesia have the common effect of suppressing the alpha rhythm [40].

2.3. Age related changes in alpha and theta reactivity

Measures of alpha or theta reactivity usually reflect power differences between two resting periods, one with eyes open, the other with eyes closed. The term alpha reactivity or suppression also is used when a resting period (eyes open or closed) is compared with a test period in which subjects have to perform some type of task. It is well known since Berger (e.g., Ref. [10]) that opening eyes and mental activity suppresses the alpha rhythm.

For children several studies have found an age related increase in alpha reactivity (e.g., Ref. [139]). Inspection of Fig. 3B,C demonstrates a strong age related increase in alpha reactivity with increasing age. However, it should also be noted that even in the delta and theta band a pronounced suppression of power can be observed (Fig. 4). This is in sharp contrast to respective findings with adults where the effects of power suppression are restricted to the alpha band. It remains an open question why power suppression during eyes open in children affects even the delta and theta band. It may be hypothesized that in children different frequency bands are not yet functionally differentiated and separated from the broad alpha frequency range and, thus respond more in an alpha-like way.

Within the age range of older subjects, it is well known that alpha reactivity or suppression tends to decrease with age (e.g., Ref. [36]). Similar effects were found when neurologically impaired subjects were compared with age matched controls (e.g., Ref. [1,11]). As an example, Sheridan et al. [136] have reported that Alzheimer demented subjects with normal alpha that is suppressed during eye opening have significantly higher WAIS Performance IQ scores than patients with irregular alpha that does not or only weakly change during eye opening. Similar findings were obtained even with learning disabled children (c.f., Ref. [41]) who show less task-related alpha attenuation than age-matched controls.

2.4. Changes in alpha and theta power during the wake–sleep cycle

The evidence reviewed so far suggests that comparatively large alpha but small theta and delta power characterize the EEG of subjects with good cognitive perfor-

mance. Thus, it appears plausible to assume that during the transition from alert wakefulness to sleep onset alpha power decreases whereas theta and delta power increase. This is indeed the case as is known since the pioneering work by Dement and Kleitman [32]. More recent studies distinguish between 9 different EEG stages within the hypnagogic state (i.e., the transition period from waking to sleeping) as is shown in Fig. 5.

By using spectral analysis and comparatively narrow bands in the extended alpha frequency range (alpha 1: 7.6–9.4 Hz; alpha 2: 9.6–11.4 Hz; alpha 3: 11.6–13.4 Hz), Tanaka et al. [154] found that absolute delta and theta power increase, whereas alpha 1 and alpha 2 decrease from EEG stage 1 to 7 (see also Ref. [56]). Power in the alpha 3 band, which already reflects parts of slow sigma activity (sigma is the frequency range of about 12.5–15 Hz where sleep spindles occur) decreases from EEG stage 1 to 6 but increases from 6 to 9. Furthermore, from stage 1 to 9, the topographical region of maximal alpha power (in all of the three bands) moved from posterior to anterior recording sites, as Fig. 6 indicates. This is reminiscent of ‘alpha anteriorization’ which was found for demented subjects (e.g., Ref. [24]). It is also interesting to note that the largest drop in alpha power was found in the alpha 2 band which corresponds to the traditional upper alpha band (when considering the mean age of subjects which was 23 years).

Sleep spindles (starting at EEG stage 8, cf. Fig. 5) usually are taken as sign for the onset of sleep. However,

sleep spindles appear rather gradually and, thus, the precise time of actual sleep onset is difficult to determine. This question was addressed in an interesting study by Ogilvie et al. [118]. Before the sleep session began, subjects were instructed to press a button if a tone was presented. As was expected, with increasing drowsiness the reaction time for pressing the button increased. During that period of increasing drowsiness (but when subjects were still responding to the tone) delta and theta power increased, whereas alpha decreased. However, when responding ceased, EEG power increased across all frequency bands. A comparison with the data of Tanaka et al. [154] suggests that actual sleep onset occurs already during EEG stage 6 and 7, much earlier than the first spindles appear. It is important to note, however, that during sleep onset alpha power shows about the same magnitude as compared to a state of very low drowsiness when subjects gave a fast response to the tone. As compared to this stage, the increase in power during actual sleep onset (measured as a percentage of increase in absolute power) for delta, theta, alpha (8–12 Hz), sigma and beta (15–25 Hz) is 56%, 211%, 3%, 177% and 56%, respectively. Thus, the abrupt increase in EEG synchronization during sleep onset occurs in a broad frequency range that only marginally affects the alpha band. As the data in Fig. 6 demonstrate, during sleep onset (at about EEG stage 6 and 7) alpha power (in the range of 7.6–11.4 Hz) is still much smaller than during alert wakefulness (EEG stage 1).

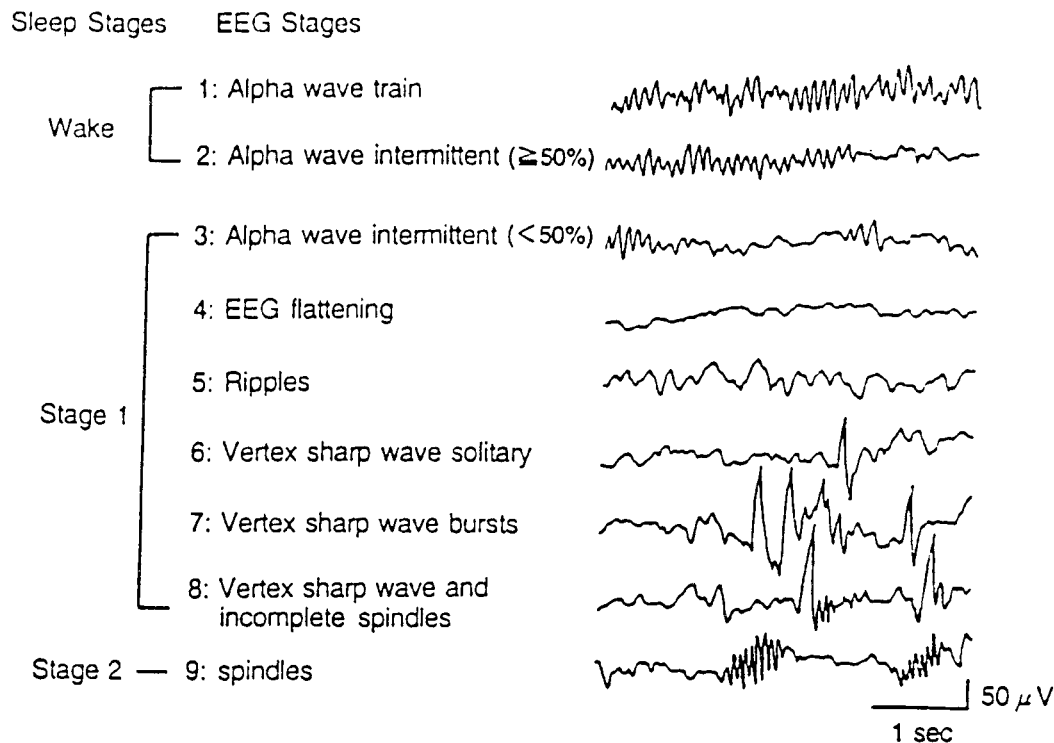


Fig. 5. Typical EEG patterns during the hypnagogic state which is the transition period from waking to sleeping (reprinted from Tanaka et al., Ref. [154], p. 524; reprinted with permission from the American Sleep Disorders Association and the Sleep Research Society, Rochester, MN (1997)). Even visual inspection of the EEG indicates that alpha activity decreases during the early EEG stages 1–4.

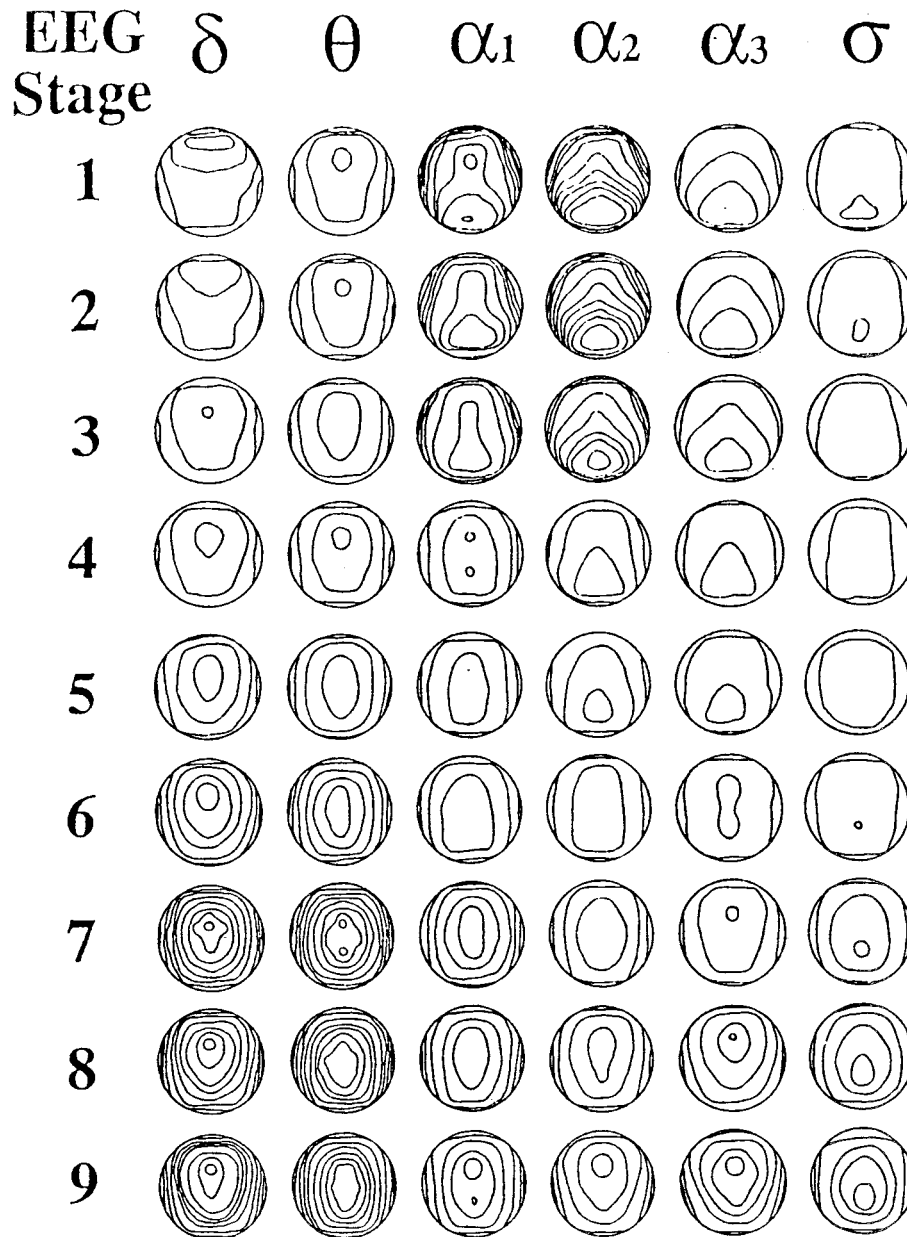


Fig. 6. Average topographic maps for six frequency bands, showing changes in absolute power during the 9 EEG stages in the hypnagogic state (reprinted from Tanaka et al., Ref. [154], p. 527; reprinted with permission from the American Sleep Disorders Association and the Sleep Research Society, Rochester, MN (1997)). As discussed in the text, actual sleep onset occurs during EEG stage 6 or 7, much earlier than the first spindles appear (cf. Fig. 5). Up to these stages alpha power (in all of the three bands) shows a strong decrease, whereas the opposite holds true for the theta and delta band. Furthermore, alpha power moves from posterior to anterior recording sites. This is reminiscent of 'alpha anteriorization' which was found for demented subjects.

REM sleep is characterized by a low voltage desynchronized EEG with an irregular pattern of bursts or trains of alpha activity particularly at occipital leads [32,145]. As compared to EEG stage 1 and 2 (cf. Fig. 5) alpha activity generally is decreased during REM sleep [50]. Because of this fact and the high probability of dreaming episodes during REM, it appears likely that the decrease in alpha during parts of the REM sleep can be interpreted in terms of an 'event-related' suppression or 'desynchronization' of

the kind that can be observed during an alert subject performing some type of task (for more details see Section 4 below). Evidence for this assumption comes from an interesting study by Chong-Hwa Hong et al. [25]. In a single subject design, 12 different dreams during REM sleep were analysed. After a dream, the subject was awakened and had to report the dream which was scored for 'language content'. The results showed that the higher the score for expressive or receptive language was, the larger

was the suppression of alpha power at those recording sites that correspond to Broca's and Wernicke's area.

During eye movements (EM's), regardless of occurring during REM or NREM sleep, alpha increases but theta decreases [27] (see also Ref. [50]). It is known that PGO spikes are highly correlated with dream activity and precede (or may even trigger) EM's. In a study conducted by Conduit et al. [28] the appearance of EM's in stage 2 sleep was used to provoke dream episodes. Their basic idea was that EM's indicate PGO spikes and to present during that period light and sound stimuli (below waking threshold) in order to provoke a dreaming episode. The results show that in the experimental condition (as compared to control conditions with EM's but no stimulation) a significant increase in alpha power and a higher frequency of imagery reports was obtained after awakening. These data suggest that the increase in alpha activity reflects some sort of visual arousal that precedes a dream with high imagery content.

The effects of sustained wakefulness and sleep deprivation on EEG power are well documented (e.g., Refs. [15,29,31,33]) and in general show that increased theta and lower alpha power reflect increased sleepiness. As an example, Cajochen et al. [22] have found that absolute EEG power within the range of 6.25–9 Hz increases monotonically during sustained wakefulness in a sample of subjects with a mean age of 53 years. Considering the age related decline in alpha frequency (cf. Ref. [88] and Fig. 2A), the expected alpha frequency for these subjects is about 9 Hz. Thus, the frequency range of 6.25–9 Hz covers the entire range of the (individually adjusted) lower alpha band. Similar findings were obtained by Torsvall and Akerstedt [157]. These results seem to indicate that an increase in lower alpha power may reflect the increased efforts (and probably difficulties) of subjects to maintain a state of alert wakefulness. This interpretation is also supported by Crawford et al. [30] who have found that in contrast to subjects with high sustained attention, low sustained attention subjects which have difficulties to inhibit distracting environmental stimuli show a significantly larger proportion of lower alpha power.

It is interesting to note that an increase in lower alpha power occurs only when subjects are not allowed to fall asleep and when they are forced to stay awake. If tired subjects are allowed to fall asleep, alpha power (including slow alpha frequencies) decreases (cf. Figs. 5 and 6). Thus, during the normal state of increased sleepiness which is correlated with increasing melatonin secretion in the respective circadian phase, we would not expect that (lower) alpha power increases selectively. During a state of decreased mental inactivity such as during increased normal sleepiness, a decrease in alpha and an increase in theta is to be expected. The results reported by Cajochen et al. [23] are in good agreement with this interpretation. These authors have shown that the administration of melatonin leads to a significant increase in absolute power in the

frequency range of 5.25–7 Hz. Considering the mean age of their subjects (which is about 25 years) indicates that the frequency range of significant power differences lies in the theta band (expected alpha frequency is about 10.5 Hz, the lower alpha band ranges from about 7–10.5 Hz). Furthermore, inspection of the time course of power changes between 1700 h and 1900 h reveals a general decrease in alpha power (cf. Ref. [23] p. 210, Fig. 1).

2.5. Alpha power in congenital blindness

Visual information processing represents an important aspect of cognitive performance. If alpha power is indeed positively related to cortical information processing, it would be expected that congenitally blind subjects lack alpha activity at occipital recording sites. This is indeed the case as the following studies indicate. Noebels et al. [113] report that in a sample of 7 congenitally blind adults, the occipital alpha rhythm was absent, whereas slow negative potentials were similar to those of normally sighted controls. Most interestingly, in blind subjects, a pronounced alpha rhythm could be observed at Cz and Fz which was larger in power than that of controls. Thus, it appears as if in more anterior cortical regions a compensatory increase in alpha activity takes place. Similar results were already reported by Birbaumer [13], who found that in congenitally blind subjects alpha activity was reduced occipitally but significantly increased frontally in relation to controls.

3. Interim discussion

If the EEG of the mature brain of young healthy adults is compared either with the developing brain, the aging brain or the brain which is affected by neurological diseases of various kinds, the conclusion is that:

- (a) alpha frequency is positively related to cognitive performance, and
- (b) large power in the range of the upper alpha band but small power in the theta frequency range indicate good cognitive performance.

These conclusions are based on findings which show that

- (a1) alpha frequency increases from early childhood to adulthood but then decreases with increasing age or age related neurological diseases,
- (a2) alpha frequency is lowered in demented subjects (as well as in patients with other types of neurological disorders),
- (a3) alpha frequency is significantly higher in subjects with good memory performance as compared to age matched controls with bad memory performance,
- (a4) alpha frequency is positively correlated with the speed of processing information,
- (b1) theta power decreases and upper alpha power increases from early childhood to adulthood,

- (b2) theta power increases and upper alpha power decreases during the late part of the lifespan,
- (b3) theta power is enhanced and alpha power lowered in subjects with a variety of different neurological disorders as compared to age matched controls (this holds true not only for demented subjects but also for children with reading/writing or spelling difficulties),
- (b4) during the hypnagogic state (i.e., the transition from waking to sleeping) when the ability to respond to external stimuli decreases, theta power increases and upper alpha power decreases.

The behavior of lower alpha shows a somewhat different pattern of results and requires some additional explanation. Old subjects (e.g., Refs. [26,101,116,117]), subjects with difficulties in maintaining a state of alert wakefulness [30] and during a state of sustained wakefulness [22], power in the lower alpha band is increased. Findings from our laboratory [72,73,75,78,83] have shown repeatedly that the lower alpha band responds selectively to attentional demands. A tonic increase of lower alpha power may, thus, reflect the attempt of old or drowsy subjects to increase their attention and alertness. Because the increase in lower alpha power may reflect an attempt to increase cognitive performance (particularly under conditions that are less favourable), large power in the alpha band is again linked to good performance in the sense that if lower alpha power would drop, cognitive performance would drop too.

The conclusions as outlined above holds true only for tonic but not for phasic changes in the EEG. The best known example of a phasic change is the suppression of the alpha rhythm during eyes opening. The results of spectral analyses show that compared to closed eyes, alpha power decreases but theta power increases. As was mentioned in Section 1, this characteristic type of a phasic change in alpha and theta band power can be observed in response to a large variety of different task demands.

At this point we arrive at an interesting paradox. During actual cognitive performance (as compared to a resting state), the EEG is characterized by increased theta but decreased alpha power and thus resembles the EEG during a tonic change that reflects decreased cognitive performance. In Section 4.4 it will be shown that the extent of an event-related change in alpha and theta depends on absolute alpha and theta power. If theta power is low, theta synchronization is large and if alpha power is large, the extent of alpha power desynchronization (suppression) is large too. It is important to note that in a pure statistical sense, the extent of an event-related band power change may very well be independent from absolute power as measured during a resting condition. Thus, the dependency of event-related on absolute power indicates a special physiological mechanism which possibly operates to increase the signal to noise ratio (from a 'reference' to a 'test' interval; cf. Section 4 below).

It will be demonstrated that alpha and theta power on the one hand and event-related changes in alpha and theta

power on the other hand show a double dissociation with cognitive performance: Large alpha power which is correlated with a pronounced decrease in event-related band power and small theta power which is correlated with a pronounced increase in band power indicate good cognitive performance. First positive evidence for the suggested hypothesis comes from age related differences in theta and particularly in alpha reactivity. As mentioned above, from early childhood to adulthood alpha power as well as alpha reactivity (suppression) increases, whereas in older subjects alpha power and alpha reactivity decrease. The complex relationship of this double dissociation is summarized in Table 2.

4. Event-related (phasic) changes in the alpha and theta band

Since the work of Berger it was suggested that visual (or other sensory) task demands and visual attention in particular are the primary factors that lead to a suppression of the alpha rhythm (e.g., Refs. [108,130]). In using event-related desynchronization (ERD), a method introduced originally by Pfurtscheller and Aranibar [123], recent research has revealed a much more complex picture.

A typical example of an EEG epoch which is used for measuring ERD is shown in Fig. 7. The subjects' task was to read a visually presented word and to make a semantic judgment by responding 'yes' to a word denoting a living and 'no' to a word denoting a non-living object. Before a word appeared a warning signal is presented. Subjects had to judge a total of 96 words. The basic principle for measuring ERD is that alpha shows a typical phasic change over the time course of a trial. After a response, the subject relaxes and awaits the presentation of the next stimulus. This state of relaxed but alert wakefulness is reflected by a pronounced alpha activity during the reference interval which precedes each trial. Even before the warning signal actually appears, the alpha rhythm becomes suppressed, because the subject anticipates the beginning of the next trial.

The measurement of ERD is done in several steps. First, the EEG is band pass filtered within defined frequency bands, the filtered data are squared and then averaged within consecutive time intervals (of e.g., 125 ms). Second, the obtained data are averaged over the number of epochs. Third, band power changes are expressed as the percentage of a decrease or increase in band power during a test as compared to a reference interval by using the following simple formula: $ERD = ((\text{band power reference} - \text{band power test}) / (\text{band power reference})) \times 100$. Note that desynchronization is reflected by positive ERD values, whereas event-related synchronization (ERS) is reflected by negative ERD values [122,124].

The appropriate selection of frequency bands is one of the most critical issues when using ERD or related measures such as changes in induced band power (IBP; cf.

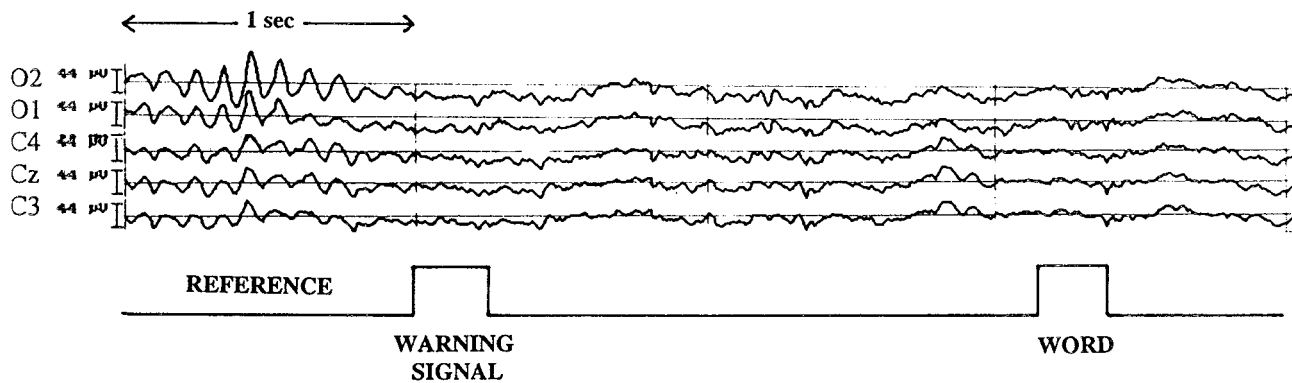


Fig. 7. Typical example of an EEG epoch, showing the basic principle of alpha desynchronization. During the first second of the epoch, which is called reference interval, the subject shows pronounced rhythmic alpha activity. Subjects run through many trials and, thus, the anticipation of the warning signal already causes alpha to desynchronize even before the warning signal actually appears. As spectral analysis shows, this attentional effect is reflected only in the lower alpha band (see Fig. 8).

Refs. [82,83]. Due to large interindividual differences of alpha frequency, large portions of alpha power may fall outside a fixed frequency window and invite misleading interpretations (cf. Fig. 1). In order to avoid these and related problems that arise with fixed frequency windows, we (e.g., Refs. [69,79–81]) suggested to use alpha frequency $f(i)$, averaged over all leads, as an anchor point to adjust frequency bands individually for each subject. Then, four frequency bands with a width of 2 Hz can be defined in relation to $f(i)$ that cover the traditional theta and alpha frequency range from about 4–12 Hz (depending on the actual $f(i)$ for each subject). The frequency bands obtained by this method are termed: theta ($f(i)-6$ to $f(i)-4$); lower 1 alpha ($f(i)-4$ to $f(i)-2$); lower 2 alpha ($f(i)-2$ to $f(i)$) and upper alpha ($f(i)$ to $f(i) + 2$). For each subject, ERD is calculated within these individually determined frequency bands. We have shown in several studies that fixed frequency bands blur the specific relationships between cognitive performance and ERD, we otherwise are able to observe (as an example, see Fig. 11).

4.1. Desynchronization in the lower alpha band reflects attention

One of our most basic findings with respect to the alpha frequency range is that alpha desynchronization is not a unitary phenomenon. If different frequency bands are distinguished within the range of the extended alpha band, two distinct patterns of desynchronization can be observed. Lower alpha desynchronization (in the range of about 6–10 Hz) is obtained in response to a variety of non-task and non-stimulus specific factors [see also Refs. [45,163]] which may be best subsumed under the term ‘attention’ (for a similar concept, see Ref. [135]). It is topographically widespread over the entire scalp and probably reflects general task demands and attentional processes. Upper alpha desynchronization (in the range of about 10–12 Hz) is topographically restricted and develops during the pro-

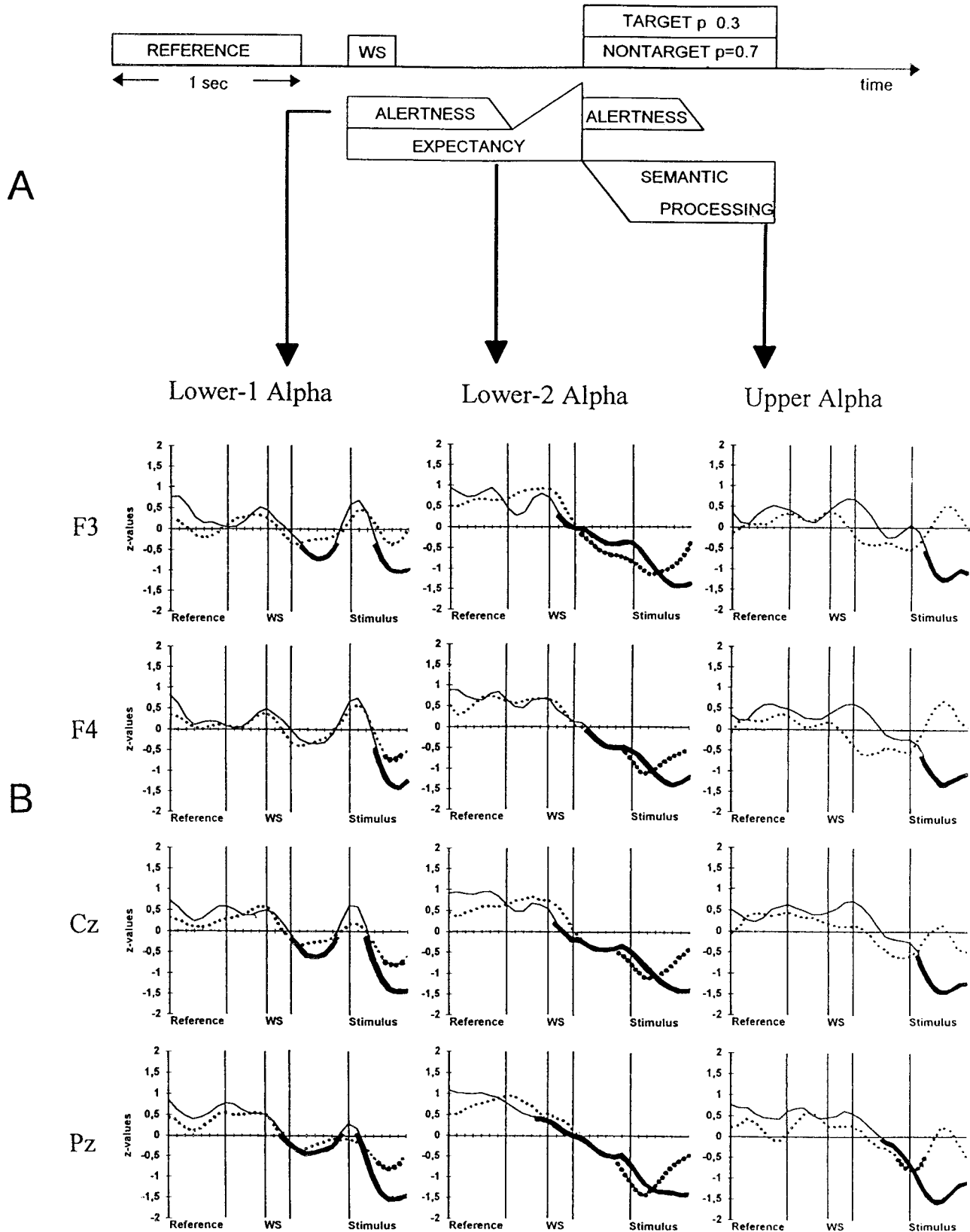
cessing of sensory-semantic information as recent evidence indicates (e.g., Refs. [72,75,78–81]).

The sensitivity of the lower alpha band with respect to attentional demands can be demonstrated by the results of a modified visual oddball task [83]. Two different components of attention, alertness (or arousal) and expectancy were studied (for a detailed cognitive analysis and definition of these terms, see Refs. [126,127]). In each trial a warning signal preceded the presentation of an imperative stimulus (target or nontarget). Subjects were asked to count the targets but to ignore nontargets. We assume that the warning signal and the target increase alertness and that the time before a target or nontarget appears reflects a state of increased expectancy. It is important to note that the presentation of targets and nontargets was not completely random. First, targets are rare and nontargets are frequent (the ratio is 30%:70%) and second, no more than three targets or nontargets were allowed to occur in succession. Thus, on the average, subjects were well able to expect (and make a good guess about) the occurrence of a target after a few trials. A large number of trials (200 stimulus presentations) was used to guarantee that subjects have enough time to get familiar with the sequence of targets and nontargets. Because it is well established that a variety of different components of event-related potentials (ERP's) are sensitive to attentional demands (cf. Ref. [98]), we in addition wanted to show whether event-related band power changes that can be observed in response to attentional demands are due to ERP components. Thus, we used IBP which is a measure that does not contain evoked EEG activity [82].

As the results depicted in Fig. 8 demonstrate, a significant response (decrease in band power) to the warning signal can be observed only in the lower-1 alpha band and when the warning signal preceded a target (note that for IBP, desynchronization is indicated by negative z -values). The finding indicates that—on the average—subjects were able to predict (expect) the occurrence of a target and that

the warning signal exerts an alerting effect primarily if it precedes a target. This alerting effect is reflected by a decrease in band power that is interrupted and, thus,

separable from the decrease in band power that occurs in response to the imperative stimulus. In contrast to the lower-1 alpha band, a steady decrease in band power



starting as early as 1000 ms before the onset of an imperative stimulus—probably reflecting expectancy—was obtained in the lower-2 alpha band. Because expectancy plays a role during the prestimulus period of both types of stimuli, there is no reason to assume that the prestimulus period will differ between target and nontarget trials. After the appearance of the imperative stimulus, however, the processing of targets and nontargets will be different. If a target appeared, subjects expect still to perform another task which is to count targets and press the response key. Thus, during the poststimulus period, targets show a somewhat larger lower-2 alpha desynchronization than nontargets.

We have found repeatedly that the upper alpha band is most sensitive to semantic or task specific effects. Thus, the largest differences between targets and nontargets are expected for the upper alpha band and during the second half of the poststimulus interval when the stimulus type is recognized and subjects start to count. This is indeed the case as Fig. 9 indicates. The findings demonstrate that three alpha bands proved useful for a better distinction between different cognitive processes. Furthermore, they replicate and extend related findings in earlier studies [72–75].

4.2. Desynchronization in the upper alpha band reflects semantic memory performance

Based on earlier findings from our laboratory (e.g., Ref. [75]), we have suggested and tested the hypothesis that upper alpha desynchronization correlates with semantic memory performance whereas theta synchronization correlates with working memory or episodic memory performance in particular. In two recently performed experiments, Klimesch et al. [79] and in a partially modified replication study [80], subjects had to judge, whether sequentially presented feature-concept pairs (such as ‘claws—eagle’, ‘wings—banana’, ‘yellow—hawk’, ‘seeds—cucumber’ etc.) are semantically congruent. It is important to note that the semantic judgment cannot be carried out before the concept word is presented. Thus, upper alpha desynchronization is expected to be significantly larger during the processing of the concept as compared to the feature word.

The results as summarized in Fig. 9 indicate that the upper alpha band is specifically related to the processing of semantic information. The most important results are that a significant increase in upper alpha desynchronization was found only during that time interval in which the semantic judgment task actually was carried out (cf. *t5* in Fig. 9) and that the theta band did not respond to semantic task demands at all. The two lower alpha bands exhibit a stepwise increase in desynchronization that exceeds the level of significance even before a semantic relationship between the feature and concept words can be detected and, thus most likely reflect the increase in attentional demands during the time course of the entire trial.

The increase in upper alpha desynchronization during the semantic task in *t5* is strictly localized over the left hemisphere. This finding is well in line with a variety of PET-studies and Tulving’s HERA model [159]. As an example, Petersen et al. [120] have shown that semantic task demands (particularly the retrieval of semantic information) are associated with a pronounced increase in the blood flow at left prefrontal regions (see also Ref. [128]). In addition, Martin et al. [104] have found that naming pictures of animals and tools (parts of the words used in the present study also represent animals, others such as weapons were similar to tools) was associated with bilateral activation of the temporal lobes and the calcarine region, the left thalamus and the left anterior insula/inferior frontal region (cf. Fig. 1 in Ref. [104]).

In Klimesch et al. [80], after a judgment task, subjects performed a semantic and episodic memory task (see also [79]). The prediction was that upper alpha desynchronization should be larger for good as compared to bad semantic memory performers. In general, we expected that upper alpha desynchronization is related to semantic memory performance, whereas theta synchronization is related to episodic memory performance.

In the semantic and the episodic memory task, the (congruent) feature words of the judgment task were presented. In the semantic task, subjects were asked to report any association that comes into their minds. In the episodic memory task, they were instructed to report only that concept word that actually was paired with a feature word. In the semantic task too, only correct responses (e.g.,

Fig. 8. (A) Structure of a single trial in a modified visual oddball task (data from Klimesch et al. [83]). An alerting warning signal precedes an imperative stimulus (target or nontarget). Subjects are asked to count targets but to ignore nontargets. (B) The assumed sequence of cognitive operations. It is predicted that the lower-1 alpha band reflects phasic alertness and responds to the WS and (imperative) stimulus with a decrease in band power (desynchronization). The lower-2 alpha band reflects expectancy and desynchronizes before the imperative stimulus appears. The upper alpha band reflects semantic processes that are related to task performance and, thus, shows maximal desynchronization in the late poststimulus interval (for targets) only. (C) Time course of changes in induced band power (IBP) for targets (bold line) and nontargets (dashed line) in three alpha bands with a width of 2 Hz each. IBP represents *z*-transformed power. Negative values indicate desynchronization, positive values synchronization. The reference interval was used to calculate confidence intervals. Thus, significant changes (marked by extra bold segments) refer to differences between the reference interval and subsequent time periods. As the results indicate, the lower-1 alpha band shows a phasic response to the WS and imperative stimulus, whereas the lower-2 alpha band exhibits a tonic increase in desynchronization that starts already before a target and nontarget appears. The upper alpha band shows the largest difference between targets and nontargets. Note that maximal desynchronization occurs in the poststimulus period for targets only. The length of the reference interval is 1 s.

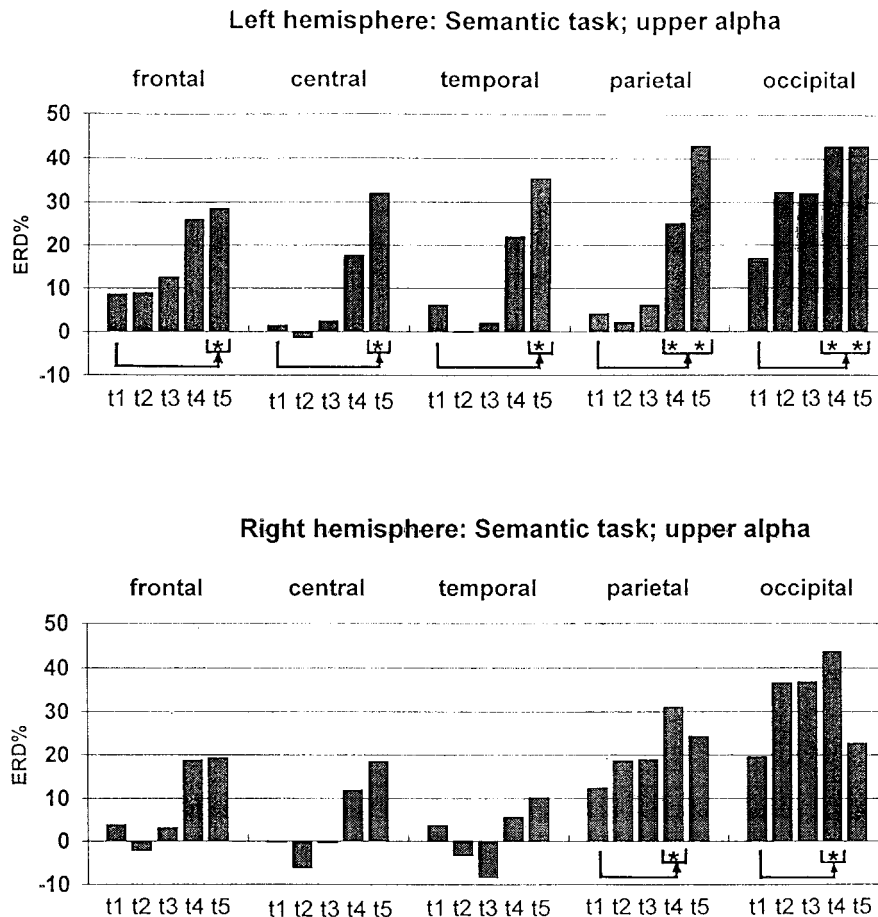


Fig. 9. Time course of event-related desynchronization (ERD) in the upper alpha band during a semantic judgment task [79]. Subjects had to judge whether a feature word (presented during t_2) is semantically congruent with a concept word (presented during t_4). Each interval (t_1 – t_5) represents a time period of 500 ms. The results show that upper alpha desynchronization (as measured by ERD) is largest during t_5 which is that time period in which the semantic judgment process actually takes place. Note the strong left hemispheric advantage (larger ERD-values over the left as compared to the right side of the scalp) particularly during t_5 .

‘eagle’ in response to ‘claws’) were counted. Thus, the only difference between the two tasks was the way subjects were instructed to retrieve information from their memory. In the semantic task, the number of correct responses was considered to reflect the strength of semantic associations. In the episodic task subjects had to focus on the specific pairing between a feature and concept. Because there are many different and semantically congruent ways a feature can be paired with a concept (e.g., ‘claws’ can also be paired with ‘hawk’) subjects had to retrieve the experimental context in which a particular feature was presented (i.e., was ‘claws’ presented in the context of ‘eagle’ or ‘hawk’?). Thus, the number of correct responses in this task was considered to reflect episodic memory performance. Subjects were divided into a group of good and a group of bad semantic memory performers. This was done on the basis of the semantic recall scores which were organized according to increasing values and were used to cut the sample into two halves. The results of this study shows again that in contrast to the theta and the two lower alpha bands, only the upper alpha responds to

semantic task demands. The most important finding of this study, however, was that upper alpha desynchronization during the semantic judgment process is significantly larger for good semantic memory performers as compared to bad performers, as Fig. 10 demonstrates. Furthermore, during the semantic judgment process, significant positive correlations were found between upper alpha desynchronization and semantic memory performance at frontal, central, temporal and parietal recording sites. Episodic memory was significantly correlated with theta synchronization. However, when the influence of episodic memory performance was removed by means of partial correlations, significant correlations between upper alpha desynchronization and semantic memory performance remained at frontal, central and parietal recording sites.

With respect to the relationship between upper alpha desynchronization and memory performance, similar findings were also obtained by Klimesch et al. [73] and Serman et al. [146] but of course not in studies using broad bands within fixed frequency limits (e.g., Ref. [132]). Finally, it should also be noted that some memory studies

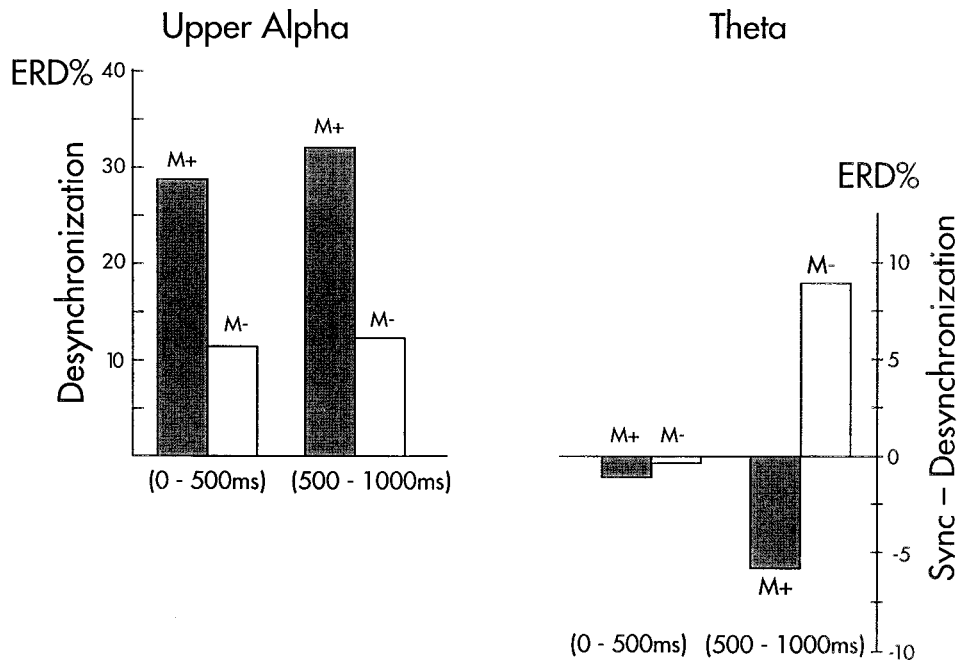


Fig. 10. Time course of event-related desynchronization (ERD) in the upper alpha and theta band during a semantic judgment task of the type used in Klimesch et al. [79], analysed separately for good (M+) and bad memory performers (M-) in a similar experiment [80]. Data are averaged for all recording sites. The time period of 0–500 ms corresponds to t_4 in Fig. 9, the period of 500–1000 ms poststimulus corresponds to t_5 in Fig. 9. The results indicate that in the upper alpha band, good memory performance (M+) is reflected by a significantly larger extent of desynchronization. The opposite holds true for the theta band where good memory performance is reflected by a larger extent of synchronization (expressed by negative ERD values).

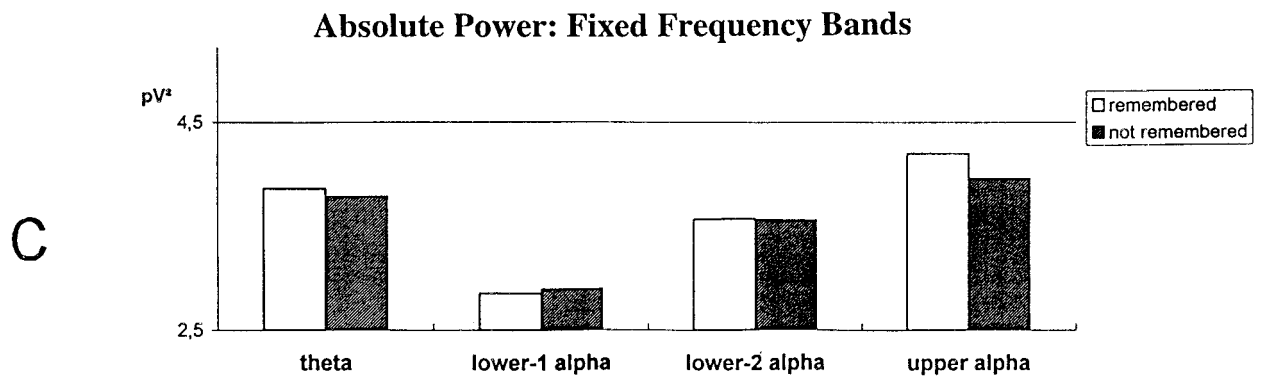
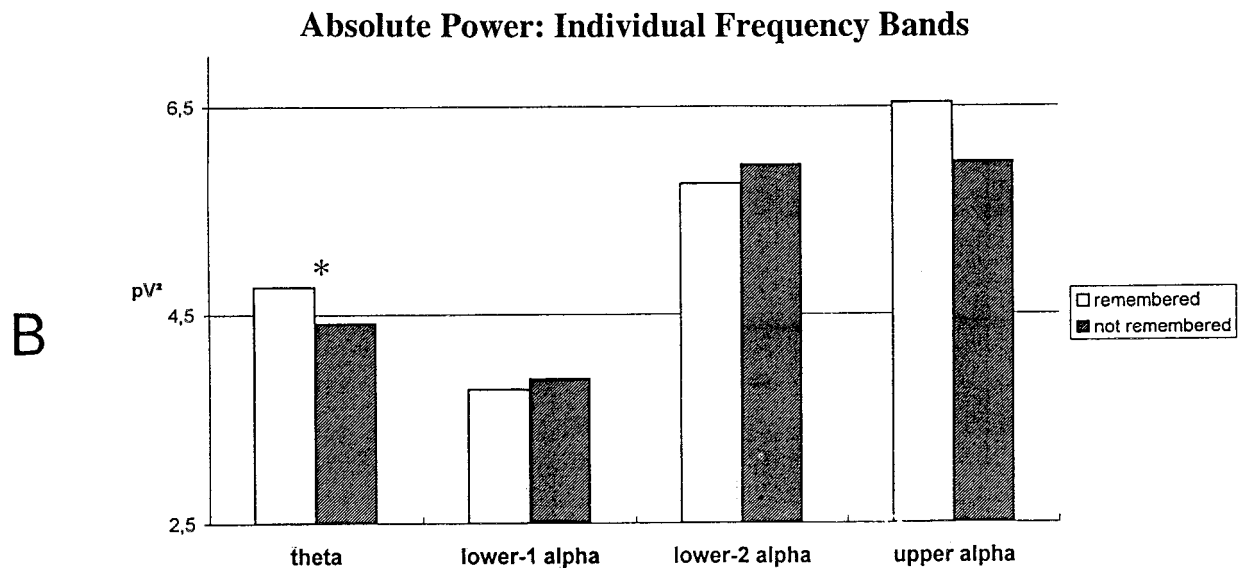
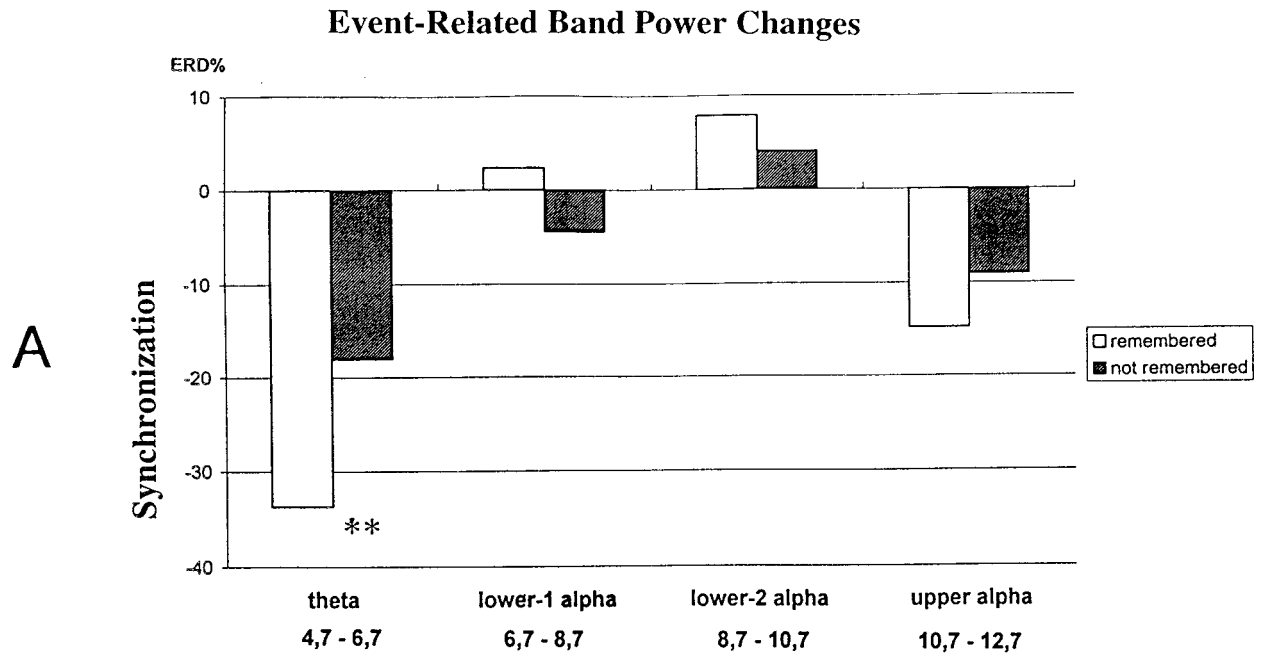
using narrow bands but acoustic stimuli (Krause et al. [89,90]) failed to replicate our findings. This failure is possibly due to the fact that simple tones such as Krause et al. used affect the tau rhythm which cannot be detected by scalp electrodes. Preliminary evidence for this view comes from an interesting study by Kaufman et al. [65] who found suppression of rhythmic activity in the alpha range over the auditory cortex when subjects scan memory for tones.

4.3. Synchronization in the theta band reflects episodic memory and the encoding of new information

Studies focusing on the hippocampal theta rhythm in animals have provided good evidence that theta power is related to the encoding of new information (cf. Refs. [20,107] for reviews) and to episodic memory in particular [47]. In a series of experiments, we were able to demonstrate that even in the human scalp EEG, the theta band responds selectively to the encoding of new information into episodic memory. This effect was first demonstrated by Klimesch et al. [75] and was meanwhile extended [45,46,76,79,81,163,168] and replicated by other research groups [18].

In the study by Klimesch et al. [76] the hypothesis was tested, whether a task related increase in theta power selectively reflects the successful encoding of new information. Because theta power increases in a large variety of different tasks (see e.g., the review in Ref. [133]) it seems

plausible to assume that theta power reflects—at least in part—unspecific factors such as e.g., attentional demands, task difficulty and cognitive load. Consequently, when trying to test the suggested hypothesis, it is important to use an experimental design which allows to control for unspecific factors. In Klimesch et al. [76], this was done by using an incidental instead of an intentional memory paradigm. During the encoding phase (i.e., the presentation of a series of words), subjects did not know that memory performance will be tested later. The crucial test for the proposed hypothesis was to calculate band power changes during the encoding stage and to compare words which can be remembered later with those which cannot be remembered later. If an increase in theta power is indeed related to a successful encoding of new information, it is to be expected that words which can be remembered in the later recall task show a significantly larger increase in theta power during encoding than words which will not be remembered later. Because all of the words used in the present study were very common, because semantic judgment tasks are very easy and because subjects did not know that their memory will be tested later, stimulus type, task difficulty, differences in mental load or specific encoding strategies can be excluded from the list of unspecific factors that influence the extent of theta synchronization. Thus, there are good reasons to assume, that the only difference between the later remembered and not remembered words refers to the actual establishment of a memory trace.



The results are plotted in Fig. 11 and demonstrate that words which could be remembered later exhibited a significantly larger extent of theta synchronization than not remembered words. Not only did theta synchronization reach significance, so did also absolute theta power, but only if frequency bands were adjusted individually. Similar findings were also obtained in a recognition task [81] where subjects knew that their memory will be tested later. Significant theta synchronization was found during the encoding phase for those words only which could be remembered later and only for correctly recognized targets during the actual recognition phase but not for distractors and not remembered targets.

4.4. The relationship between desynchronization, synchronization and absolute power

As the results by Klimesch et al. [75,76,79,80] have shown, the extent of theta synchronization and upper alpha desynchronization are related to episodic and semantic memory performance, respectively. Although these findings reveal very specific effects, they are in good agreement with the well known fact that the amount of alpha desynchronization generally is related to the relevance and/or difficulty of a task. The more demanding or relevant a task, the stronger the amount of alpha suppression or ERD (e.g., Refs. [69,14,73], cf. the review in Klimesch [68]). In a pure logical sense one would expect that the amount of desynchronization should depend on absolute power. Only if there is sufficient activity during a reference or resting interval would there be a possibility of a large extent of power suppression during task performance. A similar relationship may also be expected on the basis of physiological considerations. It would be quite plausible to assume that after a difficult task, a rebound of alpha activity takes place that lasts even into the reference interval of the next following trial (epoch). If this occurs trial after trial, the percentage of desynchronization (ERD) would clearly be linked to the power of the reference interval.

This issue was studied in a recent experiment by Doppelmayr et al. [35]. For all of the three alpha bands, the results clearly indicate that large band power in the reference interval is associated with a large amount of desynchronization (alpha suppression) during task performance. Most interestingly, the opposite holds true for the theta band. Here, small reference power is related to a large amount of synchronization or increase in power. Thus, the extent of alpha desynchronization and theta synchroniza-

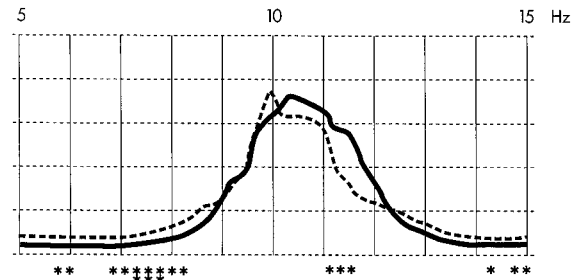


Fig. 12. Normalized percent power for good (bold line) and bad memory performers (dotted line) during memorizing words at O1 [84]. The ongoing EEG was analysed for 4 min and arbitrarily segmented in epochs of 4 s in order to achieve a frequency resolution of 0.25 Hz. Significant results (of *t*-tests between good and bad memory performers) are marked by one asterisk (for the 5%-level) or two vertically arranged asterisks (for the 1%-level). Good memory performers show significantly more upper alpha but less theta power. Similar results were found for all recording sites and even during resting sessions with eyes open and closed.

tion depend on the magnitude of absolute band power, but in opposite ways. With respect to the broad alpha band (7–14 Hz), similar findings were reported by Salenius et al. [132]. The interesting conclusion, thus, is that the reactivity in band power which reflects task performance can be predicted from the amount of absolute power as measured during a resting state.

With respect to the relationship between memory performance and absolute power, the reported findings allow us to make an important prediction. We would expect that good as compared to bad memory performers show significantly more power in the upper alpha but less power in the theta band. This result would be expected even when the EEG is measured during a resting phase. This hypothesis was clearly supported by two recent studies [161,84], as the example shown in Fig. 12 indicates. Similar findings were reported by Jausovec [61]. He found that highly intelligent subjects have significantly more absolute power in the broad alpha frequency range (7.5–13 Hz) than less intelligent subjects.

5. General conclusions and physiological considerations

The most important conclusion is that the amount of EEG power in the theta and alpha frequency range is indeed related to cognitive and memory performance in particular, if a double dissociation between absolute and event-related changes in alpha and theta power is taken

Fig. 11. ERD during the encoding phase of an incidental memory task, where subjects did not know in advance that a recall test will be carried out later. Data represent the time period of 1000 ms poststimulus after presentation onset of a word during encoding and are averaged over all recording sites. (A) Those words that can be remembered in a later recall task show a significantly larger task related increase in theta power (negative ERD values) during encoding as compared to words that cannot be remembered later. The respective differences in the three alpha bands are not significant. (B) In the theta band not only (negative) ERD (reflecting the percentage of an increase in power with respect to a reference interval) but also absolute power too is significantly larger for remembered words but only if frequency bands are adjusted individually (as for the ERD analysis) to IAF (cf. Fig. 1). (C) If instead fixed frequency windows are used, no significant differences can be observed. Data from Klimesch et al. [76].

into account. This double dissociation is characterized by the fact that during a resting state

- (i) small theta power but large alpha power (particularly in the frequency range of the upper alpha band) indicates good performance, whereas the opposite holds true for event-related changes, where
- (ii) a large increase in theta power (synchronization) but a large decrease in alpha power (desynchronization) reflect good cognitive and memory performance in particular.

A comparison with findings about the hippocampal theta rhythm in animals reveals that in response to increasing encoding demands, hippocampal theta synchronizes in a small frequency window, just as the human theta (scalp) EEG does (for an extensive review of this issue see Ref. [67]). Theta synchronization is due to an increase in the duration of multi-unit population bursts and to an increase in rhythmicity of these bursts which have the same frequency as theta. Convincing evidence for the hypothesis that theta synchronization is related to the encoding of new information comes from the fact that LTP is closely linked to the synchronous activity of the hippocampal theta rhythm:

- LTP can be best induced with stimulation patterns that mimic theta rhythm [92].
- LTP has been demonstrated in several brain regions, but it is most robust and, thus, has been studied most extensively in the hippocampus (c.f. Ref. [100]).
- The induction of LTP occurs primarily during the positive phase of the theta rhythm [119].
- The strength of the induced LTP increases linearly with increasing theta power ([100] c.f. Fig. 6 on p. 50).
- Pharmacological manipulations demonstrate that drugs which decrease theta activity also block learning [48], whereas drugs that promote the theta rhythm (and, thus, enhance the induction of LTP) also facilitate learning [142,143].

These findings support the view that hippocampal theta is important for the induction of LTP and is related to the encoding of new information in a similar way as LTP is. Consequently, we may assume that our results (e.g., Refs. [75,77,80,81] which suggest a close relationship between theta synchronization and the encoding of new information reflect theta activity that is induced into the cortex via cortico-hippocampal feedback loops (cf. Ref. [107] for a comprehensive review on this topic). Further evidence for this interpretation comes from an interesting study by Gevins et al. [46], who used a new method to spatially sharpen the EEG with magnetic resonance imaging-based finite element deblurring. These authors found a frontal midline theta rhythm which increased with increasing memory load. Most interestingly, dipole models localized this signal to the region of the anterior cingulate cortex which is part of the Papez circuit and, thus, is linked with the hippocampal formation via complex feedback or ‘reentrant’ loops.

It should be noted that there are two different types of theta synchronization. One type of synchronization is related to an increase in power within a narrow frequency band in the range of peak theta frequency. The second form of theta synchronization refers to irregular slow activity (ISA) which also is termed large irregular activity (LIA). Irregular slow activity dominates during slow wave sleep (SWS) and shows increased power outside the theta peak range (cf. Ref. [93]). This type of synchronization is not related to the increased power of a dominant rhythm within a narrow frequency band, but rather to an increase in power over a broad range. It may be explained in terms of irregular oscillatory epochs of the type Buzsaki et al. [19] have described. These irregular oscillatory epochs which occur over a comparatively broad frequency range are not coupled to the ‘coordinating’ force of the theta rhythm and are not related to the encoding of new information. It appears plausible to assume that the broad band increase in theta power reflects a state in which the ability to encode new information is reduced or even blocked (e.g., during the hypnagogic state, in SWS or in demented subjects) whereas the narrow band synchronization during regular rhythmic theta activity reflects event-related theta synchronization that is closely linked to the encoding of new information (or ‘recoding’ during REM).

In contrast to theta, the physiological mechanisms underlying alpha desynchronization appear more complex and at the first glance even paradoxical. Whereas alpha synchronization occurs during alert wakefulness, desynchronization reflects actual cognitive information processes. Alpha synchronization is a state in which millions of cortical neurons oscillate synchronously with the same phase and within a comparatively narrow frequency band. Desynchronization seems to imply that different oscillators within the alpha band are no longer coupled and start to oscillate with different frequencies. These different oscillators most likely reflect the synchronous activity of more local cortical or thalamocortical networks [97] and are, thus, termed ‘local’ or ‘functional’ alphas [7,8,114,115]. For each of the local alphas all neurons may still show a regular pattern of synchronous oscillation.

This basic EEG-phenomenon of large scale alpha synchronization (during mental inactivity) and desynchronization (during mental activity) which probably reflects a complex pattern of micro scale synchronization provides us with a preliminary but nonetheless important understanding of how information may be processed in the brain: Large scale alpha synchronization blocks information processing because very large populations of neurons oscillate with the same phase and frequency. In contrast, alpha desynchronization reflects actual cognitive processes because different neuronal networks start to oscillate at different frequencies and with different phases.

Research focusing on gamma oscillations in the visual cortex have shown that synchronous oscillatory discharge patterns reflect an elementary visual encoding process

(e.g., Ref. [49]). These results, obtained with microelectrodes, are a good example of a microscale synchronization. With respect to the human scalp EEG, it is a matter of resolution, whether or not we may speak of synchronization or desynchronization. Even if the EEG desynchronizes, a large number of different networks may still show synchronous oscillations on a microscale level. In order to discriminate between these two different types of synchronization, the synchronous activity of large cortical areas reflecting mental inactivity is termed type 1 synchronization, whereas the regular synchronous oscillatory discharge pattern of selected and comparatively small cortical areas is termed type 2 synchronization [67]. Type 1 synchronization, reflecting the summed activity of a large number of cell assemblies is a strong signal that can easily be recorded by macroelectrodes from the scalp. In contrast, the synchronous discharge of a small number of cell assemblies is a rather weak signal for the human scalp EEG. Thus, the behavior of the alpha rhythm can be explained by type 1 synchronization reflecting mental inactivity and type 2 synchronization reflecting mental activity. The behavior of the theta rhythm, on the other hand, can be described by type 2 regular synchronization (reflecting mental activity) and by type 1 irregular synchronization (reflecting mental inactivity). The general conclusion, thus, is that regular type 2 synchronization is that oscillatory mode in all of the frequency bands that reflects actual information processing in the brain.

In an attempt to integrate results from memory research in divergent fields such as cognitive psychology, neuroanatomy and neurophysiology, Klimesch [67] has suggested that type 2 synchronization, generated by thalamo-cortical and cortico-cortical feedback loops (cf. Refs. [144,97,91]) provides an ideal framework for describing spreading activation processes in semantic long-term memory. Thus, it may be assumed that type 2 synchronization as measured by (upper) alpha desynchronization reflects search and retrieval processes in semantic long-term memory which are induced into the cortex by thalamo-cortical feedback loops. For the theta band it is suggested that hippocampo-cortical pathways induce synchronous oscillations within a narrow frequency window of the theta peak into widely distributed assemblies in the cortex, thereby binding different parts of cell assemblies together. This binding process forms the basis for encoding new information (for similar conceptions, see also Refs. [107,94]). This interpretation also implies that cognitive performance is closely linked to type 2 synchronization in thalamo- and hippocampo-cortical networks.

Acknowledgements

This research was support by the Austrian Science Fund, P-11569 and P-13047.

References

- [1] C.E.D. Alloway, R.D. Ogilvie, C. Shapiro, The alpha attenuation test: assessing excessive daytime sleepiness in narcolepsy-cataplexy, *American Sleep Disorders and Sleep Research Society* 20 (1997) 258–266.
- [2] A. Anokhin, F. Vogel, EEG alpha rhythm frequency and intelligence in normal adults, *Intelligence* 23 (1996) 1–14.
- [3] A. Baddeley, Neuropsychological evidence and the semantic/episodic distinction (Commentary to Tulving), *The Behav. Brain Sci.* 7 (1984) 238–239.
- [4] A. Baddeley, Working memory, *Science* 255 (1992) 556–559.
- [5] E. Basar, Towards a renaissance of ‘alphas’, *Int. J. Psychophysiol.* 26 (1997) 1–3.
- [6] E. Basar, T.H. Bullock (Eds.), *Induced Rhythms in the Brain*, Birkhäuser, Boston, 1992.
- [7] E. Basar, R. Hari, F.H. Lopes da Silva, M. Schürmann, Brain alpha activity—new aspects and functional correlates, *Int. J. Psychophysiol.* 26 (1997) 1–482.
- [8] E. Basar, M. Schürmann, Functional correlates of alphas: panel discussion of the conference ‘Alpha Processes in the Brain’, *Int. J. Psychophysiol.* 26 (1997) 455–474.
- [9] E. Basar, M. Schürmann, C. Basar-Eroglu, S. Karakas, Alpha oscillations in brain functioning: an integrative theory, *Int. J. Psychophysiol.* 26 (1997) 5–29.
- [10] H. Berger, Über das Elektroenkephalogramm des Menschen, *Arch. Psychiat. Nervenkr.* 87 (1929) 527–570.
- [11] C. Besthorn, R. Zerfass, C. Geiger-Kabisch, H. Sattel, S. Daniel, U. Schreiter-Gasser, H. Förstl, Discrimination of Alzheimer’s disease and normal aging by EEG data, *Electroencephalogr. Clin. Neurophysiol.* 103 (1997) 241–248.
- [12] E.D. Bigler, S.C. Johnson, C. Jackson, D.D. Blatter, Aging, brain size, and IQ, *Intelligence* 21 (1995) 109–119.
- [13] N. Birbaumer, The EEG of congenitally blind adults, *Electroencephalogr. Clin. Neurophysiol.* 29 (1970) 318.
- [14] F. Boiten, J. Sergeant, R. Geuze, Event-related desynchronization: the effects of energetic and computational demands, *Electroencephalogr. Clin. Neurophysiol.* 82 (1992) 302–309.
- [15] A.A. Borbély, F. Baumann, D. Brandeis, I. Strauch, D. Lehmann, Sleep deprivation: effect on sleep stages and EEG Power density in man, *Electroencephalogr. Clin. Neurophysiol.* 51 (1981) 483–493.
- [16] R.P. Brenner, R.F. Ulrich, D.G. Spiker, R.J. Scalbassi, C.F. Reynolds III, R.S. Marin, F. Boller, Computerized EEG spectral analysis in elderly normal, demented and depressed subjects, *Electroencephalogr. Clin. Neurophysiol.* 64 (1986) 483–492.
- [17] J. Breslau, A. Starr, N. Sciotte, J. Higa, M.S. Buchsbaum, Topographic EEG changes with normal aging and SDAT, *Electroencephalogr. Clin. Neurophysiol.* 72 (1989) 281–289.
- [18] A. Burgess, J.H. Gruzeliier, Short duration synchronization of human theta rhythm during recognition memory, *NeuroReport* 8 (1997) 1039–1042.
- [19] G. Buzsáki, Z. Horvath, R. Urioste, J. Hetke, K. Wise, High-frequency network oscillation in the hippocampus, *Science* 256 (1992) 1025–1027.
- [20] G. Buzsáki, A. Bragin, J.J. Chrobak, Z. Nadasdy, A. Sik, M. Hsu, A. Ylinen, Oscillatory and intermittent synchrony in the hippocampus: relevance to memory trace formation, in: G. Buzsáki, R.R. Llinás, W. Singer, A. Berthoz, Y. Christen (Eds.), *Temporal Coding in the Brain*, Springer, Berlin, 1994, pp. 145–172.
- [21] R.F. Byring, T.K. Salmi, K.O. Sainio, H.P. Orn, EEG in children with spelling disabilities, *Electroencephalogr. Clin. Neurophysiol.* 79 (1991) 247–255.
- [22] C. Cajochen, D.P. Brunner, K. Kräuchi, P. Graw, A. Wirz-Justice, Power density in theta/alpha frequencies of the waking EEG progressively increases during sustained wakefulness, *Sleep* 18 (1995) 890–894.
- [23] C. Cajochen, K. Kräuchi, M.-A. von Arx, D. Möri, P. Graw, A.

- Wirz-Justice, Daytime melatonin administration enhances sleepiness and theta/alpha activity in the waking EEG, *Neurosci. Lett.* 207 (1996) 209–213.
- [24] R. Chiaramonti, G.C. Muscas, M. Paganini, T.J. Müller, A.J. Fallgatter, A. Versari, W.K. Strik, Correlations of topographical EEG features with clinical severity in mild and moderate dementia of Alzheimer type, *Neuropsychobiology* 36 (1997) 153–158.
- [25] C. Chong-Hwa Hong, Y. Jin, S.G. Potkin, M.S. Buchsbaum, J. Wu, G.M. Callaghan, K.L. Nudleman, C. Gillin, Dreams and alpha power: language in dreaming and regional EEG alpha power, *Sleep* 19 (1996) 232–235.
- [26] W. Christian, Das Elektroencephalogramm (EEG) im höheren Lebensalter, *Nervenarzt* 55 (1984) 517–524.
- [27] L.A. Coben, W. Danziger, M. Storandt, A longitudinal EEG study of mild senile dementia of Alzheimer type: changes at 1 year and at 2, 5 years, *Electroencephalogr. Clin. Neurophysiol.* 61 (1985) 101–112.
- [28] R. Conduit, D. Bruck, G. Coleman, Induction of visual imagery during NREM sleep, *Sleep* 20 (1997) 948–956.
- [29] M. Corsi-Cabrera, J. Ramos, C. Arce, M.A. Guevara, M. Ponce-de León, I. Lorenzo, Changes in the waking EEG as a consequence of sleep and sleep deprivation, *Sleep* 15 (1994) 550–555.
- [30] H. Crawford, T. Knebel, J. Vendemia, L. Kaplan, B. Ratcliff, EEG activation patterns during tracking and decision-making tasks: differences between low and high sustained attention. Paper presented at the 8th International Symposium on Aviation Psychology, Columbus, Ohio, April 24–27, 1995.
- [31] R.S. Daniel, Alpha and theta EEG in vigilance, *Percept. Motor Skills* 25 (1967) 697–703.
- [32] W. Dement, N. Kleitman, Cyclic variations in EEG during sleep and their relation to eye movements, body motility, and dreaming, *Electroencephalogr. Clin. Neurophysiol.* 9 (1957) 673–690.
- [33] D.J. Dijk, D.P. Brunner, D.G.M. Beersma, A.A. Borbély, Electroencephalogram power density and slow wave sleep as a function of prior waking and circadian phase, *Sleep* 13 (1990) 430–440.
- [34] M. Doppelmayr, W. Klimesch, T. Pachinger, B. Ripper, Individual differences in brain dynamics: important implications for the calculation of event-related band power measures, *Biol. Cybern.*, 1998 (in press).
- [35] M. Doppelmayr, W. Klimesch, T. Pachinger, B. Ripper, The functional significance of absolute power with respect to event-related desynchronization, *Brain Topogr.*, 1998 (in press).
- [36] F.H. Duffy, M.S. Albert, G. McNulty, A.J. Garvey, Age-related differences in brain electrical activity of healthy subjects, *Ann. Neurol.* 16 (1984) 430–438.
- [37] G.E. Edelman, *Neural Darwinism*, Oxford University Press, Oxford, 1989.
- [38] H.T. Epstein, EEG developmental stages, *Develop. Psychol.* 13 (1980) 629–631.
- [39] V.A. Feshchenko, The way to EEG-classification: transition from language of patterns to language of systems, *Int. J. Neurosci.* 79 (1994) 235–249.
- [40] V.A. Feshchenko, R.A. Veselis, R.A. Reinsel, Comparison of the EEG effects of midazolam, thiopental, and propofol: the role of underlying oscillatory systems, *Neuropsychobiology* 35 (1997) 211–220.
- [41] P.W. Fuller, Attention and the EEG alpha rhythm in learning disabled children, *J. Learn. Disab.* 11 (1978) 303–312.
- [42] T. Gasser, C. Jennen-Steinmetz, L. Sroka, R. Verleger, J. Möcks, Development of the EEG of school-age children and adolescents: II. Topography, *Electroencephalogr. Clin. Neurophysiol.* 69 (1988) 100–109.
- [43] T. Gasser, R. Verleger, P. Bächer, L. Sroka, Development of EEG of school-age children and adolescents: I. Analysis of band power, *Electroencephalogr. Clin. Neurophysiol.* 69 (1988) 91–99.
- [44] A.S. Gevins, G.M. Zeitlin, J.C. Doyle, C.D. Yingling, R.E. Schaffer, E. Callaway, C. Yeager, Electroencephalogram correlates of higher cortical functions, *Science* 203 (1979) 665–668.
- [45] A. Gevins, M.E. Smith, L. McEvoy, D. Yu, High-resolution EEG mapping of cortical activation related to working memory: effects of task difficulty, type of processing, and practice, *Cerebral Cortex* 7 (1997) 374–385.
- [46] A. Gevins, M.E. Smith, H. Leong, L. McEvoy, S. Whitfield, R. Du, G. Rush, Monitoring working memory load during computer-based tasks with EEG pattern recognition methods, *Human Factors* 40 (1998) 79–91.
- [47] B. Givens, Stimulus-evoked resetting of the dentate theta rhythm: relation to working memory, *NeuroReport* 8 (1996) 159–163.
- [48] B. Givens, D. Olton, Bidirectional modulation of scopolamine-induced working memory impairments by muscarinic activation of the medial septal area, *Neurobiol. Learn. Mem.* 63 (1995) 269–276.
- [49] C. Gray, W. Singer, Stimulus-dependent neuronal oscillations in the cat visual cortex area 17, *Neurosci. Suppl.* 22 (1987) 434.
- [50] K. Hadjiyannakis, R.D. Ogilvie, C.E.D. Alloway, C. Shapiro, FFT analysis of EEG during stage 2-to-REM transitions in narcoleptic patients and normal sleepers, *Electroencephalogr. Clin. Neurophysiol.* 103 (1997) 543–553.
- [51] R. Hari, Magnetoencephalography as a tool of clinical neurophysiology, in: E. Niedermeyer, F.H. Lopes da Silva (Eds.), *Electroencephalography: Basic Principles, Clinical Applications, and Related Fields*, Williams and Wilkins, Baltimore, 1993, pp. 1035–1061.
- [52] R. Hari, R. Salmelin, J.P. Mäkelä, S. Salenius, M. Helle, Magnetoencephalographic cortical rhythms, *Int. J. Psychophysiol.* 26 (1997) 51–62.
- [53] T. Harmony, G. Hinojosa, E. Marosi, J. Becker, M. Rodríguez, A. Reyes, C. Rocha, Correlation between EEG spectral parameters and an educational evaluation, *Int. J. Neurosci.* 54 (1990) 147–155.
- [54] T. Harmony, E. Marosi, J. Becker, M. Rodríguez, A. Reyes, T. Fernández, J. Silva, J. Bernal, Longitudinal quantitative EEG study of children with different performances on a reading–writing test, *Electroencephalogr. Clin. Neurophysiol.* 95 (1995) 426–433.
- [55] P. Hartikainen, H. Soininen, J. Partanen, E.L. Helkala, P. Riekkinen, Aging and spectral analysis of EEG in normal subjects: a link to memory and CSF AChE, *Acta Neurol. Scand.* 86 (1992) 148–150.
- [56] T. Hori, M. Hayashi, T. Morikawa, Changes of EEG patterns and reaction time during hypnagogic state, *Sleep Res.* 20 (1991) 20.
- [57] M.L. Howe, M.L. Courage, The emergence and early development of autobiographical memory, *Psychol. Rev.* 104 (1997) 499–523.
- [58] O. Hubbard, D. Sunde, E.S. Goldensohn, The EEG in centenarians, *Electroencephalogr. Clin. Neurophysiol.* 40 (1976) 407–417.
- [59] W.J. Hudspeeth, K.H. Pribram, Stages of brain and cognitive maturation, *J. Educ. Psychol.* 82 (1990) 881–884.
- [60] J.R. Hughes, Normal limits of the EEG, in: R.M. Halliday, S.R. Butler, R. Paul (Eds.), *A Textbook of Clinical Neurophysiology*, Wiley, New York, 1987, pp. 105–154.
- [61] N. Jausovec, Differences in EEG alpha activity related to giftedness, *Intelligence* 23 (1996) 159–173.
- [62] E.R. John, H. Ahn, L. Prichep, M. Trepetin, D. Brown, H. Kaye, Developmental equations for the EEG, *Science* 210 (1980) 1255–1258.
- [63] E.R. John, L. Prichep, H. Ahn, P. Easton, J. Fridman, H. Kaye, Neurometric evaluation of cognitive dysfunctions and neurological disorders in children, *Progr. Neurobiol.* 21 (1983) 239–290.
- [64] E.R. John, L. Prichep, Principles of neurometric analysis of EEG and evoked potentials, in: E. Niedermeyer, F.H. Lopes da Silva (Eds.), *Electroencephalography: Basic Principles, Clinical Applications, and Related Fields*, Williams and Wilkins, Baltimore, 1993, pp. 989–1004.
- [65] L. Kaufman, S. Curtis, J.-Z. Wang, S.J. Williamson, Changes in cortical activity when subjects scan memory for tones, *Electroencephalogr. Clin. Neurophysiol.* 82 (1992) 266–284.

- [66] W. Klimesch, The Structure of Long-term Memory: A Connectivity Model for Semantic Processing, Lawrence Erlbaum, Hillsdale, NJ, 1994.
- [67] W. Klimesch, Memory processes, brain oscillations and EEG synchronization, *Int. J. Psychophysiol.* 24 (1996) 61–100.
- [68] W. Klimesch, EEG-alpha rhythms and memory processes, *Int. J. Psychophysiol.* 26 (1997) 319–340.
- [69] W. Klimesch, G. Pfurtscheller, W. Mohl, H. Schimke, Event-related desynchronization, ERD-mapping and hemispheric differences for words and numbers, *Int. J. Psychophysiol.* 8 (1990) 297–308.
- [70] W. Klimesch, H. Schimke, G. Pfurtscheller, The topography of alpha frequency and memory performance, *J. Psychophysiol.* 4 (1990) 191–192.
- [71] W. Klimesch, H. Schimke, G. Ladurner, G. Pfurtscheller, Alpha frequency and memory performance, *J. Psychophysiol.* 4 (1990) 381–390.
- [72] W. Klimesch, G. Pfurtscheller, H. Schimke, Pre- and poststimulus processes in category judgement tasks as measured by event-related desynchronization (ERD), *J. Psychophysiol.* 6 (1992) 186–203.
- [73] W. Klimesch, H. Schimke, G. Pfurtscheller, Alpha frequency, cognitive load, and memory performance, *Brain Topogr.* 5 (1993) 241–251.
- [74] W. Klimesch, G. Pfurtscheller, H. Schimke, ERD—attentional and cognitive processes in the upper and lower alpha band, *Electroencephalogr. Clin. Neurophysiol.* 87 (1993) 133.
- [75] W. Klimesch, H. Schimke, J. Schwaiger, Episodic and semantic memory: an analysis in the EEG-theta and alpha band, *Electroencephalogr. Clin. Neurophysiol.* 91 (1994) 428–441.
- [76] W. Klimesch, M. Doppelmayr, H. Russegger, T. Pachinger, Theta band power in the human scalp EEG and the encoding of new information, *NeuroReport* 7 (1996) 1235–1240.
- [77] W. Klimesch, M. Doppelmayr, H. Schimke, T. Pachinger, Alpha frequency, reaction time and the speed of processing information, *J. Clin. Neurophysiol.* 13 (1996) 511–518.
- [78] W. Klimesch, H. Schimke, M. Doppelmayr, B. Ripper, J. Schwaiger, G. Pfurtscheller, Event-related desynchronization (ERD) and the Dm-effect: Does alpha desynchronization during encoding predict later recall performance, *Int. J. Psychophysiol.* 24 (1996) 47–60.
- [79] W. Klimesch, M. Doppelmayr, T. Pachinger, B. Ripper, Brain oscillations and human memory performance: EEG correlates in the upper alpha and theta bands, *Neurosci. Lett.* 238 (1997) 9–12.
- [80] W. Klimesch, M. Doppelmayr, T. Pachinger, H. Russegger, Event-related desynchronization in the alpha band and the processing of semantic information, *Cogn. Brain Res.* 6 (1997) 83–94.
- [81] W. Klimesch, M. Doppelmayr, H. Schimke, B. Ripper, Theta synchronization in a memory task, *Psychophysiology* 34 (1997) 169–176.
- [82] W. Klimesch, M. Doppelmayr, H. Russegger, T. Pachinger, J. Schwaiger, Induced alpha band power changes in the human EEG and attention, *Neurosci. Lett.* 244 (1998) 73–76.
- [83] W. Klimesch, H. Russegger, M. Doppelmayr, T. Pachinger, Induced and evoked band power changes in an oddball task, *Electroencephalogr. Clin. Neurophysiol.* 108 (1998) 123–130.
- [84] W. Klimesch, F. Vogt, M. Doppelmayr, Interindividual differences in alpha and theta power reflect memory performance, *Intelligence*, 1998 (in press).
- [85] R.T. Knight, Contribution of human hippocampal region to novelty detection, *Nature* 383 (1996) 256–259.
- [86] R.T. Knight, D. Scabini, Anatomic bases of event-related potentials and their relationship to novelty detection in humans, *J. Clin. Neurophysiol.* 15 (1998) 3–13.
- [87] M. Könönen, J.V. Partanen, Blocking of EEG alpha activity during visual performance in healthy adults. A quantitative study, *Electroencephalogr. Clin. Neurophysiol.* 87 (1993) 164–166.
- [88] V. Köpruner, G. Pfurtscheller, L.M. Auer, Quantitative EEG in normals and in patients with cerebral ischemia, in: G. Pfurtscheller, E.J. Jonkman, F.H. Lopes da Silva (Eds.), *Brain Ischemia: Quantitative EEG and Imaging Techniques*, Progress in Brain Research, Vol. 62, Elsevier Science Publishers, 1984, pp. 29–50.
- [89] C.M. Krause, H.A. Lang, M. Laine, M.J. Kuusisto, B. Pörn, Cortical processing of vowels and tones as measured by event-related desynchronization, *Brain Topography* 8 (1995) 47–56.
- [90] C.M. Krause, H.A. Lang, M. Laine, M.J. Kuusisto, B. Pörn, Event-related EEG desynchronization and synchronization during an auditory memory task, *Electroencephalogr. Clin. Neurophysiol.* 98 (1996) 319–326.
- [91] C.L. Larson, R.J. Davidson, H.C. Abercrombie, R.T. Ward, S.M. Schaefer, D.C. Jackson, J.E. Holden, S.B. Perlman, Relations between PET-derived measures of thalamic glucose metabolism and EEG alpha power, *Psychophysiology* 35 (1998) 162–169.
- [92] J. Larson, D. Wong, G. Lynch, Patterned stimulation at the theta frequency is optimal for the induction of hippocampal long-term potentiation, *Brain Res.* 368 (1986) 347–350.
- [93] L.W.S. Leung, F.H. Lopes da Silva, W.J. Wadman, Spectral characteristics of the hippocampal EEG in the freely moving rat, *Electroencephalogr. Clin. Neurophysiol.* 54 (1982) 203–219.
- [94] J.E. Lisman, M.A.P. Idiart, Storage of 7 + –2 short-term memories in oscillatory subcycles, *Science* 267 (1995) 1512–1515.
- [95] F.H. Lopes da Silva, The rhythmic slow activity (theta) of the limbic cortex: an oscillation in search of a function, in: E. Basar, T.H. Bullock (Eds.), *Induced Rhythms in the Brain*, Birkhäuser, Boston, 1992, pp. 83–102.
- [96] F.H. Lopes da Silva, Computer-assisted EEG diagnosis: Pattern recognition and brain mapping, in: E. Niedermeyer, F.H. Lopes da Silva (Eds.), *Electroencephalography: Basic Principles, Clinical Applications, and Related Fields*, Williams and Wilkins, Baltimore, 1993, pp. 1063–1086.
- [97] F.H. Lopes da Silva, T.H.M.T. Van Lierop, C.F. Schrijer, W. Storm van Leeuwen, Organization of thalamic and cortical alpha rhythms: spectra and coherences, *Electroencephalogr. Clin. Neurophysiol.* 35 (1973) 626–639.
- [98] G.R. Mangun, Neural mechanisms of visual selective attention, *Psychophysiology* 32 (1995) 4–18.
- [99] M.G. Marciari, M. Maschio, F. Spanedda, C. Caltagirone, G.L. Gigli, G. Bernardi, Quantitative EEG evaluation in normal elderly subjects during mental processes: age-related changes, *Int. J. Neurosci.* 76 (1994) 131–140.
- [100] S. Maren, J.P. DeCola, R.A. Swain, M.S. Fanselow, R.F. Thompson, Parallel augmentation of hippocampal long-term potentiation, theta rhythm, and contextual fear conditioning in water-deprived rats, *Behav. Neurosci.* 108 (1994) 44–56.
- [101] O.N. Markand, Alpha rhythms, *J. Clin. Neurophysiol.* 7 (1990) 163–189.
- [102] H.J. Markowitsch, M. Pritzel, The neuropathology of amnesia, *Progr. Neurobiol.* 25 (1985) 189–288.
- [103] P. Marthis, D.M. Scheffner, C. Benninger, C. Lipinski, L. Stolzis, Changes in the background activity of the electroencephalogram according to age, *Electroencephalogr. Clin. Neurophysiol.* 49 (1980) 626–635.
- [104] A. Martin, C.L. Wiggs, L.G. Ungerleider, J.V. Haxby, Neural correlates of category-specific knowledge, *Nature* 379 (1996) 649–652.
- [105] M. Matousek, I. Petersen, Automatic evaluation of EEG background activity by means of age-dependent quotients, *Electroencephalogr. Clin. Neurophysiol.* 35 (1973) 603–612.
- [106] A. Mecklinger, A.F. Kramer, D.L. Strayer, Event related potentials and EEG components in a semantic memory search task, *Psychophysiology* 29 (1992) 104–119.
- [107] R. Miller, *Cortico-Hippocampal Interplay and the Representation of Contexts in the Brain*, Springer, Berlin, 1991.
- [108] T. Mulholland, The concept of attention and the electroencephalographic alpha rhythm, in: C.R. Evans, T.B. Mulholland (Eds.),

- Attention in Neurophysiology: An International Conference, Butterworths, London, 1969, pp. 100–127.
- [109] C.A. Nelson, The ontogeny of human memory: a cognitive neuroscience perspective, *Dev. Psychol.* 31 (1995) 723–738.
- [110] E. Niedermeyer, The normal EEG of the waking adult, in: E. Niedermeyer, F.H. Lopes da Silva (Eds.), *Electroencephalography: Basic Principles, Clinical Applications, and Related Fields*, Williams and Wilkins, Baltimore, 1993, pp. 131–1520.
- [111] E. Niedermeyer, Normal aging and transient cognitive disorders in the elderly, in: E. Niedermeyer, F.H. Lopes da Silva (Eds.), *Electroencephalography: Basic Principles, Clinical Applications, and Related Fields*, Williams and Wilkins, Baltimore, 1993, pp. 329–338.
- [112] E. Niedermeyer, Maturation of the EEG: development of waking and sleep patterns, in: E. Niedermeyer, F.H. Lopes da Silva (Eds.), *Electroencephalography: Basic Principles, Clinical Applications, and Related Fields*, Williams and Wilkins, Baltimore, 1993, pp. 167–191.
- [113] J.L. Noebels, W.T. Roth, B.S. Kopell, Cortical slow potentials and the occipital EEG in congenital blindness, *J. Neurol. Sci.* 37 (1978) 51–58.
- [114] P.L. Nunez, Toward a physics of neocortex, in: P.L. Nunez (Ed.), *Neocortical Dynamics and Human EEG Rhythms*, Oxford University Press, New York, Oxford, 1995, pp. 68–132, P.L.
- [115] Nunez, L. Reid, R.G. Bickford, The relationship of head size to alpha frequency with implications to a brain wave model, *Electroencephalogr. Clin. Neurophysiol.* 44 (1978) 344–352.
- [116] W.D. Obrist, The electroencephalogram of normal aged adults, *Electroencephalogr. Clin. Neurophysiol.* 6 (1954) 235–244.
- [117] W.D. Obrist, L. Sokoloff, N.A. Lassen, M.H. Lane, R.N. Butler, I. Feinberg, Relation of EEG to cerebral blood flow and metabolism in old age, *Electroencephalogr. Clin. Neurophysiol.* 15 (1963) 610–619.
- [118] R.D. Ogilvie, I.A. Simons, R.H. Kuderian, T. MacDonald, J. Rustenburg, Behavioral, event-related potential, and EEG/FFT changes at sleep onset, *Psychophysiology* 28 (1991) 54–64.
- [119] C. Pavlides, Y.J. Greenstein, M. Grudman, J. Winson, Long-term potentiation in the dentate gyrus is induced preferentially on the positive phase of theta rhythm, *Brain Res.* 439 (1988) 383–387.
- [120] S.E. Petersen, P.T. Fox, M.I. Posner, M. Mintun, M.E. Raichle, Positron emission tomographic studies of the cortical anatomy of single-word processing, *Nature* 331 (1988) 585–589.
- [121] H. Petsche, S. Kaplan, A. von Stein, O. Filz, The possible meaning of the upper and lower alpha frequency ranges for cognitive and creative tasks, *Int. J. Psychophysiol.* 26 (1997) .
- [122] G. Pfurtscheller, Event-related synchronization (ERS): an electrophysiological correlate of cortical areas at rest, *Electroencephalogr. Clin. Neurophysiol.* 83 (1992) 62–69.
- [123] G. Pfurtscheller, A. Aranibar, Event-related cortical desynchronization detected by power measurement of scalp EEG, *Electroencephalogr. Clin. Neurophysiol.* 42 (1977) 817–826.
- [124] G. Pfurtscheller, A. Stancak Jr., C. Neuper, Event-related synchronization (ERS) in the alpha band—an electrophysiological correlate of cortical idling: a review, *Int. J. Psychophysiol.* 24 (1996) 39–46.
- [125] G. Pfurtscheller, C. Neuper, C. Andrew, G. Edlinger, Foot and hand area mu rhythms, *Int. J. Psychophysiol.* 26 (1997) 121–135.
- [126] M.I. Posner, Psychobiology of attention, in: M.S. Gazzaniga, C. Blakemore (Eds.), *Handbook of Psychobiology*, Academic Press, New York, 1975, pp. 441–480.
- [127] M.I. Posner, Attention in cognitive neuroscience: an overview, in: M.S. Gazzaniga (Ed.), *The Cognitive Neurosciences*, Bradford, MIT Press, Cambridge, MA, 1995, pp. 615–624.
- [128] M.E. Raichle, The scratchpad of the mind, *Nature* 363 (1993) 583–584.
- [129] J. Ramos, M. Corsi-Cabrera, M.A. Guevara, C. Arce, EEG activity during cognitive performance in women, *Int. J. Neurosci.* 69 (1993) 185–195.
- [130] W.J. Ray, H.W. Cole, EEG alpha activity reflects attentional demands, and beta activity reflects emotional and cognitive processes, *Science* 228 (1985) 750–752.
- [131] M.D. Rugg, A.M. Dickens, Dissociation of alpha and theta activity as a function of verbal and visuo-spatial tasks, *Electroencephalogr. Clin. Neurophysiol.* 53 (1982) 201–207.
- [132] S. Salenius, M. Kajola, W.L. Thompson, S. Kosslyn, R. Hari, Reactivity of magnetic parieto-occipital alpha rhythm during visual imagery, *Electroencephalogr. Clin. Neurophysiol.* 95 (1995) 453–462.
- [133] D.L. Schacter, EEG theta waves and psychological phenomena: a review and analysis, *Biol. Psychol.* 5 (1977) 47–83.
- [134] R.G. Schmid, W.S. Tirsch, P. Reitmeir, Correlation of developmental neurological findings with spectral analytical EEG evaluations in pre-school age children, *Electroencephalogr. Clin. Neurophysiol.* 103 (1997) 516–527.
- [135] J.C. Shaw, Intention as component of the alpha-rhythm response to mental activity, *Int. J. Psychophysiol.* 24 (1996) 7–23.
- [136] P.H. Sheridan, S. Sato, N. Foster, G. Bruno, Relation of EEG alpha background to parietal lobe function in Alzheimer's disease as measured by positron emission tomography and psychometry, *Neurology* 38 (1988) 747–750.
- [137] R.M. Shiffrin, W.S. Geisler, Visual recognition in a theory of information processing, in: R.L. Solso (Ed.), *Contemporary Issues in Cognitive Psychology*, The Loyola Symposium, Washington, 1973, pp. 53–101.
- [138] E.P. Sloan, G.W. Fenton, N.S.J. Kennedy, J.M. MacLennan, Neurophysiology and SPECT cerebral blood flow patterns in dementia, *Electroencephalogr. Clin. Neurophysiol.* 91 (1994) 163–170.
- [139] R.J.M. Somsen, B.J. Van-Klooster, M.W. Van-der-Molen, H.M. Van-Leeuwen, Growth spurts in brain maturation during middle childhood as indexed by EEG power spectra, *Biol. Psychol.* 44 (1997) 187–209.
- [140] L.R. Squire, Memory and the hippocampus: a synthesis from findings with rats, monkeys, and humans, *Psychol. Rev.* 99 (1992) 195–231.
- [141] L.R. Squire, B. Knowlton, G. Musen, The structure and organization of memory, *Ann. Rev. Psychol.* 44 (1993) 453–495.
- [142] U. Stäubli, G. Rogers, G. Lynch, Facilitation of glutamate receptors enhances memory, *Proc. Natl. Acad. Sci. USA* 91 (1994) 777–781.
- [143] U. Stäubli, B.X. Fang, Effects of 5-Ht₃ receptor antagonism on hippocampal theta rhythm, memory, and LTP induction in the freely moving rat, *J. Neurosci.* 15 (1995) 2445–2452.
- [144] M. Steriade, E. Jones, R.R. Llinás, *Thalamic Oscillations and Signaling*, Wiley, New York, 1990.
- [145] M. Steriade, D.A. McCormick, T.J. Sejnowski, Thalamocortical oscillations in the sleeping and aroused brain, *Science* 262 (1993) 679–685.
- [146] M.B. Serman, D.A. Kaiser, B. Veigel, Spectral analysis of event-related EEG responses during short-term memory performance, *Brain Topogr.* 9 (1996) 21–30.
- [147] W. Surwillo, Frequency of the alpha rhythm, reaction time and age, *Nature* 191 (1961) 823–824.
- [148] W. Surwillo, The relation of simple response time to brain-wave frequency and the effects of age, *Electroencephalogr. Clin. Neurophysiol.* 15 (1963) 105–114.
- [149] W. Surwillo, The relation of response-time variability to age and the influence of brain wave frequency, *Electroencephalogr. Clin. Neurophysiol.* 15 (1963) 1029–1032.
- [150] W. Surwillo, Some observations of the relation of response speed to frequency of photic stimulation under conditions of EEG synchronization, *Electroencephalogr. Clin. Neurophysiol.* 17 (1964) 194–198.
- [151] W. Surwillo, The relation of decision time to brain wave frequency

- and to age, *Electroencephalogr. Clin. Neurophysiol.* 16 (1964) 510–514.
- [152] W. Surwillo, Human reaction time and period of the EEG in relation to development, *Psychophysiology* 8 (1971) 468–482.
- [153] B. Szekely, R. Mielke, K. Herholz, W.-D. Heiss, Quantitative topographical EEG compared to FDG PET for classification of vascular and degenerative dementia, *Electroencephalogr. Clin. Neurophysiol.* 91 (1994) 131–139.
- [154] H. Tanaka, M. Hayashi, T. Hori, Topographical characteristics and principal component structure of the hypnagogic EEG, *Sleep* 20 (1997) 523–534.
- [155] R.W. Thatcher, Cyclic cortical reorganization during early childhood, *Brain Cogn.* 20 (1992) 24–50.
- [156] F. Torres, A. Faoro, R. Löwensohn, E. Johnson, The electroencephalogram of elderly subjects revisited, *Electroencephalogr. Clin. Neurophysiol.* 56 (1983) 391–398.
- [157] L. Torsvall, T. Akerstedt, Sleepiness on the job: continuously measured EEG changes in train drivers, *Electroencephalogr. Clin. Neurophysiol.* 66 (1987) 502–512.
- [158] E. Tulving, Precise of elements of episodic memory, *Behav. Brain Sci.* 7 (1984) 223–268.
- [159] E. Tulving, S. Kapur, F.I.M. Craik, M. Moscovitch, S. Houle, Hemispheric encoding/retrieval asymmetry in episodic memory: positron emission tomography findings, *Proc. Natl. Acad. Sci. USA* 91 (1994) 2016–2020.
- [160] B. Van Sweden, A. Wauquier, E. Niedermeyer, Normal aging and transient cognitive disorders in the elderly, in: E. Niedermeyer, F.H. Lopes da Silva (Eds.), *Electroencephalography: Basic Principles, Clinical Applications, and Related Fields*, Williams and Wilkins, Baltimore, 1993, pp. 329–338.
- [161] F. Vogt, W. Klimesch, M. Doppelmayr, High frequency components in the alpha band and memory performance, *J. Clin. Neurophysiol.* 15 (1997) 167–172.
- [162] M. Wada, T. Ogawa, H. Sonoda, K. Sato, Development of relative power contribution ratio of the EEG in normal children: a multivariate autoregressive modeling approach, *Electroencephalogr. Clin. Neurophysiol.* 98 (1996) 69–75.
- [163] S. Weiss, P. Rappelsberger, EEG coherence within the 13–18 Hz band as a correlate of a distinct lexical organisation of concrete and abstract nouns in humans, *Neurosci. Lett.* 209 (1996) 17–20.
- [164] G.H. Wierneke, C.H.A. Deinema, P. Spoelstra, W. Storm van Leeuwen, H. Versteeg, Normative spectral data on the alpha rhythm in male adults, *Electroencephalogr. Clin. Neurophysiol.* 49 (1980) 636–645.
- [165] L. Willerman, R. Schultz, J.N. Rutledge, E.D. Bigler, In vivo brain size and intelligence, *Intelligence* 15 (1991) 223–228.
- [166] S.J. Williamson, L. Kaufman, S. Curtis, Z.-L. Lu, C.M. Michel, J.-Z. Wang, Neural substrates of working memories are revealed magnetically by the local suppression of alpha rhythm, in: I. Hashimoto, Y.C. Okada, S. Ogawa (Eds.), *Visualization of Information Processing in the Human Brain: Recent Advances in MEG and Functional MRI*, EEG suppl. 47, Elsevier, Amsterdam, 1996, pp. 163–180.
- [167] S.J. Williamson, L. Kaufman, Z.L. Lu, J.Z. Wang, D. Karon, Study of human occipital alpha rhythm: the alpha hypothesis and alpha suppression, *Int. J. Psychophysiol.* 26 (1997) 63–76.
- [168] D.L. Woods, S.J. Thomas, E.W. Yund, S. Han, Visual attention modulates rhythmic brain oscillations in humans, 1998 (submitted paper).
- [169] J.Y. Yordanova, V.N. Kolev, Developmental changes in the alpha response system, *Electroencephalogr. Clin. Neurophysiol.* 95 (1996) 1–12.

EXHIBIT 21



Modification of Brain Oscillations via Rhythmic Light Stimulation Provides Evidence for Entrainment but Not for Superposition of Event-Related Responses

Annika Notbohm¹, Jürgen Kurths² and Christoph S. Herrmann^{1,3*}

¹ Experimental Psychology Lab, Center for Excellence 'Hearing4all', European Medical School, University of Oldenburg, Oldenburg, Germany, ² Potsdam Institute for Climate Impact Research, Potsdam, Germany, ³ Research Center Neurosensory Science, University of Oldenburg, Oldenburg, Germany

OPEN ACCESS

Edited by:

Lutz Jäncke,
University of Zurich, Switzerland

Reviewed by:

Peter König,
University of Osnabrück, Germany
Jonas Obleser,
University of Lübeck, Germany

*Correspondence:

Christoph S. Herrmann
Christoph.herrmann@uni-oldenburg.de

Received: 15 October 2015

Accepted: 11 January 2016

Published: 03 February 2016

Citation:

Notbohm A, Kurths J and
Herrmann CS (2016) Modification of
Brain Oscillations via Rhythmic Light
Stimulation Provides Evidence for
Entrainment but Not for Superposition
of Event-Related Responses.
Front. Hum. Neurosci. 10:10.
doi: 10.3389/fnhum.2016.00010

The functional relevance of brain oscillations in the alpha frequency range (8–13 Hz) has been repeatedly investigated through the use of rhythmic visual stimulation. The underlying mechanism of the steady-state visual evoked potential (SSVEP) measured in EEG during rhythmic stimulation, however, is not known. There are two hypotheses on the origin of SSVEPs: entrainment of brain oscillations and superposition of event-related responses (ERPs). The entrainment but not the superposition hypothesis justifies rhythmic visual stimulation as a means to manipulate brain oscillations, because superposition assumes a linear summation of single responses, independent from ongoing brain oscillations. Here, we stimulated participants with a rhythmic flickering light of different frequencies and intensities. We measured entrainment by comparing the phase coupling of brain oscillations stimulated by rhythmic visual flicker with the oscillations induced by arrhythmic jittered stimulation, varying the time, stimulation frequency, and intensity conditions. In line with a theoretical concept of entrainment (the so called *Arnold tongue*), we found the phase coupling to be more pronounced with increasing stimulation intensity as well as at stimulation frequencies closer to each participant's intrinsic frequency. Only inside the Arnold tongue did the conditions significantly differ from the jittered stimulation. Furthermore, even in a single sequence of an SSVEP, we found non-linear features (intermittency of phase locking) that contradict the linear summation of single responses, as assumed by the superposition hypothesis. Our findings provide unequivocal evidence that visual rhythmic stimulation entrains brain oscillations, thus validating the approach of rhythmic stimulation as a manipulation of brain oscillations.

Keywords: alpha, visual flicker, individual alpha frequency, Arnold tongue, intermittency, parietal cortex, steady-state visually evoked potential (SSVEP), superposition

INTRODUCTION

A relationship between ongoing alpha amplitudes and perception has been a subject of investigation since Berger's findings in the late 1920s (Berger, 1929). He described an occipital alpha-amplitude decline after stimulation, which was later shown to reflect event-related desynchronization of the ongoing alpha rhythm (Pfurtscheller and Aranibar, 1977). Experimental data largely reveal this cortical state to represent an electrophysiological correlate of activation (Arieli et al., 1996; von Stein and Sarnthein, 2000), whereas an increased amplitude in the alpha range co-occurs with inhibited perception (Klimesch et al., 2007). Besides the amplitude, alpha phase angles were found to correlate with behavior (Hanslmayr et al., 2007; Klimesch et al., 2007). These findings support the key role of brain oscillations in the perception process (Hanslmayr et al., 2005; Lakatos et al., 2008; Busch et al., 2009; Jensen and Mazaheri, 2010). It is yet unclear, however, whether oscillations indeed reflect a fundamental mechanism of information processing or rather appear as an epiphenomenon (Buzsáki and Draguhn, 2004; Herrmann et al., 2015).

Numerous studies report a modification of brain oscillations, making considerable gains in addressing this question. Besides transcranial approaches, such as magnetic stimulation (TMS; e.g., Dugué et al., 2011; Romei et al., 2011) or alternating current stimulation (tACS, Zaehle et al., 2010; Helfrich et al., 2014) a rhythmic flickering light can serve as a stimulation source. Behavioral studies show that a stream of rhythmic light stimuli improves the perception of targets presented in phase with the rhythmic stimuli (Mathewson et al., 2012; de Graaf et al., 2013; Spaak et al., 2014). Such rhythmic presentation of visual stimuli results in an electrophysiological signal, referred to as a steady-state visual evoked potential (SSVEP) in humans (Regan, 1982; Herrmann, 2001; Müller et al., 2003; Di Russo et al., 2007) as well as in animals (Mechler et al., 1998; Xu et al., 2013). The SSVEP is believed to derive from entrainment of an internal oscillator by an external visual rhythmic driving force. In the occipital cortex, this internal oscillator oscillates at the individual alpha frequency (IAF), which is then shifted toward the external frequency during entrainment.

Entrainment as the fundamental mechanism of SSVEPs is a basic requirement when applying rhythmic stimulation to investigate the causal link between oscillations and behavior (Thut et al., 2011), as the term *entrainment* implies interference with the ongoing brain oscillations. Recently, however, it has been questioned whether the SSVEP indeed reflects entrainment. While some studies report an interaction of stimulation and internal oscillations (Schwab et al., 2006; Halbleib et al., 2012), others found the stimulation to produce a series of event-related responses (ERPs), superimposing to a nearly sinusoidal oscillatory response (Capilla et al., 2011). Furthermore, Keitel et al. (2014) identified different topographies of SSVEPs and internal oscillations, thus indicating a lack of clear understanding of the underlying mechanism of the SSVEP. The superposition hypothesis entails independence of SSVEPs and the ongoing oscillations (Capilla et al., 2011). Hence, if the superposition of ERPs can indeed fully explain SSVEPs

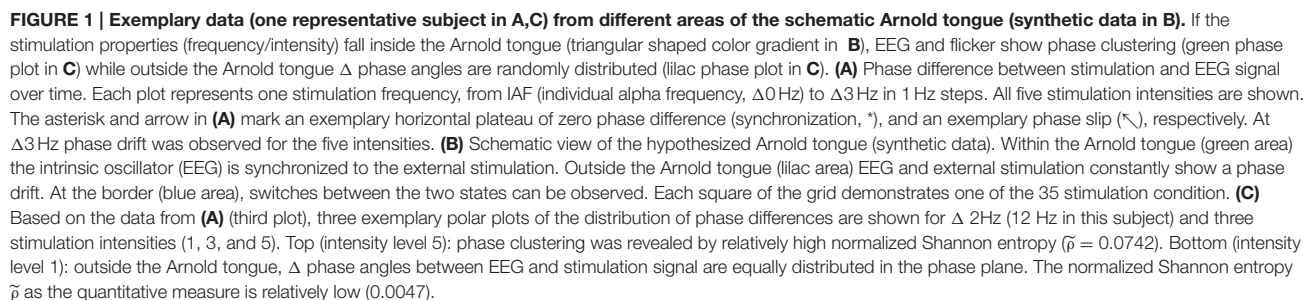
and entrainment cannot be demonstrated, altered behavior as a consequence of rhythmic light stimulation could not be considered evidence of the functional connection between oscillations and behavior.

To shed more light on this debate, here we used two physical concepts to systematically investigate the underlying mechanism of SSVEPs: the Arnold tongue and intermittency of phase locking (Pikovsky et al., 2003; **Figure 1B** shows a schematic Arnold tongue from synthetic data).

The Arnold tongue predicts the degree of synchronization (entrainment) of an oscillator coupled to a rhythmic driving force, depending on two parameters: the amplitude of the driving force (here: light intensity) and driving frequency. With a driving frequency that approaches the intrinsic frequency (here: IAF), entrainment is more likely to occur. With increasing intensity, the window of entrainment widens around the intrinsic frequency, allowing more distant stimulation frequencies to entrain the intrinsic oscillator compared to weaker stimulation intensities. This prediction would result in a triangular shaped area of entrainment when plotted as a function of driving intensity and frequency (green area in **Figure 1B**). At the border of this triangular shaped Arnold tongue (blue shaded area of **Figure 1B**) entrainment is intermitted by uncoupled time periods, so called phase slips. In other words, the intrinsic oscillator is coupled to the external stimulation phase for certain time periods, until, during constant prevailing stimulation, the internal oscillator slips back to the intrinsic frequency until it is again driven by the external stimulation. As opposed to the superposition of ERPs, the Arnold tongue predicts a non-linear response (Regan, 1982) that clearly identifies entrainment (Pikovsky et al., 2003).

Superposition of ERPs is described as processing of single events, independent of ongoing brain oscillations. Thus, we hypothesize that phase coupling should be independent of the regularity of the inter-stimulus interval at which the flicker is presented. Subjects were stimulated with 35 different conditions: five different light intensities and seven different frequencies, which were distributed around the IAF in steps of 1 Hz. Each of these rhythmic stimulation sequences was preceded by a jittered frequency with the same intensity and average number of flashes per second as the subsequent rhythmic condition. If superposition could indeed explain the SSVEP, the phase locking pattern of the 35 jittered sequences would not differ from that of rhythmic stimulation. Furthermore, a triangular entrainment region as predicted by the Arnold tongue would not be expected.

For the rhythmic stimulation conditions, phase locking was found to increase with increasing stimulation intensity as well as when the stimulation frequency approached the IAF, resulting in the triangular shaped pattern that is predicted by entrainment. Inside the triangular shape of the Arnold tongue, we found the rhythmic stimulation to show significantly stronger phase locking compared to the jittered conditions. Outside the Arnold tongue, the two hypotheses (superposition and entrainment) were indiscernible, as they both predict that no entrainment would occur, and here we found that phase locking showed no significant difference.



Thirty students from the University of Oldenburg were recruited (age 24.8 ± 3.4 years, 8 male subjects) for the study. All subjects gave written informed consent before their participation.

Two subjects' data sets had to be discarded due to technical errors. Participants in the remaining sample reported no vision deficits, psychiatric disorders, epilepsy in family history or febrile convulsions during childhood. According to the Edinburgh handedness inventory (Oldfield, 1971), five of the 28 subjects were left-handed. The experimental protocol was approved by the ethics committee of the University of Oldenburg and was conducted in accordance with the Declaration of Helsinki.

Design and Procedure

Subjects were seated in a dark sound-attenuated EEG chamber 60 cm away from an LED light, which was embedded into a black background, adjusted at individual eye-level. The experiment consisted of two parts. In the first part, EEG was recorded during resting state for 2 min in the dark. From this data, the IAF was determined (see below).

In the main experiment (after resting state measurement), participants visually fixated onto an LED which flickered at five different light intensities and seven different frequencies. The flicker was elicited in the LED by driving it with a square wave voltage (cf. **Figure 2**, Box 1A–C). We choose a square wave instead of a sine, as the linear luminance increase of the LED was located in a low voltage range, insufficient for covering the potential area of the Arnold tongue. In other words, it was not possible to drive the LED in a perfect sine using the intensities necessary to entrain the internal oscillations at multiple light intensities. This is, however, not a restriction, as Dreyer and Herrmann (2015) showed that also sine wave stimulation produces harmonics in the EEG spectrum. The five stimulation intensity levels altered in luminance between 1.42 cd/m² (minimum voltage, close to visual threshold) and either 8.34, 52.8, 326, 1756, or 7158 cd/m² (maximum voltage for the five different intensities), which corresponds to a linear increase in voltage. These intensities will henceforth be referred to as intensities 1–5. The stimulation frequency was varied from –3 to +3 Hz around the IAF, determined in the preceding resting state measurement. The LED was operated by a NIDAQ device (National Instruments Data Acquisition, National Instruments Germany GmbH, Munich, Germany), which converted the digital output generated by a script written in MATLAB R2012b (The MathWorks Inc., Natick, MA, USA) into an analog voltage.

Conditions were created with the 5 × 7 intensity–frequency combinations and each condition was presented to the participants for 30 s, followed by a 2 s pause. Preceding each single condition, a 30 s stimulation of jittered flickering light was presented, where instead of a rhythmic flicker inter stimulus intervals (ISIs) of the square wave were jittered with a maximum of ±60% (ISI from the subsequent rhythmic condition, e.g., 50 ms in the 10 Hz condition x1.6, x1.3, x1, x0.7, x0.4, resulting in 20, 35, 50, 65, or 80 ms). The ISIs were randomized with a uniform distribution over the whole stimulation period and the same ISIs never appeared twice in a row. **Figure 2A** shows an exemplary 1 s sequence of a rhythmic and a jittered stimulation interval. Below (**Figure 2B**), the averaged power spectrum (FFT, Hanning window, 1 s pieces) of the stimulation signal shows a clear peak at 10 Hz for the rhythmic stimulation (plus power

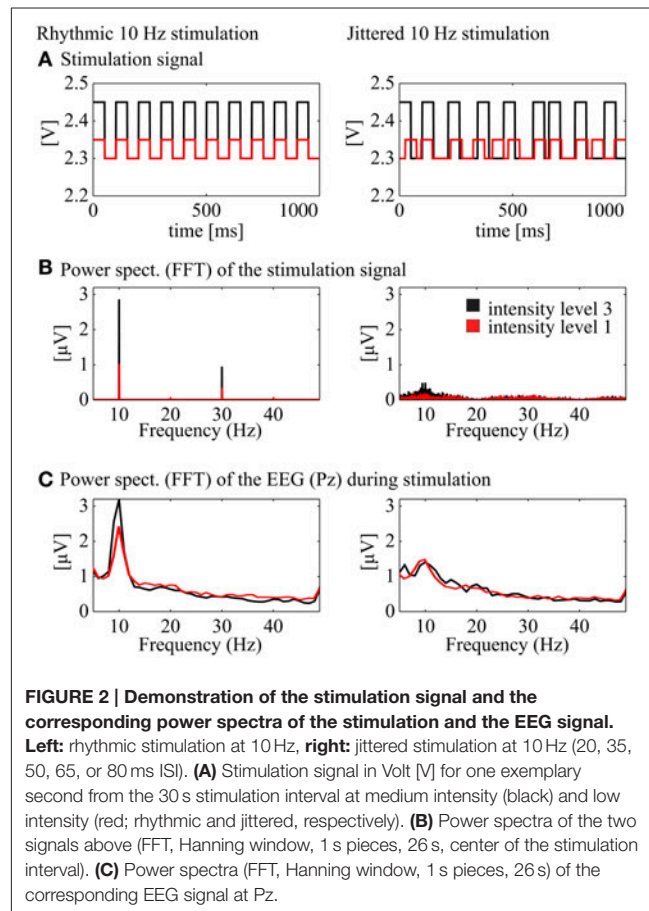


FIGURE 2 | Demonstration of the stimulation signal and the corresponding power spectra of the stimulation and the EEG signal.

Left: rhythmic stimulation at 10 Hz, **right:** jittered stimulation at 10 Hz (20, 35, 50, 65, or 80 ms ISI). **(A)** Stimulation signal in Volt [V] for one exemplary second from the 30 s stimulation interval at medium intensity (black) and low intensity (red; rhythmic and jittered, respectively). **(B)** Power spectra of the two signals above (FFT, Hanning window, 1 s pieces, 26 s, center of the stimulation interval). **(C)** Power spectra (FFT, Hanning window, 1 s pieces, 26 s) of the corresponding EEG signal at Pz.

at the harmonic frequencies). The arrhythmic character of the jittered stimulation is revealed by a flat noisy spectrum with less power at the stimulation frequency than the rhythmic stimulation at around 10 Hz. These characteristics are found likewise for the EEG spectrum at Pz (FFT, Hanning window, 1 s data pieces). The jittered stimulation was used as a control for the rhythmic condition. The order of the stimulation-jitter pairs was randomized between subjects. The main experiment was subdivided into three blocks of 12.4 min with pauses of individual length between the blocks. The duration of the whole procedure including EEG cap preparation was ~90 min.

EEG Measurement

The EEG was measured from four sintered Ag–AgCl electrodes at O1, Oz, O2, and Pz, mounted in an elastic cap (EasyCap, Falk Minow, Munich, Germany) with an extended 10–20 system layout, referenced to the nose. For further analysis steps, only Pz was chosen as the alpha oscillator has been described to show its maximum peak in a power spectrum in that region (Erdenoglu et al., 2004). Furthermore, averaging of multiple electrodes might reduce the overall effect due to phase shift between the channels. The ground electrode was placed at FPz, impedances were kept below 10 kΩ. EEG was recorded using a 16-bit Brain Amp DC amplifier and Brain Vision Recorder software (Brain Products GmbH, Gilching, Germany). An online

band pass filter of 0.016–250 Hz and a sampling rate of 5000 Hz were used. EEG was amplified in the range of $\pm 16.384 \mu\text{V}$ at a resolution of $0.5 \mu\text{V/bit}$. Stimulus markers and EEG data were stored digitally for further offline analysis. Raw exemplary EEG data is displayed in **Figure 3** (Box 1).

Data Analysis

Data were down-sampled to 1000 Hz and filtered using a windowed sinc type I linear phase FIR filter (band pass: IAF ± 3.5 Hz, filter order: 6002) and did not induce a phase shift in the alpha range (6–14 Hz). The identical filter was used for the stimulation signal and the EEG data (Widmann and Schröger, 2012). Filtered EEG data are shown in **Figure 3** (Box 2). For each condition, the first and last 2 s were discarded, since the steady-state condition has to build up and to avoid edge effects (Halbleib et al., 2012). All analysis steps were performed in MATLAB R2012b (The MathWorks Inc., Natick, MA, USA) and EEGLAB 11.0.4.3 (Delorme and Makeig, 2004).

Determination of Individual Alpha Frequency

Prior to the experiment, 2 min of resting state EEG at the Pz electrode were recorded in a dark and sound-attenuated EEG

chamber with eyes closed. A power spectrum was calculated using Fast Fourier transformation on 1 s data pieces, windowed with a rectangular taper. The induced spectra were averaged. The IAF was then defined as the maximum peak within the alpha range (9–11 Hz) in the eyes closed condition to remain within a comparable stimulation range. Ten of the 28 subjects showed no clear peak within this range. These subjects were assigned a standard IAF of 10 Hz, resulting in a mean center stimulation frequency of 9.96 ± 0.42 Hz. Furthermore, the 9 Hz subjects had to be excluded from the analysis (three subjects) as the harmonics of the IAF–3 Hz stimulation ($= 6$ Hz) lay within the band pass window, leaving 25 subjects for the analysis.

Phase Detection

To classify the degree of entrainment, we determined the phase-locking of the stimulation and the EEG signal. Each step of the analysis is depicted in **Figure 3** for two rhythmic conditions as well as one jittered condition. We used the Hilbert transform function (Matlab) on electrode Pz, because it shows the maximum alpha amplitude (Ergenoglu et al., 2004). To calculate the difference of the phase angles of the EEG data

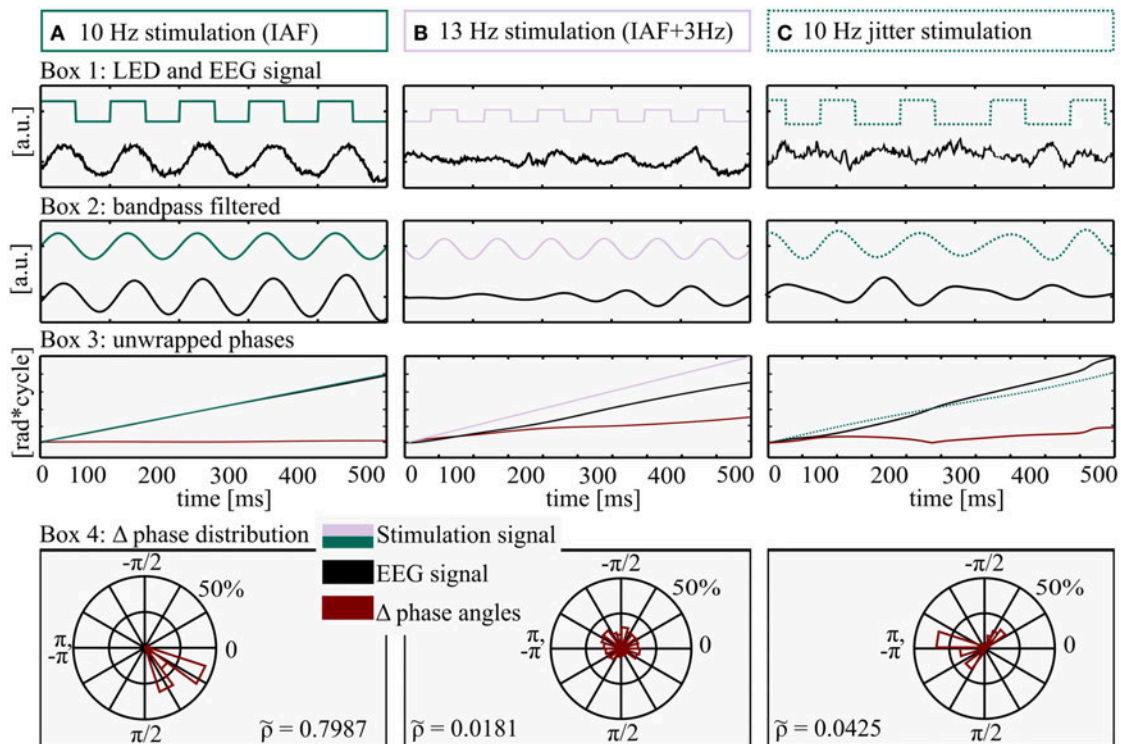


FIGURE 3 | Method for determination of Shannon entropy. All processing steps were performed on three exemplary data pieces (500 ms) from three different conditions: **(A)** Stimulation intensity 5 (max), frequency: IAF (individual alpha frequency, 10 Hz here), **(B)** Stimulation intensity 1 (min), frequency: IAF+ 3 Hz, 13 Hz here and **(C)** Jittered stimulation at 10 flashes per second. Box 1: LED stimulation signal (square wave, green/lilac) and EEG raw data (black). Box 2: filtered LED stimulation signal (green/lilac) and EEG (black). Box 3: unwrapped phase angles of LED stimulation signal (green/lilac) and EEG data (black). The red line depicts the time course of Δ phase (EEG–LED stimulation). Box 4: distribution of wrapped Δ phase angles. The almost horizontal course of Δ phase angles in Box 3A (red graph) is approaching a Dirac-like distribution, quantified by a relatively high Shannon entropy ($\tilde{p} = 0.7987$), whereas the rather uniform distributions and a lower Shannon entropy ($\tilde{p} = 0.0181$ and 0.04325) in Box 4B and 4C reflect a drift of the two phase angles (LED stimulation and EEG signal) and as a consequence an ascending Δ phase angle over time (Box 3B, red line).

and the stimulation signal (Δ phase angles), the unwrapped phase angles of the Hilbert transform (**Figure 3**, Box 3A,B) were subtracted (EEG phase minus stimulation phase) and wrapped to the range of $-\pi$ to π (**Figure 3**, Box 4). To quantify entrainment for each subject and condition, the distribution of Δ phase angles was quantified in a range between uniform distribution (complete independence of the two signals) and a Dirac-like distribution (perfect phase synchronization). Therefore, the normalized Shannon entropy (Tass et al., 1998) was determined for the Δ phase angles at each time point, condition and subject, in the range of $-\pi$ to π to quantify the phase locking over time.

The normalized Shannon entropy $\tilde{\rho}$ is defined as:

$$\tilde{\rho} = \frac{S_{\max} - S}{S_{\max}} \text{ with } S = - \sum_{k=1}^N p_k \ln p_k \text{ and } S_{\max} = \ln N,$$

where N is the number of bins ($N = 80$), p_k is the probability of the k th bin and S is the classic Shannon entropy of a fixed window between $-\pi$ to π . The normalized Shannon entropy can take values between $0 \leq \tilde{\rho} \leq 1$, where $\tilde{\rho} = 0$ corresponds to a uniform distribution and $\tilde{\rho} = 1$ to a Dirac-like distribution (Tass et al., 1998). At a glance, high entropy S (low normalized Shannon entropy $\tilde{\rho}$) reflects a rather random distribution of Δ phase angles over the bins of a polar histogram, indicating no entrainment (**Figure 3**, Box 4B), while low classic Shannon entropy (high normalized Shannon entropy $\tilde{\rho}$) results from a rather constant phase coupling (i.e., entrainment, **Figure 3**, Box 4A). Perfect coupling gathers all values within a single bin (Dirac-like distribution).

The normalized Shannon entropies were calculated for all subjects and conditions. We predicted that in case of entrainment $\tilde{\rho}$ should increase with increasing stimulation intensity and with decreasing distance from IAF. Thus, conditions were arranged in a two-dimensional plane as a function of intensity (five levels) and frequency (seven levels).

Intermittency

When the intrinsic brain oscillations are entrained by the driving force, the Δ phase angles between EEG and driving force are close to zero and, as a consequence, are considered a phase plateau. This is the case when frequency and intensity are chosen such that they are located inside the triangular shape of the Arnold tongue. Outside the Arnold tongue, the EEG is not synchronized to the driving force and Δ phase angle constantly increases over time. Intermittency is defined as an alternation of phase plateaus and phase slips (see below) and is observed at the border zone of entrainment regions. Phase plateaus are horizontal periods of the unwrapped Δ phase angles when plotted over time (see exemplary data of **Figure 1A**, marked by a *). Plateaus show increasing length with increasing driving intensity and decreasing frequency distance from IAF. To test for the effects of intensity and frequency, plateaus were identified for each sampling point by determining the slope (± 100 samples). A gradient of 0 ± 0.005 was defined as plateau and the duration was then counted. This gradient was implemented to account for noise in the data. Ten plateaus were therefore classified as such by visual inspection. The mean standard deviation of these 10 random plateaus was taken as deviation for the

plateau classifier algorithm. Stronger gradients of Δ phase angles were considered phase slips. Intermittency was quantified as the maximum plateau duration per condition and was averaged across subjects. When intermittency occurs, the characteristics of the driving oscillator (intensity and frequency) neither describe conditions outside the Arnold tongue, where the two phases linearly drift apart (constant phase slip), nor inside the triangular shape of the Arnold tongue, where the two oscillators are coupled (constant plateau).

Statistics

Normalized Shannon Entropy

In the first step, the normalized Shannon entropies $\tilde{\rho}$ of the Δ phase angles for the rhythmically stimulated conditions were tested against $\tilde{\rho}$ of the Δ phase angles for the corresponding jittered conditions. Because data failed to be normally distributed, non-parametric Mann-Whitney U -tests (Fay and Proschan, 2010) were applied. From the resulting z -values the effect sizes (r) were calculated:

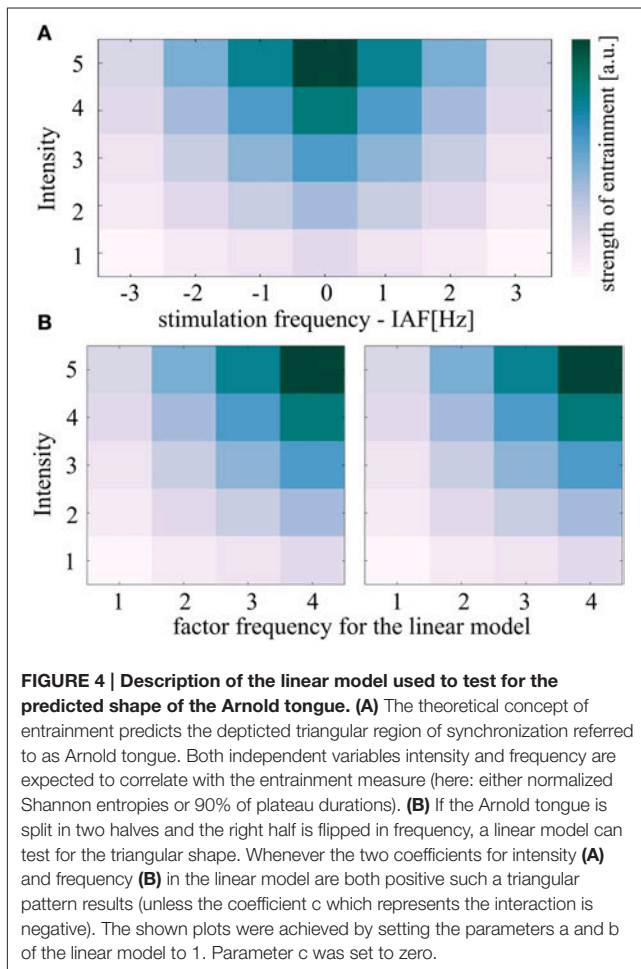
$$r = \text{abs}\left(\frac{z}{\sqrt{N}}\right), \text{ with } N = 50$$

(Fritz et al., 2012).

For the superposition hypothesis, we would expect brain responses to be independent of the driving rhythm. The resulting p -values were corrected for false discovery rate (FDR) at 0.001, 0.01, and 0.05. This procedure was applied in order to control for Type I errors by sorting the p -values, then correcting for multiple comparisons starting with the smallest p -value (Benjamini and Hochberg, 1995).

In the second step, the resulting shape of the pattern in the two-dimensional plane was tested. Therefore, $\tilde{\rho}$ -values were z -standardized subject-wise to guarantee normal distribution and reduce inter-subject variance. Then, a linear model (see below) was fitted to the normalized Shannon entropies. Based on the hypothesized pattern of the Arnold tongue, we expect the normalized Shannon entropy values to increase with increasing stimulation intensity. For the factor frequency, we expect a positive impact on the normalized Shannon entropies for the left half of the triangular shape, the closer the stimulation frequency was to the IAF (scaled from $\Delta 3 \text{ Hz} = 1$ to $\Delta 0 \text{ Hz} = 4$), the higher the $\tilde{\rho}$ (= stronger entrainment). As the factor frequency shows non-linear characteristics in the Arnold tongue (the strongest entrainment is predicted for the center of the Arnold tongue), the 5×7 (intensity \times Frequency) data structure as depicted in the two-dimensional plane of the Arnold tongue in **Figures 5A,B** was mirrored to the left side to gain linear characteristics. The linear model is depicted in **Figure 4**.

The model was then fitted to each of the 25 subjects and for both sides of the Arnold tongue (**Figure 4B**) separately, resulting in five stimulation intensities and four frequencies per linear model. The 2×25 coefficients (sides of the predicted Arnold tongue \times subjects) were concatenated into one data matrix for the independent variables intensity and frequency as well as the interaction term, respectively, resulting in 3×50 coefficients



(Intensity, Frequency and Interaction term \times coefficients of two sides for 25 subjects).

$$y = a * int + b * freq + c * int * freq$$

This procedure was repeated for both the rhythmic and the jittered stimulation. The 3×50 coefficients of the rhythmic stimulation condition were then compared to the respective jittered coefficient, using a one-sided Mann–Whitney–U-test (Fay and Proschan, 2010) as data failed to show normal distribution using a Shapiro–Wilk-test (Royston, 1993). Effect sizes r were calculated with $N = 100$ following the above described formula (Fritz et al., 2012).

Plateaus

Again the above described linear model was fitted to the 90 percentile of the sorted plateau durations for the rhythmic condition. The two-dimensional data matrix (intensity \times frequency) was therefore reshaped as described above to include the factor frequency as a linear independent variable (see Figure 4) and plateau durations were z-normalized before fitting the linear model. Then, t -tests were performed for the three coefficients (intensity, frequency, and the interaction term) to test

against zero. If it is true that plateau duration (as a measure of phase coupling over time) increases with increasing stimulation intensity, we expect the coefficients to be significantly greater than zero. Furthermore, if it was true that frequency increase (for the left half of the triangle, mirrored for the right half) has a positive impact on plateau duration, then we expect the coefficient to be significantly greater than zero. The effect sizes r were calculated by the following formula:

$$r = \sqrt{\frac{t^2}{t^2 + df}}$$

(Cohen, 1988).

RESULTS

The paradigm was designed in a way that allowed the comparison of different fields in the hypothesized plane of the Arnold tongue. Subjects were stimulated with a rhythmically flickering light at five intensity levels and at seven frequencies, centered at the IAF in steps of 1 Hz, resulting in 35 conditions. Each condition was presented for 30 s, with a preceding jittered sequence (also for 30 s).

The intrinsic frequency of the parietal brain oscillations is defined as the IAF, whose most prominent peak in the individual power spectrum is located in the parieto-occipital cortex during resting state (Berger, 1929). Following the concept of the Arnold tongue (Pikovsky et al., 2003), we expect an increased likelihood for a driving frequency close to the IAF to entrain the internal oscillator as compared to frequencies more distant to IAF. As a second factor, brighter light flicker should result in stronger phase coupling compared to weaker stimulation intensities. If these dependencies of stimulation frequency and light intensity can be shown, entrainment but not superposition of ERPs is the most likely explanation for SSVEPs.

Two measures were applied to quantify the level of entrainment, plateau duration of phase locking over time (the longer the plateau, the stronger the entrainment) and the overall phase locking, defined as the normalized Shannon entropy (the less entropy (larger value) the stronger the entrainment, because strong phase locking = entrainment). Note, that a larger value of normalized Shannon entropy indicates less entropy and stronger phase coupling, which is interpreted as stronger entrainment.

When depicting the quantified Δ phase angle distributions (normalized Shannon entropy $\tilde{\rho}$ of the phase of the EEG signal minus the visual flicker phase) as a function of frequency and intensity, a resulting triangular shape would reveal entrainment of an oscillator, as defined by the physics principle of the Arnold tongue. Additionally, the entrained areas of the Arnold tongue (inside the triangle) are expected to show a low phase difference (strong directionality of Δ phase angle distributions). The effects of stimulation intensity and frequency were tested and the shape of the resulting plot was compared to the triangular shape predicted by the Arnold tongue. Next, the plateau durations and the normalized Shannon entropies were compared to the jittered (arrhythmic) conditions.

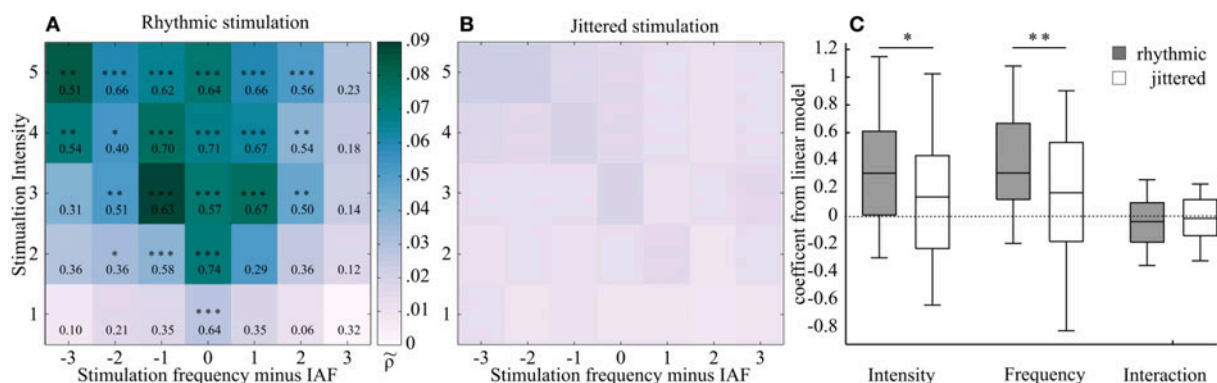


FIGURE 5 | Two two-dimensional planes showing averaged Shannon entropies (25 subjects) as a function of frequency and intensity of the external stimulation, centered at individual alpha frequency (IAF). (A) Rhythmic stimulation. Stronger phase locking is shown in darker shading (higher \tilde{p} -value). This region was found around IAF and widens with increasing intensity, resulting in a triangular shape. This shape corresponds to the hypothesized Arnold tongue. Effect sizes (r) from a Mann-Whitney U -test show the comparison between the rhythmic condition and the respective jittered condition. Asterisks mark level of significance after FDR correction (** $p < 0.00008$, ** $p < 0.0004$, * $p < 0.005$). **(B) Jittered stimulation.** No such triangular shape was observed in the jittered condition. **(C) Box plots** of the coefficients of the linear model, fitted to rhythmic (gray) and jittered (white) stimulation of the normalized Shannon entropies subjects-wise for the two sides of the triangle (see **Figure 4** for model description). A Mann-Whitney- U -test was performed to test for differences between jittered and rhythmic stimulation for the dependent variables frequency and intensity. Both factors but not the interaction term were found to differ significantly (Intensity: $r = 0.19, z = 1.92, p < 0.05$; Frequency: $r = 0.27, z = 2.66, p < 0.01$; Interaction: $r = 0.08, z = -0.78, p = 0.78$). In the plot, the middle of the box represents the median. The box represents the 95% confident interval and the whiskers the 25th and 75th percentiles.

The Normalized Shannon Entropy as a Measure of Entrainment

At the IAF, all five stimulation intensities showed constant phase locking. This phenomenon is depicted by a slope close to zero (**Figure 1A**, first plot), reflecting strong phase locking, i.e., high normalized Shannon entropy (= strong entrainment). In the schematic Arnold tongue from synthetic data in **Figure 1B** the expected position in the two-dimensional plane are indicated. On the contrary, at greater distance from IAF outside the Arnold tongue, no entrainment was expected. This was reflected in the phase of the EEG signal by (almost) unlocked phases, independently of the stimulation intensity, as shown for the exemplary dataset in **Figure 1A**, fourth plot. Thus, for these two frequency conditions (at IAF and far away from IAF) phase locking was found to be robust over time, representing entrainment by a slope close to zero in the first case and a linearly ascending slope, reflecting no entrainment in the second case.

At intermediate distance from the IAF (Δ 2Hz), the effect of intensity becomes particularly clear: at lower intensities, the phase angles of the EEG signal and the stimulation signal appeared to be similarly unlocked as in the Δ 3Hz condition, as reflected in the constant increase of Δ phase angles (cf. lilac graph in **Figure 1A**, third plot). With increasing stimulation intensity, the slopes of Δ phase angles show a weaker linear increase, indicating stronger phase locking (entrainment; cf. blue and green graph in **Figure 1A**, third plot).

Figure 1C depicts how the slopes of Δ phase angles translate to the distribution over the unit cycle, which was then expressed as normalized Shannon entropy \tilde{p} for three intensities [minimum (1), mediate (3), and maximum (5)] of the exemplary data at Δ 2Hz. The distribution of Δ phase angles was determined to quantify the phase locking over time. While the low intensity

levels are reflected by a uniform distribution of Δ phase angles (outside the Arnold tongue), the distribution becomes more directional with increasing stimulation intensity (toward areas inside the Arnold tongue). This directionality is expressed by \tilde{p} , which increases in the same ($\tilde{p}_1 = 0.0047$, $\tilde{p}_3 = 0.0085$, $\tilde{p}_5 = 0.0742$).

The \tilde{p} -values, arranged in the two-dimensional plane as a function of intensity and frequency, resulted in a triangular shape, showing increasing normalized Shannon entropy (increased synchronization) at and around the intrinsic frequency (IAF, **Figure 5**). The triangular shape was reflected by the following statistical tests:

First, the distributions of Δ phase angles from rhythmic stimulation were compared to the jittered conditions. Each of the 35 rhythmic stimulation conditions was preceded by its corresponding jittered condition with a mean frequency of the subsequent rhythmic stimulation frequency during the experiment. The intensity was also matched.

The effect sizes were found to increase gradually toward the IAF and with increasing stimulation intensity. Moreover, the normalized Shannon entropy \tilde{p} was found to significantly differ from the jittered condition only within a triangularly shaped pattern around the IAF, as revealed by Mann-Whitney U -test statistics, which were performed on each rhythmic-jitter pair. The significance level was false discovery rate (FDR)-corrected ($p < 0.00008$, $z \geq 3.96$, $r \geq 0.56$; $p < 0.00044$, $z \geq 3.54$, $r \geq 0.50$; $p < 0.00490$, $z \geq 2.55$, $r \geq 0.36$). z -values were transformed to effect sizes (r), which are shown together with the p -values for each condition in the respective field of **Figure 5A**. **Figure 5B** shows the two dimensional plane of normalized Shannon entropies for the jittered condition.

In order to test for the triangular shape in the two-dimensional plane, a linear model with the independent variables intensity and frequency was fitted to the data (see Materials and Methods Section and **Figure 4** for details) of each individual subject. The linear model was fitted to the normalized Shannon entropies from both, rhythmic and jittered stimulation conditions.

The coefficients for the rhythmic stimulation of both variables—intensity and frequency—were found to significantly differ from the jittered stimulation in a one-sided Mann-Whitney *U*-test (Intensity: $r = 0.19$, $z = 1.92$, $p < 0.05$; Frequency: $r = 0.27$, $z = 2.66$, $p < 0.01$; Interaction: $r = 0.11$, $z = -0.78$, $p = 0.78$). The box plot in **Figure 5C** shows the distribution of the coefficients. As explained in the Materials and Methods Section and shown in **Figure 4**, the positive coefficients for intensity and frequency imply a triangular shape of the region of entrainment and are thus in line with an Arnold tongue.

The Plateau Duration as a Measure of Entrainment

Besides the slope of Δ phase angles, the intermittency of phase locking is an important criterion to identify synchronization (Pikovsky et al., 2003). The phenomenon, known from entrainment of isolated physical oscillators, describes disturbed phase locking (phase slips) during constant prevailing stimulation. While a linear addition of single responses (superposition hypothesis) is expected to result in a constant EEG response, synchronization caused by entrainment can take different states of phase locking over time. The duration of the respective states depends on the frequency and intensity of the driving oscillator, as described by the Arnold tongue. Phase slips, which result from drifting apart of the two phases, are expected to be extended in time and to appear more frequent with decreasing coupling of the two oscillators (Tass et al., 1998; Pikovsky et al., 2003).

Intermittency becomes particularly obvious at the border of the Arnold tongue (light green to blue shaded area in **Figure 1B**). The data of the exemplary subject shows phase locking plateaus at higher stimulation intensities (**Figure 1A**, third plot, green curves; exemplary period marked by the asterisk) with intermittent drifting apart of the two oscillators (phase slips, one exemplary period is marked by the arrow).

Phase locking plateaus were quantified in order to test for the predicted effects of intensity and frequency. Therefore, the linear model was fitted to the *z*-normalized 90 percentiles of plateau durations subject wise. We found the independent variable intensity to significantly influence the plateau duration by testing the referring coefficients of the linear model using *t*-tests [95% CI [0.46, 0.21], 0.17 ± 0.07 , $t_{(49)} = 3.18$, $p < 0.01$, $r = 0.41$]. The coefficients for the factor frequency were also found to significantly differ from zero [95% CI [0.30, 0.52], $t_{(49)} = 7.68$, $p < 0.001$, $r = 0.74$]. No significant effects were found for the interaction term: 95% CI [-0.02, 0.05], $t_{(49)} = 0.67$, $p = 0.50$, $r = 0.10$.

DISCUSSION

The present study reveals evidence that the SSVEP reflects entrainment. Our findings support the assumption that a visual

flickering light stimulation can be applied to study the functional relevance of brain oscillations.

Sensory rhythmic stimulation is broadly accepted as an eligible tool to produce entrainment. Mathewson et al. (2010) stimulated subjects with a 12.1 Hz rhythmic flickering light and presented a masked target in phase after stimulation offset. The number of rhythmic flicker stimuli varied between 1 and 8 and was shown to positively correlate with in-phase target detection. Likewise, as a consequence of 10 Hz rhythmic stimulation Spaak et al. (2014) found the detection rate to significantly depend on stimulation phase. In their study, a 10 Hz flicker was presented to one hemifield; the other hemifield was stimulated with a flicker stream with jittered inter-flash intervals. Phase effects were found solely for the rhythmic condition. In both studies, entrainment is inferred as the fundamental mechanism of the produced SSVEP. To clearly trace back the described behavioral changes after visual rhythmic stimulation, it is however necessary to provide evidence that SSVEPs indeed reflect entrained oscillations.

The interaction of the rhythmic visual stimulation and the targeted oscillation has recently been questioned (Capilla et al., 2011; Keitel et al., 2014), which highlights the particular relevance and the timeliness of this investigation. By probing two physics concepts that unambiguously define entrainment: intermittency of phase locking and the Arnold tongue, we systematically tested the two hypotheses suggested to reflect the fundamental mechanism of SSVEPs, superposition and entrainment.

A non-rhythmic (jittered) stimulation is unable to entrain the intrinsic frequency (Parkes et al., 2004; Capilla et al., 2011). Thus, we predicted a similar pattern for the phase locking of the jittered condition and the rhythmic stimulation, assuming the superposition hypothesis was true. This was not the case. Our data were in line with the entrainment hypothesis: the normalized Shannon entropies of the rhythmic condition tested against those of the jittered condition showed an increasing effect size with increasing intensity and decreasing frequency distance to IAF in the condition wise comparison (Mann-Whitney-*U*-tests). At the maximum distance from IAF ($\Delta 3$ Hz here) and at low stimulation intensity, the two signals revealed non-distinctive phase coupling with lower effect sizes and non-significant differences between jittered and rhythmic stimulation. The fitted linear model revealed significance for the observed triangular shape of the normalized Shannon entropies, as both factors-frequency and intensity-showed a positive value (**Figure 5C**). This can only result in the predicted triangular pattern and was significantly different from the jittered stimulation condition.

The areas outside the Arnold tongue are characterized by relatively lower stimulation intensity and/or a driving frequency that is more distant to the intrinsic frequency (IAF). These characteristics are ineligible to entrain the internal oscillator. Hence, outside the Arnold tongue, stimulation responses are independent from the intrinsic alpha oscillation and thus rather resemble sequences of ERPs, as also predicted by the superposition hypothesis. Inside the Arnold tongue, however, the normalized Shannon entropy showed significantly stronger phase coupling (increased effect size *r* in a Mann-Whitney-*U*-test between jittered and rhythmic stimulation), which is

interpreted as entrainment. Oscillations are entrained, such that the intrinsic frequency is shifted toward the driving frequency. As a consequence, only under these circumstances one can investigate the function of the intrinsic oscillations. de Graaf et al. (2013) found behavioral entrainment effects at 10.6 Hz, whereas effects disappear at 7.1 Hz and below as well as at 14.2 Hz, which is in accordance with the presently identified borders of the Arnold tongue at intermediate intensity.

Intermittency of phase locking reflects a non-linear process, where the oscillator is phase locked over certain periods, but then changes its phase during constant prevailing circumstances (Pikovsky et al., 2003). In the center of the Arnold tongue, in line with the prediction of this concept, these intermittent phase slips are rather unlikely to appear, as phase locking remains robust over the stimulation period (**Figure 1A**, plot 1). The method for plateau detection was designed in a rather conservative way, which explains why the maximum plateau duration for IAF entrainment did not span over the entire stimulation period, as inferred from **Figure 1A**, plot 1. Noise eventually interrupted the plateaus, but as the procedure was identical in all conditions, the relative comparison is unaffected by noise. While the normalized Shannon entropies reflect a relative measure that identifies the shape of the Arnold tongue when comparing different intensity-frequency stimulations, intermittency is a measure that provides evidence for entrainment on a single subject level. Therefore, in order to show entrainment, it is sufficient to examine the intermittency at a stimulation condition at the border of the Arnold tongue, between the non-significant normalized Shannon entropies (suggested area outside the Arnold tongue) and the conditions expected to lie inside the Arnold tongue (**Figure 5A**). The phase slips are expected to result from a transient uncoupling of the driving oscillator (light flicker), where the intrinsic oscillator temporarily rotates at IAF. Although alpha amplitudes fluctuate over time as they correlate with cognitive functions (Worden et al., 2000; Foxe and Snyder, 2011; Klimesch, 2012) it is rather unlikely that this would cause phase slips. The effect of attention should be distributed equally over conditions. Quite on the contrary, we found the plateau duration to reveal a shape that resembles an Arnold tongue. Both factors frequency and intensity were significantly greater than zero when fitting a linear model. As depicted in **Figure 4**, this can only result in a triangular shape on the 5×4 half of the Arnold tongue.

Despite the clear triangular shape as predicted by the concept of the Arnold tongue, the maximum values were not located at the highest stimulation intensity, but rather at intermediate intensity, which might be due to intensity saturation. Buchsbaum and Pfefferbaum (1971) showed a decreased ERP amplitude when an individual threshold intensity level was exceeded. In their study, the level was highly variable between subjects. This might also explain why we did not find significant effects for the interaction term in the linear models for normalized Shannon entropies and plateau durations.

The triangular shape of normalized Shannon entropies is slightly skewed to the left. This could be due to the fact, that participants were passively stimulated without performing a demanding task, as the alpha frequency has been shown to

positively correlate with cognitive demands (Haegens et al., 2014).

The notion that SSVEPs are generated via the entrainment of an intrinsic brain oscillation also explains non-linear phenomena of SSVEPs that could not be explained by linear superposition of ERPs. For example, Herrmann (2001) demonstrated that the SSVEP in response to 80 Hz flickering light showed a clear 10 Hz oscillation. Superposition of ERPs would have predicted an SSVEP of 80 Hz. However, in case of entrainment, synchronization of the EEG to the external driving force can happen in multiple Arnold *tongues*. Synchronization typically not only occurs at the frequency of the intrinsic brain oscillator (1:1 Arnold tongue) but also harmonics ($N \times$ intrinsic frequency) and subharmonics (intrinsic frequency/ N) where N is an integer (e.g., 1:2 and 2:1). Thus, the 80 Hz flickering LED was entraining the EEG in an 8:1 manner resulting in a 10 Hz oscillation. Harmonic entrainment has been shown on a behavioral level by de Graaf et al. (2013), who found a cyclic pattern of visual detection at a 5.3 Hz entrainment as well as at 10.6 Hz, but not outside the Arnold tongue.

The reported finding of the Arnold tongue with intermittent phase locking at the border of the triangular pattern supports the assumption, that visual entrainment is a valid tool to entrain brain oscillations. Moreover, it reveals evidence for behavioral changes as a consequence of rhythmic visual stimulation to reflect causality. Furthermore, it encourages further investigation using electric and magnetic stimulation, as it confirms that oscillations can generally be entrained by an external driving force.

CONCLUSION

We showed for the first time in a systematic analysis that visual flickering stimulation results in entrainment of brain oscillations. Our data demonstrate that the visual cortex responds in a non-linear fashion when being exposed to rhythmic visual stimulation, which contradicts the hypothesis of linear superposition of ERPs. Multiple studies apply a flickering light source to investigate the causal link of brain oscillations and perception (Hanslmayr et al., 2005; Lakatos et al., 2008; Busch et al., 2009; Schroeder and Lakatos, 2009; Jensen and Mazaheri, 2010; Mathewson et al., 2011). By showing that visual rhythmic stimulation modifies ongoing brain oscillations, this study reveals evidence that visual entrainment is capable of probing causality. The effect, however, depends on the frequency's distance from the intrinsic frequency (IAF) as well as on the stimulation intensity, which should both be considered for the design of future experiments. The pattern of the Arnold tongue, as well as intermittent phase locking during rhythmic visual stimulation, reveals strong evidence for entrainment as the underlying mechanism of SSVEPs.

AUTHOR CONTRIBUTIONS

CH, JK, and AN designed research; CH and AN performed research; CH and AN analyzed data; CH, JK, and AN wrote the paper.

FUNDING

The project was supported by the PhD program “Signals and Cognition” and the Special Priority Programme 1665 of the German Research Foundation (DFG grant HE3353/8-1).

REFERENCES

- Arieli, A., Sterkin, A., Grinvald, A., and Aertsen, A. (1996). Dynamics of ongoing activity: explanation of the large variability in evoked cortical responses. *Science* 273, 1868–1871.
- Benjamini, Y., and Hochberg, Y. (1995). Controlling the false discovery rate: a practical and powerful approach to multiple testing. *J. R. Stat. Soc. B Methodol.* 57, 289–300.
- Berger, P. D. H. (1929). Über das elektroencephalogramm des menschen. *Arch. Psychiatr. Nervenkr.* 87, 527–570. doi: 10.1007/BF01797193
- Buchsbaum, M., and Pfefferbaum, A. (1971). Individual differences in stimulus intensity response. *Psychophysiology* 8, 600–611. doi: 10.1111/j.1469-8986.1971.tb00496.x
- Busch, N. A., Dubois, J., and VanRullen, R. (2009). The phase of ongoing EEG oscillations predicts visual perception. *J. Neurosci.* 29, 7869–7876. doi: 10.1523/JNEUROSCI.0113-09.2009
- Buzsáki, G., and Draguhn, A. (2004). Neuronal oscillations in cortical networks. *Science* 304, 1926–1929. doi: 10.1126/science.1099745
- Capilla, A., Pazo-Alvarez, P., Darriba, A., Campo, P., and Gross, J. (2011). Steady-state visual evoked potentials can be explained by temporal superposition of transient event-related responses. *PLoS ONE* 6:e14543. doi: 10.1371/journal.pone.0014543
- Cohen, J. (1988). *Statistical Power Analysis for the Behavioral Sciences*. Hillsdale, NJ: Lawrence Erlbaum.
- de Graaf, T. A., Gross, J., Paterson, G., Rusch, T., Sack, A. T., and Thut, G. (2013). Alpha-band rhythms in visual task performance: phase-locking by rhythmic sensory stimulation. *PLoS ONE* 8:e60035. doi: 10.1371/journal.pone.0060035
- Delorme, A., and Makeig, S. (2004). EEGLAB: an open source toolbox for analysis of single-trial EEG dynamics including independent component analysis. *J. Neurosci. Methods* 134, 9–21. doi: 10.1016/j.jneumeth.2003.10.009
- Di Russo, F., Pitzalis, S., Aprile, T., Spironi, G., Patria, F., Stella, A., et al. (2007). Spatiotemporal analysis of the cortical sources of the steady-state visual evoked potential. *Hum. Brain Mapp.* 28, 323–334. doi: 10.1002/hbm.20276
- Dreyer, A. M., and Herrmann, C. S. (2015). Frequency-modulated steady-state visual evoked potentials: a new stimulation method for brain-computer interfaces. *J. Neurosci. Methods* 241, 1–9. doi: 10.1016/j.jneumeth.2014.12.004
- Dugué, L., Marque, P., and VanRullen, R. (2011). The phase of ongoing oscillations mediates the causal relation between brain excitation and visual perception. *J. Neurosci.* 31, 11889–11893. doi: 10.1523/JNEUROSCI.1161-11.2011
- Ergenoglu, T., Demiralp, T., Bayraktaroglu, Z., Ergen, M., Beydagi, H., and Uresin, Y. (2004). Alpha rhythm of the EEG modulates visual detection performance in humans. *Cogn. Brain Res.* 20, 376–383. doi: 10.1016/j.cogbrainres.2004.03.009
- Fay, M. P., and Proschan, M. A. (2010). Wilcoxon-Mann-Whitney or t-test? On assumptions for hypothesis tests and multiple interpretations of decision rules. *Stat. Surv.* 4, 1–39. doi: 10.1214/09-SS051
- Foxe, J. J., and Snyder, A. C. (2011). The role of alpha-band brain oscillations as a sensory suppression mechanism during selective attention. *Front. Psychol.* 2:154. doi: 10.3389/fpsyg.2011.00154
- Fritz, C. O., Morris, P. E., and Richler, J. J. (2012). Effect size estimates: current use, calculations, and interpretation. *J. Exp. Psychol. Gen.* 141, 2–18. doi: 10.1037/a0024338
- Haegens, S., Cousijn, H., Wallis, G., Harrison, P. J., and Nobre, A. C. (2014). Inter- and intra-individual variability in alpha peak frequency. *Neuroimage* 92, 46–55. doi: 10.1016/j.neuroimage.2014.01.049
- Halbleib, A., Gratkowski, M., Schwab, K., Ligges, C., Witte, H., and Hauelsen, J. (2012). Topographic analysis of engagement and disengagement of neural oscillators in photic driving: a combined

ACKNOWLEDGMENTS

We thank Fabian Popp for his help with data collection and Sylvana Insua-Rieger for proof-reading the manuscript.

- electroencephalogram/magnetoencephalogram study. *J. Clin. Neurophysiol.* 29, 33–41. doi: 10.1097/WNP.0b013e318246ad6e
- Hanslmayr, S., Aslan, A., Staudigl, T., Klimesch, W., Herrmann, C. S., and Bäuml, K.-H. (2007). Prestimulus oscillations predict visual perception performance between and within subjects. *Neuroimage* 37, 1465–1473. doi: 10.1016/j.neuroimage.2007.07.011
- Hanslmayr, S., Klimesch, W., Sauseng, P., Gruber, W., Doppelmayr, M., Freunberger, R., et al. (2005). Visual discrimination performance is related to decreased alpha amplitude but increased phase locking. *Neurosci. Lett.* 375, 64–68. doi: 10.1016/j.neulet.2004.10.092
- Helfrich, R. F., Schneider, T. R., Rach, S., Trautmann-Lengsfeld, S. A., Engel, A. K., and Herrmann, C. S. (2014). Entrainment of brain oscillations by transcranial alternating current stimulation. *Curr. Biol.* 24, 333–339. doi: 10.1016/j.cub.2013.12.041
- Herrmann, C. S. (2001). Human EEG responses to 1–100 Hz flicker: resonance phenomena in visual cortex and their potential correlation to cognitive phenomena. *Exp. Brain Res.* 137, 346–353. doi: 10.1007/s002210100682
- Herrmann, C. S., Strüber, D., Helfrich, R. F., and Engel, A. K. (2015). EEG oscillations: From correlation to causality. *Int. J. Psychophysiol.* [Epub ahead of print].
- Jensen, O., and Mazaheri, A. (2010). Shaping functional architecture by oscillatory alpha activity: gating by inhibition. *Front. Hum. Neurosci.* 4:186. doi: 10.3389/fnhum.2010.00186
- Keitel, C., Quigley, C., and Ruhnau, P. (2014). Stimulus-driven brain oscillations in the alpha range: entrainment of intrinsic rhythms or frequency-following response? *J. Neurosci.* 34, 10137–10140. doi: 10.1523/JNEUROSCI.1904-14.2014
- Klimesch, W. (2012). Alpha-band oscillations, attention, and controlled access to stored information. *Trends Cogn. Sci. (Regul. Ed.)* 16, 606–617. doi: 10.1016/j.tics.2012.10.007
- Klimesch, W., Sauseng, P., and Hanslmayr, S. (2007). EEG alpha oscillations: the inhibition-timing hypothesis. *Brain Res. Rev.* 53, 63–88. doi: 10.1016/j.brainresrev.2006.06.003
- Lakatos, P., Karmos, G., Mehta, A. D., Ulbert, I., and Schroeder, C. E. (2008). Entrainment of neuronal oscillations as a mechanism of attentional selection. *Science* 320, 110–113. doi: 10.1126/science.1154735
- Mathewson, K. E., Basak, C., Maclin, E. L., Low, K. A., Boot, W. R., Kramer, A. F., et al. (2012). Different slopes for different folks: alpha and delta EEG power predict subsequent video game learning rate and improvements in cognitive control tasks. *Psychophysiology* 49, 1558–1570. doi: 10.1111/j.1469-8986.2012.01474.x
- Mathewson, K. E., Fabiani, M., Gratton, G., Beck, D. M., and Lleras, A. (2010). Rescuing stimuli from invisibility: inducing a momentary release from visual masking with pre-target entrainment. *Cognition* 115, 186–191. doi: 10.1016/j.cognition.2009.11.010
- Mathewson, K. E., Lleras, A., Beck, D. M., Fabiani, M., Ro, T., and Gratton, G. (2011). Pulsed out of awareness: EEG alpha oscillations represent a pulsed-inhibition of ongoing cortical processing. *Front. Psychol.* 2:99. doi: 10.3389/fpsyg.2011.00099
- Mechler, F., Victor, J. D., Purpura, K. P., and Shapley, R. (1998). Robust temporal coding of contrast by V1 neurons for transient but not for steady-state stimuli. *J. Neurosci.* 18, 6583–6598.
- Müller, M. M., Malinowski, P., Gruber, T., and Hillyard, S. A. (2003). Sustained division of the attentional spotlight. *Nature* 424, 309–312. doi: 10.1038/nature01812
- Oldfield, R. C. (1971). The assessment and analysis of handedness: the Edinburgh inventory. *Neuropsychologia* 9, 97–113.

- Parkes, L. M., Fries, P., Kerskens, C. M., and Norris, D. G. (2004). Reduced BOLD response to periodic visual stimulation. *Neuroimage* 21, 236–243. doi: 10.1016/j.neuroimage.2003.08.025
- Pfurtscheller, G., and Aranibar, A. (1977). Event-related cortical desynchronization detected by power measurements of scalp EEG. *Electroencephalogr. Clin. Neurophysiol.* 42, 817–826.
- Pikovsky, A., Rosenblum, M., and Kurths, J. (2003). *Synchronization: A Universal Concept in Nonlinear Sciences, Vol. 12*. Cambridge, UK: Cambridge University Press.
- Regan, D. (1982). Comparison of transient and steady-state methods*. *Ann. N. Y. Acad. Sci.* 388, 45–71. doi: 10.1111/j.1749-6632.1982.tb50784.x
- Romei, V., Driver, J., Schyns, P. G., and Thut, G. (2011). Rhythmic TMS over parietal cortex links distinct brain frequencies to global versus local visual processing. *Curr. Biol.* 21, 334–337. doi: 10.1016/j.cub.2011.01.035
- Royston, P. (1993). A pocket-calculator algorithm for the Shapiro-Francia test for non-normality: an application to medicine. *Stat. Med.* 12, 181–184.
- Schroeder, C. E., and Lakatos, P. (2009). Low-frequency neuronal oscillations as instruments of sensory selection. *Trends Neurosci.* 32, 9–18. doi: 10.1016/j.tins.2008.09.012
- Schwab, K., Ligges, C., Jungmann, T., Hilgenfeld, B., Haueisen, J., and Witte, H. (2006). Alpha entrainment in human electroencephalogram and magnetoencephalogram recordings. *Neuroreport* 17, 1829–1833. doi: 10.1097/01.wnr.0000246326.89308.ec
- Spaak, E., de Lange, F. P., and Jensen, O. (2014). Local entrainment of alpha oscillations by visual stimuli causes cyclic modulation of perception. *J. Neurosci.* 34, 3536–3544. doi: 10.1523/JNEUROSCI.4385-13.2014
- Tass, P., Rosenblum, M. G., Weule, J., Kurths, J., Pikovsky, A., Volkman, J., et al. (1998). Detection of n:m phase locking from noisy data: application to magnetoencephalography. *Phys. Rev. Lett.* 81, 3291–3294. doi: 10.1103/PhysRevLett.81.3291
- Thut, G., Schyns, P. G., and Gross, J. (2011). Entrainment of perceptually relevant brain oscillations by non-invasive rhythmic stimulation of the human brain. *Front. Psychol.* 2:170. doi: 10.3389/fpsyg.2011.00170
- von Stein, A., and Sarnthein, J. (2000). Different frequencies for different scales of cortical integration: from local gamma to long range alpha/theta synchronization. *Int. J. Psychophysiol.* 38, 301–313. doi: 10.1016/S0167-8760(00)00172-0
- Widmann, A., and Schröger, E. (2012). Filter effects and filter artifacts in the analysis of electrophysiological data. *Front. Psychol.* 3:233. doi: 10.3389/fpsyg.2012.00233
- Worden, M. S., Foxe, J. J., Wang, N., and Simpson, G. V. (2000). Anticipatory biasing of visuospatial attention indexed by retinotopically specific α -band electroencephalography increases over occipital cortex. *J. Neurosci.* 20, RC63.
- Xu, P., Tian, C., Zhang, Y., Jing, W., Wang, Z., Liu, T., et al. (2013). Cortical network properties revealed by SSVEP in anesthetized rats. *Sci. Rep.* 3:2496. doi: 10.1038/srep02496
- Zaehle, T., Rach, S., and Herrmann, C. S. (2010). Transcranial alternating current stimulation enhances individual alpha activity in human EEG. *PLoS ONE* 5:e13766. doi: 10.1371/journal.pone.0013766

Conflict of Interest Statement: The authors declare that the research was conducted in the absence of any commercial or financial relationships that could be construed as a potential conflict of interest.

Copyright © 2016 Notbohm, Kurths and Herrmann. This is an open-access article distributed under the terms of the Creative Commons Attribution License (CC BY). The use, distribution or reproduction in other forums is permitted, provided the original author(s) or licensor are credited and that the original publication in this journal is cited, in accordance with accepted academic practice. No use, distribution or reproduction is permitted which does not comply with these terms.

EXHIBIT 22



Cortical entrainment to continuous speech: functional roles and interpretations

Nai Ding^{1*} and Jonathan Z. Simon^{2,3,4*}

¹ Department of Psychology, New York University, New York, NY, USA

² Department of Electrical and Computer Engineering, University of Maryland College Park, College Park, MD, USA

³ Department of Biology, University of Maryland College Park, College Park, MD, USA

⁴ Institute for Systems Research, University of Maryland College Park, College Park, MD, USA

Edited by:

Sonja A. E. Kotz, Max Planck Institute for Human Cognitive and Brain Sciences, Germany

Reviewed by:

István Winkler, University of Szeged, Hungary

Jonas Obleser, Max Planck Institute for Human Cognitive and Brain Sciences, Germany

*Correspondence:

Nai Ding, Department of Psychology, New York University, New York, NY 10012, USA

e-mail: gahding@gmail.com;

Jonathan Z. Simon, Department of Electrical and Computer Engineering, University of Maryland College Park, College Park, MD 20742, USA

e-mail: jzsimon@umd.edu

Auditory cortical activity is entrained to the temporal envelope of speech, which corresponds to the syllabic rhythm of speech. Such entrained cortical activity can be measured from subjects naturally listening to sentences or spoken passages, providing a reliable neural marker of online speech processing. A central question still remains to be answered about whether cortical entrained activity is more closely related to speech perception or non-speech-specific auditory encoding. Here, we review a few hypotheses about the functional roles of cortical entrainment to speech, e.g., encoding acoustic features, parsing syllabic boundaries, and selecting sensory information in complex listening environments. It is likely that speech entrainment is not a homogeneous response and these hypotheses apply separately for speech entrainment generated from different neural sources. The relationship between entrained activity and speech intelligibility is also discussed. A tentative conclusion is that theta-band entrainment (4–8 Hz) encodes speech features critical for intelligibility while delta-band entrainment (1–4 Hz) is related to the perceived, non-speech-specific acoustic rhythm. To further understand the functional properties of speech entrainment, a splitter's approach will be needed to investigate (1) not just the temporal envelope but what specific acoustic features are encoded and (2) not just speech intelligibility but what specific psycholinguistic processes are encoded by entrained cortical activity. Similarly, the anatomical and spectro-temporal details of entrained activity need to be taken into account when investigating its functional properties.

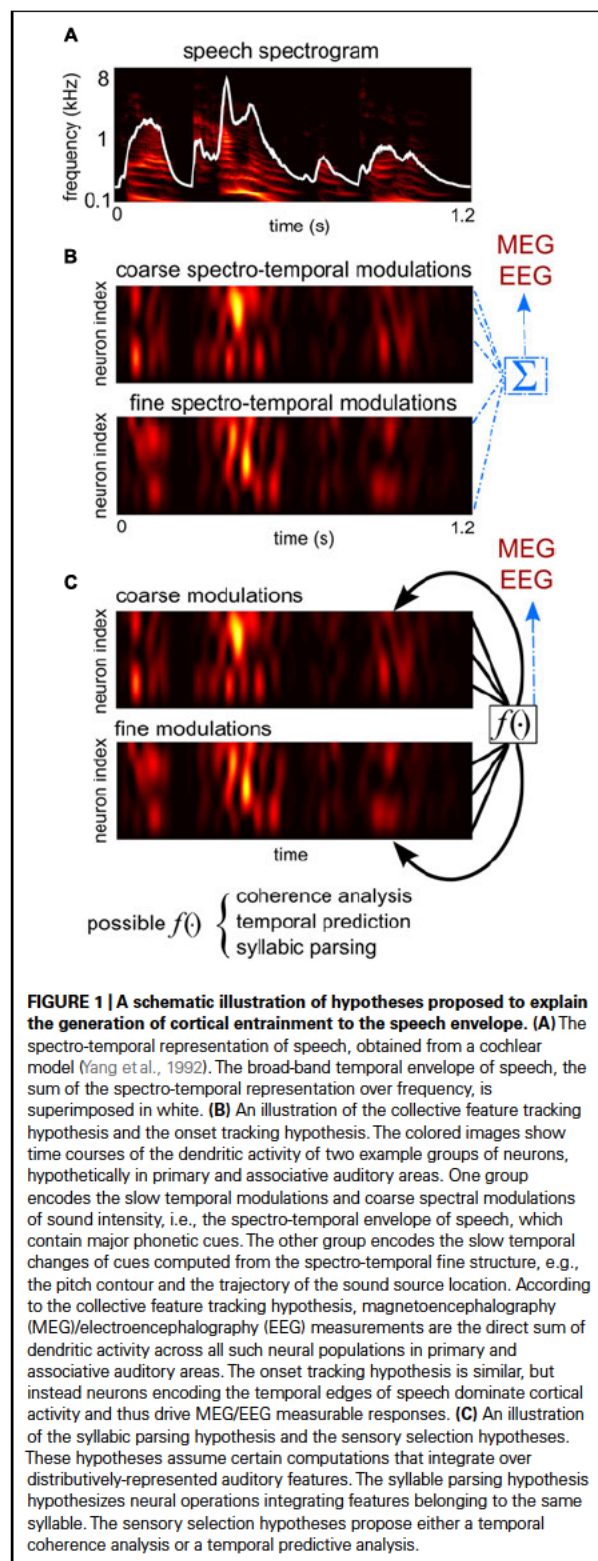
Keywords: auditory cortex, entrainment of rhythms, speech intelligibility, speech perception in noise, speech envelope, cocktail party problem

INTRODUCTION

Speech recognition is a process that maps an acoustic signal onto the underlying linguistic meaning. The acoustic properties of speech are complex and contain temporal dynamics on several time scales (Rosen, 1992; Chi et al., 2005). The time scale most critical for speech recognition is on the order of hundreds of milliseconds (1–10 Hz), and the temporal fluctuations on this time scale are usually called the *temporal envelope* (Figure 1A). Single neuron neurophysiology from animal models has shown that neurons in primary auditory cortex encode the analogous temporal envelope of other non-speech sounds by phase locked neural firing (Wang et al., 2003). In contrast, the finer scale acoustic properties that decide the pitch and timbre of speech at each time moment (acoustic fragments lasting a few 100 ms) are likely to be encoded using a spatial code, by either individual neurons (Bendor and Wang, 2005) or spatial patterns of cortical activity (Walker et al., 2011).

In the last decade or so, cortical entrainment to the temporal envelope of speech has been demonstrated in humans using magnetoencephalography (MEG; Ahissar et al., 2001; Luo and Poeppel, 2007), electroencephalography (EEG; Aiken and Picton, 2008), and electrocorticography (ECoG; Nourski et al., 2009). This envelope following response can be recorded from subjects

listening to sentences or spoken passages and therefore provides an online marker of neural processing of continuous speech. Envelope entrainment has mainly been seen in the waveform of low-frequency neural activity (<8 Hz) and in the power envelope of high-gamma activity (Pasley et al., 2012; Zion Golumbic et al., 2013). Although the phenomenon of envelope entrainment has been well established, its underlying neural mechanisms, and functional roles remain controversial. It is still under debate whether entrained cortical activity is more closely tied to the physical properties of the acoustic stimulus or to higher level language related processing that is directly related to speech perception. A number of studies have shown that cortical entrainment to speech is strongly modulated by top-down cognitive functions such as attention (Kerlin et al., 2010; Ding and Simon, 2012a; Mesgarani and Chang, 2012; Zion Golumbic et al., 2013) and therefore is not purely a bottom-up response. On the other hand, cortical entrainment to the sound envelope is seen for non-speech sound (Lalor et al., 2009; Hämäläinen et al., 2012; Millman et al., 2012; Wang et al., 2012; Steinschneider et al., 2013) and therefore does not rely on speech-specific neural processing. In this article, we first summarize a number of hypotheses about the functional roles of envelope entrainment, and then review the literature about how envelope entrainment is affected by speech intelligibility.



FUNCTIONAL ROLES OF CORTICAL ENTRAINMENT

A number of hypotheses have been proposed about what aspects of speech, ranging from its acoustic features to its linguistic meaning, are encoded by entrained cortical activity. A few dominant hypotheses are summarized and compared (Table 1). Other unresolved questions about cortical neural entrainment, e.g., what the biophysical mechanisms generating cortical entrainment are, and whether entrained neural activity is related to spontaneous neural oscillations, are not covered here (see discussions in e.g., Schroeder and Lakatos, 2009; Howard and Poeppel, 2012; Ding and Simon, 2013b).

ONSET TRACKING HYPOTHESIS

Speech is dynamic and is full of acoustic “edges,” e.g., onsets and offsets. These edges usually occur at syllable boundaries and are well characterized by the speech envelope. It is well known that a reliable macroscopic brain response can be evoked by an acoustic edge. Therefore, it has been proposed that neural entrainment to the speech envelope is a superposition of discrete, edge/onset related brain responses (Howard and Poeppel, 2010). Consistent with this hypothesis, it has been shown that the sharpness of acoustic edges, i.e., how quickly sound intensity increases, strongly influences cortical tracking of the sound envelope (Prendergast et al., 2010; Doelling et al., 2014). A challenge of this hypothesis, however, is that speech is continuously changing and it remains a problem as to which acoustic transients can be counted as edges.

If this hypothesis is true, a question naturally follows about whether envelope entrainment can provide insights that cannot be learned using the traditional event-related response approach. The answer is yes. Cortical responses, including edge/onset related auditory evoked responses, are stimulus-dependent, and quickly adapt to the spectro-temporal structure of the stimulus (Zacharias et al., 2012; Herrmann et al., 2014). Therefore, even if envelope entrainment is just a superposition of event-related responses, it can still provide insights about the properties of cortical activity when it is adapted to the acoustic properties of speech.

COLLECTIVE FEATURE TRACKING HYPOTHESIS

When sound enters the ear, it is decomposed into narrow frequency bands in the auditory periphery and is further decomposed into multi-scale acoustic features in the central auditory system, such as pitch, sound source location information, and coarse spectro-temporal modulations (Shamma, 2001; Ghitza et al., 2012). In speech, most acoustic features coherently fluctuate in time and these coherent fluctuations are captured by the speech envelope. If a neuron or a neural population encodes an acoustic feature, its activity is synchronized to the strength of that acoustic feature. As a result, neurons or neural networks that are tuned to coherently fluctuating speech features are activated coherently (Shamma et al., 2011).

Analogously to the speech envelope being the summation of the power of all speech features at each time moment, the large-scale neural entrainment to speech measured by MEG/EEG can be the summation of neural activity tracking different acoustic features of speech (Figure 1B). It is therefore plausible to hypothesize that macroscopic speech entrainment is a passive summation of microscopic neural tracking of acoustic features

Table 1 | A summary of major hypotheses about the functional roles of cortical entrainment to speech.

Hypothesis	Underlying neural computations	Reference
Onset tracking	Temporal edge detection	Howard and Poeppel (2010)
Collective feature tracking	Spectro-temporal feature coding	Ding and Simon (2012b), Ghitza et al. (2012)
Syllabic parsing	Binding features of the same syllable; discretization	Giraud and Poeppel (2012), Ghitza (2013)
Sensory selection I	Temporal coherence-based binding of auditory features	Shamma et al. (2011), Ding and Simon (2012a)
Sensory selection II	Modulation of neuronal excitability; temporal prediction	Schroeder and Lakatos (2009)

across neurons/networks (Ding and Simon, 2012b). Based on this hypothesis, the MEG/EEG speech entrainment is a marker of a collective cortical representation of speech but does not play any additional roles in regulating neuronal activity.

The onset tracking hypothesis can be viewed as a special case of the collective feature tracking hypothesis, when the acoustic features driving cortical responses are restricted to a set of discrete edges. The collective feature tracking hypothesis, however, is more general since it allows features to be continuously changing and also incorporates features that are not associated with sharp intensity changes, such as changes in the pitch contour (Obleser et al., 2012), and sound source location. Under the onset tracking hypothesis, entrained neural activity is a superposition of onset/edge-related auditory evoked responses. Under the more general collective feature tracking hypothesis, at a first-order approximation, entrained activity is a convolution between speech features, e.g., the temporal envelopes in different narrow frequency bands, and the corresponding response functions, e.g., the response evoked by a very brief tone pip in the corresponding frequency band (Lalor et al., 2009; Ding and Simon, 2012b).

SYLLABIC PARSING HYPOTHESIS

During speech recognition, the listener must segment a continuous acoustic signal into a sequence of discrete linguistic symbols, into the units of, e.g., phonemes, syllables or words. The boundaries between phonemes, and especially syllables, are relatively well encoded by the speech envelope (Stevens, 2002; Ghitza, 2013, see also Cummins, 2012). Furthermore, the average syllabic rate ranges between 5 and 8 Hz across languages (Pellegrino et al., 2011) and the rate for stressed syllables is below 4 Hz for English (Greenberg et al., 2003). Therefore it has been hypothesized that neural entrainment to the speech envelope plays a role in creating a syllabic level, discrete, representation of speech (Giraud and Poeppel, 2012). In particular, it has been hypothesized that each cycle of the cortical theta oscillation (4–8 Hz) is aligned to the portion of speech signal in between of two vowels, corresponding to two adjacent peaks in the speech envelope. Auditory features within a cycle of theta oscillation are then used to decode the phonetic information of speech (Ghitza, 2011, 2013). Therefore, according to this hypothesis, speech entrainment does not only passively track acoustic features but also reflects the language-based packaging of speech into syllable size chunks. Since syllables play different roles in segmenting syllable-timed language and stress-timed language (Cutler et al., 1986), further cross-language research may

further elucidate which of these neural processes are represented in envelope tracking activity.

SENSORY SELECTION HYPOTHESIS

In everyday listening environments, speech is often embedded in a complex acoustic background. Therefore, to understand speech, a listener must segregate speech from the listening background and process it selectively. A useful strategy for the brain would be to find and selectively process moments in time (or spectro-temporal instances in a more general framework) that are dominated by speech and ignore the moments dominated by the background (Wang, 2005; Cooke, 2006). In other words, the brain might robustly encode speech by taking glimpses at the temporal (or spectro-temporal) features that contain critical speech information. The rhythmicity of speech (Schroeder and Lakatos, 2009; Giraud and Poeppel, 2012), and the temporal coherence between acoustic features (Shamma et al., 2011), are both reflected by the speech envelope and so become critical cues for the brain to decide where the useful speech information lies. Therefore, envelope entrainment may play a critical role in the neural segregation of speech and the listening background.

In a complex listening environment, cortical entrainment to speech has been found to be largely invariant to the listening background (Ding and Simon, 2012a; Ding and Simon, 2013a). Two possible functional roles have been hypothesized for the observed background-invariant envelope entrainment. One is that the brain uses temporal coherence to bind together acoustic features belonging to the same speech stream and envelope entrainment may reflect computations related to this coherence analysis (Shamma et al., 2011; Ding and Simon, 2012a). The other is that envelope entrainment is used by the brain to predict which moments contain more information about speech than the acoustic background and then guide the brain to selectively process those moments (Schroeder et al., 2008; Schroeder and Lakatos, 2009; Zion Golumbic et al., 2012).

WHICH HYPOTHESIS IS TRUE? AN ANALYSIS-BY-SYNTHESIS ACCOUNT OF SPEECH PROCESSING

Speech processing is a complicated process that can be roughly divided into an analysis stage and a synthesis stage. In the analysis stage, speech sounds are decomposed into primitive auditory features, a process that starts from the cochlea and applies mostly equally to the auditory encoding of both speech and non-speech sounds. A later synthesis stage, in contrast, combines multiple

auditory features to create speech perception, including, e.g., binding spectro-temporal cues to determine phonemic categories, or integrating multiple acoustic cues to segregate a target speech stream from an acoustic background. The onset tracking hypothesis and the collective feature tracking hypothesis both view speech entrainment as a passive auditory encoding mechanism belonging to the analysis stage. Note, however, that the analysis stage does include some integration over separately represented features also. For example, neural processing of pitch and spectral modulations requires integrating information across frequency. Functionally, however, the purpose of integrating features in the analysis stage is to extract higher level auditory features rather than to construct linguistic/perceptual entities.

The syllabic parsing hypothesis and the sensory selection hypothesis propose functional roles of cortical entrainment in the synthesis stage. They hypothesize that cortical entrainment is involved in combining features into linguistic units, e.g., syllables, or perceptual units, e.g., speech streams (**Figure 1C**). These additional functional roles may be implemented in two ways: an active mechanism would be one that entrained cortical activity, as a large-scale voltage fluctuation, directly regulating syllabic parsing or sensory selection (Schroeder et al., 2008; Schroeder and Lakatos, 2009). A passive mechanism would be one where neural computations related to syllabic parsing or sensory selection would generate spatially coherent neural signals that are measurable by macroscopic recording tools.

Although clearly distinctive from each other, the four hypotheses may all be true for different functional areas of the brain and describe different neural generators for speech entrainment. Onset detection, feature tracking, syllabic parsing, and sensory selection are all neural computations necessary for speech recognition and all of them are likely to be synchronized to the speech rhythm carried by the envelope. Therefore, these neural computations may all be reflected by cortical entrainment to speech, and may only differ in their fine-scale neural generators. It remains unclear, however, whether these fine-scale neural generators can be resolved by macroscopic recording tools such as MEG and EEG.

Future studies are needed to explicitly test these hypotheses, or explicitly modify them, to determine which specific acoustic features and which specific psycholinguistic processes are relevant to cortical entrainment. For example, to dissociate the onset tracking hypothesis and the collective feature tracking hypothesis, one approach is to create explicit computational models for them and test which model would fit the data better. To test the syllabic parsing hypothesis, it will be important to calculate the correlation between cortical entrainment and relevant behavioral measures, e.g., misallocation of syllable boundaries (Woodfield and Akeroyd, 2010). To test the sensory selection hypothesis, stimuli that vary in their temporal probability or coherence among spectro-temporal features are likely to be revealing.

ENVELOPE ENTRAINMENT AND SPEECH INTELLIGIBILITY ENTRAINMENT AND ACOUSTIC MANIPULATION OF SPEECH

As indicated by its name, envelope entrainment is correlated with the speech envelope, an acoustic property of speech. Nevertheless, neural encoding of speech must underlie the ultimate goal of

decoding its meaning. Therefore, it is critical to identify if cortical entrainment to speech is related to any behavioral measure during speech recognition, such as speech intelligibility.

A number of studies have compared cortical activity entrained to intelligible speech and unintelligible speech. One approach is to vary the acoustic stimulus and analyze how cortical entrainment changes within individual subjects. Some studies have found that cortical entrainment to normal sentences is similar to cortical entrainment to sentences that are played backward in time (Howard and Poeppel, 2010; Peña and Melloni, 2012; though see Gross et al., 2013).

A second way to reduce intelligibility is to introduce different types of acoustic interference. When speech is presented together with stationary noise, delta-band (1–4 Hz) cortical entrainment to the speech is found to be robust to noise until the listeners can barely hear speech, while theta-band (4–8 Hz) entrainment decreases gradually as the noise level increases (Ding and Simon, 2013a). In this way, theta-band entrainment is correlated with noise level and also speech intelligibility, but delta-band entrainment is not. When speech is presented together with a competing speech stream, cortical entrainment is found to be robust against the level of the competing speech stream even though intelligibility drops (Ding and Simon, 2012a; theta- and delta-band activity was not analyzed separately there).

A third way to reduce speech intelligibility is to degrade the spectral resolution through noise-vocoding, which destroys spectro-temporal fine structure but preserves the temporal envelope (Shannon et al., 1995). When the spectral resolution of speech decreases, it has been shown that theta-band cortical entrainment reduces (Peelle et al., 2013; Ding et al., 2014) but delta-band entrainment enhances (Ding et al., 2014). In contrast, when background noise is added to speech and the speech-noise mixture is noise vocoded, it is found that both delta- and theta-band entrainment is reduced by vocoding (Ding et al., 2014).

A fourth way to vary speech intelligibility is to directly manipulate the temporal envelope (Doelling et al., 2014). When the temporal envelope in the delta-theta frequency range is corrupted, cortical entrainment in the corresponding frequency bands degrades and so does speech intelligibility. When a processed speech envelope is used to modulate a broadband noise carrier, the stimulus is not intelligible but reliable cortical entrainment is nevertheless seen.

In many of these studies investigating the correlation between cortical entrainment and intelligibility, a common issue is that stimuli which differ in intelligibility also differ in acoustic properties. This makes it difficult to determine if changes in cortical entrainment arise from changes in speech intelligibility or from changes in acoustic properties. For example, speech syllables generally have a sharper onset than offset, so reversing speech in time changes those temporal characteristics. Similarly, when the spectral resolution is reduced, neurons tuned to fine spectral features are likely to be deactivated. Therefore, based on the studies reviewed here, it can only be tentatively concluded that, when critical speech features are manipulated, speech intelligibility, and theta-band entrainment are affected in similar ways while delta-band entrainment is not. It remains unclear about

whether speech intelligibility causally modulates cortical entrainment or that auditory encoding, reflected by cortical entrainment, influences downstream language processing and therefore become indirectly related to intelligibility.

VARIABILITY BETWEEN LISTENERS

A second approach to address the correlation between neural entrainment and speech intelligibility is to investigate the variability across listeners. Peña and Melloni (2012) compared neural responses in listeners who speak the tested language and listeners who do not speak the tested language. It was found that language understanding does not significantly change the low-frequency neural responses, but it does change high-gamma band neural activity. Within the group of native speakers, the intelligibility score still varied broadly in the challenging listening conditions. Delta-band, but not theta-band, cortical entrainment has been shown to correlate with intelligibility scores for individual listeners in a number of studies (Ding and Simon, 2013a; Ding et al., 2014; Doelling et al., 2014). The advantage of investigating inter-subject variability is that it avoids modifications of the sound stimuli. Nevertheless, it still cannot identify whether the individual differences in speech recognition arise from the individual differences in auditory processing (Ruggles et al., 2011), language related processing, or cognitive control.

The speech intelligibility approach in general, suffers from a drawback that it is the end point of the entire speech recognition chain, and is not targeted at specific linguistic computations, e.g., allocating the boundaries between syllables. Furthermore, when the acoustic properties of speech are degraded, speech recognition requires additional cognitive control and the involved neural processing networks adapt (Du et al., 2011; Wild et al., 2012; Erb et al., 2013; Lee et al., 2014). Therefore, just from a change in speech intelligibility, it is difficult to trace what kinds of neural processing are affected.

DISTINCTIONS BETWEEN DELTA- AND THETA-BAND ENTRAINMENT

In summary of these different approaches, when the acoustic properties of speech are manipulated, theta-band entrainment often shows changes that correlate with speech intelligibility. For the same stimulus, however, the speech intelligibility measured from individual listeners is often correlated with delta-band entrainment. To explain this dichotomy, here we hypothesize that theta-band entrainment encodes syllabic-level acoustic features critical for speech recognition, while delta-band entrainment is more closely related to the perceived acoustic rhythm rather than the phonemic information of speech. This hypothesis is also consistent with the fact that speech modulations between 4 and 8 Hz are critical for intelligibility (Drullman et al., 1994a,b; Elliott and Theunissen, 2009) while temporal modulations below 4 Hz include prosodic information of speech (Goswami and Leong, 2013) and it is the frequency range important for music rhythm perception (Patel, 2008; Farbood et al., 2013).

ENVELOPE ENTRAINMENT TO NON-SPEECH SOUNDS

Although speech envelope entrainment may show correlated changes with speech intelligibility when the acoustic properties

of speech are manipulated, speech intelligibility is probably not a major driving force for envelope entrainment. A critical evidence is that envelope entrainment can be observed for non-speech sounds in humans and both speech and non-speech sounds in animals. Here, we briefly review human studies on envelope entrainment for non-speech sounds (see e.g., Steinschneider et al., 2013 for a comparison between envelope entrainment in human and animal models).

Traditionally, envelope entrainment has been studied using the auditory steady-state response (aSSR), a periodic neural response tracking the stimulus repetition rate or modulation rate. An aSSR at a given frequency can be elicited by, e.g., a click or tone-pip train repeating at the same frequency (Nourski et al., 2009; Xiang et al., 2010), and by amplitude or frequency modulation at that frequency (Picton et al., 1987; Ross et al., 2000; Wang et al., 2012). Although the cortical aSSR can be elicited in a broad frequency range (up to ~100 Hz), speech envelope entrainment is likely to be related to the slow aSSR in the corresponding frequency range, i.e., below 10 Hz (see Picton, 2007 for a review of the robust aSSR of 40 Hz and above). More recently, cortical entrainment has also been demonstrated for sounds modulated by an irregular envelope (Lalor et al., 2009). Low-frequency (<10 Hz) cortical entrainment to non-speech sound shares many properties with cortical entrainment to speech. For example, when envelope entrainment is modeled using a linear system-theoretic model, the neural response is qualitatively similar for speech (Power et al., 2012) and amplitude-modulated tones (Lalor et al., 2009). Furthermore, low-frequency (<10 Hz) cortical entrainment to non-speech sound is also strongly modulated by attention (Elhilali et al., 2009; Power et al., 2010; Xiang et al., 2010), and the phase of entrained activity is predictive of listeners' performance in some sound-feature detection tasks (Henry and Obleser, 2012; Ng et al., 2012).

SUMMARY

Cortical entrainment to the speech envelope provides a powerful tool to investigate online neural processing of continuous speech. It greatly extends the traditional event-related approach that can only be applied to analyze the response to isolated syllables or words. Although envelope entrainment has attracted researchers' attention in the last decade, it is still a less well-characterized cortical response than event-related responses. The basic phenomenon of envelope entrainment has been reliably seen in EEG, MEG, and ECoG, even at the single-trial level (Ding and Simon, 2012a; O'Sullivan et al., 2014). Hypotheses have been proposed about the neural mechanisms generating cortical entrainment and its functional roles, but these hypotheses remain to be explicitly tested. To test these hypotheses, a computational modeling approach is likely to be effective. For example, rather than just calculating the correlation between neural activity and the speech envelope, more explicit computational models can be proposed and used to fit the data (e.g., Ding and Simon, 2013a). Furthermore, to understand what linguistic computations are achieved by entrained cortical activity, more fine-scaled behavioral measures are likely to be required, e.g., measures related to syllable boundary allocation rather than the general measure of intelligibility. Finally, the

anatomical, temporal, and spectral specifics of cortical entrainment should be taken into account when discussing its functional roles (Peña and Melloni, 2012; Zion Golumbic et al., 2013; Ding et al., 2014).

AUTHOR CONTRIBUTIONS

Nai Ding and Jonathan Z. Simon wrote and approved the paper.

ACKNOWLEDGMENT

The work is supported by NIH grant R01 DC 008342.

REFERENCES

- Ahissar, E., Nagarajan, S., Ahissar, M., Protopapas, A., Mahncke, H., and Merzenich, M. M. (2001). Speech comprehension is correlated with temporal response patterns recorded from auditory cortex. *Proc. Natl. Acad. Sci. U.S.A.* 98, 13367–13372. doi: 10.1073/pnas.201400998
- Aiken, S. J., and Picton, T. W. (2008). Human cortical responses to the speech envelope. *Ear Hear.* 29, 139–157. doi: 10.1097/AUD.0b013e31816453dc
- Bendor, D., and Wang, X. (2005). The neuronal representation of pitch in primate auditory cortex. *Nature* 436, 1161–1165. doi: 10.1038/nature03867
- Chi, T., Ru, P., and Shamma, S. A. (2005). Multiresolution spectrotemporal analysis of complex sounds. *J. Acoust. Soc. Am.* 118, 887–906. doi: 10.1121/1.1945807
- Cooke, M. (2006). A glimpsing model of speech perception in noise. *J. Acoust. Soc. Am.* 119, 1562–1573. doi: 10.1121/1.2166600
- Cummins, F. (2012). Oscillators and syllables: a cautionary note. *Front. Psychol.* 3:364. doi: 10.3389/fpsyg.2012.00364
- Cutler, A., Mehler, J., Norris, D., and Segui, J. (1986). The syllable's differing role in the segmentation of French and English. *J. Mem. Lang.* 25, 385–400. doi: 10.1016/0749-596X(86)90033-1
- Ding, N., Chatterjee, M., and Simon, J. Z. (2014). Robust cortical entrainment to the speech envelope relies on the spectro-temporal fine structure. *Neuroimage* 88C, 41–46. doi: 10.1016/j.neuroimage.2013.10.054 [Epub ahead of print].
- Ding, N., and Simon, J. Z. (2012a). Emergence of neural encoding of auditory objects while listening to competing speakers. *Proc. Natl. Acad. Sci. U.S.A.* 109, 11854–11859. doi: 10.1073/pnas.1205381109
- Ding, N., and Simon, J. Z. (2012b). Neural coding of continuous speech in auditory cortex during monaural and dichotic listening. *J. Neurophysiol.* 107, 78–89. doi: 10.1152/jn.00297.2011
- Ding, N., and Simon, J. Z. (2013a). Adaptive temporal encoding leads to a background-insensitive cortical representation of speech. *J. Neurosci.* 33, 5728–5735. doi: 10.1523/JNEUROSCI.5297-12.2013
- Ding, N., and Simon, J. Z. (2013b). Power and phase properties of oscillatory neural responses in the presence of background activity. *J. Comput. Neurosci.* 34, 337–343. doi: 10.1007/s10827-012-0424-6
- Doelling, K., Arnal, L., Ghitza, O., and Poeppel, D. (2014). Acoustic landmarks drive delta-theta oscillations to enable speech comprehension by facilitating perceptual parsing. *Neuroimage* 85, 761–768. doi: 10.1016/j.neuroimage.2013.06.035
- Drullman, R., Festen, J. M., and Plomp, R. (1994a). Effect of reducing slow temporal modulations on speech reception. *J. Acoust. Soc. Am.* 95, 2670–2680. doi: 10.1121/1.409836
- Drullman, R., Festen, J. M., and Plomp, R. (1994b). Effect of temporal envelope smearing on speech reception. *J. Acoust. Soc. Am.* 95, 1053–1064. doi: 10.1121/1.408467
- Du, Y., He, Y., Ross, B., Bardouille, T., Wu, X., Li, L., et al. (2011). Human auditory cortex activity shows additive effects of spectral and spatial cues during speech segregation. *Cereb. Cortex* 21, 698–707. doi: 10.1093/cercor/bhq136
- Elhilali, M., Xiang, J., Shamma, S. A., and Simon, J. Z. (2009). Interaction between attention and bottom-up saliency mediates the representation of foreground and background in an auditory scene. *PLoS Biol.* 7:e1000129. doi: 10.1371/journal.pbio.1000129
- Elliott, T., and Theunissen, F. (2009). The modulation transfer function for speech intelligibility. *PLoS Comput. Biol.* 5:e1000302. doi: 10.1371/journal.pcbi.1000302
- Erb, J., Henry, M. J., Eisner, F., and Obleser, J. (2013). The brain dynamics of rapid perceptual adaptation to adverse listening conditions. *J. Neurosci.* 33, 10688–10697. doi: 10.1523/JNEUROSCI.4596-12.2013
- Farbood, M. M., Marcus, G., and Poeppel, D. (2013). Temporal dynamics and the identification of musical key. *J. Exp. Psychol. Hum. Percept. Perform.* 39, 911–918. doi: 10.1037/a0031087
- Ghitza, O. (2011). Linking speech perception and neurophysiology: speech decoding guided by cascaded oscillators locked to the input rhythm. *Front. Psychol.* 2:130. doi: 10.3389/fpsyg.2011.00130
- Ghitza, O. (2013). The theta-syllable: a unit of speech information defined by cortical function. *Front. Psychol.* 4:138. doi: 10.3389/fpsyg.2013.00138
- Ghitza, O., Giraud, A.-L., and Poeppel, D. (2012). Neuronal oscillations and speech perception: critical-band temporal envelopes are the essence. *Front. Hum. Neurosci.* 6:340. doi: 10.3389/fnhum.2012.00340
- Giraud, A.-L., and Poeppel, D. (2012). Cortical oscillations and speech processing: emerging computational principles and operations. *Nat. Neurosci.* 15, 511–517. doi: 10.1038/nn.3063
- Goswami, U., and Leong, V. (2013). Speech rhythm and temporal structure: converging perspectives? *Lab. Phonol.* 4, 67–92. doi: 10.1515/lp-2013-0004
- Greenberg, S., Carvey, H., Hitchcock, L., and Chang, S. (2003). Temporal properties of spontaneous speech – a syllable-centric perspective. *J. Phon.* 31, 465–485. doi: 10.1016/j.wocn.2003.09.005
- Gross, J., Hoogenboom, N., Thut, G., Schyns, P., Panzeri, S., Belin, P., et al. (2013). Speech rhythms and multiplexed oscillatory sensory coding in the human brain. *PLoS Biol.* 11:e1001752. doi: 10.1371/journal.pbio.1001752
- Hämäläinen, J. A., Rupp, A., Soltész, F., Szűcs, D., and Goswami, U. (2012). Reduced phase locking to slow amplitude modulation in adults with dyslexia: an MEG study. *Neuroimage* 59, 2952–2961. doi: 10.1016/j.neuroimage.2011.09.075
- Henry, M. J., and Obleser, J. (2012). Frequency modulation entrains slow neural oscillations and optimizes human listening behavior. *Proc. Natl. Acad. Sci. U.S.A.* 109, 20095–20100. doi: 10.1073/pnas.1213390109
- Herrmann, B., Schlichting, N., and Obleser, J. (2014). Dynamic range adaptation to spectral stimulus statistics in human auditory cortex. *J. Neurosci.* 34, 327–331. doi: 10.1523/JNEUROSCI.3974-13.2014
- Howard, M. F., and Poeppel, D. (2010). Discrimination of speech stimuli based on neuronal response phase patterns depends on acoustics but not comprehension. *J. Neurophysiol.* 104, 2500–2511. doi: 10.1152/jn.00251.2010
- Howard, M. F., and Poeppel, D. (2012). The neuromagnetic response to spoken sentences: co-modulation of theta band amplitude and phase. *Neuroimage* 60, 2118–2127. doi: 10.1016/j.neuroimage.2012.02.028
- Kerlin, J. R., Shahin, A. J., and Miller, L. M. (2010). Attentional gain control of ongoing cortical speech representations in a “cocktail party”. *J. Neurosci.* 30, 620–628. doi: 10.1523/JNEUROSCI.3631-09.2010
- Lalor, E. C., Power, A. J., Reilly, R. B., and Foxe, J. J. (2009). Resolving precise temporal processing properties of the auditory system using continuous stimuli. *J. Neurophysiol.* 102, 349–359. doi: 10.1152/jn.90896.2008
- Lee, A. K., Larson, E., Maddox, R. K., and Shinn-Cunningham, B. G. (2014). Using neuroimaging to understand the cortical mechanisms of auditory selective attention. *Hear. Res.* 307, 111–120. doi: 10.1016/j.heares.2013.06.010
- Luo, H., and Poeppel, D. (2007). Phase patterns of neuronal responses reliably discriminate speech in human auditory cortex. *Neuron* 54, 1001–1010. doi: 10.1016/j.neuron.2007.06.004
- Mesgarani, N., and Chang, E. F. (2012). Selective cortical representation of attended speaker in multi-talker speech perception. *Nature* 485, 233–236. doi: 10.1038/nature11020
- Millman, R. E., Prendergast, G., Hymers, M., and Green, G. G. (2012). Representations of the temporal envelope of sounds in human auditory cortex: can the results from invasive intracortical “depth” electrode recordings be replicated using non-invasive MEG “virtual electrodes”? *Neuroimage* 64, 185–196. doi: 10.1016/j.neuroimage.2012.09.017
- Ng, B. S. W., Schroeder, T., and Kayser, C. (2012). A precluding but not ensuring role of entrained low-frequency oscillations for auditory perception. *J. Neurosci.* 32, 12268–12276. doi: 10.1523/JNEUROSCI.1877-12.2012
- Nourski, K. V., Reale, R. A., Oya, H., Kawasaki, H., Kovach, C. K., Chen, H., et al. (2009). Temporal envelope of time-compressed speech represented in the human auditory cortex. *J. Neurosci.* 29, 15564–15574. doi: 10.1523/JNEUROSCI.3065-09.2009

- Obleser, J., Herrmann, B., and Henry, M. J. (2012). Neural oscillations in speech: don't be enslaved by the envelope. *Front. Hum. Neurosci.* 6:250. doi: 10.3389/fnhum.2012.00250
- O'Sullivan, J. A., Power, A. J., Mesgarani, N., Rajaram, S., Foxe, J. J., Shinn-Cunningham, B. G., et al. (2014). Attentional selection in a cocktail party environment can be decoded from single-trial EEG. *Cereb. Cortex*. doi: 10.1093/cercor/bht355
- Pasley, B. N., David, S. V., Mesgarani, N., Flinker, A., Shamma, S. A., Crone, N. E., et al. (2012). Reconstructing speech from human auditory cortex. *PLoS Biol.* 10:e1001251. doi: 10.1371/journal.pbio.1001251
- Patel, A. D. (2008). *Music, Language, and the Brain*. New York, NY: Oxford University Press.
- Peelle, J. E., Gross, J., and Davis, M. H. (2013). Phase-locked responses to speech in human auditory cortex are enhanced during comprehension. *Cereb. Cortex* 23, 1378–1387. doi: 10.1093/cercor/bhs118
- Pellegrino, F., Coupé, C., and Marsico, E. (2011). Across-language perspective on speech information rate. *Language* 87, 539–558. doi: 10.1353/lan.2011.0057
- Peña, M., and Melloni, L. (2012). Brain oscillations during spoken sentence processing. *J. Cogn. Neurosci.* 24, 1149–1164. doi: 10.1162/jocn_a_00144
- Picton, T. W. (2007). "Audiometry using auditory steady-state responses," in *Auditory Evoked Potentials: Basic Principles and Clinical Application*, eds. R. F. Burkard, J. J. Eggermont, and M. Don (Baltimore: Lippincott Williams & Wilkins), 441–462.
- Picton, T. W., Skinner, C. R., Champagne, S. C., Kellett, A. J. C., and Maiste, A. C. (1987). Potentials evoked by the sinusoidal modulation of the amplitude or frequency of a tone. *J. Acoust. Soc. Am.* 82, 165–178. doi: 10.1121/1.395560
- Power, A. J., Foxe, J. J., Forde, E. J., Reilly, R. B., and Lalor, E. C. (2012). At what time is the cocktail party? A late locus of selective attention to natural speech. *Eur. J. Neurosci.* 35, 1497–1503. doi: 10.1111/j.1460-9568.2012.08060.x
- Power, A. J., Lalor, E. C., and Reilly, R. B. (2010). Endogenous auditory spatial attention modulates obligatory sensory activity in auditory cortex. *Cereb. Cortex* 21, 1223–1230. doi: 10.1093/cercor/bhq233
- Prendergast, G., Johnson, S. R., and Green, G. G. (2010). Temporal dynamics of sinusoidal and non-sinusoidal amplitude modulation. *Eur. J. Neurosci.* 32, 1599–1607. doi: 10.1111/j.1460-9568.2010.07423.x
- Rosen, S. (1992). Temporal information in speech: acoustic, auditory and linguistic aspects. *Philos. Trans. R. Soc. Lond. B Biol. Sci.* 336, 367–373. doi: 10.1098/rstb.1992.0070
- Ross, B., Borgmann, C., Draganova, R., Roberts, L. E., and Pantev, C. (2000). A high-precision magnetoencephalographic study of human auditory steady-state responses to amplitude-modulated tones. *J. Acoust. Soc. Am.* 108, 679–691. doi: 10.1121/1.429600
- Ruggles, D., Bharadwaj, H., and Shinn-Cunningham, B. G. (2011). Normal hearing is not enough to guarantee robust encoding of suprathreshold features important in everyday communication. *Proc. Natl. Acad. Sci. U.S.A.* 108, 15516–15521. doi: 10.1073/pnas.1108912108
- Schroeder, C. E., and Lakatos, P. (2009). Low-frequency neuronal oscillations as instruments of sensory selection. *Trends Neurosci.* 32, 9–18. doi: 10.1016/j.tins.2008.09.012
- Schroeder, C. E., Lakatos, P., Kajikawa, Y., Partan, S., and Puce, A. (2008). Neuronal oscillations and visual amplification of speech. *Trends Cogn. Sci.* 12, 106–113. doi: 10.1016/j.tics.2008.01.002
- Shamma, S. (2001). On the role of space and time in auditory processing. *Trends Cogn. Sci.* 5, 340–348. doi: 10.1016/S1364-6613(00)01704-6
- Shamma, S. A., Elhilali, M., and Micheyl, C. (2011). Temporal coherence and attention in auditory scene analysis. *Trends Neurosci.* 34, 114–123. doi: 10.1016/j.tins.2010.11.002
- Shannon, R. V., Zeng, F.-G., Kamath, V., Wygonski, J., and Ekelid, M. (1995). Speech recognition with primarily temporal cues. *Science* 270, 303–304. doi: 10.1126/science.270.5234.303
- Steinschneider, M., Nourski, K. V., and Fishman, Y. I. (2013). Representation of speech in human auditory cortex: is it special? *Hear. Res.* 305, 57–73. doi: 10.1016/j.heares.2013.05.013
- Stevens, K. N. (2002). Toward a model for lexical access based on acoustic landmarks and distinctive features. *J. Acoust. Soc. Am.* 111, 1872–1891. doi: 10.1121/1.1458026
- Walker, K. M., Bizley, J. K., King, A. J., and Schnupp, J. W. (2011). Multiplexed and robust representations of sound features in auditory cortex. *J. Neurosci.* 31, 14565–14576. doi: 10.1523/JNEUROSCI.2074-11.2011
- Wang, D. (2005). "On ideal binary mask as the computational goal of auditory scene analysis," in *Speech Separation By Humans and Machines*, ed. P. Divenyi (New York: Springer), 181–197.
- Wang, X., Lu, T., and Liang, L. (2003). Cortical processing of temporal modulations. *Speech Commun.* 41, 107–121. doi: 10.1016/S0167-6393(02)00097-3
- Wang, Y., Ding, N., Ahmar, N., Xiang, J., Poeppel, D., and Simon, J. Z. (2012). Sensitivity to temporal modulation rate and spectral bandwidth in the human auditory system: MEG evidence. *J. Neurophysiol.* 107, 2033–2041. doi: 10.1152/jn.00310.2011
- Wild, C. J., Yusuf, A., Wilson, D. E., Peelle, J. E., Davis, M. H., and Johnsrude, I. S. (2012). Effortful listening: the processing of degraded speech depends critically on attention. *J. Neurosci.* 32, 14010–14021. doi: 10.1523/JNEUROSCI.1528-12.2012
- Woodfield, A., and Akeroyd, M. A. (2010). The role of segmentation difficulties in speech-in-speech understanding in older and hearing-impaired adults. *J. Acoust. Soc. Am.* 128, EL26–EL31. doi: 10.1121/1.3443570
- Xiang, J., Simon, J., and Elhilali, M. (2010). Competing streams at the cocktail Party: exploring the mechanisms of attention and temporal integration. *J. Neurosci.* 30, 12084–12093. doi: 10.1523/JNEUROSCI.0827-10.2010
- Yang, X., Wang, K., and Shamma, S. A. (1992). Auditory representations of acoustic signals. *IEEE Trans. Inf. Theory* 38, 824–839. doi: 10.1109/18.119739
- Zacharias, N., König, R., and Heil, P. (2012). Stimulation – history effects on the M100 revealed by its differential dependence on the stimulus onset interval. *Psychophysiology* 49, 909–919. doi: 10.1111/j.1469-8986.2012.01370.x
- Zion Golumbic, E. M., Ding, N., Bickel, S., Lakatos, P., Schevon, C. A., Mckhann, G. M., et al. (2013). Mechanisms underlying selective neuronal tracking of attended speech at a "cocktail party". *Neuron* 77, 980–991. doi: 10.1016/j.neuron.2012.12.037
- Zion Golumbic, E. M., Poeppel, D., and Schroeder, C. E. (2012). Temporal context in speech processing and attentional stream selection: a behavioral and neural perspective. *Brain Lang.* 122, 151–161. doi: 10.1016/j.bandl.2011.12.010

Conflict of Interest Statement: The authors declare that the research was conducted in the absence of any commercial or financial relationships that could be construed as a potential conflict of interest.

Received: 10 March 2014; accepted: 27 April 2014; published online: 28 May 2014.

Citation: Ding N and Simon JZ (2014) Cortical entrainment to continuous speech: functional roles and interpretations. *Front. Hum. Neurosci.* 8:311. doi: 10.3389/fnhum.2014.00311

This article was submitted to the journal *Frontiers in Human Neuroscience*.

Copyright © 2014 Ding and Simon. This is an open-access article distributed under the terms of the Creative Commons Attribution License (CC BY). The use, distribution or reproduction in other forums is permitted, provided the original author(s) or licensor are credited and that the original publication in this journal is cited, in accordance with accepted academic practice. No use, distribution or reproduction is permitted which does not comply with these terms.

EXHIBIT 23

CHAPTER

The discovery of human auditory–motor entrainment and its role in the development of neurologic music therapy

13

Michael H. Thaut¹

Center for Biomedical Research in Music, Colorado State University, Fort Collins, CO, USA

¹*Corresponding author: Tel.: +1-970-4915533; Fax: 970 491 7541,*

e-mail address: michael.thaut@colostate.edu

Abstract

The discovery of rhythmic auditory motor entrainment in clinical populations was a historical breakthrough in demonstrating for the first time a neurological mechanism linking music to retraining brain and behavioral functions. Early pilot studies from this research center were followed up by a systematic line of research studying rhythmic auditory stimulation on motor therapies for stroke, Parkinson's disease, traumatic brain injury, cerebral palsy, and other movement disorders. The comprehensive effects on improving multiple aspects of motor control established the first neuroscience-based clinical method in music, which became the bedrock for the later development of neurologic music therapy. The discovery of entrainment fundamentally shifted and extended the view of the therapeutic properties of music from a psychosocially dominated view to a view using the structural elements of music to retrain motor control, speech and language function, and cognitive functions such as attention and memory.

Keywords

entrainment, neurologic music therapy, neurorehabilitation, neuroscience, rhythm

1 INTRODUCTION

Entrainment is a universal phenomenon that can be observed in physical (e.g., pendulum clocks) and biological systems (e.g., fire flies) when one system's motion or signal frequency entrains the frequency of another system. The use of entrainment for therapeutic purposes was established for the first time in the early 1990s by Thaut and colleagues in several research studies, showing that the periodicity of auditory rhythmic

254 CHAPTER 13 The discovery of human auditory–motor entrainment

patterns could entrain movement patterns in patients with movement disorders (Thaut et al., 1999). Physiological, kinematic and behavioral movement analyses showed very quickly that entrainment cues not only changed the timing of movement but also improved spatial and force parameters. We know now that anticipatory rhythmic templates are critical coordinative constraints in the brain for optimal motor planning and execution. This discovery showed for the first time that a structural element in music, i.e., rhythm, could be a successful stimulus for therapeutic purposes.

Rhythmic entrainment is one of the most important underlying mechanisms for the successful application of rhythmic-musical stimuli in motor rehabilitation for movement disorders associated with stroke, Parkinson’s disease (PD), traumatic brain injury, cerebral palsy, etc. Temporal rhythmic entrainment has been successfully extended into applications in cognitive rehabilitation and speech and language rehabilitation, and thus became one of the first major neurological mechanisms linking music and rhythm to brain rehabilitation. Multiple treatment techniques in neurologic music therapy (NMT) utilize entrainment concepts in sensorimotor, cognitive, and speech/language training (Thaut and Hoemberg, 2014).

However, the discovery of structural elements in music as important mechanism facilitating therapeutic change has also motivated a previously not well-represented view to explore other elements in music as well as a language of rehabilitation: for example, the perception of melodic patterns to retrain attention and memory, singing and vocal exercises to retrain speech and language production, or elementary improvisation and composition exercises in a clinical context to train complexity thinking and facilitate executive functions. In this way, clinical rhythmic entrainment research became a model for a very different way of thinking about music in therapy and how to research it (Thaut, 2005). Approximately 25 years later, these discoveries have revolutionized how we use music successfully as a language of brain rehabilitation. The affective properties remain an important aspect of music in therapy but they are now functionally focused on dysfunctions that have critical affective and social components (Hallam et al., 2009). The clinical “music perception” model, however, has opened very new and very effective ways to apply music-based therapeutic exercises functionally to a broad range of dysfunctions of the human nervous system.

The remainder of this chapter will introduce the concept of entrainment more closely and show with examples from clinical research how profound the effects of rhythmic auditory–motor entrainment are in the rehabilitation of movement disorders. Furthermore, I will discuss why the discovery of entrainment had such a dramatic impact on changing the concepts of how music operates in therapy. Finally, illustrations will be provided how this conceptual change has led to the development of new NMT techniques in speech/language and cognitive therapy and rehabilitation.

2 WHAT IS ENTRAINMENT?

In 1666, the Dutch physicist Christian Huygens, the inventor of the pendulum clock, discovered that the pendulum frequencies of two clocks mounted on the same wall or board became synchronized to each other. He surmised that the vibrations of air

molecules would transmit small amounts of energy from one pendulum to the other and synchronize them to a common frequency (Bell, 1947; Garber, 2003). However, when set on different surfaces the synchronization effect disappeared. As it turned out, the transmitting medium was actually the vibrating board or wall. For air molecule vibrations, there would have been too much dampening of the energy transmission, as was later discovered. The effect he observed was subsequently confirmed by many other experiments and was called entrainment. In entrainment, the different amounts of energy transferred between the moving bodies due to the asynchronous movement periods cause negative feedback. This feedback drives an adjustment process, in which the energy is gradually eliminated to zero until both moving bodies move in resonant frequency or synchrony. The stronger “oscillator” locks the weaker into its frequency. When both are equally strong, the faster system slows down and the slower system speeds up until they lock into a common movement period (Pantaleone, 2002).

Technically, entrainment in physics refers to the frequency locking of two oscillating bodies, i.e., bodies that can move in stable periodic or rhythmic cycles. They have different frequencies or movement periods when moving independently, but when interacting they assume a common period. Incidentally, Huygens’ pendulums assumed a common period 180° out of phase, which he humorously called “odd sympathy.” It is now known that entrainment can occur in various phase relationships of the movement onsets of the oscillating bodies—often one can observe a stable phase relationship between the two bodies. A stable phase relationship is achieved when both bodies start and stop their movement period at the same time. However, this is not a necessary prerequisite for entrainment to occur. The deciding factor for entrainment is the common period of the oscillating movements of the two bodies. This phenomenon is of considerable importance for clinical applications of rhythmic entrainment in motor rehabilitation (Kugler and Turvey, 1987; Thaut et al., 1998a,b).

Entrainment is a common phenomenon in the physical world—e.g., coupled oscillators, fluid waves, etc. Entrainment also occurs in nature, e.g., fireflies flashing their light signal and in circadian rhythms entraining to light–dark cycles within the 24-h day period (Roenneberg et al., 2003). Unfortunately, the term entrainment is often also used loosely and has been connected to many unrelated claims—usually in the context of claims for health or healing—with little or no scientific evidence, e.g., brain wave entrainment, altered states of consciousness, trance, drum circles, or binaural beat entrainment. Therefore, it is important for the clinician who follows an evidence-based intervention model to check the scientific validity for therapeutic claims (Thaut, 2005; Thaut and Hoemberg, 2014).

3 THE AUDITORY SYSTEM AND RHYTHM PERCEPTION

The ability of the auditory system to construct stable temporal templates rapidly is well known (Thaut and Kenyon, 2003). The auditory system is superbly constructed to detect temporal patterns in auditory signals with extreme precision and speed, as

256 CHAPTER 13 The discovery of human auditory–motor entrainment

required by the nature of sound as only existing in temporal vibration patterns (Moore, 2003). The auditory system is faster and more precise than the visual and tactile systems (Shelton and Kumar, 2010). Since sound waves that are most important for speech and music and other perceptual tasks are based on periodic motions that repeat themselves in regularly recurring cycles, the auditory system is also perceptually geared toward detecting and constructing rhythmic sound patterns. However, the observation of timing in the auditory system does not stop its function there. From culture and history, we know and experience every day that the auditory and the motor system have a special relationship. For example, Thaut et al. (1998a,b) demonstrated that finger and arm movements instantaneously entrain to the period of a rhythmic stimulus (e.g., metronome beat) and stay locked to the metronome frequency even when subtle tempo changes are induced into the metronome that are not consciously perceived. These findings have been confirmed by other studies (Large et al., 2002).

Two early electrophysiological studies (Paltsev and Elnor, 1967; Rossignol and Melvill Jones, 1976) also showed how sound signals and rhythmic music can prime and time muscle activation via reticulospinal pathways. The pathway connections between the auditory and the motor system—which had not been given much emphasis when compared to visual and proprioceptive systems in motor control—have been researched much more carefully in the past 20 years, ever since our discovery between 1991 and 1993 that rhythmic entrainment in human movement is possible and can be effectively applied to improve motor function in movement disorders (Thaut et al., 1992, 1993). It is now well established that the auditory system has richly distributed fiber connections to motor centers from the spinal cord upward on brain stem, subcortical, and cortical levels (Felix et al., 2011; Koziol and Budding, 2009; Schmahman and Pandya, 2006). Clinical applications based on auditory–motor connectivity will be discussed in the next section.

4 CLINICAL APPLICATIONS OF ENTRAINMENT

In a number of experiments between 1991 and 1993, Thaut and colleagues demonstrated that auditory rhythm and music can entrain the human motor system and be used to improve functional control of movement in healthy subjects and subjects with stroke (Thaut et al., 1991, 1992, 1993). This entrainment process in human movement—especially with patients with severe motor dysfunction like stroke—was previously unknown and never applied clinically. Gait patterns in hemiparetic stroke training, however, showed massive entrainment effects resulting in highly significant improvements in velocity, stride length, cadence, and stride symmetry, as well significant reductions in variability and amplitude of motor unit recruitment (i.e., muscle activation) (Thaut et al., 1993). Based on these findings we developed a standard gait training protocol—rhythmic auditory stimulation (RAS)—which proved to be very effective when compared to traditional gait therapies (Thaut et al., 2007). Immediate entrainment effects could be translated into long-term training effects over 3 weeks (Thaut et al., 1997) and 6 weeks (Thaut et al., 2007),

respectively. Patients entered the studies in the subacute stage, approximately 2 weeks post stroke. These clinical findings have been replicated by a number of other research groups substantiating the existence of rhythmic auditory–motor circuitry for entrainment (Ford et al., 2007; Roerdink et al., 2007, 2011). RAS is now recognized among the evidence-based, state of the art motor therapies for cardiovascular accidents (Hoemberg, 2013).

Of greatest importance was the finding that the injured brain can indeed access rhythmic entrainment mechanisms. These observations led to studying rhythmic motor circuits in the brain more carefully. It is now well accepted that rhythm processing and auditory–motor interactions take place in widely distributed and hierarchically organized neural networks, extending from brain stem and spinal levels to cerebellar, basal ganglia, and cortical loops (Konoike et al., 2012; Thaut, 2003). Cortico-cerebellar networks underlying rhythmic auditory entrainment have been demonstrated by Thaut et al. (2008). Differential engagement of prefrontal (Stephan et al., 2002) and primary auditory cortex areas (Tecchio et al., 2000) have been identified mediating rhythmic motor entrainment below levels of conscious perception, depending on the magnitude of the rhythmic tempo changes. Common and distinct neural substrates for different components of musical rhythm (e.g., pattern, tempo, meter) have been described in a recent study investigating the neural basis of musical rhythm perception (Thaut et al., 2014a,b,c). The involvement of basal ganglia areas via cortico-striatal loops in the perception of harmonic changes in musical cadences was recently described for the first time by Seger et al. (2013). The involvement of the basal ganglia in auditory rhythm perception has been researched by Grahn and Brett (2009) and Grahn and Rowe (2013). Interestingly a study using rhythmic entrainment with patients with cerebellar dysfunction (Molinari et al., 2007) showed that entrainment ability, even on a subliminal level, was not affected by the presence of cerebellar damage, excluding the cerebellum as the chronometric timekeeper of the brain as had been suggested in earlier research (cf. Ivry et al., 2002).

In subsequent experiments, researchers studied rhythmic entrainment in the gaits of people with PD (McIntosh et al., 1997; Miller et al., 1996; Thaut et al., 1996). Although PD presents itself with a different neuropathology and different movement dysfunctions, we also discovered for the first time with this patient group strong entrainment effects that benefited mobility, most noticeably in improvements in bradykinesia, more stable stride symmetry and stride length, and strengthening of motor unit recruitment. Long-term maintenance of improvements over 4–5 weeks was demonstrated in a later study (McIntosh et al., 1998). RAS is now recognized as state of the art mobility treatment for PD (Archibald et al., 2013; Dietz, 2013; Hoemberg, 2005).

After successful experiments entraining endogenous biological rhythms of neural gait oscillators, a new question emerged. Can rhythmic entrainment also be applied to entrain whole body movements, especially arm and hand movements that are not driven by underlying biological rhythms? We found the answer by turning upper extremity movements, which are usually discrete and nonrhythmic by nature, into repetitive cyclical movement units which now could be matched to rhythmic time cues.

258 CHAPTER 13 The discovery of human auditory–motor entrainment

Our research group carried out two experiments studying hemiparetic arm reaching movements in patients with stroke. In one study, we investigated the immediate effect of rhythm on kinematic movement patterns, especially reaching trajectories, variability of movement timing, and elbow range of motion. Elbow range as well as both cyclical movement timing and smoothness of reaching trajectories improved significantly (Thaut et al., 2002). In a second study, we measured the effect of repetitive rhythmic arm training using a patterned sensory enhancement (PSE) protocol. Outcomes were assessed with the wolf motor function action test and the self-reporting motor activity log. Both measures were improved significantly in a within-subject design (Malcolm et al., 2009). The improvements were comparable in size to a parallel study we carried out using constraint induced therapy (CIT; Massie et al., 2009). We also compared trunk flexion and shoulder rotation in a discrete arm reaching versus cyclical reaching task cued by auditory rhythm. The rhythmic cyclical task reduced trunk flexion and increased shoulder and trunk rotation comparable to normal patterns, whereas in the discrete task subjects relied mostly on extended forward flexion of the trunk to reach the targets (Massie et al., 2009). Lastly, CIT significantly increased shoulder abduction, bringing the arm into a more circular outward motion, compared to pretest measures, whereas PSE decreased shoulder abduction, helping to bring the arm into a more forward trajectory. These findings might be interpreted as CIT being an excellent protocol to overcome nonuse of the paretic side, to stimulate associated brain plasticity, and increase quantity of movement, whereas auditory rhythm also addresses recovery of the quality of movement, such as increase in trunk rotation during reaching, which CIT does not facilitate. These findings have also been supported by similar findings in other research groups (Peng et al., 2011; Schneider et al., 2007; Whitall et al., 2000).

5 MECHANISMS OF ENTRAINMENT IN MOTOR CONTROL

The comprehensive effect of rhythmic entrainment on motor control raises some important theoretical questions as to the mechanisms modulating these changes. We know that firing rates of auditory neurons, triggered by auditory rhythms and music, entrain the firing patterns of motor neurons, thus driving the motor system into different frequency levels. However, that is not all. There are two additional mechanisms of great clinical importance in regard to entrainment. The first is that auditory stimulation primes the motor system toward a state of readiness to move. Priming increases subsequent response quality.

The second, more specific aspect of entrainment refers to the changes in motor planning and motor execution it creates. Rhythmic stimuli create stable anticipatory time scales or templates. Anticipation is a critical element in improving movement quality. Rhythm provides precise anticipatory time cues for the brain to plan ahead and be ready. Furthermore, successful movement anticipation is based on foreknowledge of the duration of the cue period. We may remember that during entrainment two movement oscillators—in our case neurally based—of different periods entrain

to a common period. In auditory entrainment, the motor period entrains to the period of the auditory rhythm. Entrainment is always driven by frequency or period entrainment—that is, the common periods may or may not be in perfect phase lock (i.e., the onset of the motor response would be perfectly synchronized to the auditory beat). Beat entrainment is a commonly misunderstood concept. Entrainment is not defined by beat or phase entrainment—it is defined by period entrainment (Large et al., 2002; Nozaradan et al., 2011; Thaut and Kenyon, 2003).

Period entrainment offers the solution to why auditory rhythm also changes the spatial kinematic and dynamic force measures of muscle activation. For a while, we lacked a conceptual link to connect time cuing via rhythmic stimuli to spatiodynamic parameters of motor control, before the analysis of acceleration and velocity profiles of our subjects offered an intriguing explanation. Why is time cuing via period entrainment so helpful for the patients' overall motor control in space, time, and force? The answer is simple and complex at the same time: rhythmic cues give the brain a time constraint—they fix the duration of the movement. Foreknowledge of the duration of the movement period changes computationally everything in motor planning for the brain. Velocity and acceleration are mathematical time derivatives of movement position. We realized that, by fixating movement time through a rhythmic interval, the brain's internal timekeeper now has an additional externally triggered timekeeper with a precise reference interval, a continuous time reference. This time period presents time information to the brain at any stage of the movement. The brain knows at any point of the movement how much time has elapsed and how much time is left, enabling better mapping and scaling of optimal velocity and acceleration parameters across the movement interval. The brain tries to optimize the movement now by matching it to the given template. This process will result not only in changes in movement speed but also in smoother and less variable movement trajectories and muscle recruitment. We can conclude that auditory rhythm, via physiological period entrainment of the motor system, acts as a forcing function to optimize all aspects of motor control. Rhythm not only influences movement timing—time as the central coordinative unit of motor control—but also modulates patterns of muscle activation and control of movement in space (Thaut et al., 1999).

With this understanding of the underlying mechanisms of entrainment it is less important if the patients synchronize their motor responses exactly to the beat—it is important that they entrain to the rhythmic period, because the period template contains critical information to optimize motor planning and motor execution. Consequently, patients might actually move, as Huygens once worded it, in any stage of “odd sympathy” to the actual beat.

6 MORE CLINICAL APPLICATIONS OF ENTRAINMENT

Rhythmic entrainment extends beyond motor control. Speech rate control affecting intelligibility, oral motor control, articulation, voice quality, and respiratory strength could greatly benefit from rhythmic entrainment using rhythm and music. Recent

260 CHAPTER 13 The discovery of human auditory–motor entrainment

findings in aphasia rehabilitation suggest that the rhythmic component in Melodic Intonation Therapy might even be as important as the activation of intact right-hemispheric speech circuitry through singing (Stahl et al., 2011). Rate control via auditory rhythmic cues has been successfully applied to fluency disorders (e.g., stuttering, cluttering), as well improvements in intelligibility in dysarthria (Lansford et al., 2011; Pilon et al., 1998; Thaut et al., 2001; Van Nueffelen et al., 2009, 2010). NMT has an excellent standardized repertoire of evidence-based techniques for speech and language training based on rhythmic entrainment mechanisms (Thaut and Hoemberg, 2014).

Lastly, the potential of temporal entrainment of cognitive function has only recently emerged as an important driver of therapeutic change. NMT techniques in cognitive rehabilitation are relying to a large extent on the role of timing in music and rhythm. For example, in the context of new research findings the time structure of music and rhythm might be considered an effective mnemonic device to improve memory functions (Kern et al., 2007; Thaut et al., 2014a,b,c; Wallace, 1994).

7 OTHER MUSICAL ELEMENTS AS THERAPEUTIC DRIVERS

Kindled by the discovery of the clinical effects of rhythmic entrainment experimenters drawing on new research concepts began to examine other musical elements for their usefulness in rehabilitation. Especially in speech/language functions and cognitive functions, additional mechanisms in music perception beyond rhythm might be needed to address therapeutic needs.

In the area of speech and language therapies, two shared functions became important from a biomedical perspective: (1) the acoustical, anatomical, and neural perception and production features shared between spoken language and vocalization in music; and (2) the ability of both systems to embed communicative functions in the auditory modality. In the research and clinical literature underlying NMT, five areas of therapeutic mechanisms and clinical applications have emerged:

1. *Differential neurologic processing of music and speech*: the fact that the neural circuitry for speaking and singing is partially overlapping but also partially segregated has led to applications, such as Melodic Intonation Therapy, especially in regard to expressive aphasia rehabilitation, where singing could engage undamaged speech circuitry in the hemisphere contra lateral to the damage.
2. *Commonalities between speech and vocal production in music*: there is evidence that common prosodic, acoustical, and physiological production features are enhanced in music versus speech. For example, singing creates a broader overtone spectrum and a stronger fundamental voice frequency. Prosodic elements are amplified leading to enhanced oral motor ranges, better phonemic enunciation, and enhanced voice control. Singing could enhance phonation, and

enhance respiratory control and capacity, due to longer durations in sound production. Longer sound durations are the basis for the slower pace in singing versus speech. Slower pacing might enhance voice control regarding articulation and intelligibility.

3. *Verbal and nonverbal auditory communication systems*: music and speech are two auditory communication systems that—in regard to certain structural elements—have common counterparts, for example, in regard to phonology, prosody, pragmatics, and rule-based systems of composition. For example, musical patterns can simulate communication gestures found in speech: dialogic turn taking, question/answer forms, expressive statements, repeating, simultaneous expressions, etc.
4. *Enhanced auditory perception through music*: music creates an enriched, complex auditory environment that can help enhance sound perception. There is research evidence that shows how musical training enhances auditory sensitivity, which can also translate into enhanced speech perception (Strait et al., 2012).
5. *Musical development mirrors speech and language development*: very interesting parallels have been found between musical and speech/language development in early childhood, showing that engaging in both can have mutually supportive developmental effects (Brandt et al., 2012). Verbalization through singing offers an additional mode of expression and language learning, which can be further integrated into other related activities, like playing musical instruments or dancing.

The role of music in cognitive rehabilitation emerged as the last rehabilitation domain in NMT. There are two likely reasons for this. Human neurocognition research could only fully develop once noninvasive research tools to study the human brain, such as brain imaging, became available. The first focus of these research endeavors was to study the neural bases of higher cognitive functions in humans before a clinical rehabilitative perspective could be established to develop neuroscience-based intervention paradigms. Second, the traditional view of music in therapy was very much characterized by an emphasis on emotional and social factors as therapeutic mechanisms and goals. Cognitive functions, such as attention or memory, were given much less interest in more psychotherapeutically oriented concepts (Thaut et al., 2014a). However, a growing body of recent research has demonstrated intriguing links between music as a complex auditory language and higher cognitive functions, including temporal sequencing (Conway et al., 2009), temporal order learning (Hitch et al., 1996), spatiotemporal reasoning (Sarntheim et al., 1997), auditory attention (Drake et al., 2000), visual discrimination (Feng et al., 2014), hemispatial neglect (Soto et al., 2009), auditory verbal memory (Thaut et al., 2014a,b,c), emotional adjustment (Kleinstaubler and Gurr, 2006), and executive control (Thaut et al., 2009). By linking music cognition and perception research to models of music learning—and finally linking music learning to retraining the injured brain, a new model has emerged that has allowed for the development of functional intervention techniques in the cognitive domain of NMT.

8 CONCLUSIONS

In conclusion, entrainment for therapeutic purposes has been used since the early 1990s, with strong research evidence that the periodicity of auditory rhythmic patterns could improve movement patterns in patients with movement disorders. Clinical research studies have demonstrated that auditory rhythmic cues elicit changes in motor patterns in gait and upper extremity movements. Changes in motor patterns are possibly due to priming of the motor system and anticipatory rhythmic templates in the brain that allow for optimal motor planning and execution with an external rhythmic cue. The ability of the brain to use rhythmic information to anticipate and plan the execution of a motor pattern has made rhythmic entrainment a valuable tool in motor rehabilitation. More recently, temporal rhythmic entrainment has been extended into applications in cognitive rehabilitation and speech and language rehabilitation, with initial successes indicating that mechanisms of rhythmic entrainment might prove to be an essential tools for rehabilitation in all domains.

The discovery of the clinical effectiveness of rhythmic motor entrainment also brought into focus for the first time that the structural elements of music have enormous potential in clinical applications to retrain the injured brain. As such, the discovery of entrainment was not just about the usefulness of entrainment, but more importantly served as a new vantage point for researching and understanding that the complex “language architecture” structure of music contains critical stimuli for effective brain rehabilitation. The new “clinical science” of music has been the bedrock for the development of NMT. Standardized clinical techniques were developed around clusters of research evidence to address motor, speech/language, and cognitive goals in brain rehabilitation. This treatment system constitutes historically the first medically endorsed form of music therapy.

REFERENCES

- Archibald, N., Miller, N., Rochester, L., 2013. Neurorehabilitation in Parkinson’s disease. In: Barnes, M.P., Good, D.C. (Eds.), *Handbook of Neurology*. In: *Neurological Rehabilitation*, vol. 110. Elsevier, New York, NY, pp. 435–442.
- Bell, A.E., 1947. *Christian Huygens and the Development of Science in the 17th Century*. Edward Arnold & Company, London.
- Brandt, A., Gebrian, M., Slevic, R.L., 2012. Music and early language acquisition. *Front. Psychol.* 3, 327. <http://dx.doi.org/10.3389/psyg.2012.00327>.
- Conway, C.M., Pisoni, D.B., Kronenberger, W.G., 2009. The importance of sound for cognitive sequencing abilities: the auditory scaffolding hypothesis. *Curr. Dir. Psychol. Sci.* 18, 275–279.
- Dietz, V., 2013. Gait disorders. In: Barnes, M.P., Good, D.C. (Eds.), *Handbook of Neurology*. In: *Neurological Rehabilitation*, vol. 110. Elsevier, New York, NY, pp. 133–144.
- Drake, C., Jones, M.R., Baruch, C., 2000. The development of rhythmic attending in auditory sequences: attunement, referent period, focal attending. *Cognition* 77, 251–288.

- Felix, R.A., Fridberger, A., Leijon, S., Berrebi, A.S., Magnusson, A.K., 2011. Sound rhythms are encoded by postinhibitory rebound spiking in the superior paraolivary nucleus. *J. Neurosci.* 31, 12566–12578.
- Feng, W., Stoermer, V.S., Martinez, A., McDonald, J.J., Hillyard, S.A., 2014. Sounds activate visual cortex and improve visual discrimination. *J. Neurosci.* 34, 9817–9824.
- Ford, M., Wagenaar, R., Newell, K., 2007. The effects of auditory rhythms and instruction on walking patterns in individuals post stroke. *Gait Posture* 26, 150–155.
- Garber, D., 2003. *The Cambridge History of Seventeenth-Century Philosophy*. Cambridge University Press, Cambridge, UK.
- Grahn, J.A., Brett, M., 2009. Impairment of beat-induced rhythm discrimination in Parkinson's disease. *Cortex* 45, 56–61.
- Grahn, J.A., Rowe, J.B., 2013. Finding and feeling the beat: striatal dissociations between detection and prediction of regularity. *Cereb. Cortex* 23, 913–921.
- Hallam, S., Cross, I., Thaut, M.H., 2009. *Oxford Handbook of Music Psychology*. Oxford University Press, Oxford, UK.
- Hitch, G.J., Burgess, N., Towse, J.N., Culpin, V., 1996. Temporal grouping effects in immediate recall: a working memory analysis. *Q. J. Exp. Psychol. A* 49, 116–139.
- Hoemberg, V., 2005. Evidence based medicine in neurological rehabilitation – a critical review. In: von Wild, K. (Ed.), *Re-Engineering of the Damaged Brain and Spinal Cord Evidence Based Neurorehabilitation*. Springer, New York, NY, pp. 3–14.
- Hoemberg, V., 2013. Neurorehabilitation approaches to facilitate motor recovery. In: Barnes, M.P., Good, D.C. (Eds.), *Handbook of Clinical Neurology*, vol. 110. Elsevier, New York, NY, pp. 161–174.
- Ivry, R.B., Spencer, R.M., Zelaznik, H.N., Diedrichsen, J., 2002. The cerebellum and event timing. *Ann. N. Y. Acad. Sci.* 978, 1085–1095.
- Kern, P., Wolery, M., Aldridge, D., 2007. Use of songs to promote independence in morning greeting routines for young children with autism. *J. Autism Dev. Disord.* 37, 1264–1271.
- Kleinstaub, M., Gurr, B., 2006. Music in brain injury rehabilitation. *J. Cogn. Rehab.* 24, 4–14.
- Konoike, N., Kotozaki, Y., Miyachi, S., Miyauchi, C.M., Yomogida, Y., Akimoto, Y., Kuraoka, K., Sugiura, M., Kawashima, R., Nakamura, K., 2012. Rhythm information represented in the fronto-parieto-cerebellar motor system. *NeuroImage* 63 (1), 328–338. <http://dx.doi.org/10.1016/j.neuroimage.2012.07.002>.
- Koziol, L.F., Budding, D.E., 2009. *Subcortical Structures and Cognition*. Springer, New York, NY.
- Kugler, P.N., Turvey, M.T., 1987. *Information, Natural Law, and the Self-Assembly of Rhythmic Movement*. Erlbaum, Hillsdale, NJ.
- Lansford, K.L., Liss, J.M., Caviness, J.N., Utianski, R.L., 2011. A cognitive-perceptual approach to conceptualizing speech intelligibility deficits and remediation practice in hypokinetic dysrthria. *Parkinsons Dis.* 2011, 150962. <http://dx.doi.org/10.4061/2011150962>.
- Large, E.W., Jones, M.R., Kelso, J.A.S., 2002. Tracking simple and complex sequences. *Psychological Research* 66, 3–17.
- Malcolm, M.P., Massie, C., Thaut, M.H., 2009. Rhythmic auditory-motor entrainment improves hemiparetic arm kinematics during reaching movements. *Top. Stroke Rehabil.* 16, 69–79.

264 CHAPTER 13 The discovery of human auditory–motor entrainment

- Massie, C., Malcolm, M., Greene, D., Thaut, M.H., 2009. Effects of constraint-induced therapy on kinematic outcomes and compensatory movement patterns: an exploratory study. *Arch. Phys. Med. Rehabil.* 90, 571–579.
- McIntosh, G.C., Brown, S.H., Rice, R.R., Thaut, M.H., 1997. Rhythmic auditory-motor facilitation of gait patterns in patients with Parkinson's Disease. *J. Neurol. Neurosurg. Psychiatry* 62, 122–126.
- McIntosh, G.C., Rice, R.R., Hurt, C.P., Thaut, M.H., 1998. Long-term training effects of rhythmic auditory stimulation on gait in patients with Parkinson's disease. *Mov. Disord.* 13, 212.
- Miller, R.A., Thaut, M.H., McIntosh, G.C., Rice, R.R., 1996. Components of EMG symmetry and variability in Parkinsonian and healthy elderly gait. *Electroencephalogr. Clin. Neurophysiol.* 101, 1–7.
- Molinari, M., Leggio, M., Thaut, M.H., 2007. The cerebellum and neural networks for rhythmic sensorimotor synchronization in the human brain. *Cerebellum* 6, 18–23.
- Moore, B.C.J., 2003. *Psychology of Hearing*. Elsevier, New York, NY.
- Nozaradan, S., Peretz, I., Missal, M., Mouraux, A., 2011. Tagging the neuronal entrainment to beat and meter. *J. Neurosci.* 31, 10234–10240.
- Paltsev, Y.I., Elnor, A.M., 1967. Change in functional state of the segmental apparatus of the spinal cord under the influence of sound stimuli and its role in voluntary movement. *Biophysics* 12, 1219–1226.
- Pantaleone, J., 2002. Synchronization of metronomes. *Am. J. Phys.* 70, 992–1000.
- Peng, Y., Lu, T., Wang, T., Chen, Y., Liao, H., Lin, K., Tang, P., 2011. Immediate effects of therapeutic music on loaded sit-to-stand movement in children with spastic diplegia. *Gait Posture* 33, 274–278.
- Pilon, M.A., McIntosh, K., Thaut, M.H., 1998. Auditory versus visual speech timing cues as external rate control to enhance verbal intelligibility in mixed spastic-ataxic-dysarthric speakers. *Brain Inj.* 12, 793–803.
- Roenneberg, T., Daan, S., Mrosovsky, M., 2003. The art of entrainment. *J. Biol. Rhythm.* 18, 183–194.
- Roerdink, M., Lamoth, C.J.C., Kwakkel, G., van Wieringen, P.C.W., Beek, P.J., 2007. Gait coordination after stroke: benefits of acoustically paced treadmill walking. *Phys. Ther.* 87, 1009–1022.
- Roerdink, M., Bank, P.J.M., Peper, C., Beek, P.J., 2011. Walking to the beat of different drums: practical implications for the use of acoustic rhythms in gait rehabilitation. *Gait Posture* 33, 690–694.
- Rossignol, S., Melville Jones, G., 1976. Audiospinal influences in man studied by the H-reflex and its possible role in rhythmic movement synchronized to sound. *Electroencephalogr. Clin. Neurophysiol.* 41, 83–92.
- Sarntheim, J., Von Stein, A., Rappelsberger, P., Petsche, H., Rauscher, F.H., Shaw, G.L., 1997. Persistent patterns of brain activity: an EEG coherence study of the positive effects of music on spatial-temporal reasoning. *Neurol. Res.* 19, 107–116.
- Schmahman, J.D., Pandya, D.N., 2006. *Fiber Pathways of the Brain*. Oxford University Press, Oxford, UK.
- Schneider, S., Schoenle, P.W., Altenmueller, E., Muentz, T., 2007. Using musical instruments to improve motor skill recovery following stroke. *J. Neurol.* 254, 1339–1346.
- Seger, C., Sperling, B.J., Sares, A.G., Quraini, S.I., Alpeter, C., David, J., Thaut, M.H., 2013. Corticostriatal contributions to musical expectancy perception. *J. Cogn. Neurosci.* 25, 1062–1077.

- Shelton, J., Kumar, G.P., 2010. Comparison between auditory and visual single reaction time. *Neurosci. Med.* 1, 30–32.
- Soto, D., Funes, M.J., Guzman-Garcia, A., Rothstein, P., Humphreys, G.W., 2009. Pleasant music overcomes the loss of awareness in patients with visual neglect. *Proc. Natl. Acad. Sci.* 106, 6011–6016.
- Stahl, B., Kotz, S.A., Henseler, I., Turner, R., Geyer, S., 2011. Rhythm in disguise: why singing may not hold the key to recovery from aphasia. *Brain* 134, 3083–3093.
- Stephan, K.M., Thaut, M.H., Wunderlich, G., Schicks, W., Tellmann, L., Herzog, H., McIntosh, G.C., Seitz, R.J., Hoemberg, V., 2002. Conscious and subconscious sensorimotor synchronization prefrontal cortex and the influence of awareness. *NeuroImage* 15, 345–352.
- Strait, D.L., Parbery-Clark, A., Hittner, E., Kraus, N., 2012. Musical training during early childhood enhances the neural encoding of speech in noise. *Brain Lang.* 123, 191–201.
- Tecchio, F., Salustri, C., Thaut, M.H., Pasqualetti, P., Rossini, P.M., 2000. Conscious and pre-conscious adaptation to rhythmic auditory stimuli: a magnetoencephalographic study of human brain responses. *Exp. Brain Res.* 135, 222–230.
- Thaut, M.H., 2003. Neural basis of rhythmic timing networks in the human brain. *Ann. N. Y. Acad. Sci.* 999, 364–373.
- Thaut, M.H., 2005. *Rhythm, Music, and the Brain: Scientific Foundations and Clinical Applications*. Routledge, New York, NY.
- Thaut, M.H., Hoemberg, V., 2014. *Oxford Handbook of Neurologic Music Therapy*. Oxford University Press, Oxford.
- Thaut, M.H., Kenyon, G.P., 2003. Rapid motor adaptations to subliminal frequency shifts in syncopated rhythmic sensorimotor synchronization. *Hum. Mov. Sci.* 22, 321–338.
- Thaut, M.H., Schleiffers, S., Davis, W.B., 1991. Analysis of EMG activity in biceps and triceps muscle in a gross motor task under the influence of auditory rhythm. *J. Music. Ther.* 28, 64–88.
- Thaut, M.H., McIntosh, G.C., Prassas, S.G., Rice, R.R., 1992. The effect of rhythmic auditory cuing on stride and EMG patterns in normal gait. *J. Neurol. Rehabil.* 6, 185–190.
- Thaut, M.H., McIntosh, G.C., Prassas, S.G., Rice, R.R., 1993. The effect of auditory rhythmic cuing on temporal stride and EMG patterns in hemiparetic gait of stroke patients. *J. Neurol. Rehabil.* 7, 9–16.
- Thaut, M.H., McIntosh, G.C., Rice, R.R., Miller, R.A., Rathbun, J., Brault, J.M., 1996. Rhythmic auditory stimulation in gait training with Parkinson's disease patients. *Mov. Disord.* 11, 193–200.
- Thaut, M.H., McIntosh, G.C., Rice, R.R., 1997. Rhythmic facilitation of gait training in hemiparetic stroke rehabilitation. *J. Neurol. Sci.* 151, 207–212.
- Thaut, M.H., Bin, T., Azimi-Sadjadi, M., 1998a. Rhythmic finger-tapping sequences to cosine-wave modulated metronome sequences. *Hum. Mov. Sci.* 17, 839–863.
- Thaut, M.H., Miller, R.A., Schauer, L.M., 1998b. Multiple synchronization strategies in rhythmic sensorimotor tasks: phase vs period adaptation. *Biol. Cybern.* 79, 241–250.
- Thaut, M.H., Kenyon, G.P., Schauer, M.L., McIntosh, G.C., 1999. The connection between rhythmicity and brain function. *IEEE. Eng. Med. Biol. Mag.* 18, 101–108.
- Thaut, M.H., McIntosh, K., McIntosh, G.C., Hoemberg, V., 2001. Auditory rhythm enhances movement and speech motor control in patients with Parkinson's disease. *Funct. Neurol.* 16, 163–172.
- Thaut, M.H., Kenyon, G.P., Hurt, C.P., McIntosh, G.C., Hoemberg, V., 2002. Kinematic optimization of spatiotemporal patterns in paretic arm training with stroke patients. *Neuropsychologia* 40 (7), 1073–1081.

266 CHAPTER 13 The discovery of human auditory–motor entrainment

- Thaut, M.H., Leins, A., Rice, R.R., Kenyon, G.P., Argstatter, H., Fetter, M., Bolay, V., 2007. Rhythmic auditory stimulation improves gait more than NDT/Bobath training in near ambulatory patients early post stroke: a single-blind randomized control trial. *Neurorehabil. Neural Repair* 21, 455–459.
- Thaut, M.H., Stephan, K.M., Wunderlich, G., Schicks, W., Tellmann, L., Herzog, H., McIntosh, G.C., Seitz, R.J., Hoemberg, V., 2008. Distinct cortico-cerebellar activations in rhythmic auditory motor synchronization. *Cortex* 45, 44–53.
- Thaut, M.H., Gardiner, J.C., Holmberg, D., Horwitz, J., Kent, L., Andrews, G., Donelan, B., McIntosh, G.C., 2009. Neurologic music therapy improves executive function and emotional adjustment in traumatic brain injury rehabilitation. *Ann. N. Y. Acad. Sci.* 1169, 406–416.
- Thaut, M.H., McIntosh, G.C., Hoemberg, V., 2014a. Neurologic music therapy: from social science to neuroscience. In: Thaut, M.H., Hoemberg, V. (Eds.), *Oxford Handbook of Neurologic Music Therapy*. Oxford University Press, Oxford, UK, pp. 1–6.
- Thaut, M.H., Peterson, D.A., McIntosh, G.C., Hoemberg, V., 2014b. Music mnemonics aid verbal memory and induce learning-related brain plasticity in multiple sclerosis. *Front. Hum. Neurosci.* 8, 395. <http://dx.doi.org/10.3389/fnhum.2014.00395>.
- Thaut, M.H., Trimarchi, D., Parsons, L.M., 2014c. Human brain basis of musical rhythm perception: common and distinct neural substrates for different rhythmic components. *Brain Sci.* 4, 428–452.
- Van Nueffelen, G., De Bodt, M., Wuyts, F., Van de Heyning, P., 2009. Effect of rate control on speech rate and intelligibility of dysarthric speech. *Folia Phoniatr. Logop.* 61, 69–75.
- Van Nueffelen, G., De Bodt, M., Vanderwegen, J., Van de Heyning, P., Wuyts, F., 2010. Effect of rate control on speech production and intelligibility in dysarthria. *Folia Phoniatr. Logop.* 62, 110–119.
- Wallace, W.T., 1994. Memory for music: effect of melody on recall of text. *J. Exp. Psychol. Learn. Mem. Cogn.* 20, 1471–1485.
- Whitall, J., McCombe Waller, S., Silver, K.H., Macko, R.F., 2000. Repetitive bilateral arm training with rhythmic auditory cuing improves motor function in chronic hemiparetic stroke. *Stroke* 31, 2390–2395.

EXHIBIT 24

EEG Modification Induced by Repetitive Transcranial Magnetic Stimulation

Hisataka Okamura, Hongkui Jing, and Morikuni Takigawa

Department of Neuropsychiatry, Faculty of Medicine, Kagoshima University, Kagoshima, Japan.

Summary: Repetitive transcranial magnetic stimulation (rTMS) is a powerful, non-invasive tool for investigating cortical physiologic functions in the brain. However, EEG spectral analysis has not been investigated extensively in rTMS study. The authors investigated the influence of rTMS on the EEG power spectrum by stimulating the left frontal cortex in 32 healthy subjects. Stimulation parameters were a 10-Hz frequency, a 3-second duration, and a 100% motor threshold. The data showed that rTMS increased the peak frequency of EEG across the scalp within 2 minutes after stimulation, whereas the value decreased at 3 to 4 minutes. The mean absolute powers within 3 minutes after rTMS did not differ from those estimated before rTMS, but increased uniformly at 4 to 5 minutes. The spectra did not change after sham stimulation. These results indicate that rTMS can influence cortical activities significantly by increasing the frequency and amplitude of EEG, and is a useful tool for helping us understand brain functions. **Key Words:** EEG—Frequency components—Power spectrum—Magnetic stimulation.

Transcranial magnetic stimulation (TMS) allows non-invasive stimulation of the human brain. A large number of studies revealed that repetitive TMS (rTMS) can influence cortical functions, and the effect depends on the stimulation parameters (Classen et al., 1995; Kujirai et al., 1993; Wassermann et al., 1993). The relationship between rTMS and EEG activity has been addressed by others (Izumi et al., 1997; Jennum et al., 1994); however, whether rTMS is capable of changing EEG activity and how rTMS affects the activity remain unclear. Bridgers (1991) declared that exposure to TMS may not have persistent effects on EEG, but transient effects may occur. In an investigation of TMS over the right motor cortex with an intensity of 5% to 10% above the motor threshold, Rossini et al. (1991) demonstrated that EEG from the left central and occipital areas showed an increase in peak frequency by approximately 1 Hz,

indicating that the neuronal networks revealed by EEG signals are affected by magnetic pulses. After improving their EEG recording technology by blocking signal input for 150 msec after TMS, Izumi et al. (1997) depicted a markedly slow wave, which occurred in 25% to 80% of records, with a duration ranging from 200 to 600 msec.

Recently, interest has focused on the delivery of repetitive magnetic stimulation. One of the reasons is that rTMS can disrupt brain functions for a relatively longer time than a single pulse, thus facilitating the detecting alteration of physiologic processes in the brain (Jahanshahi et al., 1997). Jahanshahi et al. (1997) delivered 100 trains of rTMS at 20 Hz in six healthy subjects over the left motor cortex, and no abnormalities were found on EEG after stimulation. However, several studies indicate that rTMS can induce epileptic seizures in healthy subjects (Pascual-Leone et al., 1993; Wassermann et al., 1996). Classen et al. (1995) reported a case of epileptic seizure induced by magnetic stimulation. First they delivered 30 stimuli at a 150% motor threshold over the motor cortex, and then continued with two stimuli at a

Address correspondence and reprint requests to Prof. M. Takigawa, Department of Neuropsychiatry, Faculty of Medicine, Kagoshima University, 8-35-1 Sakuragaoka, Kagoshima City 890-8520, Japan.

90% motor threshold. An epileptic seizure occurred immediately after the transfer of the second stimulus. There was no EEG record during the study; hence, it is difficult to determine when the EEG abnormality started. In another study, Bridgers (1991) summarized that rTMS is generally safe, but not entirely free from unwanted effects, and further study to define those effects is needed.

Therefore, we assumed that rTMS could influence EEG activities and that such effects varied during different periods after the stimulation. To test this hypothesis, we calculated the power spectra of EEG signals and compared the spectra before and after rTMS. We were more interested in investigating how the spectra changed during the different periods. For this purpose, the left frontal cortex of healthy subjects was stimulated. A total of 5 minutes of EEG was collected after each train. The power spectra were estimated for each minute. Frequencies and amplitudes were compared statistically with those obtained before rTMS.

METHODS AND MATERIALS

Subjects

Thirty-two healthy men were selected and screened carefully before the study to rule out neurologic or psychological disorders. They were divided randomly into two groups: the rTMS group and the sham group. Twenty subjects were included in the rTMS group (mean age, 27 years; age range, 22–38 years), and 12 in the sham group (mean age, 27 years; age range, 24–40 years). All subjects were naive to the purposes and hypothesis of this study. This study was approved by the local ethics committee, and all subjects gave written informed consent. There were no side effects reported after the study.

Stimulation

For TMS, a high-frequency magnetic stimulator (Magstim Company Limited, Wales, UK) and a figure-of-eight-shaped coil were used in the current study. The stimuli were biphasic sine wave pulses, with a rise time of 60 μ sec and a duration of 250 μ sec for each pulse. The peak magnetic field was 2 T. The stimulus parameters followed the safety guidelines set out by Wassermann (1998). In each subject, two trains (10 Hz; 3 seconds per train; interval, 300 seconds) were delivered over the left prefrontal area at an intensity of 100% of the motor threshold of the right abductor pollicis brevis muscle. The coil was in a flat position and the handle was pointed toward the occiput. The stimulated position was

5 cm to the left of and 5 cm anterior to the vertex, and it was directly beneath the intersection of the two loops of the coil where the strongest magnetic field was induced.

The sham stimulation was designed carefully according to the study of Klein et al. (1999). First, all subjects were naive to rTMS treatment. None of them had received the stimulation before. They were blind to how we handled the coil and how we delivered the stimuli. They did not know whether the coil should touch their scalp, and did not know the sensation of rTMS before the experiment. Also, they did not know whether they would receive sham or real stimulation. Second, only one subject was stimulated at each time. This prevented the subjects from exchanging their feel of rTMS pulses. Accordingly, the subjects could not differentiate the sham and real rTMS. The coil was placed perpendicular to the scalp on the left frontal area without direct contact to minimize the energy flow into the skull. Thus, only the sound artifact was elicited. The stimulation parameters were the same as the real rTMS stimulation.

EEG Data

The subjects were seated comfortably in a semireclining armchair in a quiet room. To eliminate the influences on EEG, the subjects were asked to remain in a relaxed state, avoiding any movement or muscular contraction. They were instructed to close their eyes and avoid mental activities.

Fourteen electrodes were placed on the scalp according to the International 10-20 System (F_3 , F_4 , C_3 , C_4 , P_3 , P_4 , T_3 , T_4 , T_5 , T_6 , F_z , C_z , P_z , and O_z). The linked ear electrodes were used as a common reference. Approximately 5 minutes of EEG signals were recorded before the stimulation and after each train. EEG signals were amplified by a Neurofax 4421 (Nihon-Kohden Company, Tokyo, Japan) with a passband filter of 0.1 to 30 Hz. The signals were recorded on paper and stored simultaneously on high-fidelity magnetic tapes. Off-line, the signals were sampled from tapes at a sampling rate of 500 Hz in 16-bit resolution.

EEG signals were analyzed continuously with a time window of 4 seconds. In fact, the length of the window was 2,048 points. Therefore, every two consecutive segments contained 48 overlapping points. According to the stimulation, the segments were grouped into six periods: (1) before rTMS, (2) within 1 minute after rTMS, (3) 1 to 2 minutes after rTMS, (4) 2 to 3 minutes after rTMS, (5) 3 to 4 minutes after rTMS, and (6) 4 to 5 minutes after rTMS. EEG segments contaminated by artifacts were excluded from analysis. Approximately 10 segments were calculated in each period for each rTMS train.

TABLE 1. *The effects of factors on the power spectra among different frequency bands*

Estimated parameter	Effects	δ	θ	α	β	γ
Peak frequency	F ₁	5.05 [†]	0.39	9.74 [†]	1.85*	6.64 [†]
	F ₂	3.93 [†]	9.11 [†]	57.9 [†]	2.49*	7.41 [†]
	F ₁ × F ₂	0.56	0.23	0.87	0.34	0.72
Maximal absolute power	F ₁	15.6 [†]	11.2 [†]	26.0 [†]	5.73 [†]	5.79 [†]
	F ₂	4.03 [†]	14.9 [†]	9.28 [†]	1.73	9.08 [†]
	F ₁ × F ₂	0.23	0.24	0.31	0.38	0.94
Mean absolute power	F ₁	16.7 [†]	17.8 [†]	27.9 [†]	3.65 [†]	8.78 [†]
	F ₂	4.66 [†]	13.3 [†]	6.35 [†]	2.33*	12.8 [†]
	F ₁ × F ₂	0.26	0.18	0.11	0.59	0.92
Mean relative power	F ₁	6.94 [†]	10.2 [†]	20.2 [†]	14.2 [†]	36.6 [†]
	F ₂	6.96 [†]	25.3 [†]	13.8 [†]	1.25	15.0 [†]
	F ₁ × F ₂	0.34	0.12	0.30	0.53	0.63

The data are *F* values of analysis of variance.

* 0.01 < *P* < 0.05.

[†] *P* < 0.01.

F₁, the effect of factor “channel”; F₂, the effect of factor “period”; F₁ × F₂, the interaction effect of factors “channel” and “period.”

Evaluated Parameters

EEG spectral analysis was performed with a conventional fast Fourier transformation algorithm. To observe the effects of stimulation, the spectrum was separated into five frequency bands: δ (0.5–4 Hz), θ (4–8 Hz), α (8–13 Hz), β (13–30 Hz), and γ (30–40 Hz). Four parameters were estimated on the spectra: peak frequency, maximal absolute power, mean absolute power, and relative power.

The maximal absolute power was defined as the maximal value of power calculated by fast Fourier transformation. The value was estimated for each frequency band as well as for the whole frequency range (i.e., EEG). The peak frequency corresponded to the maximal absolute power. The mean absolute power was computed for each frequency band using the following formula: (the total power of investigated band)/(the data number within the band after fast Fourier transformation). Therefore, it stood for a mean value of the absolute power and was always smaller than its corresponding maximal absolute power. The relative power was expressed as a percentage, representing how many percent of the EEG power belonged to the investigated frequency band: (the total power of investigated band)/(the total power of EEG) × 100%. In this study, we were more interested in comparing the results among the periods after rTMS.

The Kolmogorov–Smirnov test was applied to examine the normal distribution. Visual examinations using histograms were also performed on each dataset. Descriptive parameters (means and standard deviations) were calculated. Analysis of variance was performed on each frequency band in relation to two factors: “channel” × “period.” Duncan’s multiple range test was used for post hoc comparisons of individual variables. Significance was set at *P* < 0.05.

RESULTS

The Kolmogorov–Smirnov test showed normal distributions on the estimated parameters (*P* > 0.05). For the sham stimulation, there were no significant differences detected by analysis of variance on the peak frequency, maximal absolute power, mean absolute power, and relative power in the six periods (*P* > 0.05). For the rTMS group, analysis of variance showed a strong effect for the period factor. The descriptive parameter of the *F* value in analysis of variance is summarized in Table 1. Interactions between the period and channel factors were not significant (*P* > 0.05), indicating that the effect of the period factor was not modified by electrode site (i.e., EEG signals from different electrode sites had similar changes).

Table 2 shows the peak frequency before and after rTMS. Comparing the values before rTMS, the peak frequency became faster in all channels within the first 2 minutes after the trains. The shift was significant in the frontal area, where the peak frequency was increased by 1.92 Hz at F₃ (*P* < 0.01), 1.58 Hz at F₄ (*P* < 0.01), and 1.72 Hz at F₂ (*P* < 0.01). Signals recorded around the stimulated site showed similar results. For electrode C₃, the peak frequency increased by 1.34 Hz (*P* < 0.05); for T₃, by 1.585 Hz (*P* < 0.01); and for C_z, by 1.32 Hz (*P* < 0.05). Signals from electrodes far from the stimulated site also turned fast, but did not reach significance (except T₄). The values obtained at 2 to 3 minutes, 3 to 4 minutes, and 4 to 5 minutes after rTMS did not differ from those before rTMS (*P* > 0.05), indicating that the effect of rTMS weakened 2 minutes after the end of stimulation.

The mean absolute power of the α band among the electrodes was plotted in Fig. 1. The values estimated at

TABLE 2. Peak frequency of EEG recorded at different electrode sites and during different periods

Channel	Before rTMS	0–1 min after rTMS	1–2 min after rTMS	2–3 min after rTMS	3–4 min after rTMS	4–5 min after rTMS
F3	8.413 ± 1.384	10.33 ± 0.419 [†]	10.26 ± 0.355 [†]	8.900 ± 0.838	8.109 ± 1.722	8.784 ± 1.063
F4	8.570 ± 1.479	10.15 ± 0.565 [†]	10.15 ± 0.488 [†]	9.031 ± 0.837	8.589 ± 1.534	8.961 ± 0.904
C3	8.878 ± 1.336	10.22 ± 0.512*	10.18 ± 0.402*	9.243 ± 1.016	8.651 ± 1.598	9.105 ± 0.939
C4	9.228 ± 1.298	10.13 ± 0.598	10.14 ± 0.496	9.264 ± 0.911	8.721 ± 1.602	9.161 ± 1.094
P3	9.458 ± 1.434	10.22 ± 0.767	10.34 ± 0.375	9.653 ± 0.990	9.196 ± 1.790	9.658 ± 0.888
P4	9.549 ± 1.432	10.26 ± 0.817	10.25 ± 0.756	9.518 ± 0.892	9.220 ± 1.827	9.787 ± 0.856
T3	9.095 ± 1.169	10.68 ± 1.302 [†]	10.60 ± 1.242 [†]	9.534 ± 0.939	9.082 ± 1.741	9.239 ± 0.882
T4	9.369 ± 1.296	10.78 ± 1.774 [†]	10.78 ± 2.091 [†]	9.450 ± 0.787	8.930 ± 1.625	9.470 ± 0.482
T5	9.457 ± 1.599	10.32 ± 0.607	10.21 ± 0.440	9.760 ± 0.984	9.314 ± 1.539	9.721 ± 0.543
T6	9.443 ± 1.189	10.37 ± 0.518	10.38 ± 0.708	10.06 ± 1.931	9.447 ± 1.963	9.573 ± 0.738
Fz	8.509 ± 1.445	10.23 ± 0.475 [†]	10.20 ± 0.442 [†]	8.999 ± 0.864	8.514 ± 1.519	8.736 ± 1.203
Cz	8.834 ± 1.256	10.15 ± 0.589*	10.20 ± 0.444*	9.176 ± 1.001	8.548 ± 1.591	8.847 ± 1.078
Pz	9.418 ± 1.402	10.16 ± 0.675	10.25 ± 0.366	9.622 ± 1.072	9.017 ± 1.723	9.577 ± 0.908
Oz	9.701 ± 1.455	10.50 ± 0.428	10.39 ± 0.456	9.937 ± 0.901	9.749 ± 1.498	9.971 ± 0.636

Data are shown as mean ± standard deviation.

* 0.01 < *P* < 0.05.

[†] *P* < 0.01 (compare with the results calculated before rTMS).

rTMS, repetitive transcranial magnetic stimulation.

3 to 4 minutes after rTMS were uniformly lower than those estimated in other periods, whereas the estimates at 4 to 5 minutes were the highest among all channels. The powers calculated before and within 3 minutes after rTMS could not be distinguished.

An EEG example obtained from a subject (age, 24 years old) is demonstrated in Fig. 2. Although 14 channels of EEG were recorded, only four channels were demonstrated. Power spectra are displayed at two electrode sites. The peak frequency increased after rTMS, which was most obvious during the first 2 minutes. Topograms of mean absolute power and relative power of the α band were seen on all channels.

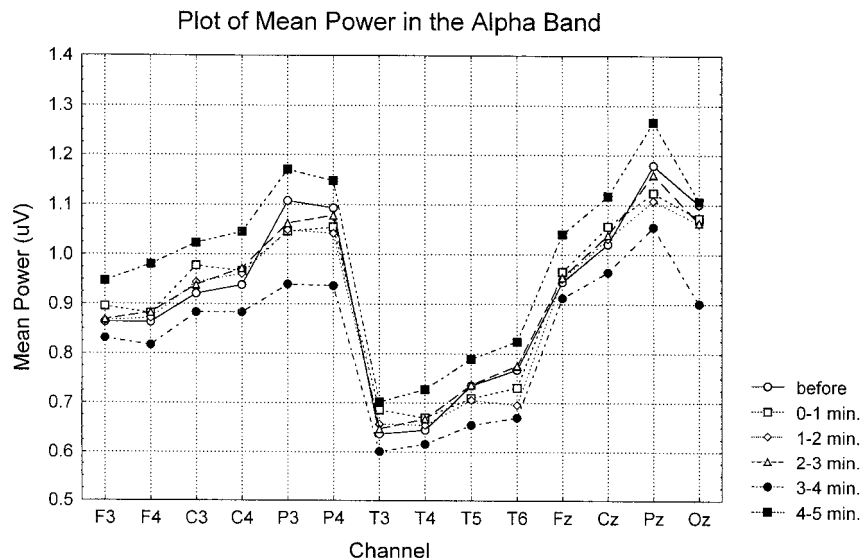
DISCUSSION

Effect of rTMS

The current study revealed that rTMS can influence EEG activities significantly, increasing the peak frequency and powers. The effect was similar over the scalp, and decreased from the second minute after stimulation.

Previous studies showed that the changes in the EEG frequency and power might reflect functional alteration of brain activities (Siegel et al., 1982), and signals from normal subjects had some characteristics of nonlinear

FIG. 1. Mean absolute power of the α band before and after repetitive transcranial magnetic stimulation (rTMS). The values obtained at 4 to 5 minutes after rTMS were uniformly higher than those calculated during other periods, whereas the minimal mean powers were yielded at 3 to 4 minutes. The values calculated before rTMS and within 3 minutes after rTMS could not be distinguished. The data were averaged for all subjects.



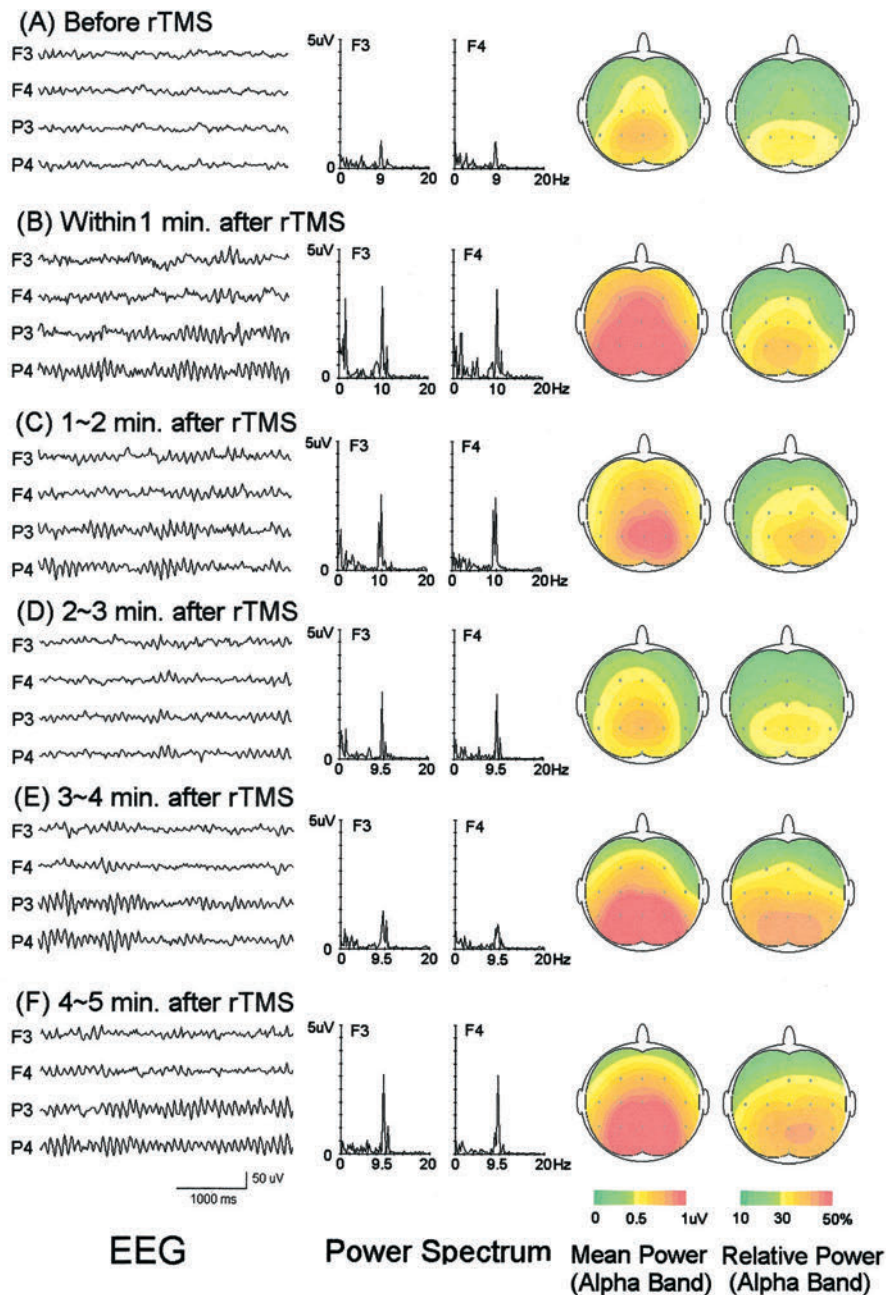


FIG. 2. EEG waves and power spectra calculated in a healthy subject. Fourteen channels of EEG signals were recorded and digitized, but only those recorded at the frontal and parietal areas are demonstrated. The power spectra displayed were estimated on the EEG obtained from the frontal area. The mean absolute power and relative power of all channels are shown in topograms. It should be noted that the values demonstrated in the topograms (left) are the mean power of the α band. Because of the average calculation, the values are lower than their corresponding maximal power.

dynamics (Jing and Takigawa, 2000b; Meyer-Lindenberg et al., 1998). Because the frequency of a nonlinear dynamic system can be altered by external influences, it is reasonable to consider that neuronal activities that show nonlinear properties may be affected by TMS pulses.

It is interesting that the changes in frequency and power were not simultaneous. First, the peak frequency increased immediately after rTMS and lasted for 2 min-

utes, but during this period, the changes in mean absolute power were not apparent. Second, at 2 to 5 minutes after rTMS, the peak frequency recovered to a level similar to that before rTMS. However, the mean absolute power obviously decreased at 3 to 4 minutes and increased at 4 to 5 minutes. These two observations suggest that EEG activity should receive attention during two periods: immediately after and 4 to 5 minutes after the stimulation. These findings were supported by the observations

of Mottaghy et al. (1998), who indicated that the influence of rTMS lasted less than 2 minutes after they delivered a 20-Hz rTMS train over Wernicke's cortex in healthy subjects.

Our results showed an increase in EEG rhythm at all electrode sites. The variation at the left central area was more obvious than that at the right central area, indicating that the influence of rTMS was stronger for the stimulated site and its surrounding areas. The influence becomes weaker in the distant cortical areas. Recently, Izumi et al. (1997) demonstrated a slow activity of EEG signals at approximately 500 msec after TMS. Our data did not contradict theirs for several reasons:

1. We applied 10-Hz rTMS with an approximate 1.4-T intensity, in contrast to their single TMS with only a 0.44-T intensity.
2. We were interested in observing the EEG changes for 5 minutes after rTMS, in contrast to only a 2-second duration in their study.
3. In the EEG segments demonstrated in their report, there was no slow activity observed from 1 second after the stimulus; the mechanisms of rhythmic changes are different.

As they explained, the slow activity was ascribed to the sum of cutaneous sensory and auditory evoked potentials (Izumi et al., 1997). Our observations are consistent with the investigation by Rossini et al. (1991), who compared power spectra of the α and β bands after the stimulation of the motor cortex. The mechanisms of effects of rTMS on EEG activities remain unclear. In a similar experiment, using the same parameters, we found that directed coherences between cerebral sites changed significantly after rTMS (Jing and Takigawa, 2000a). In that study, we focused on two periods: 1 to 3 minutes and 3 to 5 minutes after the stimulation. The directed coherence from the frontal area to the parietal area was increased significantly in both hemispheres, especially during the first period. Additionally, the effect was much stronger for the α band, with the mean directed coherence from the stimulated site to other sites increased by 32%. It was interesting that the crossed interhemispheric frontoparietal coherence (i.e., from F_3 to P_4 , from F_4 to P_3) also increased, although only the left frontal area was stimulated. A similar phenomenon was observed in the current study. The EEG power spectra changed not only at the left frontal area, but also at other cortical areas (e.g., F_4). This finding confirms the conclusion that the brain areas are not isolated from each other, regardless of whether the connections are direct (Jing and Takigawa, 2000a). For example, the nonspecific thalamic system and corpus callosum play important roles in transhemi-

spheric signal transmission (Hamada and Wada, 1998), and the brainstem also contributes to the spread of signals (Kievit and Kuypers, 1975; McIntyre and Goddard, 1973). The effect of rTMS on EEG frequency may be the result of a direct cortical effect. One mechanism is the neuronal interactions described by Pascual-Leone et al. (1993). The excitatory intracortical axons are collateral to pyramidal cells and inhibitory interneurons. The latter forms a feedback and projects to the pyramidal cells. Under normal circumstances, excitation and inhibition balance each other. rTMS upsets the balance by accumulating excitatory postsynaptic potentials temporarily, without compensation by inhibitory postsynaptic potentials because of the differences in the number of synapses and differences in the conduction along the myelinated monosynaptic excitatory collaterals (Pascual-Leone et al., 1993). This results in the spread of excitation and may even induce epileptic seizures (Classen et al., 1995). This mechanism explains the functional changes that occur during or immediately after the stimulation. However, our data revealed that the EEG frequency changes approximately tens of seconds after the rTMS and lasts for approximately 2 minutes, indicating that some other mechanisms occur in the brain. It is worth noting that similar observations have been reported by others (Fauth et al., 1992; Hömberg and Netz, 1989; Jing and Takigawa, 2000a; Kandler, 1990; Sakamoto et al., 1993). We considered that the delayed reaction may involve some complex metabolic processes or may be secondary to activation of some cerebral structures. For example, evidence from positron emission tomographic studies suggests that higher frequency stimulation (20 Hz) may increase brain glucose metabolism in a transsynaptic fashion, whereas lower frequency stimulation (1 Hz) may decrease it (Post et al., 1999; Siebner et al., 1999b), and such influence was correlated to the number of stimuli (Paus et al., 1997). Marked increase in the expression of c-fos in the different layers of the parietal cortex and hippocampus was reported recently in a chronic rTMS study (Hausmann et al., 2000), and a direct and fast connection between the cortex and brainstem was demonstrated by Meyer et al. (1997). Additionally, involvement of a multisynaptic subcortical network cannot be excluded (Siebner et al., 1999a). However, to explain the mechanism of EEG modification, one needs to perform detailed studies in the future. The limitation of our study was that only 5 minutes of EEG was recorded after each train, but our results showed that the power increased during 4 to 5 minutes, although the frequency recovered at that moment. We recognize this problem and suggest recording EEG signals for a much longer time in future studies.

Stimulation Parameters

The rTMS parameters used in the current study should be considered when extending the current results. Previous studies revealed that effects of rTMS depend on several factors: (1) intensity of stimulus, (2) frequency of stimulus, (3) duration of train, and (4) intertrain interval. These four factors are not completely independent from each other. Combinations of different values form a complex pattern. Many studies have investigated the effect of rTMS with different parameters on the functions of cerebral cortex (Chen et al., 1997; Pascual-Leone et al., 1993; Wassermann, 1998). Based on that research, it is concluded that stimulation at high intensity may cause the spread of excitation, and short intertrain interval rTMS may carry the risk of exciting the cortex, even resulting in epileptic seizures.

Other parameters that may influence the results are (1) direction of induced current flow in the brain (i.e., clockwise or counterclockwise) (Trompetto et al., 1999), (2) orientation of the coil's handle (e.g., lateromedial direction and posteroanterior direction) (Di-Lazzaro et al., 1998; Kaneko et al., 1996), and (3) the shape of the coil (Classen et al., 1995).

Considering that a number of factors may influence the effects of rTMS, it is necessary to reiterate that the modifications of EEG activities observed in the current study are based on rTMS at a frequency of 10 Hz, with a 3-second duration, and at 100% of the motor threshold.

Although the frequency and amplitude of EEG signals increased after rTMS, there were no epileptiform discharges observed in any subjects. Because of its ability to influence the activity of the cerebral cortex, rTMS is a useful tool to facilitate understanding of the mechanisms of cortical physiologic functions.

REFERENCES

- Bridgers SL. The safety of transcranial magnetic stimulation reconsidered: evidence regarding cognitive and other cerebral effects. *Electroencephalogr Clin Neurophysiol Suppl* 1991;43:170–9.
- Chen R, Gerloff C, Classen J, Wassermann EM, Hallett M, Cohen LG. Safety of different inter-train intervals for repetitive transcranial magnetic stimulation and recommendations for safe ranges of stimulation parameters. *Electroencephalogr Clin Neurophysiol* 1997;105:415–21.
- Classen J, Witte OW, Schlaug G, Seitz RJ, Holthausen H, Benecke R. Epileptic seizures triggered directly by focal transcranial magnetic stimulation. *Electroencephalogr Clin Neurophysiol* 1995;94:19–25.
- Di-Lazzaro V, Oliviero A, Profice P, et al. Comparison of descending volleys evoked by transcranial magnetic and electric stimulation in conscious humans. *Electroencephalogr Clin Neurophysiol* 1998;109:397–401.
- Fauth C, Meyer BU, Prosiegel M, Zihl J, Conrad B. Seizure induction and magnetic brain stimulation after stroke. [letter]. *Lancet* 1992; 339:362.
- Hamada K, Wada JA. Amygdaloid kindling in brainstem bisected cats. *Epilepsy Res* 1998;29:87–95.
- Hausmann A, Weis C, Marksteiner J, Hinterhuber H, Humpel C. Chronic repetitive transcranial magnetic stimulation enhances c-fos in the parietal cortex and hippocampus. *Brain Res Mol Brain Res* 2000;76:355–62.
- Hömberg V, Netz J. Generalized seizures induced by transcranial magnetic stimulation of motor cortex [letter]. *Lancet* 1989;2:1223.
- Izumi S, Takase M, Arita M, Masakado Y, Kimura A, Chino N. Transcranial magnetic stimulation-induced changes in EEG and responses recorded from the scalp of healthy humans. *Electroencephalogr Clin Neurophysiol* 1997;103:319–22.
- Jahanshahi M, Ridding MC, Limousin P, et al. Rapid rate transcranial magnetic stimulation—a safety study. *Electroencephalogr Clin Neurophysiol* 1997;105:422–9.
- Jennum P, Winkel H, Fuglsang-Frederiksen A, Dam M. EEG changes following repetitive transcranial magnetic stimulation in patients with temporal lobe epilepsy. *Epilepsy Res* 1994;18:167–73.
- Jing H, Takigawa M. Observation of EEG coherence after repetitive transcranial magnetic stimulation. *Clin Neurophysiol* 2000a;111: 1620–31.
- Jing H, Takigawa M. Comparison of human ictal, interictal and normal non-linear component analyses. *Clin Neurophysiol* 2000b;111: 1282–92.
- Kandler R. Safety of transcranial magnetic stimulation. *Lancet* 1990; 335:469–70.
- Kaneko K, Kawai S, Fuchigami Y, Morita H, Ofuji A. The effect of current direction induced by transcranial magnetic stimulation on the corticospinal excitability in human brain. *Electroencephalogr Clin Neurophysiol* 1996;101:478–82.
- Kievit J, Kuypers HG. Basal forebrain and hypothalamic connection to frontal and parietal cortex in the rhesus monkeys. *Science* 1975; 187:660–2.
- Klein E, Kreinin I, Chistyakov A, et al. Therapeutic efficacy of right prefrontal slow repetitive transcranial magnetic stimulation in major depression: a double-blind controlled study. *Arch Gen Psychiatry* 1999;56:315–20.
- Kujirai T, Caramia MD, Rothwell JC, et al. Corticocortical inhibition in human motor cortex. *J Physiol Lond* 1993;471:501–19.
- McIntyre DC, Goddard DV. Transfer, interference and spontaneous recovery of convulsions kindled from the rat amygdala. *Electroencephalogr Clin Neurophysiol* 1973;35:535–43.
- Meyer BU, Liebsch R, Roricht S. Tongue motor responses following transcranial magnetic stimulation of the motor cortex and proximal hypoglossal nerve in man. *Electroencephalogr Clin Neurophysiol* 1997;105:15–23.
- Meyer-Lindenberg A, Bauer U, Krieger S, et al. The topography of non-linear cortical dynamics at rest, in mental calculation and moving shape perception. *Brain Topogr* 1998;10:291–9.
- Mottaghy FM, Hungs M, Boroojerdi B, et al. Facilitation of picture naming induced by rTMS. *Electroencephalogr Clin Neurophysiol* 1998;107:102–3.
- Pascual-Leone A, Houser CM, Reese K, et al. Safety of rapid-rate transcranial magnetic stimulation in normal volunteers. *Electroencephalogr Clin Neurophysiol* 1993;89:120–30.
- Paus T, Jech R, Thompson CJ, Comeau R, Peters T, Evans AC. Transcranial magnetic stimulation during positron emission tomography: a new method for studying connectivity of the human cerebral cortex. *J Neurosci* 1997;17:3178–84.
- Post RM, Kimbrell TA, McCann UD, et al. Repetitive transcranial magnetic stimulation as a neuropsychiatric tool: present status and future potential. *J ECT* 1999;15:39–59.
- Rossini PM, Desiato MT, Lavaroni F, Caramia MD. Brain excitability and electroencephalographic activation: non-invasive evaluation in healthy humans via transcranial magnetic stimulation. *Brain Res* 1991;567:111–9.

- Sakamoto Y, Okamura H, Fukuzako H, Takigawa M. Does repetitive transcranial magnetic stimulation induce epileptogenesis in rabbit brain? *Epilepsia* 1993;38(suppl):63–4.
- Siebner HR, Auer C, Roeck R, Conrad B. Trigeminal sensory input elicited by electric or magnetic stimulation interferes with the central motor drive to the intrinsic hand muscles. *Clin Neurophysiol* 1999a;110:1090–9.
- Siebner HR, Peller M, Willoch F, et al. Imaging functional activation of the auditory cortex during focal repetitive transcranial magnetic stimulation of the primary motor cortex in normal subjects. *Neurosci Lett* 1999b;270:37–40.
- Siegel A, Grady CL, Mirsky AF. Prediction of spike-wave bursts in absence epilepsy by EEG power-spectrum signals. *Epilepsia* 1982;23:47–60.
- Trompetto C, Assini A, Buccolieri A, Marchese R, Abbruzzese G. Intracortical inhibition after paired transcranial magnetic stimulation depends on the current flow direction. *Clin Neurophysiol* 1999;110:1106–10.
- Wassermann EM. Risk and safety of repetitive transcranial magnetic stimulation: report and suggested guidelines from the International Workshop on the Safety of Repetitive Transcranial Magnetic Stimulation, June 5–7, 1996. *Electroencephalogr Clin Neurophysiol* 1998;108:1–16.
- Wassermann EM, Cohen LG, Flitman SS, Chen R, Hallett M. Seizures in healthy people with repeated ‘safe’ trains of transcranial magnetic stimuli. *Lancet* 1996;347:825–6.
- Wassermann EM, Pascual-Leone A, Valls-Sole J, Toro C, Cohen LG, Hallett M. Topography of the inhibitory and excitatory responses to transcranial magnetic stimulation in a hand muscle. *Electroencephalogr Clin Neurophysiol* 1993;89:424–33.

EXHIBIT 25

Rhythmic TMS Causes Local Entrainment of Natural Oscillatory Signatures

Gregor Thut,^{1,*} Domenica Veniero,^{2,3} Vincenzo Romei,^{4,5} Carlo Miniussi,^{2,3} Philippe Schyns,¹ and Joachim Gross¹

¹Centre for Cognitive Neuroimaging, Institute of Neuroscience and Psychology, University of Glasgow, Glasgow G12 8QB, UK

²Cognitive Neuroscience Section, IRCCS San Giovanni di Dio Fatebenefratelli, 25125 Brescia, Italy

³Department of Biomedical Sciences and Biotechnology, National Institute of Neuroscience, University of Brescia, 25123 Brescia, Italy

⁴Wellcome Trust Centre for Neuroimaging at UCL, Institute of Neurology, University College London, London WC1N 3BG, UK

⁵UCL Institute of Cognitive Neuroscience, University College London, London WC1N 3AR, UK

Summary

Background: Neuronal elements underlying perception, cognition, and action exhibit distinct oscillatory phenomena, measured in humans by electro- or magnetoencephalography (EEG/MEG). So far, the correlative or causal nature of the link between brain oscillations and functions has remained elusive. A compelling demonstration of causality would primarily generate oscillatory signatures that are known to correlate with particular cognitive functions and then assess the behavioral consequences. Here, we provide the first direct evidence for causal entrainment of brain oscillations by transcranial magnetic stimulation (TMS) using concurrent EEG.

Results: We used rhythmic TMS bursts to directly interact with an MEG-identified parietal α -oscillator, activated by attention and linked to perception. With TMS bursts tuned to its preferred α -frequency (α -TMS), we confirmed the three main predictions of entrainment of a natural oscillator: (1) that α -oscillations are induced during α -TMS (reproducing an oscillatory signature of the stimulated parietal cortex), (2) that there is progressive enhancement of this α -activity (synchronizing the targeted, α -generator to the α -TMS train), and (3) that this depends on the pre-TMS phase of the background α -rhythm (entrainment of natural, ongoing α -oscillations). Control conditions testing different TMS burst profiles and TMS-EEG in a phantom head confirmed specificity of α -boosting to the case of synchronization between TMS train and neural oscillator.

Conclusions: The periodic electromagnetic force that is generated during rhythmic TMS can cause local entrainment of natural brain oscillations, emulating oscillatory signatures activated by cognitive tasks. This reveals a new mechanism of online TMS action on brain activity and can account for frequency-specific behavioral TMS effects at the level of biologically relevant rhythms.

Introduction

As a method, transcranial magnetic stimulation (TMS) enables direct rhythmic stimulation of the human brain at frequencies

that characterize electro- or magnetoencephalographic (EEG/MEG) signals [1, 2]. Likewise, the alternative method of transcranial alternating current stimulation (tACS) allows stimulation of the human brain at frequencies of biologically relevant brain rhythms [1, 2]. There is now accumulating experimental support that both rhythmic TMS and tACS interact with natural brain oscillations in a frequency-specific manner [3–8]. This is based on findings that rhythmic stimulation of occipital or parietal areas results in specific (and immediate) perceptual consequences, when the stimulation frequency is tuned to the preferred oscillation frequency of the target area [3–8]. (For analogous effects within the motor system, see [9].)

The above research provides new clues on two long-standing questions: (1) How does TMS (or tACS) interact with ongoing, here oscillatory brain activity to give rise to behavioral effects, and (2), what is the functional relevance of brain oscillations? It does so by pointing toward immediate and specific behavioral consequences depending on TMS (or tACS) frequency. However, these studies [3–8] have one main limitation: they manipulated stimulation frequency (TMS or tACS) and reported behavioral outcome, but they did not study changes in brain activity, i.e., the underlying mechanisms.

Here, we present the missing piece to the puzzle of how these immediate, frequency-dependent effects on perception could come about during rhythmic TMS. Our study builds from the evidence that the behavioral effects of rhythmic TMS (or tACS) are confined to stimulation frequencies that were identified as perceptually relevant in prior EEG/MEG research [3–8]. From this 1:1 frequency locking between the most effective TMS frequency and the perceptually relevant EEG/MEG frequency derives the hypothesis that rhythmic TMS pulses may have entrained the underlying rhythmic generator. This entrainment hypothesis therefore posits that frequency-tuned rhythmic TMS causes entrainment in direct interactions with the underlying brain oscillation. As a consequence, one of the mechanisms by which rhythmic TMS exerts its action on behavior could be the reproduction of a natural oscillatory signature of brain activity (that is also functionally relevant).

Entrainment supposes (1) the induction of a distinct entrainment signature, which emerges during rhythmic TMS and whose topography and frequency reproduce the natural oscillation of the targeted generator. Entrainment also supposes that there is (2) progressive enhancement of the target oscillation in the course of the TMS train as a result of progressive synchronization by each successive TMS pulse. Finally, entrainment should (3) depend on ongoing activity of the target generator, because it is supposedly driving existing brain oscillations, as opposed to generating new artificial rhythms.

We tested the entrainment hypothesis using neuronavigated rhythmic TMS of MEG-localized brain oscillators and concurrent multichannel EEG. We first identified a parietal α -oscillator (i.e., showing oscillatory activity at α -frequency, 8–14 Hz), whose EEG/MEG amplitude is regulated by visual attention [10–13] and correlates with visual perception [13–16]. We then tested in a passive condition whether rhythmic TMS of this parietal area at its preferred frequency entrains the underlying α -generator during TMS, explaining immediate and

*Correspondence: gregor.thut@glasgow.ac.uk

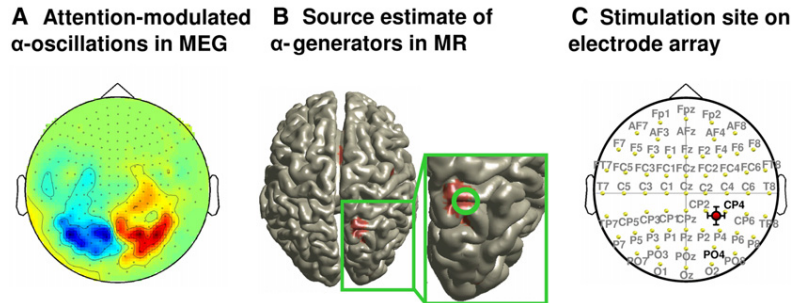
MEG α -localizer experiment

Figure 1. Identification of Parietal Target Site

(A) MEG grand average to the localizer task in sensor space (covert rightward minus leftward orienting of attention).

(B) Estimate of most prominent α -source leading to map in (A) (right hemisphere only). The source is projected on the standard MNI brain.

(C) Average position of the TMS target site projected on the electrode array (international 10–20 EEG system) that was used for EEG recordings concurrently to five-pulse TMS bursts. The TMS hot spot (coil center) was located in between CP2, CP4, P2, and P4 (closest to CP4).

frequency-specific consequences of parietal α -TMS on performance in visual tasks [3–5]. Our results are in line with the three main predictions of the entrainment hypothesis. Rhythmic TMS therefore causes entrainment in direct interactions with the underlying brain oscillations.

Results

For each participant, we first conducted a parietal α -source localizer experiment using MEG [10–13]. On the basis of individual source estimates in structural magnetic resonance (MR) images and using TMS neuronavigation, we then targeted the most prominent (individual) α -source and tuned TMS to its preferred (individual) α -frequency. Accurate placement and 1:1 frequency locking served to create ideal conditions for entrainment (for modeled interaction between stimulus parameters and oscillators, see e.g. [17, 18]).

Experimental Testing

We then ran four TMS conditions per participant while recording 62-channel EEG. In all conditions, we stimulated the same cortical α -generator with short TMS bursts (five pulses). In the main condition, we stimulated at individual α -frequency (α -TMS). During α -TMS, we oriented the TMS coil to induce currents perpendicular to the target gyrus, to maximize TMS efficacy (effect strength is enhanced with this coil orientation [19–22]). In addition to α -TMS, we ran three control conditions. In one control (called arrhythmic TMS or ar-TMS), we applied the same number of TMS pulses as in α -TMS within the same time window (same mean frequency), but with randomly jittered interpulse intervals, holding all other TMS parameters constant. This control was meant to establish that the EEG signature to α -TMS does arise from rhythmic stimulation per se, and not from a basic response of α -generators to rapid-rate TMS bursts. In α -TMS₉₀, we rotated the coil by 90° relative to α -TMS while holding the stimulation site constant (coil handle perpendicular versus parallel to the stimulated gyrus in α -TMS versus α -TMS₉₀). Based on the dependence of TMS efficacy on coil alignment (and hence orienting of induced current) relative to the underlying gyral folding pattern [19–22], we expected strongest entrainment for α -TMS relative to α -TMS₉₀, whereas unspecific effects should be identical in the two conditions. Comparing α -TMS with α -TMS₉₀ therefore allowed us to distinguish entrainment effects on neural tissue under the coil (the stimulated α -generator) from any unspecific effect that could be associated with rhythmic TMS (e.g., monitoring, TMS discomfort, rhythmic auditory clicks). Finally, we oriented the TMS coil in a sham

position (α -TMS_{sham}) to emulate the sound clicks associated with TMS without direct transcranial stimulation, to control for entrainment through rhythmic sounds. For further discussion on the choice of control conditions, see [Note S1 in the Supplemental Discussion](#) available online).

To rule out that EEG results could be of artifactual origin (note the use of a TMS-compatible EEG system [23] and artifact removal procedures; see [Experimental Procedures](#)), we also performed control TMS-EEG recordings in a phantom head using the same TMS, EEG, and postprocessing parameters as in the volunteers.

Below, we first describe localization of the parietal α -generator and how we placed the coil for the different conditions of TMS-EEG testing. We then describe the three key findings supporting TMS entrainment in the simultaneously recorded EEG: entrainment signature, progressive enhancement, and dependence on ongoing oscillations.

Parietal Target Site: Identification of α -Generator and α -Frequency via MEG

The MEG α -localizer task involved attention orienting to the left or right in anticipation of a lateralized target. Behaviorally, this led to better performance at cued versus uncued positions (main effect of cueing validity: $F_{1,7} = 12.53$; $p = 0.009$), independent of target side (cueing validity \times side: $F_{1,7} = 2.99$; $p = 0.127$). Participants responded significantly faster at attended (mean = 738.19 ms) than unattended locations (mean = 911.68 ms).

On the MEG sensor level, comparison between the two conditions (leftward versus rightward covert attention shifts) revealed in each participant the known α -signature of attention orienting (see [Figure 1A](#) for the grand average, comparable to e.g. [24]): a left-right mirror-imaged topography of α -power suppression (in blue) versus enhancement (in red) over parieto-occipital sensors when the two conditions are subtracted (attending rightward minus leftward). Anatomically, the underlying α -generators were localized in parietal areas of the attention network bilaterally (as revealed by maxima of t statistics in individual source space). TMS was then neuronavigated per participant to the right-sided, individual α -source. On average, this site was located at 31.3 ± 2.3 , -63.5 ± 3.5 , 60.3 ± 3.0 in Talairach space (x , y , z , \pm standard error of the mean [SEM]) (see also [Figures 1B](#) and [1C](#)). This location is near (1.5 cm Euclidian distance) a previous parietal target site ($x = 17$, $y = -65$, $z = 54$) measured in a functional magnetic resonance imaging (fMRI) study on attention orienting [25], and whose stimulation by α -TMS modulated perception [5]. Note that TMS of this site did not evoke phosphenes in any

of our participants, which corroborates its location in higher-order attention areas (as opposed to low-level visual areas). The average individual α -frequency across all participants was 10.1 ± 0.31 Hz (\pm SEM) (range 9–11 Hz).

For α -TMS, we oriented the coil for each participant such that its handle pointed along the sagittal plane (upward), and currents were induced in anterior-posterior (y axis) and inferior-superior directions (z axis). In contrast, during α -TMS₉₀, we oriented the coil such that its handle was pointing along the axial plane (sideways) and currents were induced in the left-right direction (x axis). These coil orientations were perpendicular (α -TMS) versus parallel to the target gyrus (α -TMS₉₀), as indicated by Figure 1B (inset, see gyral folding pattern near the average α -source in the MNI brain) and were confirmed by analysis of individual MRI scans (see Note S2 in Supplemental Discussion).

Entrainment Signature: Parietal α -TMS Bursts Mediate α -Power Enhancement at the Target Site

TMS entrainment supposes that frequency-tuned rhythmic TMS triggers a local oscillation at the target site, which cycles at the natural frequency of the targeted generator. In agreement with entrainment, time-frequency (TF) analysis of EEG during α -TMS (TMS-locked averages) shows prominent α -power boosting in a narrow α -band centered on the stimulation frequency, which was emerging over pulses 3–5 following an initial broadband response (shown for CP4 in Figure 2A, α -TMS) and was topographically restricted to the target site (Figure 2C, α -TMS). This narrow α -power boosting was absent in all three control conditions (Figures 2A and 2C, α -TMS₉₀, ar-TMS, and α -TMS_{sham}) and was not observed in recordings in a phantom head (see Note S3 in Supplemental Discussion and Supplemental Results). The latter result indicates that α -boosting during α -TMS was of neuronal origin, and not of artifactual nature.

At the beginning of the train, TMS bursts evoked brain activity over a large spectrum of frequency bands, including in a broad α -band (8–14 Hz) and in the θ - (\sim 4 Hz) and upper β -bands (\sim 25–30 Hz). These responses were transient, i.e., only present for the initial 1–2 pulses of the train (see Figure 2A, window 1 [w1]), and were condition unspecific because they were observed not only during α -TMS but also in the control conditions (Figure 2A, left panels; compare α -TMS with α -TMS₉₀, ar-TMS, and α -TMS_{sham}). In terms of topography (see Figure 2B, left scalp topographies representing α -layer activity), these early condition-unspecific responses were widespread, including frontocentral and bilateral occipital activity (see active TMS conditions: α -TMS, α -TMS₉₀, and ar-TMS). Correspondence between conditions in window w1 is further illustrated in Figures 2A and 2B by only weak differences between α -TMS and control conditions in time-frequency representations (Figure 2A, right panels, difference plots) and in topography plots (Figure 2B, middle scalp topographies, difference maps [diff maps]). These differences were all insignificant (Figure 2B, right scalp topographies, stats) except, as expected, for the comparison with inactive TMS (α -TMS_{sham}), where the differences reached significance for many electrodes (t statistics).

Critically, widespread broadband responses were absent in the second half of the train, where condition-specific responses emerged over pulses 3–5 in a narrow α -band and over the right parietal target site (Figures 2A and 2C, window 2 [w2]). These condition-specific responses were confined to α -TMS bursts, because no such α -power enhancement

existed in the control conditions (α -TMS₉₀, ar-TMS, and α -TMS_{sham}). In addition, they were centered on a narrow α -band corresponding to the preferred oscillation of the targeted generator and hence the TMS frequency (average of \sim 10 Hz; Figure 2A, upper left panel). Comparisons between conditions (subtraction and t statistics) confirmed strongest α -enhancement in w2 during α -TMS relative to all control conditions (Figure 2A, right panels), which localized over the right parietal target site (Figure 2C, middle scalp topographies for difference maps, right topographies for stats). Note in Figure 2A (upper panel) that the narrow α -band activity evoked by α -TMS is short-term, disappearing shortly after discontinuation of the train (\sim 100–150 ms later).

Progressive Enhancement of α -Oscillations during α -TMS Bursts

Although the time-frequency analysis above reveals that α -TMS evokes a response in the α -band, it does not show whether this response is a true α -oscillation (i.e., a wave evolving over one full α -cycle or more). An alternative response could be an evoked component that simply repeats at α -rate but does not constitute a full α -wave. If TMS triggers α -oscillations, TMS-induced responses should show a cyclic pattern. With the addition of other phase-aligned TMS pulses (such as with α -TMS), this α -oscillation should then become progressively enhanced (synchronizing the activity of the underlying generator). To understand the nature of the evoked responses (α -waves versus components occurring at α -rate), we filtered the EEG signal to isolate the α -band and calculated an evoked α -response to each of the five successive TMS pulses of each condition. In agreement with entrainment, the results revealed that α -TMS (but none of the control conditions) triggered α -waves with a progressive time course over the right parietal target site (Figure 3).

Figure 3A (upper panel) represents α -responses to each single pulse of the main condition (α -TMS). The five waveform plots depict responses to each of the five successive TMS pulses Tms1–Tms5 (see boxes; electrodes CP4 [in red] and PO4 [in black] are superimposed). Each one of the five waveform plots reveals a clear cyclic pattern, with α -peak topographies at 90° α -phase angle (above waveforms) and 270° α -phase angle (below waveforms) showing inverted polarity but otherwise identical topography. Corroborating the time-frequency results of α -TMS above, topographies showed widespread α -responses to the initial 1–2 pulses (Tms1 and 2) (frontocentral and occipital maxima), followed over pulses 3–5 (Tms3–5) by more local α -responses close to the stimulation site (right parietal maxima) (Figure 3A, upper panel). For statistical comparisons, we then fitted the α -maps evoked by the initial (Tms1: Map 1_{90°&270°}) and last TMS pulse (Tms5: Map 5_{90°&270°}) to individual data using spatial map fitting procedures [26] (the fitting results are depicted in Figure 3A, lower panel). The results were analyzed via three-way analysis of variance (ANOVA) on goodness of fit (factors: map [Map 1 versus 5], consecutive TMS pulses [Tms1–5], and phase angle [90° versus 270°]). This statistically confirmed induction of α -oscillations and progressive enhancement at the target site. We found that α -maps at 90° versus 270° phase angle fitted the data equally well (no effect of phase angle or interactions; all p = nonsignificant), indicating cyclic activity. We found significant differences between initial and end maps (Map 1_{90°&270°} versus Map 5_{90°&270°}) in terms of their time courses over the train [Figure 3A, fitting results; interaction map \times TMS pulse: F(4,28) = 4.87, p = 0.004]. The

Evoked activity: Time-frequency analysis and topographies

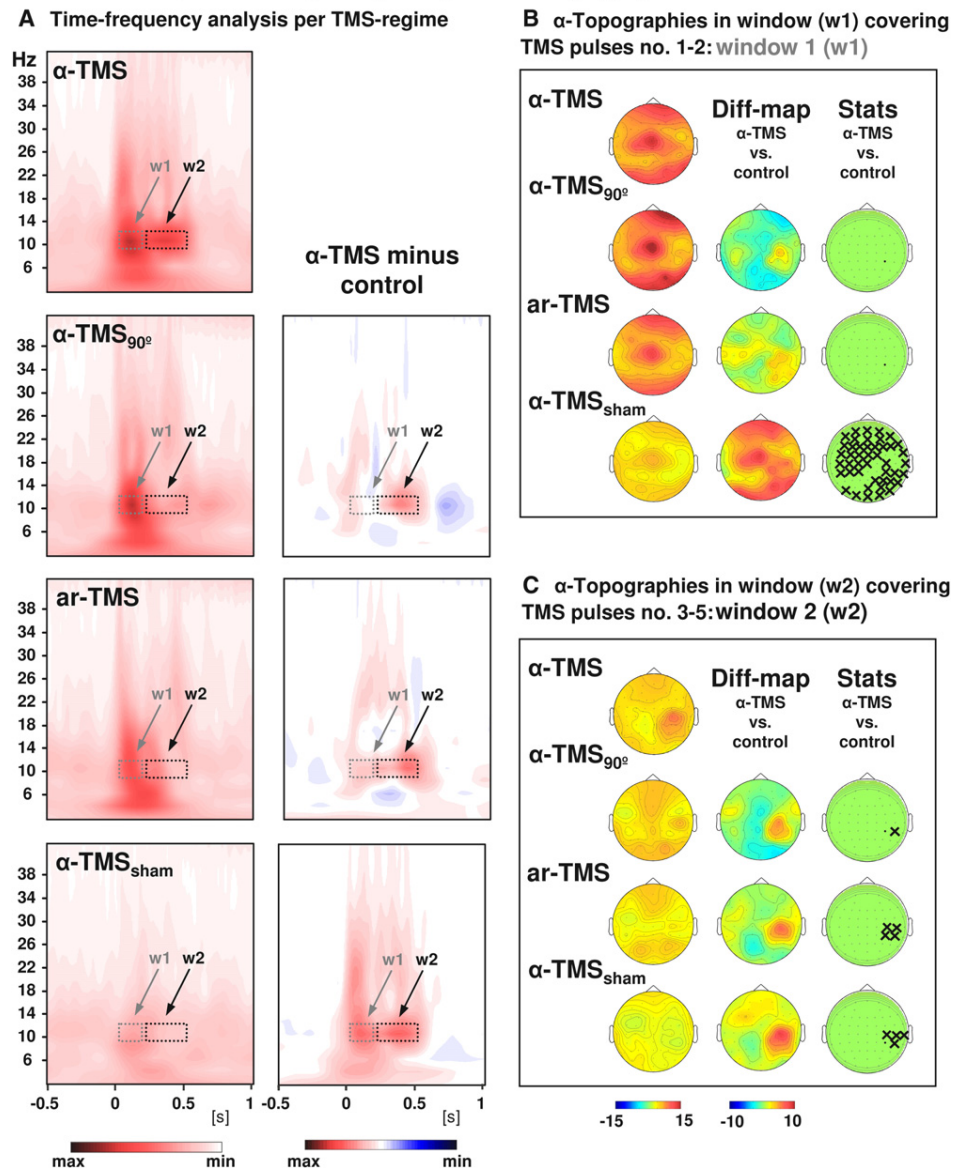


Figure 2. Grand-Averaged Time-Frequency Plots and Topographical Analysis

Comparison of α -TMS bursts (active α -TMS parallel to target gyrus), ar-TMS (active rapid-rate TMS in an arrhythmic regime perpendicular to target gyrus), and α -TMS_{sham} (inactive α -TMS).

(A) Time-frequency plots for electrode CP4 (closest to TMS hot spot) for all conditions (left panels) and subtractions (α -TMS minus control, right panels). w1 and w2 indicate windows of distinct early and late effects (the windows cover the entire train, which lasted 400 ms).

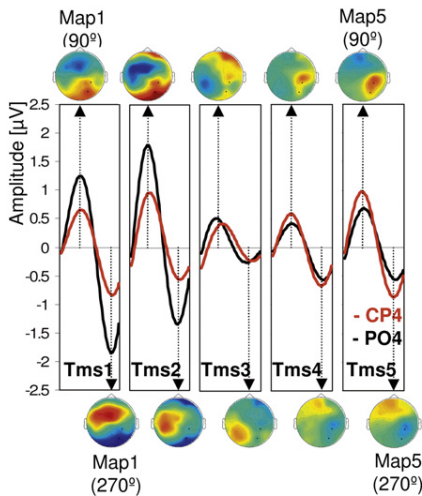
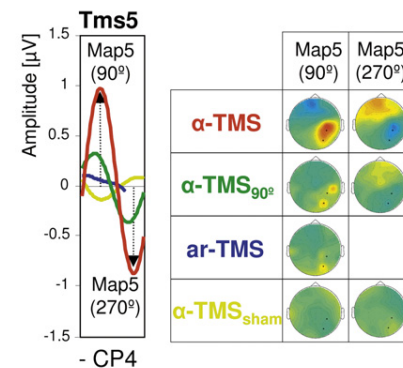
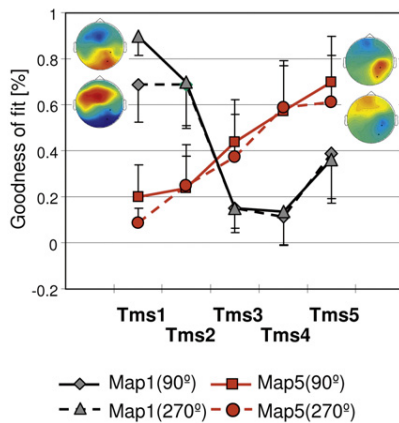
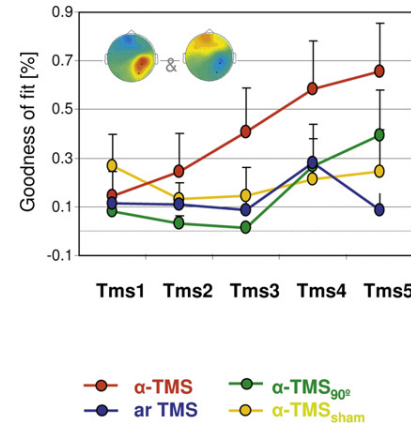
(B) Topographies of the TMS-evoked responses for α -layer activity in the early window (w1).

(C) Topographies of the TMS-evoked responses for α -layer activity in the late window (w2). The columns represent grand-average maps (left column), difference maps (α -TMS minus controls; middle columns), and corresponding t statistics (right columns). Xs indicate electrodes with statistically significant voltage differences in α -TMS relative to the corresponding control.

occipitocentral α -maps (initial Map 1_{90°&270°}) vanished after pulses 1–2 [Figure 3A, fitting results, gray lines, simple effect of TMS pulses: $F(4,28) = 5.93$, $p = 0.0014$]. In contrast, the right parietal α -maps (end Map 5_{90°&270°}) progressively appeared over the successive pulses of the train [Figure 3A, fitting results, red lines, simple effect of TMS pulses: $F(4,28) = 3.12$, $p = 0.03$; polynomial linear contrast: 7.44, $p = 0.029$].

Comparing all conditions in terms of waves and topographies evoked by the end of the train (last pulse: Tms5, end

Map 5_{90°&270°}) (Figure 3B, upper panel) revealed that only α -TMS evoked a clear α -wave (left box, red line) and a right parietal α -map (right maps, compare α -TMS with α -TMS_{90°}, ar-TMS, and α -TMS_{sham}; see Figure S2 for information across all pulses). Map fitting to individual data (fitting results depicted in Figure 3B, lower panel) statistically confirmed condition specificity. The right parietal (entrainment) maps (Map 5_{90°&270°} to α -TMS) showed a progressive time course during α -TMS, which was absent in all other conditions (Figure 3B,

Evoked activity: α -Wave forms and -topographies**A** During α -TMS for each pulse of the train (Tms1-Tms5)**B** Across all TMS regimes for the last pulse (Tms5)**Fitting results****Fitting results**

fitting results), as revealed by a significant interaction of condition \times TMS pulses [$F(12,84) = 2.02$, $p = 0.033$] and follow-up polynomial linear contrasts. The latter were significant for α -TMS [$F(1,7) = 7.44$, $p = 0.03$], but not for any control condition [α -TMS_{90°}: $F(1,7) = 2.97$, $p = 0.12$; ar-TMS: $F(1,7) = 0.43$, $p = 0.53$; α -TMS_{sham}: $F(1,7) = 0.003$, $p = 0.95$].

**Phase Alignment Depends on Ongoing Oscillations:
 α -TMS Bursts Phase Lock α -Oscillations as a Function
of Pre-TMS α -Phase**

TMS entrainment implies driving existing oscillatory processes of the brain. This should not only show in progressive synchronization of the stimulated generator to the TMS pulses (see above), but critically, this should depend on the momentary, ongoing oscillatory cycle of the underlying generator. This arises because TMS pulses will catch the stimulated generator at different stages of its cycle and therefore differentially amplify this endogenous oscillation. Specifically, entrainment performance should show a cosine-shaped function, with strong entrainment when TMS catches the ongoing oscillation at 0° and 360° of phase angle and weak entrainment at 180° .

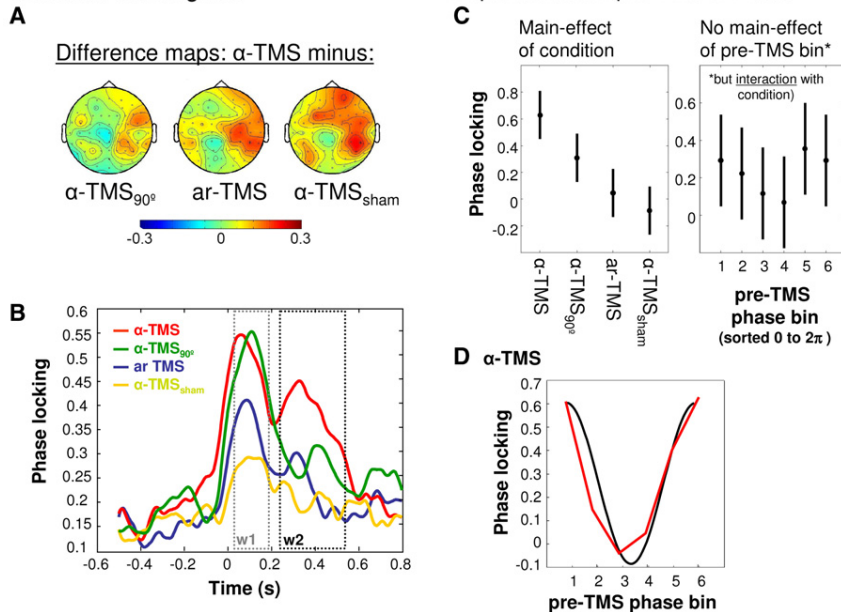
Figure 3. Evoked Activity: α -Wave Forms and Topographies

(A) Top: α -waves and topographies in response to each successive single pulse during α -TMS. Waveforms are shown for electrodes CP4 (red) and PO4 (black). Map topographies are shown for the first and second part of the α -cycle (at 90° and 270° phase angle). Bottom: result of the spatial fitting procedure (spatial map correlations) for statistical evaluation of the time course of the initial (Map 1_{90°&270°}) and end maps (Map 5_{90°&270°}). (B) Top: α -waves and topographies to the last pulse of the train (Tms5) across all conditions. Bottom: result of the spatial fitting procedure (spatial map correlations) for statistical evaluation of the end α (entrainment) maps (Map 5_{90°&270°}) across pulses (Tms1–5) per condition (α -TMS, α -TMS_{90°}, ar-TMS, and α -TMS_{sham}). Error bars represent standard error of the mean.

To fully detail the effect of our main condition (α -TMS) in terms of phase alignment and dependence on pre-TMS α -phase (and possibly α -amplitude), we computed the Hilbert transform of the band-pass-filtered (8–12 Hz) signal to obtain instantaneous phase and amplitude time series. To explore phase (Figures 4A–4D), we then calculated the phase-locking factor (PLF) [27]. PLF quantifies the consistency of the instantaneous phase across trials (with high values corresponding to high consistency). Figure 4A shows topographies of PLF differences in the α -band (α -PLF) during the second part of the TMS train (w2) between α -TMS and each control condition (left, α -TMS minus α -TMS_{90°}; middle, α -TMS minus ar-TMS; right, α -TMS minus α -TMS_{sham}). Significant phase-locking

increases in the vicinity of the stimulation site are evident (Figure 4A). The temporal evolution of α -PLF at significant electrodes (Figure 4B) shows an initial condition-unspecific increase in all conditions in window w1, followed by enhanced phase locking in window w2 during α -TMS (red line) as compared to the control conditions (green, blue, and yellow lines). This extends the results on evoked activity (Figure 2; Figure 3) by revealing that much of the condition-specific α -enhancement during α -TMS is due to increased phase locking in the course of the train. This is evidence for α -activity becoming more synchronized to the train, as opposed to unsynchronized activity increasing in power over the train.

Finally, we examined whether TMS-induced enhancement of PLF in w2 depends on pre-TMS α -phase (Figures 4C and 4D). We sorted pre-TMS α -phase (100 ms prior to TMS onset) into six equidistant bins. We computed mean α -PLFs for window w2 for each bin, condition, and participant and compared them in a two-way ANOVA. This revealed a significant main effect of condition [$F(3,7) = 10.42$, $p = 0.001$] and, importantly, a significant bin \times condition interaction [$F(5,3) = 1.85$, $p = 0.036$]. The factor bin was not significant. Population marginal means illustrate the stronger phase locking during

α -Phase locking
across all TMS-regimesFigure 4. α -Phase Locking and Dependence on Pre-TMS Phase

(A) Topographies of α -phase locking differences in window 2, expressed as change relative to baseline (left, α -TMS minus α -TMS₉₀; middle, α -TMS minus ar-TMS; right, α -TMS minus α -TMS_{sham}).

(B) Time course of relative change of phase locking at significant electrodes with respect to baseline for all four conditions.

(C) Results of two-way ANOVA on end α -phase locking (in window 2). Left: population marginal means for factor condition. Right: population marginal means for factor pre-TMS phase bin (sorted from 0 to 2π). Error bars represent 95% confidence intervals.

(D) α -TMS-specific dependence of α -phase locking (w2) on pre-TMS phase bins. The black curve represents a perfect cosine function.

α -TMS compared to all other conditions (effect of condition, Figure 4C, left panel), but no main effect for bin (Figure 4C, right panel). Further analysis of the interaction revealed a significant dependence of PLF on pre-TMS phase only for α -TMS (high correlation with a cosine function, red versus black line, Figure 4D) ($r = 0.92$, $p = 0.009$ checked by bootstrap procedure).

Analysis of amplitude based on the Hilbert transforms reproduced the condition-specific differences in α -amplitude in the vicinity of the target site in w2 obtained above (α -TMS > all three control conditions; see Figure S3), but this α -enhancement in w2 did not depend on pre-TMS α -amplitude in a condition-specific way (no significant interaction between pre-TMS α -bin and condition; data not shown). Hence, condition-specific entrainment performance (during α -TMS) was dependent only on prestimulus α -phase, but not on prestimulus α -amplitude.

Discussion

To understand the immediate effects of rhythmic TMS on perception, action, or behavior, it is necessary to identify the actions of TMS on brain activity. Here we reveal entrainment of brain oscillations in direct interaction with the underlying generator. We show local synchronization of parietal α -activity when targeting the underlying α -generator with TMS bursts at individual α -frequency (parietal entrainment signature). We demonstrate that this results from progressive synchronization of the underlying α -oscillator in the course of the TMS burst. Finally, we reveal enhanced synchronization (α -phase locking) to depend on the (pre-TMS) phase of the natural, ongoing activity of the stimulated generator. This suggests enhancement of a naturally occurring oscillation instead of the imposition of an artificial rhythm. In sum, our results show that short TMS bursts can drive natural brain oscillations by entrainment, one plausible mechanism via which TMS can act on the brain to modulate perception and performance.

α -frequency (evidence against nonrhythmic α -generation by rapid-rate bursts). Second, there was no α -synchronization with sham TMS bursts that emulate the associated rhythmic auditory events (evidence against α -entrainment through auditory input, e.g., of multisensory neurons in parietal cortex). Third, there was no α -synchronization with rhythmic TMS bursts at suboptimal coil orientations inducing currents parallel to the gyrus (evidence against other unspecific TMS-effects, such as rhythmic somatosensory input). Fourth, it is important to emphasize that the stimulated α -generator was localized in a higher-order area of the attention network, whose stimulation by TMS did not evoke any visual light sensation (phosphenes), to rule out potential visual entrainment through a TMS-induced, flickering visual percept (e.g., [28]). This therefore discounts explanations other than entrainment in direct interaction with underlying neurons.

Our EEG data reveal that short bursts of α -TMS can upregulate the targeted α -oscillations in higher-order parietal areas of the attention network, reminiscent of the α -amplitude regulation by voluntary attention orienting [10, 11], but without the need to engage the participant in an active task. Could this TMS-entrained α -signature that emulates the natural oscillations in origin and frequency also be of functional relevance? Previous EEG research revealed that the occipitoparietal α -band activity, which is amenable to attention control, also scales with visual perception [13–16] and visual cortex excitability [29]. Specifically, occipitoparietal α -power shows an inverse relationship with contralateral visual performance [13–16, 29]. Subsequent behavioral TMS research showed that parietal TMS bursts at this α -frequency (but not at control flanker frequencies) suppress visual perception, or visual representation in contralateral space [4, 5]. The present study therefore provides the missing link between a perceptually effective TMS protocol (parietal α -TMS) [4, 5] and functional EEG activity (parietal α -oscillations) [13–16, 29]. The TMS-induced parietal α -signature that we observed is therefore

likely also of functional relevance. Creating oscillatory brain signatures by TMS can open novel avenues to study not only oscillatory network interactions by means of concurrent EEG but also their functional role in perception and cognition, the latter by exploring behavioral consequences of entrainment.

As to a mechanistic account, our finding of progressive α -phase locking to TMS as a function of ongoing α -activity strongly supports phase resetting of ongoing oscillations, akin to the model of generation of sensory evoked potentials [30–32]. As a consequence of phase resetting, each TMS pulse should trigger waves that cycle at the frequency of the targeted area (approximating an oscillation kernel of entrainment). Because frequency-tuned TMS is phase aligned to these waves, they should then become progressively enhanced. Notably, TMS-aligned waves at the beginning of the train not only cycled at α -frequency but also involved oscillatory activity in the θ - and β -bands. α -oscillations only prevailed toward the end. One explanation is that the initial TMS pulses might have phase reset a multitude of parallel generators located within the same stimulated network but each cycling at a distinct frequency. This would be in keeping with evidence that single TMS pulses can probe into the natural rhythms of the stimulated area [33–35] and that parietal β - and θ -TMS leads to frequency-specific perceptual consequences, albeit ones distinct from the outcome of α -TMS [6]. Alternatively, parts of the initial responses may reflect an unspecific effect of TMS that is not necessarily of oscillatory nature (such as emotional or cognitive appraisal of TMS at the start of the bursts) rather than a genuine TMS impact on underlying neurons (see also [36]). This may be supported by our finding that the responses to the initial TMS pulses spread over several areas (including frontocentral sites). Importantly, however, over the course of the TMS train and in accord with TMS entrainment, only α -oscillations became progressively enhanced, whereas none of the other initial responses were promoted by further pulses. Importantly, also, stimulation in an arrhythmic mode did not lead to entrainment. In this condition, TMS pulses were randomly jittered around a mean α -frequency (about 10 Hz) to cover nonharmonic frequencies of 7–13 Hz (Table 1), which is likely to disrupt or even interrupt entrainment as a result of pulses being out of phase. TMS entrainment can therefore be construed as a progressive recruitment of neuronal elements cycling at the target frequency to phase align their activity to TMS. Note that the duration of entrainment that we report is in full agreement with findings that the oscillatory EEG response to one single pulse (the approximated oscillation kernel) lasts for only about one to two cycles [33, 35], the decay constant of the entrainment effect that we observe. Note also that there is no evidence for entrainment in the literature on long-term EEG aftereffects of clinical repetitive TMS protocols, given the lack of a consistent match between affected EEG and applied TMS frequency [37].

In light of our positive findings, it is of interest that previous attempts to entrain EEG oscillations to a rhythmic TMS train were unsuccessful [38]. It is unlikely that this discrepancy is simply explained by our selection of individual parameters for careful targeting of the generators. Although individual source estimation and 1:1 frequency matching between applied and preferred α -frequency is likely ideal for obtaining entrainment, parietal α -TMS leads to frequency-specific perceptual consequences also with fixed, not strictly individualized (10 Hz) frequency [4, 5]. Physiologically, this may be explained by trial-by-trial fluctuations around the average individual

α -frequency. In addition, computational work shows that the tight relationship between effective stimulation frequency and preferred frequency loosens up as stimulus intensity increases, meaning that with increasing stimulus intensity, entrainment may occur from a progressively larger bandwidth, albeit one centered on the natural frequencies of the stimulated cortex (giving rise to the so-called Arnold tongues) (e.g., [17, 18]). This suggests that entrainment should also work when TMS frequency is slightly off the individual α -frequency. One explanation of previous null results of entrainment may be the use of overly conservative artifact-removal procedures (e.g., independent component analysis, as in [38]), as may be required in certain EEG devices with slow recovery times after TMS. This may eliminate not only the artifacts but also TMS-evoked activity. Alternatively, entrainment may have been complicated by the choice of a suboptimal coil orientation. Further research will need to study in detail the parameter space within which a natural oscillatory signature can be entrained.

Conclusion

Our data show that short rhythmic TMS bursts can directly entrain underlying brain rhythms. This sheds new light on the direct interaction of rhythmic TMS with brain oscillations and significantly adds to an emerging literature on entrainment via alternative transcranial stimulation protocols, such as tACS [7–9, 39–42]. Our data show that TMS entrainment can evoke spatially specific and frequency-specific signatures. The evoked signatures mimic naturally occurring, task-related modulations that are of functional significance. This may prove highly beneficial for the study of human brain oscillations.

Experimental Procedures

Participants

Ten healthy adult volunteers participated, of whom two had to be excluded from EEG analysis because of excessive eye blinks (artifacts) triggered by TMS. The remaining participants (five females, three males) had a mean age of 27.1 years (21–33 years) and were predominantly right handed by self report (one left handed). None had contraindications to TMS. All gave written informed consent prior to the study, which was approved by the ethics committee of the Faculty of Information & Mathematical Sciences of the University of Glasgow. The TMS protocol used accords with current safety guidelines and is of widespread use in studies on cognition [43].

MEG Localizer Experiment

Participants performed in a symbolically cued visual-spatial attention-orienting paradigm, in anticipation of an upcoming, lateralized visual target. In short, a central visual cue of 0.2 s duration (randomly pointing either to the lower left or right visual field) prompted covert shifts of visual attention to the indicated position. After 1.7 s, the target appeared more often at cued than noncued locations (80% versus 20% of trials). The targets consisted of either an “x” or a “+,” whose luminance contrast with the background was chosen to give rise to perithreshold performance per participant. The participants were required to discriminate the two targets (giving left index responses for “x” and right index responses for “+”). There was a 3 s delay between the manual response and the next cue. Participants were asked to keep central fixation, to covertly direct and maintain attention to the cued position, and to respond to targets at cued and noncued locations.

MEG data of 100 trials were collected for each of the two attention conditions (randomly intermixed within five blocks of approximately 4 min duration each) using a 248-channel magnetometer whole-head MEG system (Magnes 3600 WH, 4-D Neuroimaging). Data were collected at 508 Hz sampling rate and online high-pass filtered at 0.1 Hz.

MEG data analysis focused on attention-related signals in the cue-target interval, normalized to baseline before cue onset. To this end, we epoched MEG signals time locked to cue onset (–1 to 2.5 s) and linearly detrended them prior to regression-based denoising using the signals from the reference sensors. Trials contaminated with artifacts were rejected after visual

Rhythmic TMS Drives Brain Oscillations

1183

Table 1. TMS Conditions

	TMS Mode	TMS Regime	TMS Pulses	Train Duration	Frequency	IPI	Coil Handle Relative to Target Gyrus	Coil Surface Relative to Scalp
α -TMS	active	rhythmic	n = 5	4 × IAF cycle	IAF	fixed to 1000/IAF	perpendicular	tangential
α -TMS _{90°}	active	rhythmic	n = 5	4 × IAF cycle	IAF	fixed to 1000/IAF	parallel	tangential
ar-TMS	active	arrhythmic	n = 5	4 × IAF cycle	NA	jittered by 0.7 × IPI, 0.8 × IPI, 1.2 × IPI, 1.3 × IPI	perpendicular	tangential
α -TMS _{sham}	inactive	rhythmic	n = 5	4 × IAF cycle	IAF	fixed to 1000/IAF	NA	radial

The following abbreviations are used: IPI, interpulse interval; IAF, individual α -frequency; NA, not applicable. Note: in the formula for calculating individual jitter in ar-TMS, IPI refers to individual IPIs of the rhythmic regimes (= 1000/IAF). The presentation order of the four resulting, variable IPIs was randomized within each trial.

inspection. Spectral analysis was performed on two 1 s data segments (−1 s to 0 s and 0.5 s to 1.5 s) after applying Hanning tapers. Spectra for left-cue and right-cue trials were averaged separately and subtracted. The difference spectral plot was used to identify the individual α -generator (in the 5–15 Hz range) that showed strongest modulation by visual spatial attention.

Source localization was performed using dynamic imaging of coherent sources (DICS; [44]) on a 6 mm³ grid at individual α -frequency to localize the strongest generators of the α -modulation associated with the shift of spatial attention. To this end, a t statistic was computed for the single-trial difference between precue and postcue α -power. The 3D map of t values was visualized on the standardized structural MRI, and the coordinates of the global maximum were identified.

To control for adequate task performance, behavioral data were analyzed using repeated-measure ANOVA. Reaction times to targets were subjected to ANOVA with factors cueing validity (for targets appearing at cued versus noncued positions) and target side (left versus right). Post hoc tests were Bonferroni corrected. See [Supplemental Experimental Procedures](#) for more details.

TMS-EEG

TMS Paradigm

TMS was applied at rest. Participants were comfortably seated with their chin positioned in a chin rest, their eyes open, and their gaze centered on a continuously displayed fixation cross (black on a gray background, RGB 192). Participants were asked to maintain central fixation and to minimize eye blinks and other movements during the recording blocks.

Short TMS bursts were delivered under the main (α -TMS) and three control conditions (α -TMS_{90°}, ar-TMS, and α -TMS_{sham}). Each control condition differed in one aspect from the main condition. See text and [Table 1](#) for details.

We neuronavigated the TMS coil (70 mm figure-of-eight coil connected to a Magstim Rapid2 Stimulator) in all conditions to the Talairach coordinates of the most prominent posterior α -generator of the right hemisphere (obtained from the MEG localizer task) viaBrainsight (Rogue Research). Neuronavigation was based on individual source estimates and the individual structural MR scans.

TMS intensity was at 100% phosphene threshold, determined in blindfolded participants. Under blindfolding, occipital stimulation at experimental TMS intensity therefore evoked weak phosphenes in 50% of trials. With TMS over the α -generators that were localized in parietal cortex for all participants, no phosphene perceptions could be evoked (replicating [5]). The average stimulation intensity was 63.25% of maximum stimulator output (range 58%–66%).

The four TMS conditions were tested in a block design. In each block, 18 five-pulse TMS trains were given with an intertrain interval of 20 s, leading to 90 pulses per block over a block duration of about 6 min. All four conditions were tested in a series of four blocks (order of conditions randomized). This was repeated three times, leading to a total of 810 active TMS pulses with 54 trials per condition.

The duration of the experiment was 1.5–2 hr of recording, plus 1 hr for mounting the 64 EEG electrodes.

EEG Recording

Using TMS-compatible equipment (BrainAmp 64 MRplus, BrainProducts), EEG was continuously acquired from 62 channels (plus ground and reference electrodes). TMS-compatible sintered Ag/AgCl-pin electrodes were used. The signal was band-pass filtered at DC to 1000 Hz and digitized at a sampling rate of 5 kHz. Skin/electrode impedance was maintained below 5 k Ω .

EEG Analysis

Analysis was performed using the FieldTrip software package (<http://fieldtrip.fcdonders.nl>), custom-made MATLAB code, BrainVision Analyzer 1 (BrainProducts), and Cartool software (<http://sites.google.com/site/fbmlab/cartool>).

Preprocessing and Artifact Removal. Preprocessing epochs were of 4 s duration (−2 s to +2 s from TMS train onset). Epochs with excessively noisy EEG, eye movement artifacts (blinks or saccades), or muscle artifacts were excluded (mean acceptance rate 68%). The 50 Hz artifact was removed from remaining trials by fitting and subtracting a 50 Hz sine/cosine function. Subsequently, data were rereferenced to common average reference. After these steps, the remaining artifacts associated with the TMS pulses consisted of brief high-voltage peaks. These artifacts, which were generally of about 5–8 ms duration (replicating e.g. [23] using the same EEG equipment), were then removed using cubic interpolation for a conservative 15 ms interval following the TMS pulse. The same procedure was applied to remove the shorter and smaller rTMS recharge artifact [23], interpolating a 3 ms interval after ~20 ms from each magnetic pulse (latencies varied across subjects according to TMS intensity). Single trials were carefully inspected to ensure absence of residual TMS artifacts. See also [Note S3 in the Supplemental Discussion](#) on TMS-induced artifacts.

Wavelet Analysis across the Entire Epoch. To analyze the oscillatory activity evoked by the TMS train, we calculated the average responses for an epoch of −0.5 s pre to +1 s post train onset and processed them with complex Morlet wavelets (2–40 Hz, 20 frequency steps, $c = 5$). Based on the results and in order to evaluate the entrainment of α -oscillations, we extracted the frequency range between 8 and 12 Hz for each subject from the wavelet dataset. Their spatial map topographies were plotted and compared across conditions (α -TMS versus controls) using subtraction plots (subtraction maps) and electrode-wise t statistics (t/p maps). The analysis revealed a biphasic response pattern (broadband response in an early time window, narrow α -band response in a later time window). Analyses were therefore performed on two windows (window w1 and w2), each centered on these responses. The early window (40–190 ms into the train) covered pulses 1–2, the later window (240–540 ms) pulses 3–5.

Analysis of α -Waves to Each Successive TMS Pulse. To analyze the spatio-temporal characteristics of α -waves, we band-pass filtered artifact-free data 8–12 Hz (Butterworth zero-phase filters, slope 48 dB/oct) and rearranged them to five epochs locked to the onset of each single pulse (epoch duration depending on individual α -frequency [IAF] and condition, minimum 0–90 ms post-TMS for IAF of 11 Hz, minimum 0.7 × 90 ms = 63 ms for ar-TMS). The average α -wave was then analyzed in terms of evolution of its topographies over the five pulses and in terms of differences across conditions. To this end, we performed spatial map fitting between the grand-average scalp topographies at the two α -peaks within an α -cycle (90° and 270°) and the corresponding individual α -peaks of the same or corresponding control conditions (intercorrelation between peak topographies). The fitting results were then analyzed to evaluate goodness of fit of grand-average maps (gmMap) in individual data to statistically secure their condition specificity (see e.g. [11] for application; see [26] for review). To this end, we computed ANOVAs on the fitting results (goodness of fit). To evaluate the evolution of α -waves across TMS pulses in the main condition (α -TMS), we conducted a 2 × 5 × 2 ANOVA with evoked map (start versus end), TMS pulse (Tms1–5) and phase (90° versus 270°) as within-subject factors. To compare α -waves across all conditions, we conducted a 4 × 5 × 2 ANOVA on fitting of map 5 with condition (α -TMS, α -TMS_{90°}, ar-TMS, and α -TMS_{sham}), TMS pulse (Tms1–5) and phase (90° versus 270°) as within-subject factors.

Analysis of Dependence on Ongoing Oscillations prior to TMS. Artifact-free data were band-pass filtered 8–12 Hz and subjected to Hilbert

transform for computation of instantaneous phase and amplitude. Intertrial phase locking was computed from the instantaneous phase ϕ as the absolute value of the mean of $\exp(i\phi)$ across trials, also called phase-locking factor (PLF) [27]. PLF and amplitudes were individually averaged across trials (amplitudes were normalized by computing change relative to baseline [−500 ms to −100 ms]). Differences between conditions were tested for all electrodes in window w2. As a conservative significance estimate, we only considered electrodes with $p < 0.05$ (t tests) in all three comparisons (α -TMS minus α -TMS₉₀, α -TMS minus ar-TMS, and α -TMS minus α -TMS_{sham}) to be significant.

In a next step, trials were sorted into six bins of increasing pre-TMS α -phase (spanning from 0 to 2π) or pre-TMS α -amplitude (spanning from min to max) (100 ms before TMS onset). Ongoing α -activity prior to TMS showed a widespread distribution over occipital and parietal sites bilaterally (data not shown), in contrast to α -phase locking during TMS, which was spatially restricted to electrodes over the right parietal target site (Figure 4A), indicating local entrainment. The ongoing right parietal signal was therefore likely distorted by volume conductance from adjacent posterior sites (right occipital and left parietal). To decrease contributions from (possibly stronger) more distant α -sources prior to TMS and to thereby obtain a more reliable estimate of the ongoing α -phase and α -amplitude of the right parietal source (to be related to entrainment measures over right parietal sites), we computed pre-TMS phase and amplitude calculations for sorting on a bipolar montage (C4 – CP4) – (CP4 – P4). α -phase locking and α -amplitudes were averaged across window w2 and significant electrodes for each participant, condition, and bin separately before being subjected to 6×4 ANOVAs with factors bin and condition. Population marginal means of main factors were computed using the multcompare function in MATLAB (MathWorks).

To analyze whether the strength of phase locking was consistently modulated by pre-TMS phase, we computed the maximum cross-correlation between the six PLF values (one for each phase bin) and a cosine function for all four conditions (α -TMS, α -TMS₉₀, ar-TMS, and α -TMS_{sham}) and compared them to the 95th percentile of the null distribution for each condition separately. The null distribution was created by computing the maximum cross-correlation (across all lags) for 500 random permutations of the six PLF values. Significant cross-correlation was obtained only for α -TMS (Figure 4D).

Supplemental Information

Supplemental Information includes Supplemental Results, Supplemental Discussion, three figures, and Supplemental Experimental Procedures and can be found with this article online at doi:10.1016/j.cub.2011.05.049.

Acknowledgments

This work was supported by the Biotechnology and Biological Sciences Research Council (BB/I006494/1) and the Wellcome Trust (091928 and 084067).

Received: February 19, 2011

Revised: April 21, 2011

Accepted: May 26, 2011

Published online: June 30, 2011

References

- Thut, G., and Miniussi, C. (2009). New insights into rhythmic brain activity from TMS-EEG studies. *Trends Cogn. Sci. (Regul. Ed.)* 13, 182–189.
- Siebnner, H.R., and Ziemann, U. (2010). Rippling the cortex with high-frequency (>100 Hz) alternating current stimulation. *J. Physiol.* 588, 4851–4852.
- Klimesch, W., Sauseng, P., and Gerloff, C. (2003). Enhancing cognitive performance with repetitive transcranial magnetic stimulation at human individual alpha frequency. *Eur. J. Neurosci.* 17, 1129–1133.
- Sauseng, P., Klimesch, W., Heise, K.F., Gruber, W.R., Holz, E., Karim, A.A., Glennon, M., Gerloff, C., Birbaumer, N., and Hummel, F.C. (2009). Brain oscillatory substrates of visual short-term memory capacity. *Curr. Biol.* 19, 1846–1852.
- Romei, V., Gross, J., and Thut, G. (2010). On the role of prestimulus alpha rhythms over occipito-parietal areas in visual input regulation: Correlation or causation? *J. Neurosci.* 30, 8692–8697.

- Romei, V., Driver, J., Schyns, P.G., and Thut, G. (2011). Rhythmic TMS over parietal cortex links distinct brain frequencies to global versus local visual processing. *Curr. Biol.* 21, 334–337.
- Kanai, R., Chaieb, L., Antal, A., Walsh, V., and Paulus, W. (2008). Frequency-dependent electrical stimulation of the visual cortex. *Curr. Biol.* 18, 1839–1843.
- Feurra, M., Paulus, W., Walsh, V., and Kanai, R. (2011). Frequency specific modulation of human somatosensory cortex. *Front. Psychol.* 2, 13.
- Pogosyan, A., Gaynor, L.D., Eusebio, A., and Brown, P. (2009). Boosting cortical activity at beta-band frequencies slows movement in humans. *Curr. Biol.* 19, 1637–1641.
- Kelly, S.P., Lalor, E.C., Reilly, R.B., and Foxe, J.J. (2006). Increases in alpha oscillatory power reflect an active retinotopic mechanism for distracter suppression during sustained visuospatial attention. *J. Neurophysiol.* 95, 3844–3851.
- Rihs, T.A., Michel, C.M., and Thut, G. (2009). A bias for posterior alpha-band power suppression versus enhancement during shifting versus maintenance of spatial attention. *Neuroimage* 44, 190–199.
- Sauseng, P., Klimesch, W., Stadler, W., Schabus, M., Doppelmayr, M., Hanslmayr, S., Gruber, W.R., and Birbaumer, N. (2005). A shift of visual spatial attention is selectively associated with human EEG alpha activity. *Eur. J. Neurosci.* 22, 2917–2926.
- Thut, G., Nietzel, A., Brandt, S.A., and Pascual-Leone, A. (2006). Alpha-band electroencephalographic activity over occipital cortex indexes visuospatial attention bias and predicts visual target detection. *J. Neurosci.* 26, 9494–9502.
- van Dijk, H., Schoffelen, J.M., Oostenveld, R., and Jensen, O. (2008). Prestimulus oscillatory activity in the alpha band predicts visual discrimination ability. *J. Neurosci.* 28, 1816–1823.
- Hanslmayr, S., Aslan, A., Staudigl, T., Klimesch, W., Herrmann, C.S., and Bäuml, K.H. (2007). Prestimulus oscillations predict visual perception performance between and within subjects. *Neuroimage* 37, 1465–1473.
- Mathewson, K.E., Gratton, G., Fabiani, M., Beck, D.M., and Ro, T. (2009). To see or not to see: Prestimulus alpha phase predicts visual awareness. *J. Neurosci.* 29, 2725–2732.
- Glass, L. (2001). Synchronization and rhythmic processes in physiology. *Nature* 410, 277–284.
- Gouwens, N.W., Zeberg, H., Tsumoto, K., Tateno, T., Aihara, K., and Robinson, H.P. (2010). Synchronization of firing in cortical fast-spiking interneurons at gamma frequencies: A phase-resetting analysis. *PLoS Comput. Biol.* 6, e1000951.
- Brasil-Neto, J.P., Cohen, L.G., Panizza, M., Nilsson, J., Roth, B.J., and Hallett, M. (1992). Optimal focal transcranial magnetic activation of the human motor cortex: Effects of coil orientation, shape of the induced current pulse, and stimulus intensity. *J. Clin. Neurophysiol.* 9, 132–136.
- Mills, K.R., Boniface, S.J., and Schubert, M. (1992). Magnetic brain stimulation with a double coil: The importance of coil orientation. *Electroencephalogr. Clin. Neurophysiol.* 85, 17–21.
- Kammer, T., Vorwerk, M., and Herrmberger, B. (2007). Anisotropy in the visual cortex investigated by neuronavigated transcranial magnetic stimulation. *Neuroimage* 36, 313–321.
- Thielscher, A., Opitz, A., and Windhoff, M. (2011). Impact of the gyral geometry on the electric field induced by transcranial magnetic stimulation. *Neuroimage* 54, 234–243.
- Veniero, D., Bortoletto, M., and Miniussi, C. (2009). TMS-EEG co-registration: On TMS-induced artifact. *Clin. Neurophysiol.* 120, 1392–1399.
- Bahramisharif, A., van Gerven, M., Heskes, T., and Jensen, O. (2010). Covert attention allows for continuous control of brain-computer interfaces. *Eur. J. Neurosci.* 31, 1501–1508.
- Corbetta, M., Akbudak, E., Conturo, T.E., Snyder, A.Z., Ollinger, J.M., Drury, H.A., Linenweber, M.R., Petersen, S.E., Raichle, M.E., Van Essen, D.C., and Shulman, G.L. (1998). A common network of functional areas for attention and eye movements. *Neuron* 21, 761–773.
- Murray, M.M., Brunet, D., and Michel, C.M. (2008). Topographic ERP analyses: A step-by-step tutorial review. *Brain Topogr.* 20, 249–264.
- Tallon-Baudry, C., Bertrand, O., Delpeuch, C., and Pernier, J. (1996). Stimulus specificity of phase-locked and non-phase-locked 40 Hz visual responses in human. *J. Neurosci.* 16, 4240–4249.
- Herrmann, C.S. (2001). Human EEG responses to 1–100 Hz flicker: Resonance phenomena in visual cortex and their potential correlation to cognitive phenomena. *Exp. Brain Res.* 137, 346–353.
- Romei, V., Brodbeck, V., Michel, C., Amedi, A., Pascual-Leone, A., and Thut, G. (2008). Spontaneous fluctuations in posterior alpha-band

Rhythmic TMS Drives Brain Oscillations

1185

- EEG activity reflect variability in excitability of human visual areas. *Cereb. Cortex* 18, 2010–2018.
30. Sayers, B.M., Beagley, H.A., and Henshall, W.R. (1974). The mechanism of auditory evoked EEG responses. *Nature* 247, 481–483.
 31. Makeig, S., Westerfield, M., Jung, T.P., Enghoff, S., Townsend, J., Courchesne, E., and Sejnowski, T.J. (2002). Dynamic brain sources of visual evoked responses. *Science* 295, 690–694.
 32. Klimesch, W., Sauseng, P., Hanslmayr, S., Gruber, W., and Freunberger, R. (2007). Event-related phase reorganization may explain evoked neural dynamics. *Neurosci. Biobehav. Rev.* 31, 1003–1016.
 33. Paus, T., Sipila, P.K., and Strafella, A.P. (2001). Synchronization of neuronal activity in the human primary motor cortex by transcranial magnetic stimulation: An EEG study. *J. Neurophysiol.* 86, 1983–1990.
 34. Fuggetta, G., Fiaschi, A., and Manganotti, P. (2005). Modulation of cortical oscillatory activities induced by varying single-pulse transcranial magnetic stimulation intensity over the left primary motor area: a combined EEG and TMS study. *Neuroimage* 27, 896–908.
 35. Rosanova, M., Casali, A., Bellina, V., Resta, F., Mariotti, M., and Massimini, M. (2009). Natural frequencies of human corticothalamic circuits. *J. Neurosci.* 29, 7679–7685.
 36. Hamidi, M., Slagter, H.A., Tononi, G., and Postle, B.R. (2010). Brain responses evoked by high-frequency repetitive transcranial magnetic stimulation: An event-related potential study. *Brain Stimulat.* 3, 2–14.
 37. Thut, G., and Pascual-Leone, A. (2010). A review of combined TMS-EEG studies to characterize lasting effects of repetitive TMS and assess their usefulness in cognitive and clinical neuroscience. *Brain Topogr.* 22, 219–232.
 38. Johnson, J.S., Hamidi, M., and Postle, B.R. (2010). Using EEG to explore how rTMS produces its effects on behavior. *Brain Topogr.* 22, 281–293.
 39. Marshall, L., Helgadottir, H., Mölle, M., and Born, J. (2006). Boosting slow oscillations during sleep potentiates memory. *Nature* 444, 610–613.
 40. Bergmann, T.O., Groppa, S., Seeger, M., Mölle, M., Marshall, L., and Siebner, H.R. (2009). Acute changes in motor cortical excitability during slow oscillatory and constant anodal transcranial direct current stimulation. *J. Neurophysiol.* 102, 2303–2311.
 41. Ozen, S., Sirota, A., Belluscio, M.A., Anastassiou, C.A., Stark, E., Koch, C., and Buzsáki, G. (2010). Transcranial electric stimulation entrains cortical neuronal populations in rats. *J. Neurosci.* 30, 11476–11485.
 42. Zaehle, T., Rach, S., and Herrmann, C.S. (2010b). Transcranial alternating current stimulation enhances individual alpha activity in human EEG. *PLoS ONE* 5, e13766.
 43. Rossi, S., Hallett, M., Rossini, P.M., and Pascual-Leone, A.; Safety of TMS Consensus Group. (2009). Safety, ethical considerations, and application guidelines for the use of transcranial magnetic stimulation in clinical practice and research. *Clin. Neurophysiol.* 120, 2008–2039.
 44. Gross, J., Kujala, J., Hamalainen, M., Timmermann, L., Schnitzler, A., and Salmelin, R. (2001). Dynamic imaging of coherent sources: Studying neural interactions in the human brain. *Proc. Natl. Acad. Sci. USA* 98, 694–699.

EXHIBIT 26



HHS Public Access

Author manuscript

Brain Stimul. Author manuscript; available in PMC 2023 March 01.

Published in final edited form as:

Brain Stimul. 2022 ; 15(2): 458–471. doi:10.1016/j.brs.2022.02.008.

Daily prefrontal closed-loop repetitive transcranial magnetic stimulation (rTMS) produces progressive EEG quasi-alpha phase entrainment in depressed adults

Josef Faller^{*,1}, Jayce Doose^{*,2}, Xiaoxiao Sun^{*,1,3}, James R. McIntosh^{1,4}, Golbarg T. Saber^{5,6}, Yida Lin⁷, Joshua B. Teves⁵, Aidan Blankenship⁵, Sarah Huffman⁸, Robin I. Goldman⁹, Mark S. George^{8,10}, Truman R. Brown^{2,5}, Paul Sajda^{1,11,12,13}

¹Department of Biomedical Engineering, Columbia University, New York, NY 10027, USA

²Center for Biomedical Imaging, Medical University of South Carolina, Charleston, SC 29425, USA

³US DEVCOM Army Research Laboratory, Aberdeen Proving Ground, MD 20115, USA

⁴Department of Orthopaedic Surgery, Columbia University Irving Medical Center, New York, NY 10032, USA

⁵Department of Radiology and Radiological Science, Medical University of South Carolina, Charleston, SC 29425, USA

⁶Department of Neurology, University of Chicago, Chicago, IL 60637, USA

⁷Department of Computer Science, Columbia University, New York, NY 10027, USA

⁸Department of Psychiatry and Behavioral Sciences, Medical University of South Carolina, Charleston, SC 29425, USA

⁹Center for Healthy Minds, University of Wisconsin-Madison, Madison, WI 53705, USA

¹⁰Ralph H. Johnson VA Medical Center, Charleston, SC 29401, USA

* contributed equally

All persons who meet authorship criteria are listed as authors, and all authors certify that they have participated sufficiently in the work to take public responsibility for the content, including participation in the concept, design, analysis, writing, or revision of the manuscript.

Josef Faller: conceptualization, methodology, software, writing-original draft

Jayce Doose: conceptualization, investigation, data curation, writing-original draft, writing-review & editing

Xiaoxiao Sun: methodology, formal analysis, writing-original draft, writing-review & editing, Visualization

James McIntosh: conceptualization, methodology, software, data curation, writing-review & editing

Golbarg T.Saber: conceptualization, methodology, data curation

Yida Lin: software

Joshua B. Teves: investigation, data curation

Aidan Blankenship: investigation, data curation

Sarah Huffman: investigation

Robin Goldman: conceptualization, methodology, writing-review & editing, funding acquisition, project administration, supervision

Mark S. George: conceptualization, methodology, writing-review & editing, funding acquisition, project administration, supervision

Truman R. Brown: conceptualization, methodology, writing-review & editing, funding acquisition, project administration, supervision

Paul Sajda: conceptualization, methodology, writing-original draft, writing-review & editing, funding acquisition, project administration, supervision

Publisher's Disclaimer: This is a PDF file of an unedited manuscript that has been accepted for publication. As a service to our customers we are providing this early version of the manuscript. The manuscript will undergo copyediting, typesetting, and review of the resulting proof before it is published in its final form. Please note that during the production process errors may be discovered which could affect the content, and all legal disclaimers that apply to the journal pertain.

¹¹Department of Radiology, Columbia University Irving Medical Center, New York, NY 10032, USA

¹²Department of Electrical Engineering, Columbia University, New York, NY 10027, USA

¹³Data Science Institute, Columbia University, New York, NY 10027, USA

Abstract

Background: Transcranial magnetic stimulation (TMS) is a non-invasive neuromodulation modality that can treat depression, obsessive-compulsive disorder, or help smoking cessation. Research suggests that timing the delivery of TMS relative to an endogenous brain state may affect efficacy and short-term brain dynamics.

Objective: To investigate whether, for a multi-week daily treatment of repetitive TMS (rTMS), there is an effect on brain dynamics that depends on the timing of the TMS relative to individuals' prefrontal EEG quasi-alpha rhythm (between 6 to 13 Hz).

Method: We developed a novel closed-loop system that delivers personalized EEG-triggered rTMS to patients undergoing treatment for major depressive disorder. In a double blind study, patients received daily treatments of rTMS over a period of six weeks and were randomly assigned to either a synchronized or unsynchronized treatment group, where synchronization of rTMS was to their prefrontal EEG quasi-alpha rhythm.

Results: When rTMS is applied over the dorsal lateral prefrontal cortex (DLPFC) and synchronized to the patient's prefrontal quasi-alpha rhythm, patients develop strong phase entrainment over a period of weeks, both over the stimulation site as well as in a subset of areas distal to the stimulation site. In addition, at the end of the course of treatment, this group's entrainment phase shifts to be closer to the phase that optimally engages the distal target, namely the anterior cingulate cortex (ACC). These entrainment effects are not observed in the group that is given rTMS without initial EEG synchronization of each TMS train.

Conclusions: The entrainment effects build over the course of days/weeks, suggesting that these effects engage neuroplastic changes which may have clinical consequences in depression or other diseases.

Keywords

Closed-loop Neurostimulation; Electroencephalography (EEG); Repetitive Transcranial Magnetic Stimulation (rTMS); Inter-trial Phase Coherence (ITPC); Major Depressive Disorder (MDD)

INTRODUCTION

Several forms of targeted neurostimulation can treat multiple diseases and psychiatric conditions (George et al., 2000; Rodriguez-Martin et al., 2002; Kobayashi and Pascual-Leone, 2003; Hallett, 2007; George et al., 2010). An important issue for these approaches is how to focus the stimulation in both space (location) and time (relative to other brain events) (Pascual-Leone and Walsh, 2002; Walsh and Pascual-Leone, 2003; Sliwinska et al., 2014). This is particularly true in non-invasive neurostimulation such as TMS, where the ultimate therapeutic target site might be deep in the brain while the initial stimulation site is often

located superficially. In the case of pharmacologically resistant major depressive disorder (MDD), the Food and Drug Administration (FDA) approved repetitive transcranial magnetic stimulation (rTMS) at 10 Hz over the left dorsolateral prefrontal cortex (DLPFC) as a treatment (O'Reardon et al., 2007; Markowitz et al., 2010; George et al., 2010; Wo niak-Kwa niewska et al., 2014). One of the earliest hypotheses held that rTMS might be an effective antidepressant because the proximal stimulation over DLPFC could cause changes in a circuit involving distal brain regions including the anterior cingulate cortex (ACC) and the subgenual ACC (sgACC), where these distal regions are believed to be linked to the disease state (George et al., 1994; Fox et al., 1997; Mayberg et al., 1997). Evidence in support of this theory was reported by George and others (George et al., 2010; Raco et al., 2016).

The therapeutic mechanisms of TMS are thought to be mediated by connectivity between the stimulation site and deeper brain structures (Drysdale et al., 2017). Functional imaging studies have observed significant functional connectivity between the ACC and DLPFC (Barbas et al., 2002; Rushworth et al., 2011; Medalla and Barbas, 2012; Caspers et al., 2017). However, it is also well-known that functional connectivity can be dynamic, and thus the ability to affect distal regions via stimulation is likely impacted by these dynamics, i.e., the dose of the neurostimulation to the target area may depend on the timing of the rTMS to the stimulation site relative to the dynamics of the functional connectivity between the two sites.

A candidate for tracking the dynamics of the functional connectivity between the DLPFC and ACC is prefrontal alpha oscillation. Alpha oscillations have been implicated in network connectivity, with the phase of alpha linked to activation and release of inhibition across and within networks (Hinkley et al., 2011; Klimesch, 2012; Sadaghiani et al., 2012; Medalla and Barbas, 2012; George et al., 2019). Alpha phase could therefore act as a gating mechanism where different phases in the cycle are associated with states of low and high excitability within the network. Hypothetically, there may be certain, potentially even subject-specific, phases in the alpha cycle where stimulation over DLPFC causes a greater effect at distal brain regions. This idea is consistent with research showing that the timing of stimulus onset relative to the phase of the alpha cycle influences perception (Busch et al., 2009; Milton and Pleydell-Pearce, 2016; Ronconi et al., 2018).

An important and relatively under-explored question is whether it matters what phase the brain is in when a TMS pulse is delivered. Several groups have investigated synchronized TMS delivery to the alpha phase (or the mu/beta rhythm in the motor system) and have shown acute/transient effects suggesting that excitability is indexed by phase (Zrenner et al., 2018, 2020; Torrecillos et al., 2020). There are, however, ongoing debates, including over the size and anatomical location of effects (Thut et al., 2011; Wagner et al., 2019; Samaha et al., 2020). All these studies assessed phase effects at relatively short time scales and have not examined effects of phase-synchronized rTMS applied over multiple weeks as part of a clinical intervention. Most have also studied the motor system and have used motor evoked potentials as their output marker. Notably, we have found in previous work that TMS-evoked BOLD response, particularly in the dorsal ACC, depends on the frontal alpha phase prior to TMS delivery (Saber et al., 2018; George et al., 2019). The data we

report here is part of a randomized, active-comparator controlled clinical trial in depression we are currently completing comparing phase dependent prefrontal TMS to the standard approach that does not take phase-dependence into account. The results from this clinical trial will show whether state-dependent, phase-locked stimulation may be more effective than conventional rTMS treatments.

In this paper, we consider whether phase dependent effects – entrainment – might persist across weeks when rTMS is synchronized to ongoing quasi-alpha (6 to 13 Hz) activity in the prefrontal cortex. Note that we have defined quasi-alpha as a slightly expanded bandwidth version of the traditional definition of alpha (8 to 12 Hz) due to early system tests trying to maximize prefrontal signal and be inclusive of more subjects (see Discussion section). We developed a novel closed-loop neurostimulation system (see Figure 1) and used it to test the hypothesis that synchronized application across weeks of rTMS treatment might yield increased entrainment, as observed by the EEG dynamics after stimulation. We assessed entrainment using the inter-trial phase coherence (ITPC) measure, which is a metric to capture how consistent oscillatory phase is across an ensemble of event-locked trials (Papenberg et al., 2013; van Diepen and Mazaheri, 2018), and examined how this measure changes over a period of weeks as rTMS is periodically applied either synchronized or unsynchronized to the preferred prefrontal quasi-alpha phase of an individual.

We investigated this hypothesis in a group of MDD patients as part of an ongoing double-blind clinical study, where one group receives rTMS synchronized to their quasi-alpha activity (SYNC), while another group receives the same stimulation, but the initial pulse in each train is not synchronized (UNSYNC). The phase at which we synchronized the first pulse in each TMS pulse train is based on a unique targeting approach using an integrated fMRI-EEG-TMS (fET) system (see Faller et al. (2019); Saber et al. (2018); George et al. (2019) and supplemental material; another separate manuscript about the fET system is also in preparation), where the preferred prefrontal alpha phase ϕ_{pre} is the phase which yielded the strongest BOLD fMRI activation in the ACC. The method used to estimate ϕ_{pre} is described in the Materials and Methods section and the supplementary material (see S.1 in supplementary material for details). In this report, we focus on whether rTMS applied synchronized or unsynchronized to this preferred phase over 30 sessions of treatment impacts entrainment over time.

MATERIALS AND METHODS

Subjects

This is an interim blinded analysis of an ongoing clinical trial. All EEG data for this randomized, double-blind, active comparator-controlled clinical trial ([ClinicalTrials.gov](https://clinicaltrials.gov/ct2/show/study/NCT03421808) ID: [NCT03421808](https://clinicaltrials.gov/ct2/show/study/NCT03421808)) was collected at the Medical University of South Carolina, SC, USA. 23 patients were consented and enrolled in the study, and 15 (see Table 1) were able to complete the rTMS treatment. 8 subjects dropped out for reasons including claustrophobia (N=2, i.e., could not complete MRI), hospital admission due to severe depressive episodes (N=1), and some participants could no longer make the time commitment for the study (N=5). During enrollment, all patients were randomly assigned to the SYNC or UNSYNC group before treatment. The inclusion criteria included diagnosis of unipolar MDD in a

current major depressive episode, Hamilton Rating Scale for Depression (HRSD) score 20, age between 21 to 70, and fixed and stable antidepressant medications for 3 weeks prior to and during the trial. Patients also needed to show a moderate level of resistance to antidepressant treatment, defined as failure of one to four adequate medication trials, or intolerance to at least three trials. Primary exclusion criteria were that patients had to be able to undergo a 3T MRI scan as well as TMS treatment safely. To ensure that baseline level of depression severity was stable at the time of study enrollment, patients were dropped from the study if they showed more than 30% improvement in the HRSD score from the time of their initial screening to the baseline assessment. A full list of inclusion and exclusion criteria can be found on [ClinicalTrials.gov](https://clinicaltrials.gov/ct2/show/NCT03421808). (<https://clinicaltrials.gov/ct2/show/NCT03421808>). This study was reviewed and approved by the Institutional Review Board of Medical University South Carolina and written informed consent was obtained from all study participants prior to enrollment.

EEG setup for closed-loop EEG-rTMS

Head circumference was used to select an appropriately sized cap with 32 active EEG sensors (ActiCap Slim, Brain Products GmbH, Munich, Germany; Jasper (1958)), which was placed on the patient's head. Cap placement was verified by making sure the EEG sensor for channel Cz was located midway between nasion and inion as well as between the left and right preauricular points. Impedance was reduced to less than $10k\Omega$ for each electrode. EEG was sampled at 10 kHz using a biosignal amplifier (ActiChamp, Brain Products GmbH, Munich, Germany). This amplifier is designed to recover from electromagnetic artifacts related to a TMS pulse in less than 1 ms (see also Sekiguchi et al. (2011)). No additional high-pass filters were applied before recording the data. Synchronized acquisition of all signals and experimental events was accomplished through the software framework Labstreaming Layer (LSL; see Kothe (2014)) and all data was stored in extensible data format (XDF; Kothe and Brunner (2014)) files. Additional detailed information about the equipment setup and conduct with closed-loop EEG-rTMS system are available in S.1 to S.5 of the supplementary materials.

EEG preprocessing for post-hoc analysis

Prior to EEG analysis, a double exponential model was fit to the average post-pulse response from $t = 17.5$ ms to $t = t_{ipr}$, which is the interval between pulses in a train, i.e., $1/IAF$. This fit was then subtracted from the post-pulse response for all pulses in a session in order to suppress a slow instantaneous TMS artifact present in the EEG. This instantaneous TMS artifact was interpolated from -1 ms to 17.5 ms. The entire EEG session was then low-pass filtered with a cut-off at 50 Hz and down-sampled to 250 Hz. Infomax-based Independent Component Analysis (ICA; see Makeig et al. (1996)) was then performed on each session for each subject independently. The CORRMAP (Viola et al., 2009) plugin for the EEGLAB MATLAB toolbox (Delorme and Makeig, 2004) was used to identify ocular artifacts across sessions and those components were subsequently removed from the EEG data. For consistency with other studies in this project, data was then re-referenced to electrode location TP10 (close to the right mastoid). The arithmetic mean was computed separately for every EEG channel and subtracted from every point in the time series for that channel.

Next, EEG data was segmented into two separate datasets (**Pre** and **Post**) for two separate calculations (see Figure 2 and Figure 3). For dataset **Pre**, epochs were extracted from the intervals between two rTMS pulse trains. Only epochs of 2.5 seconds or longer were considered, and the longest epoch was 186.0 seconds long. The mean epoch length (interval between two rTMS pulse trains) was 15.6 s at a standard deviation of 75.3 s. For dataset **Post**, epochs were extracted from a time window [0,2.5]s relative to the last (i.e., 40th) pulse of each pulse train. A band-pass filter (FIR, 6 to 13 Hz, order 63) was applied bi-directionally to attenuate oscillatory signal components at frequencies outside the alpha band (McIntosh and Sajda, 2020).

Trial weighted inter-trial phase coherence

Inter-trial phase coherence (ITPC) is commonly used for quantifying event-related phase modulation (Niso et al., 2013). ITPC is a scalar value that ranges from [0, 1] and is derived from an ensemble of phase values at a particular time point in trials. A value closer to 0 indicates low phase alignment among the trials at that particular time point, while an ITPC value closer to 1 indicates high alignment of phase angles across trials (Delorme and Makeig, 2004) at that point. As a simple example, if there is a systematic effect across N trials where at time point $t_{example}$ oscillatory activity shows similar phase (e.g., close to “peak” of a sine wave), we would expect for the single ITPC value we derive at time point $t_{example}$ for these N trials to be closer to 1 rather than 0. In order to identify effects most relevant to the rTMS treatment, we focused our analysis on electrodes at (F3) and adjacent to (FP1, F7) the stimulation site over DLPFC (the same channels were previously used to determine IAF).

The accuracy of the phase estimation of the Hilbert transform for each pulse train from each session is dependent on the signal to noise ratio (SNR) of each pulse train (the ratio of the quasi-alpha (6 to 13 Hz) wave to other EEG components (1 to 30 Hz)). This approximation based on fast Fourier transform (FFT) has errors in the energy sense due to the fact that Hilbert transformation is a unitary operator in the L^2 space (Rahman, 2007; Mo et al., 2015), so instead of averaging across trials for the phase coherence calculation, each trial was first weighted by its power in the inter pulse train period (epoched dataset **Pre**; see Figure 2). Relative power was used to calculate the trial weight of phase for each pulse interval with the consideration of consistency and comparability within one session. Relative power was defined as the ratio of absolute quasi-alpha power to the total power calculated from 1 to 30 Hz (spanning delta, theta, alpha and beta bands, see eq (2)). Quasi-alpha power was calculated as the integrated power between 6 to 13Hz which is the range used to identify the IAF for each subject during the rTMS triggering. The power of the entire spectrum (1 to 30 Hz) was calculated by Welch’s power spectral density (PSD) estimation method, for which the complete epoch was segmented into eight windows that overlapped 50%. The approximate integrals of absolute quasi-alpha power (6 to 13 Hz) and total frequency band (1 to 30 Hz) were calculated with the trapezoidal method of non-unit but uniform spacing which is determined by the frequency resolution (frequency resolution was 0.2441 Hz). More formally, trial weight was calculated as follows:

$$\alpha_{n,S} = \int_6^{13} P_{n,S,f}^{targeted} df = \int_6^{13} \frac{1}{3} (P_{n,S,f}^{FP1} + P_{n,S,f}^{F3} + P_{n,S,f}^{F7}) df \quad (1)$$

$$\bar{\alpha}_{n,S} = \frac{\alpha_{n,S}}{\int_1^{30} P_{n,S,f}^{targeted} df} \quad (2)$$

$$\omega_{n,S} = \frac{\bar{\alpha}_{n,S}}{\sum_{n=1}^n \bar{\alpha}_{n,S}} \quad (3)$$

where $\alpha_{n,S}$ is the absolute quasi-alpha power for trial n from session S ; $\int_1^{f2} P_{n,S,f}^j df$ is the integral of power between frequency $f1$ and $f2$ of channel j for trial n from session S , $j = \{FP1, F3, F7\}$; *targeted* refers to the near targeted area which includes FP1, F3, and F7; $\bar{\alpha}_{n,S}$ is the relative power for trial n from session S ; $\omega_{n,S}$ is the trial weight for trial n from session S .

After the trial weight calculation, the Hilbert Transform ($H\{\cdot\}$) was applied to the dataset **Post** (see Figure 2) to estimate the instantaneous phase $\phi_{n,j}(t)$ of signal $x_{n,j}(t)$ locked to the last TMS pulse for trial n and channel j , where $t \in [0, 2.5](s)$, $\phi(t) \in [-\pi, \pi]$.

$$\phi(t) = \arctan\left(\frac{H\{x(t)\}}{x(t)}\right), \quad \phi(t) \in [-\pi, \pi] \quad (4)$$

We then transformed the phase angle back to the analytic signal $Z_{n,j}(t)$ in the real and complex domain using Euler's formula.

$$Z_{n,j}(t) = re^{i\phi_{n,j}(t)} = r\cos(\phi_{n,j}(t)) + i \times r\sin(\phi_{n,j}(t)), \quad r = 1 \quad (5)$$

Our approach of calculating ITPC was slightly modified from the standard approach introduced by van Diepen and Mazaheri (2018). Instead of simply averaging $Z_{n,j}(t)$ across the trials (i.e., subscript n), we calculated a weighted average, where the analytic signal for each trial was weighted by coefficients $\omega_{n,S}$ that were derived based on relative quasi-alpha power for that trial, as described earlier (see Equation (3)). That way the absolute part of the intermediate result, $\bar{Z}_{j,S}(t)$, represented trial weighted ITPC for channel (electrode) j , which resulted in a 3×625 matrix of ITPC values for each session. Each row represents one channel (FP1, F3, and F7) and columns represent the samples in a trial (width of epoch of dataset **Post**, $2.5 \text{ s} \times 250 \text{ Hz}$ sampling rate). Finally, for the spatial average, we calculate the circular mean across these three EEG channels and obtain the absolute value, which is the post-stimulation $ITPC_S(t)$ of the near target region. Based on these resulting time series, we determined the ITPC for the time range $[0, 2.5]s$ post rTMS pulse train (see Figure 3).

$$\bar{Z}_{j,S}(t) = \sum_{n=1}^{n=75} e^{i \times \phi_{n,S,j}(t)} \times \omega_{n,S} \quad (6)$$

$$ITPC_S(t) = \left| \frac{1}{3} \sum_{j=1}^{j=3} \bar{Z}_{j,S}(t) \right| = \left| \frac{1}{3} \sum_{j=1}^{j=3} \sum_{n=1}^{n=75} e^{i \times \phi_{n,S,j}(t)} \times \omega_{n,S} \right| \quad (7)$$

where $ITPC_S(t)$ refers to the average ITPC value for session S at time t post rTMS; $|\bar{Z}_{j,S}|$ refers to the ITPC value of channel j from session S ; $\phi_{n,S,j}(t)$ is the instantaneous phase of channel j from trial n of session S ; $\omega_{n,S}$ is the trial weight for trial n of session S .

Correlation between first post-stimulation ITPC peak and treatment session

At the subject level, in order to see how this brain synchronization after an rTMS pulse train changes across sessions, Spearman correlation (Spearman's ρ) was used to capture the relationship between the first post-stimulation ITPC peak (referred as $ITPC^{max[1]}$, which is defined as the first local maximum of the ITPC following the last TMS pulse in a train, see Figure 3 and the details of first peak detection is available in S.6 of supplementary materials) and the treatment session number (Corder and Foreman, 2014). The range of Spearman's ρ is $[-1,1]$, with 1 indicating perfect correlation, -1 perfect anticorrelation and 0 that there is no monotonic association between two variables (Daniel et al., 1990).

Generalized linear mixed-effects model

We used a generalized linear mixed-effects model (GLMM) to analyze changes in $ITPC^{max[1]}$ across sessions as a function of treatment arm (SYNC vs UNSYNC). A GLMM is an extension to the generalized linear model (GLM) in which the linear predictor contains random effects in addition to the usual fixed effects (Breslow and Clayton, 1993). The general form of a GLMM as per (Jiang, 2007) is as follows:

$$y = X\beta + Z\mu + \varepsilon \quad (8)$$

Where y is the outcome variable; X represents the predictor variables; β is a column vector of the fixed-effects regression coefficients; Z is the design matrix for the random effects (the random complement to the fixed X); μ is a vector of the random effects (the random complement to the fixed β); and ε is a column vector of the residuals.

We used the GLMM in Matlab (Statistics and Machine Learning Toolbox, Matlab 2018b, Mathworks, USA) to investigate the relationship between $ITPC^{max[1]}$ and the corresponding independent variables which include stimulation frequency (IAF), relative quasi-alpha power $\bar{\alpha}_P$, session number of each treatment, and subject's treatment group (SYNC or UNSYNC). The fixed-effects in the model included stimulation frequency, relative quasi-alpha power, treatment group, session number, the interaction between treatment group and relative power, and the interaction between treatment group and session number. The subject difference was modeled by grouping variable *sub* as random-effects. Therefore, the final model is:

$$\ln\left(\frac{ITPC^{max[1]}}{1 - ITPC^{max[1]}}\right) \sim stim\ f + (session + \bar{\alpha}_P) * condition + (1 | sub) + \epsilon, \quad (9)$$

$$\ln\left(\frac{ITPC^{max[1]}}{1 - ITPC^{max[1]}}\right) \in [0, 1]$$

where $ITPC^{max[1]}$ refers to the first post-stimulation ITPC peak value for each session; $stim\ f$ refers to the stimulation frequency for each session; $session$ is the corresponding session number (e.g., the first treatment is 1); $\bar{\alpha}_P$ is the relative quasi-alpha power for each session; $condition$ is the SYNC(1) or UNSYNC(-1) group; sub represents each subject (e.g., the first subject is 1). In addition, because the range of $ITPC^{max[1]}$ is between 0 and 1 ($ITPC \in [0,1] \Rightarrow ITPC^{max[1]} \in [0,1]$), the logit link function is applied in this linear model.

RESULTS

Fifteen treatment-resistant depressed patients (part of a double-blind clinical trial, see Material and Method Section) were enrolled and assigned randomly to either of the two treatment arms, SYNC (experimental treatment) or UNSYNC (active comparator) (see Table 1). A preferred phase of quasi-alpha EEG, defined as the phase at which a TMS pulse to left DLPFC evoked strongest activity in dorsal anterior cingulate cortex (dACC), was determined for every subject in a single session of combined fET (see S.1 in supplementary materials for details). Patients participated in 30 treatment sessions, only one session per work day for six weeks (extended to seven weeks if sessions were skipped). For these treatment sessions, participants were seated comfortably in an adjustable armchair with the EEG-rTMS setup (see Figure 1). Every closed-loop EEG-rTMS treatment session (see Figure 2) started with 5 minutes of resting state recording where an individual alpha frequency (IAF) and triggering threshold (RMSE) was determined (see S.4 in supplementary materials for details). The closed-loop EEG-rTMS treatment for one session lasted approximately 30 minutes, and patients received 75 pulse trains of rTMS, with 40 pulses per train over the left DLPFC at 120% of intensity relative to their individual motor threshold (see S.3 in supplementary materials for how motor threshold was determined). The interval between pulses in a pulse train was set to $t_{ipi} = 1/IAF$ (e.g., 125 ms for a patient with alpha frequency of 8 Hz) for both the SYNC and UNSYNC groups. For patients who were assigned to the group SYNC, the first TMS pulse in each train of 40 pulses was triggered at the individual's preferred phase, as determined from the initial fET session ($\phi_{targ} = \phi_{pre}$). For patients in the UNSYNC group, the preferred phase was not targeted, but instead the target phase was drawn randomly from a uniform distribution over the range $[0, 2\pi]$ for the first pulse in every rTMS pulse train ($\phi_{targ} \sim U(0, 2\pi)$). The hardware setup and software used to administer the EEG-guided rTMS is described in more detail in S.2 of supplementary materials (also see Faller et al. (2019); George et al. (2019)).

SYNC patients show increased inter-trial phase coherence over sessions and decreased phase difference relative to the optimal phase for the therapeutic target.

Figure 4 shows examples of how the ITPC, for a given session, is estimated from the raw data for both SYNC and UNSYNC subjects. Post-stimulation, we observed an increase

across sessions in the first ITPC peak (or $ITPC^{max[1]}$) around the stimulation site (left DLPFC; based on electrodes F3, FP1 and F7) for SYNC patients relative to the control group UNSYNC (Spearman's rank correlation coefficient, Table 3). Specifically, for the SYNC experimental group, three of seven subjects showed a statistically significant ($p < 0.05$) increase in the post-stimulation $ITPC^{max[1]}$ over sessions (see Table 3), suggesting that more days of treatment with phase synchronized rTMS was associated with increasingly greater post-stimulation alignment in quasi-alpha phase between trials. For the UNSYNC control group, this effect was observed for only one of eight subjects (see Table 3). Figure 5 compares the changes in the post-stimulation $ITPC^{max[1]}$ for SYNC and UNSYNC groups both by session and by week. We see that five SYNC group subjects show an increase in quasi-alpha entrainment represented by positive $ITPC^{max[1]}$ between the first and last session (where the first session value was subtracted as baseline, see Figure 5 (A)). Group level effects were tested with non-parametric tests. A two-sided Wilcoxon signed rank test was used to test the difference between the first and last session within each group, where the null hypothesis was that the difference between the first and last session comes from a distribution with zero median (Wilcoxon, 1992). A Wilcoxon rank sum test was also used to test the difference between the first and last session across groups, with the null hypothesis being they come from the same population (Wilcoxon, 1992). As there may be noise/variation in the measurement of each single treatment session, we also did a similar analysis by averaging sessions across week. This analysis was similar to the session comparison, except $ITPC^{max[1]}$ was calculated between the first and last week (where all sessions in a week were averaged and the ITPC of the first week was subtracted as baseline, see Figure 5 (B)). The group level effect is the most significant ($p = 0.0059$) between SYNC and UNSYNC groups in the week comparison. This indicates that though the impact may be variable across individual days, EEG synchronized rTMS treatment is associated with greater post-stimulation quasi-alpha entrainment, compared to unsynchronized treatment, over the long-term across multiple sessions extending over weeks.

We also investigated the relationship between each subject's peak quasi-alpha entrainment phase (ϕ_{ent}) and their individual preferred phase that maximally engaged the ACC target (ϕ_{pre} from pre-treatment scan and ϕ_{post} from post-treatment scan). Here, ϕ_{ent} is the corresponding phase at the time when the first post-stimulation ITPC peak, $ITPC^{max[1]}$, was found (see Figure 4, i.e., the entrainment phase calculated based on electrode F3 for subject #P09, #Session 18 is 316.4724 degrees). Specifically, we looked at the difference, both at the beginning of the treatment and at the end of the six weeks, between the ϕ_{ent} and the phase eliciting the maximal response in the ACC target region. As mentioned earlier, the pre-treatment preferred phase (ϕ_{pre}) was determined using a simultaneous fET scan. We also performed a second post-treatment fET scan at the end of the six-week treatments to determine the preferred phase at that point (ϕ_{post}), since treatment itself could potentially affect the phase relationship between the TMS and the activity at the therapeutic target, namely the ACC. First, we obtained the corresponding ϕ_{ent} at the time that $ITPC^{max[1]}$ was detected for the treatments of the first and last week, where each week included 5 treatment sessions. Then the circular mean was calculated to represent the entrainment phase of the first ($\phi_{ent,1st}$) and last week ($\phi_{ent,6th}$). For the first week we computed the differences, for each subject, of $\phi_{ent,1st}$ and ϕ_{pre} computed pre-treatment, while for the

last week we computed the differences of $\phi_{ent,6th}$ relative to ϕ_{post} . Figure 5 (C) and (D) show the results for each treatment group. For the SYNC group, 5 out of 7 subjects' phase differences (entrainment phase minus preferred target phase) decrease from the first to the last week, indicating that the entrainment phase and preferred target phase are converging over the treatment sessions. Conversely, in the UNSYNC group, we see this convergence in only 1 out of 6 subjects. Note that two UNSYNC subjects are excluded here because their post-treatment fET scans were not available. A Kruskal-Wallis test was used to test the null hypothesis that the phase difference in the first and last week in each group (SYNC vs UNSYNC) comes from the same distribution (Kruskal and Wallis, 1952). Treating the direction of the phase changes (clockwise vs counterclockwise) as different and considering the magnitude of the differences, we find we can reject the null hypothesis ($p = 0.0455$) at the 5% significance level. We performed a second test to investigate whether an increase/decrease of phase was different across the groups, regardless of the magnitude of the individual changes for each subject. We applied Fisher's exact test to Table 2 to test if there are nonrandom associations between the categorical findings of increase/decrease of phase difference in SYNC and UNSYNC groups. The result of Fisher's test is $p = 0.1026$, thus we cannot reject the null hypothesis of no nonrandom association between the categorical variables (SYNC vs UNSYNC) at the 5% significance level. This finding, together with the analysis taking the magnitude of the phase difference into account and the significant increase in entrainment over time, is consistent with an interpretation that there is a shift in phase that is induced in the SYNC group. Thus the individual entrainment phase appears to move toward the individual preferred phase, i.e., toward the phase associated with the strongest BOLD activation in the ACC after subjects received rTMS treatment synchronized to their quasi-alpha activity (mainly alpha activity).

Evidence for entrainment both locally over the stimulation site and distally over the therapeutic target.

In support of our hypothesis, we found a significant group level effect, where $ITPC^{max[1]}$ increased across sessions only when rTMS was synchronized to individual preferred phase (SYNC group). Specifically, we observed a statistically significant effect of the interaction between the factors session-number (1 to 30) and treatment group (SYNC and UNSYNC) on $ITPC^{max[1]}$ as the dependent variable (generalized linear mixed effects model; $\beta = 0.0307$, $p = 0.0000$, $R^2 = 0.4329$; see Table 4). Figure 6 (A) shows the marginal effect of session-number on $ITPC^{max[1]}$ for the SYNC group on the near target region which includes electrodes FP1, F7 and F3 ($ITPC_{1st}^{max[1]} = 0.2980$, $ITPC_{30th}^{max[1]} = 0.5182$, $ITPC^{max[1]} = 0.2202$; see Figure 6 (A)). No significant effect was observed for an increasing session-number on $ITPC^{max[1]}$ for the UNSYNC group ($ITPC_{1st}^{max[1]} = 0.3204$, $ITPC_{30th}^{max[1]} = 0.3289$, $ITPC^{max[1]} = 0.0085$; see Figure 6 (A)). No significant effects were found for stimulation frequency (IAF) or session-number and treatment group alone. Random effects covariance parameters are shown in Table 5. We conducted the same analysis as a function of the EEG channels used to compute the post-stimulation $ITPC^{max[1]}$ (e.g. contralateral to rTMS target, see Figure 6 (B)). The $ITPC^{max[1]}$ increase across sessions ($ITPC^{max[1]}$) is largest near the

rTMS targeted area and fades to be non-significant in the area contralateral to the rTMS target (see Figure 6).

DISCUSSION

In this paper, differences in the consistency of TMS phase-locked responses were evaluated using an ITPC comparison between patients in SYNC versus UNSYNC groups. We showed that $ITPC^{max[1]}$ observed after TMS pulse trains over the left DLPFC region significantly increased across treatment sessions for patients who received SYNC rTMS treatment, while it did not for patients in the active control condition UNSYNC. This result suggests that long-term continuous synchronized rTMS treatments over left DLPFC could lead to greater brain synchronization and entrainment in the near targeted area in treatment-refractory MDD patients.

Despite rTMS being approved as a treatment for MDD, there continues to be a need to improve its efficacy (O'Reardon et al., 2007; Markowitz et al., 2010; Anderson et al., 2016). In a recent study, Sackeim et al. (2020) reported on over 5000 patients treated at more than 100 private practice sites since FDA approval. Four to six weeks of daily rTMS resulted in 28 to 62 percent remission, and 58 to 83 percent response (over 50% reduction in symptoms). These results are impressive. However, around 20 percent of patients with medication-refractory depression do not respond to rTMS treatment as it is delivered today, which ignores the EEG phase of delivery and treatment length. As suggested by our prior studies using the fET system, synchronizing the TMS pulse to an individual's brain state over long periods of time is a method that is important for reaching deep areas such as the ACC, so it may more efficiently engage the therapeutic target and affect the dynamics of the circuit that includes more than the DLPFC. (Saber et al., 2018; George et al., 2019). As this is a blinded ongoing trial, we are not yet able to test whether the entrainment effect seen here is linked to improved clinical response.

The observed increasing phase alignment over sessions may be attributable to neuroplasticity in the brain circuitry that gives rise to the prefrontal quasi-alpha oscillation (Lewis, 2009; Liu et al., 2015). We hypothesized that the phase of prefrontal alpha represents a gating mechanism (Veniero et al., 2011; Kundu et al., 2014; Saber et al., 2018; George et al., 2019), such that certain phases in the alpha are linked to states of greater excitability in which a higher dosage of TMS administered over the DLPFC will reach distal target structures such as the ACC. In practice, the EEG-rTMS system targeted frequencies in a wider range (6 to 13 Hz) than is classically defined for alpha (8 to 12 Hz). In system tests performed prior to the clinical trial using the alpha range, we found the system would not meet targeting specifications on many subjects. Since we did not know a-priori what the ideal frequency target would be for this population, and our mastoid montage optimized prefrontal alpha power partially at the expense of focality thus making our signal different from classically defined occipital alpha, it was decided to expand the range. As a result, our findings here suggest that there may be an increasing quasi-alpha entrainment to the stimulation. It is possible this may increase sensitivity/excitability at the target site at a certain preferred alpha phase for stimulation. Through this increasing alignment of phase across the stimulation sessions, the pulses may more frequently fall closer to the phase that

is associated with a state of greater excitability, where treatment effects at distal target brain structures may also be greater.

Several studies have examined aspects of how the timing of stimulation relative to spectral phase may impact subsequent oscillatory dynamics. For example, spectral analysis by Paus et al. (2001) suggested that single-pulse TMS induces a brief period of synchronized activity in the beta range (15 to 30 Hz) at the stimulation site. Leuchter et al. (2013) have hypothesized that the entrainment of cerebral oscillations caused by exogenous stimulation can reset cortical oscillators, possibly enhancing neuroplasticity, normalizing cerebral blood flow, and ultimately ameliorating depressive symptoms so as to increase the efficiency of rTMS treatment. A behavioral study by Samaha et al. (2020) has shown that entrainment (phase-locking) of ongoing quasi-alpha neuronal oscillations to rhythmic stimuli is a potential mechanism for enhancing neuronal responses and perceptual sensitivity. Another study observed a sustained oscillatory echo in the left inferior frontal gyri (IFG) when stimulated at the beta frequency, with subjects having stronger entrainment showing more memory impairment (Hanslmayr et al., 2014). Since our study is a double-blind clinical trial of MDD patients, the entrainment we observe can be examined relative to clinical improvement (such as higher rates of depression remission or response rate) and will provide a rigorous test of the hypothesis that entrainment effects are clinically meaningful.

Our results also show that the level of quasi-alpha entrainment post phase-locked rTMS treatment depends on whether rTMS was consistently locked to a specific phase in the cycle or not (i.e., SYNC or UNSYNC). Multiple studies have demonstrated that the modulation of brain excitability can depend on phase. Raco et al. (2016), for example, designed a close-loop system which combines different neuromodulation techniques (TMS and transcranial Alternating Current Stimulation (tACS)) and demonstrated that it can precisely hit the target phase to induce a phase dependent motor evoked potential (MEP) modulation with a phase lag. Desideri et al. (2017) found that cortico-cortical excitability is influenced by the phase of oscillatory activity at the time of the stimulus. Using a closed-loop EEG-TMS system, Zrenner et al. (2018) showed that the efficacy of TMS-induced plasticity in human motor cortex is determined by real-time EEG-defined excitability states. Furthermore, Hosseini et al. (2021) reported that by applying controllable phase-synchronized rTMS with tACS, they were able to induce and stabilize neuro-oscillatory resting-state activity at targeted frequencies. It is noteworthy that these previous studies investigated effects that were tied to phase targets that were fixed and the same for all subjects (e.g. $+90^\circ$ and -90°). In contrast, here we selected a subject specific preferred phase by determining the phase that maximized BOLD response in the ACC. We found that there was some inter-subject variability in terms of which preferred phase elicited the strongest BOLD response to TMS. Our findings further complement the existing body of research, which has focused on short-term/immediate effects, with evidence that points to long-term entrainment effects.

Differences in brain synchronization changes, measured as post-stimulation quasi-alpha entrainment across treatment sessions in the targeted region, were found between SYNC and UNSYNC groups. For patients that received SYNC condition treatment (i.e., onset of rTMS time-locked to preferred instead of random phase), the consistency of the TMS phase-locked response across trials increased as the number of treatment sessions increased. This was

observed as an increase in the first ITPC peak value post-stimulation, $ITPC^{max[1]}$, across sessions. For patients in the UNSYNC group, no such effect was observed. Interestingly, on subject-level, one participant in the UNSYNC group showed statistically significant phase entrainment at a considerable correlation strength ($p = 0.0110$; $\rho = 0.46$). From reviewing demographic information and EEG data that are available at this stage of this single-blind study we have no explanation yet for this outlier. Other studies also investigated condition-specific brain synchronization differences after rTMS treatment with phase-focused measurements: Zuchowicz et al. (2019), for example, found frequency-dependent brain connectivity changes in MDD-responders and MDD-non-responders after rTMS sessions using the Phase Locking Value (PLV). This result suggests that an increase in phase synchronization in the EEG after rTMS treatment could indicate which patients are more likely to respond with a clinically significant improvement in MDD-symptoms. Similar results have been shown by Olbrich et al. (2014) based on another metric called Phase Lag Index (PLI). In a recent study, Lin et al. (2021) provided evidence for TMS-induced entrainment of alpha activity in occipital cortex using the ITPC metric. In accordance with the findings of these previous studies, we also found evidence in support of phase entrainment, specifically on a longer time scale of multi-week synchronized rTMS treatments.

Limitations

While these findings are promising, there are a number of limitations to this study that should be considered when interpreting these findings more broadly. Specifically, while we found evidence for quasi-alpha phase entrainment in the condition SYNC, our study was not designed to determine whether any randomly chosen phase, rather than the predetermined subject-specific preferred phase, would accomplish the same effect as long as it is kept fixed across the treatment sessions. Moreover, in a separate analysis of BOLD changes in ACC (manuscript in preparation), we found that there is a correlation between phase and the peak of BOLD activation at the group level, indicating it is possible that there is a general preferred phase which is not subject-specific. This would be consistent with previous findings from Zrenner et al. (2018), which showed that across subjects, a negative μ -rhythm phase is associated with high corticospinal excitability, while positive μ -rhythm phase connects with low excitability. Future studies with adapted designs are needed to test whether rTMS can induce entrainment also if phase is fixed instead of tuned to the subject.

It is also noteworthy, as was mentioned above, that we defined the range of the individual alpha frequency between 6 and 13 Hz for this study, which is broader than the typical 8 to 12 Hz alpha range. This broadening may have incorporated high theta frequencies in addition to alpha, which is why they are referred to as “quasi-alpha” rather than alpha EEG. In fact, the two subjects who presented the highest effect size from the intervention had average target frequencies in the range of high theta frequencies, further suggesting not only prefrontal alpha oscillation but other physiologically meaningful oscillatory activities might have been included, which requires further investigation. Another limitation of this study is our relatively small sample size, and future studies replicating these results in larger samples are warranted. In addition, the patients receiving rTMS treatment continued to take their medication during the experiment. This was consistent across treatment arms but could

conceivably influence patients' brain activity. In this study, we measured the first ITPC peak after rTMS offset to index and track brain synchronization across sessions. Future research could include other non-linear measurements like PLV or complexity analysis such as Higuchi fractal dimension (FD) and Lempel-Ziv Complexity. In fact, several studies have shown brain connectivity differences in MDD-responders after receiving rTMS treatment (Zuchowicz et al., 2019) and EEG complexity differences after rTMS between MDD-responders and non-responders based on FD (Akar et al., 2015; Bachmann et al., 2018) or Lempel-Ziv complexity (Arns et al., 2014).

An additional limitation is the selection of the right mastoid as the reference. Prior to the start of the clinical trial, multiple re-referencing methods were considered, including Laplacian, common average reference (CAR), and mastoids. Preliminary analyses indicated choosing the right mastoid provided the most stable alpha signal for system targeting. This provided an increase in SNR at the possible cost of being less certain if the quasi-alpha oscillation was primarily frontal, driven by posterior regions due to volume conduction, or mixed with oscillation in the motor area. While initial analyses comparing the phase of occipital and parietal regions to the phase of F3 suggest these more posterior regions are not the primary drivers of the frontal quasi-alpha signal studied, it is possible that this prefrontal oscillation is mixed with oscillations near motor area for several subjects. More investigation into optimized brain region and EEG signal targets, referencing schemes, and motor area is required (see S.10 in supplemental material). There is also a need for additional sham control conditions in TMS studies: TMS is a considerable source of sensory stimulation and sham-based control conditions are important so that findings in TMS-based experiments can be interpreted correctly and potential confounds can be ruled out (Siebner et al., 2019; Belardinelli et al., 2019). During the original experimental design, an additional control condition that included sham TMS was considered, but we were unable to practically add additional arms to the study. Future experiments must include sham-based controls to rule out any potential confounds from the sensory stimulation associated with TMS. Though hypothetical, it is also possible the most relevant brain activity changes after rTMS occurred during the first 128 ms of EEG data immediately after the TMS pulse train, then we could have missed them as this time window was not included in our ITPC analysis due to the noise induced by bandpass filtering on each TMS pulse train segment. Novel and more powerful signal processing methods would be required to study relevant effects in these time windows. Finally, once our double-blind clinical trial is completed, clinical results on changes in depression scores should be included and compared.

CONCLUSIONS

To our knowledge, this is the first study to track changes in brain synchronization reflecting phase entrainment at 6 to 13 Hz across multiple weeks of rTMS treatments (6 to 7 weeks of 30 sessions). The observed increase in brain synchronization across treatments suggests that the efficacy of rTMS may be improved with synchronized rTMS pulse triggering. Moreover, combining fET and EEG-rTMS proved to be valuable for exploring the physiological and therapeutic effects of phase-synchronized stimulation in patients with MDD, especially those with treatment-refractory depression.

Supplementary Material

Refer to Web version on PubMed Central for supplementary material.

ACKNOWLEDGMENTS

This work was funded by the National Institute of Mental Health (MH106775) and a Vannevar Bush Faculty Fellowship from the US Department of Defense (N00014-20-1-2027). We would like to thank Spiro P. Pantazatos for reviewing and providing feedback on the manuscript draft. We would like to thank Daniel Cook for his help with initial data collection with closed-loop EEG-rTMS. We would like to thank Michael Milici for his help with building the safety circuit box and ActiChamp testing. We would like to thank DeeAnn Guo for her help with ActiChamp testing and initial EEG data collection.

REFERENCES

- Akar SA, Kara S, Agambayev S, and Bilgiç V (2015). Nonlinear analysis of EEGs of patients with major depression during different emotional states. *Computers in biology and medicine*, 67:49–60. [PubMed: 26496702]
- Anderson RJ, Hoy KE, Daskalakis ZJ, and Fitzgerald PB (2016). Repetitive transcranial magnetic stimulation for treatment resistant depression: Re-establishing connections. *Clinical Neurophysiology*, 127(11):3394–3405. [PubMed: 27672727]
- Arns M, Cerquera A, Gutiérrez RM, Hasselman F, and Freund JA (2014). Non-linear EEG analyses predict non-response to rTMS treatment in major depressive disorder. *Clinical Neurophysiology*, 125(7):1392–1399. [PubMed: 24360132]
- Bachmann M, Päeske L, Kalev K, Aarma K, Lehtmets A, Ööpik P, Lass J, and Hinrikus H (2018). Methods for classifying depression in single channel EEG using linear and nonlinear signal analysis. *Computer methods and programs in biomedicine*, 155:11–17. [PubMed: 29512491]
- Barbas H, Ghashghaei H, Rempel-Clower N, and Xiao D (2002). Anatomic basis of functional specialization in prefrontal cortices in primates. *Handbook of neuropsychology*, 7:1–28.
- Belardinelli P, Biabani M, Blumberger D, Bortoletto M, Casarotto S, and David O (2019). Reproducibility in TMS-EEG studies: a call for data sharing, standard procedures and effective experimental control. *Brain Stimulation*, 12(3):787–790. [PubMed: 30738777]
- Breslow NE and Clayton DG (1993). Approximate inference in generalized linear mixed models. *Journal of the American statistical Association*, 88(421):9–25.
- Busch NA, Dubois J, and VanRullen R (2009). The phase of ongoing EEG oscillations predicts visual perception. *Journal of Neuroscience*, 29(24):7869–7876. [PubMed: 19535598]
- Caspers J, Mathys C, Hoffstaedter F, Südmeyer M, Cieslik EC, Rubbert C, Hartmann CJ, Eickhoff CR, Reetz K, Grefkes C, et al. (2017). Differential functional connectivity alterations of two subdivisions within the right dlPFC in Parkinson's disease. *Frontiers in human neuroscience*, 11:288. [PubMed: 28611616]
- Corder GW and Foreman DI (2014). *Nonparametric statistics: A step-by-step approach*. John Wiley & Sons.
- Daniel WW et al. (1990). *Applied Nonparametric Statistics*. PWS-Kent Pub. Boston, 2nd edition.
- Delorme A and Makeig S (2004). EEGLAB: an open source toolbox for analysis of single-trial EEG dynamics including independent component analysis. *Journal of neuroscience methods*, 134(1):9–21. [PubMed: 15102499]
- Desideri D, Belardinelli P, Zrenner C, and Ziemann U (2017). Cortico-cortical excitability is influenced by the phase of oscillatory activity at the time of the stimulus. *Brain Stimulation: Basic, Translational, and Clinical Research in Neuromodulation*, 10(2):491.
- Drysdale AT, Grosenick L, Downar J, Dunlop K, Mansouri F, Meng Y, Fetcho RN, Zebley B, Oathes DJ, Etkin A, et al. (2017). Erratum: Resting-state connectivity biomarkers define neurophysiological subtypes of depression. *Nature medicine*, 23(2):264.

- Faller J, Lin Y, Doose J, Saber T, G., McIntosh J, Teves J, Goldman R, George M, Sajda P, and Brown T (2019). An EEG-fMRI-TMS instrument to investigate bold response to eeg guided stimulation. pages 1054–1057.
- Fox P, Ingham R, George MS, Mayberg H, Ingham J, Roby J, Martin C, and Jerabek P (1997). Imaging human intra-cerebral connectivity by PET during TMS. *Neuroreport*, 8(12):2787–2791. [PubMed: 9295118]
- George M, Saber G, McIntosh J, Doose J, Faller J, Lin Y, Moss H, Goldman R, Sajda P, and Brown T (2019). Combined TMS-EEG-fMRI. the level of TMS-evoked activation in anterior cingulate cortex depends on timing of TMS delivery relative to frontal alpha phase. *Brain Stimulation: Basic, Translational, and Clinical Research in Neuromodulation*, 12(2):580.
- George MS, Ketter TA, and Post RM (1994). Prefrontal cortex dysfunction in clinical depression. *Depression*, 2(2):59–72.
- George MS, Lisanby SH, Avery D, McDonald WM, Durkalski V, Pavlicova M, Anderson B, Nahas Z, Bulow P, Zarkowski P, et al. (2010). Daily left prefrontal transcranial magnetic stimulation therapy for major depressive disorder: a sham-controlled randomized trial. *Archives of general psychiatry*, 67(5):507–516. [PubMed: 20439832]
- George MS, Nahas Z, Molloy M, Speer AM, Oliver NC, Li X-B, Arana GW, Risch SC, and Ballenger JC (2000). A controlled trial of daily left prefrontal cortex TMS for treating depression. *Biological psychiatry*, 48(10):962–970. [PubMed: 11082469]
- Hallett M (2007). Transcranial magnetic stimulation: a primer. *Neuron*, 55(2):187–199. [PubMed: 17640522]
- Hanslmayr S, Matuschek J, and Fellner M-C (2014). Entrainment of prefrontal beta oscillations induces an endogenous echo and impairs memory formation. *Current biology*, 24(8):904–909. [PubMed: 24684933]
- Hinkley LB, Vinogradov S, Guggisberg AG, Fisher M, Findlay AM, and Nagarajan SS (2011). Clinical symptoms and alpha band resting-state functional connectivity imaging in patients with schizophrenia: implications for novel approaches to treatment. *Biological psychiatry*, 70(12):1134–1142. [PubMed: 21861988]
- Hosseini T, Yavari F, Biagi MC, Kuo M-F, Ruffini G, Nitsche MA, and Jamil A (2021). External induction and stabilization of brain oscillations in the human. *Brain Stimulation*.
- Jasper HH (1958). The ten-twenty electrode system of the International Federation. *Electroencephalogr. Clin. Neurophysiol*, 10:370–375.
- Jiang J (2007). Linear and generalized linear mixed models and their applications. Springer Science & Business Media.
- Klimesch W (2012). Alpha-band oscillations, attention, and controlled access to stored information. *Trends in cognitive sciences*, 16(12):606–617. [PubMed: 23141428]
- Kobayashi M and Pascual-Leone A (2003). Transcranial magnetic stimulation in neurology. *The Lancet Neurology*, 2(3):145–156. [PubMed: 12849236]
- Kothe C (2014). Lab streaming layer (LSL). <https://github.com/scn/labstreaminglayer>. Accessed on October.
- Kothe C and Brunner C (2014). Lab streaming layer (LSL): A system for unified collection of measurement time series in research experiments. <https://github.com/scn/xdf>. Accessed on October.
- Kruskal WH and Wallis WA (1952). Use of ranks in one-criterion variance analysis. *Journal of the American statistical Association*, 47(260):583–621.
- Kundu B, Johnson JS, and Postle BR (2014). Prestimulation phase predicts the TMS-evoked response. *Journal of neurophysiology*, 112(8):1885–1893. [PubMed: 25008413]
- Leuchter AF, Cook IA, Jin Y, and Phillips B (2013). The relationship between brain oscillatory activity and therapeutic effectiveness of transcranial magnetic stimulation in the treatment of major depressive disorder. *Frontiers in human neuroscience*, 7:37. [PubMed: 23550274]
- Lewis DA (2009). Neuroplasticity of excitatory and inhibitory cortical circuits in schizophrenia. *Dialogues in clinical neuroscience*, 11(3):269. [PubMed: 19877495]
- Lin Y-J, Shukla L, Dugué L, Valero-Cabré A, and Carrasco M (2021). TMS entrains occipital alpha activity: Individual alpha frequency predicts the strength of entrained phase-locking. *bioRxiv*.

- Liu KK, Bartsch RP, Lin A, Mantegna RN, and Ivanov PC (2015). Plasticity of brain wave network interactions and evolution across physiologic states. *Frontiers in neural circuits*, 9:62. [PubMed: 26578891]
- Makeig S, Bell AJ, Jung T-P, and Sejnowski TJ (1996). Independent component analysis of electroencephalographic data. In *Advances in neural information processing systems*, pages 145–151.
- Markowitz JC, Rosenbaum JF, Thase ME, Gelenberg AJ, and Freeman CMP (2010). *Practice Guideline for the Treatment of Patients With Major Depressive Disorder*. American Psychiatric Association, Washington, DC, 3rd edition.
- Mayberg HS, Brannan SK, Mahurin RK, Jerabek PA, Brickman JS, Tekell JL, Silva JA, McGinnis S, Glass TG, Martin CC, et al. (1997). Cingulate function in depression: a potential predictor of treatment response. *Neuroreport*, 8(4):1057–1061. [PubMed: 9141092]
- McIntosh JR and Sajda P (2020). Estimation of phase in EEG rhythms for real-time applications. *Journal of Neural Engineering*, 17(3):034002. [PubMed: 32244233]
- Medalla M and Barbas H (2012). The anterior cingulate cortex may enhance inhibition of lateral prefrontal cortex via m2 cholinergic receptors at dual synaptic sites. *Journal of Neuroscience*, 32(44):15611–15625. [PubMed: 23115196]
- Milton A and Pleydell-Pearce CW (2016). The phase of pre-stimulus alpha oscillations influences the visual perception of stimulus timing. *Neuroimage*, 133:53–61. [PubMed: 26924284]
- Mo Y, Qian T, Mai W, and Chen Q (2015). The AFD methods to compute Hilbert transform. *Applied Mathematics Letters*, 45:18–24.
- Niso G, Bruña R, Pereda E, Gutiérrez R, Bajo R, Maestú F, and Del-Pozo F (2013). HERMES: towards an integrated toolbox to characterize functional and effective brain connectivity. *Neuroinformatics*, 11(4):405–434. [PubMed: 23812847]
- Olbrich S, Tränkner A, Chittka T, Hegerl U, and Schönknecht P (2014). Functional connectivity in major depression: increased phase synchronization between frontal cortical EEG-source estimates. *Psychiatry Research: Neuroimaging*, 222(1–2):91–99.
- O'Reardon JP, Solvason HB, Janicak PG, Sampson S, Isenberg KE, Nahas Z, McDonald WM, Avery D, Fitzgerald PB, Loo C, et al. (2007). Efficacy and safety of transcranial magnetic stimulation in the acute treatment of major depression: a multisite randomized controlled trial. *Biological psychiatry*, 62(11):1208–1216. [PubMed: 17573044]
- Papenberg G, Hämmerer D, Müller V, Lindenberger U, and Li S-C (2013). Lower theta inter-trial phase coherence during performance monitoring is related to higher reaction time variability: a lifespan study. *NeuroImage*, 83:912–920. [PubMed: 23876249]
- Pascual-Leone A and Walsh V (2002). 11 - Transcranial Magnetic Stimulation. In Toga AW and Mazziotta JC, editors, *Brain Mapping: The Methods* (Second Edition), pages 255–290. Academic Press, San Diego, second edition edition.
- Paus T, Sipila P, and Strafella A (2001). Synchronization of neuronal activity in the human primary motor cortex by transcranial magnetic stimulation: an EEG study. *Journal of Neurophysiology*, 86(4):1983–1990. [PubMed: 11600655]
- Raco V, Bauer R, Tharsan S, and Gharabaghi A (2016). Combining TMS and tACS for closed-loop phase-dependent modulation of corticospinal excitability: a feasibility study. *Frontiers in Cellular Neuroscience*, 10:143. [PubMed: 27252625]
- Rahman M (2007). *Integral equations and their applications*. WIT press.
- Rodriguez-Martin JL, Barbanoj JM, Schlaepfer TE, Clos SS, Perez V, Kulisevsky J, and Gironell A (2002). Transcranial magnetic stimulation for treating depression. *Cochrane Database of Systematic Reviews*, (2).
- Ronconi L, Busch NA, and Melcher D (2018). Alpha-band sensory entrainment alters the duration of temporal windows in visual perception. *Scientific reports*, 8(1):1–10. [PubMed: 29311619]
- Rushworth MF, Noonan MP, Boorman ED, Walton ME, and Behrens TE (2011). Frontal cortex and reward-guided learning and decision-making. *Neuron*, 70(6):1054–1069. [PubMed: 21689594]
- Saber G, McIntosh J, Doose J, Faller J, Lin Y, Moss H, Goldman R, George M, Sajda P, and Brown T (2018). Level of TMS-evoked activation in anterior cingulate cortex depends on timing of TMS

delivery relative to frontal alpha phase. *Proceedings of the International Society for Magnetic Resonance in Medicine*, 26:4518.

Sackeim HA, Aaronson ST, Carpenter LL, Hutton TM, Mina M, Pages K, Verdoliva S, and West WS (2020). Clinical outcomes in a large registry of patients with major depressive disorder treated with Transcranial Magnetic Stimulation. *Journal of Affective Disorders*, 277:65–74. [PubMed: 32799106]

Sadaghiani S, Scheeringa R, Lehongre K, Morillon B, Giraud A-L, d'Esposito M, and Kleinschmidt A (2012). Alpha-band phase synchrony is related to activity in the fronto-parietal adaptive control network. *Journal of Neuroscience*, 32(41):14305–14310. [PubMed: 23055501]

Samaha J, Iemi L, Haegens S, and Busch NA (2020). Spontaneous brain oscillations and perceptual decision-making. *Trends in cognitive sciences*.

Sekiguchi H, Takeuchi S, Kadota H, Kohno Y, and Nakajima Y (2011). Tms-induced artifacts on EEG can be reduced by rearrangement of the electrode's lead wire before recording. *Clinical Neurophysiology*, 122(5):984–990. [PubMed: 20920887]

Siebner H, Conde V, Tomasevic L, Thielscher A, and Bergmann T (2019). Distilling the essence of TMS-evoked EEG potentials (TEPS): A call for securing mechanistic specificity and experimental rigor. *Brain Stimulation*, 12(4):1051–1054. [PubMed: 30962028]

Sliwinska MW, Vitello S, and Devlin JT (2014). Transcranial magnetic stimulation for investigating causal brain-behavioral relationships and their time course. *Journal of visualized experiments: JoVE*, (89).

Thut G, Veniero D, Romei V, Miniussi C, Schyns P, and Gross J (2011). Rhythmic TMS causes local entrainment of natural oscillatory signatures. *Current biology*, 21(14):1176–1185. [PubMed: 21723129]

Torrecillos F, Falato E, Pogosyan A, West T, Di Lazzaro V, and Brown P (2020). Motor cortex inputs at the optimum phase of beta cortical oscillations undergo more rapid and less variable corticospinal propagation. *Journal of Neuroscience*, 40(2):369–381. [PubMed: 31754012]

van Diepen RM and Mazaheri A (2018). The caveats of observing inter-trial phase-coherence in cognitive neuroscience. *Scientific reports*, 8(1):1–9. [PubMed: 29311619]

Veniero D, Brignani D, Thut G, and Miniussi C (2011). Alpha-generation as basic response-signature to transcranial magnetic stimulation (TMS) targeting the human resting motor cortex: A TMS/EEG co-registration study. *Psychophysiology*, 48(10):1381–1389. [PubMed: 21542853]

Viola FC, Thorne J, Edmonds B, Schneider T, Eichele T, and Debener S (2009). Semi-automatic identification of independent components representing EEG artifact. *Clinical Neurophysiology*, 120(5):868–877. [PubMed: 19345611]

Wagner J, Makeig S, Hoopes D, and Gola M (2019). Can oscillatory alpha-gamma phase-amplitude coupling be used to understand and enhance TMS effects? *Frontiers in human neuroscience*, 13:263. [PubMed: 31427937]

Walsh V and Pascual-Leone A (2003). *Transcranial magnetic stimulation: a neurochronometrics of mind*. MIT press.

Wilcoxon F (1992). Individual comparisons by ranking methods. In *Breakthroughs in statistics*, pages 196–202. Springer.

Woniak-Kwańska A, Szekely D, Aussedat P, Bougerol T, and David O (2014). Changes of oscillatory brain activity induced by repetitive transcranial magnetic stimulation of the left dorsolateral prefrontal cortex in healthy subjects. *Neuroimage*, 88:91–99. [PubMed: 24269574]

Zrenner B, Zrenner C, Gordon PC, Belardinelli P, McDermott EJ, Soekadar SR, Fallgatter AJ, Ziemann U, and Müller-Dahlhaus F (2020). Brain oscillation-synchronized stimulation of the left dorsolateral prefrontal cortex in depression using real-time EEG-triggered TMS. *Brain Stimulation*, 13(1):197–205. [PubMed: 31631058]

Zrenner C, Desideri D, Belardinelli P, and Ziemann U (2018). Real-time EEG-defined excitability states determine efficacy of TMS-induced plasticity in human motor cortex. *Brain stimulation*, 11(2):374–389. [PubMed: 29191438]

Zuchowicz U, Wozniak-Kwasniewska A, Szekely D, Olejarczyk E, and David O (2019). EEG phase synchronization in persons with depression subjected to transcranial magnetic stimulation. *Frontiers in neuroscience*, 12:1037. [PubMed: 30692906]

Author Manuscript

Author Manuscript

Author Manuscript

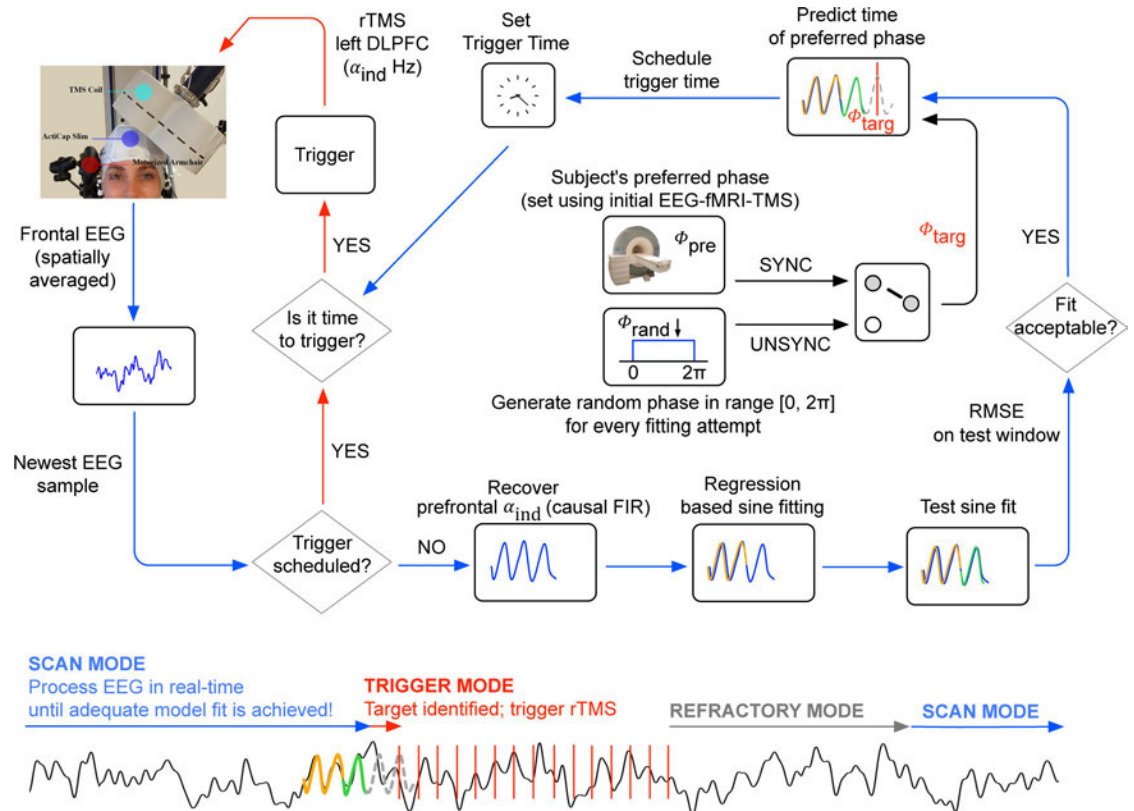
Author Manuscript

EEG-triggered repetitive TMS (rTMS) was applied over DLPFC either synchronously or asynchronous timed to an individual's quasi-alpha oscillation phase for patients' undergoing treatment for major depressive disorder.

Patients that received synchronous rTMS showed increased entrainment over sessions across days and decreased phase difference relative to the optimal phase for the therapeutic target (anterior cingulate).

Entrainment was observed both locally over the stimulation site and distally over the therapeutic target.

The entrainment effects build over the course of days/weeks, suggesting that these effects engage neuroplastic changes.

**Figure 1.**

Logic of the closed-loop stimulation system that synchronizes the onset of rTMS to EEG alpha phase. The system continuously processes EEG in real-time, where the EEG is sampled at 10 kHz. To optimize throughput, data is read from the amplifier in chunks of 20 data points (i.e., samples). Subsequently, a low-pass antialiasing filter is applied with a cut-off at 50 Hz and the signal is downsampled to 500 Hz. For EEG processing, the logic switches between three operation modes, SCAN MODE (blue arrows), TRIGGER MODE (red arrows) and REFRACTORY MODE (grey arrow). Model fitting in SCAN MODE is performed in parallel to reading new data (multi-threading) and every new fitting attempt is always performed on the newest available data. Starting in SCAN MODE, the system fits multiple single-sine function models on to the individual's prefrontal quasi-alpha signal (α_{ind} 6 to 13 Hz; spatial average of FP1, F7 and F3) in a time window $[-300, \sim -100]$ ms relative to the newest EEG sample (see S.2 in supplementary material). The resulting model that achieves the lowest root mean square error (RMSE) on that training signal is used for prediction on a more recent test signal in the time window $[-100, 0]$ ms, again relative to the newest EEG sample. If the RMSE on that test signal does not reach below a pre-determined, subject-specific threshold (see S.4 in supplementary material), the logic continues with a new fitting attempt, but now again using data relative to the newest EEG data that arrived in real-time. Otherwise, if and only if the RMSE on that test signal is below this threshold, the single-sine model is used to predict the prefrontal quasi-alpha wave up to 123 ms into the future. The targeted phase, ϕ_{targ} , then depends on the randomized treatment arm for that patient. For SYNC, ϕ_{targ} is the subject specific preferred phase ϕ_{pre} that was determined in an initial combined fMRI-EEG-TMS experiment (see S.1 in supplementary material).

For UNSYNC, ϕ_{targ} is drawn from a uniform random distribution over the range $[0, 2\pi]$ at every prediction ($\phi_{targ} \sim U(0, 2\pi)$). Taking into account the group delay of causal filtering and processing time, the logic then schedules the rTMS trigger onset at the predicted future time of ϕ_{targ} and switches into TRIGGER MODE. In TRIGGER MODE, no model fitting is attempted. Instead the logic keeps reading new data samples. Whenever the scheduled trigger time has arrived, a train of 40 TMS pulses is triggered where the inter-pulse-interval is the reciprocal of the subject's individual alpha frequency (IAF, $t_{ipi} = 1/IAF$). Directly after the 40th pulse has been triggered, the logic switches into REFRACTORY MODE, where the system does nothing other than reading in new EEG samples for $2 \times 40 \times \frac{1}{IAF}$ or twice the amount of time it took to deliver 40 TMS pulses, after which the logic again switches into SCAN MODE.

Author Manuscript

Author Manuscript

Author Manuscript

Author Manuscript

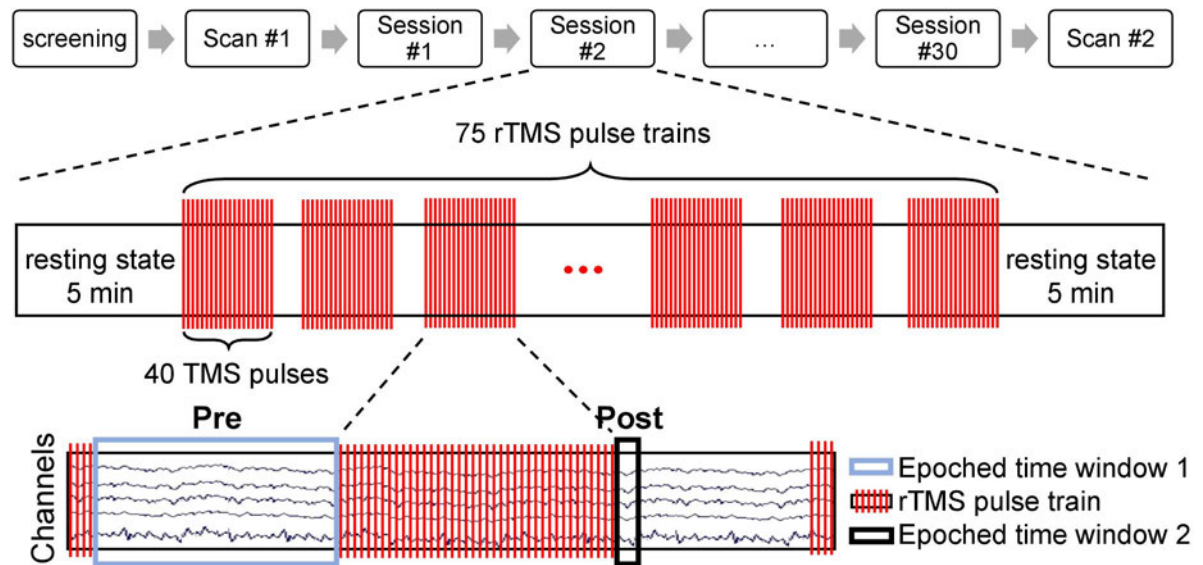
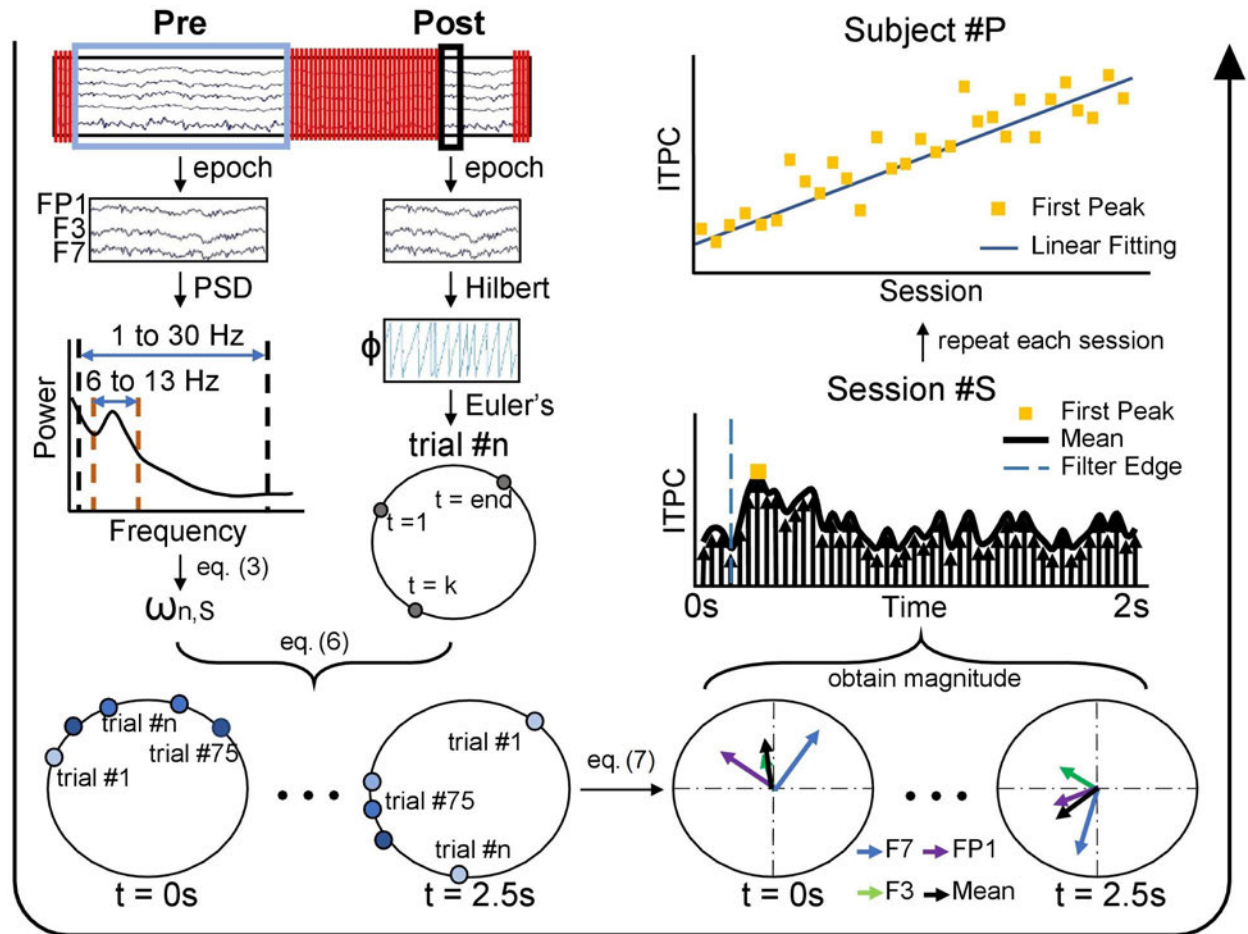


Figure 2.

Longitudinal treatment design. Before the pre-treatment scan (scan #1), all subjects were screened to meet both inclusion and exclusion criterion described in Materials and Methods section (see **Subjects** section for details). Then the first scan was done with the fET system to determine the pre-treatment preferred phase ϕ_{pre} , which was then used as the individual target phase ϕ_{targ} for subjects in SYNC group during the entire EEG-rTMS treatment. During the six to seven week treatment period, each subject received a total of 30 rTMS treatment sessions (one treatment each weekday). In each session, there were two five-minute rest periods (before the first and after the last pulse train). Each treatment consisted of 75 rTMS pulse trains/session (3000 pulses/session). In each rTMS pulse train, 40 TMS pulses were delivered at the IAF for each subject. Two datasets were split off from the EEG recordings during the treatment session: **Pre** was used for estimating the trial weight of each pulse train, **Post** was used for computing the post-stimulation trial weighted inter-trial phase coherence. After all treatment sessions, another scan (scan #2) was done with the fET system to obtain the post-treatment preferred phase ϕ_{post} .

**Figure 3.**

Flowchart of trial-weighted inter-trial phase coherence (ITPC) calculation. Processing flow is indicated by the large black arrow which starts at the upper left and goes counterclockwise to the upper right. First, two datasets were generated, one **Pre** and one **Post** with respect to the TMS pulse train. The **Pre** data was used for the trial weight calculation and the **Post** segment was used for the post-stimulation phase calculation. For each pulse train, the trial weight, $\omega_{n,S}$, was calculated based on relative alpha power of the **Pre** segment. The phase of the **Post** segment was obtained by a Hilbert transform, shown in polar coordinate by applying Euler's formula. This process was repeated for each pulse train of one session, and the results of each pulse train were combined via Equation (6) resulting in the trial weighted-phases, shown as polar coordinates, from $t = 0$ s to $t = 2.5$ s post rTMS pulse train. In the figure, trials with greater weight are shown with darker blue, while a smaller trial weight is shown as lighter blue. Using Equation (7), the trial weighted ITPC was calculated for each electrode in a region (shown here is the target region including electrodes FP1, F3, and F7) and the mean of the ITPC was also calculated across the three electrodes. The magnitude of vectors (mean, black) were plotted in the time window $t = [0, 2]$ s and the first peak of ITPC ($ITPC^{max[1]}$) was taken to present the post-stimulation ITPC value for that session. Finally, we analyzed how this time series of $ITPC^{max[1]}$ changes across sessions for

each subject #P, as shown in the upper right corner which uses a SYNC subject who has increasing phase entrainment as an example.

Author Manuscript

Author Manuscript

Author Manuscript

Author Manuscript

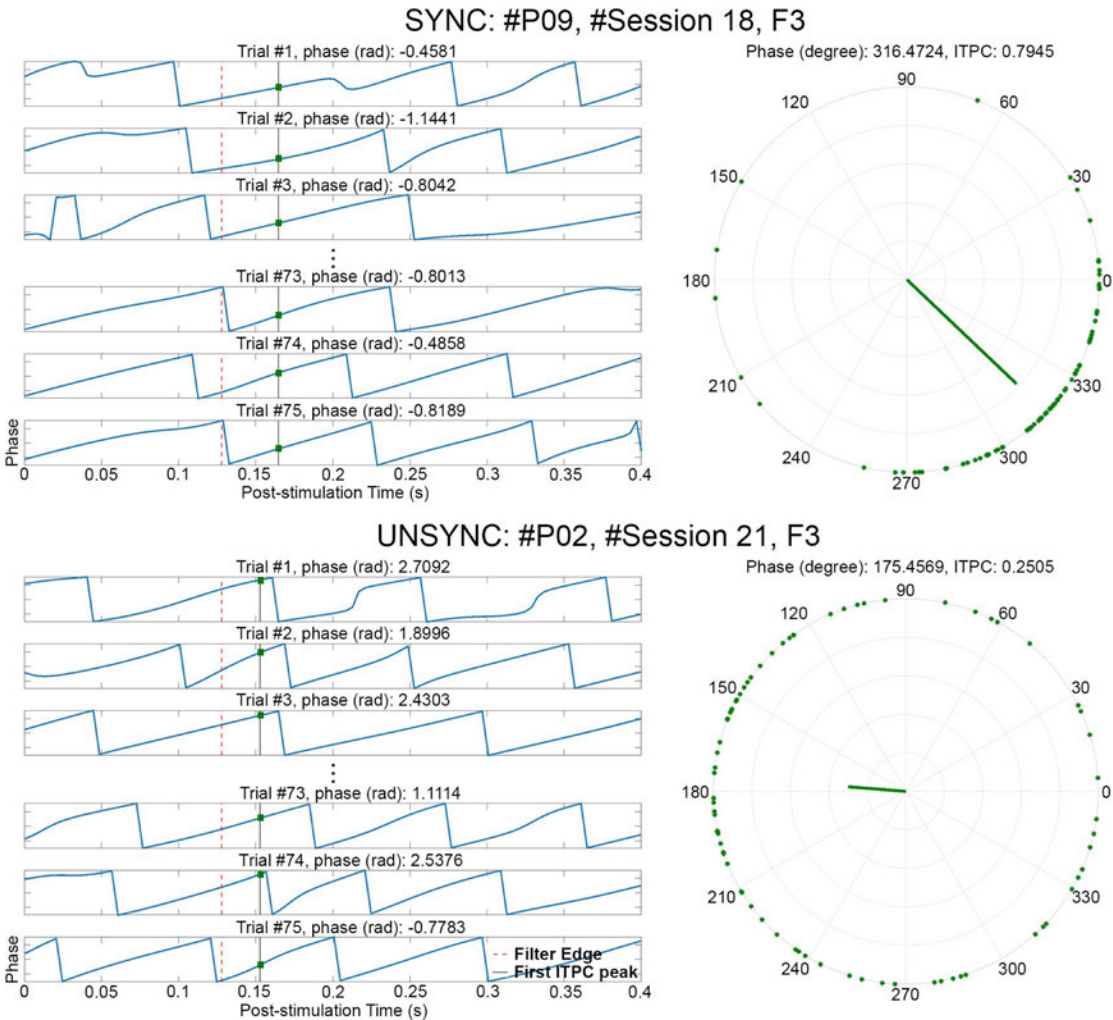
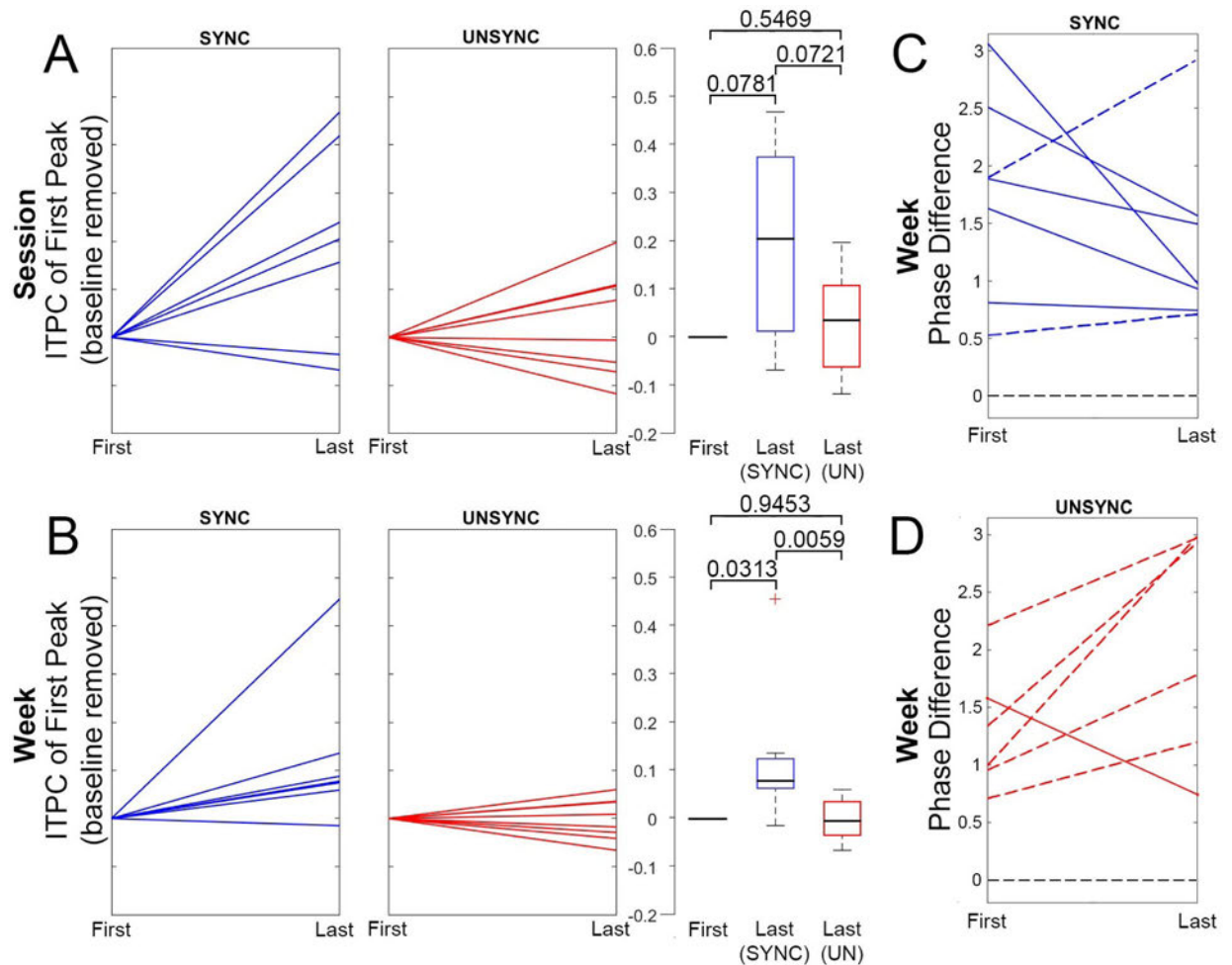


Figure 4. Estimate of phase entrainment in the quasi-alpha band (6 to 13 Hz) at the target electrode (F3). One session from a SYNC subject (#P09, #Session 18) and one session from an UNSYNC subject (#P02, #Session 21) are presented. For each trial of a session, the phase of the Post stimulation segment was obtained via Hilbert transform after alpha-band filtering, with the phase value shown (blue line) in each subpanel on the left. $t = 0$ refers to the end of one rTMS pulse train and the red dashed line in each subpanel indicates the filter edge ($t = 0.128$ s). The black solid line is the corresponding time point where the first post-stimulation ITPC peak ($ITPC^{max[1]}$) was detected (one value was calculated per session). The intersection (green dot) of the blue line and black line is the corresponding phase value of $ITPC^{max[1]}$. These points, across all trials of a session, are combined via Equation (5) resulting in the phase points shown as the green dots on the polar coordinates ($r = 1$) on the right. Using Equation (6) and (7), the trial weighted $ITPC^{max[1]}$ (green bar) is calculated for electrode F3 based on these points. In this example, the value of $ITPC^{max[1]}$ for this SYNC subject is two times greater ($ITPC^{max[1]} = 0.7945$) than this UNSYNC subject ($ITPC^{max[1]} = 0.2505$) indicating much greater entrainment on F3.

**Figure 5.**

Longitudinal changes in quasi-alpha entrainment for SYNC and UNSYNC groups. (A) Change in quasi-alpha entrainment between the first and last session, as measured by $ITPC^{max[1]}$. In each panel, blue represents the SYNC group and red represents the UNSYNC group. Each line is an individual subject (7 SYNC subjects and 8 UNSYNC subjects). Boxplots of data are shown on the right, together with the corresponding p-values of non-parametric tests of group level effects. Boxplots include the minimum, first (lower) quartile, median, third (upper) quartile, and maximum value of $ITPC^{max[1]}$, where the middle black line shows the median, the hinges represent first and third quartile and whiskers span from smallest to largest value in the data but reach out no further than 1.5 times the interquartile range. The data located outside of this range is indicated with a red cross. Panel (B) is similar to (A), except that pre- and post-treatment $ITPC^{max[1]}$ values are not derived from single sessions (i.e., the first and the last) but instead more robustly from an average across all sessions of one week (i.e., first vs last treatment week). (C) For the SYNC group (blue), this panel shows the difference ($\phi \in [0, \pi]$) between the preferred phases (ϕ_{pre} and ϕ_{post}) and the phases at which ITPC peaked post-rTMS (see Figure 3, center right) at two time points, before and after six weeks of treatment ($\phi_{ent,1st}$ presents the first week and $\phi_{ent,6th}$ presents the last week). Pre- and post-treatment preferred phase (ϕ_{pre} and ϕ_{post})

were obtained from two separate fET sessions acquired before (pre) and after (post) the full treatment course. Each line represents one subject, and seven subjects are included. A solid line indicates that the phase average of the last treatment week is closer to the preferred phase ($|\phi_{ent,6th} - \phi_{post}| < |\phi_{ent,1st} - \phi_{pre}|$), while a dashed line indicates that the phase average of the last week is further away from the preferred phase ($|\phi_{ent,6th} - \phi_{post}| > |\phi_{ent,1st} - \phi_{pre}|$). The black dashed line at phase difference $\phi = 0$ at the bottom represents the point where post-rTMS ITPC peak phase is exactly at the individual's preferred phase ($|\phi_{ent,6th} - \phi_{post}| = |\phi_{ent,1st} - \phi_{pre}| = 0$). Panel (D) is similar to (C), except that the comparison is performed for the UNSYNC group (red) which includes six subjects with complete data.

Author Manuscript

Author Manuscript

Author Manuscript

Author Manuscript

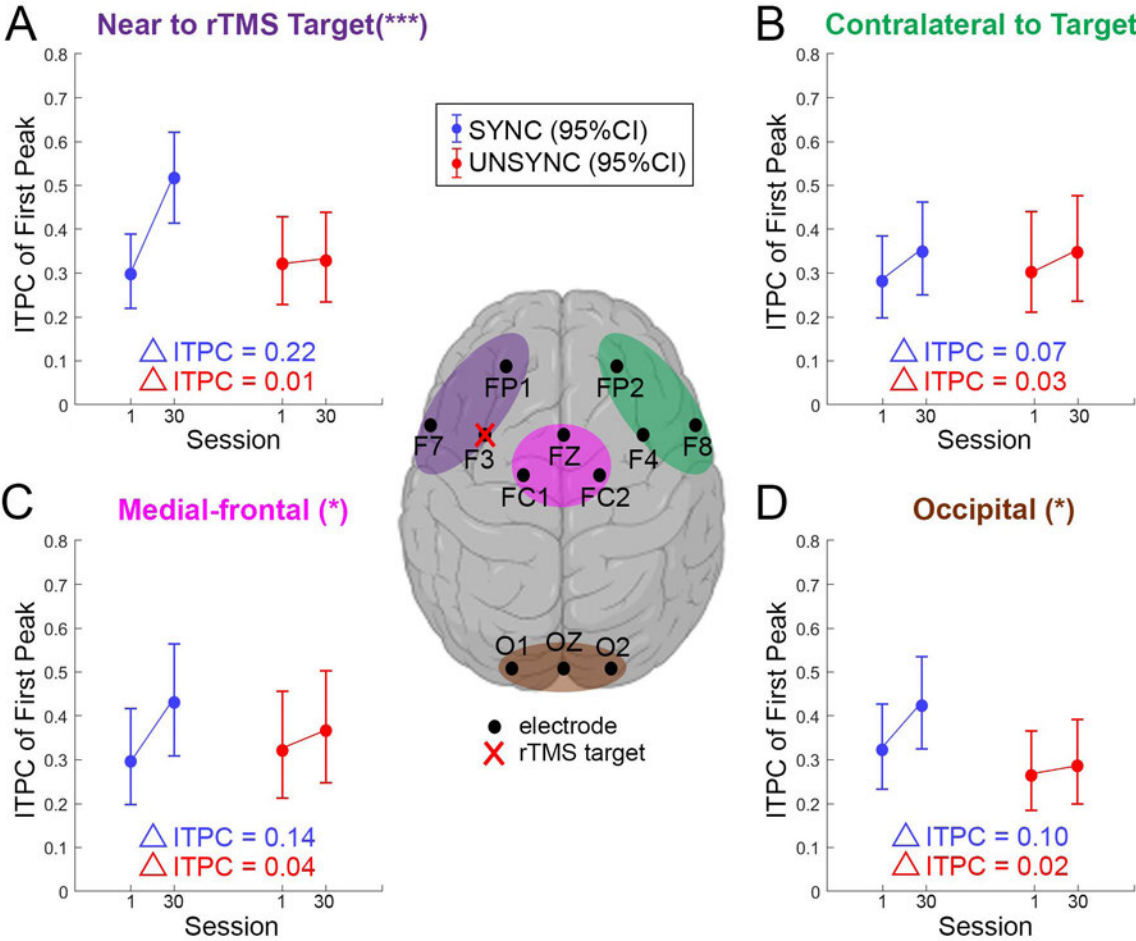


Figure 6. Following the significant effect observed for the interaction between session and group (see Table 4), we here show the effect of treatment session separately for UNSYNC and SYNC groups (i.e., marginal effect) across four different regions of interest (ROIs) based on the GLMM prediction. The central figure defines the ROIs and the electrodes used in the analysis. All ROIs consist of three electrodes. rTMS is applied over the left DLPFC (over electrode F3) for all subjects. (A) The model prediction of changes in ITPC^{max[1]} between the first and last session for SYNC and UNSYNC groups at the ROI near the rTMS target ROI, (B) contralateral to the target ROI, (C) in the medial-frontal ROI and (D) in the occipital ROI. The interaction-term of session and SYNC/UNSYNC group in the GLMM was highly significant in (A) (***, $p < 0.01$), significant in (C) and (D) (*, $0.01 < p < 0.05$) but not significant in (B).

Table 1.

Number of patients in every group, average age, gender, and average (\pm standard deviation) duration of the current depressive episode in weeks are shown. The duration of the current depressive episode is used to describe how long an individual patient has been depressed during the present depressive episode. There is no significant difference between the SYNC and UNSYNC groups in age ($p = 0.4803$) or duration of current depressive episode ($p = 0.7034$).

	# of Patients	Age (y)	Sex	Duration of Current Depressive Episode
SYNC	7	50.1 \pm 10.5	6 F, 1 M	50.1 \pm 39.9 weeks
UNSYNC	8	45.0 \pm 15.9	6 F, 2 M	60.6 \pm 60.5 weeks
Total	15	47.4 \pm 13.4	12 F, 3 M	55.7 \pm 50.4 weeks

Author Manuscript

Author Manuscript

Author Manuscript

Author Manuscript

Table 2.

Number of patients in different phase change direction for each group.

Phase Difference	SYNC	UNSYNC
Closer	5	1
Farther	2	5

Author Manuscript

Author Manuscript

Author Manuscript

Author Manuscript

Table 3.

Spearman correlation between post-stimulation trial weighted first post-stimulation ITPC peak (ITPC^{max}[1]) and Session

Subject	Condition	ρ	p-value
P01	unsync	0.4612	0.0110(*)
P02	unsync	0.1462	0.4392
P03	unsync	0.0670	0.7244
P04	unsync	0.0056	0.9775
P05	unsync	-0.0478	0.8015
P06	unsync	-0.0216	0.9102
P07	unsync	-0.0170	0.9323
P08	unsync	-0.2796	0.1343
P09	sync	0.7320	0.0000(***)
P10	sync	0.4585	0.0115(*)
P11	sync	0.4011	0.0391(*)
P12	sync	0.3112	0.0944(.)
P13	sync	0.1773	0.3471
P14	sync	0.0553	0.7795
P15	sync	-0.1430	0.4492

(***) indicates significant under a 99.9% confidence level

(**) indicates significant under a 99% confidence level

(*) indicates significant under a 95% confidence level

(.) indicates significant under a 90% confidence level.

Table 4.

Fixed effects coefficients (95% CIs)

Name	Estimate	SE	t-Stat.	DF	p-Value	Lower CI	Upper CI
(Intercept)	−0.3929	0.3371	−1.1655	435	0.2445	−1.0556	0.2697
stimf	−0.0405	0.0256	−1.5803	435	0.1148	−0.0909	0.0099
$\bar{\alpha}_P$	−0.3128	0.5875	−0.5323	435	0.5948	−1.4675	0.8420
session	0.0013	0.0038	0.3487	435	0.7275	−0.0062	0.0089
condition	−0.1355	0.3145	−0.4309	435	0.6668	−0.7537	0.4827
$\bar{\alpha}_P$:condition	−1.5174	0.8257	−1.8378	435	0.0668	−3.1401	0.1054
session:condition	0.0307	0.0058	5.2647	435	0.0000	0.0192	0.0422

Author Manuscript

Author Manuscript

Author Manuscript

Author Manuscript

Table 5.

Random effects

			Type	Estimate
Group: sub (15 Levels)	(Intercept)	(Intercept)	std	0.33875
Group: Error	sqrt(Dispersion)	-	-	0.10561

Author Manuscript

Author Manuscript

Author Manuscript

Author Manuscript

EXHIBIT 27

Electronic Circuits: Fundamentals and Applications

Electronic Circuits: Fundamentals and Applications

Second edition

Michael Tooley, BA

Director of Learning Technology
Brooklands College




Newnes

OXFORD AUCKLAND BOSTON JOHANNESBURG MELBOURNE NEW DELHI

EX. 27
000378

Newnes
An imprint of Butterworth-Heinemann
Linacre House, Jordan Hill, Oxford OX2 8DP
225 Wildwood Avenue, Woburn, MA 01801-2041
A division of Reed Educational and Professional Publishing Ltd

 A member of the Reed Elsevier plc group

First published 1995 as *Electronic Circuits Student Handbook*
Reprinted 1999
Second edition 2002

© Michael Tooley 1995, 2002

All rights reserved. No part of this publication may be reproduced in any material form (including photocopying or storing in any medium by electronic means and whether or not transiently or incidentally to some other use of this publication) without the written permission of the copyright holder except in accordance with the provisions of the Copyright, Design and Patents Act 1988 or under the terms of a licence issued by the Copyright Licensing Agency Ltd, 90 Tottenham Court Road, London, England W1P 0LP. Applications for the copyright holder's written permission to reproduce any part of this publication should be addressed to the publishers

British Library Cataloguing in Publication Data

A catalogue record for this book is available from the British Library

ISBN 0 7506 5394 9

Typeset by Integra Software Services Pvt. Ltd., Pondicherry 605 005, India
www.integra-india.com
Printed and bound in Great Britain



EX. 27
000379

Contents

Preface	vii	11 Microprocessor systems	177
A word about safety	ix	12 The 555 timer	192
1 Electrical fundamentals	1	13 Radio	201
2 Passive components	18	14 Test equipment and measurements	216
3 D.C. circuits	46	Appendix 1 Student assignments	246
4 Alternating voltage and current	66	Appendix 2 Revision problems	250
5 Semiconductors	80	Appendix 3 Answers to problems	260
6 Power supplies	105	Appendix 4 Semiconductor pin connections	263
7 Amplifiers	116	Appendix 5 Decibels	265
8 Operational amplifiers	138	Appendix 6 Mathematics for electronics	267
9 Oscillators	151	Appendix 7 Useful web links	292
10 Logic circuits	161	Index	294

Resonance

The frequency at which the impedance is minimum for a series resonant circuit or maximum in the case of a parallel resonant circuit is known as the resonant frequency. The resonant frequency is given by:

$$f_0 = \frac{1}{2\pi\sqrt{LC}} \text{ Hz}$$

where f_0 is the resonant frequency (in hertz), L is the inductance (in henries) and C is the capacitance (in farads).

Typical impedance frequency characteristics for series and parallel tuned circuits are shown in Figs

4.17 and 4.18. The series $L-C-R$ tuned circuit has a minimum impedance at resonance (equal to R) and thus maximum current will flow. The circuit is consequently known as an **acceptor circuit**. The parallel $L-C-R$ tuned circuit has a maximum impedance at resonance (equal to R) and thus minimum current will flow. The circuit is consequently known as a **rejector circuit**.

Quality factor

The quality of a resonant (or tuned) circuit is measured by its **Q -factor**. The higher the Q -factor, the sharper the response (narrower bandwidth), conversely the lower the Q -factor, the flatter the

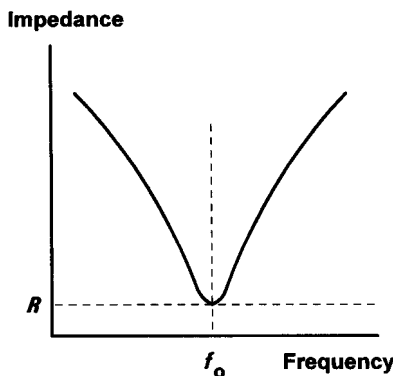


Figure 4.17 Impedance versus frequency for a series $L-C-R$ acceptor circuit

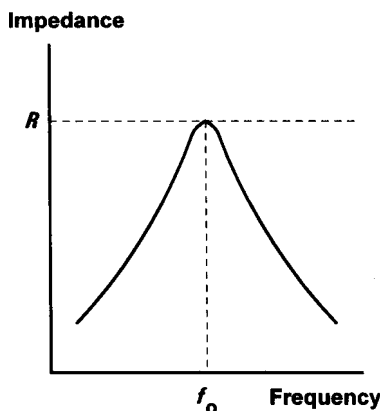
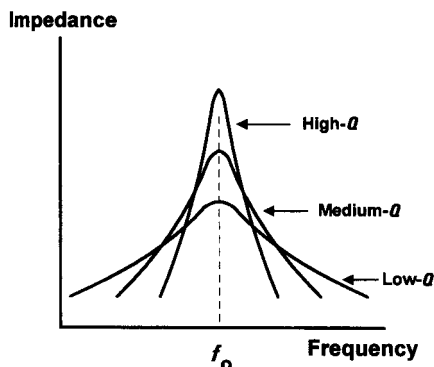
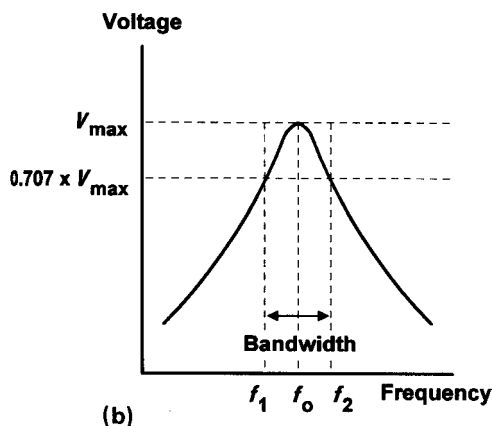


Figure 4.18 Impedance versus frequency for a parallel $L-C-R$ rejector circuit



(a)



(b)

Figure 4.19 (a) Effect of Q -factor on the response of a parallel resonant circuit (the response is similar, but inverted, for a series resonant circuit); (b) bandwidth

response (wider bandwidth), see Fig. 4.19. In the case of the series tuned circuit, the Q -factor will increase as the resistance, R , decreases. In the case of the parallel tuned circuit, the Q -factor will increase as the resistance, R , increases.

The response of a tuned circuit can be modified by incorporating a resistance of appropriate value either to 'dampen' or 'sharpen' the response.

The relationship between bandwidth and Q -factor is:

$$\text{bandwidth} = f_2 - f_1 = \frac{f_0}{Q} \text{ Hz}$$

Example 4.13

A parallel L – C circuit is to be resonant at a frequency of 400 Hz. If a 100 mH inductor is available, determine the value of capacitance required.

Solution

Re-arranging the formula $f_0 = 1/2\pi\sqrt{LC}$ to make C the subject gives:

$$C = \frac{1}{f_0^2(2\pi)^2 L}$$

Thus

$$C = \frac{1}{400^2 \times 39.4 \times 100 \times 10^{-3}} \text{ F}$$

or

$$C = \frac{1}{160 \times 10^3 \times 39.4 \times 100 \times 10^{-3}} \text{ F}$$

Hence $C = 1.58 \mu\text{F}$.

This value can be realized from preferred values using a $2.2 \mu\text{F}$ capacitor connected in series with a $5.6 \mu\text{F}$ capacitor.

Example 4.14

A series L – C – R circuit comprises an inductor of 20 mH, a capacitor of 10 nF, and a resistor of 100Ω . If the circuit is supplied with a sinusoidal signal of 1.5 V at a frequency of 2 kHz, determine the current supplied and the voltage developed across the resistor.

Solution

First we need to determine the values of inductive reactance (X_L) and capacitive reactance (X_C):

$$X_L = 2\pi fL = 6.28 \times 2 \times 10^3 \times 20 \times 10^{-3}$$

Thus $X_L = 251.2 \Omega$.

$$X_C = \frac{1}{2\pi fC} = \frac{1}{6.28 \times 2 \times 10^3 \times 100 \times 10^{-9}}$$

Thus $X_C = 796.2 \Omega$.

The impedance of the series circuit can now be calculated:

$$\begin{aligned} Z &= \sqrt{R^2 + (X_L - X_C)^2} \\ &= \sqrt{100^2 + (251.2 - 796.2)^2} \end{aligned}$$

thus

$$Z = \sqrt{10\,000 + 297\,025} = \sqrt{307\,025} = 554 \Omega$$

The current flowing in the series circuit will be given by:

$$I = V/Z = 1.5/554 = 2.7 \text{ mA}$$

The voltage developed across the resistor can now be calculated using:

$$V = IR = 2.7 \text{ mA} \times 100 \Omega = 270 \text{ mV}$$

Transformers

Transformers provide us with a means of coupling a.c. power or signals from one circuit to another. Voltage may be **stepped-up** (secondary voltage greater than primary voltage) or **stepped-down** (secondary voltage less than primary voltage). Since no increase in power is possible (transformers are passive components like resistors, capacitors and inductors) an increase in secondary voltage can only be achieved at the expense of a corresponding reduction in secondary current, and vice versa (in fact, the secondary power will be very slightly less than the primary power due to losses within the transformer). Typical applications for transformers include stepping-up or stepping-down mains voltages in power supplies, coupling signals in AF amplifiers to achieve impedance matching and to isolate d.c. potentials associated with active components. The electrical characteristics of a transformer are determined by a number of factors including the core material and physical dimensions.

The specifications for a transformer usually include the rated primary and secondary voltages and currents the required power rating (i.e. the

EXHIBIT 28

SPECIAL ISSUE

ABSTRACTS OF THE XX INTERNATIONAL CONGRESS ON SCHIZOPHRENIA RESEARCH

April 2–April 6, 2005, Savannah, Georgia

Contents

Introduction	185
1. Diagnosis	187
2. Phenomenology	195
3. Epidemiology	215
4. Neuroanatomy, Animal	245
5. Neuropathology, Biochemistry	248
6. Neuropathology, Histology	257
7. Genetics, Clinical	264
8. Genetics, Basic	281
9. Neurochemistry, Clinical	287
10. Neurochemistry, Animal	295
11. Psychology, Neuro-	315
12. Psychology, Cognitive	348
13. Neuroimaging, Structural	382
14. Neuroimaging, Functional	410
15. Neuroimaging, Neurochemical	442
16. Electrophysiology	449
17. Eye Movement Physiology	469
18. Therapeutics: Treatment Trials	474
19. Therapeutics: Pharmacologic Probes	509
20. Therapeutics: Psychosocial Trials	518
21. Health Economics & Services Research	537
22. Drug Side Effects & Tardive Dyskinesia	557
Author Index	576
Keyword Index	596

Introduction

INTERNATIONAL CONGRESS ON SCHIZOPHRENIA RESEARCH

The International Congress on Schizophrenia Research began meeting in April 1987, as part of the National Plan for Schizophrenia. It developed as the U.S. sister meeting of the Winter Workshop on Schizophrenia held in Europe every other year, organized by Steven Hirsch and Tim Crow. At the time of its inception, there was no scientific group in the U.S. which was organized around the discovery of mechanisms and treatments for schizophrenia. The meeting's goals were to allow scientists to exchange ideas, plan research projects, and see new treatment developments. The first meeting was small, numbering only 187, and each subsequent Congress has grown in attendance, to more than 1,500.

The goals of the meetings are to provide a forum for active investigators from around the world from academia, government, and industry to exchange information, be exposed to new ideas in neuroscience, and socialize. Ultimately we want the Congress to promote research activity and provide a scientific base and technical breadth to the field of schizophrenia research. Several practical goals are of utmost importance in this pursuit, first among which is to foster growth and interest among young scientists so they will invest their careers in this field. To this end, we began the Young Investigator Award Program in 1987, and have to date, including those awardees for our 2003 meeting, sponsored more than 281 young scientists to attend the Congress. Many of these scientists and clinicians are now established investigators in the field and devoted Congress participants. Another goal is to have a mixed group of basic and applied scientists, so that a true opportunity for informed translational research can transpire. At each of the recent meetings, approximately one third of the scientists are bench experimentalists and two thirds are clinical scientists. A third goal is to have scientists attend from around the world, since schizophrenia is an illness of worldwide incidence and concern. That goal is gradually being met, with 45 countries being represented at our last Congress and greater than 50% of attendees being outside the U.S. The Congress has facilitated collaborations across countries and continents and helped increase the scientific stature of research around the world.

To facilitate all of these goals, the setting for the International Congress is a matter of serious consideration for the Organizers. Characteristics of natural beauty, recreational possibilities, and cultural interest are important to complement the scientific goals. The Organizers recognize the capable and hard work of the Congress staff, without which this meeting could never occur. Over the lifetime of the Congress, the National Institute of Mental Health, the William K. Warren Foundation, several very faithful pharmaceutical companies, the University of Maryland's MPRC (serving as the operating institution), Case Western Reserve University through 1999, and now the University of Minnesota have all made the entire project feasible. But the most valuable resources of the Congress are the schizophrenia investigators from around the world, whose abstracts are represented in this volume, and whose science has drawn the attention of investigators, schizophrenia voluntaries, foundations, governments, newspapers, and politicians in all countries to this very needy area of medical research.

Carol A Tamminga, M.D.
University of Maryland School of Medicine
Maryland Psychiatric Research Center

S. Charles Schulz, M.D.
Chairman, Department of Psychiatry
University of Minnesota Medical School

16. Electrophysiology

455

EVENT-RELATED POTENTIALS IN SCHIZOPHRENIA: SPATIOTEMPORAL FACTOR STRUCTURE IN EMOTION RECOGNITION

T. Indersmitten,* C. G. Kohler, R. C. Gur, R. E. Gur, B. I. Turetsky

Psychiatry, University of Pennsylvania, Philadelphia, PA, USA

Emotion recognition deficits are well established in schizophrenia. However, few studies exist that examine brain related processing of emotional stimuli in schizophrenia. 20 schizophrenia subjects (6 female, 14 male) and 10 healthy controls (4 female, 6 male) had to recognize faces with happy, sad and neutral emotional expressions in mild and extreme intensities. Electrophysiological data was obtained using a 64-channel EEG. Principal Component Analyses were performed yielding 2 spatial and 4 temporal factors. Repeated measures ANOVAs were performed between patient and control groups for behavioral and electrophysiological data. Schizophrenia subjects performed worse on recognition of emotions. During emotion recognition, principal components analyses found fronto-central activations at 120 ms, 240 ms and 540 ms and a posterior activation at 410 ms. Patients had lower activations frontally at 240 ms, specifically for sad faces, and posterior at 410 ms. At 410 ms and 540 ms, emotion specific activations could be found. In addition, severity of negative symptoms, in particular alogia and anhedonia, were negatively correlated with recognition of happy faces and with activation at 410 ms. In schizophrenia subjects compared to controls, we found lower brain activations associated with emotion processing, suggesting a dysfunctional linkage between anterior and posterior areas. Emotion recognition performance and brain activation patterns at 540 ms were related to negative symptoms, suggestive of associations between brain based processing, emotion recognition and experience. NIMH MH01839.

RESTING FRONTAL BRAIN ACTIVATION ASYMMETRY AND SHYNESS AND SOCIABILITY IN SCHIZOPHRENIA

M. K. Jetha,* L. A. Schmidt, J. O. Goldberg

Psychology, McMaster University, Hamilton, ON, Canada

A number of recent studies have shown that the pattern of resting frontal EEG alpha (8 to 13 Hz) asymmetry is predictive of individual differences in affective style in healthy adults and children and some clinically depressed and anxious populations even when their symptoms are in remission. Individuals who exhibit stable patterns of greater relative right frontal EEG activity at rest are known to be at risk for depression and anxiety-related disorders, while individuals who exhibit stable left frontal EEG activity at rest are more successful in regulating stress and are sociable and outgoing. Using recent frontal activation/affective style models as a theoretical platform, we attempted to extend these findings to adults with schizophrenia. The relations among the pattern of resting regional EEG alpha activity, Cheek and Buss trait shyness and sociability, and positive and negative symptoms scores (PANSS) were examined in 20 adults with schizophrenia who attend a community-based treatment and rehabilitation center. Baseline regional EEG was measured continuously for 2 min (1 min eye-open, 1 min eye-closed) using a lycra stretchable cap from the left and right mid-frontal (F3, F4), central (C3, C4), parietal (P3, P4), and occipital (O1, O2) sites. We found that high trait shyness was related to greater relative resting right frontal EEG activity ($p < .05$), whereas high trait sociability was related to greater relative resting left frontal EEG activity ($p < .05$), only in those adults with schizophrenia who were classified as having low positive symptoms. These findings were specific to the mid-frontal

asymmetry measure. The relations with posterior asymmetry measures and trait personality measures were not significant. The present findings extend earlier work noting relations between the pattern of resting frontal EEG alpha asymmetry and personality in healthy individuals to a clinical population characterized by major psychosis. Findings are discussed in terms of the use of frontal EEG asymmetry as a metric for personality in schizophrenia.

ALPHA EEG SELECTIVITY PREDICTS EFFICACY OF RTMS IN SCHIZOPHRENIA

Y. Jin,* S. G. Potkin, S. Huerta, A. Kemp, G. Alva,

J. Sievers, W. E. Bunney

Psychiatry, University of California Irvine, Irvine, CA, USA

Human alpha EEG has a strong resonant feature. Changes in the EEG activity in schizophrenia have been found to be associated with negative symptoms. The present study showed that individualized rTMS could tune the alpha EEG and improve the negative symptoms. The selectivity of a resonant system can be described by quality factor, Q . For small damping it can be identified with $Q = f_p/(f_1 - f_2)$, where f_p is the resonant frequency, and $f_1 - f_2$ is a half-power bandwidth (HPB) around the resonance. Eight first-break drug-naïve schizophrenic patients in a separate study showed a significant reduction in alpha EEG selectivity as compared with age and gender matched controls. In this rTMS study, 16 schizophrenic patients with predominantly negative symptoms were included. rTMS rate was set at the alpha EEG resonant frequency. Magnetic pulses (80% motor threshold) were delivered bilaterally through a 9cm circular coil at prefrontal area. Treatment was consisted of 10 daily sessions for active or sham condition followed by a 2-week washout between treatments. During each session, rTMS was given 2 seconds per minute for a total of 20 minutes. Sham stimulation was conducted in the similar manner except that the coil was not plugged into the electricity. A separate coil placed 2 ft away was charged to simulate the acoustic effect of the active stimulation. Clinical symptoms and EEG were evaluated at baseline and after 10 treatments at each condition. Analysis of EEG at Fz revealed a significant increase in alpha EEG selectivity ($Q = 2.60$, $sd = 0.61$; $t_{14} = 19$, $p = 0.001$) after the active rTMS as compared with baseline ($Q = 2.17$, $sd = 0.42$). Power density at peak frequency was also increased ($p = 0.07$). No significant changes in EEG selectivity and power were found with sham. Using 11 cases who had completed both EEG and clinical evaluations, we found that the clinical improvement in negative symptoms was significantly correlated with the degree of increase in Q factor ($R = 0.61$, $p = 0.04$; $n = 11$). These data provide evidence that human alpha EEG can be tuned by direct electromagnetic stimulation. The association between changes in the alpha selectivity and clinical symptoms suggests that the timing (purity and persistence) of rhythmic brain activity may play a critical role in cognitive process. The potential role of EEG tuning in symptom improvement will be discussed in light of other supportive materials.

RELATIONSHIPS BETWEEN N100 AND M100 SENSORY GATING DEFICITS IN SCHIZOPHRENIA

A. P. Jones,* F. M. Hanlon, R. J. Thoma, M. P. Weisend, M. X. Huang, K. Martin, A. Smith, R. A. Yeo, G. A. Miller, J. M. Canive

Psychiatry, New Mexico VA Healthcare System, Albuquerque, NM, USA

A failure to filter out redundant auditory sensory stimuli is a hallmark deficit in schizophrenia. This sensory gating deficit has been

EXHIBIT 29



document 1 of 1

Full Text | Scholarly Journal

Improvement in Alpha EEG Selectivity and Negative Symptoms in Schizophrenia Following rTMS Treatment

Jin, Y; Potkin, S G; Huerta, S; Kemp, A; et al. Clinical EEG and Neuroscience; **Wheaton** Vol. 35, Iss. 4, (Oct 2004): 224-225.

Find a copy



http://getit.library.nyu.edu/resolve?url_ver=Z39.88-2004&rft_val_fmt=info:ofi/fmt:kev:mtx:journal&genre=article&sid=ProQ:ProQ%3Ahealthcompleteshell&atitle=Improvement+in+Alpha+EEG+Select+10-01&volume=35&issue=4&spage=224&au=Jin%2C+Y%3BPotkin%2C+S+G%3BHuerta%2C+S%3BKemp%2C+A%3Bet+al&isbn=&jtitle=Clinical+EEG

Abstract

None available.

Full Text

Introduction: rTMS has demonstrated value in altering symptoms of neuropsychiatric illness. Negative symptoms of schizophrenia are among the most difficult to treat with pharmacological intervention. We report that rTMS can tune the alpha EEG and improve negative symptoms of schizophrenia. The purity (bandwidth) and the persistence (ring-down time) of a resonant system can be described by quality factor, Q , defined as $Q = (\text{Stored Energy} / \text{Energy Lost Per Cycle})$. The greater the Q , the higher the selectivity (i.e., purer oscillation and longer ring-down). For small damping it can be identified with $Q = f^{\text{sub } p} / (f^{\text{sub } 1} - f^{\text{sub } 2})$, where $f^{\text{sub } p}$ is the resonant frequency, and $f^{\text{sub } 1} - f^{\text{sub } 2}$ is a half-power bandwidth (HPB) around the resonance. Human EEG has been demonstrated to have strong resonant features, especially in the alpha frequency band.

Methods: In this sham-controlled and crossover study, we used rTMS to challenge the alpha activity to identify the quality of EEG resonance in schizophrenic patients ($N = 16$) with predominantly negative symptoms. rTMS rate was set at subject's peak frequency. Magnetic pulses at 80% motor threshold intensity were delivered through a 9-cm circular coil at bilaterally prefrontal area. Treatment was consisted of 10 daily sessions for each condition followed by a 2-week washout between treatments. During each session, rTMS was given 2 seconds per minute for a total of 20 minutes. Sham stimulation was conducted in the similar manner except that the coil was not plugged into the electricity. A separate coil placed 2 ft away was charged to simulate the acoustic effect of the active stimulation. Clinical symptoms and EEG were evaluated at baseline and after 10 treatments at each condition.

Results: Analysis of single channel EEG at Fz showed a significant increase in patients' alpha EEG selectivity ($Q = 2.60 \pm 0.61$; $t^{\text{sub } 14} = 19$, $p = 0.001$) after rTMS as compared with baseline ($Q = 2.17 \pm 0.42$). Power density at peak frequency was also increased but did not reach statistical significance ($p = 0.07$). No significant changes in EEG selectivity or power were observed with sham. Using 11 cases who had completed both EEG and clinical evaluations, clinical improvement in negative symptoms was predicted by the degree of increase in Q factor ($R = 0.61$, $p = 0.04$; $n = 11$).

Conclusions: These data provide evidence that human alpha EEG can be tuned by direct electromagnetic stimulation. The association between changes in the alpha selectivity and clinical symptoms suggests that the timing (purity and persistence) of rhythmic brain activity may play a critical role in cognitive process. The potential role of EEG tuning in symptom improvement will be discussed in light of other supportive materials.

Author Affiliation

Jin Y, Potkin SG, Huerta S, Kemp A, Alva G, Sievers J, Bunney WE, Jr, University of California at Irvine, Irvine, California, USA

Copyright EEG and Clinical Neuroscience Society (ECNS) Oct 2004

Title Improvement in Alpha EEG Selectivity and Negative Symptoms in Schizophrenia Following rTMS Treatment
Author Jin, Y; Potkin, S G; Huerta, S; Kemp, A; et al
Publication title Clinical EEG and Neuroscience; Wheaton
Volume 35
Issue 4
Pages 224-225
Number of pages 2
Publication year 2004
Publication date Oct 2004
Publisher SAGE PUBLICATIONS, INC.
Place of publication Wheaton
Country of publication United States, Wheaton
Publication subject Medical Sciences--Psychiatry And Neurology
ISSN 15500594
e-ISSN 21695202
Source type Scholarly Journal
Language of publication English
Document type General Information
ProQuest document ID 206319285
Document URL <http://proxy.library.nyu.edu/login?url=https%3A%2F%2Fwww.proquest.com%2Fscholarly-journals%2Fimprovement-alpha-eeg-selectivity-negative%2Fdocview%2F206319285%2Fse-2%3Faccountid%3D12768>
Copyright Copyright EEG and Clinical Neuroscience Society (ECNS) Oct 2004
Last updated 2023-07-03
Database ProQuest Central

Database copyright © 2024 ProQuest LLC. All rights reserved. Terms and Conditions